Cellular and molecular bases of Vibrio / Crassostrea gigas interactions in healthy and pathological context

Daniel Oyanedel Trigo

THÈSE POUR OBTENIR LE GRADE DE DOCTEUR DE L'UNIVERSITÉ DE MONTPELLIER

En Biologie des Interactions (BDI)

École doctorale

GAÏA

Unité de recherche

UMR 5244, Interactions Hôtes Pathogènes Environnements (IHPE)

Bases moléculaires et cellulaires des interactions *Vibrio* / *Crassostrea gigas* en contexte sain et pathologique

Présentée par Daniel OYANEDEL TRIGO

Le 16 octobre 2020

Sous la direction de Delphine DESTOUMIEUX-GARZON et Guillaume CHARRIERE

Devant le jury composé de

Prof. Carmen AMARO GONZALEZ, Université de Valencia, Espagne	Rapporteur
Prof. François LALLIER, Sorbonne Université	Président du jury
Dr. Sophie GAUDRIAULT, INRAe	Examinateur
Dr. François DELAVAT, Université de Nantes	Examinateur
Dr. Annick JACQ, CNRS	Examinateur
Dr. Guillaume CHARRIERE, Université de Montpellier	Co-directeur de thèse
Dr. Delphine DESTOUMIEUX-GARZON, CNRS	Directrice de thèse

UNIVERSITÉ DE MONTPELLIER

Remerciements

Je n´aurais pas pu réaliser cette thèse sans l´aide des nombreuses personnes qui ont collaboré professionnellement et personnellement mener à terme ce projet. C´est pourquoi que je voudrais exprimer mes sincères remerciements à tous ceux qui m'ont aidé avec leur connaissance, patience, volonté, gentillesse et soutien pendant ces quatre années.

En premier lieu, je voudrais remercier Madame Carmen Amaro et Monsieur François Lallier pour m´avoir fait l´honneur d´accepter d'être les rapporteurs de ce manuscrit. Je voudrais également remercier Madame Sophie Gaudriault, Monsieur François Delavat et Madame Annick Jacq pour avoir accepté de participer au jury de cette thèse.

Merci également aux membres de mon comité de suivi : Madame Frédérique Le Roux, Monsieur Hervé Cottet, Monsieur Jérôme Nigou, et Monsieur Alain Givaudan qui ont su partager avec moi leurs connaissances, et me prodiguer tout au long de ma thèse leurs conseils avisés.

Je souhaite remercier particulièrement Madame Frédérique Le Roux à la Station biologique de Roscoff pour ses précieux conseils, son engagement et sa volonté de collaborer en apportant son expertise au développement de ma thèse. Merci à Monsieur Yannick Labreuche pour m´avoir transmis ses connaissances sur la mutagénèse, pour sa patience et ses qualités didactiques avec lesquelles il a su répondre à mes doutes, mille fois. Merci aussi à Monsieur Maxime Bruto pour son aide en bioinformatique.

Je voudrais aussi remercier Madame Marie-Agnès Travers, Monsieur Benjamin Morga et Madame Delphine Toubiez du Laboratoire de Génétique et Pathologie des Mollusques marins à La Tremblade pour tous les conseils précieux, leur accueil et leur collaboration. Merci de m'avoir accueilli dans votre laboratoire pour la réalisation d'une partie importante de mon travail.

Je remercie aussi les membres de la plateforme Microbex du laboratoire Marbec pour m'avoir permis de travailler dans leurs locaux lors des travaux de rénovation effectués dans notre laboratoire.

Je tiens à remercier l´Université de Montpellier, et l´école doctorale Gaia pour m'avoir permis de réaliser cette thèse et m'avoir accompagné tout au long de celle-ci.

Je suis très reconnaissant au Département Conicyt, du Ministère d´Education au Chili pour m´avoir donné le financement pour la réalisation de mes études.

Je remercie également le CNRS (PEPS blanc INEE, projet Like inhospitality), l´Ifremer (politique de site, projet Diversivib), l'Agence National de la Recherche (projet Decipher, ANR-14-CE19-0023) et l´Union Européenne (projet Vivaldi, H2020, subvention n° 678589) pour avoir financé mes travaux de recherche au travers de divers projets.

Je remercie Messieurs Guillaume Mitta et Yannick Gueguen pour m´avoir accueilli au sein du laboratoire IHPE dans leur unité de recherche.

Je souhaite exprimer ma gratitude envers Madame Delphine Destoumieux-Garzón. Tu as toujours été présente à chaque étape de ma formation, dans ton rôle de directrice de thèse

et de responsable d'équipe. Tu m´as montré à travers ta passion, ta discipline et ta rigueur quel doit être le chemin d'un vrai scientifique. Pendant ces 4 ans, j'ai toujours été étonné de ton niveau d´organisation et de ton sens des responsabilités. J´espère qu´un jour je pourrai faire de même pour les autres. Merci beaucoup pour ta patience pendant les moments et les situations compliquées. Tu as su me pousser à donner le meilleur de moi-même surtout au stade de la rédaction de ce manuscrit. Merci.

Au niveau personnel, j'apprécie les bons moments que j'ai partagés avec toi et ta famille, je n'oublierai jamais ta douceur et ton enthousiasme dans les réunions amicales en dehors du laboratoire, tels que la paella, la raclette et les invitations personnelles où Edwin nous a fait sentir chez nous.

Je tiens aussi à exprimer ma reconnaissance à Monsieur Guillaume Charrière, co-directeur de cette thèse. Je te remercie de tes conseils toujours opportuns, plein de références bibliographiques et ton expertise pratique. Toi et Delphine faites une excellente équipe d'encadrants et je crois que tous les étudiants qui ont été guidés pour vous conviennent que vous nous donnez un exemple à suivre.

Maintenant, je voudrais remercier tous les étudiants avec qui j´ai partagé mon bureau. Un grand merci à Etienne, Maxime, Aude, Samuel et Tristan, mes compagnons de la première étape. Je vous remercie pour votre accueil à mon arrivée, votre gentillesse et bonne humeur. Particulièrement je dis merci beaucoup à Maxime et Etienne pour les invitations personnelles qui m'ont aidé à rejoindre l'équipe et qui m'ont permis de découvrir la gastronomie française. Également, je donne un grand merci à mes compagnons de la deuxième étape ; Pierre-Louis, Maurine, Jean, Cairé, Janan, Maurine, Aurélie et Noémie pour tous les bons moments que nous avons partagés et où nous avons rigolé ensemble.

Je tiens à remercier Marco pour son rôle indispensable dans le laboratoire et aussi pour ses sympathiques histoires. Avec toi pas d'autre option que le français. Avec quelques « hola amigo que pasa » pour communiquer, tu m'as permis de dépasser ma honte et j'ai commencé à pratiquer le français. Je remercie aussi Philippe, à mon arrivée il a également été l'un des premiers avec qui j'ai pu partager. Ta patience et ta gentillesse m'ont beaucoup aidé le temps que je m'habitue à un nouveau laboratoire, ville, pays et continent. Je ne peux pas ne pas nommer Cristian. Merci pour la surprise de trouver un compatriote si loin, ton aide au travail mais surtout merci de m'avoir invité à partager chez vous et rencontrer ta belle famille.

Merci beaucoup à toute l'équipe IHPE. Je pense que je n'ai jamais eu de question ou de demande d'aide (scientifique, technique, de répétition ou de relecture) qui soit restée sans réponse. Pendant mon séjour j'ai pu voir un renouvellement important du personnel de l'équipe. Pourtant, étant en mesure de voir cette équipe un peu plus de l'extérieur, je me rends bien compte que l'atmosphère de convivialité qui y règne est quelque chose de précieux, que tous les laboratoires n'ont pas. J'espère que c'est quelque chose qui vous accompagnera toujours.

Je souhaite remercier aussi mes amis chiliens qui m'ont encouragé pendant cette période. Surtout je voudrais remercier ma famille pour m´avoir donné sa force et son soutien, toujours. Je remercie très affectueusement mes parents Cecilia et Jorge et ma sœur Vanessa pour m´a apporté leur aide, confiance, soutien et amour pendant toute ma vie, mais surtout dans

ce défi de venir étudier à Montpellier. Merci.

Je voudrais remercier Madame Paulina Schmitt qui m'a motivé pour venir ici poursuivre ma formation professionnelle et qui m'a recommandé à Delphine afin de rejoindre son équipe de recherche. Assis à côté du congélateur du laboratoire au Chili, alors que je regardais un mauvais résultat très probable, tu m'as demandé ce que j'allais faire après le master, qui allait imaginer que ta question pouvait se terminer par une telle aventure. Merci Pauli et on se revoit bientôt !

Finalement, je voudrais te remercier toi, Genezareth. Bien que nous ayons décidé cette aventure ensemble, comme la petite famille que nous venions de former, tu as complètement changé ta vie pour que je puisse arriver à la fin de cette thèse, et c'est sans aucun doute un sacrifice que je garde dans mon cœur. Je suis heureux que ce voyage ait été l'occasion pour toi de redécouvrir tous tes talents en dehors de ceux académiques. Tu m'as montré que la vie est pleine de surprises qu'il faut savoir embrasser. Merci pour ta patience infinie, toi qui as su me supporter quand j'étais stressé, en manque de confiance et insupportable. Je t'aime sans conditions et j'ai hâte de ce qui nous attend lorsque notre foyer va être de retour au Chili.

« J'aime les étudiants qui vont au laboratoire/ ils découvrent ce qui se cache à l'intérieur du confessionnal »

Violeta Parra

TABLE OF CONTENTS

LIST OF FIGURES AND TABLES

FIGURES

TABLES

LIST OF ABBREVIATIONS

AhpC	Alkyl hydroperoxide reductase C
AMPs	Antimicrobial Peptides
BPI	Bactericidal Permeability Increasing Protein
cDNA	Complementary Permeability Increasing Protein
CFU	Colony Forming Units
Cm	Chloramphenicol
DAMPs	Damage Associated Molecular Patterns
Dap	Diaminopimelic acid
DAPI	4´,6-diamidino-2-phenylindole
DNA	Deoxyribonucleic Acid
DUOX	Dual Oxidase
ECP	Extra Cellular Product
FAO	Food and Agriculture Organisation
GFP	Green Fluorescent Protein
IFN	Interferon
IL-17	Interleukin 17
Kda	Kilodalton
LPS	Lipopolysaccharides
LRR	Leucine-rich repeats
MARTX	Multifunctional Autoprocessing Repeats-in-Toxin
MIC	Minimal Inhibitory Concentration
NETs	Neuthropil Extracellular Traps
OMV	Outer Membrane Vesicule
ORF	Open Reading Frame
OsHV-1	*Ostreid* HerpesVirus-1
OTU	Operational Taxonomic Unit
PAMPs	Pathogen Associated Molecular Patterns
PGRP	Peptide Glycan Recognition Protein
PRP	Pattern Recognition Protein
Prp	Proline Rich Peptide
PRR	Pattern Recognition Receptor
q-PCR	Quantitative Polymerase Chain Reaction
RNA	Acid Ribonucleic
RNS	Reactive Nitrogen Species
ROS	Reactive Oxygen Species
SDS-PAGE	SDS PolyAcrylamide Gel Electrophoresis
SOD	Super Oxyde Dismutase
Spc	Spectinomycin
T2SS	Type 2 Secretion System
T3SS	Type 3 Secretion System
T6SS	Type 6 Secretion System
TLR	Toll Like Receptor
TNF	Tumor Necrosis Factor
UDP-GlcNAc	UDP-N-acetylglucosamine
UDP-MurNAG	UDP-N-acetylmuramyl Acid

RESUMÉ

CHAPITRE 1 : SYNTHESE BIBLIOGRAPHIQUE

Les bactéries du genre *Vibrio* sont des γ-proteobactéries ubiquitaires des milieux aquatiques. Elles possèdent une plasticité génomique et phénotypique remarquable, donnant lieu à une diversité de spécialisation de niche, allant des formes de vie libres à des associations mutualistes, commensales ou parasitaires avec des hôtes métazoaires et protozoaires (Takemura *et al*., 2014 ; Le Roux et Blokesch, 2018). Les vibrios font partie du microbiote naturel des animaux marins comme les coraux, les éponges et diverses espèces de bivalves. Même si certaines espèces établissent des symbioses mutualistes à l'exemple de *Vibrio fischeri* avec les calamars sépiloïdes (Ceccarelli et Colwell, 2014 ; McFall-Ngai, 2014), de nombreuses espèces sont des agents pathogènes, dont certaines bien connues chez l'homme (*V. cholerae* est l'agent étiologique du cholera), et d'autres sont responsables de vibrioses chez les organismes aquatiques, avec un impact fort sur la pisciculture et la conchyliculture dans le monde (Romalde et Barja, 2010).

L'huître du Pacifique *Crassostrea gigas* est produite tout le long de la côte française pour la consommation humaine. Depuis 2008, les populations d'huîtres d'élevage subissent des épisodes sévères de mortalité affectant particulièrement les huîtres juvéniles de moins de 18 mois ; les taux de mortalité pouvant atteindre 100% dans les exploitations françaises (Segarra et al., 2010). Cette maladie est connue sous le nom de syndrome de mortalité des huîtres du Pacifique (POMS). Son complexe étiologie implique l'interaction entre la génétique et l'état physiologique de l'hôte, l'environnement et des agents pathogènes, en particulier des microvariants du virus de l'herpès ostreid OsHV-1 et des bactéries opportunistes, dont des vibrios (Samain and McCombie, 2008 ; Petton *et al*., 2015). Le POMS survient de façon saisonnière, dans une fenêtre de température de l'eau de mer permissive allant de 16 ° C à 24 ° C (Pernet *et al.,* 2012). Les mortalités suivent une séquence d'événements qui commence par la réplication intense d'OsHV-1 dans l'huître conduisant à un état d'immunosuppression qui bénéficie à des bactéries opportunistes, dont certaines espèces de *Vibrio*, favorisant une infection secondaire entraînant la mort de l'hôte (de Lorgeril *et al*., 2018). La question de savoir si ces espèces de *Vibrio* sont de simples opportunistes ou participent activement au processus infectieux (agents pathogènes opportunistes) n'était pas résolue au démarrage de cette thèse.

Néanmoins, les interactions entre les huîtres et les vibrios ne se limitent pas à des interactions pathogènes. Ainsi, la structure des populations de vibrios présentes dans différentes fractions de la colonne d'eau et dans les tissus de l'huître montre que certaines populations de *Vibrio* présentent une association préférentielle avec l'huître même en dehors d'un contexte pathologique, avec peu ou pas de chevauchement des populations entre les huîtres malades et saines (Bruto *et al*., 2017). Ceci suggère que sans l'influence de facteurs de stress

majeurs tels que la température (Green *et al*., 2019) ou d'agents pathogènes tels que OsHV-1 µvar, les huîtres possèdent une capacité remarquable à maintenir l'homéostasie immunitaire avec son microbiote résident (Schmitt *et al*., 2011), ce qui devrait avoir un impact sur les génomes des groupes bactériens (ici des bactéries du genre *Vibrio*) capables d'établir une interaction stable avec les huîtres en tant qu'hôte (Chow *et al*., 2010).

L'objectif de la thèse a été de caractériser les mécanismes sous-jacents à l'association de l'huître C. *gigas* avec les populations de vibrios en contexte sain et pathologique.

CHAPITRE 2 : RESULTATS

SECTION I. DETERMINANTS DE LA COLONISATION ET PERSISTANCE ENVIRONNEMENTALE CHEZ *V. SPLENDIDUS* ASSOCIES A DES HUITRES SAINES

En raison de leurs conséquences importantes sur l'ostréiculture, les associations entre les vibrios et les huîtres ont été principalement étudiées dans le but d'identifier leur rôle en tant qu'agents étiologiques dans les maladies des huîtres. Le travail de notre proche collaboratrice Frédérique Le Roux à l'Ifremer (laboratoire de biologie intégrative des modèles marins, Station Biologique de Roscoff) a révélé que les espèces de *Vibrio* associées aux POMS expriment un potentiel de virulence contre l'huître, et que des populations virulentes de *Vibrio* formant des unités taxonomiquement et fonctionnellement proches, colonisent les huîtres affectée par le POMS (Bruto et al., 2017). Leurs travaux et les autres ont permis l'identification des déterminants de la pathogénicité de populations de vibrios pathogènes (Binesse *et al*., 2008 ; Duperthuy *et al*., 2011 ; Vanhove *et al*., 2016 ; Bruto *et al*., 2017, 2018 ; Piel *et al*., 2019). Néanmoins ces travaux ont aussi révélé qu'en rade de Brest (façade Atlantique), certaines populations de vibrios s'associent préférentiellement aux huîtres au printemps en l'absence de mortalités massives d'huîtres dues au POMS. Par conséquent, nous avons voulu étudier les espèces de *Vibrio* colonisant les huîtres en dehors du contexte pathologique pour dévoiler les déterminants clés de la colonisation des huîtres immunocompétentes. Pour cela, nous avons bénéficié des populations de vibrios caractérisées par Bruto et al. (2017). Nous nous sommes intéressés en particulier à une population affiliée taxonomiquement à *V. splendidus* (population #23), isolée d'huitres saines, et phylogénétiquement proche de *V. splendidus* (population #24) trouvée dans les huitres pendant le POMS. La population #23 présente un potentiel de virulence modéré.

Par une étude de génomique comparative et d'invalidation fonctionnelle de gène, nous avons montré que deux loci, un complexe MARTX (*Multifunctional Autoprocessing Repeats-in-Toxin*) et un système de sécrétion de type 6 (T6SS) étaient nécessaires à la virulence modérée de cette population. Ces résultats ont été publiés dans **l'article 1**. Nous avons ainsi découvert que chez *V. splendidus*, la capacité de colonisation et la virulence étaient limitées par une structure de l'antigène O (qui décore les lipopolysaccharides à la membrane externe de la bactérie). Leur structure est plus facilement reconnue par le système

immunitaire de l'huître par rapport à d'autres structures alternatives, avec un effet délétère sur la virulence mais qui confère une résistance aux prédateurs environnementaux que sont les amibes marines. Ainsi, nos résultats suggèrent une évolution de *V. splendidus* vers une virulence modérée comme compromis entre la « fitness » chez l'huître en tant qu'hôte et la résistance à ses prédateurs dans l'environnement. Les données des **résultats complémentaires 1** ont confirmé cette hypothèse dans un fond génétique de *Vibrio* différent.

Dans les **résultats complémentaires 2** (« short letter », en préparation), nous avons utilisé des populations supplémentaires de *Vibrio* associées positivement et négativement aux huîtres pour interroger si la résistance aux puissantes défenses antimicrobiennes de l'huître est un facteur suffisant pour déterminer la capacité des *Vibrio* à coloniser l'habitat hostile que représente l'huitre sain. Dans l'ensemble, nos résultats ne permettent pas de discrimer les associations vibrio-huître sur la base du seul caractère de résistance, sans doute parce que les multiples interactions biotiques qui ont lieu dans le milieu aquatique exercent des pressions similaires sur les populations qui ne sont pas associées aux huitres. Néanmoins, en considérant toutes les souches de vibrios indépendamment de leur affiliation taxonomique, les principaux facteurs expliquant l'association aux huîtres étaient : La résistance aux ROS, la virulence et la charge de surface.

SECTION II. LE ROLE DE LA CYTOTOXICITE CHEZ LES VIBRIOS DU CLADE SPLENDIDUS ASSOCIES AU POMS

Les huîtres possèdent une capacité remarquable à maintenir une homéostasie immunitaire en présence des communautés microbiennes abondantes et diversifiées associées à leurs tissus (Schmitt *et al*., 2012). Les facteurs biotiques et abiotiques pouvant conduire à la perte de cette homéostasie, comme l'infection à OsHV-1 µvar (de Lorgeril et al., 2018), sont des facteurs de risque clés pour l'apparition de mortalités massives. Parmi les bactéries associées à cette dysbiose, les vibrios du clade Splendidus, notamment *V. tasmaniensis* et *V. crassostreae*, sont les plus étudiés. *V. tasmaniensis* LGP32, souche isolée à l'origine d'un événement de mortalité en 2004, présente un important potentiel de virulence, causant la mort des huîtres en infections expérimentales, par injection (Gay *et al*. 2004). Notre équipe a montré qu'il s'agit d'un pathogène intracellulaire facultatif cytotoxique pour les hémocytes (Duperthuy *et al*., 2011 ; Vanhove *et al*., 2016), dont sa cytotoxicité dépend de l'étape de phagocytose. Aujourd'hui cette souche est utilisée comme modèle d'interaction hémocyte-vibrio dans un contexte pathogène (Duperthuy et al., 2010, 2011 ; Vanhove et al., 2015, 2016).

Une autre espèce à fort potentiel de virulence, *V. crassostreae*, a été caractérisée pour sa capacité à remplacer les communautés commensales de l'huître pendant le POMS. Une protéine extracellulaire de fonction inconnue, codée par le gène *r5.7*, et un plasmide (pGV1512), sont nécessaires pour la virulence de la souche *V. crassostreae* J2-9 en infection

expérimentale, par injection (Bruto *et al*., 2017). Toutefois, ces deux déterminants de virulence sont absents chez V. *tasmaniensis*. Ceci suggère que la virulence de ces deux espèces résulte de différents mécanismes. Au départ de ma thèse, les mécanismes d'interaction de J2-9 avec les hémocytes venaient d'être révélés par Tristan Rubio qui avait mis en évidence une cytotoxicité vis à vis des hémocytes, comme précédemment observé pour *V. tasmaniensis* LGP32. Cette cytotoxicité ne dépendait pas toutefois de la phagocytose mais du simple contact avec les hémocytes, indiquant un mécanisme extracellulaire (Rubio, 2018)

Dans l'**article 2** nous avons ainsi développé une étude intégrative et comparative de l'interaction hôte-microbe de *V. crassostreae* et *V. tasmaniensis* avec les huîtres. Nous avons pu décrire les interactions cellulaires et les changements moléculaires qui se produisent chez l'hôte et les bactéries au cours de la phase intra-hôte de l'infection. Ceci a été rendu possible grâce à la mise au point d'un dual RNAseq *in vivo*. J'ai pu réaliser la validation fonctionnelle des gènes candidats bactériens nouvellement identifiés par l'invalidation de ces gènes (collaboration avec l'équipe de Frédérique Le Roux) et le phénotypage des interactions *in vivo* et *in vitro* entre les huîtres ou leurs hémocytes et les mutants bactériens obtenus. Nos données (article 2) nous ont permis de conclure qu'au sein du clade Splendidus, *V. crassostreae* et *V. tasmaniensis* ont acquis des mécanismes spécifiques à l'espèce qui semblent converger vers la suppression des défenses cellulaires des huîtres. Ces phénotypes cytotoxiques sont nécessaires aux deux espèces pour la colonisation des tissus d'huitres conduisant à la mort, et sont caractéristiques des souches virulentes. Ils reposent sur R5.7 chez *V. crassostreae,* dont l'expression est induite lors de la colonisation, et sur un système de sécrétion de type 6 (T6SS) nouvellement identifié chez *V. tasmaniensis*. Dans des résultats complémentaires de cette section, j'ai identifié un effecteur associé au $T6SS_{Chr1\text{-}LGP32}$ responsable de la cytotoxicité de *V. tasmaniensis* envers les hemocytes. Cependant, cet effecteur ne semble pas nécessaire pour la virulence *in vivo*. Ces résultats préliminaires ouvrent la voie à de nouveaux projets sur la caractérisation des effecteurs T6SS impliqués dans la pathogenèse de *V. tasmaniensis*.

SECTION III. COMPORTEMENT DE TRICHEURS DE VIBRIOS ASSOCIES AUX POMS

Le POMS a été largement caractérisé en rade de Brest, sur le littoral Atlantique français, où des espèces de *Vibrio* appartenant au clade Splendidus ont été régulièrement trouvées associées aux huîtres moribondes qui contribuent de manière significative à l'infection systémique conduisant à la mort des huîtres (Gay *et al*., 2004 ; Saulnier et al., 2010 ; Lemire *et al*., 2015 ; Bruto *et al*., 2017, 2018). Néanmoins, le POMS affecte l'élevage d'huîtres dans le monde entier, dans des environnements aux écologies différentes où des variations dans la composition de la communauté du *Vibrio* sont attendues (Turner *et al*., 2009 ; Takemura *et al*., 2014 ; Li *et al*., 2020). Nous nous sommes donc demandés si différents assemblages microbiens contribuaient au POMS dans différents écosystèmes exploités pour l'ostréiculture, et si oui, qu'elles étaient les fonctions exprimées par les vibrios participant à la pathogenèse

dans ces différents environnements. Pour cela, nous avons étudié les communautés de vibrios associés au POMS dans La lagune de Thau. Cette lagune est un écosystème marin méditerranéen avec une activité ostréicole importante qui souffre également depuis 2008 d'épisodes répétés de POMS affectant les hûitres juvéniles avec une forte présence d'OsHV-1 restreinte aux zones d'élevage (20% de la surface totale) (Pernet *et al*., 2012). La lagune de Thau a une écologie qui diffère de la rade de Brest, avec notamment une salinité plus élevée et un régime de température qui pendant la moitié des années varie entre 16 et 30 ° C (Lopez-Joven et al., 2018).

Une série d'échantillonnages a été réalisée dans la lagon de Thau par Philippe Haffner, en commençant par un épisode POMS à l'automne 2015, confirmé par la présence d'OsHV-1 dans les huîtres moribondes. Les échantillonnages suivants ont été réalisés en 2016 pendant et en dehors des périodes de mortalité. En collaboration avec Maxime Bruto, Arnaud Lagorce a caractérisé la structure des populations de vibrios dans les huîtres et la colonne d'eau. Mon travail a consisté à (i) phénotyper les principales espèces retrouvées pour leur capacité à coloniser les huîtres dans des infections écologiquement réalistes (balnéation) mettant en jeu le partenaire viral OsHV-1 µvar et (ii) à déterminer les bases moléculaires sous-jacentes aux associations mises en jeu par les espèces colonisatrices.

Dans **l'article 3** (en préparation), les résultats présentés montrent que dans la lagune de Thau, l'infection par OsHV-1 µvar était associée à une prévalence particulière des membres du clade Harveyi, avec des souches affiliées taxonomiquement aux espèces de *Vibrio harveyi* et *V. rotiferianus* préférentiellement associées aux tissus d'huîtres tandis que *V. jasicida* et *V. owensii* étaient présents dans la colonne d'eau et exclus des huîtres moribondes. La reproduction de cette infection polymicrobienne en mésocosme et une étude fonctionnelle de cette collection de souches nous ont permis de montrer que seules les espèces *V. harveyi* et *V. rotiferianus* colonisaient les huitres infectées par OsHV-1 µvar, reproduisant ainsi en condition expérimentale l'observation de terrain. Lors de cette colonisation, l'hôte manipulé par le virus n'en demeure pas moins un habitat que seules certaines espèces de *Vibrio* ont la capacité de coloniser. L'analyse des génomes des espèces colonisatrices et des tests fonctionnels de cytotoxicité et de production/acquisition de sidérophores nous permettent de proposer que deux stratégies différentes de colonisation soient présentes parmi ces deux espèces de *Vibrio*. D'une part, l'espèce *V. harveyi* au fort potentiel de virulence utilise des propriétés cytotoxiques pour affaiblir les défenses cellulaires de l'huître, comme déjà observé dans le clade Splendidus. D'autre part, l'espèce au faible potentiel de virulence, *V. rotiferianus,* emploierait une stratégie de tricheur pour acquérir le fer nécessaire à sa croissance de manière non coopérative, grâce aux sidérophores produits par *V. harveyi*. De manière remarquable ces mécanismes ne sont efficaces que pour coloniser l'huître infectée par le virus, avec qui ces espèces exercent une activité synergique qui se traduit par une pathogénèse accélérée. En l'absence de virus, la communauté des vibrios qui pénèterent

l'huitre de manière transitoire, n'induisent pas de réponse immunitaire, révélant une tolérance très importante de l'huitre aux communautés bactériennes.

CHAPITRE 3. DISCUSSION GENERALE ET PERSPECTIVES FUTURES.

Dans l'état d'homéostasie immunitaire qui caractérise les huîtres saines, des associations préférentielles et positives de populations de vibrios peuvent être maintenues dans les huîtres sans développement de maladie (Schmitt et al., 2012). Cependant, les facteurs abiotiques et biotiques agissant sur l'holobionte (l'huître et son microbiote associé) peuvent déclencher une dysbiose dans laquelle la prolifération d'espèces opportunistes de vibrios entraîne la mort de l'hôte. Dans cette thèse, nous nous sommes intéressés à caractériser ces deux états différents, qui questionnent la tolérance du système immunitaire de l'huître et sa manipulation par les vibrios. La section suivante abordera les principaux résultats de la thèse, qui sont mis en perspective de la littérature disponible. Je décris également un certain nombre de développements futurs découlant de nos conclusions.

DES ARMES SPECIFIQUES AUX ESPECES DE VIBRIO POUR LYSER LES CELLULES IMMUNITAIRES ET AFFAIBLIR LES DEFENSES IMMUNITAIRES DES HUITRES

Nous avons étudié ici des vibrios associés au POMS issus de deux milieux marins côtiers différents qui abritent une activité ostréicole importante, à savoir la rade de Brest sur la côte atlantique française et la lagune de Thau, sur la côte méditerranéenne. Les espèces de vibrios pathogènes pour les huîtres appartiennent au clade Splendidus dans l'Atlantique (Lemire *et al*., 2015 ; Bruto *et al*., 2017) et au clade Harveyi dans la lagune de Thau (Oyanedel en préparation). Nous avons constaté que pour l'ensemble des populations virulentes de vibrios que nous avons étudié, celles-ci expriment une cytotoxicité envers les cellules immunitaires des huîtres, les hemocytes (Rubio *et al*., 2019, Oyanedel en préparation).

Nos résultats de **l'article 2**, ont montré que les espèces virulentes de vibrios, *V. crassostreae* et *V. tasmaniensis* sont caractérisées par des mécanismes spécifiques à l'espèce leur permettant d'affaiblir les défenses cellulaires de l'huître et d'ouvrir la voie à des infections systémiques. Au contraire, les souches non cytotoxiques des mêmes espèces de *Vibrio* sont rapidement contrôlées par les hémocytes par phagocytose et agglutination cellulaire, empêchant ainsi une infection systémique. Cette capacité à supprimer les défenses cellulaires des huîtres a également été mise en évidence chez *V. harveyi* (**article 3**), une espèce qui colonise efficacement les huîtres infectées par OsHV-1 à la fois sur le terrain et dans des expériences au mésocosme. Virulence et cytotoxicité apparaissent donc étroitement liées, probablement parce qu'elles déterminent le succès de la colonisation, comme nous l'avons démontré dans le clade Splendidus (Rubio *et al*., 2019).

L'activité cytotoxique des bactéries pathogènes peut mettre en jeu une diversité de mécanismes et d'effecteurs. De manière générale elle est liée l'activité de toxines qui sont

soit exportées par les bactéries dans le milieu extracellulaire, soit injectées ou administrées par voie intracellulaire dans les cellules cibles via des systèmes de sécrétion spécialisés (Ma et al., 2009 ; Osorio, 2018). Comme développé dans **l'article 2**, les déterminants de la cytotoxicité des vibrios envers les hémocytes ont évolué indépendamment chez *V. crassostreae* et *V. tasmaniensis*. Chez *V. crassostreae*, la cytotoxicité et la virulence dépendent fortement de la protéine R5.7 (absente de *V. tasmaniensis*), même si la protéine elle-même n'est pas cytotoxique (Bruto et al., 2018). De plus cette cytotoxicité de *V. crassostreae* exprimant R5.7 nécessite un contact physique direct avec les hémocytes (Rubio et al., 2019). Dans le cas de *V. tasmaniensis* qui se comporte comme un pathogène intracellulaire facultatif des hémocytes d'huître (Duperthuy et al., 2011), la perte du gène ancestral *r5.7*, aurait été compensée par l'acquisition d'un $T6SS_{Chr1\text{-}LGP32}$ qui délivre des effecteurs putatifs participant à la virulence et la cytotoxicité du *V. tasmaniensis*. De plus, nous avons potentiellement identifié l'effecteur putatif du $T6SS_{Chr1\text{-}LGP32}$ présent dans toutes les souches virulentes de *V. tasmaniensis* qui est l'orthologue evpP sécrété par le T6SS du pathogène du poisson *Edwardsiella tarda* (Hu *et al.*, 2014). La délétion d'evpP chez *V. tasmaniensis* altère son potentiel de cytotoxicité, cependant, il n'a montré aucune atténuation de la virulence lors d'infections expérimentales (**données complémentaires, section II.3**). Des expériences de complémentation ectopique sont à prévoir pour valider ces phénotypes.

Chez l'espèce *V. harveyi* associée aux POMS de la lagune de Thau, qui elle aussi est cytotoxique, la génomique comparative nous a permis d'émettre l'hypothèse que la distribution différentielle d'un système de sécrétion de type III dans le chromosome 1 (T3SS1) et les effecteurs cytotoxiques associés putatifs précédemment identifiés chez *V. parahaemolyticus* (Broberg *et al.*, 2010 ; Osorio, 2018 ; Wu *et al.*, 2020), pourraient contribuer à leur cytotoxicité. Chez *V. harveyi* et *V. jasicida*, qui contiennent le deux les gènes structuraux du T3SS, mais présentent une cytotoxicité contrastée (*V. jasicida* n'est pas cytotoxique), la principale différence que nous avons pu identifier est le nombre plus élevé d'effecteurs cytotoxiques putatifs présents chez *V. harveyi* (Arginine ADP-ribosyl transférase, VopQ, VopR, VopS et VPA0450) par rapport à *V. jasicida* (VopQ et VopS). La délétion ou l'invalidation ciblée des éléments structuraux de ce T3SS1 et des effecteurs putatifs associés devraient aider à clarifier leurs rôles respectifs dans la cytotoxicité et la virulence. Récemment, des méthodes de manipulation génétique de *V. harveyi* ont été développées avec succès (Delavat *et al.*, 2018), ce qui devrait être envisagé pour de futurs travaux de manipulation de gènes dans des souches Harveyi d'intérêt.

Dans l'ensemble, nos données sur des populations distinctes de *Vibrio* (*V. tasmaniensis*, *V. crassostreae*, *V. harveyi*) montrent que des armes spécifiques à l'espèce sont utilisées pour supprimer les cellules immunitaires des huîtres au cours du POMS. Cela suggère que *V. tasmaniensis*, *V. crassostreae* et *V. harveyi* sont probablement des agents pathogènes

opportunistes et non de simples colonisateurs bénéficiant de l'immunosuppression de l'OsHV-1.

AU DELA DES SOUCHES CYTOTOXIQUES, DES TRICHEURS BENEFICIENT DE L'INFECTION PAR OsHV-1

En réalisant des études en mésocosmes pour réaliser des infections expérimentales écologiquement réalistes. Les huîtres ont été exposées à de l'eau de mer contenant le virus OsHV-1 et une communauté *Vibrio*, au lieu des traditionnelles injections intramusculaires de pathogènes donnés, ce qui nous a permis d'observer de nouveaux comportements parmi les vibrios associés aux POMS. Dans un contexte, polymicrobien, il peut arriver que de multiples interactions hôte-bactéries et bactéries-bactéries modifient les pressions sélectives intra-hôtes agissant sur les colonisateurs potentiels (Alizon, 2013). Dans **l'article 3**, nos résultats ont montré que tous les vibrios capables de coloniser les huîtres ne sont pas cytotoxiques, mais que certains d'entre eux peuvent bénéficier de l'activité du microbiote, qui non seulement affaiblir les défenses immunitaires des huîtres mais produire également des « biens publics » utilisables par des tricheurs opportunistes.

C'est ainsi que l'espèce V. rotiferianus semble adopter un comportement de tricheur pour l'acquisition du fer (Kramer et al., 2020) par absorption du sidérophore vibrioferrine. Cette espèce, qui colonise efficacement les huîtres, n'est pas cytotoxique et elle a perdu le cluster de synthèse de la vibrioferrine présent chez V. *harveyi* tout en conservant le gène codant pour le récepteur apparenté, ce qui serait un exemple d'évolution des dépendances par perte de gène adaptative, également connu comme l'hypothèse de la reine noire (Morris, 2015). Nous avons confirmé *in vitro* que la croissance peut être restaurée dans des conditions de limitation du fer par les produits extracellulaires de *V. harveyi*, un producteur de vibrioferrine. Ce résultat nous amène à proposer qu'en tant que population moyennement virulente et cytotoxique, *V. rotiferianus* bénéficie de l'état physiologique altéré de l'hôte causé par des populations virulentes comme *V. harveyi* mais aussi de l'acquisition non coopérative de biens publics tels que les sidérophores pour coloniser l'huître par une stratégie purement opportuniste. Il sera nécessaire de confirmer ces hypothèses en réalisant des expériences supplémentaires avec des combinaisons isolées et spécifiques de populations de vibrios pour répondre à deux questions en suspens : (i) La colonisation de l'hôte par *V. rotiferianus* résulte-t-elle d'une stratégie opportuniste qui dépend de la présence de V. harveyi ? (ii) Quels facteurs expliquent l'exclusion de *V. owensii* et *V. jasicida* des huîtres ? Est-ce dû à des contraintes physiologiques (par exemple des exigences métaboliques) ou via l'exclusion grâce à l'action antagoniste des membres du microbiote de l'hôte ?

L'IMMUNOSUPPRESSION PAR L'OSHV-1 ET LA MODIFICATION DE L'HUITRE EN TANT QU'HABITAT

Dans le cas de l'infection expérimentale en mésocosme, la charge en vibrios n'augmente que de façon transitoire dans les tissus d'huître pour diminuer plus tard de 48 h en absence du

virus OsHV-1. De manière surprenante, nous n'avons pas observé d'expression génique différentielle significative entre les huîtres naïves et les huîtres exposées aux vibrios dans ce contexte, contrairement aux fortes réponses transcriptionnelles qui sont induites par l'injection de vibrios virulents ou non virulents (**articles 2**). Comme si le système immunitaire des huîtres ne détectait pas l'augmentation des charges de vibrios lorsqu'ils sont acquis par des voies naturelles d'infection. La raison pour laquelle les vibrios n'induisent pas la réponse immunitaire dans les configurations d'infection naturelle reste inconnue. Une hypothèse possible est la production par l'hôte de PGRP à activité amidase (PGRP-LB), dont il a été démontré qu'elle supprime la signalisation immunitaire conférant une tolérance au microbiote, chez d'autres invertébrés (Zaidman-Rémy et al., 2006). En l'absence de changements transcriptomiques de l'hôte, la réfractivité des huîtres à une colonisation stable par des vibrios exogènes nous a incités à spéculer que l'huître représentait un habitat hostile à coloniser par des vibrios sans l'effet perturbateur de facteurs supplémentaires tels que l'immunosuppression par OsHV -1. Ceci est étayé par nos données supplémentaires sur la tolérance au cuivre, au zinc et au ROS (**chapitre 2, section I, 4**) et discuté plus en détail dans notre mini-revue (**article 4**). Cette hypothèse est en outre étayée par la reprogrammation transcriptionnelle des huîtres en présence d'OsHV-1, qui permet une colonisation stable des vibrios. Pour aider à clarifier la dynamique d'association des vibrios avec les huîtres saines, nous proposons de suivre la localisation histologique des bactéries exprimant la GFP chez les huîtres saines et affectées par le POMS, au cours de la cinétique d'exposition de la même manière que les vibrios ont été localisés par immunohistologie dans **l'article 2.**

LA CYTOTOXICITÉ DE V. SPLENDIDUS COLONISANT DES HUÎTRES SAINES : UN FACTEUR DE COLONISATION PLUTÔT QU'UN DÉTERMINANT DE LA VIRULENCE

En étudiant la population de V. splendidus #23 qui est associée aux huîtres en dehors des périodes de mortalités, et qui présente un potentiel de virulence modéré par rapport aux populations de *V. crassostreae ou V. splendidus # 24* collectées en période de mortalités estivales, nous avons pu montrer que toutes les souches de Pop #23 étaient cytotoxiques vis-à-vis des hémocytes *in vitro*, y compris la souche 4G1_4 considérée comme non virulente (survie des huîtres> 82% six jours après injection). Cette souche non virulente est caractérisée par l'absence de deux loci codants pour des facteurs de virulence potentiels, un complexe MARTX et un T6SS. Dans le cadre de **l'article 1** la caractérisation des déterminants de la cytoxicité de *V. splendidus* n'a pas été ralisée. Cependant, comment il est présent dans toutes les souches de Pop#23, nous pensons que R5.7 pourrait être impliqué dans la cytotoxicité de *V. splendidus*, comme montré chez *V. crassostreae*, (Bruto et al., 2017, 2018) où il agit indépendamment de la présence du $T6SS_{pGV1512}$ pour provoquer la lyse hémocytaire (Piel et al., 2019). Nos résultats montrent que la cytotoxicité envers les hémocytes est présente dans les vibrios non virulents appartenant au microbiote des huîtres saines (hors périodes de mortalités). Ces résultats suggèrent que la cytotoxicité est essentielle dans les vibrios du clade

Splendidus pour coloniser les huîtres, mais ils montrent également que la cytotoxicité n'est pas un indicateur suffisant de virulence ; il contribuerait plutôt à rendre l'huitre moins hostile à sa colonisation.

TRADE-OFFS AGISSANT SUR LA VIRULENCE DES VIBRIOS COLONISANT DES HUÎTRES SAINES

Nous avons été intrigués par les souches de *V. splendidus* Pop #23 qui affichent une virulence modérée tout en portant des facteurs de virulence tels qu'un MARTX et un $T6SS_{4G4\_4}$. Nous avons pu identifier des différences dans le contenu du cluster génique hypervariable *wbe,* responsable de la synthèse de l'antigène O du LPS, entre les souches moyennement virulentes et non virulentes. En raison de sa localisation dans la membrane externe, l'antigène O est soumis à des pressions sélectives de la part des prédateurs environnementaux et des effecteurs antimicrobiens des hôtes métazoaires (Wildschutte et al., 2004 ; March et al., 2013). Les résultats présentés dans **l'article 1** indiquent que la sélection pour la résistance à la prédation par modifications de l'antigène O peut être en conflit avec la virulence, contrairement à la sélection coïncidente identifiée dans *V. tasmaniensis* LGP32 pour des facteurs de virulence chez l'huître également impliqués dans la résistance aux amibes (Robino *et al*., 2019).

Le POMS semble sélectionner majoritairement des bactéries aux phénotypes virulents, cytotoxiques, capables de coloniser des huîtres immunodéprimées, à l'exception des tricheurs opportunistes identifiés en milieu méditerranéen (**article 3**). Étant donné que le virus OsHV-1 se transmet rapidement parmi les populations d'huîtres sensibles (Fleury et al., 2020), on s'attend à ce que dans ce contexte, la mort rapide de l'hôte favorise la transmission du virus aux individus permissifs proximaux, assurant ainsi de nouvelles niches réplicatives pour le développement des populations virulentes. Il en va de même pour les populations bactériennes qui colonisent les huitres infectées par le virus, armées pour se répliquer dans l'hôte immunodéprimé. Dans ce cas, la virulence dépendant de la cytotoxicité envers les hémocytes favorise la multiplication et la transmission bactérienne. En revanche, un raisonnement opposé pourrait s'appliquer aux populations qui colonisent les huîtres juvéniles saines. Ces animaux sont en effet hostiles aux bactéries colonisatrices et donc l'expression d'un potentiel de virulence élevé conduisant à la mort de l'hôte peut être dans ce cas mal adapté (Alizon et Michalakis, 2015) car elle élimine la niche bactérienne obligeant les vibrios à devoir coloniser de nouveaux hôtes immunocompétents avec un microbiote stable ou de nouvelles niches réplicatives dans l'environment en dehors de cet hôte. Ainsi, l'évolution vers une virulence modérée et une résistance à la prédation, illustrée par Pop # 23, pourrait se traduire par une « fitness » globale plus élevée que celle résultant de la sélection pour la virulence chez les populations colonisant des huîtres saines.

PATHOGÈNES OPPORTUNISTES ASSOCIES AU POMS EN DEHORS DU GENRE *VIBRIO*

Récemment, des études indépendantes sur les mortalités massives de *C. gigas* ont permis

d'identifier que, bien que les vibrios soient effectivement présents chez les animaux malades, ils ne sont pas le seul groupe bactérien à se développer dans les huîtres malades affectées par des facteurs de stress environnementaux biotiques et abiotiques tels que l'OsHV-1 ou de hautes températures (de Lorgeril *et al*., 2018 ; Green *et al*., 2019 ; King *et al*., 2019). Parmi eux, le genre *Arcobacter* a été régulièrement trouvé enrichi dans les huîtres malades. En outre, *Arcobacter* bénéficie de la perturbation du microbiote et de la physiologie de l'hôte provoquée par une injection de Vibrio pour dominer le microbiote associé à l'hémolymphe (Lokmer and Wegner 2015). Parmi *Arcobacter* spp., la résistance aux antimicrobiens et aux métaux ainsi que des facteurs de virulence ayant des effets cytotoxiques envers les cellules de mammifères ont été décrites (Brückner *et al*., 2020). Compte tenu de ces caractéristiques, il est probable qu'Arcobacter pourrait remplacer fonctionnellement *Vibrio* comme pathogène opportuniste des huîtres malades, cependant nous ignorons toujours si les souches associées aux POMS expriment un potentiel de virulence ou si elles ont un comportement opportuniste par acquisition de ressources. Avec le développement de la métatranscriptomique appliquée au POMS par Annick Jacq et a sa collaboration avec notre laboratoire, nous espérons en savoir plus sur la complémentarité fonctionnelle et/ou la coopération des populations microbiennes contribuant à l'issue fatale du POMS.

CONCLUSION

L'objectif de cette thèse était de caractériser les mécanismes d'interaction entre l'huître *Crassostrea gigas* et les vibrios dans un contexte sain ou pathologique. Si la plupart des vibrios pénètrent le système circulatoire des huitres de manière transitoire, sans induire de réponse immunitaire, certaines espèces montrent des associations préférentielles. Nos études montrent que si la résistance aux antimicrobiens est un trait partagé par les populations de vibrios associés aux huîtres, elle n'est pas suffisante pour la colonisation d'huîtres saines. En revanche chez les vibrios colonisant les huitres saines, une virulence modérée pourrait être avantageuse. Ainsi, chez certains vibrios, certaines structures de l'antigène O favorisent la résistance aux prédateurs environnementaux mais entraînent une activation accrue du système immunitaire des huîtres qui réduit la virulence et la capacité de colonisation des *Vibrio* chez cet hôte. En parallèle, en explorant les populations de vibrios associés aux huîtres dans un contexte pathologique, suite à la perturbation de de l'huître par le virus OsHV-1, nous avons montré que la cytotoxicité envers les hémocytes de l'huître était un déterminant clé de la colonisation. Cette cytotoxicité est étroitement (mais pas exclusivement) associée à la virulence et favorise la colonisation des huitres par des vibrios pathogènes capables de lyser les cellules immunitaires de leur hôte. Une autre stratégie basée sur l'utilisation non coopérative des biens publics a également été observée chez une espèce de vibrios capable de coloniser les huitres affectées par le POMS. Il est vraisemblable que la synergie du virus OsHV-1 et des vibrios virulents associés au POMS, en accélérant la mort des huîtres, favorise la transmission des pathogènes à de nouveaux hôtes.

GENERAL INTRODUCTION

Bacteria of the *Vibrio* genus are ubiquitous inhabitants of aquatic environments that possess a remarkable genomic and phenotypic plasticity, which allows them to undergo into a wide range of niche specialization going from free-living forms to mutualistic, commensal and pathogenic association with plants and animals (Takemura *et al.*, 2014; Le Roux and Blokesch, 2018). In their association with animals, vibrios are part of the natural microbiota of healthy marine organisms like corals, sponges and diverse species of bivalves as well as intimate mutualistic symbionts of sepiloid squids (Ceccarelli and Colwell, 2014; McFall-Ngai, 2014). Nonetheless, several *Vibrio* species are well-known human pathogens and causative agents of vibrioses in aquatic organisms with severe impact on fish and shellfish farming worldwide (Romalde and Barja, 2010).

The Pacific Oyster *Crassostrea gigas* is a valuable product for human consumption that is produced all along the French coast. Since 2008, farmed populations of oysters had suffered from severe episodes of summer mortalities specially affecting juvenile oysters of less than 18 months, reaching mortality rates as high as 100% in French farms (Segarra *et al.*, 2010). This disease is known as the Pacific Oyster Mortality Syndrome (POMS). It has a complex etiology, which involves the interaction between the host genetics and physiological state, the environment, and pathogens, specifically microvariants of the ostreid herpes virus OsHV-1 and opportunistic bacteria including vibrios (Petton *et al.*, 2015). POMS occur seasonally, during a permissive seawater temperature window ranging from 16°C to 24°C and follows a sequence of events that starts with the intense replication of OsHV-1 within the host leading to an immunosuppressed state that is used for opportunistic bacteria, among them vibrios, to mount a secondary infection that causes the death of the host (de Lorgeril *et al.*, 2018). Whether these *Vibrio* species are simple opportunists or actively participate in the infectious process (opportunistic pathogens) has been highly debated.

Nonetheless pathogenicity does not summarize the interaction between the oysters and vibrios. The population structure of the vibrio community present in different fraction of the water column and in the oyster tissues shows that certain vibrio populations show preferential association with the oyster even outside a pathological context, with little or no overlapping in populations between diseased and healthy oysters (Bruto *et al.*, 2017). Without the influence of major stressors such as temperature (Green *et al.*, 2019) or pathogens such as OsHV-1 µvar, oysters possess a remarkable capacity to maintain immune homeostasis with its resident microbiota (Schmitt *et al.*, 2011), which should have shaped the genomes of the bacterial groups able to establish a stable interaction with oysters as a host (Chow *et al.*,

2010).

The objective of the present thesis was to characterize the mechanisms underlying the association of the oyster *C. gigas* with vibrio populations in health and disease. For this, we studied vibrio populations that display a preferential association to the oyster tissues but are isolated from contrasted contexts; i.e. the absence of mass mortalities when seawater temperature is below 16°C, and the POMS outbreaks characterized by warmer waters (above 16°C).

In **CHAPTER 1** of my thesis, I present a review of **(I)** the main characteristic of the *Vibrio* genus, the diversity of association that *Vibrio* establish in the environment and the mechanisms of colonization with metazoan hosts, **(II)** the biology and immune defenses of our model host, the oyster *C. gigas* and **(III)** the latest knowledge about the POMS, the polymicrobial disease that affects juvenile oysters whose etiology involves the OsHV-1 µvar virus and opportunistic vibrios.

In **CHAPTER 2**, I present the results obtained during my thesis, divided into three section. **Section I** describes a moderately virulent species of *V. splendidus* associated with healthy oysters. We explore the tradeoffs existing between virulence and environmental persistence in this species (**article 1, Env. Microbiol.**). We also investigate whether the resistance to oyster antibacterial defenses determines the capacity of vibrios to colonize healthy oysters (**short letter, in prep**). In **section II,** we present a comparative study of the mechanism of virulence of *V. crassostreae* and *V. tasmaniensis,* two vibrio species associated with mortality outbreaks in the Atlantic marine ecosystem. We show by which means these virulent species subvert the host defenses enabling systemic infection (**article 2, PNAS**). Finally, in **section III**, we characterize the *Vibrio* community associated with POMS in the Mediterranean oyster-farming site whose ecology differs from that of the Atlantic. We identify the strategies of those *Vibrio* species that are able to benefit from the OsHV-1 immunosuppressed state of the host, both killers and cheaters, to successfully colonize and infect oysters (**article 3, in prep**).

CHAPTER 3 presents a general discussion of the results obtained as a well as perspectives to further explore the colonization of the oyster *C. gigas* by vibrios, considering the diversity of biological and ecological contexts in which this process occurs.

This thesis manuscript ends with a minireview on *Vibrio*-bivalve interactions (**article 4, Env. Microbiol., ANNEX 1**), in which we compare *Vibrio* interactions with important aquaculture species, the oyster *C. gigas* and the mussels *Mytilus edulis* and *M. galloprovincialis.*

CHAPTER 1. STATE OF THE ART

I. THE GENUS VIBRIO

I.1 VIBRIO BIOLOGY AND DIVERSITY

Members of the family *Vibrioneaceae* (thereafter vibrios) are natural and ubiquitous inhabitants of temperate marine, freshwater and estuarine environments where they contribute to the carbon cycle, rhizospheric nitrogen fixation and display a wide range of niche specialization that goes from free-living forms to biotic associations establishing mutualistic, commensal and pathogenic association with plants and animals (Johnson, 2013; Ceccarelli *et al.*, 2019). Several *Vibrio* species are well-known human pathogens causing gastrointestinal diseases and wound infections (Osunla and Okoh, 2017) as well as causative agents of vibrioses in aquatic organisms with severe impact on fish and shellfish farming worldwide (Travers *et al.*, 2015; Abdelaziz *et al.*, 2017). However, vibrios are also part of the natural microbiota of healthy marine organisms like, corals, sponges and diverse species of bivalves (Boyd *et al.*, 2015). As for example, the well-known bobtail squid-*Vibrio fischeri* (now *Aliivibrio fischeri)* association represents a case of intimate mutualistic symbiosis (Nyholm and McFall-Ngai, 2004).

Vibrios are small (0.5-0.8 µm wide, 1.4-2.6 µm long) straight or curved rod-shaped gram-negative bacteria, with a single polar flagellum enclosed in a sheath (Thompson *et al.*, 2009) (Figure 1A and B). Median genome size in vibrios is around 5 Mbp and it is distributed in two independently-replicating chromosomes of unequal size. This bipartite genomic structure, which is an exception to the rule in bacterial genomes (Okada *et al.*, 2005), is conserved among vibrios, despite some naturally occurring chromosomes fusion events described in isolates of *V. cholerae* (Chapman *et al.*, 2015). While the larger chromosome (chromosome 1) usually carries most of the essential genes, the smaller one (chromosome 2) displays adaptive, species-specific genes and it would have been acquired as a mega plasmid before the diversification of *Vibrionaceae* (Reen *et al.*, 2006).

Vibrios use a chemosensory system to sense environmental signals and actively move towards dissolved or particulate organic matter in search for nutritional sources or escape from harmful substances, in a process called chemotaxis (Takemura *et al.*, 2014; Ringgaard *et al.*, 2018). Locomotion is mediated by the flagella, which in vibrios correspond to a sodium-driven molecular machine that can spin at up to 1,700 Hz, conferring them a higher speed and motility relative to other bacteria like salmonella, which posses a proton-driven flagellum with spin frequencies around 300 Hz (Minamino and Imada, 2015).

They are heterotrophic bacteria with a facultative anaerobic metabolism (Gomez-Gil *et al.*, 2014). In the marine environment they mostly rely on catabolizing carbohydrates, proteins and lipids and are able to hydrolyze sugars and amino acids, when available (Grimes, 2020).

The majority of vibrios can degrade the chitin polymer (Gooday, 1990; Keyhani and Roseman, 1999), which is the most abundant biopolymer in the aquatic environment, composed of β-(1,4)-linked N-acetyl-D-glucosamine (Le Roux and Blokesch, 2018), as well as, to a lesser extent, algal and plant polysaccharides (Takemura *et al.*, 2017). As an example of specialization to algal exploitation, *V. breoganii*, which has lost the ability to degrade chitin, is able to catabolize alginate, laminarin and additional glycans present in the cell wall of brown algae (Corzett *et al.*, 2018). Additionally, the production of extracellular proteases allow them to effectively utilize some abundant animal resources such as collagens, which all vibrios are able to catabolize (Grimes, 2020).

The study of environmental dynamics of *Vibrio* species, has mainly focused on species pathogenic to humans. It was shown that salinity and temperature are the two main drivers of Vibrio dynamics (Takemura *et al.*, 2014). Vibrios inhabit temperate waters growing in a temperature range that goes from 15 to 40°C with an optimum between 25-30°C (Sawabe *et al.*, 2013). They are mesophilic bacteria and most species are halophilic and require saline medium for growth (Thompson *et al*., 2004). The minimal concentration of Na+ for optimal growth varies between 5 and 700 mM, depending on the species (Farmer *et al.,* 2015). It is estimated that vibrios constitute 10% of the total culturable marine bacteria, thus representing one of the most abundant culturable fraction of marine bacteria (Eilers *et al.*, 2000). In the water column, culture dependent studies estimate an average of 10^3 to 10^6 CFU L^{-1} while culture independent methods estimate 10^4 to 10^8 16S rRNA copies L^{-1} representing 1% of the total bacterioplankton in coastal waters (Rehnstam *et al.*, 1993).

Vibrios are easily cultured on both selective and non-selective standard media and this had allowed research activities over the pre-molecular era of microbiology (Takemura *et al.*, 2014) and more recently, DNA sequencing and culture-independent approaches has unraveled the outstanding genetic diversity that characterize environmental vibrios (Dryselius *et al.*, 2007).

I.2 VIBRIO TAXONOMIC ORGANIZATION

The *Vibrionaceae* is a family of γ-proteobacteria that gathers, to date, 155 validly published species distributed among 11 genus: *Aliivibrio* (6 spp), *Catenococcus* (1 spp), *Echinomonas* (1 spp), *Enterovibrio* (5 spp), *Grimontia* (3 spp), *Listonella* (2 spp), *Paraphotobacterium, Photobacterium* (1 spp), *Salinivibrio* (6 spp), *Thaumaslovibrio* (2 spp) and *Vibrio* (128 spp)

https://lpsn.dsmz.de/family/vibrionaceae.

This represents a wide and diversified family of bacteria belonging to many different closely related species. This limits the interspecies resolution using 16S rRNA gene polymorphism; hence several faster evolving and highly polymorphic protein-coding genes have been used in Multi Locus Sequence Analysis (MLSA) to reconstruct the phylogenetic relationships, to assess biodiversity and to infer the evolutionary history of this group (Sawabe *et al.*, 2007; Gabriel *et al.*, 2014). By using a MLSA approach based on the analysis of 9 housekeeping genes (*ftsZ*, *gapA*, *gyrB*, *mreB*, *pyrH*, *recA*, *rpoA*, *topA* and the 16S RNA gene) over 58 strains, Sawabe and collaborators defined 14 monophyletic clades and more than 60 vibrio species (Sawabe *et al.,* 2007). This phylogeny was improved further more recently (Sawabe *et al.,* 2013) by using 86 vibrio strains, 10 vibrio genomes, and 8 housekeeping genes: eight new clades were identified and 9 others were updated (Figure 1C).

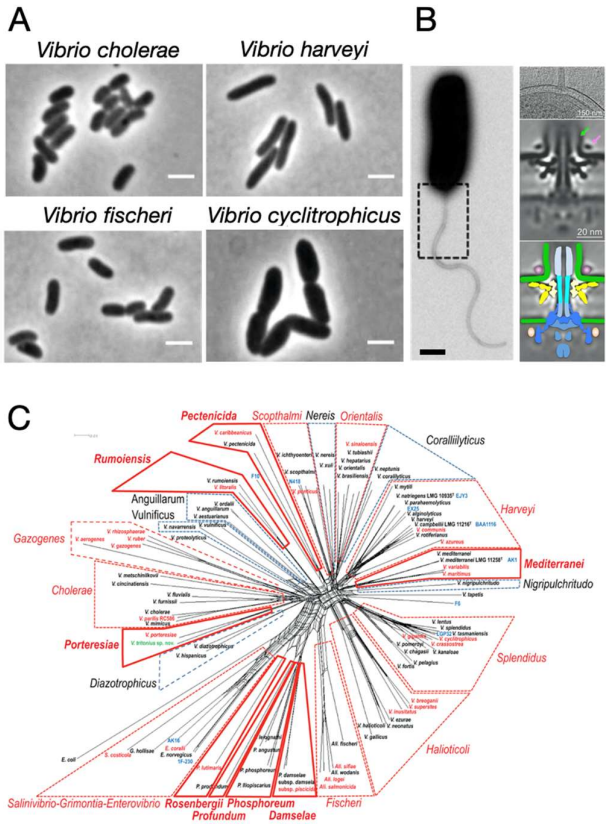

Figure 1. Morphological traits and taxonomy of vibrios

(A) Light microscopy images of Vibrios species, scale bars are 2 µm. (B) Transmission Electron Microscopy image of negatively stained *V. alginolyticus* showing the polar flagellum, scale bar 0.5 µm (right), Imaging of a single sheathed polar flagellum of *V. alginolyticus* (scale bar 0.15 µm) showing the detailed motor structure (scale bar 0.2 µm) (left) (modified from Zhu *et al.*, 2017). (C) Phylogenetic tree of *Vibrionaceae* based on 86 strains, 10 sequenced genomes and 8 housekeeping genes (*ftsZ, gapA,*

gyrB, merB, pyrH, rpoA,topA and the 16S rRNA) (taken from Sawabe *et al., 2013)*.

I.3 VIBRIO ECOLOGICAL POPULATIONS: BRINGING TOGETHER GENETIC RELATEDNESS AND ECOLOGICAL FUNCTION

Taxonomic classification of bacterial isolates relies on a polyphasic identification of species that integrates all available phenotypic and genotypic information (Gillis *et al.*, 2015). This approach often fails to integrate fine scale information about bacteria-scale potential habitats (Preheim *et al.*, 2011b). Although the physical space that a group of organisms occupies is key information to characterize the ecology of a species, this aspect remains limited for bacteria including vibrios. Pioneering work has coupled ecological sampling with high resolution genotyping, showing that vibrios whose coexist in the water column following different lifestyles (free-living or attached to particles or zooplankton) can be partitioned according to genetic and ecological similarities and thus, define vibrio ecological populations constituted by genotypic clusters sharing temporal or spatial common habitats which are connected by dispersal (Hunt *et al.*, 2008; Preheim *et al.*, 2011b). Due to this connection between habitats by dispersal, a metapopulation framework can be applied to consider possible overlaps or differences of populations isolated from distinct habitats (Preheim *et al.*, 2011a).

Moreover, it has been demonstrated that these ecological populations also represent units of gene flow where the recombination rate is higher within than between populations, which allows adaptive genes to spread in a population-specific way (Le Roux *et al.*, 2016). In the context of vibrios interactions with oysters, this ecological population framework has allowed to study how vibrio populations assemble into the oyster during health and disease and to identify functional units of pathogenesis in vibrios by mapping virulence determinants onto population structure (Lemire *et al.*, 2015; Bruto *et al.*, 2017, 2018).

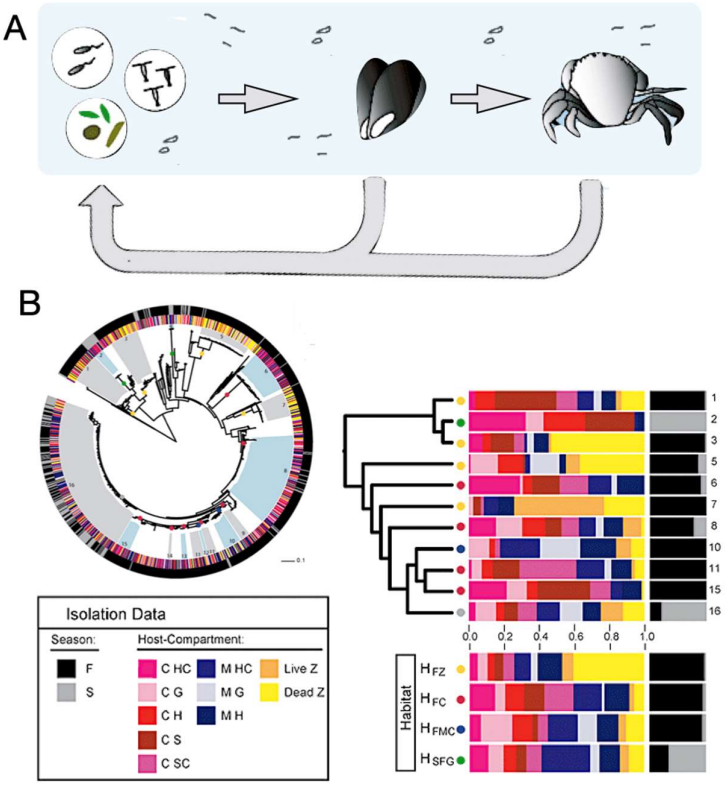

Figure 2. Metapopulation structure of vibrios.

(A) Dispersal routes of bacterial populations through food chain interactions proposed by Preheim *et al.,* 2011, and used as a sampling strategy to define and compare the population structure of vibrios across animal host and the water column. (B) Prediction of the population structure based on the ecological sampling showed in (A). Maximum likelihood gene tree constructed by concatenated protein-coding genes used for the MLST genotyping. Phylogenetic tree constructed trough MLST genotyping with 1753 vibrio isolates integrating season of sampling (grey or black outer ring) and predicted habitat categories (colored inner ring). The right panel indicated the distribution of each of the identified populations across seasons and predicted habitats. It highlights the overlap of populations among different habitats. Color code for the predicted habitats and live or death condition of the host is indicated in the "Isolation data" box. Abbreviation : F, fall ; S, Spring ; C, Crab ; M, Mussel ; G, Gill ; S, Stomach Tissue ; SC, Stomach Contents ; H, Hindgut Tissue ; HC, Hindgut Contents ; Z, Zooplankton.

I.4 Diversity of vibrio interactions in the environment

Vibrios belong to one of the two major groups that constitute the prokaryotic picoplankton at the ocean surface. While the first group, which includes *Pelagibacter* (SAR11), *Prochlorococcus*, and *Synechococcus* corresponds to relatively small cells with streamlined genomes and low biomass, vibrios are characterized by their lower abundance but high

biomass per cell, metabolic diversity and phenotypic plasticity (Leroux and Blokesch, 2018).

Although it was first proposed that the presence of vibrio in the water column was mainly a consequence of their excretion on animal feces (Takemura *et al.*, 2014), It was later evidenced that their genetic diversity and phenotypic plasticity allow them to adopt a variety of complex associations in the environment; while tight associations with animals do exist for some *Vibrio* species, other can be loosely associated with metazoans (Preheim *et al.*, 2011a).

I.4.1 FREE-LIVING AND PARTICLE ATTACHED LIFESTYLES

In microcosms, purely dissolved nutrients, derived from algal exudates, are able to sustain the proliferation of vibrios in a free-living state, overcoming competition and predation by grazers (Mouriño-Pérez *et al.*, 2003; Worden *et al.*, 2006; Eiler *et al.*, 2007). Although able to proliferate from dissolved nutrient, vibrios are more frequently found attached to biotic and abiotic surfaces, and this lifestyle has been related to their environmental persistence (Reen *et al.*, 2006). Dead biomass of small planktonic organisms, fecal pellets and polymer aggregates such as marine snows may represent microhabitats for vibrios and provide resources for growth (Takemura *et al.*, 2014).

Two sympatric ecological populations of *V. cyclitrophicus* presenting different food-seeking behavior have been shown to favor early stages of differentiation through a gene-specific selective sweep mechanism leading to gradual genome wide differentiation (Shapiro *et al.*, 2012). Behavioral confirmation defined two distinct populations, the L population, which is specialized in growing attached to large particles, and the S population, which benefits from rapid detection and swarming towards transient patches of dissolved nutrients (Figure 3A). The recent gain or loss of 2 gene clusters exclusive to the L population related to attachments (*msh* gene cluster) and biofilm formation (*syp* gene cluster) have been proposed to explain the behavioral differences between L and S that impose boundaries to previous unrestricted recombination within the parental populations, triggering an ecological differentiation that may lead to speciation (VanInsberghe *et al.*, 2020).

As certain vibrio population transiently associate to organic particles and planktonic hosts (both metazoans and protozoans), this can increase the colonization efficiency of filter feeding organisms that show size-dependent retention of particles such as oysters or mussels (Duinker and Cranford, 2012; Bruto *et al.*, 2017). It has been recently demonstrated that the association of *V. vulnificus* with artificial marine snow (AMS) can dramatically increase the colonization success of the oyster *C. gigas* (Figure 3B). While this study was applied to the human pathogen *V. vulnificus,* this novel mechanism enhancing bivalve colonization may be

extended to other vibrio species that are pathogenic for oysters.

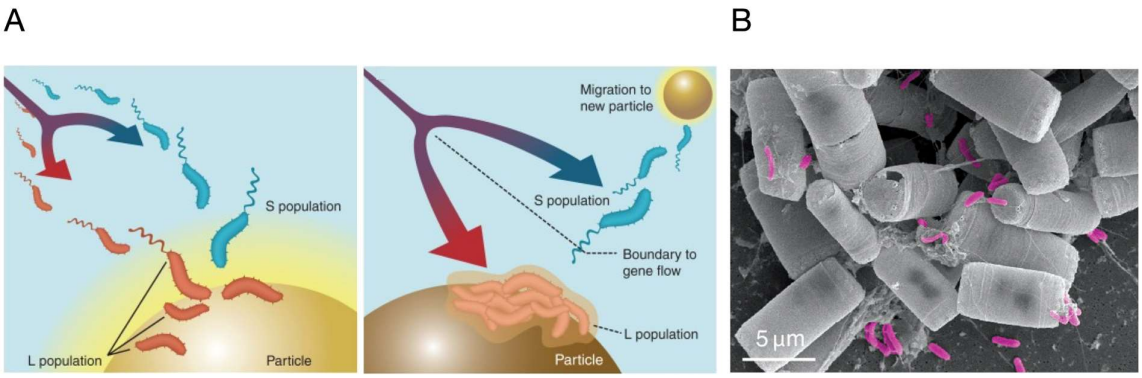

Figure 3. Free-living and particle-associated dynamics of vibrios.

(A) Model for behavioral adaptations of two sympatric *V. cyclitrophicus* populations. Both populations respond to nutrient gradient but only the L population carrying key genes linked to adhesion and biofilm-producing genes are able to establish in the particle while the S populations stay around the particle benefiting from the dissolved nutrient patch. In proximity of a new nutrient rich particle, the free-swimming S population is able to readily migrate (Modified from Shapiro and Polz. 2015). (B) Scanning electron microscopy photograph of *V. vulnificus* bacteria (in pink) attached to artificial marine snow particles (Modified from Hubert and Michell. 2020).

I.4.2 BIOTIC ASSOCIATIONS

While capable of thriving in a free-living or particle associated state, vibrio can also take advantage of the association with plants, algae, zooplankton and other animals that sustain proliferation and dispersion (Figure 4A) (Takemura *et al.*, 2014; Le Roux and Blokesch, 2018), nonetheless, for most of these examples the formal demonstration of an intimate host microbe interaction and the underlying molecular mechanisms are often lacking (Le Roux and Blokesch, 2018).

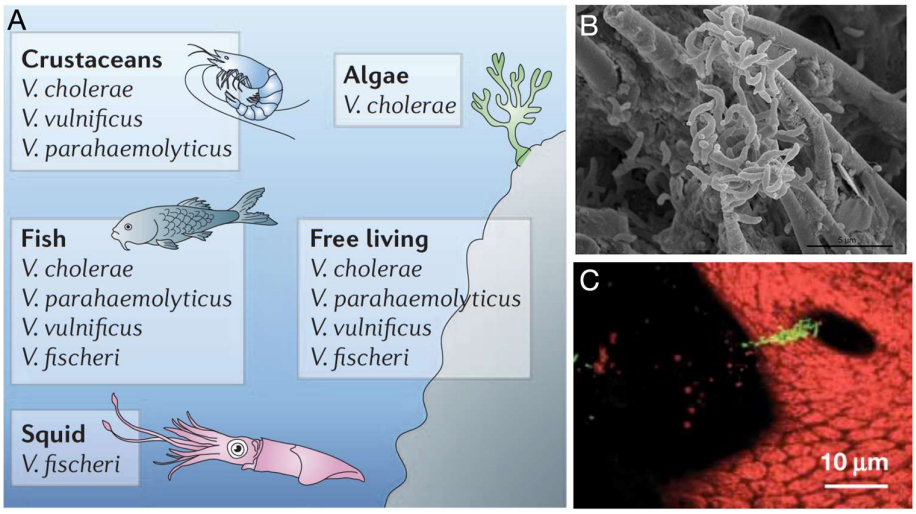

Figure 4. Environmental dynamics of vibrios association with biotic surfaces.

(A) The wide range of associations of vibrios exemplified with four well described *Vibrio* species (modified from Reen *et al.,* 2006). (B) SEM image of *V. cholerae* biofilm formed in chitin derived from crab shells, bar 5µm (modified from Echazarra and Klore. 2019. (C) Migration of *Vibrio fischeri* (in green) through the pores that connect with the light organ 2-5 hours after the initial aggregation, bar 10 µm (modified from Nyholm and Macfall-Ngai. 2004).

Associations with Phyto and zooplankton

Vibrios have a numerical dominance on phytoplankton surfaces, as demonstrated by culture-based studies, but direct physical association with specific phytoplankton has only been described for *V. cholerae* with two microalgal species, the freshwater *Rhizoclonium fontanum* (Islam et al., 1989) and *Anabaena sp,* both in freshwater (Islam et al., 1999) and saline condition (Ferdous, 2009).

Associations with zooplankton have also been studied, attachment of *V. cholerae* to copepods species such *Ascartia* and *Eurytemora* has been evidenced while exploring the potential role of these planktonic species as a reservoir of *V. cholerae*. It has been proposed a role of the main virulence factors of *V. cholerae*, the cholera toxin (CT) and the toxin co-regulated pilus (TCP) in a mutualistic relationship with copepods, where attachment to the chitinous exoskeleton is mediated by the TCP, providing a growth substrate to *V. cholerae*, and the increased Cl- secretion and reduced Na+ absorption produced by the CT has an advantageous osmoregulatory effect for the crustacean host moving towards increasing salinities (Reen *et al.*, 2006).

Other than copepods, cladocerans have been described also as a possible host for *V.*

cholerae with the potential to enhance growth when added to the mesocosm. The number of vibrios attached per individual cladoceran was 100 times higher compared to copepods. Nevertheless, there was no evidence of an enrichment of vibrios attached to cladocerans compared to the water column and therefore the authors suggested that frequent dispersal and no permanent attachment characterize this supported growth of vibrios by cladocerans (Kirschner *et al.,* 2011).

Beyond *V. cholerae*, in a comprehensive study on the metapopulation structure of *Vibronacea* among invertebrates (Figure 2A), Preheim et al. (2011) showed that the crustacean zooplanktonic fraction of the water column contained the lesser diverse but more specific assembly of vibrio populations compared to other invertebrates such as crabs and mussels. Interestingly, the authors distinguished dead from alive zooplankton. While vibrios were found associated with both dead and alive specimens, they displayed a higher relative frequency in dead individuals. This suggests a preferential saprophytic lifestyle benefiting from the degradation of the dead host tissues and the chitinaceous carapaces, thanks to the already discussed capacity of vibrios to degrade chitin. Overall, both phyto and zooplankton appear to be able to support vibrio growth in a free-living state by providing dissolved organic carbon but also participating in direct physical interaction with vibrios. Still, for the majority of these associations a clear distinction between transitory or specialized and stable associations is missing.

ASSOCIATION WITH ANIMALS

Historically, since the first observation of *V. cholerae* by Filippo Pacini from cholera stools in 1854 and its later isolation by Robert Koch in 1883, vibrios have been mainly studied as vertebrate and invertebrate pathogens (Thompson *et al*., 2004). The four well-known species, *V. cholerae, V. vulnificus, V. parahaemolyticus* and *V. alginolyticus,* have been defined based on their incidence and severity of the disease that they cause to humans; and several other species, such as *V. splendidus, V. crassostreae, V. harveyi, V. coralliilyticus, V. aestuarianus, V. anguillarum* have been associated with infectious diseases affecting marine organisms like fish, bivalves and corals (Le Roux *et al.*, 2015).

In contrast, for some of them an exchange of benefits between vibrios and the host has been suggested to represent true mutualistic relationships. The mutualism of luminescent vibrios with certain squid species has served as models to disentangle the mechanisms underpinning this type of symbiotic association (Figure 4B) (Ruby and Lee, 1998). The symbiosis between the *V. fischeri* and the bobtail *Euprymna scolopes* being the most documented one. While not an obligatory relationship, the light organ of the squid, provides a safe and nutritious environment for *V. fischeri* while the squid uses the light produced by the bacteria in a

counter illumination strategy to avoid predators during the night (Nyholm and McFall-Ngai, 2004). The establishment, development and maintenance of *V. fischeri* in the light organ results from an intricate interplay between the symbionts and the host. *V. fischeri* cells use chemotaxis and aggregate in biofilms in the mucus secreted by the ciliated epithelia of the surface of the light organ. Next, symbionts migrate into the pores and through the ducts that connect to the light organ crypts where *V. fischeri* is exposed to oxidative stress. Symbionts are able to attenuate the nitric oxide production and induce, through peptidoglycan and lipopolysaccharide signaling, a morphogenesis of the epithelial fields that discourage subsequent colonization (Figure 5A). From there, symbionts go through daily cycles of expulsion and regrowth. The continuous discovery of novel symbiotic determinants in this model has shown that copper efflux is also determinant for *V. fischeri* resilience in the light organ (Brooks *et al.*, 2014) and that different *V. fischeri* genotypes can undergo into bacterial competition, which could underlie the observation that the vibrio populations in the light organ are often dominated by a single strain (Figure 5B) (Speare *et al.*, 2018).

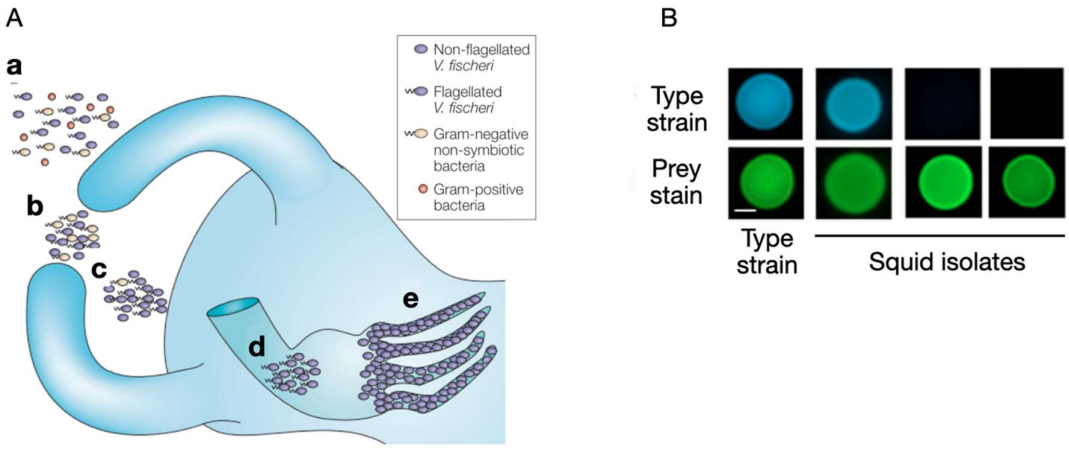

Figure 5. The paradigmatic vibrio-squid mutualism.

(A) Model of colonization of the light organ of *E. scolopes* (a) Mucus secretion by *E. scolopes* in response to bacterial presence (b) Only Gram-negative bacteria aggregate in the mucus (c) Gram-positive bacteria exclusion from aggregates (d) Viable and motile *V. fischeri* migrate through the pores that connect with the light organ (e) Successful colonizers become non-motile and induce morphological changes in the host that inhibits further colonization (Modified from Nyholm and McFall-Ngai. 2004). (B) Symbionts *V. fischeri* are able to compete with conspecifics through a strain-specific Type VI secretion system. Co-incubation of the non-lethal type strain ES114 with different *V. fischeri* strains isolated from the light organ show a strain-specific killing activity.

Among animals, interactions of vibrios with diverse benthic organisms have been well documented also, such as interactions with diverse bivalves (Lokmer and Mathias Wegner, 2015; Lokmer *et al.*, 2016a), gastropods (Sawabe*,* 2006) and crustaceans (Davis and Sizemore, 1982; Sullivan and Neigel, 2018). There are evidences that suggest the stable gut colonization of the herbivorous *Haliotis* abalone by *V. haliotis,* based on specificity of occurrence only in *Haliotis* and a possible role of the alginolytic activity of *V. haliotis* in the digestion of algal polysaccharides in the abalone (Takemura *et al.*, 2014). In contrast other vibrio species such as *V. harveyi* and *V. parahaemolyticus* are the etiological agents of severe vibriosis in *Haliotis* species (Cardinaud *et al.*, 2014; Lu *et al.*, 2017). The same is true for filter feeding organisms like oyster and mussels where vibrios are part of the normal microbiota of healthy individual but also, especially in the case of oysters, are responsible for severe vibriosis in larvae, juveniles and adults (Hasegawa *et al.*, 2008; Bruto *et al.*, 2017; Lupo *et al.*, 2019). We will see these interactions in further details in a dedicated section below.

Accidental infections in humans

Humans can also become hosts for vibrio through the accidental ingestion of contaminated water or seafood, but also by the mere exposure of open wound to contaminated water. The most common disease caused by the 11 recognized species pathogenic for humans are gastroenteritis and wound infections, which can be deadly specially in immunocompromised individuals.

V. cholerae

Cholera is the most famous disease caused by any vibrio in humans as it can cause epidemic outbreaks. It is a severe diarrheal disease caused by *V. cholerae* for which it has been described more than 200 serogroups, but only O1 and O139 serogroups have been responsible for large scale cholera outbreaks. Upon pathogen entrance through ingestion, *V. cholerae* colonizes the small intestine thanks to a lipopolysaccharide (LPS) mediated resistance to complement and the expression of the toxin co-regulated pilus (TCP) that promote bacteria-bacteria interaction and the formation of microcolonies on the surface of epithelial cells. Once stablished, the expression of the cholera toxin promotes a massive fluid and electrolyte efflux that causes the severe diarrhea that characterizes the cholera disease (Saha and LaRocque, 2012).

V. parahaemolyticus

Acute gastroenteritis caused by *V. parahaemolyticus* is also linked to the consumption of raw or uncooked fish and shellfish (Lee *et al.*, 2003). The vibrio colonizes the human small intestine presumably through the expression of a series of virulence factors including adhesins,

hemolysins (TDH and TRH) and effectors involved in attachment and cytotoxic activity toward the host cells which are secreted through a specialized protein delivery nanomachine called type III secretion system (de Souza Santos and Orth, 2014). *V. parahaemolyticus* can eventually infect wounds which is related to higher mortality risk due to septicemia. In shrimps, *V. parahaemolyticus* is the causative agent of an acute hepatopancreatic disease (AHPND) which is currently threatening shrimp culture worldwide. The highly virulent strains of *V. parahaemolyticus* associated with this disease, express two deadly toxins, PirA and PirB, encoded in the virulence plasmid pVA1, which has been suggested to have been either lost or acquired through horizontal gene transfer (Lee *et al.*, 2015) and has been identified in other *Vibrio* species pathogenic for shrimps such as *V. campbellii, V. harveyi* and *V. owensii* (Peña-Navarro *et al.*, 2020).

V. VULNIFICUS

V. vulnificus is a rarely infecting but highly lethal opportunistic pathogen for humans which naturally inhabits the coastal marine environment and an emergent pathogen for aquaculture species (Jones and Oliver, 2009; Le Roux and Blokesch, 2018). Strains are classified based on biochemical, serological and host range characteristics in three different biotypes. Biotypes 1 is mostly associated with disease in humans and commonly found associated from shellfish, biotype 2 associated with disease in eels but also an opportunistic pathogen for humans (Amaro and Biosca, 1996) and a third one with strains genetically distinct from biotype 1 and 2 and limited to Israel (Bisharat *et al*., 1999).

Consumption of contaminated seafood or open wound exposure can lead to severe systemic infection and septic shock linked to the coordinated expression of several putative virulence factors such as capsular polysaccharide, cytotoxic MARTX (Multifunctional-Autoprocessing Repeats-in-ToXin) toxins, hemolysin, the metalloprotease VVP, essential for mucus colonization in fish and siderophores for iron acquisition under limiting conditions, (Hernández-Cabanyero and Amaro, 2020 ; Li and Wang, 2020). Survival of *V. vulnificus* in the human blood is directly linked to elevated iron concentration in the serum due to hematological conditions such as hemochromatosis and thalassemia (Strom and Paranjpye, 2000). Despite the number of putative virulence factors identified, the majority of *V. vulnificus* isolated are non-pathogenic to humans and the factors described above have not been reliably correlated with disease in humans (Li and Wang, 2020).

I.4.3 VIBRIO ASSOCIATIONS WITH BIVALVES IN HEALTH AND DISEASE

Bivalves are the second largest group in the Phyllum Mollusca and have a fundamental role in ecology marine ecosystem including nutrient recycling, habitat creation and influence over food webs (Vaughn and Hoellein, 2018). They include farmed species of economic importance and represent a unique model to study colonization and disease dynamics in

vibrios (Le Roux *et al.*, 2016).

Most bivalves adopt a sessile lifestyle in their adult stages and therefore, they cannot escape predation. They take up large amounts of water for feeding and oxygen assimilation purpose, thus are unavoidably submitted to the dynamic of the diverse microbial communities in close proximity (Takeuchi *et al.*, 2016). From this microbe-rich environment, bivalves are colonized by a diverse and rich microbiota composed of species from various genera like *Vibrio, Pseudomonas, Acinetobacter, Photobacterium, Moraxella, Aeromonas, Micrococcus* and *Bacillus* (Romalde *et al.*, 2014). This composition has been determined by culture-independent methods based on the sequencing of the 16S rRNA gene in oysters, clams and mussels showing that the gut microbiota possesses a community composition that differs from that of the proximal water column (Lokmer *et al.*, 2016b). In the oyster, where other tissues such as the gills, mantle, muscle and hemolymph have been studied, the latter is characterized by a similar evenness but higher species richness than the solid-tissues. Despite this apparent selectivity imposed by the host to microbial assembly, the existence of a host-specific microbiota in oysters is still debated as its composition varies according to the seasonal and local variations of the environmental microflora (Schmitt *et al.*, 2012b). Moreover, depuration in UV-treated water decreases the concentration of some vibrio species like *V. vulnificus* in oysters (Tamplin and Capers 1992), while other vibrio species resist to this treatment in other edible bivalves (Pruzzo *et al.*, 2005; Vezzulli *et al.*, 2018), which suggests that they could belong to a persistent microbiota in oysters (Schmitt, Rosa, *et al.*, 2012). Paradoxically, vibrios that are able to enter the circulatory system of bivalves, coexist in the invertebrate analog of blood, the hemolymph, with immunocompetent cells and soluble antimicrobial effectors which through complex mechanisms of recognition and regulation, are able to tolerate the presence of a diversity of bacterial groups while limiting the proliferation and infection of potentially pathogenic bacteria (Bachère *et al.*, 2015).

Vibrios include opportunistic pathogens which under certain conditions proliferate and invade deeper tissues causing systemic infection (Lemire *et al.*, 2015; Bruto *et al.*, 2017). Mortality outbreaks associated with several vibrio species have been registered in cultivated bivalves such as oyster, clams and mussels (Saulnier *et al.*, 2010; Travers *et al.*, 2015; Le Roux *et al.*, 2016; Dubert *et al.*, 2017; Green *et al.*, 2019). Susceptibility to vibrio infection is not homogeneous among bivalves. While oysters are frequently affected by recurrent and seasonal vibriosis, few cases of mortality outbreaks are reported for mussels (Gestal *et al.*, 2008; Watermann *et al.*, 2008) despite that, just like in oysters, vibrios concentrate on their tissues (Stabili *et al.*, 2005). More recently a *Vibrio* strain (10/068) associated with one of these outbreaks was isolated and used to evaluate the response to infection mussel, which previously had been only evaluated with strains pathogenic to the oyster. *Vibrio* 10/068 was

shown to be rapidly internalized by the phagocytes of the mussel but it inhibited defense-related functions such as ROS production through the secretion of extracellular products that still remain to be characterized (Ben Cheikh *et al.*, 2016).

A thorough analysis of vibrio population structure between the oyster tissues and the water column was made by comparing the frequency and abundance of defined vibrio population between these two main compartments in the spring and summer season. This allowed to define first, that some vibrio populations are preferentially associated with the oyster tissues in the spring seasons in absence of juvenile mortalities and second, that the vibrio population structure in both the water column and the oyster is highly defined by the season with *V. crassostreae* particularly abundant in diseased animals in summer showing a clear correlation of pathogenicity with the presence of a large mobilizable plasmid (Bruto *et al.,* 2017).

I.5 VIBRIO ECO-EVOLUTIONARY DYNAMICS

It is typically assumed that evolution and population dynamics are processes that occur at such different timescales that they are considered as de-coupled, nevertheless growing evidence has shown that rapid changes in allelic frequencies within microbial population can in fact cause noticeable ecological changes establishing an eco-evolutionary dynamics (Bohannan and Lenski, 2000; Sanchez and Gore, 2013).

We have discussed so far, the diversity of interactions of vibrios within the environment. In this dynamics, biotic and abiotic factors in the environment shape the evolution of vibrio populations by selecting genomic events (deletion, duplication or horizontal gene transfer), thus generating phenotypic diversity (Le Roux and Blokesch, 2018).

Among the events that contribute to genomic variation in vibrio, intensive horizontal gene transfer has ben described has a major player in the eco-evolutionary dynamics of vibrios, driving niche adaptation and speciation (Le Roux and Blokesch, 2018; Chibani *et al.*, 2020).

I.5.1 HORIZONTAL GENE TRANSFER

In an ecological population framework, closely related vibrio strains share a common habitat and gene pool, exchanging genes by horizontal gene transfer at a sufficiently high rate to evolve as gene flow units where gene flow boundaries are strong enough for adaptive genes to spread in a population-specific way (Le Roux *et al.*, 2016). This gene flow boundaries specifically refers to the magnitude of gene flow that occurs between microbial populations and which is mainly determined by the genetic similarity and ecological overlap between the strains that make up those populations (Shapiro and Polz, 2015). Here again, genetics

interlinks with ecology as efficiency of homologous recombination of genes acquired by HGT decrease exponentially with sequence divergence but the transfer probability increases with the greater physical contact that characterize strains that share the same habitat (VanInsberghe *et al.,* 2020).

Through the study of genome plasticity, it has been demonstrated that the three major and most studied mechanisms of HGT in prokaryotes, namely natural competence for transformation, conjugation and transduction, occur in vibrios. The principal characteristics of these mechanisms are briefly described below.

NATURAL COMPETENCE FOR TRANSFORMATION

This mechanism describes the physiological state in which a DNA-uptake nanomachine enables its uptake from the surroundings. Briefly, it includes a type IV pilus adherence structure, an extendable appendage that binds extracellular DNA, and upon retraction, is thought to open the outer membrane secretin pore from which the extracellular DNA is internalized and pulled into the cytoplasm by a periplasmic DNA-binding protein (Blokesch, 2016). If the incoming DNA is successfully integrated into the chromosome by homologous recombination the bacterial genome is considered naturally transformed (Lo Scrudato and Blokesch, 2012; Metzger and Blokesch, 2016; Le Roux and Blokesch, 2018). The abundance of the chitinous polysaccharides in the marine environment could favor such HGT events, as chitin can induce the state of natural competence for transformation in several vibrio species (*V. cholerae, V. fischeri, V. parahaemolyticus, and V. vulnificus*) upon growth on chitin. The characterization of this developmental program in *V. cholerae* has shown that additional environmental cues such as a high cell density and the absence of catabolite-repressing sugars are necessary for entering the natural competence state (Lo Scrudato and Blokesch, 2012).

CONJUGATION

Transfer of genetic material by conjugation requires direct cell-to-cell contact and the synthesis of a multiple-protein mating pilus between the donor and recipient bacteria. This type of transfer represents the primary mode by which plasmid-borne antibiotic resistant gene are transfer by HGT (Le Roux and Blokesch, 2018).

TRANSDUCTION

Bacteriophages not only represent a predatory agent for bacteria but also mediate horizontal gene transfer. During phage replication, due to the low fidelity of DNA packaging, pieces of host DNA can result encapsidated in a new viral particle and be transferred from one cell to another (Le Roux and Blokesch, 2018; Chiang *et al.*, 2019).

I.5.2 EVOLUTION OF VIBRIOS BY HGT

The horizontal acquisition of mobile genetic elements was shown to play a key role in the virulence of vibrios. Typical examples like the acquisition of prophages, seroconversion and multidrug resistance are described below.

PROPHAGE ACQUISITION

Lysogenic prophages and genomic islands have been shown to be determinant for the development of virulence. The "pandemic genome" (PG) group that reunite the pathogenic clones of *V. cholerae* that are able to cause cholera disease in humans, have emerged through the acquisition, by HGT, of two key mobile genetic elements, the CTXΦ prophage, that encodes the CTX and the Zonula occludens toxin (zot), and the Vibrio Pathogenicity Island-1, which encodes the toxin-co-regulated pilus (TCP)(O'Shea and Boyd, 2002; Castillo *et al.*, 2018).

The acquisition of phage-associated toxins is not restricted to *V. cholerae* but also occur in other several marine vibrio species such as *V. coralliilyticus* (Weynberg *et al.*, 2015), *V. anguillarum* (Castillo *et al.*, 2017), *V. harveyi* (Munro *et al.*, 2003) and *V. parahaemolyticus* (Nasu *et al.*, 2000) suggesting that prophages harbor diverse genetic elements with a large dissemination potential among the *Vibrio* group. To further explore the prophage influence in *Vibrio* adaptation, Castillo et al. (2018) characterized prophage-like elements in 1874 available whole genome sequenced *Vibrio* strains showing that, indeed, prophage-encoded genes potentially conferring virulence, niche adaptations and antibiotic resistance, are not restricted to human pathogens but extensively exchanged among the *Vibrio* genus.

The acquisition of prophage-associated virulence factors in *V. parahaemolyticus* named above, specifically refers to the emergence of the pandemic strain O3:K6 which has been attributed to a generalized acquisition of virulence factors by HGT. Analysis of pandemic and pre-pandemic isolates suggested that the founder strain,a nonpathogenic O3:K6 initially acquired a new virulence regulator thought the *toxRS* operon and subsequently at least seven genomic islands (Espejo *et al.*, 2017) and the 80-kb pathogenicity island Vp-PAI (Izutsu *et al.*, 2008).

SEROCONVERSION BASED ON O-ANTIGEN CLUSTER EXCHANGE

Essential membrane determinants can be affected by horizontal exchange of genes. *V. parahaemolyticus* serotype O3:06 underwent rapid changes in the O-antigen (O) and capsular antigen (K) after its transcontinental spreading, resulting in more than 20 serovariants (Chen *et al.*, 2010). This O and K antigen correspond to two types of polysaccharides that decorate the outer membrane of Gram-negative bacteria. The K or capsular antigen is composed of high molecular weight polysaccharides that form a loosely attached coat outside the bacterial cell contributing to the resistance to phagocytosis and to the

complement system (Chen *et al.*, 2010). In contrast, the O-antigen constitutes the distal component of the lipopolysaccharide and is composed of up to 50 repeating units of two to eight sugars (Wildschutte *et al.*, 2010). From the three structural domains of LPS (Lipid A, core-oligosaccharide and O-antigen) the O-antigen is the most variable, with diverse monosaccharides composition, linkage and number of these repeating units (Figure 6B).

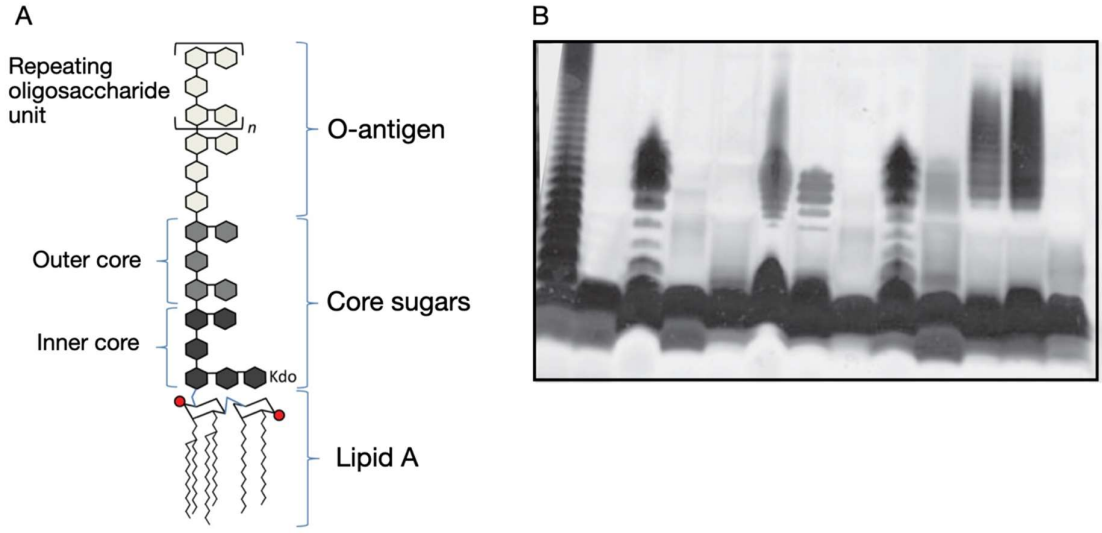

Figure 6. LPS structure and the O-antigen structural diversity.

(A) Basic structure of lipopolysaccharide : At the bottom the Lipid A moiety with the di-glucosamine headgroup indicated by the polygonal structures, the acyl chains represented by zigzag lines, and the negatively charged phosphate groups indicated by red dots. Inner and outer core consisting of repeating units and the O-antigen including a bracket with an "n" that indicates the variable number of repeating units that form the outermost structure of the LPS (modified from Maeshima and Fernandez, 2013. (B) O-antigen profiles, indicating divergence from the general structure show in (A) can be resolved by migration of LPS extracts in SDS-PAGE gels and visualization by silver staining profiles. The image shows the diversity of O-antigen structure associated with different vibrio isolates associated with different marine organisms (modified from Wildschutte *et al,* 2010).

The high phenotypic diversity observed in the O-antigen structure is the product of the hypervariability of the *wb** region which was discovered to encode the products responsible for its synthesis in *V.cholerae* O1(*wbe*) and later in the seroconverted O139 strain (*wbf*) which emerged in 1992 and caused cholera outbreaks in India and Bangladesh and spread through Asia replacing the ancestral O1 El Tor strain in the environment (Popovic *et al.*, 1995). Comparative genomics between vibrios with different O-antigen structures showed that shared genes differ based on mutations, while non-homologous genes are the result of

horizontal transfer (Wildschutte *et al.*, 2010). The *wb** region presents a cassette-like organization with conserved genes (*gmhD* and *rjg)* flanking the variable region (Sozhamannan *et al.*, 1999). Therefore, fragment acquisition by natural transformation, followed by homologous recombination has been proposed as a possible mechanism of lateral transfer of O-antigen synthesis genes occurring in the aquatic environment, since through the induction by chitin, it can mediate the seroconversion of *V. cholerae* O1 through a serogroup specific gene cluster exchange with the *V. cholerae* O139 strain (Blokesch and Schoolnik, 2007). The acquisition of this gene cluster, which encodes for a novel O-antigen structure, and the ability to synthesize a capsular polysaccharide, confers resistance to bacteriolysis by a O1-specific bacteriophage, suggesting that it simultaneously granted the ability to the O193 strain to infect individuals already immunized with the O1 strain and an advantage for its persistence in aquatic habitat that could explain its rapid environmental dominance after its emergence (Blokesch and Schoolnik, 2007).

Divergence in O-antigen structure is not restricted to pathogenic species of human health interest, like *V. cholerae* but it has also been characterized in a collection of coastal *V. splendidus* isolates collected from diverse microhabitats (Wildschutte *et al.*, 2010). In this work, genetic diversity of the *wbe* region correlated with phenotypic variation in the O-antigen structure. As the O-antigen structure is at the interphase between the vibrio and its environment, it is therefore subjected to different types of selective pressures characteristic of each of the diverse associations that vibrio establish, ranging from the predation activity of bacteriophages and protist grazers to the reactivity of the innate defenses of metazoan hosts. In consequence, the ability to diversify the O-antigen structure trough HGT may offer fitness advantages in specific environments with possible tradeoffs due to conflicting selective pressures targeting O-antigen structure. As an example, *Salmonella enterica* is able to epigenetically control the length of its O-antigen conferring resistance to bacteriophage predation at the expense of a transient reduction in pathogenicity (Cota *et al.*, 2015).

MULTIDRUG RESISTANCE

Mobile genetic elements are also major drivers in the emergence of multidrug resistant strains (MDR). MDR has been identified in more than 99% of recent *V. cholerae* isolates from stool samples (Verma *et al.*, 2019), identified in environmental non-O1/non-O139 strains (Lepuschitz *et al.*, 2019). MDR is also found in *Vibrio spp* isolated from reared fish (Scarano *et al.*, 2014; Deng *et al.*, 2019; Mohamad *et al.*, 2019), and wild and farmed mollusks (Banerjee and Farber, 2018). MDR can be achieved through the reduction of the intracellular concentration of the antibiotic, through reduced permeability or active drug efflux, through the alteration or the protection of the target site, or through the direct inactivation of the antibiotic molecule. These mechanisms can be acquired through vertical gene transfer but also disseminated to

more distantly related species through HGT (Verma *et al.*, 2019). Therefore both, the overuse and misuse of antibiotics for treatment of human infections, but also in the control of diseases in aquaculture, represent a driver for the development of antibiotic resistance in the *Vibrio* group which is submitted to extensive gene exchange in the environments such as the hatcheries of cultures bivalves (Dubert *et al.*, 2017).

In an ecological context, horizontal gene transfer has been also linked to the socially cohesive behavior of ecological populations of *Vibrio,* where antagonism, due the production of broad-range antibiotics, occur between rather than within populations. The establishment of a network of antibiotic-mediated antagonistic interaction among populations of *V. ordalii, V. crassostreae* and *V. tasmaniensis*, showed that within the *V. ordalii* population collaboration to compete with the other co-occurring populations can occur by the production of broad-range antibiotics only by a subset of the population while the rest of the strains are resistant. As the resistance gene is coded in a different region than the antimicrobial gene it is suggested that only the antibiotic resistant individuals within the populations can acquire the antimicrobial coding gene (Cordero *et al.*, 2012b).

II. COLONIZATION PROCESS IN VIBRIOS, ADAPTABILITY TO THE HOST'S HOSTILE ENVIRONMENT

The transition of vibrios from a free-living or particle-associated state to the colonization of a metazoan capable of non-self-recognition, requires specific adaptations to respond to the new environment. In this process, colonization is a necessary step that precedes proliferation (and eventually infection) of metazoan hosts, which can be aquatic organisms or humans in the case of vibrios. Aside from the well characterized vibrio-squid mutualistic symbiosis, colonization has been mainly characterized in the context of pathogenesis. In *C. gigas,* studies have mainly focused on factors that determine the virulence potential of strains associated with mortality outbreaks by means of experimental infections by injection. Nevertheless, high resolution population structure of vibrios has established that certain populations have the ability to transition between environmental and host associations (Bruto *et al.*, 2017), although the mechanisms involved in the transition are mostly unknown. However, what we know about the colonization process of mutualistic and pathogenic vibrios can serve as a guiding framework to future research on the colonization process of the diverse *Vibrio* populations that have been recently identified associated with *C. gigas.*

II.1 RESPONSE TO ENVIRONMENTAL CHANGES

Sensing environmental changes correspond to a key feature that allows vibrios to respond to the dynamic coastal waters where they establish a plethora of different interactions. As examples, responding to environmental and host cues is essential in the transition from an aquatic of *V. cholerae* to a human habitat and of *V. vulnificus* to human serum (Williams *et al.*, 2014), and the establishment of *V. fischeri* as a mutualist of the bobtail squid (Visick and Skoufos, 2001; Hussa *et al.*, 2007).

Transmembrane signaling systems sense these environmental cues and transduce them into intracellular signals that regulate cellular functions in response to the extracellular stimuli. One-component signaling systems (Figure 7A) (OCS), two-component systems (TCS) (Figure 7B) and extracytoplasmic function (ECF) sigma factors (σ) (Figure 7C) are the three major types of transmembrane signaling systems in bacteria (Jung *et al.*, 2018).

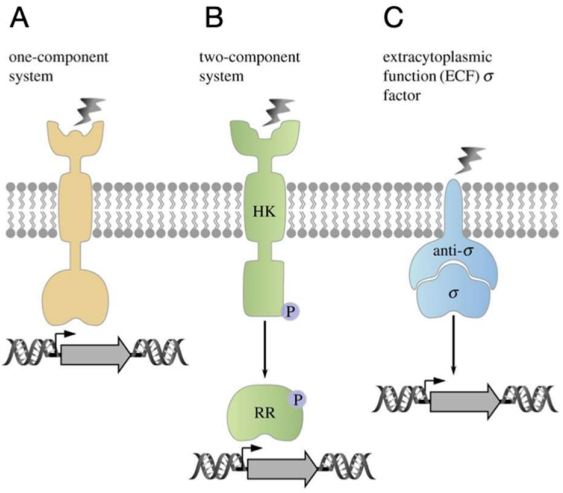

Figure 7. The three major transmembrane signaling system in bacteria.
(A) One-component systems reunite an extracellular sensor input domain and an intracellular signal output binding domain in a single molecule. (B) Two-component systems present a membrane-integrated histidine kinase (HK) and a response regulator (RR). (C) Extracytoplasmic function (ECF) sigma factors (σ) are released from the anti-sigma factor (anti- σ) upon stimulus (modified from Jung *et al*, 2018).

In simple TCSs, a signaling event leads to the activation of a receptor kinase activity and the autophorylation of a specific histidine residue, this phosphoryl group is subsequently transferred to a conserved aspartate residue of the cognate response regulator (RR) which mediates the cellular response, through DNA binding as well as non-DNA binding activities (Figure 7B) (Hussa *et al.*, 2007). In the facultative mutualist *V. fischeri* a comprehensive identification and functional characterization, by gene disruption, of 39 putative RRs,

identified 12 RRs that are linked to colonization success of the squid's light organ (Hussa *et al.,* 2007).

Members of the ToxR family receptors are examples of one-component systems and include major regulators of virulence such as ToxR/S and TcpP/H in *V. cholerae,* PsaE in *Yersinia tuberculosis*, *WmpR* in *Pseudoalteromonas tunicate* and the pH sensor CadC identified in *E. coli* and *Vibrio* species (Brameyer *et al.*, 2019). The periplasmic sensors ToxR/S and TcpP/H regulate the expression of virulence proteins in *V. cholerae* through the regulation of the AraC-like transcriptional activator ToxT which is coded in the *Vibrio* pathogenicity island-1, and is induced upon sensing of the intestinal environment (Childers and Klose, 2007) (Figure 8).

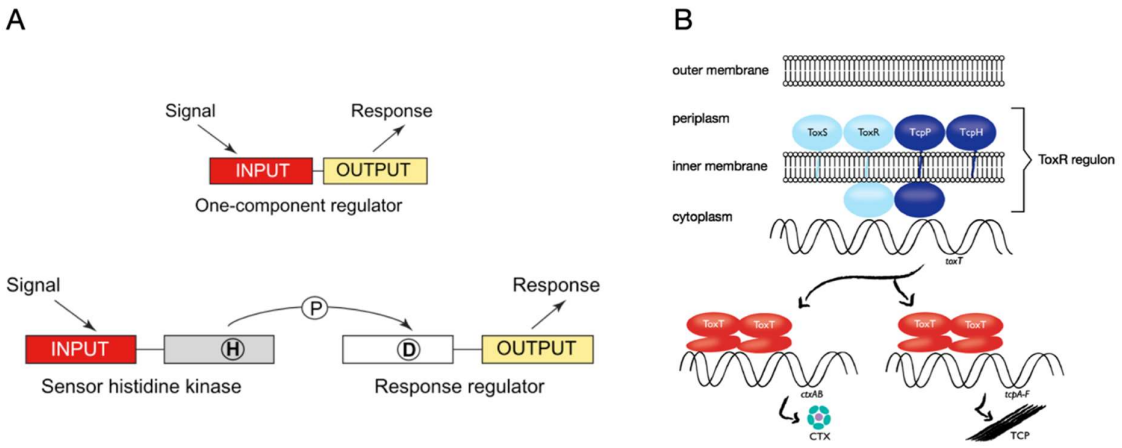

Figure 8. One and two component signaling system.

(A) Signal transduction in one (upper) and two (lower) component systems. (A) One component system consists of a single protein that possesses an input and output domain but it lacks the His-Asp phosphotransfer domain (grey boxes). Two component system containing the input domain that receives the signal and the output domain located in two different proteins that communicate through the His-Asp phosphotranfer domain (grey bowes) (modified from Schaller *et al.*, 2011) (B) One-component system ToxR/S and TcpP/H (ToxR regulon) controls the expression of virulence proteins in *V. cholerae*. ToxR and TcpP are inner-membrane proteins that binds to the *toxT* promoter activating its transcription. In turn ToxT activates the transcription of ctxAB and tcpA-F coding for the cholera toxin and the toxin-regulated pilus, respectively (taken from Haas *et al.*, 2014)

Two-component signal transduction systems have been identified in the *Vibrio* genus sensing nutrient availability, pH, osmolarity, host factors, and the environment, These systems lead to modulation of motility, bioluminescence, as well as biofilm production and the onset of virulence. (Hussa *et al.*, 2007). The two-component system VarA/VarS is known to regulate viru-

lence in *V. cholerae* and luminescent in *V. harveyi* but also in the oyster associated pathogens *V. aestuarianus,* and *V. tasmaniensis* LGP32. In *V. aestuarianus a* single mutation in the regulator VarS is sufficient to impact the secretion of the Vam metalloprotease impairing pathogenicity (Goudenège *et al.*, 2015). In *V. tasmaniensis* LGP32 the production of two proteases related to strain virulence and toxicity, Vsm and PrtV, is modulated by a complex regulatory network that involves VarA/VasS signaling, both dependent and independent of CsrB. CsrB are conserved multiple-copy noncoding small RNAs that normally are regulated by the VasA/VasS signaling and mediate changes in gene expression (Nguyen *et al.*, 2018).

II.2 QUORUM SENSING

Quorum sensing (QS) is a cellular communication mechanism that allows a wide diversity of bacteria to switch from individual to coordinated population behaviors through collective changes in gene expression in response to cell density (Rutherford 2011). Coordination is achieved through the extracellular accumulation of signaling molecules, referred to as autoinducers (Figure 9), which are produced constitutively by the bacterial populations. Their recognition is mediated by perisplasmic sensors that resemble two component systems with transmembrane histidine kinase and a response regulator domain but with no DNA-binding domain.

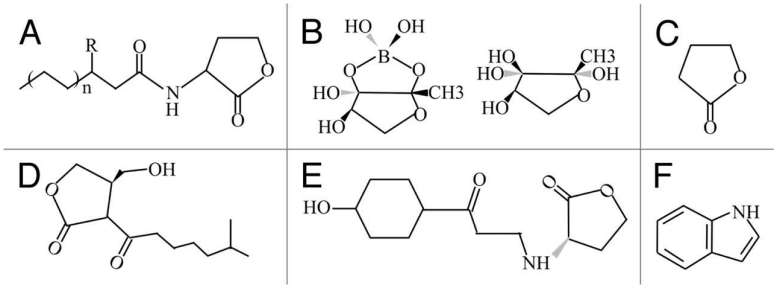

Figure 9. Representative quorum sensing autoinducers.
(A) *N*-Acyl-L-homoserine lactone (AHL). (B) Autoinducer-2 (AI-2). (C) γ-Butyrolactones. (D) A-factor. (E) *p*-Coumaryl homoserine lactone (*p*C-HSL). (F) Indole.

The analysis of QS sensing network in several *Vibrio* species (*V. fischeri*, *V. harveyi*, *V. cholerae*, *V. anguillarum* and *V. vulnificus*) identified a diversity in the type of signal networks and different regulatory responses that reflects the diversity of environmental roles and kinds of associations within the *Vibrio* group (Milton, 2006). Three different species *V. fischeri*, *V. harveyi* and *V. cholerae* can serve as examples for the role of quorum sensing in *Vibrio* symbiosis and pathogenesis towards both, animal and human hosts.

The phenomenon of quorum sensing was originally described in *V. fischeri* and referred to as "autoinduction" due to the capacity of culture media supernatants to induce bioluminescence in freshly inoculated *V. fischeri* of the same strain (Ulrich and Koonin, 2005). Bioluminescence induction, along with early and late colonization factors such as motility and biofilm formation, are critical for the *Vibrio*-squid symbiosis. Its regulation is achieved in *V. fischeri* though three QS systems; LuxI/R, AinS/R and LuxS/Q that form a regulation network essential for colonization of the light organ. While paradigmatic in the QS systems described for Gram-negative bacteria, the LuxI/R system is not present in all vibrios (Milton, 2006).

V. harveyi is also capable of luminescence and is considered as a common pathogen of diverse marine vertebrate and invertebrate organisms such as fishes, crustaceans and mollusks (Kraxberger-Beatty *et al.*, 1990; Balebona *et al.*, 1995; Saeed, 1995; Hispano *et al.*, 1997; Company *et al.*, 1999; Diggles *et al.*, 2000; Alcaide *et al.*, 2001; Tendencia, 2002). Both luminescence and expression of virulence factors linked to its pathogenicity potential are sensitive to cell density-dependent regulations through a three-channel QS network composed of LuxM/N, LuxS/PQ and CqsA/S each one with its own autoinducer (Figure 10). Interestingly, in the *V. campbelli* strain ATCC BAA-1116 (originally classified as *V. harveyi*), pathogenic for the larvae of the brine shrimp *Artemia franciscana,* it has been shown that *in vitro* conditions of high cellular density positively regulates bioluminescence production and synthesis of metalloproteases, siderophores, exopolysaccharides but represses expression of the type III secretion system (Detailed in section II.8 Secretion systems)(Milton, 2006).

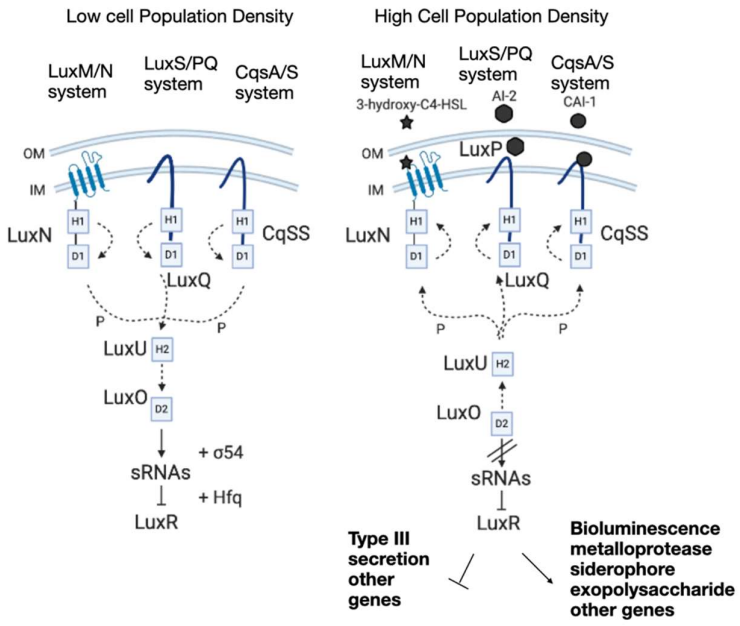

Figure 10. Cell-density dependent regulationof cellular functions in *V. campbelli* BAA-1116.
QS is regulated by three two-component signaling systems that work in parallel to regulate virulence and bioluminescence. At low cellular densities, in absence of signaling molecules, LuxN, LuxQ and CqsS madiate the phosphorylation of the σ^{54} -dependent activator LuxO, which activates the expression of small regulatory RNAs that contribute to the destabilization of the mRNA encoding LuxR the master regulator. High cellular densities promote the productions of signaling molecules by the LuxM, LuxS and CqsA synthases, autoinduciers accumulate in the cytoplasm to be diffused or transported to the periplasmic region and is believed that they bind to their respective sensors which converts LuxN, LuxQ and CqsS into phosphatases that, leading to the dephosphorylation and inactivation of LuxO and LuxR transcription (modified from Milton *et al.,* 2006)

In *V. cholerae,* QS is at the top of the signaling cascade leading to virulence gene expression. During the transition to a human host downstream gene expression is regulated through four parallel QS systems (CqsS, LuxPQ, CqsR and VpsS) that converge at LuxO for gene regulation. At a high cellular density that characterizes the passing through the upper digestive track, biofilm production is induced to increase acid resistance. After a substantial bacterial elimination in the upper gut, *V. cholerae* arrives to the small intestine and detaches from the biofilm and colonizing the intestine in a low cellular density that activates the expression of CT and TCP. Upon successful colonization and increase in population density, QS modulates the repression of virulence factors and the production of the HA protease that leads to detachment from the epithelium and exiting from the host into the environment (Milton, 2006; Watve *et al.*, 2020).

II.3 ADHESION MOLECULES AND BIOFILM FORMATION

Planktonic vibrio species are able to explore surfaces thanks to the presence of the haemagglutinin pili (MSHA), Type IV pili (TFP) and the flagellum. Upon recognition of a suitable surface, cells attach to it and the loss of flagellum triggers the production of extracellular matrix substances (Rodrigues *et al.*, 2018).

Physical adhesion of bacteria to host cells is considered as the essential step of colonization of an encountered organism, specifically for pathogens, a prerequisite for the delivery of effectors and induction of signaling events facilitate pathogen invasion (Stones and Krachler, 2016). Attachment is achieved through adhesive appendages such as pili and flagella, and molecules such as chitin-binding proteins and capsular polysaccharides which are widespread among vibrios (Ceccarelli *et al.*, 2019).

Vibrio tasmaniensis LGP32, which is a facultative intracellular pathogen, uses the OmpU porin as an adhesin/invasin that binds to the RGD motif of the major plasma opsonin Cg-EcSOD to promote phagocytosis and a β-integrin mediated invasion of the hemocytes of the oyster *C. gigas*, a key event in the expression of its pathogenicity in the oyster (Duperthuy *et al.*, 2011). The adhesion properties and role in pathogenesis of OmpU were also found in *V. cholerae* where OmpU binding to fibronectin was investigated in the context of colonization of mice and rabbit intestinal epithelium (Sperandio *et al.*, 1995; Nakasone and Iwanaga, 1998).

Exopolysaccharides are polymeric carbohydrates that are present on the surface of many bacteria, they form an interbacterial matrix that support biofilm formation. QS systems LuxS/LuxPQ and CqsA/CqsS regulate biofilm formation in several vibrio species such as *V. fischeri*, *V. harveyi*, *V. anguillarum*, *V. cholerae*, and *V. vulnificus* (Milton, 2006). They are a preferential life-style in bacteria as it facilitates nutrient access and confers protection from predators, shields bacteria from antimicrobials, (Yildiz and Visick, 2009)but also promote gene exchange by HGT specially when interbacterial competition ocurr and free DNA is liberated from prey bacterias (Le Roux and Blokesch, 2018).

II.4 METAL HOMEOSTASIS.

Bacteria have a dichotomic relationship with metals: while metal ions are essential for many reactions in the bacterial metabolism, at high concentrations they can become toxic (Z. Ma *et al.*, 2009). As this concentration-dependent toxicity of metals is used as a defense mechanism by the innate defenses of metazoans which have the ability to sequester iron in response to infections, bacteria have evolved mechanism to cope with metal concentration variations and maintain homeostasis mainly by transport of metals from in and out of the cell.

In a metal deprivation state, bacteria increase metal intake, mobilize stored metals and switch to metabolic pathway that are independent of the limiting metal. To face metal excess, bacteria respond by the activation of efflux-systems for detoxification (Takemura *et al.*, 2014).

Zinc, iron and manganese are considered among the three most important transition metals for bacterial metabolisms and therefore extensive literature is available devoted to characterize sensing and response to changes in ion metal status in model organisms such as *Bacillus subtilis*. Among mutualistic and pathogenic vibrio, copper and iron homeostasis appears as tightly associated with their colonization capacity (Brooks *et al*., 2014; Vanhove *et al*., 2016; Kramer *et al*., 2020)

COPPER HOMEOSTASIS AND COLONIZATION SUCCESS

In the oyster facultative intracellular pathogen, *V. tasmaniensis* LGP32, invasion of the hemocytes, the oyster immune cells, depends on copper homeostasis through the P-type ATPase A, CopA, and to a lower extent the CusABC efflux machinery. CopA is essential for LGP32 intracellular survival and virulence expression (Vanhove *et al.*, 2016).

Similarly, in *V. fischeri,* the global discovery of determinants of symbiosis through a transposon insertion strategy, allowed to identify two genes related to copper efflux systems (*cusC* and *copA*) as implicated in the colonization success of *V. fischeri*. Interestingly, oxygen arrives to the crypts of the light organ carried by hemocyanin, a metalloprotein that coordinates copper ions to reversibly bind to oxygen. If this copper coordination is conserved in *E. scolopes,* as predicted (Brooks *et al.*, 2014), it could explain the copper presence in the crypts and therefore the relevance of copper detoxification in the persistence of *V. fischeri* in the light organ.

IRON ACQUISITION

Iron plays an essential role in bacterial metabolism as a cofactor in the catalysis of redox reactions that are part of vital processes like respiration, DNA synthesis and detoxification of reactive oxygen species. Despite its abundance, many natural environments are characterized by neutral and basic levels of pH at which the predominant oxidized ferric (Fe^{3+}) state of iron is highly insoluble making it not readily bioavailable for bacterial assimilations (Kramer *et al.*, 2020). Its dissolved concentration in ocean open waters can reach as low as 20 to 30 pM, well below the 0.1 to 0.5 µM range for standard optimal growth under laboratory conditions (Payne *et al.*, 2016). Moreover, bacteria not only have to face iron scarcity in the environment but also during colonization of metazoan hosts that present levels of freely available iron under the minimum required for bacterial growth, with most of it associated with high affinity iron binding proteins. As iron withholding capacity is induced

under infection it is considered as a form of nutritional immunity in response to pathogen invasion (Hood and Skaar, 2012).

The model for iron acquisition in vibrios is *V. cholerae* with more than 1% of its genome dedicated to iron transport systems (Payne *et al.*, 2016). While vibrios possess transporters for ferric (Fe^{3+}) or ferrous (Fe^{2+}) iron and also for iron complexes with organic molecules such as citrate or heme, they also synthesize small high-affinity iron chelators, called siderophores, as well as their cognate receptors and transport proteins (Figure 11). The Ferric uptake regulator *fur* is the transcription factor that represses siderophore synthesis in presence of Fe^{2+} (Troxell and Hassan, 2013).

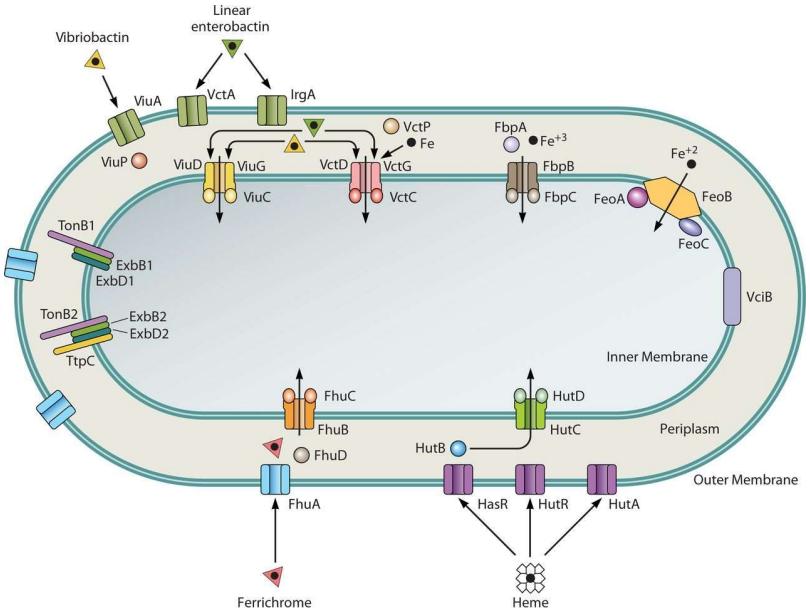

Figure 11. Diversity of *V. cholerae* iron transport system.

Localization of each iron transporting system respect to the cell envelope and the compound transported is shown. The names of the siderophores recognized by the specific transporters are indicated outside the bacterial cell. The TonB-ExbB-ExbD complex located at the inner membrane allows energy transduction to the specific siderophore receptors located at the outer membrane (taken from Payne *et al.,* 2016)

Once secreted, siderophores scavenge iron either freely in the extracellular medium or bound to the vibrio surface. Upon iron binding, the ferrisiderophore complex is recognized by its cognate receptor and transported across the outer membrane into the periplasm in an energy-dependent manner which is powered by the coupling of the receptor with the inner membrane complex TonB-ExbB-ExbD. In the periplasm, the iron complex bound to a periplasmic binding protein is transferred to the cytoplasm by less specific membrane

permeases. Finally, iron reduction or enzymatic cleavage release iron from the siderophore making it available to the cell. Thus, the successful fight for iron through the synthesis of siderophores is identified as a virulence determinant in vibrios including *V. parahaemolyticus*, *V. harveyi*, and *V. alginolyticus*.

Interestingly, in a community of natural bacterioplankton populations of vibrios the distribution of siderophore was identified as unevenly distributed across isolates. Only clusters of strains associated with animal hosts present a high frequency of siderophore producers, which is expected because of iron-limiting environment, that host represent as part of their infection-limiting strategies (Hood and Skaar, 2012). Despite that siderophore and receptor synthesis genes are often co-localized in large clusters, non-producers showed to evolved by a selective loss of only the biosynthesis genes but retention of the associated receptor allowing a cheating behavior for iron acquisition (Cordero *et al.*, 2012a).

This social interaction based on "public goods" shows to be better supported in larger particle sizes of organic matter that offer a more stable community structure, allowing the emergence of dependence through selective gene loss. Whether this social interaction between producers and cheaters can occur during host colonization remains to be explored.

II.5 EVASION AND RESISTANCE TO PHAGOCYTOSIS

On its way to establishment on either vertebrate or invertebrate hosts, bacteria will inevitably encounter specialized phagocytic cells armed with diverse antimicrobial effectors to kill invaders inside the phagolysosome, where an oxidative and degradative milieu is configured upon microbe internalization.

To evade control by phaogocytes, bacteria have evolved mechanisms to interfere with this process at any step between recognition and phagosome maturation, or even physical scape from the phagosome. Phagocytosis evasion at different steps has been mainly characterized on relevant extra and intracellular human pathogens such as *S. aureus*, *M. tuberculosis* and *L. monocytogenes* (Uribe-Quero and Rosales, 2017) while available examples in vibrios remain fragmentary based on different vibrio species infecting different hosts.

In human infection by *V. vulnificus* and *V. cholerae,* the pathogens were shown *to* directly suppress phagocytes through cytotoxicity. Apoptosis of murine macrophages was evidenced to be induced by *V. vulnificus* although the underlying mechanisms were not explored (Kashimoto *et al.*, 2003) while in a more recent article the secretion of a RTX toxin shown to confer protection from phagocytosis enhancing pathogen survival (Lo *et al.*, 2011).

Clinical and environmental isolates of *V. cholerae* contain a T6SS considered among the

group of accessory virulent factor whose contribution to cholera disease is not fully understood and roles for environmental fitness are proposed. Vibrio internalization by phagocytic cells is required for the T6SS-dependent secretion of VgrG-1 protein into the cytosol. This VgrG-1 contains an Actin Crosslinking Domain (ACD) that cross-links G-actin causing F-actin depolymerization and leading to an irreversible cytoskeleton compromise and deactivated phagocytic capacity (A. T. Ma *et al.*, 2009).

In *V. anguillarum* the O-antigen of the LPS prevents phagocytosis by the skin epithelial cells of the rainbow trout protecting bacteria during the early stages of skin infection (Lindell *et al.*, 2012).

In *C. gigas* the extracellular products (ECPs)of *V. aestuarianus* 01/32 are lethal when injected into oysters and cause immunosuppression by causing morphological changes in hemocytes that inhibit phagocytosis (Labreuche *et al.*, 2006a; Labreuche *et al.*, 2006b). It was demonstrated that the Vam zinc metalloprotease constitutes a major contributor to the impairment of the cellular functions caused by the ECPs of *V. aestuarianus* (Labreuche *et al.*, 2010).

A more detailed characterization of phagocyte manipulation by vibrios has been produced in the study of *V. tasmaniensis* LGP32, a facultative intracellular pathogen of juvenile oysters. After entrance into the circulatory system, LGP32 is opsonized in the oyster hemolymph by the protein Cg-EcSOD which binds to the OmpU porin. The formed complex is recognized by hemocyte β-integrins, which mediate vibrio internalization. Inside the hemocytes LGP32 resist degradation through the a combined inhibition of vacuole acidification, limiting of ROS production, antioxidant activity, copper efflux and resistance to AMPs (Figure 12) (Duperthuy *et al.*, 2011; Vanhove *et al.*, 2015, 2016).

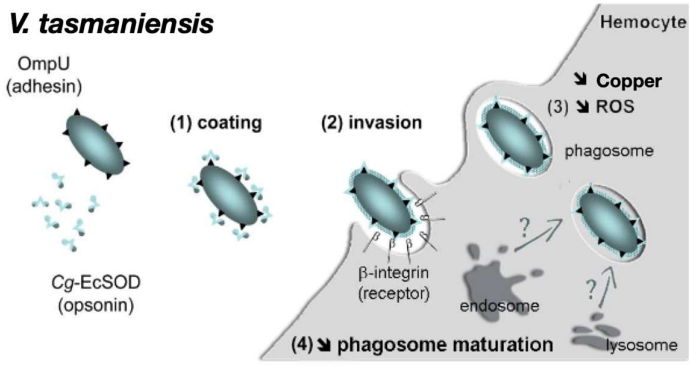

Figure 12. Internalization of *V. tasmaniensis* LGP32

V. tasmaniensis LGP32 uses the OmpU porin as an adhesin that facilitates the internalization into hemocytes. (1) The OmpU porin is recognized by the plasmatic protein *Cg*-EcSOD that will cover the

bacteria serving as an opsonin. (2) internalization is dependent into the recognition of the OmpU/*Cg*-EcSOD complex by the β-integrin receptors in the membrane of hemocytes (3) Inside the phagosome LPG32 uses different strategies to evade the oxidate stress (SodA, Alkyl hydroperxide reductase C), copper acummulation (CopA) and pH disminution by (4) inhibition of phagosome acidification (Duperthuy *et al.*, 2011; Vanhove *et al.*, 2015,2016). (modified from Duperthuy, 2010)

II.6 RESISTANCE TO HOST ANTIMICROBIALS

Several strategies have been described in colonizing vibrios that allows them to cope with the presence of the diverse antimicrobial effectors that are produced by their host to control the proliferation of resident and invasive microbes.

Among bactericidal effectors, antimicrobial peptides are a diverse group that mostly comprises cationic molecules with the common characteristic of being able to interact electrostatically with the bacterial surface and insert into the membrane bilayer forming deleterious pores, binding to essential components of the membrane or translocate into the cytoplasm where they can interfere in vital cellular processes (Schmitt *et al.*, 2012b).

The initial electrostatic interaction of AMPs in gram negative bacteria, like vibrios, is possible thanks to the negatively-charged LPS that constitutes a major and essential component of outer membrane. The hydrophobic domain of LPS named Lipid A (Figure 6) anchors the molecule to the membrane and confers the negative charge to the molecule (Steimle *et al.*, 2016). A strategy used by bacteria to impair the initial interaction with cationic antimicrobial peptides is to lower the net negative charge of the membrane by modifying the Lipid A. In some strains of *V. cholerae* resistant to AMPs, the VprA/B two component system regulates the substitution of Lipid A with glycine or diglycine residues, altering the bacterial surface charge, upon the sensing of host cues such as bile, mildly acidic pH and cationic antimicrobial peptides. Both the VprA/B and the *almEFG* operon that encodes genes for glycine substitution are necessary for host colonization (Herrera *et al.*, 2014). This strategy is also employed by *V. fischeri* which is able to sense the acidic pH experienced in the transition from environmental to host association and trigger the substitution of Lipid A with positively charged ethanolamine residues which confer resistance to polymyxin B, a well-known prokaryotic AMP, and increase colonization of *V. fischeri in-vivo* (Schwartzman *et al.*, 2019).

Another protective response against AMPs was described in the oyster pathogen *V. tasmaniensis* LGP32, which otherwise lacks the genetic determinants to substitute its Lipid A with glycine or diglycine residues. In response to membrane damage, LGP32 secretes ECPs that contain an insoluble fraction consisting of outer membrane vesicles (OMVs). OMV

release was observed both in the extracellular milieu and inside the phagosomes (Figure 13). These OMVs entrap periplasmic content during extrusion from the cell envelope. In LGP32 they contain a vesicular serine protease (Vsp) that participates in the virulence of LGP32, but does not degrade AMPs. Nonetheless the released OMVs are highly protective against AMPs which are entrapped in the membranes of the released vesicles. It is therefore believed that OMVs can confer protection against AMPs produced by the oyster or by the resident microbiota, thereby conferring a colonization advantage to LGP32 (Vanhove *et al.*, 2015).

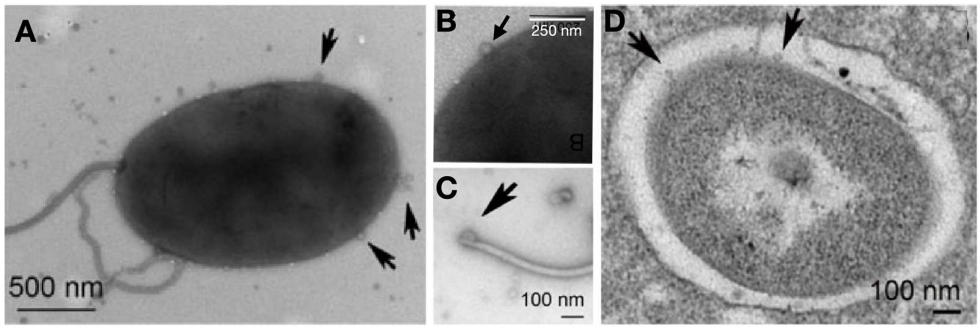

Figure 13. Secretion of outer membrane vesicles by *V. tasmaniensis* LGP32

Negatively stained LPG32 cultures in logarithmic phase and phagocyted bacteria observed by electron microscopy. (A) Outer membrane vesicles (OMV) produced by LGP32 indicated by black arrows. (B) Detail of OMVs detaching from the outer membrane or (B) from the the polar flagellum (modified from Vanhove *et al*., 2015)

II.7 RESISTANCE TO OXIDATIVE STRESS

Reactive Oxygen and Nitrogen Species (ROS and RNS) are other highly toxic compounds produced as defense molecules, which in absence of efficient antioxidant mechanisms, can seriously damage cells and tissues.

V. cholerae probably has to face ROS during infection, as cholera patients show a decreased level of antioxidant enzymes and an activation of oxidative stress-related enzymes, but also in the environment after escape from the human host (H. Wang *et al.*, 2017). Two LysR-family transcriptional regulators, OxyR1/2 regulate the expression of genes essential for resistance of *V. cholerae* to oxidative stress. The firstly identified, OxyR1 activate the expression of peroxiredoxin PrxA, DPS (DNA-binding protein from starved cell) and the catalases KatG and KatB, all of them involved on in-host resistance to oxidative damage in response to H_2O_2. The later identified OxyR2, regulates the expression of the

alkylhydroperoxide reductase gene *ahpC* in a H_20_2-independent way, which directly regulates OxyR1 and allows *V. cholerae* to better adapt to the low levels of oxidative stress of the environment after host escape (H. Wang *et al.*, 2017).

V. fischeri is exposed to two different types of oxidative stress on its migration towards the crypts of the light organ. Nitric oxide (NO) is present in toxic concentration in the ciliated fields, ducts and the crypts antechambers and the deep crypts present halide peroxidase that can generate bactericidal hypohalous acid (Davidson *et al.*, 2004; Nyholm and McFall-Ngai, 2004). The daily exudate that is expelled from the light organ containing bacterial symbionts and host cells was used to characterize the proteomic characteristic linked to this association. The study revealed the presence of detoxification proteins (eg. alkyl hydroperoxide reductase, C22, thioredoxin reductase, hydroperoxidase KatA, FeSOD, thioredoxin-dependent thiol peroxidase, nitric oxide dioxygenase, thioredoxin peroxidase) for ROS and RNS supporting the role of oxidative stress protection among the determinants factors that ensure the symbiotic persistence of *V. fischeri* in the bob-tail squid (Schleicher and Nyholm, 2011).

Vibrios adopting intracellular stages experience strong oxidative stress. This was shown by a transcriptomic analysis of the intracellular stages of the oyster pathogen *V. tasmaniensis* LGP32, which survives into the oyster phagocytes. Inside the hemocytes, LGP32 undergoes a significant gene expression reprograming. Among the overexpressed genes, superoxide dismutase [Mn] (sodA) and alkyl hydroperoxide reductase C (*ahpC*) were associated with oxidative stress resistance. Deletion mutants confirmed that MnSOD (*sodA*), which catalyzes the conversion of superoxide ($O_2^{-\cdot}$) to hydroperoxide (H_2O_2) and dioxygen (O_2), was essential for LGP32 survival in and cytotoxicity to oyster phagocytes (Vanhove *et al*., 2016)

II.8 SECRETION SYSTEMS

Transport of proteins between compartments, into the environment or to other bacteria is an essential function in prokaryotic cells. Dedicated bacterial secretion systems assist this transfer of cargo proteins and are essential for growth of bacteria but also implicated on interbacterial competition or virulence against eukaryotic cells when toxic effectors are the cargo proteins that are delivered through the secretion system. Different classes of secretion systems have been identified that are exclusive of gram-negative bacteria, that assist the translocation of protein substrates across 1, 2 or 3 membranes, depending on the apparatus (Figure 14).

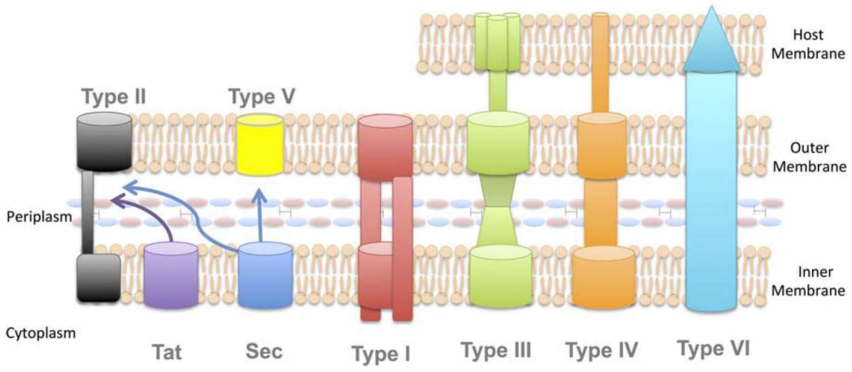

Figure 14. Class of secretion systems of Gram-negative bacteria
(taken from Green and Mecsas, 2015)

Essential functions of *Vibrio* biotic interactions have been associated with the activity of secretion systems of the type II, III and VI.

Not going further from the model of *Vibrio* pathogenesis, the cholera toxin is secreted through a **type II secretion system (T2SS)** along with several degradative enzymes such as chitinases, proteases, lipases/esterases, phospholipases, nucleases, pilin and matrix proteins for biofilm formation (Johnson *et al.*, 2014). In the transient life-styles of *V. cholerae* between a mammalian host and the aquatic environment, adhesion to mucins covering epithelial cells and chitinous surfaces is facilitated by the secretion of the N-acetyl-D-glucosamine binding protein (GbpA), therefore, considered a broad-host colonization factor (Sikora, 2013). The zinc metalloprotein HapA displays proteolytic activity that could facilitate obtaining nutrients in different environmental contexts but also a determinant factor for the detachment of *V. cholerae* from the intestinal cell layer and the successful exit from the host (Silva *et al.*, 2003). Expression of T2SS has been, until recently suggested to be constitutive; however, it is now known to be regulated by the high concentration of the bacterial second messenger cyclic diguanylate monophosphate (c-di-GMP), which in turn is regulated by QS and related to high cell density. Remarkably, overexpression of T2SS was not related with higher toxin secretion or biofilm formation (Sloup *et al.*, 2017). Taken all together secretion of T2SS effectors appears to strongly contribute to the fitness of *V. cholerae* in different ecological niches (Sikora, 2013).

Type III secretion (T3SS) systems have been identified in several *Vibrio* species. First identified in *V. parahaemolyticus,* two T3SS gene clusters (T3SS1 and T3SS2), one on each chromosome were discovered (Makino *et al.*, 2003), with T3SS1 found in all strains while T3SS2 was restricted to KP-positive strains (hemolysis of blood-agar produced by the presence of the thermostable direct haemolysin). Subsequently T3SS clusters where identified in non-O1/non-O139 and non-toxigenic O1 *V. cholerae, V. alginolyticus, V. mimicus, V. harveyi* and *V. tubiashii*. Several

cytotoxic effectors have been characterized to be secreted in a T3SS-dependent manner. Among them, T3SS1 secreted toxins identified are VopQ, VopR, VopS, VP1659 and VPA0450 which have been characterized to induce autophagy, cell rounding, cell lysis and cell death in eukaryotic cells (Whitaker *et al.*, 2012).

V. campbelli strain BB120 (originally assigned to the species *V. harveyi*) posseses one T3SS locus, whose expression and transcriptional control has been investigated *in vitro* using nutrient rich synthetic growth media and *in-vivo* during infection of gnotobiotic brine shrimp larvae of *Artemia franciscana* (Ruwandeepika *et al.,* 2011). QS regulation at high cell density was shown to inhibit the expression of T3SS genes *in vitro* (Figure 10)(Henke and Bassler, 2004). T3SS expression is regulated by QS through the master regulators LuxR and AphA. Both are repressors of the expression of T3SS, but while LuxR transcription is upregulated by high cell density, AphA transcription is repressed under this condition and induced al low cellular densities (Ruwandeepika *et al.*, 2011), Using an *in-vivo* model of infection, Ruwandeepike *et al.,* (2011) showed that *in-vivo* levels of expression at low and high cellular density are more similar between them and <1000 fold higher than in the *in vitro* conditions, suggesting that additional host cues are integrated in the regulation of the T3SS during infection to only express this energy consuming mechanism when there is a host present. It is proposed that the repression by LuxR at higher cellular densities helps to silence the expression of T3SS inside biofilms in absence of a host and the repression by AphA to silence T3SS expression at low cellular densities when bacteria are in planktonic life style.

The **Type 6 secretion system** was discovered in the interaction of *V. cholerae* with the model amoeba *Dictyostellium discoideum*. *D. discoideum* is used as a model of eukaryotic cell that mimics mammalian macrophages to study several environmental pathogens that display mechanisms of killing or intracellular resistance to amoeba and mammalian cells. Here, mechanism of cytotoxicity dependent on a cell to cell contact is associated with the presence of gene cluster coding for a new secretion system that was named type 6 secretion system in relation to the previously characterized microbial secretion systems (Pukatzki *et al.*, 2006).

The T6SS is a syringe-like molecular nanomachine consisting of two main complexes: a membrane-associated complex that include elements homologue to the type IV secretion system and a second complex that structurally resemble a bacteriophage sheath, tube and tail spike proteins that work together to translocate effector proteins across the membranes of the donor cell and through the outer membrane of the recipient cell (Russell *et al.*, 2014). These secreted effector proteins are recruited to the spike-tube complex through the VgrG and/or PAAR-repeat proteins and incorporated into the Hcp tube. Extracellular signals that

trigger the contraction of the sheath cause the ejection of the spike-tube complex carrying the effectors across the donor and target membranes into the recipient cell (Navarro-Garcia *et al.*, 2019).

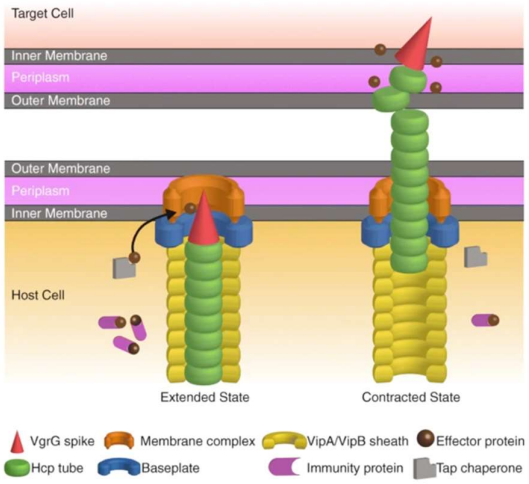

Figure 15. Type VI secretion system (T6SS) model of *V. cholerae*.
Diagram of the extended and contracted state of the T6SS. It is composed of a membrane and baseplate complex; the outer contractile sheath is composed by protein VipA/B and the inner needle complex by the Hcp and VgrV spike. Following the contraction of the VipA/VipB sheath, the VgrG, Hcp and associated toxins are injected into the target cell (Taken from Crisan *et al*., 2019).

Since its discovery T6SS-encoding genes have been identified over a fourth of sequenced Gram-negative genomes and while virulence-associated functions have been characterized linked to the secretion of toxic effectors, the discovery of T6SSs in non-pathogenic or even mutualistic bacteria has highlighted roles for this secretion system different from virulence towards eukaryotic hosts (Jani and Cotter, 2010). Anti-inflammatory (Chow and Mazmanian, 2010), interbacterial cooperation (Konovalova *et al.*, 2010) and competition are among the novel functions associated with T6SS, with the latter possibly been specially relevant, as most of the secreted effectors discovered have antibacterial activity (Jana *et al.*, 2019).

Cytotoxic activity towards eukaryotic cells has been mainly attributed to the presence of a C-terminal actin crosslinking domain in the VgrG-1 protein that is required both for T6SS-dependent secretion but also secreted through the system by only internalized bacteria. The with the ACD not required for secretion but necessary for the occurrence of T6SS-dependent phenotypes (A. T. Ma *et al.*, 2009). Moreover, the induction of T6SS-encoding genes after bacterial uptake by host cells has been observed in several other species such as *Burkholderia pseudomallei, B. cenocepacia and Salmonella enterica serovar* Typhimurium

(Jani and Cotter, 2010).

T6SS-mediated antagonistic interaction between bacteria are linked to the presence of toxin-antitoxin or effector-immunity pairs modules constituted by effector proteins reported to mainly target cell wall components (muramidases and glycoside hydrolases), cellular membranes (lipases) or nucleic acids (nucleases) and a cognate immunity protein that prevent self-intoxication of the toxin-producing cell (Yang *et al.*, 2018).

The relevance of the interbacterial competition in the final step of colonization, that is establishment, has been exemplified above in the examples of *V. vulnificus* T6SS1-positive strains able to kill T6SS-negative strains within the oyster and the contribution of a T6SS2 to the successful colonization of the light organ by specific strains of *V. fischeri.*

II.9 Opportunism, Environmental interactions and selection of virulence traits

As described above, vibrios can use a variety of strategies to overcome host defenses favoring colonization of new hosts. As opportunists, they interact in the environment with a diversity of biotic and abiotic components that could participate to the selection of traits that will provide advantages for colonizing animals.

Resistance to phages

Bacterial mortality in the environment is rarely caused by a lack of resources, and specially *Vibrios* are characterized by having a remarkable ability to survive in oligotrophic conditions and rapidly recover in response to nutrient pulses (Pernthaler, 2005; Takemura *et al.*, 2014). Instead, it is considered that activity of bacteriophages and predation by heterotrophic protist are the major causes of mortality in bacterial populations and a key environmental pressure that has promoted the evolution of a number of strategies for resistance to predation, on which it largely depends the survival and persistence of bacteria in the environment (Sun *et al.*, 2013).

As reviewed earlier, bacteriophages can contribute to evolution of bacteria by mediating HGT, but also trough bactericidal selection. Membrane receptors, porins, LPS, flagella and pili are components of the cell wall that mediate attachment of bacteriophages to the cell and thus are submitted to important selective preassures (Dy *et al.*, 2014).

During cholera disease, phages expand in the intestine and are release in stool back in the environment making cholera epidemics self-limiting (Le Roux and Blokesch, 2018),

Nevertheless, *V. cholerae* strains resistant to phage predation have emerged through the modification of the O-antigen structure that serve as receptors for phage adsorption and entrance (Knirel *et al.*, 2015), along with the horizontal acquisition of phage-inducible chromosomal island-like elements that reduces phage replication and accelerates bacterial cell lysis, limiting phage propagation (O'Hara *et al.*, 2017)

PREDATION BY ENVIRONMENTAL GRAZERS

Grazing activity by phagotrophic protists involves several steps that go from prey encounter, internalization in food vesicles and digestion. In this process, different bacterial species have evolved resistance to predation either by pre-ingestional or post-ingestional strategies to avoid elimination (Matz and Kjelleberg, 2005). Among pre-ingestional adaptations motility, reduction in size, cell wall structure, morphology, secretion of exopolymers, and cell-cell communication are among the phenotypes described with evidence of providing protection from protist predation. Post-ingestional adaptation include inhibition of vacuolar trafficking and scape from vacuoles together with toxin release.

One remarkable aspect of this predator-prey dynamic is that the phagocytic processes of protist as remained conserved in the immune cells of metazoans at the cellular and molecular level. Therefore, it has been hypothesized that strategies evolved by bacteria to resist protist predation and more precisely survival to intracellular degradation favoring the emergence of intracellular pathogens. Related to our model, *C. gigas*, it has recently been described that the detoxifying copper p-ATPase CopA (Vanhove et al., 2016) and the secreted protease Vsm (Binesse et al., 2008), that are among the virulence factors expressed by the intracellular pathogen of the oyster, *V. tasmaniensis* LGP32, also confer resistance against grazing by the marine amoeba *Vannella* sp. This constitute a first insight into an hypothetical environmental selection of virulence factors in the emergence of vibrio pathogenic to the oyster (Robino et al., 2019). Use of the newly developed population framework and high-resolution sampling, genetic manipulation tools and readily available NGS technologies, will allow to explore further the contribution of predators in the eco-evolutionary dynamic of vibrio populations.

III. THE PACIFIC OYSTER CRASSOSTREA GIGAS

III.1 THE OYSTER BIOLOGY

The Pacific cupped oyster *Crassostrea gigas* is a Lophotrochozoan belonging to the phylum Mollusca, class Bivalvia. After a swimming larval stage, juvenile and adult stages are sessile and adopt a benthic life-style showing a settlement preference on firm rocky bottoms of low

intertidal to subtidal estuaries, but they can also be found on muddy or sandy bottoms as epibionts of natural beds of other organisms like mussels (Diederich *et al.*, 2005). Oyster display a wide range of tolerance for varying environmental conditions such as temperature and salinity (Strand *et al.*, 2011), particularly adults, which can survive to temperatures between -2°C and 38°C, and salinity between 15‰ and 41‰ (EFSA. 2015).

The global aquaculture industry has promoted the introduction of this species, originating from Japan, worldwide. It has benefited from remarkable culturing traits like fast growth, important reproductive performances, physiologic adaptations and resistance to diseases like bonamiasis, which affects other oyster farmed species like *Ostrea edulis* (Kennedy and Roberts, 1999). *C. gigas* was introduced in Europe in the 1970's to mitigate the decrease in stock of the Portuguese oyster *Crassostrea angulata* caused by an iridovirus (Grize and Héra, 1991). Similarly *C. angulata* was previously introduced to France in response to the overexploitation and mortality outbreaks affecting the indigenous flat oyster *Ostrea edulis* (Cognie *et al.*, 2006). Despite its subtropical origin, *C. gigas* has been successfully introduced in regions outside its native range. Nowadays the species shows a near-global distribution and establishes wild populations in the introduction sites due to escape from aquaculture facilities (Escapa *et al.*, 2004; Stagličić *et al.*, 2020).

III.1.1 MORPHOLOGY, ANATOMY AND PHYSIOLOGY

The soft body mass of the oyster is enclosed and protected inside two hinged asymmetric valves composed of calcium carbonate and a proteinaceous matrix, which are joined by the hinge and the adductor muscle (Gosling, 2015). The valves are solid, extensively fluted with the superior valve deeply cupped and concave, and the inferior valve flat or slightly convex. The opening and closing of the shell are controlled by the action of the elastic ligament of the hinge that forces the valves to separate and the contraction of the adductor muscle that brings them together in a hermetic closing, which is essential during periods of emersion (Figure 16A).

The bilateral body of the oyster is divided into 4 sections; the visceral mass, the adductor muscle, the gills and two asymmetric mantle lobes (Evseev *et al.*, 1996) (Figure 13B).

The mantle presents well-developed hemolymph vessels, nerves and muscles, and is responsible for the synthesis of the shell and to perform sensory, particle sorting and oxygen intake functions. The two mantle lobs join at the dorsal zone, they close the hinge and cover the internal body organs enclosing the animal within the shell. The space between these two lobes is called the palleal cavity, a semi-closed space divided by the gills into the entrance and cloacal chamber. The oyster possesses two gills that are curtain-like structures suspended from the ctenidial axis that runs along the dorsal margin of the mantle from the labial palps to

the adductor muscle (Godfrey, 2005). Each gill is composed of several W-shaped filaments with divided in two V-shaped demibranchs made of one inner descending filament and one outer ascending filament called lamellae. Thanks to the ciliated filaments, the water flow passes from the inhalant chamber ventral to the filament and connected to the inhalant area of the mantle edge to the exhalant chamber, inside each demibranch, which connects with the exhalant area of the mantle edge. From the water current gills assimilate oxygen and move food particles to the labials palps that precede the mouth.

Directly from the mouth, food passes through the esophagus and into the stomach, a two-chamber sac-like organ embedded in the digestive gland that connects with the stomach by several ducts that allow a continuous two-way flow where food particles enter the digestive gland for intracellular digestion and absorption and waste leaves to the stomach and towards the intestine to be eliminated as feaces through the anus located next to the adductor muscle.

The gonadal tissue, site of gamete production, is located around the surface of the digestive gland with a structure that varies depending on the specific phase of the reproductive cycle, which is seasonal (Fabioux *et al.*, 2005).

The circulatory system of the oyster is considered as semi-open (Schmitt *et al*., 2012b). The hearth is located inside the pericardic cavity next to the adductor muscle; it pumps the hemolymph through arteries and veins into sinuses that connect through the conjunctive tissue forming the hemocoelic cavity. Here the hemolymph is in direct contact with the cell membrane of the tissues.

The major functions of the hemolymph are related to the transport of dissolved oxygen, in the absence of respiratory pigments, nutrient supply, waste removal and immune defense mainly due to the presence of circulating immune-competent phagocytes, the hemocytes (Schmitt *et al.*, 2011).

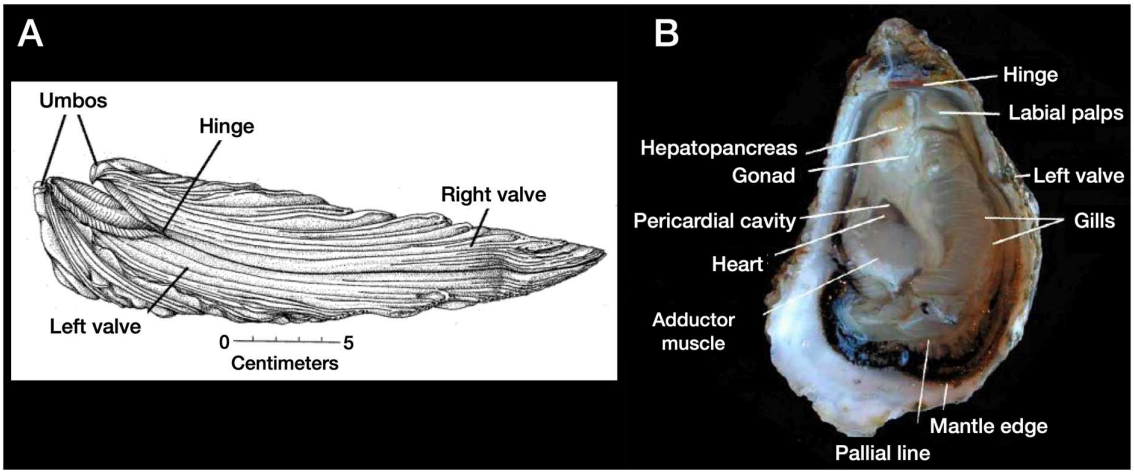

Figure 16. *Crassostrea gigas* anatomy

(A) External morphology (modified from galtsoff, 1964). (B) Internal view of the left valve of an adult oyster showing the organ disposition (modified from Kennedy et al., 1996).

IIII.1.2 REPRODUCTION AND LIFE CYCLE

C. gigas oyster present sequential hermaphroditism, meaning that male and female gametes are produced at different periods of its life. Despite a proposed bias in the primary sex ratio towards males (protandry) has been proposed, female bias (protogyny) can also be found in the literature (Broquard *et al.*, 2020). Oysters have an annual reproductive cycle where environmental temperature and photoperiod play a determinant role on the regulation of gametogenesis (Fabioux *et al.*, 2005) in parallel with the availability and quality of food which fuels this energetically demanding process (Ubertini *et al.*, 2017). As oysters are ectotherm animals (they do not regulate their temperature), the favorable temperature for gamete production is determined by the season (Fabioux *et al.*, 2005).

After spawning, gametes are released in the water column where fecundation occurs. The embryo develops into a ciliated trochophore larvae after 6 h and into a D-stage larva at 24h that remains ciliated but has acquired the velum which also participates in mobility. From the 2nd until the 20th day, a veliger larva develops, which remains pelagic thanks to the cilia and a full developed velum. Around day 20, the pediveliger larva has developed, starting the transition between the pelagic and benthonic life-style by the development of the foot. The pediveliger larva actively sinks to the bottom and uses the newly developed foot search for a suitable substrate to settle. Once the substrate is selected, the larva attaches and metamorphosis occur involving and internal counterclockwise reorganization of the organs and a switch from aragonite to calcite for shell calcification (Baker and Mann, 1994; Ginger *et al.*, 2013). After metamorphosis the oyster larva enters the juvenile stage until the first

spawning cycle that occurs within the first year of age. From there, oysters will develop into adults by only experiencing growth in size (Figure 17).

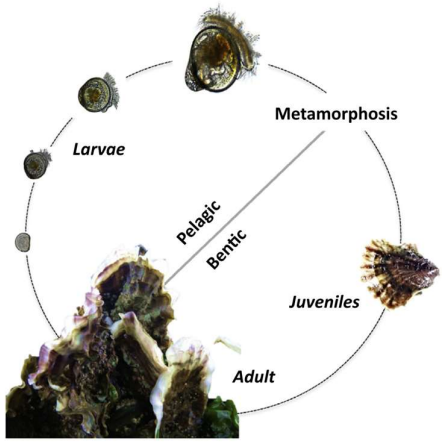

Figure 17. Life cycle of the oyster *Crassostrea gigas*.
(Taken from Le Roux *et al*, 2016)

III.1.3 IMMUNITY

III.1.3.1 OVERVIEW

The immune defense of *C. gigas*, as for all invertebrates, is considered to rely entirely on innate immunity, i.e mechanisms to respond to infection without the development of a lymphocyte mediated immune memory against the re-exposure to a particular antigen (Rowley and Powell, 2007). However, oysters are capable of immune memory, a phenomenon known as immune priming, in which prior exposure to a sublethal dose or pathogen-associated material confers protection against a subsequent infection, either within or between generations, the latter being referred to as trans-generational immune priming (Lafont *et al.*, 2017, 2019; Robinson and Green, 2020). This priming capacity, which still requires a mechanistic characterization (the cellular support of the immune memory remains unknown), adds a new complexity layer to the more thoroughly described but not fully understood immune mechanisms and regulatory networks of the oyster defenses.

Functionally oyster immune defenses rely on multiple components, tissues, cellular and molecular effectors. Water intake, which is necessary for feeding and gas exchange, also represents an abundant and continuous source of microorganisms towards exposed epithelial surfaces such as gills and mantle, which are also part of the first line of defense against infection. These epithelia harbor a diverse bacterial community and produce antimicrobial effectors that offer a hostile environment to potential pathogens (Bachère *et al.*, 2015). Upon breaching of these barriers, bacteria encounter hemocytes, the oyster immune cells that circulate into the hemolymph and infiltrate tissues in response to infection.

In these tissues, both humoral and cellular defenses act together to limit pathogen proliferation and systemic invasion. Given that healthy oysters harbor a microbiota associated with immunocompetent tissues, they must harbor a complex system of recognition and regulations of the immune response to allow the presence of advantageous microorganisms while controlling pathogenic ones in the constant dynamic of maintaining an immune homeostasis. The comprehensive annotation of the oyster genome revealed that the multigene families that make up the immunome are characterized by large-scale gene duplication events and functional divergence, which is suggested to be evolutionary driven by both biotic and abiotic stressors. Such a functional diversification seems determinant to mount highly specific responses towards bacterial, viral or abiotic stressors, mediated by the differential expression of specialized genes within these expanded multigene families (Zhang *et al.*, 2015).

III.1.3.2 EPITHELIA, HEMOLYMPH AND HEMOCYTES

Epithelia of various organs are able to express non-self-recognition receptors and also produce immune effectors with microbicidal activity (Bachère *et al.*, 2015; Wang *et al.*, 2018). For instance, several cDNA sequences identified as peptidoglycan recognition proteins (PGRP) have been identified in the epithelium of the gills, digestive tissue and digestive gland of the oyster (Itoh and Takahashi, 2008) where they specifically binds to peptidoglycan and produce bacterial death by inducing production of ROS, depletion of antioxidant thiols and incrementing the concentration of metal concentration, by overactivating two component systems and exploiting the stress defense response of bacteria (Dziarski *et* al., 2012, Kashyap *et* al., 2014). In addition to recognition proteins, epithelial tissues produce antimicrobial effectors such as lysozyme (Matsumoto et al., 2006, Itoh and Takahashi 2007, Xue et al., 2010), hydrolytic enzymes (Itoh and Takahashi 2007, Itoh *et al.*, 2010b) and antimicrobial peptides (summarized in Wang et al., 2018). The presence of recognition proteins and antimicrobial effectors upport an active role of epithelial surfaces in the defense against invading microorganisms.

Hemolymph, in the immune context, constitutes an important interface of interaction between microorganisms and the immune system (Dupont *et al.*, 2020). Remarkably, it harbors both the hemocytes, i.e the principal cellular mediators of immunity, and an abundant and diverse microbial community (Dupont *et al.*, 2020). Although the hemolymph is devoid of clotting factors, the hemocytes, which display a strong aggregation capacity, perform a reversible cellular cloth in response to wounding (Bachere et al., 1988). The composition of the plasmatic fraction of the hemolymph is dominated by proteins with homologies with a metalloenzyme known as extracellular Superoxide Dismutase (EcSODs). While it has not been confirmed that all the SOD-related proteins found in the oyster plasma

possess a SOD activity, their role in non-self-recognition and opsonization of bacteria have been shown for the Cu/Zn Cg-EcSOD, the major plasma protein found in the oyster (Gonzalez *et al.*, 2005; Duperthuy *et al.*, 2011).

Hemocytes, the oyster circulating immune cells, are transported by the hemolymph across the semi-open circulatory system from where they are able to migrate by diapedesis from sinuses through the conjunctive tissue to the surface of, particularly, mantle and gills where they are discarded (Bachère *et al.*, 2004; Schmitt *et al.*, 2011). In addition to their key immune functions described in the following chapters, hemocytes mediate vital functions such as wound and shell repair, gamete reabsorption, nutrient transport, digestion and excretion (Bachère *et al.*, 2004). Upon infection or wounding, hemocytes rapidly migrate to sites of infection through chemotaxis towards a C1q domain containing protein (H. Li *et al.*, 2019). To date there is no consensus on the hematopoietic site and the life-cycle of hemocytes in bivalves has not being established (Vogt, 2012). An origin on the connective tissue (Cheng, 1981), the endothelial cells of vessels and arteries (Tirapé *et al.*, 2007) and more recently the tubules of the gill filaments have been proposed for the hemocytes of *C. gigas* (Jemaa *et al.*, 2014; Li *et al.*, 2017). The proposition of gills as the hematopoietic organ of the oyster is supported by the finding of abundant stem-like cells associated with an irregular folded structure (IFS) in the gill epithelium. These cells were found to be actively going under replication (BrdU-labeled) and positive for the stemness marker SOX-2 and the hemocyte-specific enzyme Cu/Zn CgEc-SOD. Associated with this potential hemocyte precursor, the presence of large BruU-labeled cells positives for Cu/Zn CgEc-SOD and the protein filamin specific for hemocytes was considered by the authors as the evidence connecting the replicative activity the stem-like cells and their differentiation into hemocytes. A transcription factors, the Stem Cell Leukemia gene (SCL), having relevant hematopoietic functions in vertebrates, has been found to be highly expressed in hemocytes and necessary for the expression of hemocyte-specific genes (Song *et al.*, 2016).

There is no general consensus in the number of different cell types that compose the cellular fraction of the hemolymph of *C. gigas*, nonetheless, two clearly differentiable populations of granular and agranular hemocytes are consistently reported in the literature. From this simple categorization two subpopulations of granulocytes (basophils and eosinophils) and three of agranulocytes (blast-like cells, agranular basophils and macrophage-like hyalinocytes) have been proposed. Among them, a particular population behaves as professional phagocytes with strong phagocytic activity (Jiang *et al.*, 2016; Takahashi *et al.*, 2017; W. Wang *et al.*, 2017).

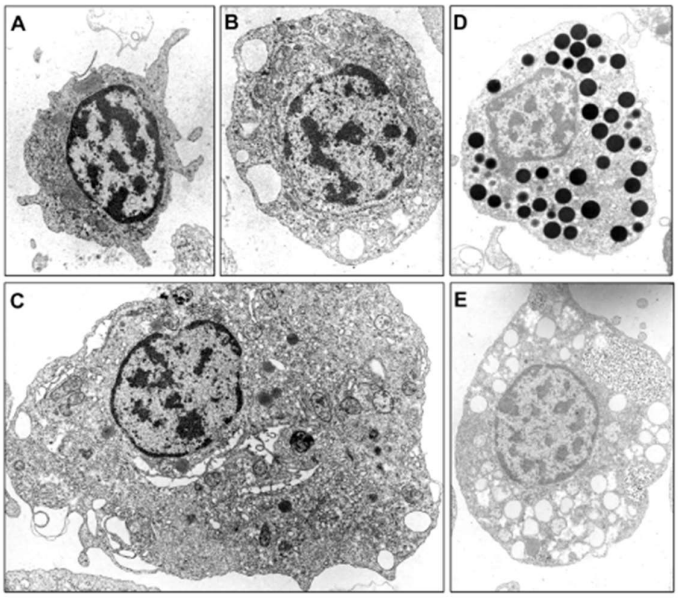

Figure 18. Types of circulating hemocytes of *C. gigas* observed by transmission electron microscopy. (A) Small, probably young hyalinocyte. (B) Hyalinocyte. (C) Large Hyalinocyte. (D) Granulocyte with electron-dense granules. (E) Granulocyte displaying electron lucent granules and numerous cytoplasmic bodies apparently corresponding to phagocytic residues (modified from Bachère et al., 2004).

The discovery of novel genetic markers, thanks to the availability of the oyster genome, the development of single cell RNAseq, together with the implementation of techniques such as single cell RNA-seq, which already has been in the study of hemocytes of other invertebrates such as insects, will help to unravel further the origin, lifecycle and functional relationships of the oyster hemocytes.

III.1.3.3 Recognition of non-self and damage-related patters

The initial step that can trigger the immune response involves the recognition of two types of signals, either conserved molecules from microorganisms absent from the host (MAMPS), recognized as non-self by the immune system, or molecules released by dying or damaged cells (DAMPS), recognized as signals of danger (Newton and Dixit, 2012).

As oyters immunity relies only on innate immunity, this recognition is mediated by germline encoded pattern recognition molecules that can be soluble (Pattern Recognition Proteins, PRPs) or associated with the cellular membrane (Pattern Recognition Receptors, PRRs).

A diversity of MAMPs can be recognized by PRPs and PRRs like peptidoglycan, the major structural polymer of the bacterial cell wall, lipopolysaccharides that extensively cover the

outer membrane of Gram-negative bacteria, lipoteichoic acids that are present in the cell wall of gram-positive bacteria, but also proteins like bacterial flagellin, or sugars like β-glucans from the cell wall of fungi. Some nucleic acids can also play a role as MAMPs, like double stranded RNA (dsRNA) involved in the replication cycle of certain viruses (Beutler, 2004).

The reliance of invertebrates on innate mechanisms of defense does not imply by any means an impaired immunocompetence against infection, compared to vertebrates. Oysters possess a vast repertoire of both PRRs and PRPs with most of them able to perform not only immune recognition but also exert antibacterial activity towards microbes. The functional divergence that characterizes the oyster immunome is suggested to be a source of innovation and adaptability (Zhang *et al.*, 2015).

So far, the list of PRR/Ps identified in the oyster, includes peptidoglycan recognition proteins, carbohydrate binding lectins, Toll-like receptors, Gram-negative binding proteins, scavenger receptors, and fibrinogen-related proteins (FREPs) (Wang *et al.*, 2018).

A recent survey of PRR/P using the latest genome version available (V9, size: 581 Mb, ORFs: 26.811 [X. Wang *et al*., 2019]) identified a total of 1084 genes assigned to recognition function distributed in at least 12 gene families. The transcriptomic profile of this set of PRR/P in response to LPS, peptidoglycan, glucan, and poly I:C (which mimics dsRNA) was examined by RNA-seq. Overall, the principal gene families involved in the response to MAMPs were C1q-domain containing proteins (C1qDCs), C-type lectins (CTLs) and FREPs with a dynamic and specific regulation of numerous PRR/Ps in response to the stimulus (Wang *et al.*, 2019).

C1q-domain containing proteins (C1qDC) have begun to be considered as key players in the immune response of bivalves. The C1q domain is present in the C1 complex that initiates the classical complement pathway in vertebrates by the binding of the C1q domain to antigen-antibody complexes (Cooper, 1985). A larger number of proteins containing the globular C1qDC motif are found in metazoans that lack an adaptive immune system, specially species of bivalve mollusks, which can harbor up to 1000 different C1qDC proteins (Gerdol *et al.*, 2019). This highly expanded gene binds a wide range MAMPs from bacteria, virus and fungi (Gerdol *et al.*, 2019). Nonetheless, it is not clear whether all the members are involved in immune recognition (Gerdol *et al.*, 2015) as they have also been associated with the response to environmental pollutants and involved into shell mineralization (Hattan et al., 2001; Liu et al., 2007; Yin et al 2005), which suggests functional diversification following gene expansion in the oyster (Gerdol *et al.*, 2015, 2019).

The oyster *C. gigas* harbors in its genome more than 300 C1qDC proteins (Zhang *et al.*, 2015; Gerdol *et al.*, 2019; Wang *et al.*, 2019), which are mainly categorized into two subgroups:

those containing only one globular head C1q domain (ghC1q) and those who also presenting a collagen region N-terminal to the C1q domain (C1q-like), which is characteristic of the vertebrate C1 complex. According to the study of the expansion of the C1q gene family in *C. gigas* by Gerdol and coll. (2015), most of the C1qDC genes have, to some extent, a tissue-specific expression. From a total of 337 annotated C1qDC proteins, 156 were associated with the digestive gland, 73 to the gills, 5 to hemocytes, 5 to the mantle tissue and 91 with non-tissue-specific expression. Function-wise, five CgC1qDC that only contain the ghC1q motif and one that also carries a collagen-like domain (*Cg*C1qDC-6) are involved in either the enhancement of phagocytosis towards *V. splendidus*, direct antimicrobial activity, or cell migration (Lv *et al.*, 2018; H. Li *et al.*, 2019). Finally, a transcriptomic analysis in response to LPS, identified several homologues of the complement system of vertebrates in *C. gigas*, including a C3 protein which is responsible for the activation of the alternative complement pathway. This suggests the existence of a multi-component complement system in the oyster (L. Wang *et al.*, 2017).

Glycans are found in several MAMPs, such as glycoproteins, glycolipids, and polysaccharides which are bound with high affinity by lectins that also participate in agglutination, immobilization and complement-mediated opsonization. C-type, P-type, F-type, I-type, galectins, ficolins, and chitinase-like are the seven groups of lectins identified in the oyster (Wang *et al.*, 2011).

C-type lectins (CTLs) bind carbohydrates in a calcium dependent manner and contain at least one carbohydrate-recognition domain. Seven different CTLs have been identified in the oyster (Yamaura *et al.*, 2008; Jia *et al.*, 2016). Among them, CgCLT-2 possesses only one CRD and the recombinant protein can trigger hemocyte phagocytosis. CgCLT-4 and CgCLT-5 are secreted and intracellular lectins, respectively, both induced by LPS. Both recombinant proteins display a broad MAMP, bacteria-binding and agglutinating ability, but only CgLec-4 exerts antimicrobial activity against bacteria and fungi (Jia et al., 2016).

Fibrinogen-related proteins (FREPs) contain one or more fibrinogen-like (FBG) domain which display high sequence similarity with the soluble plasma protein fibrinogen involved in blood coagulation in vertebrates. FREPs are widespread in vertebrates, urochordates and invertebrates. Their inducibility and binding activity in organisms like the scallop *Argopecten purpuratus* and the snail *Biomphalaria glabrata* has been shown to display specificity to the type of pathogen related stimuli (Zhang *et al.*, 2008, 2009). The first report of complete FREPs coding sequence in *C. gigas* was identified through a cloning strategy: 5 different FREPs-like sequences were amplified using a single pair of primers, suggesting a high sequence diversity of this gene family (Zhang *et al.*, 2012). Genomic studies allowed to found a total of 202

predicted protein identified in the oyster genome (Wang *et al.*, 2019) ; they were found to be highly expressed in the gill tissue, thus suggesting an important role in the response towards potential microbial invaders.

Toll-like receptors (TLR) are type I membrane proteins, where a transmembrane domain connects an extracellular domain that contains leucine rich repeats (LRR), with a cytoplasmatic domain (TIR) that resembles the Interleukin -1 receptor. TLR are considered main mediators of the innate immunity (Satake and Sekiguchi, 2012).

They present an important level of expansion with 83 TLR genes predicted to be part of the oyster genome. They are distributed in five groups according to their sequence similarity (Wang *et al.*, 2018). From the large repertoire of predicted TLRs only six have been identify as involved in the immune response based on their induction in response to MAMPs (*Cg*Toll-1), their ability to activate NF-κB in transfected HEK293 cells (*Cg*TLR1-4) and their broad recognition capacity towards bacteria, fungi, LPS and PGN (*Cg*TLR-6) (Wang *et al.*, 2016).

Retinoic acid-inducible gene I (RIG-I)-like receptor (RLRs) contribute to the recognition of viral nucleic acids by sensing non-self RNA in the cellular cytoplasm. Search for homologues of the three human RLRs members, RIG-I, MDA5 and LGP2 identified thirteen candidate *Cg*RLRs annotated as RIG-I family members with an unusual diversity of domain architecture. The first RLR identified in *C. gigas*, *Cg*RIG-I, has the typically conserved domains, *i.e.* the caspase activation and recruitment domains (CARDs), a helicase domain and a C-terminal regulatory domain (RD) (Y. Y. Zhang *et al.*, 2014). It is exclusively induced by the dsRNA analog polyI:C among a repertoire of other MAMPs and its promoter region contains predicted sites for NF-kB, IRF and STAT binding, sustaining the responsiveness to polyI:C (Y. Y. Zhang *et al.*, 2014). RLR pathways are involved in the antiviral response that characterized the ostreid-herpes virus 1 infection of juvenile oyster (Lafont *et al.*, 2017); it contributes to the protective effect of polyI:C priming in OsHV-1 infected oysters (Lafont *et al.*, 2020) and falls within the group of immune genes whose higher basal expression has been linked to oyster survival against OsHV-1 infection (Lorgeril *et al.*, 2020).

Nine **PGRPs (peptidoglycan recognition proteins)** have been identified in the oyster (Wang *et al.*, 2019). They recognize peptidoglycan, which forms the bacterial cell wall as a mesh-like structure consisting of a carbohydrate backbone cross-linked to peptides. Peptidoglycan monomers are composed of two joined units of N-acetylglucosamine (NAM) and N-acetylmuramic acid with a pentapeptide attached to the NAM unit. This essential bacterial motif is bound by peptidoglycan recognition proteins. Six out of the nine oyster PGRPs are

short PGRP type carrying a conserved PGRP/amidase domain in then C-terminus, suggesting a PGN lysis activity (Itoh and Takahashi, 2008). This amidase activity plays an important role in microbiota tolerance as demonstrated in *Drosophila*, where PRGP-LB degrades Gram-negative bacteria peptidoglycan to attenuate immune activation (Zaidman *et al*., 2006). While all the oyster PGRPs show conservation of the amidase domain, the residues directly involved in PGN binding present a degree of mutation that could translate into a more flexible response towards microbial challenges.

The Gram-Negative Binding Protein (GNBP) are inducible by immune challenge and includes members that bind to Gram-negative bacteria, lipopolysaccharide (LPS) and β-1,3-glucan. Two β-1,3-glucan binding proteins (βGBP) have been identified in *C. gigas*, CgβGBP-1 and CgβGBP-2 have been suggested to have different immunological functions based on *in vitro* investigations using recombinant proteins (Itoh *et al.*, 2010a).

Scavenger receptors (SR) are endocytic PRR with the ability to recognize host-modified low-density lipoproteins and various bacterial ligands. The Scavenger Receptor Cystein-Rich (SRCR) domain is an ancient and highly conserved domain of typically 110 amino acids in length with six or eight cysteine residues connected by three or four interdomain disulfide bonds. SRCRs are found in SRs but are also common to a large variety of molecules restricted to immune cells (Mukhopadhyay and Gordon, 2004). In the genome of *C. gigas,* 71 different predicted SRCRs have been identified. The contribution of SR to the adaptation to multiple stressors have been proposed, as several of them are up-regulated during the Pacific Oyster Mortality Syndrome affecting *C. gigas* juveniles (Fleury et al., 2010), during hypoxia (David et al., 2005) and during bacterial challenge (McDowelll et al., 2014).

III.1.3.4 Cellular communication

The signals recognized by the different receptor described above activate different signaling pathways to mount humoral and cellular responses, which usually depend on the type of stimuli.

Toll-like receptors signaling pathway

Although details of the TLRs signaling and involvement in the immune response still need to be investigated with greater details in oyster, several components of the signaling pathways coupled to this type of PRR have been identified in the genome of *C. gigas,* namely MyD88, IRAK, TRAF, ECSIT, IKK and members of the canonical pathway for Nuclear factor-kappaB (NF-κB) activation (see section below). The Myeloid differentiation factor 88 (MyD88) corresponds to a cytosolic adaptor that links, through protein-protein interaction, the IL-1R domain to the

IL-1R-associated kinases (IRAK) family kinases, which in turn can activate NF-κB, MAPK and AP-I. Ten MyD88 genes have been annotated with some of them either induced or suppressed by bacterial challenge. A blocking peptide designed against the TIR domain of *Cg*MyD88 impaired NF-kB activation in HEK293 cell transfected with *Cg*TLR1 and *Cg*MyD88 but also inhibit hemocyte degranulation and *Cg*TNF expression in response to *V. parahaemolyticus* injection (Zhang et al. 2013).

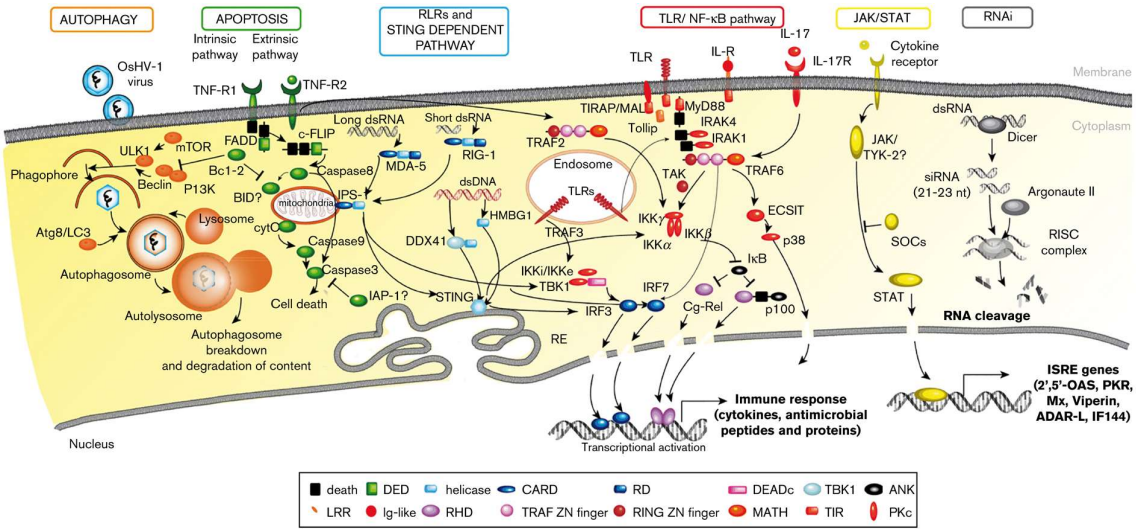

Figure 19. Reconstruction of signaling pathways in *C. gigas*.

The presented diagram was constructed based on the identification of conserved sequences in the oyster genome and most interactions between signaling componentes have been inferred from vertebrate and insect literature (taken from Green and Montagnani 2015).

The canonical pathway for NF-κB activation

One major group of inducible transcription factors is composed by members of the Rel family of DNA-binding proteins that are collectively named NF-κB which regulate the expression of a large array of immune-related genes.

In vertebrates the nuclear translocation of NF-κB is activated through two different independent pathways named canonical and alternative. The canonical pathway is triggered by recognition of MAMPs by diverse PRRs, including TLRs, and through the action of pro-inflammatory cytokines (Lui *et al*., 2017).

Three essential components of the canonical pathway have been identified in *C. gigas,* the

transcription factor Rel/NF-κB itself (Huang et al 2012., Montagnani et al., 2004; Wu et al., 2007), three IκB proteins (CgIkB1-3) that inhibit NF-kB activation in HEK293 cells, in agreement with their putative ability to sequester Rel proteins in the cytoplasm (Xu et al., 2015; Zhang et al., 2009). Finally, two IKKa/β and one IκB kinase-like (oIKK) were found that should mediate the inducible degradation of IκB and release of NF-κB along with the unmasking of its nuclear localization signal. Transfection of oIKK successfully promoted the translocation of NF-kB to the nucleus, activity that was dependent on the kinase activity of the oIKK (Montagnani *et al.*, 2004). The IKKa/β-2 homologues have been suggested to be involved in the oyster interferon (IFN)-like antiviral pathway as it was found that they are able to interact with the interferon regulatory factor (Huang *et al.*, 2019).

Mitogen-Activated Protein Kinases (MAPK) pathway

MAPKs belong to a family of conserved protein kinases that are activated by several PRRs, with the best studied example being TLRs. A p38 MAPK was identified in *C. gigas* closely related to the *Ch*P38 from *C. hongkongensis*. *Cg*p38 is inducible by both LPS and *V. splendidus* stimulation and it was shown to regulate positively the expression of pro-inflammatory cytokines including *Cg*IL17-1,2,3,4,6, and *Cg*TNF (Sun *et al.*, 2019).

The interferon (IFN) pathway

The interferon (IFN) family cytokines are produced upon recognition of MAMPs related to viral infection, such as dsRNA and viral glycoproteins which promotes, through the JAK/STAT signaling, the translocation of interferon regulatory factors (IRFs) and other transcription factors to the cell nucleus (Randall and Goodbourn, 2008; Martins, 2020). The production of interferon in turn leads to the induction of IFN-stimulated genes that stimulate an amplification loop of IFN production and also antiviral mechanisms such as apoptosis or autophagy to limits the viral replication (Sadler and Williams, 2008).

C. gigas possesses a complex antiviral response that involves several components of the interferon pathway which includes related sensors molecules such as cytoplasmic TLRs, RIG-1 and cGAS, the MyD88 and IkKB signal transducers, IRFs, stimulator of interferon genes (STING), JAK/STAT signaling components and effectors such as OAS, Viperin and Mx. Interestingly, a sustained activation of this pathway in the oyster can be induced by the injection of dsRNA or by its synthetic analog the polyI:C that confers protection against OsHV-1 infection over months. This phenomenon relates to immune priming; see below (Lafont *et al.*, 2017, 2020).

Cytokines

Following the activation of the innate immune system, the response is regulated by the action

of several soluble factors which include cytokines and chemokines that fine tune the humoral and cellular response of the host. In the *C. gigas* genome, six interleukin-17 (*Cg*IL17) (Roberts *et al.*, 2008), one Interferon like protein (CgIFNLP) and 23 tumor necrosis factor homologs have been annotated so far. In vertebrates, IL-17 is a major pro-inflammatory cytokine in the innate and adaptive immunity of vertebrates. It is involved in recruiting neutrophils to the site of infection and it can induce the production of antimicrobial peptides (Veldhoen, 2017). All the six IL-17 homologues found in *C. gigas* are differentially regulated by MAMPs (Li *et al.*, 2014; Sun *et al.*, 2019) and most of them have been shown to be responsive to the regulation by the NF-kB/Rel transcription factor, *CgRel* in hemocytes of oysters injected with LPS (Y. Li *et al.*, 2019). Furthermore, IL17-5 is able to activate NF-kB, CREB and ATF-1 in HEK293T cells and induce IL6 in HuVEC cells (Xin *et al.*, 2015).

The **interferon-like protein (*Cg*IFNLP**) and its cognate receptor interact *in vitro* and both transcripts are induced in response to polyI:C. As *Cg*IFNR-3 is able to activate the JAK/STAT pathway in oyster and *Cg*IFNLP induces phagocytosis and apoptosis in hemocytes, they are likely part of the antiviral response in oysters (Green *et al.*, 2015). From the 23 TNF homologues, 15 are oyster-specific and one (rCgTNF-1) regulates apoptosis and antibacterial activities in hemocytes (Sun *et al.*, 2014).

III.1.3.5 Effector mechanisms of oyster defense

Several cellular and humoral responses can be mounted by hemocytes in response to MAMPs or DAMPs recognition.

Hemocytes are very reactive, and they can migrate rapidly towards the site of injury or infection. This allows hemocytes to concentrate in the affected site and through aggregation, phagocytosis and production of defense molecules control either pathogen invasion or tissue injury (Schmitt *et al.*, 2012b; Bachère *et al.*, 2015).

Phagocytosis.

Phagocytosis is a highly conserved process that has been thoroughly characterized in vertebrates. It is utilized by diverse types of cell to ingest particles usually larger than 0.5 µm (Rosales and Uribe-Querol, 2017). The key events of attachment, formation of pseudopods and phagosome internalization, and finally phagosome maturation into a degradative phagolysosome are conserved in hemocytes and all of them involve a coordinated

reorganization of the cytoskeleton membrane trafficking (Underhill and Goodridge, 2012). Six genes, *Cg*Integrin, *Cg*PI3K, *Cg*Rho J, *Cg*MAPKK, *Cg*Rab 32, and *Cg*NADPH, putatively involved in phagocytosis are inducible by stimulation with *V. splendidus* and are responsive to a second exposure by an enhance overexpression (T. Zhang *et al.*, 2014). Furthermore, a member of the Nimrod family receptor was described for its role in hemocyte phagocytosis like in other invertebrates. *Cg*NimC harbors binding capacity towards LPS and Gram-negative bacteria. Moreover, monoclonal antibodies raised against *Cg*NimC significatively reduced the phagocytic index of Gram-negative bacteria (Wang *et al.*, 2015).

Certain oyster pathogens like *V. aesturianus* are able to inhibit hemocyte phagocytosis to evade immune control (Labreuche, Lambert, *et al.*, 2006) but others like *V. tasmaniensis* LGP32 benefit from phagocytosis to adopt an intracellular stage thanks to several resistance mechanism to phagolysosomal degradation (Duperthuy *et al.*, 2011; Vanhove *et al.*, 2015, 2016).

Reactive species of oxygen and nitrogen

Reactive oxygen/nitrogen species (ROS/RNS) are normally produced by all aerobic organisms and have important roles in the host physiology including defense due to their toxicity at high concentration that can be employed by the host in bacterial killing. During phagocytosis, transmembrane NADPH oxidases together with Dual oxidases (DUOX) participate in a respiratory burst that will generate highly reactive superoxide (O^{-}_{2}) resulting in a variety of intermediate ROS such as hydrogen peroxide (H_2O_2), hydroxyl radicals, hypochlorous acid and singlet oxygen that will accumulate in the phagolysosome configuring a highly oxidative environment. The production of RNS is catalyzed by inducible nitric oxide synthases (NO) that use L-arginine and oxygen to produce nitric oxide. Both ROS and RNS can synergize inside the phagolysosome to create a highly oxidative environment for phagocyted microorganisms (X. Zhang *et al*., 2019).

While valuable for host defense, the toxicity of ROS and RNS has no specificity and can also generate significant damage to host macromolecules such as proteins, lipids and specially DNA (Kohen and Nyska, 2002). One important group of antioxidant enzyme identified in the oyster are Superoxide dismutases (SOD), i.e. metalloenzymes that convert the superoxide into hydrogen peroxide (H_2O_2) and O_2. Two SOD types have been identified and characterized in the oyster according to their metal content, a Manganese and Copper/Zinc SOD (MnSOD, Cu/ZnSOD) which serve as antioxidants but also as PRR as it has been described for the extracellular EcSOD which is able to bind LPS, PGN, and poly (I:C) and promotes the

internalization of *V. tasmaniensis* LGP32 by bridging the vibrio virulence factor OmpU (a major outer membrane protein required to enter oyster hemocytes) with the host *Cg*Integrin (Duperthuy *et al.*, 2011; Vanhove *et al.*, 2016).

It was reported that the expression of the DUOX genes in hemocytes was associated with survival of oyster to *Vibrio* infection (de Lorgeril *et al.*, 2011) and that higher extracellular SOD expression is a trait selected by oyster families resistant to field mortalities (Fleury and Huvet, 2012), supporting the contribution of the respiratory burst to the antimicrobial capacity of *C. gigas*. However, some pathogenic *Vibrios* such as *V. aesturianus* and *V. tasmaniensis* LGP32 are able to suppress the production of ROS, which contributes to their virulence to the oyster. The ability of pathogenic vibrios to the oyster to evade ROS activity suggests a major role of ROS in the defenses of the host.

Lysozymes

Lysozymes belong to a family of hydrolases which specific substrate is the peptidoglycan of the bacterial cell wall catalyzing the hydrolysis of the β-1,4 glycosidic bond of the peptidoglycan (Itoh *et al*., 2010b). In addition to their direct role as bacteriolytic agents they have been described involved in immunomodulation and as important digestive enzymes in some species. So far, three invertebrate-type (i-type) lysozymes have been reported (CGL-1, CGL-2, CGL-3). CGL-2 mRNA is expressed in all oyster tissues except the adductor muscle, while the expression in the digestive gland is restricted to the basophil cell of the gland tubule (Matsumoto *et al.*, 2006). CGL-1 and 3 were found mainly expressed in the mantle tissue and the recombinant protein showed antibacterial activity in mantle extract of *C. gigas* (Itoh *et al.*, 2010b)

Antimicrobial peptides

Antimicrobial peptides (AMPs) are evolutionary ancient small proteins (<10kDa) with a broad spectrum of antibacterial and immunomodulatory activities that are ubiquitous among metazoans (Spohn *et al.*, 2019). Several but not all AMP classes from eukaryotic origin adopt an amphipathic design of clusters of hydrophobic and cationic amino acids (Zasloff, 2002). They are usually cationic, thereby exploiting the intrinsic negative charge of the outermost bilayer membrane of bacteria to initiate a primary interaction that either leads to membrane permeabilization by pore formation or their seamlessly translocation to their cytoplasm where they can interfere with the bacterial metabolism (Spohn *et al.*, 2019).

The oyster genome contains AMPs families that have been characterized to variable extent. CSaβ-defensins (characterized by a cysteine stabilized alpha beta motif broadly found in plant and arthropod defensins) and Big Defensins (multidomain defensins mostly found in species of marine invertebrates and cephalochordates) are among the best studied AMPs from *C. gigas* (Schmitt *et al*., 2012b)). Members of the CSaβ-defensins are the mantle defensin *Cg*-Defm (Gueguen *et al*., 2006) and two hemocyte defensins, *Cg*-Defh1 and *Cg*-Defh2 (Gonzalez et al. 2007), which act by inhibiting the biosynthesis of peptidoglycan (Schmitt et al., 2012). Big defensins are multi-domain polypeptides (Schmitt, *et* al., 2016); they contain a hydrophobic N-terminal domain and a cationic C-terminal domain. *C. gigas* possesses a diversity of Big defensins (Gerdol et al., 2020) among which *Cg*BigDef-1 and -2 are specifically expressed in circulating and infiltrating hemocytes, after bacterial challenge (Rosa et al. 2011). *Cg*BigDef-1 was shown to entrap and kill bacteria into elongated fibrils called nanonets induced by contact with bacteria (Loth et al., 2019).

Bactericidal/permeability-increasing protein

Bactericidal permeability-increasing protein (BPI) and lipopolysaccharide (LPS)-binding protein (LBP) are considered to be members of a family of lipid-binding proteins. Vertebrate BPI and LBP bind to the Lipid A moiety of LPS but they also display antagonistic pro-inflammatory and anti-inflammatory activities upon recognition, respectively (Bingle and Craven, 2004). Two homologues of the human BPI (hBPI) have been identified in the oyster (*Cg*-BPI1 and *Cg*-BPI2), they are constitutively expressed in various tissues and they are induced in hemocytes after immune challenge presenting different temporal expression profiles. Recombinants *Cg*-BPI1 and 2 show both antibacterial activities exclusively towards Gram-negative bacteria (Gonzalez *et al.*, 2007; Zhang *et al.*, 2011). Cg-BPI1 acts by permeabilizing the bacterial membranes (Gonzalez *et al*. 2007).

Diversity of mechanism and synergism

Synergistic activities have been described between different families of oyster AMPs. As a notable example, synthetic proline-rich AMPs identified in hemocytes have poor activity against Gram-positive and no activity towards Gram-negative bacteria, but they act synergistically with *Cg-Defs* and *Cg*-BPI against both Gram-positive and Gram-negative bacteria (Gueguen *et al.*, 2009; Schmitt *et al.*, 2012a). The migratory behavior and infiltration response of hemocytes has been proposed to contribute to the colocalization of diverse antimicrobial thus allowing synergy, as different AMPs are expressed in hemocytes and different tissues like mantle, during injury or infection (Schmitt *et al.*, 2012a).

III.1.3.6 IMMUNE PRIMING

Evidences have accumulated over the years supporting the existence of an immune memory in invertebrates where re-exposure to a microbial stimulus generates a faster and more effective immune response relative to naive individuals, which can translate in an increased survival to infection (Melillo *et al.*, 2018). As the concept of immune memory is paradigmatically linked to the cellular (lymphocytes) and humoral components (antibodies) of adaptive immunity in vertebrates, that are missing in invertebrates, this phenomenon requires to redefine immune memory in a way that is independent of the underlying mechanisms (Milutinović and Kurtz, 2016).

Although phenotypic evidences of an immune memory have accumulated across different taxa, the remaining controversy is mainly due to the lack of knowledge about the underlying molecular and cellular mechanisms (Hauton and Smith, 2007).

In the oyster *C. gigas* antiviral immune priming was evidenced in response to dsRNA. This response confers to juvenile oysters a specific and long-lasting protection to juvenile oysters against the infection by the ostreid herpes virus 1 (OsHV-1) by blocking viral replication (Lafont *et al.*, 2017, 2020). This translates into enhanced field survival to the mass mortalities of the Pacific Oyster Mortality Syndrome. The molecular bases of this immune priming phenomenon have been recently studied; results showed that a sustained upregulation of gene expression is triggered after priming that can still be observed after 4 months after priming. This sustained alert state is proposed to allow an effective early immune response towards OsHV-1 (Lafont *et al., 2020)*.

In addition, a maternal transgenerational priming phenomenon has been evidenced in *C. gigas*. Upon genitor stimulation with polyI:C, only mothers are able to transfer immunity to the next generation conferring larvae with higher resistance to OsHV-1 infection. This phenomenon could be the result of the maternal provisioning of the eggs with antiviral compounds (Green *et al.*, 2016; Lafont *et al.*, 2019). Nevertheless, a tradeoff in maternal offspring protection has been recently identified, where improved larval survival is linked with impaired growth and a higher *Vibrio* loads compared with trans-generationally unprimed offspring (Robinson and Green, 2020).

Immune priming by bacterial components has also been studied in the oyster. Although immune functions have been shown to be enhanced upon re-exposure to bacteria, no evidence of enhanced survival of primed oyster has been reported so far making debatable the functional relevance of this primed response against bacterial infection (T. Zhang *et al.*, 2014; Li *et al.*, 2017; Wang *et al.*, 2020).

III.2. THE PACIFIC OYSTER MORTALITY SYNDROME (POMS) AS A MODEL FOR POLYMICROBIAL HOST-MICROBE INTERACTIONS

Over the past twenty years, two main different infectious diseases have affected juvenile and adult *C. gigas* oysters causing mortality outbreaks on reared oysters. These diseases have been considered to challenge the sustainability of *C. gigas* farming in France and worldwide (Dégremont *et al.*, 2020). Since 2012 adult mortalities have been caused by *V. aestuarianus*, a bacterial species that is suggested to have re-emerged as an oyster pathogen after a period of low detection in moribund oysters between 2008 and 2012 (Goudenège *et al.*, 2015).

In contrast, a disease of a higher etiological complexity, able to cause 100% mortality in farmed juveniles has severely affected oyster farming since 2008. This severity is associated with the emergence of a microvariant genotype of the previously identified Ostreid herpesvirus 1 (Segarra *et al.*, 2010). This microvariant refreed to as OsHV-1 µvar is the etiological agent of the Pacific Oyster Mortality Syndrome (POMS), a polymicrobial disease that integrates complex interaction between the environment, host and pathogens. In this infectious disease OsHV-1 is necessary for the onset while opportunistic bacterial pathogens, notably vibrios, determine its fatal outcome (de Lorgeril *et al.*, 2018; Petton *et al.*, 2019).

POMS occur seasonaly, during a permissive seawater temperature window ranging from 16°C to 24°C (Pernet *et al*., 2012). Susceptible oysters reared in the intertidal farming sites become infected by the OsHV-1 virus, which starts replicating exponentially during the first 24h. This promotes the shedding of virions into the water column which are then dispersed towards other hosts. Mortalities start around day 3 post infection, following a viral-driven suppression of antimicrobial defenses. The destabilization of the host microbiota and a fatal systemic infection due to the replacement of the commensal bacteria communities with virulent populations (de Lorgeril *et al*., 2018), among which *Vibrio crassostreae* have been repeatedly isolated from mortality episodes and extensively characterized with respect to its ecology and the evolution and mechanics of its virulence determinants towards the oysters (Lemire *et al*., 2015; Bruto *et al*., 2017, 2018; Piel *et al*., 2019).

III.2.1 RISK FACTORS OF POMS

POMS is a multifactorial disease, not only dependent on multiple microorganisms (viral and bacterial pathogens) but also on distinct environmental and host variables that contribute to the expression and severity of this syndrome. Initial approaches to characterize the disease have relied on direct injection of the different viral and bacterial pathogens into specific pathogen free oysters. Although this methodology allowed primary characterization of the

microorganisms involved, it did not correctly represent the natural way of infection neither the polymicrobial complexity of the field. An ecologically realistic infection protocol was therefore developed over the past years by Bruno Petton and collaborators (Petton *et al.,* 2013,2015) to study the full complexity of the disease. Specific pathogen-free oysters were used to naturally "catch" the disease by deploying them on the field during mortality season. Once they were naturally infected, they were placed in cohabitation with naive oysters under controlled conditions and the disease dynamics was monitored in the recipient oysters. This methodology to effectively transfer POMS into the laboratory has allowed characterizing in details several risk factors associated with the development of the syndrome.

A now well-established environmental determinant of POMS is **seawater temperature** (Petton *et al.*, 2013). Seasonal outbreaks occur in the summer season when seawater temperature is in a 16°C to 24°C range, which is permissive for virus replication and transmission (Pernet *et al.*, 2012; Petton *et al.*, 2013). This factor, which is undoubtedly the main trigger of disease outbreaks in the field, is currently explored for its role on the whole pathosystem (ANR project Decicomp, led by Guillaume Mitta).

Two other key factors controlling disease expression are currently investigated.

The first factor is **Oyster age.** It was shown to determine the susceptibility of oysters to POMS. Indeed, resistance is suspected to be acquired between 15 and 25 months (Azema *et al., 2017,* Petton *et al*., 2015)

The second one is **diet restriction,** which can influence host or pathogen physiology. Energetic reserves (carbohydrates and neutral lipids) have already been associated with mortality risk during oyster epizootics (Corporeau *et al*., 2014, Pernet *et* al., 2014b, Young *et al*., 2017). Preliminary results obtained by Petton and collaborators showed a huge influence of oyster diet in the susceptibility to POMS. A starvation of two weeks was sufficient to prevent POMS expression (personal communication).

Beyond these key factors, other possible determinants of the disease have been investigated.

Oysters are exposed to high variations in **seawater salinity**, driven by warm periods and precipitation, showing a remarkable tolerance range that goes from below 10‰ up to 35‰ (Helm 2005). Although not as strong as temperature as a trigger, salinity could modify oyster susceptibility POMS. Indeed, acclimation of oysters to salinity of 10‰ showed to increase survival rate to 95.8% compared to the 73.2, 43.2 and 61% of oysters acclimated at 15, 25, 35‰ respectively (Fuhrmann et al., 2016). The physiological changes associated with this survival success was later studied, and were shown to be associated with an increased water content, protein level and energetic reserves along with the inhibition of hexokinase activity,

involved in glycolysis, and decreased catalase activity (Fuhrmann *et al.*, 2018).

Rearing practices (including densities) also have important consequences on POMS severity. The level of oyster mortalities also varies among farming sites that present different farming practices. Pernet and collaborator (2012) showed that oysters that are kept in open waters of the Mediterranean Sea during the window of permissive temperatures (17°C to 24°C) did not experienced mortalities and presented a low level of OsHV-1 detection. Contrastingly, oysters kept within the farming area of the Thau Lagoon suffered from severe mortality outbreaks while those maintained also in the lagoon but outside the farming area presented sporadic mortalities that correlated with their connection with the farming sites through water currents. Within the farming sites poor water renewal, high oyster density and the transfer of asymptomatic virus carriers between sites, have been proposed to have important implications in the mortality risk in farming sites and therefore candidates to be considered in disease management initiatives (Pernet *et al.*, 2012, 2014a; Petton *et al.*, 2015).

III.2.2. OSTREID HERPES VIRUS MICROVARIANT (OSHV-1 MVAR)

The Ostreid herpesvirus type 1 was firstly identified during 1991 in *C. gigas* larvae affected by mass mortalities in French and New Zeland hatcheries (Vigneron *et al.*, 2004).

Extracellular viruses are usually enveloped and present a diameter of 100-180 nm. Infected oysters present circular or polygonal empty capsids and nucleocapsids of 70-80 nm of diameter scattered in the nucleus of infected cells while cytoplasmic vesicles contain single or groups of enveloped virions (Renault, 2016). Cryo-electron microscopy was used to reconstruct the icosahedral capsid, revealing the characteristic triangulation number of T=16 of herpesviruses. Isolated virions were used to obtain the first complete genome sequence of the virus which corresponds to the reference type (Davison *et al.*, 2005). Although the overall genome structure and aminoacidic sequences demonstrated a distant relationship with vertebrate herpesviruses, based on morphological features, capsid structure and the presence of a putative terminase gene, it was classified under the name Ostreid herpesvirus 1 representing the first of the 2 species that compose the Malacoherpesviridae family within the order *Herpesvirales* (Davison *et al.*, 2005; Renault, 2016).

A more virulent microvariant of the ostreid herpesvirus 1 (OsHV-1 µVar) was identified in 2008 associated with mass mortality events of juvenile oysters in France and defined by a series of mutations relative to the reference type (Segarra *et al.*, 2010).

Recently, Delmotte *et al.* evidenced distinct populations of OsHV-1 µvar in the French Mediterranean and Atlantic farms (Delmotte et al., 2020). How specific genetic differences in

OsHV-1 µvar populations influence the outcome of the POMS remains to be elucidated.

III.2.3 BACTERIA

Until recently, the bacterial component of POMS has mainly been studied through cultural approaches. *Vibrio* species are among the cultural bacteria those that have been more clearly associated with POMS. Members of the Splendidus clade (e.g., *V. tasmaniensis, V. splendidus, V. cyclitrophicus* and *V. crassostreae*) have been systematically isolated from diseased juvenile oyster during summer mortalities and to lower extent, *V. harveyi* and *V. aestuarianus,* which fall outside the clade (Saulnier *et al.*, 2010; Segarra *et al.*, 2010; Bruto *et al.*, 2017; Go *et al.*, 2017). Their association to POMS has promoted extensive research to characterize the particular role and contribution of vibrios to mortalities.

Initial approaches demonstrated the pathogenic potential of *Vibrio* isolates from disease animals and achieved to identify some relevant factors that contribute to virulence in oysters. From there, in a pioneer work by the group of Frédérique Le Roux and collaborators, which used pathogen free oyster spats, allowed field-based approaches. The authors characterized the population structure of *Vibrio* species found in naturally infected oysters during mortality season in the Atlantic French coast, and characterized the population structure of vibrios associated with the development of POMS (Lemire *et al.*, 2015). They evidenced the replacement of the resident microbiota of the oyster by a genetically diverse but phylogenetically coherent vibrio population of *Vibrio crassostreae* that was established as a unit of pathogenesis. The isolation of related non-virulent *V. crassostreae* strains allowed to confirm, by injection, the previous observation that non-pathogenic strain can act synergistically with pathogenic ones to increase mortality suggesting that a similar phenomenon could occur during the natural development of POMS derived bacterial dysbiosis (Gay *et al.*, 2004; Lemire *et al.*, 2015).

This field-based approach was further applied to characterize, through genomics, simultaneously the population structure of the vibrio community in the oyster tissues and different fractions of the water column at two different dates in the spring season in absence of mortalities and during mortality episodes in the summer season (Bruto *et al.*, 2017). This confirmed the predominance of the *V. crassostreae* population during mortality season and its almost exclusive association to the oyster tissues, but also evidenced the seasonality of the vibrio population structure between the spring and summer season, the presence of *Vibrio* populations from the Splendidus clades in healthy oysters during the spring season and a set of populations that are preferentially association to the water column fractions, apparently no founding the oyster as a suitable host for colonization. The mechanisms of association of vibrio populations in absence of disease and alternative colonization determinants other than

virulence-related are aspect of vibrio/oyster interaction that have not been explored so far in the oyster. *Vibrios* have been the unique bacterial group to be studied in detail as one of the etiological agent of POMS, nonetheless other groups such as *Arcobacter* and *Shewanella* have been also found associated with mortalities but their particular contribution and potential synergisms with other bacterial communities that participate in the fatal dysbiosis in oyster is still unknown (Go *et al.*, 2017; de Lorgeril *et al.*, 2018; Lasa *et al.*, 2019).

CHAPTER 2. RESULTS

SECTION I. COLONIZATION DETERMINANTS AND ENVIRONMENTAL PERSISTENCE IN *V. SPLENDIDUS* ASSOCIATED WITH HEALTHY OYSTERS

I.1. CONTEXT AND OBJECTIVE OF THE STUDY

The association between vibrios and oysters have been studied mainly in a pathological context, due to important consequences on oyster farming. Vibrios have been systematically isolated from moribund oysters and studied to identify their potential role as etiological agents of oyster disease. The large amount of knowledge produced by our close collaborator Frédérique Le Roux at Ifremer (laboratoire de biologie integrative des modèles marins, Station Biologique d Roscoff) has revealed that *Vibrio* species associated with POMS express virulence potential; this precious biological material enabled the identification of determinants of *Vibrio* pathogenicity both by her group and our research unit (Binesse *et al.*, 2008; Duperthuy *et al*., 2011; Vanhove *et al.*, 2016; Bruto *et al.*, 2017, 2018; Piel *et al.*, 2019).

However, since the elucidation of the complexity of POMS pathogenesis in our laboratory, we know that vibrios associated with POMS colonize oysters whose immunity is altered by the OsHV-1 virus (de Lorgeril *et al*. 2018). Therefore, analyzing *Vibrio* species colonizing oysters outside this pathological context is of great importance to unveil key determinants of *Vibrio* colonization in oysters with an intact immune system. The use of *Vibrio* species of known ecology was therefore key to undertake this exploration.

As reviewed in the introduction, vibrios are a diverse group of heterotrophic bacteria that are part of planktonic and animal-associated microbial communities. Population genetic coupled to ecological sampling applied to vibrios have shown that they can be grouped in closely related genetic units distributed differentially among predicted habitats but connected by the high degree of dispersal that characterize the marine environment (Hunt *et al.*, 2008; Preheim *et al.*, 2011; Szabo *et al.*, 2013; Shapiro and Polz, 2014).

This population framework has allowed to determine the population structure of vibrios in the oyster tissues and the surrounding seawater as well as how functionally and cohesive vibrio population assembly in the oyster during disease (Bruto *et al.*, 2017). These studies have unraveled that, in the Atlantic marine ecosystem, some **vibrio populations do preferentially associate to oysters during the spring season in absence of massive oyster mortalities**,

whereas the vibrio populations that colonize the oysters during POMS tend to harbor more virulent phenotypes.

The assessment of virulence potential of the vibrio populations characterized by Bruto *et al*. (2017) showed that **one population taxonomically assigned to *V. splendidus* (population #23)**, that is phylogenetically close to *V. splendidus* (population #24) found during POMS, displayed a moderate virulence potential and belonged to the microbiota associated with healthy oysters in the spring season.

So far, virulence and cytotoxicity have been characterized as determinant for the ability of vibrios to colonize oysters, but in a pathological context were the host's defenses are disturbed by the OsHV-1 virus and leads to the death of the host.

We were interested in exploring the alternative context of association of vibrios with healthy oysters using *V. splendidus* population #23.

In article 1, we studied this particular association searching for the **molecular determinants of this moderate virulence and possible tradeoffs involved in the maintenance of such phenotype**. We discovered that in *V. splendidus*, certain structures of O-antigen are more easily recognized by the immune system of the host and constrain colonization and virulence, but confer resistance to environmental grazers, thus providing an additional advantage to this vibrio population for environmental persistence. We indeed found that O-antigen structures that favour resistance to environmental predators result in an increased activation of the oyster immune system and a reduced virulence in that host. Our results suggest an evolution of *V. splendidus* towards moderate virulence as a compromise between fitness in the oyster as a host, and resistance to its predators in the environment. Data in **complementary results 1** confirmed this hypothesis in a different *Vibrio* genetic background.

In complementary results 2 (unpublished results that will be submitted for publication as a short letter, in preparation), we used the same biological material and additional *Vibrio* populations positively and negatively associated with oysters to ask one fundamental question: **Are vibrios able to colonize characterized by resistance traits that explain their capacity to cope with an intact immune system?** Overall, our results illustrate that the multiple biotic interaction taking place in the aquatic environment do not allow for discrimination of vibrio oyster-association on the basis of the only resistance trait. When considering all vibrio strains independent of their taxonomic affiliation, the main factors explaining association to oysters were resistance to ROS, virulence and surface charge.

I.2. ARTICLE N°1. VIBRIO SPLENDIDUS O-ANTIGEN STRUCTURE: A TRADE-OFF BETWEEN VIRULENCE TO OYSTERS AND RESISTANCE TO GRAZERS.

By **Oyanedel, D**., Labreuche, Y., Bruto, M., Amraoui, H., Robino, E., Haffner, P., Rubio, T., Charrière., G.M., Le Roux, F., Destoumieux-Garzón, D. (2020). Environmental Microbiology, doi: 10.1111/1462-2920.14996

environmental microbiology

Environmental Microbiology (2020) **00**(00), 00–00 doi:10.1111/1462-2920.14996

Vibrio splendidus O-antigen structure: a trade-off between virulence to oysters and resistance to grazers

Daniel Oyanedel,[1] Yannick Labreuche,[2,3] Maxime Bruto,[2,3] Hajar Amraoui,[1] Etienne Robino,[1] Philippe Haffner,[1] Tristan Rubio,[1,4] Guillaume M. Charrière,[1] Frédérique Le Roux[2,3*] and Delphine Destoumieux-Garzón[1*]

[1]*IHPE, Univ Montpellier, CNRS, Ifremer, Université de Perpignan Via Domitia, Montpellier, France.*

[2]*Ifremer, Unité Physiologie Fonctionnelle des Organismes Marins, ZI de la Pointe du Diable, CS 10070, F-29280, Plouzané, France.*

[3]*Sorbonne Universités, UPMC Paris 06, CNRS, UMR 8227, Integrative Biology of Marine Models, Station Biologique de Roscoff, CS 90074, F-29688, Roscoff cedex, France.*

[4]*Molecular Microbiology and Structural Biochemistry (UMR 5086). CNRS, University of Lyon, 69367, Lyon, France.*

Summary

A major debate in evolutionary biology is whether virulence is maintained as an adaptive trait and/or evolves to non-virulence. In the environment, virulence traits of non-obligatory parasites are subjected to diverse selective pressures and trade-offs. Here, we focus on a population of *Vibrio splendidus* that displays moderate virulence for oysters. A MARTX (Multifunctional-autoprocessing repeats-in-toxin) and a type-six secretion system (T6SS) were found to be necessary for virulence toward oysters, while a region (wbe) involved in O-antigen synthesis is necessary for resistance to predation against amoebae. Gene inactivation within the wbe region had major consequences on the O-antigen structure, conferring lower immunogenicity, competitive advantage and increased virulence in oyster experimental infections. Therefore, O-antigen structures that favour resistance to environmental predators result in an increased activation of the oyster immune system and a reduced virulence in that host. These trade-offs likely contribute to maintaining O-antigen diversity in the marine environment by favouring genomic plasticity of the wbe region. The results of this study indicate an evolution of *V. splendidus* towards moderate virulence as a compromise between fitness in the oyster as a host, and resistance to its predators in the environment.

Received 20 January, 2020; revised 13 March, 2020; accepted 22 March, 2020. *For correspondence. E-mail ddestoum@ifremer.fr; frederique.le-roux@sb-roscoff.fr

Introduction

Parasite virulence encompasses two features of a disease producing capacity, (i) infectivity, that is, the capacity to colonize a host and (ii) the ability to cause damage in a host (Pirofski and Casadevall, 2012). A major debate in evolutionary biology is whether virulence can evolve to non-virulence while maintaining the ability to provide other adaptive advantages (Bull and Lauring, 2014; Alizon and Michalakis, 2015; Cressler *et al*., 2016). On the one hand, as virulence affects host fitness, it may select for host resistance leading to a permanent non-virulence state. On the other hand, as a parasite evolves, it may counteract host resistance and maintain (or increase) virulence in a co-evolutionary arms race. For non-obligatory infectious agents, selection upon virulence traits will continue outside the host (Levin, 1996; Matz and Kjelleberg, 2005; Brown *et al*., 2012). This condition is exemplified by coincidental selection of bacterial genes involved in resistance to grazing in the environment and cytotoxicity to host immune cells, for example, the macrophage (Adiba *et al*., 2010). However, experimental evolution in the context of single or multiple predators has revealed that the resultant bacterial resistance is frequently associated with an accompanying attenuation of virulence through pleiotropic effects on growth or infectivity (Friman *et al*., 2009; Mikonranta *et al*., 2012; Friman and Buckling, 2014), extending the long-standing debate regarding virulence evolution. Indeed, in the environment, virulence traits can be subjected to a multitude of pressures, yet relevant theories lack empirical data on the mechanisms of virulence gene acquisition, maintenance or loss (Ferenci, 2016).

Species of *Vibrionaceae* (herein named vibrio) are marine heterotrophic bacteria that are ecologically and metabolically diverse members of planktonic and animal-

associated microbial communities (Takemura *et al*., 2014). The genus encompasses the well-studied human pathogen, *V. cholerae*, as well as some very important albeit less thoroughly characterized animal pathogens (Le Roux and Blokesch, 2018). Vibrio-associated diseases in *Crassostreae gigas* have been steadily rising over the past decade (Le Roux *et al*., 2015) and this oyster species is now considered as a model in which to explore vibrio disease dynamics in wild animals (Le Roux *et al*., 2016). Moreover, vibrios have been subjected to population genetic analyses, which have allowed the delineation of functionally and genetically cohesive ecological populations (Cordero and Polz, 2014; Shapiro and Polz, 2014). This population genetic structure provides a framework for the mapping of disease properties, the analysis of vibrio ecological and evolutionary dynamics, and the interpretation of selective mechanisms. We previously showed that some vibrio populations are preferentially associated with oyster tissues compared to the surrounding water (Bruto *et al*., 2017). Within the diverse Splendidus clade, virulence represents an ancestral trait that has been lost in several populations (Bruto *et al*., 2018). We identified diverse loci that are necessary for virulence, resulting in population-specific mechanisms that converge to a common end: cytotoxicity to immune cells and immune evasion (Piel *et al*., 2019; Rubio *et al*., 2019). To date the non-virulence status of Splendidus-related strains has been related to gene loss (Bruto *et al*., 2018); however, whether and why gene acquisition could result in virulence attenuation remains to be determined.

Here we focused on a population taxonomically assigned to the marine species *V. splendidus* and positively associated with oysters (Bruto *et al*., 2017). All members of this population were isolated in Spring, before oyster disease events. This sampling approach precludes biases associated with the selection of bacterial genotypes encoding high virulence potential (Bruto *et al*., 2017). We show that, while members of this population display moderate virulence, at least one strain is non-virulent. Two loci, a MARTX gene cluster and a type six secretion system (T6SS), were found necessary for virulence. A third locus (wbe), involved in O-antigen synthesis, distinguished between strains based on their combination of virulence and O-antigen structure. Gene inactivation within the wbe region resulted in increased virulence, competitive advantage and lower immunogenicity in oyster, whereas it suppressed protection against grazing by marine amoebae. Our results suggest that a conversion of O-antigen structure resulting from wbe genes shuffling is involved in a trade-off between resistance to environmental grazing and virulence to oysters.

Results

Despite the presence of two virulence loci, V. splendidus *strains can show a relatively moderate virulence towards oysters*

We previously demonstrated the coincidence of vibrio ecological population delineation with virulence for oyster (Bruto *et al*., 2018). Here we focused on three populations positively associated with oysters. Strains of *V. splendidus* (population #23), associated to healthy oysters in spring, were significantly less virulent (82.1% mean survival rate 24 hpi, ANOVA, $p < 0.05$ and Tukey HSD test) than populations isolated from diseased oysters in the summer (Bruto *et al*., 2017, 2018) (Fig. 1A). Moreover, contrasting virulence phenotypes were observed between strains of *V. splendidus* #23 when generating Kaplan–Meier survival curves over 6 days (Fig. 1B). Indeed, only 40%–60% of oysters injected with strains 4G4_4, 4D1_8 and 3T8_11 were alive at day 3, and generally remained viable until day 6. To contrast with *V. crassostreae* and *V. splendidus* #24 (Fig. 1A), we classify these strains as moderately virulent. By comparison, strain 4G1_8 had no significant effect on oyster survival (survival >82%, Log-rank *p*-value = 0,035, Bonferroni corrected for 10 comparisons) over the 6 days.

We performed comparative genome analyses between the moderately virulent strains (3T8_11, 4D1_8, 4G4_4) and the non-virulent strain (4G1_8) to investigate the genetic bases of this moderately virulent phenotype. A total of 419 genes were found to be specific to the moderately virulent strains (maxLrap >0.8; identity >60%) (Table S1). Among these genes, 38 clustered in two loci potentially involved in virulence. A first locus (*rtxACHBDE*, gene labels GV4G44_v1_300029 to 300,034 in 4G4_4) encodes a putative toxin (MARTX, gene *rtxA)*, a putative acyltransferase (*rtxC*), an uncharacterized protein (*rtxH*), and a putative type I secretion system (*rtxBDE*) (Fig. S1A). The MARTXs found in 3T8_11, 4D1_8, 4G4_4 (5088 amino acids) show a 97.88% of identity with the MARTX found in *V. splendidus* strain ZS185 (Bruto *et al*., 2018) and contain a core structure composed of two conserved regions at the amino- and carboxyl-termini, a cysteine-protease domain (CPD), a Ras/Rap1-specific endopeptidase (RRSP), an actin cross-linking domain (ACD), an α/β hydrolase (ABH) and two other cysteine-protease effector domains (MCF) (Fig. S1B). We assessed genetically the importance of the MARTX encoding gene for *V. splendidus* #23 virulence in strain 4G4_4 by inactivation of the *rtxA (rtxA-i)*. Inactivation did not impair growth in culture media (Fig. S2) but increased significantly survival of infected oysters, from 71.7% to 82.5%, when determined 24 hpi ($p < 0.05$) (Fig. 2).

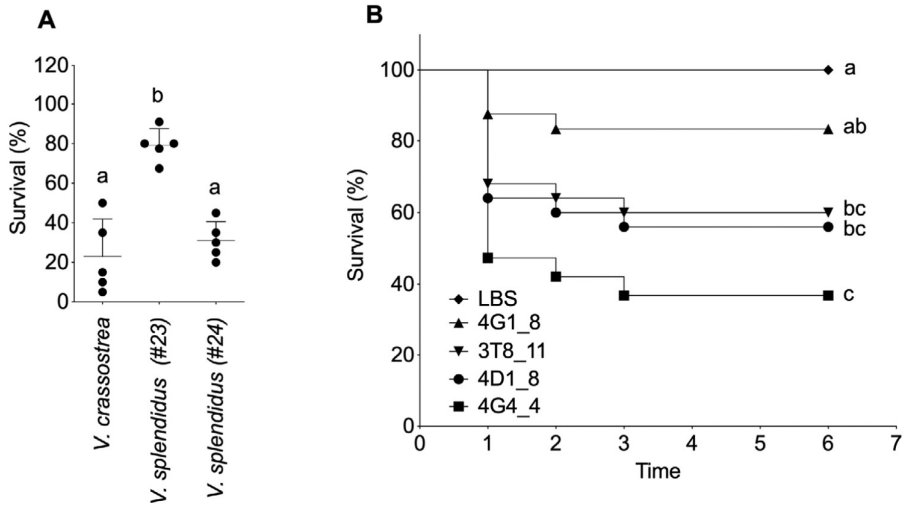

Fig. 1. *V. splendidus* #23 shows moderate virulence in oyster experimental infections.
A. Oyster survival was measured after injection with 15 *Vibrio* strains representative of three ecological populations (x-axis). Strains from *V. splendidus* #23 have been isolated from healthy oysters in spring, while strains from *V. crassostreae* and *V. splendidus* #24 have been isolated from diseased oysters in summer. A dose of 10^7 CFU was injected intramuscularly to individual juvenile oysters and the percentage of survival was measured after 24 h (y axis). A significantly higher oyster survival was observed for *V. splendidus* #23, which appeared less virulent than the two other populations tested, (ANOVA, $p < 0.05$ and Tukey HSD test). Experiment was performed in duplicate and repeated once.
B. Kaplan Meier survival curves were generated for four strains of *V. splendidus* #23 (2×10^7 CFU per oyster). Mortalities were counted daily in two tanks containing 20 oysters for 6 days. Significant difference in survival curves (Log-rank *p*-value = 0.0016, Bonferroni corrected for 10 comparisons) was recorded for strains 4G1_8 (non-virulent) and 4G4_4 (moderately virulent). Data are representative of two independent experiments.

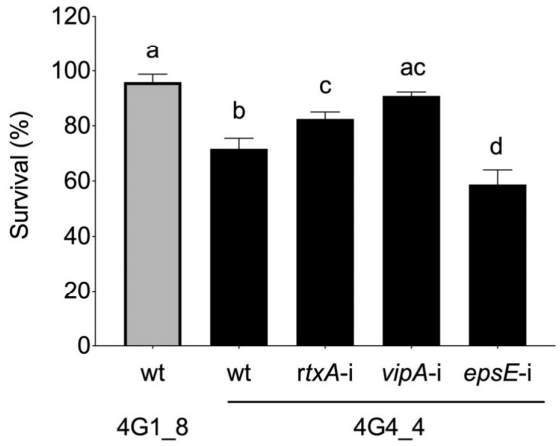

Fig. 2. Oyster mortality in response to experimental infection with *Vibrio* wild type (wt) strains and isogenic mutants. The *rtxA*, *vipA* and *epsE* genes were inactivated in *V. splendidus* #23 strain 4G4_4. The wild type strains 4G4_4 (virulent) and 4G1_8 (non-virulent), and the 4G4_4 mutants were injected to 40 oysters (2.10^7 CFU per animal). Data represent the survival percentage measured 24 h post injection in three independent experiments. Mean values are displayed ± SD. Different letters indicate a significant difference between them (ANOVA, $p < 0.05$ and Tukey HSD test). The *rtxA-i* and *vipA-i* mutants are attenuated (higher oyster survival) in contrast to the *epsE-i* mutant, which is more virulent than the wild type 4G4_4 strain (lower oyster survival).

A second locus (GV4G44_v1_320001 to GV4G44_v1_320032 in 4G4_4) encodes a type VI secretion system (T6SS), a contact-dependent contractile nanomachine used by many Gram-negative bacteria as weapons against a variety of prokaryotic and eukaryotic organisms (Cianfanelli *et al*., 2016). The locus (herein named $T6SS_{4G4\_4}$) is organized into, at least, three operons containing genes involved in the structure and assembly of the contractile complex (Fig. S3). Specifically, for the strain 4G4_4 next to the gene encoding a PAAR-motif protein (DUF4150 domain and 380 amino acid extension of unknown function), we identified a putative immunity system for nucleic acid degrading toxins. The putative effector (GV4G44_v1_320031 in 4G4_4) contains an AHH (Ala-His-His) nuclease domain found in bacterial polymorphic toxin systems (Zhang *et al*., 2011). In many bacterial models, T6SSs are involved in killing competing bacteria (Cianfanelli *et al*., 2016). Here, we did not observe inter-bacterial killing *in vitro* when using 4G4_4 as a predator and *E. coli* ML35p (Lehrer *et al*., 1988) as a prey (Supporting Information Fig. S8). This result suggests that this $T6SS_{4G4\_4}$ may not function in bacterial killing or are restricted to congeners. Alternatively, $T6SS_{4G4\_4}$ expression could be restricted to specific conditions such as oyster infection. We also tested whether $T6SS_{4G4\_4}$ could mediate toxicity towards eukaryotic cells. We showed that the three moderately virulent strains of *V. splendidus* #23, as well as the non-virulent strain 4G1_8, which lacks the $T6SS_{4G4\_4}$ were all significantly cytotoxic, as they induced 25.9% to 51.3% hemocyte lysis over 18 h ($p < 0.05$), as opposed to 4.1% for the negative control *V. tasmaniensis* $LMG20012^T$ (Supporting Information Fig. S4A). Consistent

with this observation, we found that inactivation of *vipA* in 4G4_4 (GV4G44_v1_320017), which encodes a component of the $T6SS_{4G4\_4}$ contractile sheath, did not alter strain cytotoxicity, in contrast to the *vipA1-i* inactivation of $T6SS_{chr1\text{-}LGP32}$ in *V. tasmaniensis* LGP32 (Fig. S4B). On the other hand, the 4G4_4 *vipA-i* mutant showed attenuated virulence, as determined by a significant increase in oyster survival after vibrio injection, from 71.7% (wild-type 4G4_4) to 90.8% (4G4_4 *vipA-i*), $p < 0.05$ (Fig. 2). Hence, the presence of $T6SS_{4G4\_4}$ affects virulence in the oyster, although its molecular mechanisms and cellular target(s) remain to be determined.

Specific O-antigen structure antagonizes with V. splendidus *virulence*

The O-antigen is a highly diverse structure of the lipopolysaccharide (LPS) molecules, and is displayed at the outer surface of Gram-negative bacteria. In *V. splendidus*, the wbe region involved in O-antigen synthesis was previously shown to exhibit extensive genetic diversity (Wildschutte *et al*., 2010). Here, we found that the moderately virulent strains of *V. splendidus* #23 present a wbe region structure (GV4G44_v1_410010 to GV4G44_v1_370009 in 4G4_4) that highly differs from that of the strain 4G1_8 (Table 1). To assess the possible consequences of wbe genetic organization on O-antigen structure, we analysed the electrophoretic profiles of the LPS expressed by four strains of *V. splendidus* #23. All LPS were of smooth type (Pupo and Hardy, 2007), as indicated by the typical ladder-like electrophoretic profiles of molecules containing different numbers of O-antigen repeating units (Raetz and Whitfield, 2002) (Fig. 3A). Short-chain molecular species containing only lipid A and core oligosaccharides migrated to the bottom of the gel, and were observed in all bacterial strains. However, several major differences were observed between the non-virulent strain 4G1_8 and the three moderately virulent strains (4G4_4, 3T8_11 and 4D1_8). First, the non-virulent 4G1_8 displayed an LPS of higher molecular weight with a lower number of monosaccharide residues per O-antigen repeating unit, as indicated by the tighter spacing between bands (Fig. 3A). Second, the LPS profile of all moderately virulent strains showed a prominent band of molecules of moderate size that may indicate the attachment to the core of a fixed number of O-antigen repeating units, or of an oligosaccharide side chain. In contrast to the polysaccharide moieties, no difference could be evidenced in the Lipid A anchor, as determined by MALDI-TOF-MS (Fig. S5). To determine the functional consequences of such distinct LPS structures, we compared the ability of *V. splendidus* #23 strains to bind to cytochrome C, a cationic molecule that binds to the negatively-charged membranes of bacteria (Saar-Dover *et al*., 2012; Cullen *et al*., 2015). Cytochrome C bound significantly more to the non-virulent 4G1_8 (80.8%) than to the three moderately virulent strains, which all showed a similar degree of binding (25.3% to 34.6%), $p < 0.001$ (Fig. 3B). This result strongly suggests that genetic diversity in the wbe region of *V. splendidus* #23 strains determines strain O-antigen structure, with consequences on the strain's ability to interact with macromolecules (Fig. 3B).

The importance of the wbe region for O-antigen synthesis and strain serotypes was further addressed genetically. To this aim, a gene encoding a glycosyltransferase *(epsE*, GV4G44_v1_370043 in 4G4_4) was inactivated in two strains. The LPS structure of the *epsE-i* mutant showed a reduced number of monosaccharides per repeating units (tighter spacing of the bands) as well as a higher molecular weight than the wild-type 4G4_4 (Fig. 3A), confirming that the wbe region determines the O-antigen profile. Moreover, *epsE* inactivation in strain 4G4_4 was sufficient to increase cytochrome C binding from 33.7% in the wild type strain 4G4_4 to 71.6% in *epsE-i* ($p < 0.001$) reflecting important changes in the bacterial surface properties. Identical phenotypes on O-antigen structure and binding capacity were obtained for the *epsE-i* mutant derived from another moderately virulent strain, 4D1_8 (Fig. S6).

We next explored the effect of *epsE* inactivation on virulence. The *epsE-i* mutant was found significantly more virulent that the wild type strain 4G4_4 in oyster experimental infections. Indeed, oyster survival rate dropped from 71.7% when injected with wild type 4G4_4 down to 58.8% upon 4G4_4 *epsE-i* injection, $p < 0.05$ (Fig. 2). In addition, the *epsE-i* mutant showed a significant competitive advantage over their wild-type parents, 4G4_4 and 4G1_8 in oyster colonization, as indicated by competitive index values >0.5 (Fig. 4A).

Because the O-antigen is a well-known determinant of bacterial immunogenicity (Chatterjee and Chaudhuri, 2011), we next asked whether the oyster immune response depended upon the O-antigen structure. Cells of 4G4_4 wild type and *epsE-i* mutant were injected into juvenile oysters after removing all traces of culture medium (potentially immunogenic). Oyster immune gene expression was then measured by RT-qPCR 2 hpi to capture the oyster's early response to infection. We selected eight genes (IL 17–1, IL 17R, NFκB, MyD88, TNF-14, *Cg*LBP, *Cg*BPI, *Cg*BigDef-1) involved in recognition, immune signalling and pathogen control that were previously shown to respond to vibrio infections (Gonzalez *et al*., 2007; Rosa *et al*., 2011; Rubio *et al*., 2019; Sun *et al*., 2019). Only genes encoding cytokines or involved in signalling pathways, namely IL 17–1, MyD88 and TNF-14, were significantly more induced by injection of the wild type 4G4_4 cells relative to an injection of sterile seawater (SSW) (Fig. 4B; Supporting

Table 1. Gene content of the wbe regions from *V. splendidus* 4G4_4, 4G1_8, and *V. tasmaniensis* LGP32. The *epsE* gene mutated in 4G4_4 appears in boldface. Gene labels of strain 4G4_4 are used to represent the homologue genes of the moderately virulent strains of *V. splendidus* Pop#23.

Pop#23 ORF#	Locus tag	Putative function or gene name	4G1_8 ORF#	Locus tag	% nt similarity	LGP32 ORF#	Locus tag	% nt similarity
1	GV4G44_v1_410010	*gmhD*	1	GV4G18_v1_20068	97.4	1	VS_0201	94.9
2	GV4G44_v1_410009	UDP-glucose 6-dehydrogenase	2	GV4G18_v1_20067	94.8		_	
3	GV4G44_v1_410008	Transcriptional regulator	3	GV4G18_v1_20066	100	2	VS_0202	98.1
4	GV4G44_v1_410007	Protein of unknown function	_				_	
5	GV4G44_v1_410006	Peptidase	4	GV4G18_v1_20065	97.1	3	VS_0203	89.6
6	GV4G44_v1_410005	Serine acetyltransferase	5	GV4G18_v1_20064	100	4	VS_0204	100
7	GV4G44_v1_410004	NAD(P)H-glycerol-3-phosphate dehydrogenase	6	GV4G18_v1_20063	95.1	5	VS_0205	95.4
8	GV4G44_v1_410003	Export protein SecB	7	GV4G18_v1_20062	97.5	6	VS_0206	98.1
9	GV4G44_v1_410002	Rhodanese-related sulfurtransferase	8	GV4G18_v1_20061	99.3	7	VS_0207	100
10	GV4G44_v1_370056	protein of unknown function	_				_	
11	GV4G44_v1_370055	GDP-mannose mannosyl hydrolase	_				_	
12	GV4G44_v1_370054	Mannose-1-phosphate guanyltransferase	_				_	
13	GV4G44_v1_370053	Phosphomannomutase	_				_	
14	GV4G44_v1_370052	GDP-D-mannose dehydratase, NAD(P)-binding	_				_	
15	GV4G44_v1_370051	Bifunctional GDP-fucose synthetase	_				_	
16	GV4G44_v1_370050	O-unit flippase	_				_	
17	GV4G44_v1_370049	CDP-4-dehydro-6-deoxy-D-glucose 3-dehydratase (fragment)	_				_	
18	GV4G44_v1_370048	Membrane protein of unknown function; putative O-atigen flippase	15	GV4G18_v1_20054	18.6		_	
19	GV4G44_v1_370047	Putative glycosyl transferase family 11	_				_	
20	GV4G44_v1_370046	Putative Uncharacterized glycosyltransferase HI_1578	_				_	
21	GV4G44_v1_370045	Putative glycosyltransferase	37	GV4G18_v1_20032	26.5		_	
22	GV4G44_v1_370044	Putative glycosyltransferase	_				_	
23	GV4G44_v1_370043	Putative Glycosyl transferase, group 2 family *epsE*	_				_	
24	GV4G44_v1_370042	Putative glycosiltranferase	13	GV4G18_v1_20056	29.2		_	
25	GV4G44_v1_370041	O-antigen polymerase Wzy				19	VS_0220	22.3
26	GV4G44_v1_370040	Putative glycosyltransferase	12	GV4G18_v1_20057	37.3		_	
27	GV4G44_v1_370039	UDP-GlcNAc:undecaprenylphosphate GlcNAc-1-phosphate transferase	18	GV4G18_v1_20051	81.1		_	
28	GV4G44_v1_370038	Regulator of length of O-antigen component of lipopolysaccharide chains	19	GV4G18_v1_20050	68.9		_	
29	GV4G44_v1_370037	Conserved membrane protein of unknown function	_			8	VS_0208	84
30	GV4G44_v1_370036	Outer membrane lipoprotein	_			9	VS_0209	95.7
31	GV4G44_v1_370035	Conserved hypothetical protein	_			10	VS_0210	85.3
32	GV4G44_v1_370034	Lipoprotein	22	GV4G18_v1_20047	20.3	11	VS_0212	93.9
33	GV4G44_v1_370033	*wza*	23	GV4G18_v1_20046	94.7	12	VS_0213	90.5
34	GV4G44_v1_370032	*wzb*	24	GV4G18_v1_20045	98.6	13	VS_0214	93.8
35	GV4G44_v1_370031	*wzc*	25	GV4G18_v1_20044	97.4	14	VS_0215	92.2
36	GV4G44_v1_370030	Conserved protein of unknown function	26	GV4G18_v1_20043	96.4		_	
37	GV4G44_v1_370029	Protein of unknown function	_				_	
38	GV4G44_v1_370028	N-acetylmuramoyl-L-alanine amidase	29	GV4G18_v1_20040	91.8		_	
39	GV4G44_v1_370027	Conserved protein of unknown function	30	GV4G18_v1_20039	90.5		_	
40	GV4G44_v1_370026	Conserved protein of unknown function	32	GV4G18_v1_20037	71.8		_	
41	GV4G44_v1_370025	Conserved protein of unknown function	33	GV4G18_v1_20036	95.2		_	
42	GV4G44_v1_370024	HAD hydrolase, family IIA (fragment)					_	

(Continues)

Table 1. Continued

Pop#23 ORF#	Locus tag	Putative function or gene name	4G1_8 ORF#	Locus tag	% nt similarity	LGP32 ORF#	Locus tag	% nt similarity
43	GV4G44_v1_370023	HAD hydrolase, family IIA (fragment)						
44	GV4G44_v1_370022	Protein of unknown function						
45	GV4G44_v1_370021	Protein of unknown function						
46	GV4G44_v1_370020	Putative CDP-glycerol:poly glycerophosphotransferase						
47	GV4G44_v1_370019	Membrane protein of unknown function	35	GV4G18_v1_20034	24.6			
48	GV4G44_v1_370018	Family 2 glycosyltransferase						
49	GV4G44_v1_370017	Membrane protein of unknown function						
50	GV4G44_v1_370016	Conserved protein of unknown function						
51	GV4G44_v1_370015	Putative glycosyl transferase, group 1	39	GV4G18_v1_20030	31.1			
52	GV4G44_v1_370014	Galactosyl-transferase	40	GV4G18_v1_20029	79.5	32	VS_0233	37.1
53	GV4G44_v1_370013	Putative acetyltransferase	41	GV4G18_v1_20028	89.9			
54	GV4G44_v1_370012	Perosamine synthetase (WeeJ)	42	GV4G18_v1_20027	93.6			
55	GV4G44_v1_370011	Mannosyl-transferase	43	GV4G18_v1_20026	96.3	33	VS_0234	89.2
56	GV4G44_v1_370010	Conserved protein of unknown function	44	GV4G18_v1_20025	98			
57	GV4G44_v1_370009	Phosphoglyceromutase	45	GV4G18_v1_20024	99.2	34	VS_0235	97.3

Information Fig. S7). Interestingly none of these important immune pathways was significantly induced by the 4G4_4 *epsE-i* mutant at this early time point. Therefore, the LPS structure harboured by the moderately virulent strains appears as more immunogenic than that of the corresponding *epsE-i* mutant. This lower immunogenicity could be responsible for the higher competitiveness and virulence of the 4G4_4 *epsE-i* mutant in oyster experimental infections (Figs 2 and 4A).

Trade-off between immunogenicity and grazing resistance is mediated by O-antigen structure

As non-obligate parasites, vibrios can encounter a variety of hosts and predators in the marine environment. To determine whether the O-antigen structure of *V. splendidus* #23 affects other biotic interactions, we tested each strain's resistance to grazing by a marine amoeba isolated from the oyster environment (Robino *et al*., 2019). The wild-type 4G4_4 was resistant to grazing by *Vannella* sp. AP1411, as indicated by a stable relative fluorescence of the bacterial strain up to 10 days after the beginning of the grazing experiment (Fig. 5A). In agreement *Vannella* sp. AP1411 did not grow on a 4G4_4 grazing lawn (Fig. 5B). In contrast, the GFP-expressing *epsE-i* derivative was significantly grazed, as indicated by the decrease of the relative fluorescence down to 46.8% ($p < 0.05$) of the vibrio lawn (Fig. 5A) and enabled a significant amoeba growth (407 cells mm^{-2}, $p < 0.05$) after 12 days (Fig. 5B). The grazer-susceptible control, the GFP-expressing *V. tasmaniensis* LMG20012^T, was almost completely grazed in the same time span, giving rise to a significant level of amoeba growth at day 12 (651 cells mm^{-2}, $p < 0.05$) (Fig.5). Taken altogether, these results show that the LPS structure present in moderately virulent strains *of V. splendidus* #23 is protective against amoeba grazing but immunogenic during the interaction with oysters.

Discussion

In the environment, vibrios are exposed to a diversity of selective pressures, that may have effects on their virulence (Cui *et al*., 2015; Shapiro *et al*., 2016; Roig *et al*., 2018; Sakib *et al*., 2018; López-Pérez *et al*., 2019) Here, we identified in a population of vibrios, trade-offs between traits needed for resistance to a grazer and traits involved in virulence to oysters. Illustrating the 'conflicting selection hypothesis' (Mikonranta *et al*., 2012), an O-antigen structure conferring resistance to predation by marine amoebae showed increased immunogenicity, and lower competitiveness and virulence in oysters, showing that selection in the outside-host environment might conflict with optimized pathogenicity.

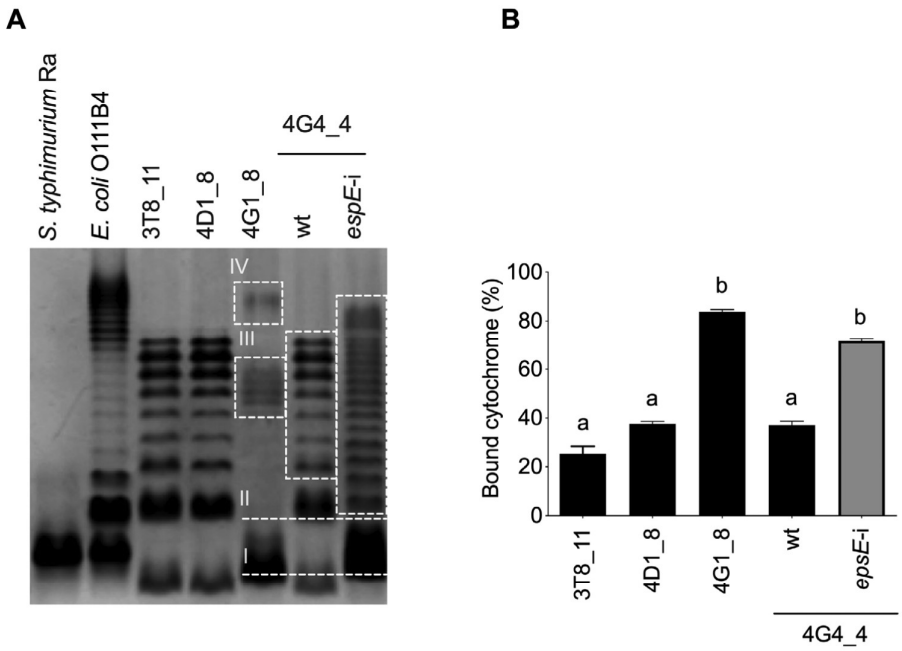

Fig. 3. Distinct gene contents in the wbe region are responsible for LPS variability in *V. splendidus* #23.
A. Silver-stained 4%–15% polyacrylamide gel of LPS extracted from bacterial stationary phase cultures. *Salmonella typhimurium* Ra (rough type LPS lacking O-antigen) and *Escherichia coli* O111B4 (smooth type LPS containing O-antigen polysaccharides) are included as references. All strains from *V. splendidus* #23 are smooth type (presence of O-antigen). Strain 4G1_8 shows an LPS profile distinct from the rest of *V. splendidus* #23. The main differences between strains are highlighted with roman numerals. I shows different sizes of the Lipid A -oligosaccharide core (low size bands). II and III show differences in the O-antigen structure both at intermediate (II) and high size (III and IV). The *epsE-i* mutant shows important modifications of the O-antigen structure.
B. Cytochrome C binding unravelling the effect of O-antigen structure on the interaction of bacteria with macromolecules. The ability of bacterial strains to bind cytochrome C is displayed. Data represent mean values of 3 independent experiments ± SD. Different letters indicate a significant difference (ANOVA, $p < 0.05$ and Tukey HSD test).

V. splendidus population #23 has been previously described as preferentially associated with oyster tissues, suggesting that oysters represent a permissive habitat for this population. This is supported here by the ability of all tested strains to kill the oyster hemocytes and thus potentially evade the host immune response. To date cytotoxicity toward the oyster hemocytes has been described as a common trait of virulent vibrios, although based on population-specific molecular determinants (Piel *et al*., 2019; Rubio *et al*., 2019). The present study shows that dampening of oyster cellular defences is a trait not restricted to virulent populations but shared by moderately and non-virulent strains that constitute the microbiota of healthy oysters.

Although less virulent than vibrios associated to disease (*V. splendidus* #24 and *V. crassostreae*), some *V. splendidus* #23 strains were able to affect oyster survival in experimental infections. This moderate degree of virulence results at least in part from the acquisition of two loci encoding effector delivery systems, a MARTX gene complex and a T6SS. The MARTX toxins are multifunctional effector cargo translocation, processing and delivery machines that can deliver functionally diverse cytopathic bacterial effectors to target eukaryotic cell (Satchell, 2015). In *V. splendidus* #23, MARTX effector domains are potentially involved in: (i) modulation of small GTPases and manipulation of host cell signalling (RRSP); (ii) disruption of cytoskeletal integrity (ACD); (iii) inhibition of endocytic trafficking and autophagy (ABH); and (iv) induction of apoptotic cell death (MCF) (Gavin and Satchell, 2015). The *V. splendidus* #23 MARTX shares the same overall structure as *V. vulnificus* MARTX type III, *i.e*. an MCF domain, an ABH domain, and then a second copy of MCF follows the ACD domain. In *V. vulnificus* the MARTXs appear to be essential for protection both from fish phagocytic cells and from predation by amoeba (Lee *et al*., 2013).

The T6SS nanomachines and its effectors are highly diverse in vibrios, acting against bacterial competitors (Unterweger *et al*., 2014), amoeba or phagocytic cells during an intracellular stage (Ma *et al*., 2009) or directly by contact with the target eukaryotic cell. Our cytotoxicity assays suggest that in *V. splendidus* #23, the T6SS does not target oyster hemocytes, in contrast to *V. tasmaniensis* or *V. crassostreae* (Piel *et al*., 2019; Rubio *et al*., 2019). The

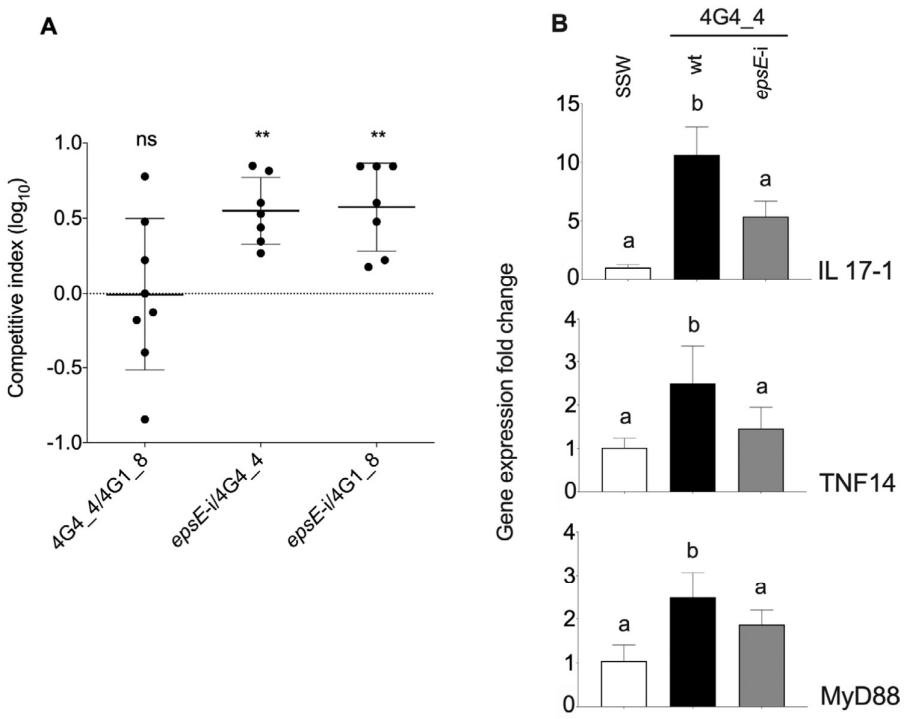

Fig. 4. O-antigen structure influences bacterial fitness and immune recognition in oysters.
A. Competitive index (CI) between wild type strains and *epsE-i* mutant of *V. splendidus*. Randomly selected colonies isolated from injected animals were identified by PCR. The competitive index was calculated as the ratio of the strains in the input inoculum over the ratio of the strains in the output at 24 hpi. Each dot represents the log_{10} of the CI obtained from colonies isolated from individual oysters. Means significantly higher than value 0 (t-test, $p < 0.01$) were considered as a competitive advantage of the strain. B- Relative expression of immune genes in response to *Vibrio* injection. Four pools of 10 oysters were sampled 2 h after being injected either with sterile seawater (SSW) or wild type (wt) and *epsE-i* mutant of *V. splendidus* (2×10^7 CFU/animal). RNA was extracted from the four pools. For each pool, RT-qPCR was performed on immune genes to determine their expression relative to the elongation factor 1 alpha (EF1-α). The $\Delta\Delta^{ct}$ method was used (Pfaffl, 2001). Data are presented as the mean ± SD. Different letters indicate a significant difference between them (ANOVA, $p < 0.05$ and Tukey HSD test).

presence of toxin and immunity modules in the T6SS loci would rather indicate anti-bacterial activity. However the T6SS might also be tightly regulated transcriptionally or post-translationally by lifestyle of the bacterium, or by membrane damage due to conjugation or membrane-targeting antibiotics (Ho *et al*., 2013). Indeed a within-host restricted expression was previously observed in *V. tasmaniensis* for $T6SS_{Chr2\text{-}LGP32}$, one of the two chromosomal T6SS identified in this population (Rubio *et al*., 2019). Future work should explore the environmental conditions necessary for its expression and function in order to formally demonstrate its role in inter-bacteria competition. Overall, the selection of specific effector domains within the T6SS or MARTX loci may arise as a result of the evolutionary arms race between bacteria, competitors and predators and could have correlative effects on bacterial virulence, hence supporting the 'coincidental selection hypothesis' (Levin, 1996; Matz and Kjelleberg, 2005; Brown *et al*., 2012).

Various biotic interactions can also lead to a trade-off on virulence (Friman *et al*., 2009; Mikonranta *et al*., 2012; Friman and Buckling, 2014). We showed here that the acquisition of genes involved in the synthesis of the LPS O-antigen confers a phenotype resistant to predation by an amoeba but results in a reduced virulence in the oyster. LPS is a major component of the outer membrane in Gram-negative bacteria. These molecules are composed of a conserved lipid structure that is embedded in the outer membrane, and a polysaccharide referred to as the O-antigen (Raetz and Whitfield, 2002). O-antigen structures are highly variable across strains of a species (Seif *et al*., 2019) and the wbe region was identified as a hypervariable locus in *V. splendidus*, contributing to structural variations of O-antigen (Wildschutte *et al*., 2010). Wildschutte *et al*. observed extensive gene shuffling in the wbe region, which provides a means for O-antigen structure selection. However, they did not find any predominant serotype within hosts but conversely observed closely related serotypes, expressing the same O-antigen, among different hosts (Wildschutte *et al*., 2010), which raises the questions about whether/how the

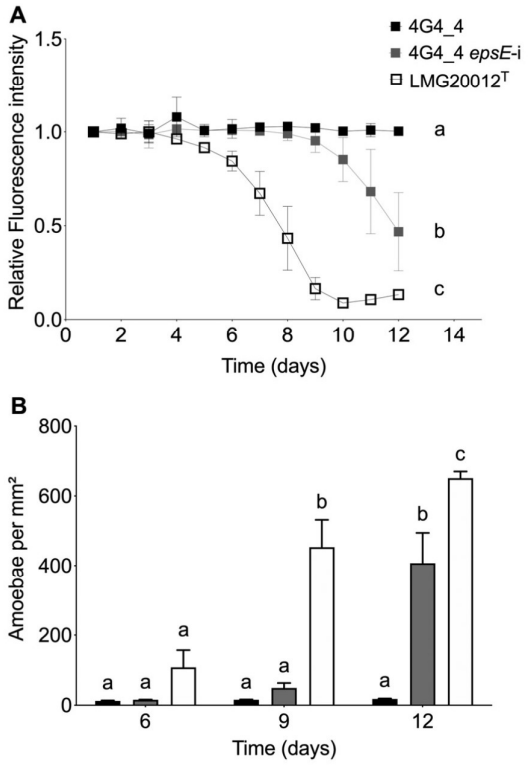

Fig. 5. Resistance to grazing by marine amoeba is dependent on LPS structure.

A. Bacterial resistance to grazing by *Vannella* sp. AP1411 was assessed for *V. splendidus strains* 4G4_4 and *epsE-i* by measuring the fluorescence of the GFP-expressing bacteria after contact with amoebae over 12 days. The strain *V. tasmaniensis* LMG20012T was used as a grazing-susceptible control. Results show the mean of three technical replicates ± SD. Data are representative of three independent experiments. Different letters indicate a significant difference, $p < 0.001$ (RM-ANOVA).

B. Amoeba growth was monitored at day 6, 9 and 12 by manual counting under phase light microscopy. Each condition was counted in three technical replicates. The results shown are representative of three independent experiments. For each time point, different letters indicate a significant difference (ANOVA, $p < 0.001$ and Tukey HSD test).

selection of O-antigen structures occurs outside the host. In nature this outer membrane structure directly interacts with ambient surfaces in the environment and, thus is subject to environmental selective pressures (Wildschutte *et al*., 2004; March *et al*., 2013). Indeed O-antigens constitute a first line of defence against predators (Simkovsky *et al*., 2016) and have been shown to mediate antimicrobial resistance (Band and Weiss, 2015). Here we found that mutation of the wbe region was detrimental to the resistance of amoeba grazing. Indeed, a *V. splendidus* #23 strain lost its resistance to grazing upon mutation of the wbe region. Therefore, selective forces exerted by environmental predators may have favoured the maintenance of this wbe encoded O-antigen structure.

In the host, O-antigens play a key role in both the activation of innate immunity and resistance to host immune effectors (Raetz and Whitfield, 2002). This dual function has important consequences on disease outcomes. In the rainbow trout (*Oncorhynchus mykiss*) pathogen *Vibrio anguillarum*, O-antigen polysaccharides were reported to determine the capacity to evade phagocytosis by skin epithelial cells (Lindell *et al*., 2012). In *Vibrio vulnificus*, O-antigen polysaccharides are protective against serum complement, playing a key role in virulence for eels (Amaro *et al*., 1997). Here, mutation of the wbe region yielded a modified O-antigen structure that significantly increased strain competitiveness and virulence. The O-antigen modification affected the polysaccharide structure and reduced strain immunogenicity, as indicated by the lack of induction of important oyster immune pathways involved in vibrio recognition (Rubio *et al*., 2019) during early infection stages. This result indicates that strains of *V. splendidus* #23 with moderate virulence harbour an O-antigen structure easily recognized by the oyster immune system, leading to suboptimal colonization capacity. A trade-off between virulence and resistance to predators outside of host tissue was previously reported for *Salmonella enterica* O-antigen structure, which is under epigenetic control (Cota *et al*., 2015). In this species, the O-antigen is a receptor for phage, and resistance is acquired by phase variation of O-antigen chain length, that is, phenotypic plasticity. Similar phase variation affecting the wbe region was shown to modulate O-antigen expression in *V. cholerae* (Seed *et al*., 2012). Adaptations to phage predation involving trade-offs in evolutionary fitness and virulence have also been described for in this specie. Resistance to the lytic phage ICP2 results from mutations within either *ompU*, which encodes the major outer membrane porin, or its direct regulator *toxR* and results in virulence attenuation (Seed *et al*., 2014).

Epidemiological success of non-obligate parasites depends on their environmental persistence in addition to the ability to produce major virulence factors. In complex microbial ecosystem such as the marine environment or the oyster microbiota, the outcomes for virulence trait selection can be positive (coincidental selection), neutral (relaxed selection) or negative (conflicting selection) (Mikonranta *et al*., 2012). It has been argued that high virulence resulting in rapid killing of the host can be maladaptive as it does not allow parasite niche maintenance by the parasite (Alizon and Michalakis, 2015). Our genomic and phenotypic data suggest that *V. splendidus* #23 has evolved as a moderately virulent population with high fitness in its host, thereby supporting the theoretical

prediction that moderate virulence can maximize parasite overall fitness (Alizon and Michalakis, 2015).

Experimental procedures

Strains, plasmid and primers

Vibrio strains used in this study were *V. splendidus* 3T8_11, *V. splendidus* 4D1_8, *V. splendidus* 4G1_8, *V. splendidus* 4G4_4 (Bruto *et al.*, 2018). Vibrio strains were cultured at 20°C in Luria Bertani medium (LB) supplemented with 0.5 M NaCl (LBS). For *Vibrio splendidus* strains carrying either the integrative suicide plasmid pSW23T (Demarre *et al.*, 2005) or the pMRB-P_{LAC}*GFP* replicative plasmid (Le Roux *et al.*, 2011), the culture media were supplemented with 5 μg ml^{-1} of Chloramphenicol (Cm). For strains carrying a pMRB-P_{LAC}*GFP* replicative plasmid with a spectinomycin (Spc) resistance cassette, 100 μg mL^{-1} Spc was used. *Escherichia coli* strains were cultured at 37°C in LB medium. Marine amoebae *Vannella* sp. AP1411 (Robino *et al.*, 2019) was grown for 3 days prior experiments at 18°C in 70% sterile seawater (70% SSW), using *E. coli* SBS363 as a nutritive source. Other strains, plasmids and primers used are included in Tables S2-S4.

Animals

For experimental infections, we used *Crassostrea gigas* diploid oysters from a batch of standardized Ifremer spats (NSI) produced from a pool of 120 genitors. Animals were from both sexes. For hemocyte cytotoxicity assays, hemolymph was collected from adults (18 months old) produced from a pool of 120 genitors (ASI). All oysters were produced at the Ifremer hatchery in Argenton, France.

Experimental infections

Experimental infections were performed at 20°C, as previously described (Rubio *et al.*, 2019). Juvenile oysters (1.5–2 cm) were anaesthetised for 3 h by immersion in seawater with 50 g L^{-1} $MgCl_2$ (Suquet *et al.*, 2009). Stationary phase cultures (20 h at 20°C with agitation at 150 rpm) were prepared for injection into the adductor muscle. For survival curves, two groups of 20 individuals were used. Each animal received an intramuscular injection of stationary phase culture (2 x 10^7 CFU per animal) or an equivalent volume of fresh culture medium. Each group of injected oysters was placed in a separate tank containing 3 l of seawater. Mortalities were monitored at 24 h or daily for a 6-day period. The non-parametric Kaplan Meier test was used to estimate log-rank, including Bonferroni *p*-value correction for multiple comparison. Each phenotyping was repeated twice. For gene-expression analysis, stationary phase culture were washed three times in sterile seawater (SSW) and adjusted to 2 x 10^7 CFU ml^{-1} before injection into oyster adductor muscle. For each condition tested, 40 oysters were injected with 100 μl of the washed bacterial culture or SSW only. Four pools of 10 oysters were collected at time 0 (untreated controls) and at 2 h post injection (hpi) for each experimental condition. Pools of oyster tissues were snap frozen in liquid nitrogen and pulverized with a bead mixer mill (Retsch MM400). Pulverized pools were kept at −80 until RNA extraction. Experimental infections were performed according to the Ifremer animal care guidelines and policy.

Growth curves

Strains from −80°C stocks were plated on LB NaCl agar plates and incubated at 20°C for 24 h. Single colonies were used to seed LB NaCl broth. After overnight at 20°C with agitation at 150 rpm, cultures were adjusted to an OD_{600} of 0,1 in fresh LB NaCl 0.5 M broth. For each bacterial suspension, 300 μl were disposed in triplicate in a 96-well platen and OD_{600} was measured every 15 min in a TECAN infinite plate reader for 18 h.

Killing assay

Vibrios strains were grown at 20°C in LBS media containing 5 μg mL^{-1} chloramphenicol when needed and *E. coli* ML35p was grown at 37°C in LB media containing 100 μg mL^{-1} ampicillin.

Cultures of predator and prey strains were normalized to an OD_{600} of 1 and mixed at a MOI of 10. 50 μl of cell suspension were spotted on a 0.45 μm membrane (MF-Milipore™ MCE) placed in LBS agar to allow cell to cell contact and incubated at 20°C for 5 h. Filters were recovered and bacteria re-suspended in LBS media. CFU of surviving *E. coli* per millilitre was determined by plating serial dilutions and selective growth at 37°C on LB agar containing 100 μg mL^{-1} ampicillin.

Competitive index in mixed infections

For competitive assays of mix infections, adult oysters (ASI) were anaesthetised and injected as described above with a 1:1 mixture of strains (2 x 10^7 CFU total) in LB NaCl medium. Under 24 hpi, 8 oysters per group were sampled and homogenized with an ULTRA-TURRAX® homogenizer after adding 1 ml of SSW per g of flesh. Tissue homogenates were serially diluted in SSW and plated onto TCBS agar plates. Colonies were randomly selected after 48 h at 20°C and tested by PCR with strain-specific primers (Supporting Information Table S4) to determine the ratio of strains present on each individual. Multiplex PCR with

strain-specific primer couples 4G4_4F: 5′- TGCTATTG-AGGAGGGACTGG-3′/4G4_4R: 5′- CACCTGAACCCAAA-AATCGT-3′ and 4G1_8F:5′-CAGAACTCTCTGGGCA TGTG-3′/4G1_8R: 5′- AAAATCACACCCGACTCGAC -3′, were used to discriminate between strains 4G4_4 and 4G1_8. To discriminate between 4G4_4 and 4G4_4*epsE*-i, the external primers used for mutant control Ext**epsE*-F: 5′-TCTCTGATGACTGCTCAACTG –3′ and Ext**epsE*-R: 5′-TAAATAGACACGAAGGACCC -3′ were used to identify *epsE*-i strains from wild type. To discriminate between 4G1_8 and 4G4_4 *epsE*-i a first multiplex PCR was performed to differentiate between 4G4_4 and 4G1_8 strains and a second pcr with the *epsE*-i control primers to confirm that 4G4_4 identified colonies corresponded to *esp*E-i mutants. The competitive index was calculated as the ratio of the strains in the input inoculum over the ratio of the strains in the output obtained after 24 hpi. Competitive indices were then log transformed. Significant differences from a hypothetical value of 0 (no fitness advantage between strains) were determined with a one sample Student's t-test.

Molecular microbiology

Vibrio strains were grown at 20°C in LB NaCl medium. *Escherichia coli* strains were grown at 37°C in LB medium for cloning and conjugation experiments. Chloramphenicol (Cm) at 5 or 25 μg mL^{-1} depending on the strain, Spectinomycin (Spc) at 100 μg mL^{-1}, thymidine (0.3 mM) and diaminopimelate (0.3 mM) were added as supplements when necessary. Conjugations between *E. coli* and *Vibrio* were performed at 30°C as described previously (Le Roux *et al*., 2007). Gene inactivation was performed by cloning ~ 500 bp of the target gene in pSW23T (Demarre *et al*., 2005) and selecting on Cm (5 μg ml^{-1}) the suicide plasmid integration obtained by a single recombination (Le Roux *et al*., 2009). Mutants were screened for insertion of the suicide vector by PCR using external primers flanking the different targeted sequence for plasmid insertion (Supporting Information Table S4). To label bacteria with fluorescent emission, strains were transformed with the pMRB plasmid containing the green fluorescent protein (*gfp)* gene known to be stable in *Vibrio spp* (Le Roux *et al*., 2011) resulting in a constitutive expression from a P_{lac} promoter under chloramphenicol or spectinomycin selection.

Grazing assay and monitoring of amoeba growth

To prepare the co-culture of GFP-expressing vibrios and amoebae, 1 ml of vibrio overnight culture (3 x 10^9 CFU ml^{-1}) was mixed with 100 μl of a 3 day-old *Vannella* sp. AP1411 culture (5 × 10^5 cells ml^{-1}) resuspended in 70% SSW. For the control without amoeba, the vibrio culture was mixed with 100 μl of 70% SSW. For grazing experiments, 500 μl of 70% SSW containing 1% agar were deposited in the wells of a 24-well plate (transparent flat bottom). Each well was covered with 50 μl of the mixed vibrio/amoeba cultures and let dry for 4 h at 20°C under a sterile laminar flow. The 24-well plates were then incubated at 18°C in a humid atmosphere. GFP fluorescence intensity was measured daily over 12 days using a TECAN plate reader (λex 480 nm/λem 520 nm). To estimate the effect of the amoebae grazing activity on the abundance of GFP-expressing vibrios, the fluorescence intensity of the wells containing amoebae was compared with the fluorescence of vibrios lawn without amoebae, and expressed as a ratio. Each condition was performed in technical triplicates, and the more representative experiment is depicted out of at least three independent experiments. Error bars represent the standard deviation of the mean ± SD. Statistical analysis was performed using RM-ANOVA and Tukey's HSD comparison test.

The proliferation of *Vannella* sp. AP1411 was monitored at days 6, 9 and 12 in grazing assays. Amoebae were directly imaged by phase-contrast microscopy and enumerated in triplicate for each condition. Every experiment was performed in technical triplicates, and the more representative experiment is depicted out of at least three independent experiments. Error bars represent the ± SD. Statistical analysis was performed using ANOVA, $p < 0.001$ and Tukey HSD test.

LPS isolation and molecular characterization

LPS were prepared from 4 l of stationary phase cultures of vibrios growth in LB NaCl 0.5 M. Cultures were centrifuged at 1500 g for 20 min and bacterial pellets were washed with SSW before fixation with 2% paraformaldehyde (18 h at 4°C). Fixed bacteria were centrifuged (3000 g for 20 min) and washed twice with 0.1 M phosphate buffer saline before shipping in dry ice to LPS Bioscience, University Paris Sud, 91400 Orsay France. LPS structures were characterized by electrophoresis and/or MALDI-TOF-MS by as described in (Hankins *et al*., 2012). Briefly, Lipids A were isolated from lyophilized bacteria by mild acid hydrolysis followed by an extraction with an appropriate chloroform-methanol–water mixture. Bacterial lysates were treated with Proteinase K and loaded to a 4%–15% polyacrylamide gel for electrophoresis. Gels were silver-stained. MALDI-TOF-MS analysis was performed in negative-ion [M-H]- / linear mode. A purified lipid A from *Escherichia coli* was used as a standard for external calibration of *V. splendidus* lipids A mass-spectra.

RT qPCR monitoring of immune gene expression

Total RNA was extracted from 10 mg of pulverized oysters using Direct-zol RNA extraction kit (Zymo research). cDNA was synthetized using M-MLV RT (Invitrogen) with 1 μg of RNA and 250 ng of random primers (Promega). Real-time qPCR was performed on 40 ng μl^{-1} of cDNA at the qPHd plateform of qPCR in Montpellier with the LightCycler 480 System (Roche) and using the oyster gene specific primers (Table S4). Relative expression was calculated using the $2^{-\Delta\Delta Cq}$ method (Pfaffl, 2001), with normalization to the *C. gigas* EF1-α (GenBank AB123066). One-way ANOVA followed by Tukey HSD test for multiple comparisons was used to analyse the data.

In vitro *cytotoxicity assays*

Hemolymph was collected from the oyster adductor muscle sinus using a 2 ml ice cold-syringe equipped with a 23-G needle to prevent cellular aggregation. Hemocytes were counted in a KOVA® slide and plated onto 96 well-plates to create a cell monolayer (2×10^5cells per well). After 1 h at 20°C, plasma was removed and 5 μg μl^{-1} Sytox Green (Molecular Probes) diluted in 200 μl sterile seawater was added to each well. Cell-free hemolymph (plasma) was obtained by centrifugation (3000 g, 15 min, 4°C) and filtration through a 0.2 μm syringe filter. Vibrios were centrifuged and resuspended in the cell free plasma for opsonization (60 min at 20°C). The OD_{600} of the vibrio suspension was normalized in SSW to 1 (10^9 CFU mL^{-1}) and vibrio were added to the wells at a MOI of 50:1. Hemocytes were incubated at 20°C for 18 h after which the Sytox fluorescence was measured (λex 480 nm/λem 550 nm) using a TECAN infinite microplate reader. Fluorescence intensity was compared to the total cytolysis determined in control wells where hemocytes were lysed by adding 0.1% Triton X-100. An ANOVA followed by a Tukey's HDS test was perform on the data.

Cytochrome C binding assay

Stationary phase cultures (20 h, 20°C, 150 rpm) were wash twice by centrifugation (1500 g, 20°C) with 20 mM MOPS buffer (pH 7,2) supplemented with sucrose for a final osmolarity of 450 mOsm to make it compatible with the hyper saline environment of marine bacteria but to eliminate interfering charged salts. After washing by centrifugation (1500 g, 20 min), bacterial pellets were suspended in MOPS sucrose buffer and the suspension was adjusted to an OD_{600} of 6. Cytochrome C solution was prepared in MOPS-Sucrose buffer to a concentration of 5 mg mL^{-1}. Then, 900 μl of bacterial suspension were placed in 1.5 ml polypropylene microcentrifuge tubes with 0.5 mg mL^{-1} cytochrome c. Tubes were incubated for 15 min at 20°C and then centrifuged at 6000 g at room temperature for 15 min. The OD_{530} of the supernatants was measured in a TECAN microplate reader (300 μl transferred in triplicates to 96-well plates). The percentage of bound cytochrome c to bacteria was calculated relative to the OD_{530} value of a 0.5 mg ml^{-1} cytochrome c control solution not exposed to bacteria.

Acknowledgements

We warmly thank Prof. Edward G. Ruby (University of Hawai'i, USA) for critical reading of the manuscript. We thank Prof. Hervé Cottet from the *IBMM* (Montpellier, France), Dr. Jeremie Vidal-Dupiol and Dr. Yannick Gueguen from *IHPE* (Montpellier, France) as well as Dr. Agnès Delmas from the *CBM* (Orléans, France) for fruitful discussions. We are indebted to Marc Leroy from *IHPE* for precious technical assistance, to Dr. Martine Caroff and Dr. Alexey Novikov from *LPS biosciences* (Orsay, France) for lipopolysaccharide characterization, and to Philippe Clair at the qPHD platform/Montpellier genomix (Montpellier, France) for access to qPCR. We thank Bruno Petton, Matthias Huber and Jacqueline Le Grand from the Ifremer for providing standardized oyster spats for experimental infections and adults for cellular biology. This work was supported by the European Union's Horizon 2020 Research and Innovation Program Grant *Vivaldi* 678589; the CNRS, PEPS Blanc 2016 (project *Like Inhospitality*); CONICYT PFCHA/Doctorado En El Extranjero Becas Chile/2016-72170430 to D.O.; AMIBADAPT project funded by LABEX CeMEB; The Agence Nationale de la Recherche (Revenge project, ANR-16-CE32-0008-01) to F.L.R., and the University of Montpellier (Doctoral School Gaia; to E.R. and T.R.). This study is set within the framework of the 'Laboratoires d'Excellence (LABEX)' Tulip (ANR-10-LABX-41).

Conflict of Interest

The authors declare that there are no conflicts of interests related to this work.

References

Adiba, S., Nizak, C., van Baalen, M., Denamur, E., and Depaulis, F. (2010) From grazing resistance to pathogenesis: the coincidental evolution of virulence factors. *PLoS One* **5**: 1–10.

Alizon, S., and Michalakis, Y. (2015) Adaptive virulence evolution: the good old fitness-based approach. *Trends Ecol Evol* **30**: 248–254.

Amaro, C., Fouz, B., Biosca, E.G., Marco-Noales, E., and Collado, R. (1997) The lipopolysaccharide O side chain of Vibrio vulnificus serogroup E is a virulence determinant for eels. *Infect Immun* **65**: 2475–2479.

Band, V.I., and Weiss, D.S. (2015) Mechanisms of antimicrobial peptide resistance in gram-negative bacteria. *Antibiot (Basel, Switzerland)* **4**: 18–41.

Brown, S.P., Cornforth, D.M., and Mideo, N. (2012) Evolution of virulence in opportunistic pathogens: Generalism, plasticity, and control. *Trends Microbiol* **20**: 336–342.

Bruto, M., James, A., Petton, B., Labreuche, Y., Chenivesse, S., Alunno-Bruscia, M., *et al*. (2017) Vibrio crassostreae, a benign oyster colonizer turned into a pathogen after plasmid acquisition. *ISME J* **11**: 1043–1052.

Bruto, M., Labreuche, Y., James, A., Piel, D., Chenivesse, S., Petton, B., *et al*. (2018) Ancestral gene acquisition as the key to virulence potential in environmental {vibrio} populations. *ISME J* **12**: 2954–2966.

Bull, J.J., and Lauring, A.S. (2014) Theory and empiricism in virulence evolution. *PLoS Pathog* **10**: e1004387.

Chatterjee, D., and Chaudhuri, K. (2011) Association of cholera toxin with vibrio cholerae outer membrane vesicles which are internalized by human intestinal epithelial cells. *FEBS Lett* **585**: 1357–1362.

Cianfanelli, F.R., Monlezun, L., and Coulthurst, S.J. (2016) Aim, load, fire: the type VI secretion system, a bacterial Nanoweapon. *Trends Microbiol* **24**: 51–62.

Cordero, O.X., and Polz, M.F. (2014) Explaining microbial genomic diversity in light of evolutionary ecology. *Nat Rev Microbiol* **12**: 263–273.

Cota, I., Sánchez-Romero, M.A., Hernández, S.B., Pucciarelli, M.G., García-Del Portillo, F., and Casadesús, J. (2015) Epigenetic control of *Salmonella enterica* O-antigen chain length: a tradeoff between virulence and bacteriophage resistance. *PLoS Genet* **11**: e1005667–e1005667.

Cressler, C.E., McLeod, D.V., Rozins, C., VAN DEN Hoogen, J., and Day, T. (2016) The adaptive evolution of virulence: a review of theoretical predictions and empirical tests. *Parasitology* **143**: 915–930.

Cui, Y., Yang, X., Didelot, X., Guo, C., Li, D., Yan, Y., *et al*. (2015) Epidemic clones, oceanic gene pools, and eco-LD in the free living marine pathogen *Vibrio parahaemolyticus*. *Mol Biol Evol* **32**: 1396–1410.

Cullen, T.W., Schofield, W.B., Barry, N.A., Putnam, E.E., Rundell, E.A., Trent, M.S., *et al*. (2015) Antimicrobial peptide resistance mediates resilience of prominent gut commensals during inflammation. *Science (80-)* **347**: 170–175.

Demarre, G., Guérout, A.M., Matsumoto-Mashimo, C., Rowe-Magnus, D.A., Marlière, P., and Mazel, D. (2005) A new family of mobilizable suicide plasmids based on broad host range R388 plasmid (IncW) and RP4 plasmid (IncPα) conjugative machineries and their cognate *Escherichia coli* host strains. *Res Microbiol* **156**: 245–255.

Ferenci, T. (2016) Trade-off mechanisms shaping the diversity of bacteria. *Trends Microbiol* **24**: 209–223.

Friman, V.-P., and Buckling, A. (2014) Phages can constrain protist predation-driven attenuation of *Pseudomonas aeruginosa* virulence in multienemy communities. *ISME J* **8**: 1820–1830.

Friman, V.-P., Lindstedt, C., Hiltunen, T., Laakso, J., and Mappes, J. (2009) Predation on multiple trophic levels shapes the evolution of pathogen virulence. *PLoS One* **4**: e6761.

Gavin, H.E., and Satchell, K.J.F. (2015) MARTX toxins as effector delivery platforms. *Pathog Dis* **73**: ftv092–ftv092.

Gonzalez, M., Gueguen, Y., Desserre, G., de Lorgeril, J., Romestand, B., and Bachère, E. (2007) Molecular characterization of two isoforms of defensin from hemocytes of the oyster *Crassostrea gigas*. *Dev Comp Immunol* **31**: 332–339.

Hankins, J.V., Madsen, J.A., Giles, D.K., Brodbelt, J.S., and Trent, M.S. (2012) Amino acid addition to Vibrio cholerae LPS establishes a link between surface remodeling in Gram-positive and Gram-negative bacteria. *Proc Natl Acad Sci* **109**: 8722–8727.

Ho, B.T., Basler, M., and Mekalanos, J.J. (2013) Type 6 secretion system–mediated immunity to type 4 secretion system–mediated gene transfer. *Science (80-)* **342**: 250–253.

Le Roux, F., and Blokesch, M. (2018) Eco-evolutionary dynamics linked to horizontal gene transfer in Vibrios. *Annu Rev Microbiol* **72**: 89–110.

Le Roux, F., Binesse, J., Saulnier, D., and Mazel, D. (2007) Construction of a Vibrio splendidus mutant lacking the metalloprotease gene vsm by use of a novel counterselectable suicide vector. *Appl Environ Microbiol* **73**: 777–784.

Le Roux, F., Zouine, M., Chakroun, N., Binesse, J., Saulnier, D., Bouchier, C., *et al*. (2009) Genome sequence of Vibrio splendidus: an abundant planctonic marine species with a large genotypic diversity. *Environ Microbiol* **11**: 1959–1970.

Le Roux, F., Labreuche, Y., Davis, B.M., Iqbal, N., Mangenot, S., Goarant, C., *et al*. (2011) Virulence of an emerging pathogenic lineage of vibrio nigripulchritudo is dependent on two plasmids. *Environ Microbiol* **13**: 296–306.

Le Roux, F., Wegner, K.M., Baker-Austin, C., Vezzulli, L., Osorio, C.R., Amaro, C., *et al*. (2015) The emergence of vibrio pathogens in Europe: ecology, evolution and pathogenesis (Paris, 11-12 March 2015). *Front Microbiol* **6**: 1–8.

Le Roux, F., Wegner, K.M., and Polz, M.F. (2016) Oysters and Vibrios as a model for disease dynamics in wild animals. *Trends Microbiol* **24**: 568–580.

Lee, C.-T., Pajuelo, D., Llorens, A., Chen, Y.-H., Leiro, J.M., Padrós, F., *et al*. (2013) MARTX of Vibrio vulnificus biotype 2 is a virulence and survival factor. *Environ Microbiol* **15**: 419–432.

Lehrer, R.I., Barton, A., and Ganz, T. (1988) Concurrent assessment of inner and outer membrane permeabilization and bacteriolysis in *E. coli* by multiple-wavelength spectrophotometry. *J Immunol Methods* **108**: 153–158.

Levin, B.R. (1996) The evolution and maintenance of virulence in microparasites. *Emerg Infect Dis* **2**: 93–102.

Lindell, K., Fahlgren, A., Hjerde, E., Willassen, N.-P., Fällman, M., and Milton, D.L. (2012) Lipopolysaccharide O-antigen prevents phagocytosis of vibrio anguillarum by rainbow trout (*Oncorhynchus mykiss*) skin epithelial cells. *PLoS One* **7**: e37678–e37678.

López-Pérez, M., Jayakumar, J.M., Haro-Moreno, J.M., Zaragoza-Solas, A., Reddi, G., Rodriguez-Valera, F., *et al*. (2019) Evolutionary model of cluster divergence of the emergent marine pathogen Vibrio vulnificus: from genotype to ecotype. *MBio* **10**: e02852–e02818.

Ma, A.T., McAuley, S., Pukatzki, S., and Mekalanos, J.J. (2009) Translocation of a vibrio cholerae type VI secretion effector requires bacterial endocytosis by host cells. *Cell Host Microbe* **5**: 234–243.

March, C., Cano, V., Moranta, D., Llobet, E., Pérez-Gutiérrez, C., Tomás, J.M., *et al*. (2013) Role of bacterial surface structures on the interaction of *Klebsiella pneumoniae* with phagocytes. *PLoS One* **8**: e56847.

Matz, C., and Kjelleberg, S. (2005) Off the hook - how bacteria survive protozoan grazing. *Trends Microbiol* **13**: 302–307.

Mikonranta, L., Friman, V.-P., and Laakso, J. (2012) Life history trade-offs and relaxed selection can decrease bacterial virulence in environmental reservoirs. *PLoS One* **7**: e43801.

Pfaffl, M.W. (2001) A new mathematical model for relative quantification in real-time RT–PCR. *Nucleic Acids Res* **29**: e45–e45, 445.

Piel, D., Bruto, M., James, A., Labreuche, Y., Lambert, C., Janicot, A., Chenivesse S., Petton B., Wegner K.M., Stoudmann C., Blokesch M., le Roux F. (2019) Selection of vibrio crassostreae relies on a plasmid expressing a type 6 secretion system cytotoxic for host immune cells. *Environ Microbiol*. https://doi.org/10.1111/1462-2920.14776

Pirofski, L., and Casadevall, A. (2012) Q and a: what is a pathogen? A question that begs the point. *BMC Biol* **10**: 6.

Pupo, E., and Hardy, E. (2007) Isolation of smooth-type lipopolysaccharides to electrophoretic homogeneity. *Electrophoresis* **28**: 2351–2357.

Raetz, C.R.H., and Whitfield, C. (2002) Lipopolysaccharide Endotoxins. *Annu Rev Biochem* **71**: 635–700.

Robino, E., Poirier, A.C., Amraoui, H., Le Bissonnais, S., Perret, A., Lopez-Joven, C., *et al*. (2019) Resistance of the oyster pathogen Vibrio tasmaniensis LGP32 against grazing by Vannella sp. marine amoeba involves Vsm and CopA virulence factors. *Environ Microbiol*. https://doi.org/10.1111/1462-2920.14770

Roig, F.J., González-candelas, F., Sanjuán, E., and Fouz, B. (2018) Phylogeny of Vibrio vulnificus from the analysis of the core-genome: implications for intra-species taxonomy. *Front Microbiol* **8**: 1–13.

Rosa, R.D., Santini, A., Fievet, J., Bulet, P., Destoumieux-Garzón, D., and Bachère, E. (2011) Big defensins, a diverse family of antimicrobial peptides that follows different patterns of expression in hemocytes of the oyster *Crassostrea gigas*. *PLoS One* **6**: e25594–e25594.

Rubio, T., Oyanedel, D., Labreuche, Y., Toulza, E., Luo, X., Bruto, M., *et al*. (2019) Species-specific mechanisms of cytotoxicity toward immune cells determine the successful outcome of vibrio infections. *Proc Natl Acad Sci* **116**: 14238–14247.

Saar-Dover, R., Bitler, A., Nezer, R., Shmuel-Galia, L., Firon, A., Shimoni, E., *et al*. (2012) D-Alanylation of lipoteichoic acids confers resistance to cationic peptides in group B streptococcus by increasing the cell wall density. *PLoS Pathog* **8**: e1002891.

Sakib, S.N., Reddi, G., and Almagro-Moreno, S. (2018) Environmental role of pathogenic traits in vibrio cholerae. *J Bacteriol* **200**: 1–12.

Satchell, K.J.F. (2015) Multifunctional-autoprocessing repeats-in-toxin (MARTX) toxins of Vibrios. *Microbiol Spectr* **3**. https://doi.org/10.1128/microbiolspec.VE-0002-2014

Seed, K.D., Faruque, S.M., Mekalanos, J.J., Calderwood, S.B., Qadri, F., and Camilli, A. (2012) Phase Variable O Antigen Biosynthetic Genes Control Expression of the Major Protective Antigen and Bacteriophage Receptor in Vibrio cholerae O1. *PLoS Pathog* **8**(9): e1002917.

Seed, K.D., Yen, M., Shapiro, B.J., Hilaire, I.J., Charles, R. C., Teng, J.E., *et al*. (2014) Evolutionary consequences of intra-patient phage predation on microbial populations. *Elife* **3**: e03497–e03497.

Seif, Y., Monk, J.M., Machado, H., Kavvas, E., and Palsson, B.O. (2019) Systems biology and pangenome of salmonella O-antigens. *MBio* **10**: e01247–e01219.

Shapiro, B.J., and Polz, M.F. (2014) Ordering microbial diversity into ecologically and genetically cohesive units. *Trends Microbiol* **22**: 235–247.

Shapiro, B.J., Levade, I., Kovacikova, G., Taylor, R.K., and Almagro-moreno, S. (2016) Origins of pandemic vibrio cholerae from environmental gene pools. *Nat Microbiol* **2**: 16240.

Simkovsky, R., Effner, E.E., Iglesias-Sánchez, M.J., and Golden, S.S. (2016) Mutations in novel lipopolysaccharide biogenesis genes confer resistance to amoebal grazing in *Synechococcus elongatus*. *Appl Environ Microbiol* **82**: 2738–2750.

Sun, J., Wang, L., Wu, Z., Han, S., Wang, L., Li, M., *et al*. (2019) P38 is involved in immune response by regulating inflammatory cytokine expressions in the Pacific oyster *Crassostrea gigas*. *Dev Comp Immunol* **91**: 108–114.

Suquet, M., de Kermoysan, G., Araya, R.G., Queau, I., Lebrun, L., Le Souchu, P., and Mingant, C. (2009) Anesthesia in Pacific oyster, *Crassostrea gigas*. *Aquat Living Resour* **22**: 29–34.

Takemura, A., Chien, D., and Polz, M. (2014) Associations and dynamics of Vibrionaceae in the environment, from the genus to the population level. *Front Microbiol* **5**: 38.

Unterweger, D., Miyata, S.T., Bachmann, V., Brooks, T.M., Mullins, T., Kostiuk, B., *et al*. (2014) The vibrio cholerae type VI secretion system employs diverse effector modules for intraspecific competition. *Nat Commun* **5**: 3549.

Wildschutte, H., Wolfe, D.M., Tamewitz, A., and Lawrence, J.G. (2004) Protozoan predation, diversifying selection, and the evolution of antigenic diversity in salmonella. *Proc Natl Acad Sci U S A* **101**: 10644–10649.

Wildschutte, H., Preheim, S.P., Hernandez, Y., and Polz, M. F. (2010) O-antigen diversity and lateral transfer of the wbe region among Vibrio splendidus isolates. *Environ Microbiol* **12**: 2977–2987.

Zhang, D., Iyer, L.M., and Aravind, L. (2011) A novel immunity system for bacterial nucleic acid degrading toxins and its recruitment in various eukaryotic and DNA viral systems. *Nucleic Acids Res* **39**: 4532–4552.

Supporting Information

Additional Supporting Information may be found in the online version of this article at the publisher's web-site:

Table S1 Genes specific to moderately virulent strains of *V. splendidus* Pop#23.

Genes listed below are present in the genomes of 3T8_11, 4D1_8 and 4G4_4 but absent from the 4G1_8 genome.

Table S2 Bacterial strains

Table S3 Plasmids

Table S4 Oligonucleotides

Figure S1 The *rtxACHBDE* cluster in *V. splendidus* #23.

A- The figure shows gene replacement between non-virulent and moderately virulent strains leading to loss/acquisition of the MARTX encoding genes cluster. B- MARTX effector domains. The domain abbreviations are: Rtx = Repeats-in toxin; ACD = Actin Cross-linking Domain; ABH = α/β Hydrolase; MCF = Makes Caterpillars Floppy; RRSP = Ras/Rap1-specific endopeptidase; CPD = Cysteine Protease Domain (Satchell, 2015)

Figure S2 Growth curves of mutants versus wild type strains in LB NaCl medium.

Data show mean values of technical triplicates $\pm$ SD.

Figure S3 Genetic organization of the T6SS cluster in *V. splendidus* #23.

The figure shows gene replacements (in blue) between non-virulent and moderately virulent strains leading to loss/acquisition of a chromosomal T6SS-encoding gene cluster. Genes in green are specifically found in the non-virulent strain 4G1-8. Genes in red are specifically found in virulent strains and contain the T6SS genes. The gene cluster of the virulent strains is present on two contigs (genes GV4G44_380041 - GV4G44_380047 and GV4G44_320001 - GV4G44_320044). From the complete genome of *V. tasmaniensis* LGP32, which contains the same gene cluster, we found that genes GV4G44_380047 and GV4G44_320001 (hatched red genes) form a single large gene that is splitted in our assemblies due to numerous repeats.

Figure S4 Strains of *V. splendidus* #23 are cytotoxic toward hemocytes.

Maximum cytotoxicity exerted by *V. splendidus* over oyster hemocytes *in vitro*. A hemocyte monolayer was exposed to vibrios at a MOI of 1:50 and the percentage of cell lysis was monitored by the SYTOX Green assay. (A) shows that the four strains of *V. splendidus* #23 are cytotoxic toward hemocytes. Data are representative of five independent experiments. (B) shows that the *vipA-i* mutant derived from *V. splendidus* 4G4_4 does not show any attenuation of its cytotoxicity toward hemocytes, unlike the *vipA1-I* mutant derived from *V. tasmaniensis* LGP32. Data are representative of three independent experiments. Mean values of three technical replicates are displayed $\pm$ SD. Identical letters indicate a non-significant difference (ANOVA, $p < 0.05$ and Tukey HSD test).

Figure S5 Lipid A inferred structure does not differ between strains 4G1_8 and 4G4_4.

(A) Data show the MALDI-TOF spectra of 4G1_8 and 4G4_4 Lipid A. MALDI-TOF-MS analysis was performed in negative-ion [M-H]- / linear mode. A major Lipid A molecular species was observed at m/z 1740.1–1740.7, which by analogy with *V. cholerae* Lipid A could be attributed to a hexa-acyl (6 FA) molecular species (Hankins *et al.*, 2011, 2015), with one suggested exception *i.e.* the presence of non-hydroxylated 12:0 fatty acid at the secondary C3' position. As a consequence, no molecular species with Glycine substitution was found in either strain. Moreover, no substitution of phosphate groups with charged amino derivatives such as phosphoethanolamine or aminoarabinose could be inferred from our MS spectra. An additional peak, common to both strains was observed at m/z 1976.1–1977.4, which could be tentatively attributed to a hepta-acyl Lipid A molecular species (7 FA) carrying an additional 16:0 or 16:1 fatty acid. This molecular species appeared more intense in the virulent 4G4_4 than in the non-virulent 4G1_8. (B) Lipid A structure from *Vibrio cholerae* O1 adapted from Hankins *et al.* (2012), Fig.. The upper panel shows the MALDI-TOF spectra of *V. cholerae* Lipid A with a major molecular species at m/z 1756.1. The lowel panel shows the corresponding hexa-acyl molecular species (6 FA). Numbers indicate the number of carbons per acyl chain.

Figure S6 Inactivation of *epsE* in strains 4G4_4 and 4D1_8 generates the same O-antigen modifications and cytochrome C binding phenotype.

(a) SDS PAGE electrophoresis of LPS extractions from bacterial cultures in stationary phase. (b) Percentage of cytochrome C bound to the bacterial surface of wild type strains and *epsE-i* isogenic mutants. Data represent mean values of 3 independent experiments $\pm$ SD. Different letters indicate a significant difference (ANOVA, $p < 0.05$ and Tukey HSD test).

Figure S7 Immune genes that do not respond to early infection by *V. splendidus*. 4 pools of 10 oysters were sampled 2 h after being injected either with sterile seawater (SSW) or vibrio strains ($2x10^7$ CFU per animal). RNA was extracted from the 4 pools. For each pool, RT-qPCR was performed on immune genes to determine their expression relative to the elongation factor 1 alpha (EF1-α). The $\Delta\Delta^{ct}$ method was used (Pfaffl, 2015). Data are presented as the mean $\pm$ SD. Different letters indicate a significant difference (ANOVA, $p < 0.05$ and Tukey HSD test).

Figure S8 Strain 4G4-4 do not show killing activity against *E. coli* ML35p *in-vitro*. Cells were co-incubated in agar media for 4 h to allow cell to cell contact and T6SS mediated killing. Bars represent the mean CFU per millilitre of surviving *E. coli* from two replicates ($\pm$ SD). Means were compared by a Student's t-test ^{ns} = p > 0,05

I.2.1. SUPPLEMENTAL FIGURES

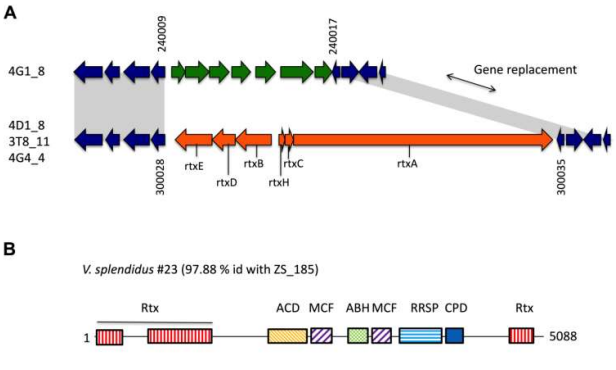

Figure S1. The *rtxACHBDE* cluster in *V. splendidus* #23**.** A- The figure shows gene replacement between non-virulent and moderately virulent strains leading to loss/acquisition of the MARTX encoding genes cluster. B- MARTX effector domains. The domain abbreviations are: Rtx = Repeats-in toxin; ACD = Actin Cross-linking Domain; ABH = α/β Hydrolase; MCF = Makes Caterpillars Floppy; RRSP = Ras/Rap1-specific endopeptidase; CPD = Cysteine Protease Domain (Satchell, 2015)

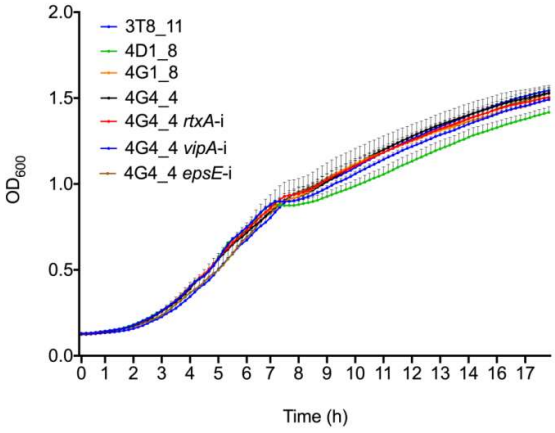

Figure S2. Growth curves of mutants versus wild type strains in LB NaCl medium. Data show mean values of technical triplicates ± SD.

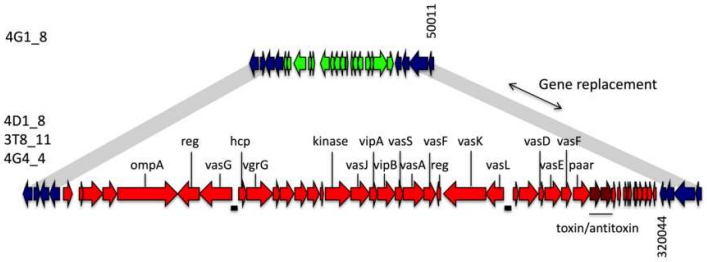

Figure S3. Genetic organization of the T6SS cluster in *V. splendidus* #23. The figure shows gene replacements (in blue) between non-virulent and moderately virulent strains leading to loss/acquisition of a chromosomal T6SS-encoding gene cluster. Genes in green are specifically found in the non-virulent strain 4G1-8. Genes in red are specifically found in virulent strains and contain the T6SS genes. The gene cluster of the virulent strains is present on two contigs (genes GV4G44_380041 - GV4G44_380047 and GV4G44_320001 - GV4G44_320044). From the complete genome of *V. tasmaniensis* LGP32, which contains the same gene cluster, we found that genes GV4G44_380047 and GV4G44_320001 (hatched red genes) form a single large gene that is splitted in our assemblies due to numerous repeats.

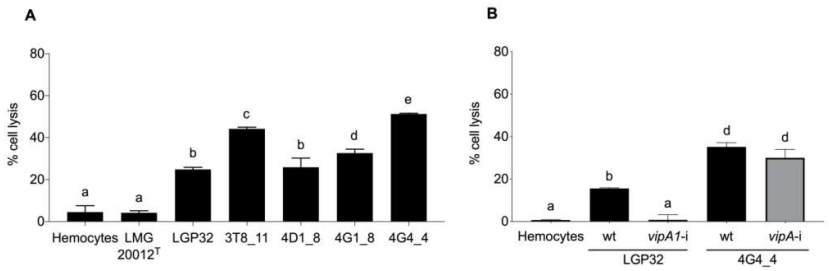

Figure S4. Strains of *V. splendidus* #23 are cytotoxic towards hemocytes. Maximum cytotoxicity exerted by *V. splendidus* over oyster hemocytes *in vitro*. A hemocyte monolayer was exposed to vibrios at a MOI of 1:50 and the percentage of cell lysis was monitored by the SYTOX Green assay. (A) shows that the four strains of *V. splendidus* #23 are cytotoxic towards hemocytes. Data are representative of five independent experiments. (B) shows that the *vipA-i* mutant derived from *V. splendidus* 4G4_4 does not show any attenuation of its cytotoxicity towards hemocytes, unlike the *vipA1-I* mutant derived from *V. tasmaniensis* LGP32. Data are representative of three independent experiments. Mean values of three technical replicates are displayed ± SD. Identical letters indicate a non-significant difference (ANOVA, $p < 0.05$ and Tukey HSD test).

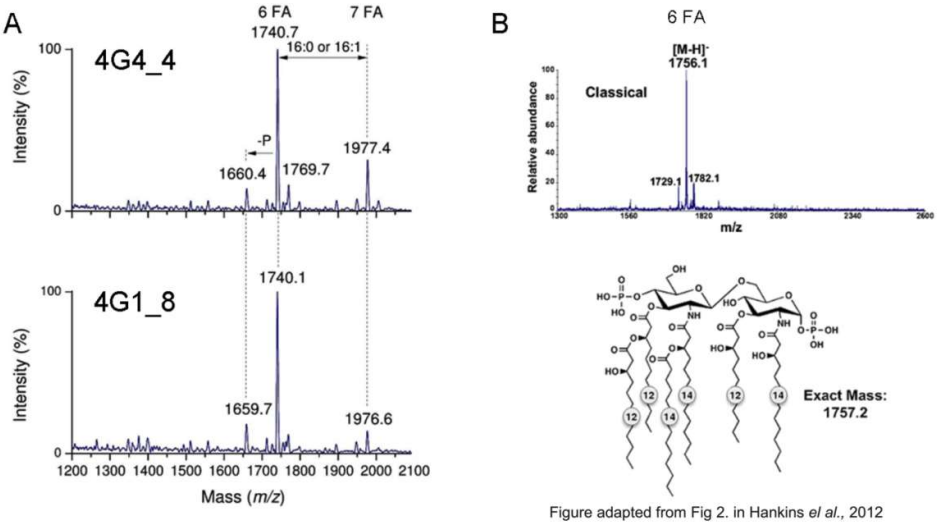

Figure S5. Lipid A inferred structure does not differ between strains 4G1_8 and 4G4_4. (A) Data show the MALDI-TOF spectra of 4G1_8 and 4G4_4 Lipid A. MALDI-TOF-MS analysis was performed in negative-ion [M-H]- / linear mode. A major Lipid A molecular species was observed at m/z 1740.1-1740.7, which by analogy with *V. cholerae* Lipid A could be attributed to a hexa-acyl (6 FA) molecular species (Hankins *et al.*, 2011, 2012), with one suggested exception *i.e.* the presence of non-hydroxylated 12:0 fatty acid at the secondary C3' position. As a consequence, no molecular species with Glycine substitution was found in either strain. Moreover, no substitution of phosphate groups with charged amino derivatives such as phosphoethanolamine or aminoarabinose could be inferred from our MS spectra. An additional peak, common to both strains was observed at m/z 1976.1-1977.4, which could be tentatively attributed to a hepta-acyl Lipid A molecular species (7 FA) carrying an additional 16:0 or 16:1 fatty acid. This molecular species appeared more intense in the virulent 4G4_4 than in the non-virulent 4G1_8. (B) Lipid A structure from *Vibrio cholerae* O1 adapted from Hankins et al. (2012), Fig.2. The upper panel shows

the MALDI-TOF spectra of *V. cholerae* Lipid A with a major molecular species at m/z 1756.1. The lower panel shows the corresponding hexa-acyl molecular species (6 FA). Numbers indicate the number of carbons per acyl chain.

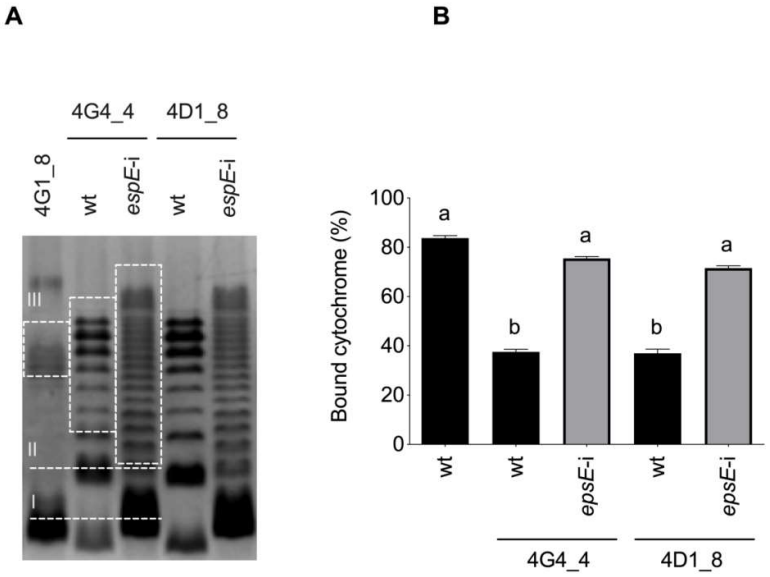

Figure S6. Inactivation of *epsE* in strains 4G4_4 and 4D1_8 generates the same O-antigen modifications and cytochrome C binding phenotype. (A) SDS PAGE electrophoresis of LPS extractions from bacterial cultures in stationary phase. (B) Percentage of cytochrome C bound to the bacterial surface of wild type strains and *epsE-i* isogenic mutants. Data represent mean values of 3 independent experiments ± SD. Different letters indicate a significant difference (ANOVA, $p < 0.05$ and Tukey HSD test).

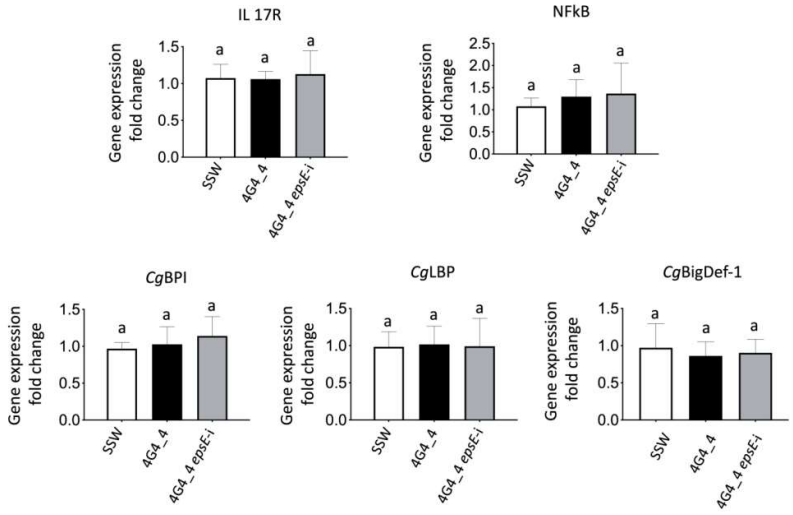

Figure S7. Immune genes that do not respond to early infection by *V. splendidus*. 4 pools of 10 oysters were sampled 2 h after being injected either with sterile seawater (SSW) or vibrio strains (2x10^7 CFU per

animal). RNA was extracted from the 4 pools. For each pool, RT-qPCR was performed on immune genes to determine their expression relative to the elongation factor 1 alpha (EF1-a). The $\Delta\Delta^{ct}$ method was used (Pffafl., 2001). Data are presented as the mean ± SD. Different letters indicate a significant difference (ANOVA, $p < 0.05$ and Tukey HSD test).

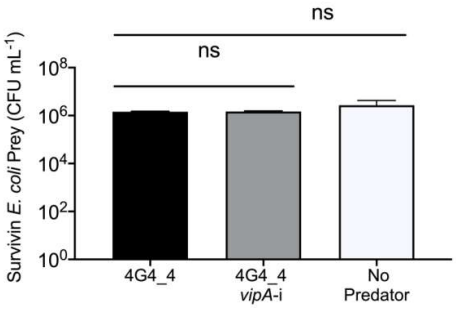

Figure S8. Strain 4G4-4 do not show killing activity against *E. coli* ML35p *in vitro*. Cells were co-incubated in agar media for 4 h to allow cell to cell contact and T6SS mediated killing. Bars represent the mean cfu per milliliter of surviving *E. coli* from two replicates (± SD). Means were compared by a Student's t-test, ns= $p > 0.05$

Table S1. Genes specific to moderately virulent strains of *V. splendidus* Pop#23.
Genes listed below are present in the genomes of 3T8_11, 4D1_8 and 4G4_4 but absent from the 4G1_8 genome.

Locus tag	*Gene*	Putative function or gene name
GV4G44_v1_10002	_	protein of unknown function
GV4G44_v1_10024	_	protein of unknown function
GV4G44_v1_10046	*bsn*	Extracellular ribonuclease *bsn*
GV4G44_v1_10050	_	Unknown
GV4G44_v1_10056	_	Unknown
GV4G44_v1_10057	_	Radical SAM
GV4G44_v1_10058	_	Unknown
GV4G44_v1_10132	_	Unknown
GV4G44_v1_10136	_	Outer membrane protein
GV4G44_v1_10152	_	Unknown
GV4G44_v1_10162	_	ABC-type uncharacterized transport system, periplasmic component
GV4G44_v1_10163	_	conserved exported protein of unknown function
GV4G44_v1_10207	_	Alpha-amylase
GV4G44_v1_10262	_	Two-component system sensory/regulatory protein-like protein (Hybrid family)
GV4G44_v1_20013	_	Uncharacterized conserved membrane protein
GV4G44_v1_20017	_	protein of unknown function
GV4G44_v1_20041	_	protein of unknown function
GV4G44_v1_20042	_	conserved protein of unknown function
GV4G44_v1_20043	_	protein of unknown function
GV4G44_v1_20080	_	conserved exported protein of unknown function
GV4G44_v1_20081	_	Transcriptional regulatory protein
GV4G44_v1_20082	_	putative 17-beta-estradiol 17-dehydrogenase
GV4G44_v1_20083	_	Lysophospholipase
GV4G44_v1_20084	_	conserved protein of unknown function
GV4G44_v1_20249	_	protein of unknown function
GV4G44_v1_20250	_	conserved protein of unknown function
GV4G44_v1_30001	_	Predicted PE--lipooligosaccharide phosphorylethanolaminetransferase
GV4G44_v1_30002	_	conserved protein of unknown function
GV4G44_v1_30019	_	conserved exported protein of unknown function
GV4G44_v1_30127	_	Outer membrane protein
GV4G44_v1_40019	_	protein of unknown function
GV4G44_v1_40020	_	putative ferrichrome-iron receptor
GV4G44_v1_40059	_	putative adhesin

GV4G44_v1_40060	_	putative AraC-family transcriptional regulatory protein
GV4G44_v1_40070	_	protein of unknown function
GV4G44_v1_40162	_	protein of unknown function
GV4G44_v1_50053	_	conserved protein of unknown function
GV4G44_v1_50069	_	putative Type IV pilin
GV4G44_v1_50071	_	conserved protein of unknown function
GV4G44_v1_50072	_	Pili retraction protein PilT
GV4G44_v1_50073	_	Pili subunit
GV4G44_v1_50076	_	putative alginate lyase
GV4G44_v1_50145	_	Methyl-accepting chemotaxis protein I (Serine chemoreceptor protein)
GV4G44_v1_60017	_	conserved protein of unknown function
GV4G44_v1_60019	_	conserved protein of unknown function
GV4G44_v1_60034	_	protein of unknown function
GV4G44_v1_60058	_	conserved protein of unknown function
GV4G44_v1_60071	_	protein of unknown function
GV4G44_v1_60073	_	conserved protein of unknown function
GV4G44_v1_60074	_	conserved membrane protein of unknown function
GV4G44_v1_60075	_	conserved protein of unknown function
GV4G44_v1_60076	_	conserved protein of unknown function
GV4G44_v1_60078	*relE*	Toxin of the RelE-RelB toxin-antitoxin system; Qin prophage
GV4G44_v1_60079	_	Prevent-host-death family protein
GV4G44_v1_60080	_	transposase
GV4G44_v1_60081	_	protein of unknown function
GV4G44_v1_60082	_	conserved protein of unknown function
GV4G44_v1_60087	_	putative c-di-GMP phosphodiesterase A-related protein
GV4G44_v1_60091	_	protein of unknown function
GV4G44_v1_60147	_	protein of unknown function
GV4G44_v1_70001	_	conserved protein of unknown function
GV4G44_v1_70002	_	conserved membrane protein of unknown function
GV4G44_v1_70003	_	conserved exported protein of unknown function
GV4G44_v1_70004	_	conserved protein of unknown function
GV4G44_v1_70005	_	conserved protein of unknown function
GV4G44_v1_70006	_	conserved protein of unknown function
GV4G44_v1_70007	*vspR*	Transcriptional regulator VspR
GV4G44_v1_70008	_	putative transcriptional regulator
GV4G44_v1_70009	_	transposase (fragment)
GV4G44_v1_70010	_	protein of unknown function
GV4G44_v1_70011	_	transposase (fragment)
GV4G44_v1_70039	*yeiJ*	putative sodium/proton nucleoside transporter
GV4G44_v1_70040	*ahcY*	Adenosylhomocysteinase
GV4G44_v1_70041	_	Regulatory protein LysR:LysR substrate-binding
GV4G44_v1_70042	_	Bifunctional 2',3'-cyclic nucleotide 2'-phosphodiesterase/3'-nucleotidase periplasmic protein
GV4G44_v1_70043	_	conserved protein of unknown function
GV4G44_v1_70044	_	conserved protein of unknown function
GV4G44_v1_70158	_	Transcriptional regulators, LysR family
GV4G44_v1_70159	_	conserved exported protein of unknown function
GV4G44_v1_80003	_	conserved protein of unknown function
GV4G44_v1_80004	_	protein of unknown function
GV4G44_v1_80005	_	Prophage MuSo1 transcriptional regulator Cro/CI family (fragment)
GV4G44_v1_80036	_	conserved protein of unknown function
GV4G44_v1_80037	_	membrane protein of unknown function
GV4G44_v1_80038	_	exported protein of unknown function
GV4G44_v1_80039	_	protein of unknown function
GV4G44_v1_80074	_	conserved protein of unknown function
GV4G44_v1_80091	_	protein of unknown function
GV4G44_v1_80099	_	conserved protein of unknown function
GV4G44_v1_80100	_	membrane protein of unknown function
GV4G44_v1_80101	_	protein of unknown function
GV4G44_v1_90039	_	protein of unknown function
GV4G44_v1_90069	_	protein of unknown function
GV4G44_v1_90070	*ectA*	L-2,4-diaminobutyric acid acetyltransferase
GV4G44_v1_90071	*ectB*	Diaminobutyrate--2-oxoglutarate transaminase
GV4G44_v1_90072	*ectC*	L-ectoine synthase
GV4G44_v1_90073	_	Aspartokinase associated with ectoine biosynthesis
GV4G44_v1_90074	_	putative sigma-54 interacting response regulator transcription regulator protein
GV4G44_v1_90075	_	putative hyperosmotically inducible periplasmic protein
GV4G44_v1_90076	_	conserved protein of unknown function
GV4G44_v1_90077	_	conserved exported protein of unknown function
GV4G44_v1_90078	_	conserved protein of unknown function
GV4G44_v1_90079	_	Methylglyoxal synthase

GV4G44_v1_90080	_	Potassium efflux system KefA protein / Small-conductance mechanosensitive channel
GV4G44_v1_90081	_	conserved protein of unknown function
GV4G44_v1_90082	_	conserved protein of unknown function
GV4G44_v1_90083	_	conserved protein of unknown function
GV4G44_v1_90084	_	conserved protein of unknown function
GV4G44_v1_90085	_	conserved protein of unknown function
GV4G44_v1_90086	_	putative permease protein
GV4G44_v1_90119	_	Site-specific recombinase, phage integrase family (fragment)
GV4G44_v1_90120	_	protein of unknown function
GV4G44_v1_110106	_	conserved protein of unknown function
GV4G44_v1_110108	_	conserved protein of unknown function
GV4G44_v1_110109	_	protein of unknown function
GV4G44_v1_110110	*int*	Integrase/recombinase
GV4G44_v1_120079	_	protein of unknown function
GV4G44_v1_120085	_	Outer membrane protein
GV4G44_v1_120086	_	putative Flp pilus assembly protein TadG
GV4G44_v1_120087	_	conserved protein of unknown function
GV4G44_v1_120088	_	putative Flp pilus assembly protein TadE
GV4G44_v1_120089	_	putative Flp pilus assembly protein TadD
GV4G44_v1_120090	_	putative Flp pilus assembly protein TadC
GV4G44_v1_120091	_	putative Flp pilus assembly protein TadB
GV4G44_v1_120092	_	Flp pilus assembly protein
GV4G44_v1_120093	_	ATPase involved in chromosome partitioning
GV4G44_v1_120094	_	conserved protein of unknown function
GV4G44_v1_120095	_	Flp pilus assembly protein
GV4G44_v1_120096	_	conserved protein of unknown function
GV4G44_v1_120097	_	conserved protein of unknown function
GV4G44_v1_120098	_	putative membrane protein
GV4G44_v1_120100	_	Transcriptional regulator
GV4G44_v1_120101	_	conserved exported protein of unknown function
GV4G44_v1_130004	_	conserved protein of unknown function
GV4G44_v1_130031	_	conserved membrane protein of unknown function
GV4G44_v1_130046	_	protein of unknown function
GV4G44_v1_140001	_	protein of unknown function
GV4G44_v1_140002	_	Transcriptional repressor of sporulation, septation and degradative enzyme
GV4G44_v1_140003	_	transposase
GV4G44_v1_140004	_	transposase
GV4G44_v1_140005	_	membrane protein of unknown function
GV4G44_v1_140006	_	conserved protein of unknown function
GV4G44_v1_140007	_	protein of unknown function
GV4G44_v1_140061	_	protein of unknown function
GV4G44_v1_140064	_	protein of unknown function
GV4G44_v1_140068	_	protein of unknown function
GV4G44_v1_140069	_	conserved protein of unknown function
GV4G44_v1_150005	_	protein of unknown function
GV4G44_v1_150025	_	Sensory box/GGDEF family protein
GV4G44_v1_160049	_	protein of unknown function
GV4G44_v1_160073	_	Selenoprotein W-related protein
GV4G44_v1_160084	_	conserved exported protein of unknown function
GV4G44_v1_170011	_	protein of unknown function
GV4G44_v1_170086	_	conserved membrane protein of unknown function
GV4G44_v1_170087	_	Prophage Lp2 protein 6
GV4G44_v1_180039	_	protein of unknown function
GV4G44_v1_180040	_	Maltose operon periplasmic protein MalM
GV4G44_v1_180041	*lamB*	Maltoporin
GV4G44_v1_190001	_	protein of unknown function
GV4G44_v1_190015	*yfbR*	deoxyribonucleoside 5'-monophosphatase
GV4G44_v1_190016	_	conserved protein of unknown function
GV4G44_v1_190017	_	conserved protein of unknown function
GV4G44_v1_190018	_	conserved membrane protein of unknown function
GV4G44_v1_190020	*bdcA*	Cyclic-di-GMP-binding biofilm dispersal mediator protein
GV4G44_v1_190021	_	putative transcriptional regulator, LysR family protein
GV4G44_v1_190022	_	conserved protein of unknown function
GV4G44_v1_190023	_	Cellobiose phosphotransferase system CelC
GV4G44_v1_190024	_	Transcriptional regulator
GV4G44_v1_190025	_	protein of unknown function
GV4G44_v1_190026	_	putative sugar transport protein
GV4G44_v1_190027	_	protein of unknown function
GV4G44_v1_190028	_	conserved exported protein of unknown function
GV4G44_v1_190029	_	protein of unknown function

GV4G44_v1_190030	_	membrane protein of unknown function
GV4G44_v1_190031	_	exported protein of unknown function
GV4G44_v1_190032	_	conserved protein of unknown function
GV4G44_v1_190033	_	conserved protein of unknown function
GV4G44_v1_190034	_	conserved protein of unknown function
GV4G44_v1_190035	_	conserved protein of unknown function
GV4G44_v1_190036	_	conserved protein of unknown function
GV4G44_v1_190037	_	Site-specific recombinase, phage integrase family
GV4G44_v1_190038	_	conserved protein of unknown function
GV4G44_v1_190039	_	conserved protein of unknown function
GV4G44_v1_190041	_	conserved protein of unknown function
GV4G44_v1_190042	_	conserved protein of unknown function
GV4G44_v1_190044	_	conserved protein of unknown function
GV4G44_v1_190045	_	protein of unknown function
GV4G44_v1_200038	_	protein of unknown function
GV4G44_v1_200075	_	conserved protein of unknown function
GV4G44_v1_200076	_	conserved protein of unknown function
GV4G44_v1_200077	_	conserved protein of unknown function
GV4G44_v1_200088	_	transposase (fragment)
GV4G44_v1_220015	_	protein of unknown function
GV4G44_v1_230011	*yefM*	antitoxin of the YoeB-YefM toxin-antitoxin system
GV4G44_v1_230012	*yoeB*	toxin of the YoeB-YefM toxin-antitoxin system
GV4G44_v1_230029	_	conserved protein of unknown function
GV4G44_v1_230031	_	ThiJ/PfpI family protein
GV4G44_v1_230032	_	conserved exported protein of unknown function
GV4G44_v1_230063	_	putative Phage integrase family protein
GV4G44_v1_230064	_	conserved protein of unknown function
GV4G44_v1_230065	_	conserved protein of unknown function
GV4G44_v1_230066	_	conserved protein of unknown function
GV4G44_v1_230067	_	conserved protein of unknown function
GV4G44_v1_230068	_	conserved protein of unknown function
GV4G44_v1_230069	_	conserved protein of unknown function
GV4G44_v1_240031	_	conserved exported protein of unknown function
GV4G44_v1_240071	_	Predicted membrane protein
GV4G44_v1_240072	_	Zn-dependent protease with chaperone function
GV4G44_v1_270001	_	conserved protein of unknown function
GV4G44_v1_270021	_	conserved exported protein of unknown function
GV4G44_v1_270067	_	protein of unknown function
GV4G44_v1_280014	_	conserved protein of unknown function
GV4G44_v1_280018	_	conserved exported protein of unknown function
GV4G44_v1_280044	_	conserved exported protein of unknown function
GV4G44_v1_280045	_	conserved exported protein of unknown function
GV4G44_v1_280059	_	conserved protein of unknown function
GV4G44_v1_280060	_	conserved protein of unknown function
GV4G44_v1_290030	_	protein of unknown function
GV4G44_v1_290047	_	protein of unknown function
GV4G44_v1_290060	_	protein of unknown function
GV4G44_v1_300029	*rtxE*	Leukotoxin translocation ATP-binding protein LktB
GV4G44_v1_300030	*rtxD*	RTX toxin transporter
GV4G44_v1_300031	*rtxB*	Cyclolysin secretion/processing ATP-binding protein CyaB
GV4G44_v1_300032	*rtxH*	conserved protein of unknown function
GV4G44_v1_300033	*rtxC*	Cytolysin-activating lysine-acyltransferase RtxC
GV4G44_v1_300034	*rtxA*	protein of unknown function
GV4G44_v1_310021	_	MSHA pilin protein MshA
GV4G44_v1_310022	_	putative MSHA pilin protein MshC
GV4G44_v1_310023	_	MSHA pilin protein MshD
GV4G44_v1_310024	_	putative type IV prepilin, MshO
GV4G44_v1_310025	_	MSHA biogenesis protein MshP
GV4G44_v1_310026	_	MSHA biogenesis protein MshQ
GV4G44_v1_320001	_	protein of unknown function
GV4G44_v1_320002	_	protein of unknown function
GV4G44_v1_320003	_	conserved protein of unknown function
GV4G44_v1_320004	_	conserved exported protein of unknown function
GV4G44_v1_320005	*ompA*	OmpA family protein
GV4G44_v1_320006	_	Sigma 54 dependant transcriptional regulator
GV4G44_v1_320007	*vasG*	Protein ClpV1
GV4G44_v1_320008	*hcpC*	hcp
GV4G44_v1_320009	*vgrG*	putative Vgr protein
GV4G44_v1_320010	_	Protein of unknown function (structural homology with vgrG tip)
GV4G44_v1_320011	_	conserved protein of unknown function

GV4G44_v1_320012	_	conserved protein of unknown function
GV4G44_v1_320013	_	conserved protein of unknown function
GV4G44_v1_320015	_	kinase
GV4G44_v1_320016	*vasJ*	Type VI secretion system vasJ
GV4G44_v1_320017	*vipA*	Type VI secretion system vipA
GV4G44_v1_320018	*vipB*	Type VI secretion system vipB
GV4G44_v1_320019	*vasS*	Type VI secretion system vasS
GV4G44_v1_320020	*vasA*	Type VI secretion system VasA
GV4G44_v1_320021	*vasF*	Type VI secretion system vasF
GV4G44_v1_320022	_	putative HTH-type transcriptional regulator
GV4G44_v1_320023	*vasK*	Putative Type VI secretion system protein IcmF
GV4G44_v1_320024	*vasL*	Type VI secretion system vasL
GV4G44_v1_320025	_	Type VI secretion system protein of unknown function
GV4G44_v1_320026	_	Type VI secretion system forkhead-associated protein
GV4G44_v1_320027	*vasD*	Type VI secretion system vasD
GV4G44_v1_320028	*vasE*	Type VI secretion system vasE
GV4G44_v1_320029	*vasF*	Type VI Secretion System, VasF
GV4G44_v1_320030	*paar*	Type VI secretion system protein with PAAR domain + unknown extension
GV4G44_v1_320031*	_	Putative bacterial toxin system with endonuclease activity
GV4G44_v1_320032*	_	Putative immunity protein
GV4G44_v1_320038	_	protein of unknown function
GV4G44_v1_320039	_	protein of unknown function
GV4G44_v1_320042	_	conserved protein of unknown function
GV4G44_v1_320043	_	Cytochrome c553
GV4G44_v1_330027	_	protein of unknown function
GV4G44_v1_340001	_	Putative RTX protein (fragment)
GV4G44_v1_340025	_	protein of unknown function
GV4G44_v1_340035	_	conserved exported protein of unknown function
GV4G44_v1_340044	*tnpA*	transposase
GV4G44_v1_340045	_	protein of unknown function
GV4G44_v1_340048	_	conserved membrane protein of unknown function
GV4G44_v1_360022	_	conserved protein of unknown function
GV4G44_v1_360039	_	protein of unknown function
GV4G44_v1_370003	_	conserved protein of unknown function
GV4G44_v1_370006	*groES*	Co-chaperonin GroES
GV4G44_v1_370014	_	putative UDP-galactose phosphate transferase (WeeH)
GV4G44_v1_370034	*yjbH*	putative porin
GV4G44_v1_370035	_	conserved exported protein of unknown function
GV4G44_v1_370036	_	putative regulator
GV4G44_v1_370037	*ymcD*	conserved hypothetical protein; putative inner membrane protein
GV4G44_v1_370038	_	Regulator of length of O-antigen component of lipopolysaccharide chains
GV4G44_v1_370040	_	conserved protein of unknown function
GV4G44_v1_370041	_	membrane protein of unknown function
GV4G44_v1_370042	*wbcM*	WbcM protein
GV4G44_v1_370043	_	putative Glycosyl transferase, group 2 family
GV4G44_v1_370044	_	protein of unknown function
GV4G44_v1_370045	_	protein of unknown function
GV4G44_v1_370046	_	putative Uncharacterized glycosyltransferase HI_1578
GV4G44_v1_370047	_	putative Glycosyl transferase family 11
GV4G44_v1_370048	_	membrane protein of unknown function
GV4G44_v1_370049	_	CDP-4-dehydro-6-deoxy-D-glucose 3-dehydratase (fragment)
GV4G44_v1_370051	*fcl*	bifunctional GDP-fucose synthetase:
GV4G44_v1_370052	*gmd*	GDP-D-mannose dehydratase, NAD(P)-binding
GV4G44_v1_370053	*manB*	Phosphomannomutase
GV4G44_v1_370054	*cpsB*	mannose-1-phosphate guanyltransferase
GV4G44_v1_370055	*nudD*	GDP-mannose mannosyl hydrolase
GV4G44_v1_370056	_	protein of unknown function
GV4G44_v1_380016	_	protein of unknown function
GV4G44_v1_380046	_	conserved protein of unknown function
GV4G44_v1_380047	_	conserved exported protein of unknown function
GV4G44_v1_390025	_	protein of unknown function
GV4G44_v1_400018	_	conserved protein of unknown function
GV4G44_v1_410007	_	protein of unknown function
GV4G44_v1_410014	_	putative capsular polysaccharide biosynthesis protein
GV4G44_v1_410015	_	conserved protein of unknown function
GV4G44_v1_420016	_	conserved exported protein of unknown function
GV4G44_v1_450042	_	protein of unknown function
GV4G44_v1_460001	_	conserved protein of unknown function
GV4G44_v1_460004	_	Metallophosphoesterase
GV4G44_v1_470021	_	protein of unknown function

GV4G44_v1_480041	_	ABC-type uncharacterized transport system component
GV4G44_v1_480042	_	putative Outer membrane protein
GV4G44_v1_480043	_	Agglutination protein
GV4G44_v1_480044	_	conserved protein of unknown function
GV4G44_v1_490006	_	conserved protein of unknown function
GV4G44_v1_490015	_	Long-chain fatty acid transport protein
GV4G44_v1_510029	_	conserved protein of unknown function
GV4G44_v1_510030	_	conserved protein of unknown function
GV4G44_v1_520009	_	protein of unknown function
GV4G44_v1_520014	_	conserved exported protein of unknown function
GV4G44_v1_520015	_	protein of unknown function
GV4G44_v1_520025	_	exported protein of unknown function
GV4G44_v1_580014	*agaR*	DNA-binding transcriptional dual regulator
GV4G44_v1_580015	*agaR*	DNA-binding transcriptional dual regulator
GV4G44_v1_580016	*kbaZ*	tagatose 6-phosphate aldolase 1, kbaZ subunit
GV4G44_v1_580017	*agaS*	tagatose-6-phosphate ketose/aldose isomerase
GV4G44_v1_580018	*agaV*	N-acetylgalactosamine-specific enzyme IIB component of PTS
GV4G44_v1_580019	_	putative N-acetylgalactosamine-specific IID component, PTS system
GV4G44_v1_580020	*agaD*	N-acetylgalactosamine-specific enzyme IID component of PTS
GV4G44_v1_580021	_	Phosphotransferase system, mannose/fructose-specific component IIA
GV4G44_v1_580022	*manD*	N-acetylglucosamine-6-phosphate deacetylase
GV4G44_v1_580023	*kbaY*	tagatose 6-phosphate aldolase 1, kbaY subunit
GV4G44_v1_580035	_	Transcriptional regulator
GV4G44_v1_580036	_	conserved protein of unknown function
GV4G44_v1_580037	_	conserved exported protein of unknown function
GV4G44_v1_580038	_	protein of unknown function
GV4G44_v1_620024	*pilA*	Fimbrial protein
GV4G44_v1_630001	_	conserved protein of unknown function
GV4G44_v1_630004	_	Restriction endonuclease family protein
GV4G44_v1_630005	_	conserved protein of unknown function
GV4G44_v1_630006	_	conserved protein of unknown function
GV4G44_v1_630007	_	conserved protein of unknown function
GV4G44_v1_630008	_	conserved protein of unknown function
GV4G44_v1_630009	_	DNA polymerase I
GV4G44_v1_630010	_	conserved protein of unknown function
GV4G44_v1_630011	_	conserved protein of unknown function
GV4G44_v1_630012	_	protein of unknown function
GV4G44_v1_630013	_	protein of unknown function
GV4G44_v1_630014	_	conserved exported protein of unknown function
GV4G44_v1_630015	_	conserved protein of unknown function
GV4G44_v1_630016	_	conserved protein of unknown function
GV4G44_v1_630017	_	conserved protein of unknown function
GV4G44_v1_630018	_	conserved protein of unknown function
GV4G44_v1_630019	_	Site-specific recombinase XerD-like
GV4G44_v1_630020	_	protein of unknown function
GV4G44_v1_630021	_	putative thiol peroxidase (fragment)
GV4G44_v1_630022	_	Nucleoside 2-deoxyribosyltransferase
GV4G44_v1_630023	_	exported protein of unknown function
GV4G44_v1_630026	_	protein of unknown function
GV4G44_v1_640021	_	conserved protein of unknown function
GV4G44_v1_650021	_	conserved exported protein of unknown function
GV4G44_v1_670015	_	DNA mismatch repair protein MutT
GV4G44_v1_670027	_	conserved protein of unknown function
GV4G44_v1_710001	_	exported protein of unknown function
GV4G44_v1_730016	_	conserved membrane protein of unknown function
GV4G44_v1_730017	_	conserved protein of unknown function
GV4G44_v1_740016	_	conserved protein of unknown function
GV4G44_v1_760001	_	conserved membrane protein of unknown function
GV4G44_v1_760002	_	conserved protein of unknown function
GV4G44_v1_760003	_	conserved protein of unknown function
GV4G44_v1_760004	_	conserved protein of unknown function
GV4G44_v1_760005	_	conserved protein of unknown function
GV4G44_v1_760006	_	Bacteriophage P7 related protein
GV4G44_v1_760007	_	conserved protein of unknown function
GV4G44_v1_760008	_	conserved protein of unknown function
GV4G44_v1_760009	_	conserved protein of unknown function
GV4G44_v1_760013	_	Outer membrane receptor protein
GV4G44_v1_760014	_	conserved protein of unknown function
GV4G44_v1_760015	_	conserved protein of unknown function
GV4G44_v1_760016	_	conserved protein of unknown function

GV4G44_v1_760017	_	conserved protein of unknown function
GV4G44_v1_760018	_	conserved protein of unknown function
GV4G44_v1_760019	_	putative replication initiation protein, phage-related
GV4G44_v1_760020	_	conserved protein of unknown function
GV4G44_v1_760021	_	conserved protein of unknown function
GV4G44_v1_760022	_	conserved protein of unknown function
GV4G44_v1_760023	_	conserved protein of unknown function
GV4G44_v1_760024	_	conserved protein of unknown function
GV4G44_v1_760025	_	conserved protein of unknown function
GV4G44_v1_760026	_	Integrase
GV4G44_v1_790009	_	protein of unknown function
GV4G44_v1_790010	_	protein of unknown function
GV4G44_v1_800001	_	Metal-dependent phosphohydrolase, HD subdomain
GV4G44_v1_800002	_	conserved protein of unknown function
GV4G44_v1_800003	_	protein of unknown function
GV4G44_v1_800004	_	conserved protein of unknown function
GV4G44_v1_800005	_	protein of unknown function
GV4G44_v1_800006	_	protein of unknown function
GV4G44_v1_800007	_	putative caffeoyl-CoA O-methyltransferase (fragment)
GV4G44_v1_800008	_	putative caffeoyl-CoA O-methyltransferase (fragment)
GV4G44_v1_800009	_	RNA-directed DNA polymerase (fragment)
GV4G44_v1_800010	_	conserved protein of unknown function
GV4G44_v1_800011	_	Methyl-accepting chemotaxis protein
GV4G44_v1_800012	_	protein of unknown function
GV4G44_v1_830008	_	Internal scaffolding protein B
GV4G44_v1_840003	_	protein of unknown function
GV4G44_v1_880001	_	conserved protein of unknown function
GV4G44_v1_880002	_	Helix-turn-helix family protein
GV4G44_v1_880003	_	conserved protein of unknown function
GV4G44_v1_920001	_	conserved protein of unknown function
GV4G44_v1_990001	_	Acetyltransferase family protein
GV4G44_v1_1010001	_	transposase (fragment)
GV4G44_v1_1060001	_	conserved membrane protein of unknown function

GV4G44_v1_320031 and GV4G44_v1_320032 indicated with an * in the locus tag are genes exclusive of strain 4G4_4

Table S3. Bacterial strains

Strain	Description	Mutated gene	Reference
E. coli Π3813	lacIQ, thi1, supE44, endA1, recA1, hsdR17, gyrA462, zei298::Tn10, DthyA::(erm-pir116) [TcR Erm R]		Le Roux *et al*., 2007
E. coli β3914	(F -) RP4-2-Tc::Mu ΔdapA ::(erm-pir116), gyrA462, zei298::Tn10 [KmR EmR TcR]		Le Roux *et al*., 2007
E. coli SBS3	K12, derived from E. coli D22, F- Ro reverse Trp+, galU129 (short-chain LPS)		Saclay Bacterial strain bank
E. coli ML-35p	i-, y-, z+ + pBR-322[AmpR]		Lehrer *et al.,* 1988
GV 2390	3T8_11, *V. splendidus* Pop #23		Bruto *el al*., 2017
GV 2386	4D1_8, *V. splendidus* Pop #23		Bruto *el al*., 2017
4D1_8 **epsE*-i	Δ*epsE*::pSW23T [Cm^R]	GV4D18_v1_120057	This study
GV 2388	4G1_8, *V. splendidus* Pop #23		Bruto *el al*., 2017
GV 2389	4G4_4, *V. splendidus* Pop #23		Bruto *el al*., 2017
4G4_4 **rtxA*-i	**rtxA*::pSW23T [Cm^R]	GV4G44_v1_300034	This study
4G4_4 **vipA*-i	**vipA*::pSW23T [Cm^R]	GV4G44_v1_320017	This study

4G4_4 **epsE*-i	**espE*::pSW23T [Cm^R]	GV4G44_v1_370043	This study
4G4_4 **epsE*-i GFP	**espE*::pSW23T [Cm^R] + pMRB-P_{LAC}*gfp* [Spt^R]		This study
LMG20012T GFP	pMRB-P_{LAC}*gfp*[Cm^R]		Vanhove *et al.,* 2016

Table S4. Plasmids

Plasmid	Description	Reference
pSW23T	$oriV_{R6K\gamma}$; $oriT_{RP4}$; [Cm^R]	Demarre *et al*., 2005
pSWδ*rtxA*	pSW23T; Δ*rtxA GV4G44_v1_300034*	This study
pSWδ*vipA*	pSW23T; Δ*vipA GV4G44_v1_320017*	This study
pSWδ*epsE*	pSW23T; Δ*gtf2 GV4G44_v1_370043*	This study
pMRB-P_{LAC}*gfp*	$oriV_{R6K\gamma}$; $oriT_{RP4}$; $oriV_{pB1067}$; P_{lac}*gfp* [Cm^R]	Le Roux et al., 2011
pMRB-P_{LAC}*gfp*	$oriV_{R6K\gamma}$; $oriT_{RP4}$; $oriV_{pB1067}$; P_{lac}*gfp* [Spt^R]	Le Roux et al., 2011

Table S5. Oligonucleotides

Oligonucleotide	Gene id	Sequence 5'-3'	Description	Organism	Use
EFUfw	AB122066	GAGCGTGAACGTGGTATCAC	EF-1α	*C. gigas*	RT-qPCR of host genes
EFUrv	AB122066	ACAGCACAGTCAGCCTGTGA	EF-1α	*C. gigas*	RT-qPCR of host genes
CGI_10025754 F1	CGI_10025754	GCCCACGAATCTTGCTGAAC	Interleukin 17-1	*C.gigas*	RT-qPCR of host genes
CGI_10025754 R1	CGI_10025754	TTTGGGTAGCGGGTGGAAAG	Interleukin 17-1	*C. gigas*	RT-qPCR of host genes
IL-17 R-86 F	CGI_10021486	CTGTCGCTGCAATGTGATCT	Interleukin 17 receptor	*C. gigas*	RT-qPCR of host genes
IL-17 R-86 R	CGI_10021486	TTTCTTGCCATTCGTTTTCC	Interleukin 17 receptor	*C. gigas*	RT-qPCR of host genes
MyD88like-22_F	CGI_10012722	CGATTGGATTCCACAGAGGT	Myeloid differentiation primary response 88-like	*C. gigas*	RT-qPCR of host genes
MyD88like-22_R	CGI_10012722	CCGGAAGTGACACAGCTTTT	Myeloid differentiation primary response 88-like	*C. gigas*	RT-qPCR of host genes
TNF14-07 F	CGI_10028807	TCCGCTAGGAAGTGCCTTTA	Tumor necrosis factor ligand superfamily	*C. gigas*	RT-qPCR of host genes
TNF14-07 R	CGI_10028807	GGGCTGTATAGCCTTGCAGA	Tumor necrosis factor ligand superfamily	*C. gigas*	RT-qPCR of host genes
NF-kB-49 F	CGI_10016949	CCCAAACAGGAGAAGGTCAA	Nuclear factor-kappa B	*C. gigas*	RT-qPCR of host genes
NF-kB-49 R	CGI_10016949	TTCTTTTGCTCCATGGCTCT	Nuclear factor-kappa B	*C. gigas*	RT-qPCR of host genes
CgLBP F	XM_011416094	AAGTTGTCGACCCGAACACG	Lipopolysaccharide binding protein	*C. gigas*	RT-qPCR of host genes
CgLBP R	XM_011416094	ACGCTAATAACTGGCACTGG	Lipopolysaccharide binding protein	*C. gigas*	RT-qPCR of host genes
CgBPI F	AAN84552.1	GATAGAAATAGGAATGGACGG	Bactericidal permeability increasing protein	*C. gigas*	RT-qPCR of host genes
CgBPI R	AAN84552.1	GTTATAGATCCACGGTGCTCC	Bactericidal permeability increasing protein	*C. gigas*	RT-qPCR of host genes
CgBigdef-1 F	AEE92772.1	TTCGCCTGCTTCCATAATGG	Big defensin-1	*C. gigas*	RT-qPCR of host genes
CgBigdef-1 R	AEE92772.1	GAATAAGGAGTGACCATGAC	Big defensin-1	*C. gigas*	RT-qPCR of host genes
*rtxA-F	GV4G44_v1_300034	GtatcgataagcttgatatcgaattcTTCCG ATCTAGGAGACGGGC	RtxA protein from MARTX cluster	*V. splendidus* 4G4_4	Mutagenesis
*rtxA-R	GV4G44_v1_300034	CccccgggctgcaggaattcTTCTATTCGG TTGCTGCCAG	RtxA protein from MARTX cluster	*V. splendidus* 4G4_4	Mutagenesis
Exr *rtxA-F	GV4G44_v1_300034	AGCCTAGCCGTCGCGTCAAG	RtxA protein from MARTX cluster	*V. splendidus* 4G4_4	Control of mutagenesis

Ext *rtxA-R	GV4G44_v1_300034	TGGCGATCGGCTTCCGCTCG	RtxA protein from MARTX cluster	*V. splendidus* 4G4_4	Control of mutagenesis
*vipA-F	GV4G44_v1_320017	Gtatcgataagcttgatatcgaattc TTCCAGCAACAGGCGATGCG	VipA protein from T6SS	*V. splendidus* 4G4_4	Mutagenesis
*vipA-R	GV4G44_v1_320017	Ccccgggctgcaggaattc ACGGAAAGCAGGTACATTCC	VipA protein from T6SS	*V. splendidus* 4G4_4	Mutagenesis
Ext *vipA-F	GV4G44_v1_320017	ACGTGATGGCTCGGTGGCTC	VipA protein from T6SS	*V. splendidus* 4G4_4	Control of mutagenesis
Ext *vipA-R	GV4G44_v1_320017	TCTGCACCAATGCTTAGTTC	VipA protein from T6SS	*V. splendidus* 4G4_4	Control of mutagenesis
*epsE-F	GV4G44_v1_370043	Gtatcgataagcttgatatcgaattc TTGAGGAGGGACTGGCGCAC	Glycosyltransferase from wbe region	*V. splendidus* 4G4_4	Mutagenesis
*epsE-R	GV4G44_v1_370043	Ccccgggctgcaggaattc CTTGACGGATGAGGGTTACG	Glycosyltransferase from wbe region	*V. splendidus* 4G4_4	Mutagenesis
Ext *epsE-F	GV4G44_v1_370043	TCTCTGATGACTGCTCAACTG	Glycosyltransferase from wbe region	*V. splendidus* 4G4_4	Control of mutagenesis
Ext *epsE-R	GV4G44_v1_370043	TAAATAGACACGAAGGACCC	Glycosyltransferase from wbe region	*V. splendidus* 4G4_4	Control of mutagenesis
4G4_4-370043F	GV4G44_v1_370043	TGCTATTGAGGAGGGACTGG	Glycosyltransferase from wbe region	*V. splendidus* 4G4_4	Strain identification
4G4_4-370043R	GV4G44_v1_370044	CACCTGAACCCAAAAATCGT	Glycosyltransferase from wbe region	*V. splendidus* 4G4_4	Strain identification
4G1_8-10031F	GV4G18_v1_10031	CAGAACTCTCTGGGCATGTG	LysR family transcriptional regulator	*V. splendidus* 4G1_8	Strain identification
4G1_8-10031R	GV4G18_v1_10032	AAAATCACACCCGACTCGAC	LysR family transcriptional regulator	*V. splendidus* 4G1_8	Strain identification

I.3. Complementary result 1. Assessment of the susceptibility to grazing due to O-antigen modifications, in a different genetic background of the population #23

We confirmed that the modification of the O-antigen structure was also determinant in the susceptibility to amoeba grazing in other genetic background within population #23. In the supplemental results of article 1, presented above, we show that the mutation of the *wbe* region results in highly similar O-antigen profiles in two different mutant strains of population #23 and here we corroborate that this alternative structure is also determinant for the susceptibility to grazing of strain 4D1_8.

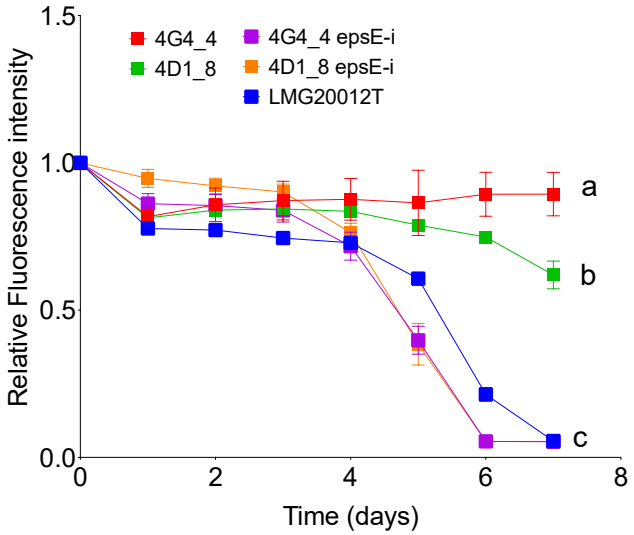

Figure 20. Bacterial resistance to grazing by *Vanella sp* 1411.

Ressistance to amoeba grazing was assessed for *V. splendidus strains* 4D1_8 and *epsE-i* by measuring the fluorescence of the GFP-expressing bacteria after contact with amoebae over 7 days. The strain *V. tasmaniensis* LMG20012T and the published mutant 4G4_4 *epsE-i* were used as a grazing-susceptible and grazing-resistance control, respectively. Results show the mean of three technical replicates ± SD. Data are representative of two independent experiments. Different letters indicate a significant difference, $p<0.001$ (RM-ANOVA).

I.4. COMPLEMENTARY RESULTS 2. RESISTANCE OF VIBRIO POPULATIONS TO OYSTER ANTIMICROBIAL DEFENSES IS INSUFFICIENT TO EXPLAIN HOST ASSOCIATION

These results will be submitted for publication as a short letter, in preparation

Resistance of vibrio populations to oyster antimicrobial defenses is insufficient to explain host association

Daniel Oyanedel-Trigo[1], Laura Chapelet[1], Frédérique Le Roux[2,3], Yannick Gueguen[1], Jérémie Vidal-Dupiol[1], Agnès Delmas[4], Hervé Cottet[5], Guillaume M. Charrière[1] and Delphine Destoumieux-Garzón[1]

[1] Interactions Hôtes-Pathogènes-Environnements (IHPE), Université de Montpellier, CNRS, Ifremer, Université de Perpignan Via Domitia, Montpellier, France.

[2] Ifremer, Unité Physiologie Fonctionnelle des Organismes Marins, ZI de la Pointe du Diable, CS 10070, F-29280 Plouzané, France.

[3] Sorbonne Universités, UPMC Paris 06, CNRS, UMR 8227, Integrative Biology of Marine Models, Station Biologique de Roscoff, CS 90074, F-29688, Roscoff cedex, France.

[4] CNRS UPR 4301, Centre de Biophysique Moléculaire, Rue Charles Sadron, Orléans, France.

[5] IBMM, Université de Montpellier, CNRS, ENSCM, Montpellier, France

Introduction

The capacity to colonize a host is multifactorial. It depends on both host and pathogen factors. As they encounter a new host, microorganisms need to overcome a series of innate immune mechanisms that are conserved across metazoans and serve as a first line of immune defense. These include antimicrobial peptides (AMPs) and pattern-recognition receptors (PRRs) that initiate cellular-based signal transduction cascades connecting microbe recognition signals to expression and secretion of immunomodulatory cytokines and chemokines (Reddick and Alto, 2014). Conversely microbes employ strategies to evade, inhibit or manipulate the innate immune responses. Commonly, counter-measures to host innate immunity include resistance/tolerance to antimicrobials, escape from host recognition (usually by disguising their immunogenic surface components) or active dampening of immune defense, i.e. immune suppression. Those mechanisms have been described and reviewed for a series of human pathogens (Hornef et al., 2002; Reddick and Alto, 2014).

In the continuum of symbiotic interactions, from mutualisms to pathogenicity, microorganisms have evolved the capacity to establish stable interactions with metazoan hosts by selecting

one or several of these strategies to avoid elimination by their host immune system. In marine aquatic environments, vibrios have co-evolved with a diversity of sessile and planktonic metazoans hosts. A thorough analysis of vibrio ecological associations has been recently published by Bruto et al. (2016) in a marine coastal environment used for oyster farming. Some vibrio populations were shown to be positively associated with oysters in health and/or disease, indicating they have evolved the capacity to tolerate their host defenses, which only rely on innate immune mechanisms in the case of mollusks. In contrast, other populations were shown to be negatively-associated with oysters indicating they find better ecological niches in other host species present in phytoplankton and zooplankton, or adopt a free-living style, maybe as a consequence of their inability to tolerate the immune defenses of metazoan hosts present in the ecosystem.

Among vibrios colonizing oysters, one strain referred to as *V. tasmaniensis* LGP32 (Splendidus clade) adopts an original life-style as it enters oyster immune cell as part of its pathogenic process (Duperthuy *et al.*, 2011). As a possible requirement for its intracellular stages, LGP32 was shown to be equipped with mechanisms of resistance to oyster AMPs (Duperthuy *et al.*, 2010; Vanhove *et al.*, 2015). The most potent mechanism relies on trapping of AMPs through secretion of outer membrane vesicles that bind and sequester AMPs (Vanhove *et al.*, 2015). *V. tasmaniensis* LGP32 was also shown to resist ROS and heavy metals present in oyster phagocytes and/or plasma, and these mechanisms of resistance are required for efficient host colonization (Vanhove *et al.*, 2016). Thus, resistance/tolerance to antimicrobials is essential for LGP32 to colonize oysters. In other species of vibrios colonizing oysters, some virulence factors were shown to play a role in host colonization. In the species *V. crassostreae* and *V. splendidus* (Lemire *et al.*, 2015; Bruto *et al.*, 2018), virulence factors include toxins of the MARTX family as well as proteins of unknown functions such as the R5-7 protein (Bruto *et al.*, 2017, 2018). Still, the relative weight of virulence and resistance to host defenses in favoring colonization of oysters by environmental vibrios remains unknown. Moreover, little attention has been paid until now to non-virulent strains that may use alternative ways of immune evasion like avoiding host recognition to efficiently colonize their host. Exploring the diversity of immune evasion processes along a gradient of virulence in natural populations of vibrios is now needed to understand the multiple factors that govern host colonization and may distinguish the evolution towards commensalism versus virulence among vibrios.

With that objective, we explored the complex interface between vibrios and a metazoan host, the oyster. We used a series of 6 ecological populations of vibrios known to be positively (*V. crassotreae, V. splendidus* pop23 and pop24) or negatively-associated with oysters (*V. breogani, V. orientalis, A. fisheri*) although present in the oyster environmental waters. By phenotyping strains for resistance to antimicrobials (AMPs, ROS, and heavy metals) we

showed that resistance to oyster antimicrobials is a population-specific trait insufficient to recapitulate host associations. Overall, the main factors explaining association to oysters were resistance to ROS, virulence and surface charge.

Materials and methods

Strains and growth conditions

Vibrio populations used in this part of the study were taxonomically assigned to the species *V. crassostreae*, *V. splendidus*, *V. breogani*, *V. orientalis* and *V. fischeri* (Bruto *et al.*, 2017). Strains were grown at 20°C in Zobell broth or agar (4g/L bactopeptone and 1g/L of yeast extract in artificial seawater, pH 7.6) and with agitation at 150 rpm. Modified Zobell broth used for Minimal Inhibitory Concentration tests contained 1.3g/L bactopeptone and 0.3 g/L of yeast extract in artificial seawater, pH 7.6. Saline Peptone Water (SPW) medium agar was used for copper and zinc sensibility assays (bacto peptone 1.5% P7vol Bio-Rad, NaCl 2.92% P/vol Bio-Rad, Agar 1.5% P/vol Bio-Rad, pH 7.2)

Cg-BigDef1 synthesis

The antimicrobial peptide Cg-BigDef1 (10.7 kDa) secreted by oyster hemocytes was produced by chemical synthesis by Agnès Delmas in the Center of Molecular Biophysics (CMB) of the CNRS in Orléans – UPR 4301 according to the recently published procedure (Loth *et al.*, 2020).

Determination of the Minimal Inhibitory Concentration

From stationary phase bacterial cultures, fresh cultures were started with a 1:100 ratio of inoculum in Zobell medium, respectively. Cultures were incubated at 20° and 150 rpm until an OD_{600} between 0,2 - 0,4 corresponding to exponential phase of growth. Cultures in exponential phase were adjusted to a theoretical OD_{600} :0.001 in modified Zobell medium. Of this bacterial suspension 90 µl were placed into 96 well plates and 10 µl of a serial dilution of *Cg*BigDef-1 were added to each well. Plates were incubated 18 hrs at 20° C with shaking at 150 rpm. After incubation time, plates were read at OD_{600} to determine the minimal inhibitory concentration of *Cg*BigDef-1 for each strain.

Susceptibility to Copper and Zinc

Bacterial cultures in stationary phase were washed twice with sterile seawater (SSW), by centrifugation at 1500 x g, 20ºC, to eliminate Zobell medium from cultures. After, the OD600 was measured and adjusted to 1 in SSW. After adjusting the OD, 500 µl of each culture were added to Saline Peptone Water (SPW) medium agar plates supplemented with NaCl to a final concentration of 0.5M (bacto peptone 1.5% P7vol Bio-Rad, NaCl 2.92% P/vol Bio-Rad, Agar 1.5% P/vol Bio-Rad, pH 7.2)

Cultures were homogeneously spread, and the excess liquid not absorbed was removed. After, in sterile conditions, air-dried cellulose disc previously soaked for 30 min in a 0.2 µM filtrated 50 mM copper sulfate (CuSO4) or 50 mM Zinc sulfate solution (cupric sulfate pentahydrate, 99%, C-7631 Sigma – Aldrich; Zinc sulfate heptahydrate, 99%, 205986-50g Sigma – Aldrich) were placed per plate. Petri dishes were incubated for 18 h at 20ºC and the size of the inhibition zone was measured for each strain with a digital caliper.

Susceptibility to oxygen reactive species. Bacterial cultures (100ul) in stationary phase were homogeneously plated in Zobell agar. A cellulose disc soaked with 10ul of a solution of cumene hydroperoxide at 160 uM (technical grade 80%, reference 247502-100G Sigma-Aldrich was placed in the center of the petri dish. After 18 hours of incubation at 20ºC, the size of the inhibition zone was measured. The results represent the average of three independent experiments.

Cytochrome C binding assay. Cytochrome C has a net charge of +8 and two different type of interaction characterized in model membranes bearing acid phospholipids like cardiolipin present in mitochondrial and bacterial membranes (Mileykovskaya and Dowhan, 2010). At neutral pH the interaction is electrostatic and dependent on the negative surface charge density and reversible by the addition of competing anionic species like ATP with the A-site of cyt c, by other hand, at acidic pH cyt c bound by its C-site by hydrogen bonds and hydrophobic interaction that cannot be reversed by ATP or salt addition. Stationary phase cultures were wash twice by centrifugation (1500 x g, 20ºC) with 20 mM MOPS buffer supplemented with sucrose for a final osmolarity of 450 mOsm to make it compatible with the hyper saline environment of marine bacteria. After washing, OD600 was measured, cultures were centrifuged and pellet suspended in MOPS sucrose buffer adjusting to an OD600 = 6. After, 900 µl of bacterial suspension were placed in 1.5 mL polipropilene microcentrifuge tubes. Cytochrome c solution was prepared in MOPS Sucrose buffer to a concentration of 5 mg/mL and added to bacterial suspension for a final concentration of cytochrome c of 0.5

mg/mL. Tubes were incubated 15 minutes at 20ºC and then centrifuged at 6000 x g at room temperature for 15 min, finally 300 ul of supernatant were placed in triplicate in to 96 wells plates and the OD530 was measured in a TECAN micro plate reader. The percentage of cytochrome C bound to bacteria was calculated relative to the OD530 value of a 0.5 mg/mL cytochrome c control solution not exposed to bacteria.

Statistical analyses

Redundancy analysis (hereafter named RDA) was used to investigate the assemblage of the different bacterial strains (positive or negative association to oysters). RDA was performed on AMP resistance, ROS resistance, copper resistance, zinc resistance, surface charge and virulence. Then significant variables (i.e., variables that significantly explained changes in the distribution of strains, oyster versus water-column) were identified using a forward-selection procedure (999 permutations), implemented in the R "vegan" package and in the "rda" and "ordiR2step" functions. For all analyses, the threshold significance level was set at 0.05.

Results

In our work with the collection of vibrio populations characterized by Bruto *et* al. (2017), we hypothesized that resistance to oyster antimicrobial defenses could be a major explicative factor for the preferential association of certain populations to the oyster tissues, while susceptibility to these antimicrobials could be a common trait of vibrio populations that are excluded from the oyster. For that, we used 30 strains representative of six populations of vibrios that display positive (*V. crassostreae, V. splendidus* Pop #23 and Pop #24) or negative associations (*V. breogani, V. orientalis, A. fisheri*) with oyster tissues (Bruto *et al.*, 2017). These included both virulent and non-virulent populations of vibrios (Bruto et al., 2016). Every strain was phenotyped for its resistance to the oyster antimicrobial peptide Cg-BigDef1, ROS (cumene hydroperoxyde), copper and zinc, which all participate in oyster immune cell defenses against pathogenic vibrios (Vanhove et al., 2016).

Individual resistance phenotypes were found to be population-specific traits presenting little to no intra-population variability (Figure 21A). For some populations, resistance perfectly fitted with our initial hypothesis. Thus, strains of *V. splendidus* pop23, a population positively associated with oysters were highly resistant to antimicrobial peptides, ROS and heavy metals. By contrast, strains of *V. breogani*, a population negatively associated with oysters, were among the most susceptible to ROS and heavy metals. However, some other population like the virulent *V. splendidus* pop24, positively associated with oysters, showed more mosaic traits of resistance (e.g. high resistance to heavy metals and ROS but low

resistance to AMPs.

Overall, when considering all vibrio strains independent of their taxonomic affiliation, only resistance to ROS discriminated significantly vibrios according to their known association with oysters ($p<0.0001$) (Figure 22A).

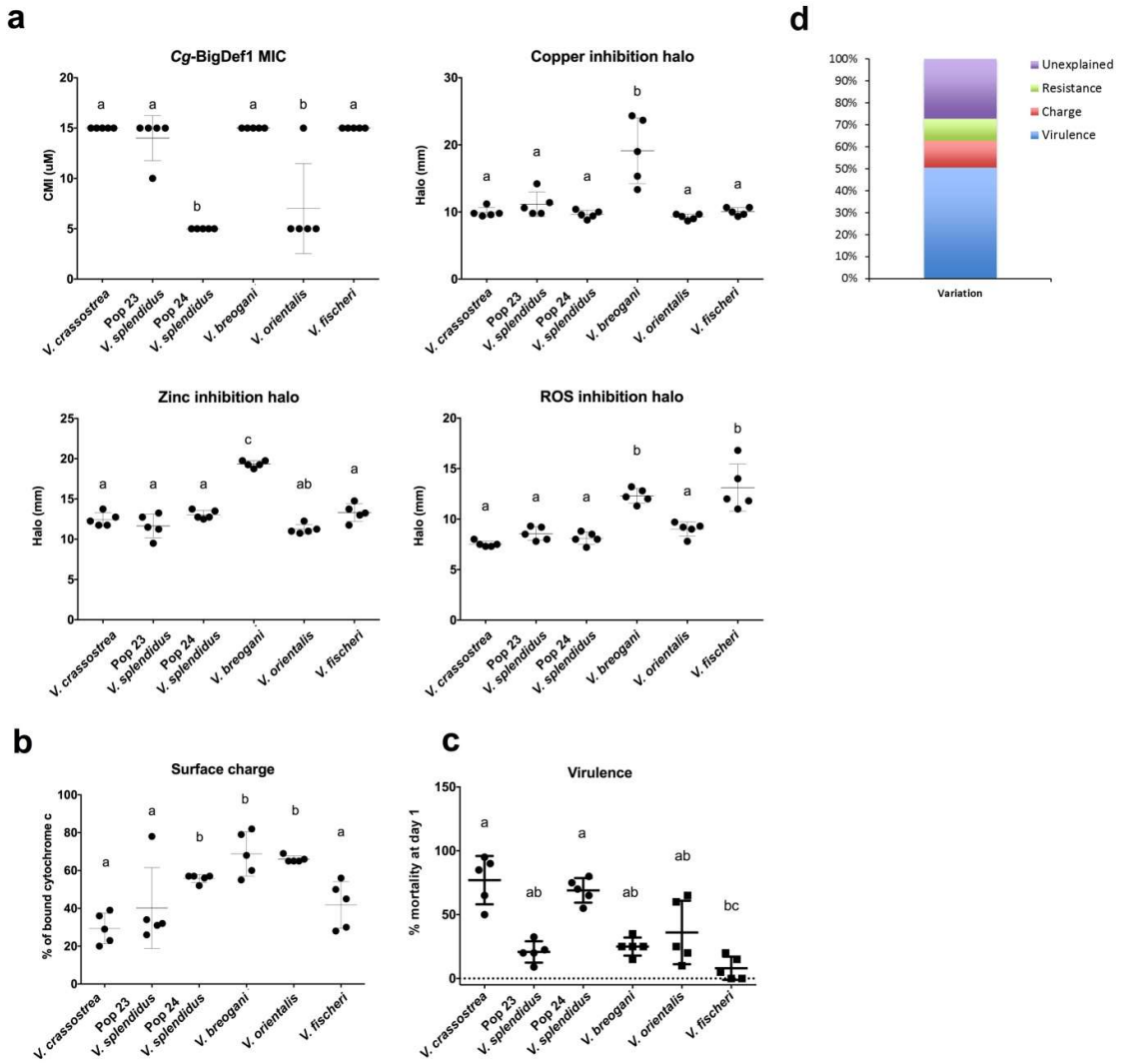

Figure 21. Relative weight of resistance to antimicrobials, virulence and surface charge in vibrio association to oysters.

6 vibrio populations (30 strains) were phenotyped. (a) Resistance to antimicrobials. Minimum Inhibitory Concentration of Cg-Bigdefensin1, inhibition halo of Copper, Zinc and ROS (cumene hydroperoxide). Statistical significance ($p<0.05$) were determined by ANOVA one-way with a Holm-Sidak's post test and designated by different letters. (b) Relative surface charge of vibrio strains revealed by cytochrome c binding. Statistical significance ($p<0.05$) determined by non-parametric Mann Whitney and designated by an asterisk. (c) General lineal model generated including antimicrobial resistance, surface charge and virulence data. (c) Virulence in oyster experimental infections. Mortalities were monitored at day 1

after infection. (d) RDA analysis of factors contributing to vibrio association to oysters. All parameters of resistance, virulence and surface charge were included.

To better estimate the relative weight of resistance to host antimicrobials in the capacity of vibrios to colonize oysters, we included **other parameters influencing host-microbe interactions such as strain virulence and surface charge**. As a proxy of strain resistance, we used a resistance index defined as the sum of every single resistance trait. For strain virulence, we used the mortality induced by intramuscular injection of vibrios, previously determined (Bruto et al., 2017). Finally, for surface charge we used the strain ability to bind to the cationic protein cytochrome C as a proxy (Saar-Dover *et al*., 201; Cullen *et al*., 2015). Only the last two parameters discriminated significantly ($p<0.01$) vibrio strains according to habitat. By using a general linear model, we showed that vibrio association to oysters are explained at 50.4 % by strain virulence while surface charge explains 12.3 % and resistance to host antimicrobials only 10 % of the association to oysters (Figure 21D). Therefore, the capacity of vibrios to colonize oysters depends on a multiplicity of factors that includes resistance to ROS, virulence factors and surface determinants, which are evocative of distinct strategies of avoidance of the host immune system.

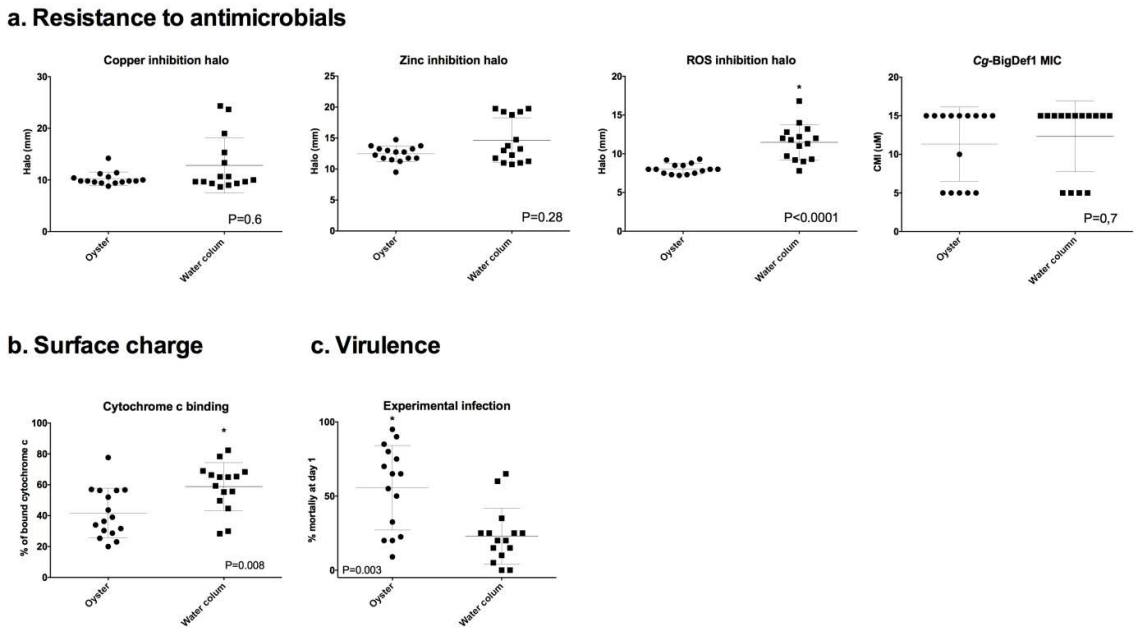

Figure 22. Resistance to ROS, virulence and surface charge discriminate vibrios according to association to oysters

6 vibrio populations (30 strains) were phenotyped and grouped by preferential habitat (a) Resistance to

antimicrobials. Minimum Inhibitory Concentration of Cg-Bigdefensin1, inhibition halo of Copper, Zinc and ROS (cumene hydroperoxide). (b) Relative surface charge of vibrio strains revealed by cytochrome c binding. (c) Virulence in oyster experimental infections. Mortalities were monitored at day 1 after infection.Statistical significance ($p<0.05$) determined by non-parametric Mann Whitney and designated by an asterisk.

Discussion

Based on an *in vitro* approach, which obviously does not recapitulate the complexity of *in vivo* interactions, we found that resistance to oyster innate antimicrobial defenses was insufficient to discriminate environmental vibrios according to their known association with oysters. This result contrasted with the many examples of both commensal and pathogenic interactions between bacteria and metazoan hosts that have been shown to depend on such resistance phenotypes. For instance, resilience of Bacteroidetes in the mammalian gut was shown to depend on resistance to AMPs (Cullen *et al*., 2015); *Mycobacterium tuberculosis* survival inside macrophages depends on resistance to copper and zinc (Neyrolles *et al*., 2015), etc. It also contrasted with our earlier studies of the oyster opportunistic pathogen *V. tasmanienis* LGP32, which identified diverse mechanisms of resistance to oyster AMPs, ROS, and heavy metals, the later having important consequences on the capacity of LGP32 to colonize its host (Duperthuy *et al*., 2010; Vanhove *et al*., 2015; Vanhove *et al*., 2016).

Interestingly, resistance to oyster innate antimicrobial defenses was shown here to be a population-specific trait, and until now only *V. tasmaniensis* LGP32 has been studied in details for its host-pathogen interactions with oysters. This strain has evolved the capacity to enter and survive inside oyster immune cells, the hemocytes, as a necessary stage in its infectious process (Duperthuy *et al*., 2011). It is therefore likely that resistance to antimicrobials is a trait essential for vibrios adopting hemocyte intraphagosomal stages, the phagosome being the recipient of hydrolytic enzymes, AMPs and heavy metals (Bachère *et al*., 2015). Likewise, *V. crassostreae* was also reported to inhabit hemolymph and gills (Bruto *et al*., 2017), which are antimicrobial tissues in oysters (Destoumieux-Garzón *et al*., 2014) and not surprisingly we found it highly resistant to antimicrobials in the present study. But little is still known on the tissue niches of other vibrio-populations associated with oysters such as the *V. splendidus* pop23 and 24 from this study.

Resistance to antimicrobials may therefore be not as discriminant for vibrio populations having different tissue tropism, for example populations that would colonize tissue poor in antimicrobials (i.e. not colonizing hemolymph nor epithelia). An interesting finding is the contrast between *V. splendidus* pop23 (associated with oysters outside infectious events) and

pop24 (associated with oysters during mortality events) in terms of resistance to Cg-BigDef1. We recently showed that Cg-BigDef1 is repressed by OsHV-1 virus, which triggers bacterial colonization during infectious episodes (de Lorgeril *et al.* 2018). It is therefore likely that opportunistic pathogens including strains of pop24 benefit from such a repression of oyster antimicrobial defenses, whereas other resident population like pop23 have intrinsic resistance capacities that help them colonize oyster tissues of healthy oysters. Finally, outside the oyster-vibrio interactions studied here, we cannot ignore that interactions with other metazoan hosts occur in the water column (e.g. copepods), which share many innate immune effectors with mollusks. By applying similar selective pressures, these interactions have likely shaped resistance phenotypes among populations negatively associated with oysters. Altogether, this illustrates that the multiple biotic interaction taking place in the aquatic environment do not allow for discrimination of vibrio oyster-association on the basis of the only resistance trait.

Individual resistance phenotypes were found to coincide with vibrio population delineation, showing low to no variability within each population. Populations negatively associated with oysters were susceptible to at least one the main antimicrobial tested (Figure 21A). Strains of the algal specialist, *V. breogani,* were among the most susceptible to ROS and heavy metals. In contrast, two out of three populations positively associated with oysters, namely *V. splendidus* Pop #23 and *V. crassostreae*, were highly resistant to all antimicrobials tested (*Cg*BigDef-1, ROS, zinc and copper), which may confer a great advantage in colonizing their molluscan host. Only *V. splendidus* Pop #24, positively associated with oysters, showed high resistance to copper, zinc and ROS but lower resistance to *Cg*BigDef-1). Noteworthy, this population, like *V. crassotreae* (Lemire *et al.*, 2015), colonizes oysters affected by the POMS (Bruto *et al.*, 2017), a disease in which the OsHV-1 virus suppresses *Cg*BigDef-1 expression (de Lorgeril *et al.*, 2018). Therefore, the resistance profile of vibrio populations positively associated with oysters agrees with their ecology and variations of their niche biochemical landscape (determined by the physiology of their healthy or immune-compromized host). This suggests a role of homeostasis of antimicrobial defenses in shaping the *Vibrio* communities associated with oysters.

To determine the contribution of Big-defensins in control of the commensal microbiota and opportunistic pathogens like vibrios, is one of the objectives of the doctoral project of Noémie de San Nicolas, that is currently been developed in our team. Through an RNAi approach, they aim to block *in vivo* the transcription of Big-defensins and evaluate how it affects the stability of the associated microbiota and the success of infection of known opportunistic pathogens, functionally testing the immunosuppression hypothesis.

SECTION II. THE ROLE OF CYTOTOXICITY IN *VIBRIO* OF THE SPLENDIDUS CLADE ASSOCIATED WITH POMS

II.1. CONTEXT AND OBJECTIVE OF THE STUDY

Oysters possess a remarkable capacity to maintain an immune homeostasis in the presence of the abundant and diverse microbial communities that are associated with its tissues. The biotic and abiotic factors that can lead into the loss of this homeostasis are of particular interest as they are key risk factors for the onset of mass mortalities.

As described earlier, during POMS, the OsHV-1 infection of oysters causes immunosuppression disrupting immune homeostasis and favoring proliferation of pathogenic bacteria (de Lorgeril *et al*, 2018).

Within the bacteria associated with this dysbiosis, vibrios from the Splendidus clade, notably *V. tasmaniensis* and *Vibrio crassostreae,* are among the most studied.

One strain, *V. tasmaniensis* LGP32, originally isolated from a mortality event in 2004 causes mortalities when injected into oysters (Gay *et al*. 2004). It is a facultative intracellular pathogen cytotoxic to hemocytes (Duperthuy *et al*., 2011; Vanhove et al. 2016). The sequencing of its genome and the development of molecular tools for genetics investigations (Le Roux *et al.* 2007, 2009) established this strain as a model of hemocyte-vibrio interaction in a pathogenic context (Duperthuy *et al*., 2010, 2011; Vanhove *et al*., 2015, 2016).

The other well described species, *V. crassostreae,* has not been characterized on its specific interactions with hemocytes. Yet, it has been shown that functionally cohesive populations of *V. crassostreae* replace the commensal communities in the oyster during disease and share virulence as a core function with an extracellular protein of unknown function, encoded by the gene *r5.7,* and a plasmid (pGV1512), both necessary for full virulence (Bruto *et al*., 2017). These virulence mechanisms were characterized in the strain *V. crassostreae J2-9* isolated by Lemire *et al*. (2015). Interestingly *r5.7* which is widely distributed among virulent populations of the Splendidus clade, and the virulence plasmid pGV1512, characteristic of virulent *V. crassostreae* strains are absent from *V. tasmaniensis,* suggesting that virulence in this these two species is achieved through different mechanisms that determine the success of infection.

Puzzled by the varrying association of these two *Vibrio* spieces to POMS-diseased oysters, we performed a broader study to characterize the pathogenic mechanisms used by *V.*

crassostreae and *V. tasmaniensis.* We used 4 virulent strains as well a non-virulent strain from each species with which we developed an integrative study of the host-microbe interaction. We described the cellular interactions and molecular changes that occur in the host and the bacteria during the within-host phase of the infection (*in vivo* dual RNAseq), along with functional validation of the bacterial candidate genes newly identified (gene knock-down).

In article 2, we present the results of this study. Our data, allowed us to conclude that within the Splendidus clade, *V. crassostreae* and *V. tasmaniensis* had acquired species-specific mechanisms that seems to converge in a common objective, which is to suppress the cellular defenses of the oysters using different cytotoxic mechanisms for a successful colonization during pathogenesis. These species-specific mechanisms rely on R5.7 in *V. crassostreae* and a newly identified T6SS encoded by chromosome 1 in *V. tasmaniensis.*

In complementrary results, we have identified a T6SS-secreted effector responsible for *V. tasmaniensis* cytotoxicity toward hemocyte. However, this effector does not seem to be required for virulence *in vivo*. These preliminary results open the way to new projects on the characterization of T6SS effectors involved in *V. tasmaniensis* pathogenesis

II.2. ARTICLE N°2. SPECIES-SPECIFIC MECHANISMS OF CYTOTOXICITY TOWARD IMMUNE CELLS DETERMINE THE SUCCESSFUL OUTCOME OF VIBRIO INFECTIONS.

By Rubio, T.*, **Oyanedel, D.*,** Labreuche, Y., Toulza, E., Luo, X., Bruto, M., Chaparro, C., Torres, M., de Lorgeril, J., Haffner, P., Vidal-Dupiol, J., Lagorce, A., Petton, B., Guillaume, M., Jacq, A., Le Roux, F., Charrière, G.M., Destoumieux-Garzón, D. (2019).

* co-first authors

Proceedings of the National Academy of Sciences, 116(28), 14238–14247.

Species-specific mechanisms of cytotoxicity toward immune cells determine the successful outcome of *Vibrio* infections

Tristan Rubio[a,1], Daniel Oyanedel[a,1], Yannick Labreuche[b,c], Eve Toulza[a], Xing Luo[d], Maxime Bruto[c], Cristian Chaparro[a], Marta Torres[a,d,e], Julien de Lorgeril[a], Philippe Haffner[a], Jeremie Vidal-Dupiol[a], Arnaud Lagorce[a], Bruno Petton[b], Guillaume Mitta[a], Annick Jacq[d], Frédérique Le Roux[b,c,2], Guillaume M. Charrière[a,2], and Delphine Destoumieux-Garzón[a,2]

[a]Interactions Hôtes Pathogènes Environnements (IHPE), University Montpellier, CNRS, Ifremer, University Perpignan Via Domitia, F-34090 Montpellier, France; [b]Unité Physiologie Fonctionnelle des Organismes Marins, Ifremer, F-29280 Plouzané, France; [c]Station Biologique de Roscoff, Integrative Biology of Marine Models, UMR 8227, CNRS, Université Pierre et Marie Curie Paris 06, Sorbonne Universités, 29688 Roscoff, France; [d]Institute for Integrative Biology of the Cell, Commissariat à l'Énergie Atomique et aux Énergies Alternatives, CNRS, University Paris-Sud, Université Paris–Saclay, 91198 Gif-sur-Yvette, France; and [e]Department of Microbiology, Faculty of Pharmacy, University of Granada, 18071 Granada, Spain

Edited by Margaret J. McFall-Ngai, University of Hawaii at Manoa, Honolulu, HI, and approved May 21, 2019 (received for review April 5, 2019)

Vibrio **species cause infectious diseases in humans and animals, but they can also live as commensals within their host tissues. How *Vibrio* subverts the host defenses to mount a successful infection remains poorly understood, and this knowledge is critical for predicting and managing disease. Here, we have investigated the cellular and molecular mechanisms underpinning infection and colonization of 2 virulent *Vibrio* species in an ecologically relevant host model, oyster, to study interactions with marine *Vibrio* species. All *Vibrio* strains were recognized by the immune system, but only nonvirulent strains were controlled. We showed that virulent strains were cytotoxic to hemocytes, oyster immune cells. By analyzing host and bacterial transcriptional responses to infection, together with *Vibrio* gene knock-outs, we discovered that *Vibrio crassostreae* and *Vibrio tasmaniensis* use distinct mechanisms to cause hemocyte lysis. Whereas *V. crassostreae* cytotoxicity is dependent on a direct contact with hemocytes and requires an ancestral gene encoding a protein of unknown function, *r5.7*, *V. tasmaniensis* cytotoxicity is dependent on phagocytosis and requires intracellular secretion of T6SS effectors. We conclude that proliferation of commensal vibrios is controlled by the host immune system, preventing systemic infections in oysters, whereas the successful infection of virulent strains relies on *Vibrio* species-specific molecular determinants that converge to compromise host immune cell function, allowing evasion of the host immune system.**

T6SS | toxin | dual RNA-seq | cytolysis | pathogenesis

Vibrionaceae (hereafter vibrios) are ɣ-proteobacteria ubiquitous in oceans and marine coastal environments. They are free-living or associated with organic particles (sea snows) and organisms (1), in the latter case establishing a wide range of mutualistic, commensal, and pathogenic interactions with their hosts. The partnership between the luminous bacterium *Vibrio fischeri* and the Hawaiian bobtail squid *Euprymna scolopes* has been used to study mutualistic symbiosis in animals (2, 3). In contrast, some *Vibrio* species, including *Vibrio cholerae*, cause disease in humans (4). Other *Vibrio* species cause disease in wild and farmed marine animals including corals, shrimp, mollusks, and fishes, having significant ecological and economic consequences (5–7). In this context, the oyster *Crassostrea gigas* provides a model for studying the interactions of *Vibrio* species with an ecologically relevant host, specifically to understand their disease-causing properties (8).

In oysters, maintenance of homeostatic interactions between the microbiota and host immunity is poorly understood (9), and can be disrupted by abiotic and biotic factors, including pathogenic agents. For example, in oysters with Pacific oyster mortality syndrome, a *Herpes* virus was shown to cause immune suppression, enabling microbiome dysbiosis and proliferation of bacteria such as *Vibrio crassostreae* (10). This species and other closely related species of the Splendidus clade (e.g., *Vibrio splendidus*, *Vibrio tasmaniensis*, and *Vibrio cyclitrophicus*) have been repeatedly isolated from diseased oysters, and their virulence confirmed in experimental oyster infections (11–14).

Most oyster–vibrio interactions have been studied by using a single strain, *V. tasmaniensis* LGP32, as a model. This strain is a facultative intracellular pathogen of hemocytes, oyster immune cells (15). Several LGP32 genes conferring resistance to reactive oxygen species (ROS) and heavy metals were shown to be required for protection against killing by hemocytes (16). Moreover, inside phagosomes, the LGP32 strain undergoes membrane remodeling

Significance

Vibrio **species are causal agents of important infectious diseases in humans and animals. Here, we have studied *Vibrio* infections in an ecologically relevant model host, oyster, for which natural virulent *Vibrio* strains are available. We have shown that virulent *Vibrio* species use different mechanisms to evade host cellular defenses. These mechanisms relied on distinct molecular determinants shared between strains of the same *Vibrio* species, but not between different species. The different mechanisms nonetheless converged on the same crucial outcome, immune cell lysis. Such cytotoxicity enabled virulent strains to cause systemic infections. Species-specific mechanisms that actively target host immunity could be more common than thought among *Vibrio* species, including human pathogens.**

Author contributions: A.J., F.L.R., G.M.C., and D.D.-G. designed research; T.R., D.O., Y.L., E.T., X.L., M.B., M.T., J.d.L., P.H., A.L., B.P., A.J., F.L.R., G.M.C., and D.D.-G. performed research; C.C. contributed new analytic tools; T.R., D.O., E.T., M.B., C.C., J.V.-D., A.L., G.M., A.J., F.L.R., G.M.C., and D.D.-G. analyzed data; and T.R., D.O., Y.L., E.T., G.M., A.J., F.L.R., G.M.C., and D.D.-G. wrote the paper.

The authors declare no conflict of interest.

This article is a PNAS Direct Submission.

Data deposition: The data reported in this paper have been deposited in the Genbank database (nucleotide accession nos. SEOP00000000, SESM00000000, SESL00000000, and VARQ00000000) and SRA database (BioProject accession no. PRJNA515169, SRA accession nos. SRR8551076–SRR8551093; BioProject accession no. PRJNA521688, SRA accession nos. SRR8567597–SRR8567602; BioProject accession no. PRJNA521693; SRA accession nos. SRR8573808–SRR8573813).

[1]T.R. and D.O. contributed equally to this work.

[2]To whom correspondence may be addressed. Email: frederique.le-roux@sb-roscoff.fr, guillaume.charriere@umontpellier.fr, or ddestoum@ifremer.fr.

This article contains supporting information online at www.pnas.org/lookup/suppl/doi:10.1073/pnas.1905747116/-/DCSupplemental.

that confers resistance to host antimicrobial peptides (17). This strain was shown to be cytotoxic to hemocytes (16), but the mechanisms causing cytotoxicity remain unknown, and it remains unclear whether other strains belonging to *V. tasmaniensis* or to the Splendidus clade as a whole are also intracellular pathogens and cytotoxic to hemocytes. Within the Splendidus clade, virulence is an ancestral trait that has been lost in several species (12). The ancestrally acquired *r5.7* gene, which encodes for an exported protein of unknown function, is necessary for virulence across the entire Splendidus clade (12, 14). The *r5.7* gene is absent from *V. tasmaniensis*, although this species includes virulent strains, suggesting that virulence relies, at least in part, on alternative mechanisms. Thus, to understand the basis of *Vibrio*-driven diseases, it is necessary to identify the specific determinants of virulence of the species belonging to the Splendidus clade and their potential host target(s).

An effective strategy to characterize different virulence pathways is to compare the genomes of closely related strains with potentially distinct virulence mechanisms. Complementary information can be obtained through global analyses of bacterial and host transcriptional responses, i.e., dual transcriptomics. Indeed, bacterial colonization has been shown to have substantial transcriptional effects on host and microorganisms. Thus, simultaneously measuring host and pathogen gene expression by using dual RNA-seq provides useful insights into the physiological changes that occur during the course of an infection, as well as the response of such changes to each other (18), which can be tested by using gene knock-out experiments.

In the present study, we have characterized the within-host cellular and molecular mechanisms leading to colonization success in oysters infected with 2 *Vibrio* species belonging to the Splendidus clade, *V. tasmaniensis* and *V. crassostreae.* By using an integrative approach, we provide a cellular and molecular description of the changes occurring in host and bacterial physiologies during the infection. Our results show that all virulent strains from both species actively repress host cellular defenses by killing hemocytes and colonize oyster tissues. We have found that the process of immune evasion and colonization is accompanied by the repression of a series of antibacterial defenses and manipulation of metal and ROS homeostasis. Interestingly, we have also identified distinct genetic determinants required for bacterial virulence and cytotoxicity in both vibrio species. Taken together, our results show that vibrios have acquired species-specific virulence mechanisms that converge in a common end, i.e., alteration in key cellular defenses in oysters.

Results and Discussion

Differential Cytotoxicity of Virulent *Vibrio* Strains. Upon being phagocytized, the virulent *V. tasmaniensis* LGP32 strain causes high levels of hemocyte cytotoxicity (16). To determine if hemocyte cytotoxicity is a common feature of *V. tasmaniensis* and *V. crassostreae*, hemocytes were exposed to 4 virulent strains of each species, as well as a closely related but nonvirulent strain as a control (Fig. 1*A*). Only virulent strains induced hemocyte lysis (Fig. 1*B*). Nonetheless, the *V. crassostreae* J2-9 strain induced hemocyte lysis significantly more rapidly than the *V. tasmaniensis* LGP32 strain (Fig. 1*C*), Furthermore, treatment of hemocytes with cytochalasin D, which inhibits phagocytosis, strongly reduced the cytotoxicity of all *V. tasmaniensis* strains (RM-ANOVA P value $<$ 0.001; Fig. 1*B*) but had no effect on *V. crassostreae* cytotoxicity. *V. crassostreae* J2-9 secretion products alone were unable to induce cytotoxicity (*SI Appendix*, Fig. S1), prompting us to ask whether cellular contact was required for J2-9 to kill hemocytes. Transwell experiments revealed that J2-9 cytotoxicity was significantly reduced in the absence of contact with hemocytes (RM-ANOVA P value < 0.01; Fig. 1*D*). Thus, although both species have major lytic effects on oyster hemocytes, their cytotoxicity is exerted through different mechanisms.

Virulent Vibrios Escape Hemocyte Aggregation and Cause Systemic Infection. To explore the pathogenesis of the virulent strains, we compared their histopathological effects versus those of nonvirulent strains. Strains were first injected into oysters from the same biparental family to reduce host genetic variability. Virulent strains (*V. tasmaniensis* LGP32 and *V. crassostreae* J2-9) induced mortality within 1 d and reached a plateau after 2–3 d (Fig. 2*A*). No significant differences were observed in the kinetics and rate of mortality induced by either of the strains, with ∼40% of oysters surviving after 3 d (log-rank test, $P = 0.802$; Fig. 2*A*). No mortalities were recorded in oysters injected with nonvirulent strains (LMG20012T, J2-8; Fig. 2*A*). The similarity in virulence of the 2 strains was confirmed in 2 other families of oysters, suggesting that virulence phenotypes do not depend on the genetic background of the oysters (*SI Appendix*, Fig. S2).

Bacterial load and tissue damages were analyzed 8 h after injection, before the first mortality occurred. Similar bacterial loads were observed for virulent and nonvirulent vibrios, with 1 copy of the vibrio genome per 25–50 copies of the oyster genome (*SI Appendix*, Table S1). However, localization of bacteria and damages to oyster tissues differed markedly between virulent and nonvirulent strains. Both virulent strains, LGP32 and J2-9, spread between muscle fibers and caused tissue disorder with loss of cellular integrity in the adductor muscle around the injection site (Fig. 2*B*). Moreover, a systemic and massive colonization of the conjunctive tissue was observed around the kidney, the digestive gland, the gonad, and under the basal lamina of the gut (Fig. 2*B*). In contrast, the nonvirulent strains LMG20012T and J2-8 did not cause any detectable tissue damage beyond the lesion caused by the needle injection in the muscle. These strains were not detected in histological sections or were restricted to the needle path within the adductor muscle (Fig. 2*B*). Instead, they were found in large hemocyte aggregates in the pericardial cavity, and, for J2-8, the kidney, aggregates that were not observed in oysters injected with virulent strains (Figs. 2*B* and 3*A*). These cell aggregates are reminiscent of extracellular DNA traps [referred to as Neutrophil extracellular traps (NETs) in mammals], which can bind and neutralize pathogenic bacteria and microorganisms, a defense mechanism conserved across species and recently observed in mollusks (19). In oysters, such DNA traps were shown to contain antimicrobial H1- and H5-like histones active against vibrios (20). Thus, our data suggest that virulent vibrios escape from hemocyte control and invade the oyster conjunctive tissue, whereas nonvirulent vibrios are contained within hemocyte aggregates, which we hypothesize prevent tissue colonization and associated tissue damage. In vivo, both virulent strains were highly cytotoxic to hemocytes. Indeed, *V. crassostreae* J2-9, but not the nonvirulent J2-8 strain, caused significant damage to circulating hemocytes within 8 h of oyster infection (Fig. 3*B*), consistent with previous observations for *V. tasmaniensis* LGP32 (16). In histological sections, *V. crassostreae* J2-9 was mainly observed outside hemocytes whereas *V. tasmaniensis* LGP32 and the nonvirulent strains J2-8 and LMG20012T were observed to have been heavily phagocytized (Fig. 3*A*). Therefore, our in vivo data are consistent with the cell contact-dependent and phagocytosis-dependent cytotoxicity observed in vitro for *V. crassostreae* and *V. tasmaniensis*, respectively (Fig. 1).

Virulent Vibrios Bypass Host Defenses. The outcome of an infection depends on a series of complex host and bacterial factors that coordinate and fine-tune host–pathogen interactions (21, 22). Herein, by implementing dual RNA-seq in an in vivo infection, we were able to analyze the mechanisms underpinning colonization success by vibrios in pathological and nonpathological contexts.

We focused on host responses by comparing the transcriptomes of oysters injected with vibrios (virulent strains LGP32 or J2-9 or nonvirulent strains LMG20012T or J2-8) versus that of mock-infected

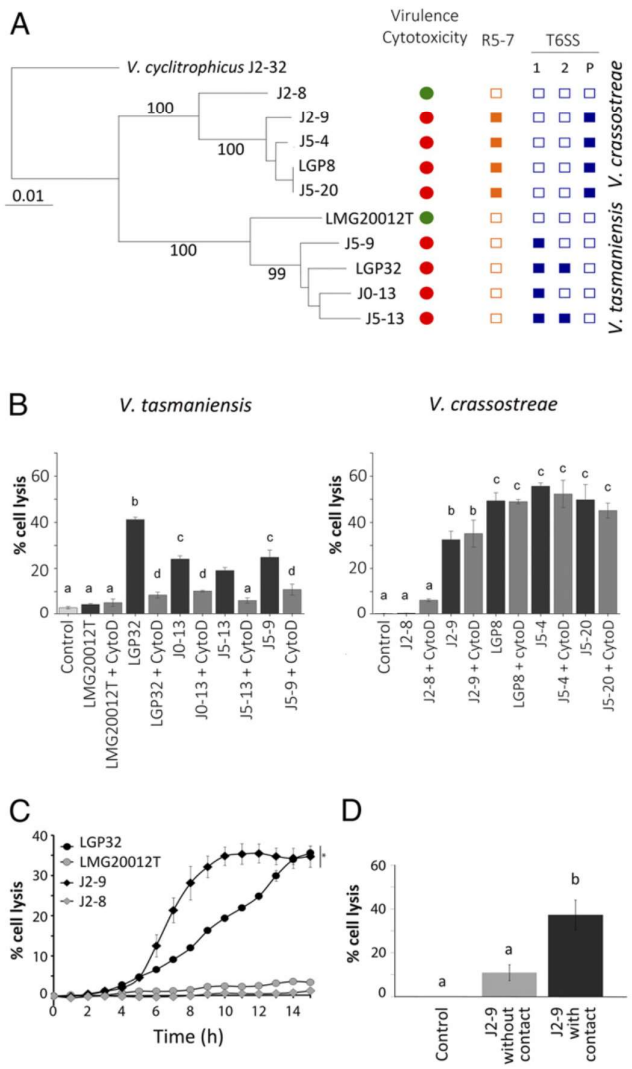

Fig. 1. Species-specific mechanisms of cytotoxicity in *V. crassostreae* and *V. tasmaniensis*. (*A*) Multilocus sequence typing tree of *V. crassostreae* and *V. tasmaniensis* with closely related nonvirulent strains. The tree was reconstructed with maximum-likelihood method from a concatenated alignment of 6 core genes (*gyrB*, *hsp60*, *mreB*, *recA*, *rpoD*, and *topA*) representing 10,626 sites. Node support was assessed with 100 bootstrap replicates. The strain cytotoxicity, which correlates with strain virulence (*B*), is indicated by a red circle, whereas absence of these phenotypes is indicated by a green circle. A filled orange square indicates the presence of the *r5.7* gene, which encodes for a known virulence factor. The effect of the presence of T6SS systems on the different replicons (1, on chromosome 1; 2, on chromosome 2; P, on a plasmid) is indicated by a filled blue square. (*B–D*) Cytotoxicity of vibrios on a monolayer of hemocytes was monitored by the SYTOX Green assay for 15 h. Cells were infected with bacteria at a multiplicity of infection (MOI) of 50:1. (*B*) Maximum cytotoxicity exerted by *V. tasmaniensis* or *V. crassostreae* strains in the presence (gray bars) or absence (back bars) of cytochalasin D, which was used as an inhibitor of phagocytosis. Error bars represent the SD of the mean (RM-ANOVA, $P < 0.001$). All virulent strains are cytotoxic. Cytotoxicity appears to be dependent on phagocytosis for *V. tasmaniensis* virulent strains only. The cytotoxicity exerted by *V. crassostreae* was found to be higher than that of *V. tasmaniensis*. (*C*) Time-course analysis of cytotoxicity of J2-9 (black diamond), LGP32 (black circle), J2-8 (gray diamond), and LMG20 012T (gray circle) strains. J2-9 cytotoxicity is faster than LGP32 cytotoxicity. J2-8 and LMG20 012T are noncytotoxic. The error bar represents the SD of the mean (RM-ANOVA, $P < 0.05$). (*D*) Maximum cytotoxicity for J2-9 strain was observed when in contact with hemocytes (black bars) vs. a Transwell plate without hemocyte contact (gray bars). The contact between hemocytes and vibrios is necessary for significant expression of J2-9 cytotoxicity. The error bar represents the SD of the mean (RM-ANOVA, $P < 0.01$; *SI Appendix*, Fig. S1).

oysters (injected with sterile seawater). Oysters were killed 8 h after the infection and before the onset of mortality. From 3 independent experimental infections of the same family of oysters, we observed significant differential expression [false discovery rate (FDR) < 0.05] for 331 host genes in response to vibrios (Dataset S1). RNA-seq data were validated by qRT-PCR (correlation $R^2 = 0.92$; linear regression test, $P < 0.001$; *SI Appendix*, Fig. S4).

All vibrios induced an immune response in oysters independently of their virulence. Among the 331 genes differentially expressed in response to vibrios, 129 responded similarly to all strains (Fig. 4*A*), with 25.6% of them being involved in immunity (Fig. 4*B* and Dataset S1). We observed an overrepresentation of transcripts from 3 major immune signaling pathways, the interleukin 17 (IL-17), tumor necrosis factor (TNF), and Toll-like receptor (TLR) pathways (Dataset S1). This includes transcripts homologous to TLR13 and TLR4, which have been shown to recognize bacterial 23S ribosomal RNA and LPS, respectively, in mammals (23, 24). IL-17 is also recognized as a key player in the immune response of oysters against bacterial infections (25). Consequently, all vibrio infections induced oyster antimicrobial defenses mainly based on antimicrobial peptides (big defensins) (26) (*SI Appendix*, Fig. S5), ROS (dual oxidase DUOX expression; Dataset S1), and heavy metals (metallothioneins and zinc transporters; Dataset S1). These antimicrobial functions are believed to control bacterial infections in oysters (10, 16) and more generally microbiome homeostasis across animal species (27, 28).

However, a set of shared antibacterial responses was specifically repressed in oysters infected by the virulent *V. tasmaniensis* LGP32 and *V. crassostreae* J2-9 strains, suggesting a common strategy of immune evasion. Overall, a much more extensive response was induced against infection by virulent vibrios (132 differentially expressed host genes) compared with that by nonvirulent strains (20 differentially expressed host genes: Fig. 4*A*). This response clustered according to vibrio virulence rather than their phylogenetic relatedness (Fig. 4*C*). Host responses were similarly altered by both virulent strains (57 genes; Fig. 4*A*) encompassing 4 main functional categories: metabolism, cell proliferation and differentiation, immunity, and extracellular remodeling (Fig. 4*B* and Dataset S1). Immune genes involved in antibacterial defenses were repressed (Dataset S1). These included the NADPH-mediated production of ROS, C-type lectin-mediated antibacterial immunity, and Deleted in Malignant Brain Tumors 1 (DMBT-1)-mediated mucosal immunity. We recently demonstrated the role that repression of ROS in oyster hemocytes plays in survival of *Vibrio tasmaniensis* (16). C-type lectin domain family 4 proteins, which display aggregation and direct antibacterial properties in oysters (29), are involved in the maintenance of microbiome homeostasis (30, 31). The DMBT-1 mucosal fluid protein functions in mucosal immunity, involving bacterial recognition and countering invasion (32), and has been shown to suppress the virulence of *P. aeruginosa* (33). These antibacterial defenses may play a role in controlling commensal bacteria, and their repression by virulent vibrios likely represents an important strategy to bypass the host defense mechanisms and avoid clearance.

Oyster responses to vibrios revealed the existence of virulence mechanisms specific to each species. *V. tasmaniensis* LGP32 infection was characterized by multiple specific host responses (48 genes) falling into 5 main categories: metabolism, stress response, cell proliferation and differentiation, metal homeostasis (mainly induced genes), and extracellular matrix remodeling (both induced and repressed genes; Fig. 4*C* and Dataset S1). The LGP32-specific modulation of genes belonging to "cytoskeleton dynamics" is consistent with the phagocytosis-mediated cytotoxicity of LGP32 (16). Likewise, specific induction of zinc transporters and metallothioneins revealed the involvement of "metal homeostasis" in LGP32 pathogenesis (Fig. 4*C* and Dataset S1). On the contrary, specific responses to *V. crassostreae* J2-9 (27 genes) mostly fell

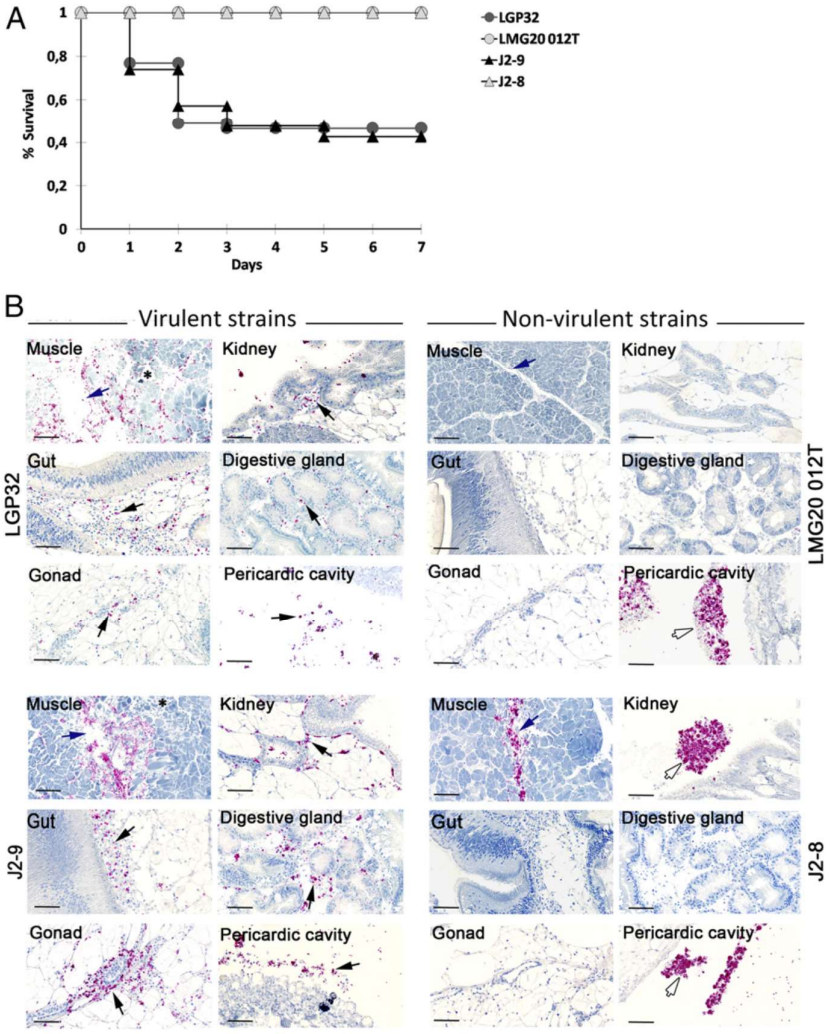

Fig. 2. Virulent strains LGP32 and J2-9 colonize oyster connective tissues and cause damage to the adductor muscle (*SI Appendix*, Fig. S2). (*A*) Kaplan–Meier survival curves were generated from a biparental family of juvenile oysters (Decipher family 14) injected with the virulent LGP32 or J2-9 or the nonvirulent LMG20 012T or J2-8 (7.5×10^7 CFU per oyster). Mortalities were counted daily over 7 d in 2 tanks containing 20 oysters each. Only J2-9 and LGP32 induced significant mortalities in oysters. (*B*) Tissue localization and histopathology of oysters infected with vibrios. Juvenile oysters were injected with 7.5×10^7 CFU of GFP-expressing LGP32, GFP-expressing J2-9, GFP-expressing LMG20012T, or GFP-expressing J2-8. After 8 h, oyster tissues were fixed and stained with hematoxylin. Vibrios were stained on histological sections with anti-GFP antibodies coupled to alkaline phosphatase (red staining). Photographs were taken with a NanoZoomer scanner. Virulent vibrios J2-9 and LGP32 were found in the pericardial cavity and in the connective tissue surrounding the kidney, the gut, the digestive gland, and the gonad (black arrow). Histological damage was observed in the adductor muscle near the site of injection, where virulent vibrios were abundant (blue arrow). No histological damage was recorded in oysters infected with nonvirulent strains. J2-8 was controlled by hemocyte aggregates in the muscle, the kidney, and the pericardial cavity, whereas LMG20012T was controlled by hemocyte aggregates in the pericardial cavity only (white arrow). (Scale bar: 20 μm.)

into the "immunity" category, representing 33% of the specific responses to J2-9 (Fig. 4 *B* and *C*). Immune genes were generally repressed, particularly those encoding C1q domain-containing (C1qDC) proteins (Dataset S1), a family of complement-related proteins, which, in oysters, can serve as opsonins that enhance vibrio phagocytosis (34). Their repression is consistent with the low levels of phagocytosis of *V. crassostreae* J2-9 (Fig. 3*A*). Genes in the category "cell signaling and adhesion" tended to be repressed by intracellular LGP32, whereas they were induced by J2-9. Thus, even though virulence appeared as the major criterion discriminating oyster responses to vibrios, specific signatures were also observed in the host response to distinct *Vibrio* species.

Overall, our oyster transcriptomics analyses suggest that the ability of virulent vibrios to escape hemocyte control and colonize oysters does not rely on the escape from immune recognition but rather on an active repression of a set of antibacterial defenses. Moreover, we found that vibrio strategies to bypass host defenses rely, at least in part, on a species-specific alteration of host responses.

***Vibrio* Gene Expression Support Species-Specific Virulence Mechanisms.** Global changes in bacterial gene expression can be monitored to explore mechanisms driving colonization success during pathogenesis. We used bacterial RNA-seq to analyze the transcriptomes of virulent vibrios (LGP32 and J2-9) in infected oysters. *V. tasmaniensis* LGP32 and *V. crassostreae* J2-9 showed substantial transcriptomic reprogramming inside the host, with 46.7% (2,266 genes) and 50.1% (2,815 genes) differentially expressed genes, respectively, compared with time 0 (before injection; fold change ≥2, FDR < 0.05; Fig. 5*A*). Overall within-host transcriptomes were comparable between the 2 virulent strains in terms of functional category distribution. A

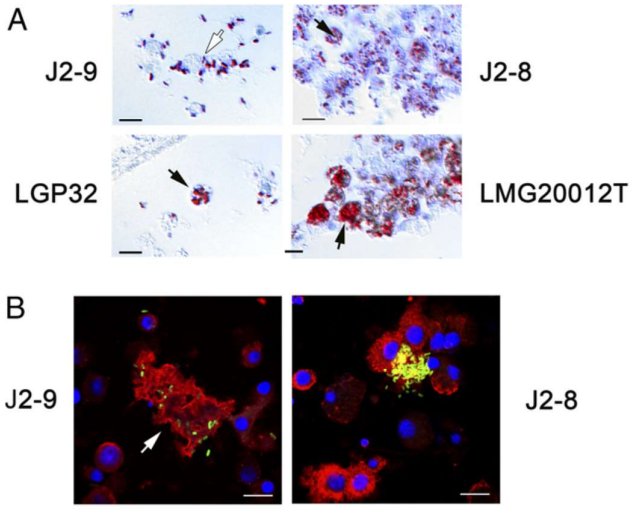

Fig. 3. Virulent strains cause damage to hemocytes and escape hemocyte aggregates in vivo. (*A*) Juvenile oysters were injected with 7.5×10^7 CFU of GFP-expressing LGP32, GFP-expressing J2-9, GFP-expressing LMG20012T, or GFP-expressing J2-8. After 8 h, oyster tissues were fixed and stained with hematoxylin. Photographs of hemocytes were taken in histological sections by using differential interference contrast (DIC) microscopy. Hemocytes and vibrios appear in blue and red, respectively. J2-9 is present inside and outside the hemocytes, whereas LGP32 and the nonvirulent vibrios are massively phagocytized. Hemocyte aggregates are observed with nonvirulent vibrios only. (Scale bar: 10 μm.) (*B*) Confocal microscopy of hemolymph collected from animals infected with *V. crassostreae* J2-9 or the nonvirulent control J2-8. Juvenile oysters were injected with 1.5×10^8 CFU of GFP-expressing vibrios. For each experimental condition, hemolymph was withdrawn from 5 oysters 2 h, 4 h, and 8 h after injection. Hemocytes were observed by confocal microscopy on Cyto-Spin glass slides after the staining of nuclei and actin cytoskeleton with DAPI and phalloidin-TRITC, respectively. In oysters injected with J2-9, J2-9 cells were often found associated with hemocyte lysis (mostly observed at 4 h and 8 h; white arrow), which was absent in J2-8–injected oysters at any time point. In contrast to J2-9, the nonvirulent J2-8 was massively phagocytized at 2 h and 4 h, often inside hemocyte aggregates; it became almost undetectable in the oyster hemolymph at 8 h, whereas J2-9 was still present (*SI Appendix*, Fig. S3). (Scale bar: 10 μm.) Similar observations of in vivo hemocyte lysis have been recorded for LGP32 in a previous study (16).

common group of orthologous genes differentially expressed during oyster infection was identified, which encompassed 340 repressed and 501 induced genes (Fig. 5 *B* and *C* and Dataset S2). Most induced genes encoded proteins involved in "carbon compound and carbohydrate utilization" and "amino acid transport and metabolism" (Fig. 5*C*), reflecting a major metabolic shift in response to the host as a new environment (35). "Defense mechanisms" and "metal homeostasis" were also strongly induced in the *Vibrio* species, particularly genes encoding efflux machineries (multidrug, copper, and zinc transporters), siderophores, and iron uptake systems (Fig. 5*C* and Dataset S2). Therefore, gene expression of both virulent strains in oyster is consistent with a competitive behavior in a hostile environment that is poor in the essential iron but rich in zinc, copper, and other antimicrobials (Fig. 4*C* and *SI Appendix*, Fig. S4).

V. tasmaniensis LGP32 and *V. crassostreae* J2-9 also displayed species-specific responses to colonization, which were mostly clearly observed when considering the 200 most highly induced genes of both strains (*SI Appendix*, Fig. S6). The *V. tasmaniensis* LGP32 response was characterized by a strong induction of genes involved in cell wall biogenesis, transport, regulation, and redox homeostasis (*SI Appendix*, Fig. S6). This result is in agreement with the known protective remodeling of vibrio membranes, and strong induction of antioxidants inside the phagosomes of oyster hemocytes (16, 17). Several adhesins, including *mshM* (VS_0329) and the type IV pilin assembly protein *pilB* (VS_2548), were induced (Dataset S3), which may favor LGP32 attachment to hemocytes and promote phagocytosis, as previously shown for the major adhesin OmpU (15). Various expression patterns were observed for genes encoding putative RTX toxins. For example, the gene *VS_II0512* was highly expressed inside and outside the host whereas *VS_1394* was induced during colonization (Dataset S3). Oyster colonization had significant effects on the expression of genes encoding type 6 secretion systems (T6SS; reviewed in refs. 36–40) localized on the first (T6SS1) and second (T6SS2) chromosomes in *V. tasmaniensis*. T6SS is a multiprotein secretion system responsible for the transport and delivery of toxins (effectors) into recipient cells (39). It has been shown to contribute to pathogenicity toward plant and animal cells as well as to take part in interbacterial competition. T6SS2 genes were expressed only inside the host (Dataset S4), whereas T6SS1 genes were highly expressed outside the host and decreased to the levels of T6SS2 expression inside oysters (similar numbers of normalized counts; Dataset S4). The high preinfection expression levels of T6SS1 and the within-host expression of T6SS2 were confirmed over 24 h in oysters experimentally infected with *V. tasmaniensis* LGP32 (*SI Appendix*, Fig. S7).

The response of *V. crassostreae* J2-9 to host colonization was characterized by a strong induction of adhesion genes (*SI Appendix*, Fig. S7), including a type IV pilus cluster, further supporting the role of attachment of the bacteria to the host target cells during the infection process (Dataset S2). The *r5.7* gene (VCR9J2v1_730268) encoding an exported protein of unknown function, which has been previously shown to be necessary for virulence in *V. crassostreae* (12, 14), was one of the most highly induced virulence genes in J2-9 inside the host (Dataset S3). A number of genes encoding putative RTX toxins were highly expressed outside and inside the host, whereas other toxins and toxin secretion systems were expressed only inside the host (Dataset S3). In particular, a NAD-arginine ADP ribosyltransferase (putative toxin, VCR9J2v1_730029) and 2 toxin secretion membrane fusion proteins (VCR9J2v1_740022, VCR9J2v1_740023) were expressed only inside the host (Dataset S3). Genes encoding a T6SS, carried by the virulence plasmid pGV1512 (11), were induced in oyster (Dataset S4). Genes related to the mobile genetic elements (Fig. 5*C*), particularly those involved in conjugative transfer, were very highly induced in J2-9 during oyster colonization (Dataset S2), suggesting that horizontal gene transfer between infecting *V. crassostreae* could occur during host colonization.

Taken together, cellular and molecular data highlight 2 strategies evolved by virulent vibrios in the Splendidus clade: *V. tasmaniensis* acts as an intracellular pathogen that subverts cellular functions and kills oyster phagocytes as part of its pathogenic process, whereas *V. crassostreae* acts as an extracellular pathogen that uses cell contact-dependent cytotoxicity to overcome the cellular defenses of its host. These results indicate that, within the Splendidus clade, distinct virulent species have acquired the capacity to compromise hemocyte functions to mount successful infections.

Species-Specific Virulence Converges to Impair Host Defenses. To confirm our conclusions that *V. tasmaniensis* LGP32 and *V. crassostreae* J2-9 use species-specific virulence determinants, we sought to identify genes responsible for virulence and cytotoxicity by using a gene knock-out approach. Candidate genes were selected based on their high expression or induction levels upon oyster colonization (Datasets S3 and S4). None of the mutants showed impaired bacterial growth in culture media (*SI Appendix*, Figs. S8*A* and S9*A*).

We knocked out potential adhesins and toxins. In *V. tasmaniensis* LGP32, the inactivation of an adhesin (*mshM*, VS_0329), a type IV pilin assembly protein *pilB* (VS_2548), and putative RTX toxins (VS_II0512 and VS_1394) did not significantly attenuate virulence in the experimental infection of oysters (*SI Appendix*, Fig. S8*B*).

MICROBIOLOGY

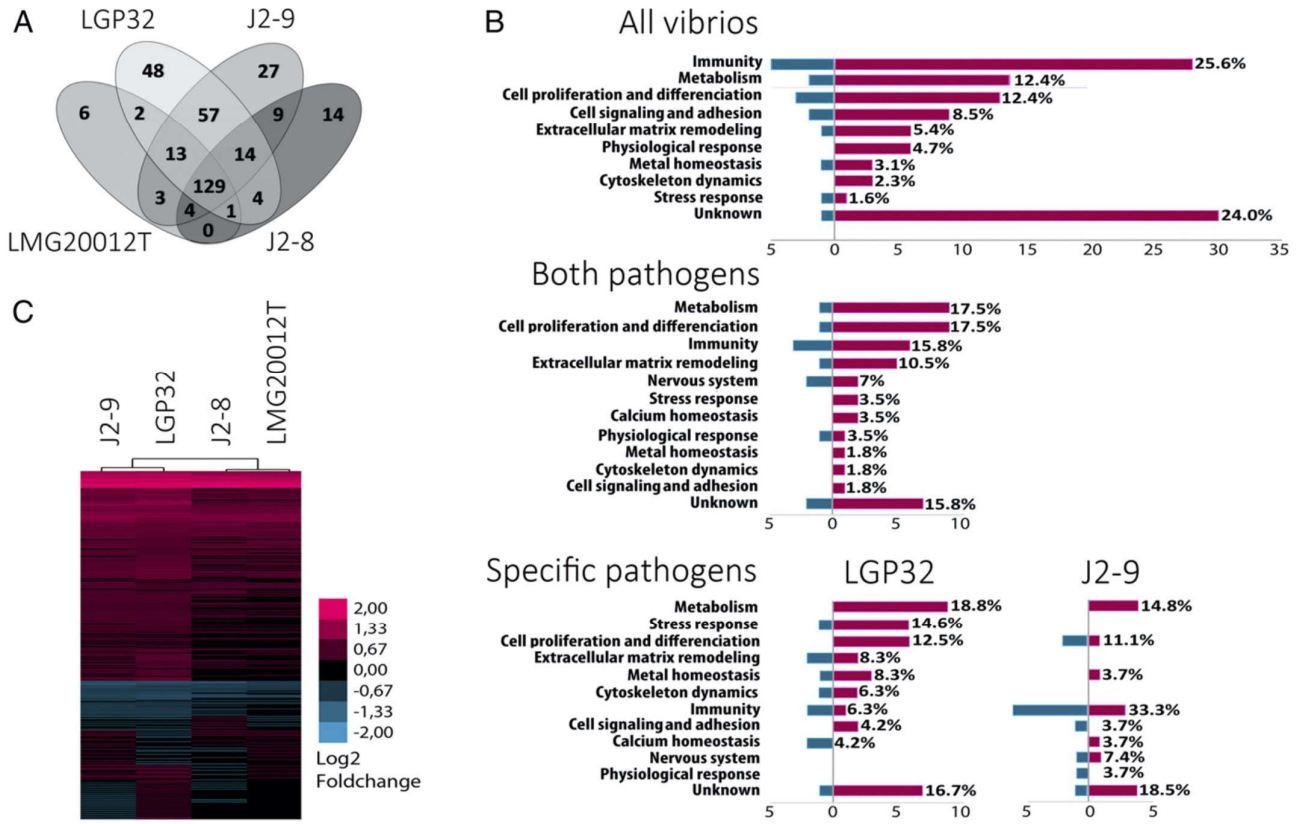

Fig. 4. *Vibrio* virulence status dictates the oyster transcriptional responses to infection. Transcriptional responses of juvenile oysters (fulsib family Decipher 14) to virulent or nonvirulent strains of the Splendidus clade were compared. In 3 independent experiments, groups of 30 oysters were injected with 7.5×10^7 CFU of LGP32, LMG20012T, J2-9, J2-8, or sterile seawater (mock-infected oysters). RNA-seq was performed on pools of 30 oysters collected 8 h after injection for each experiment under each condition. Transcriptomes of vibrio-infected oysters were compared with mock-infected oysters. RNA-seq results showed a significant modulation of 331 genes (Benjamini–Hochberg procedure, which controls FDR, $P < 0.05$). (*A*) Venn diagram showing the number of modulated genes in oysters injected with each vibrio strain. Virulent vibrios LGP32 and J2-9 induce a greater transcriptomic response than nonvirulent vibrios. (*B*) Functional categories of differentially expressed genes. Histograms show the percentage of differentially expressed genes that respond similarly to all vibrio infections, to virulent vibrios only (J2-9 and LGP32), or specifically to strains J2-9 and LGP32. Induced genes are shown in pink, and repressed genes are shown in blue. (*C*) Heat map representing the mean of differential expression (log2 fold change) of genes significantly induced (red) or repressed (blue) in 3 independent experiments (DESeq2: FDR < 0.05). Data show that oyster transcriptomes cluster according to vibrio virulence status. *SI Appendix*, Fig. S5 provides antimicrobial peptide expression (Dataset S1).

Similarly, in *V. crassostreae* J2-9, inactivation of a NAD-arginine ADP ribosyltransferase (VCR9J2v1_730029) and a membrane fusion protein involved in toxin secretion (VCR9J2v1_740022) had no significant effect on virulence (*SI Appendix*, Fig. S9*B*).

We next examined the role of T6SS in both virulent strains, as this secretion system expressed by LGP32 and J2-9 is well known for the delivery of effectors (toxins) into recipient cells (39). T6SS is encoded by cluster(s) of 15–20 genes that includes components of a contractile nanomachine, as well as regulators and effectors (36–40). The constituents of the phage-like subassembly are required for T6SS function (*SI Appendix*, Fig. S10). The VipA/B proteins act as a phage contractile sheath. The hemolysin coregulated proteins (Hcp) form a tail-tube. The valine-glycine repeat protein G (VgrG), a fusion of gp5 and gp27 phage-like domains, forms a cell-puncturing tip. Proteins from the proline-alanine-alanine-arginine repeat (PAAR) superfamily interact with VgrG, forming the canonical tip of the puncturing device complex. Effectors can be delivered to the target cell as a complex with VgrG/PAAR spikes or through the Hcp channel. The C-terminal domains of several VgrG and PAAR proteins (referred to as "evolved" VgrG or PAAR proteins) are predicted to have various enzymatic activities toxic for prokaryotic and eukaryotic cells.

In *V. tasmaniensis* LGP32, the constitutively expressed T6SS1 was identified in 3 other virulent strains of the species, but was absent from the nonvirulent strain (Fig. 1*A*, *SI Appendix*, Fig. S10, and Dataset S4). In all virulent strains, *vgrG* and *paar*-encoded proteins do not contain C-terminal effector domains (*SI Appendix*, Figs. S10–S12). However, all of them contain an *evpP* ortholog (VS_2123 in LGP32), as revealed by searching for potential T6SS effectors in a public database (http://db-mml.sjtu.edu.cn/SecReT6/). In the intracellular pathogen *Edwardsiella tarda*, *evpP* encodes a non-VgrG non-PAAR T6SS effector that is involved in cell invasion (41) and inhibition of the host immune response (42). Together these data suggest a role for T6SS1 in *V. tasmaniensis* virulence.

As we predicted, inactivation of the T6SS1 *vipA* gene resulted in a substantial loss of virulence in oyster experimental infections and cytotoxicity toward oyster hemocytes ($P < 0.01$; Fig. 6). This is reminiscent of the *Burkholderia* sp. T6SS5/T6SS1, which is essential for virulence in the host (43). Thus, our data indicate that the phagocytosis-dependent cytotoxicity of *V. tasmaniensis* toward immune cells requires the intracellular secretion of T6SS1 cytotoxic effectors. Likewise, studies by Ma and Mekalanos reported a role for the *V. cholerae* T6SS in inducing macrophage death (44), whose activation required bacterial phagocytosis by the

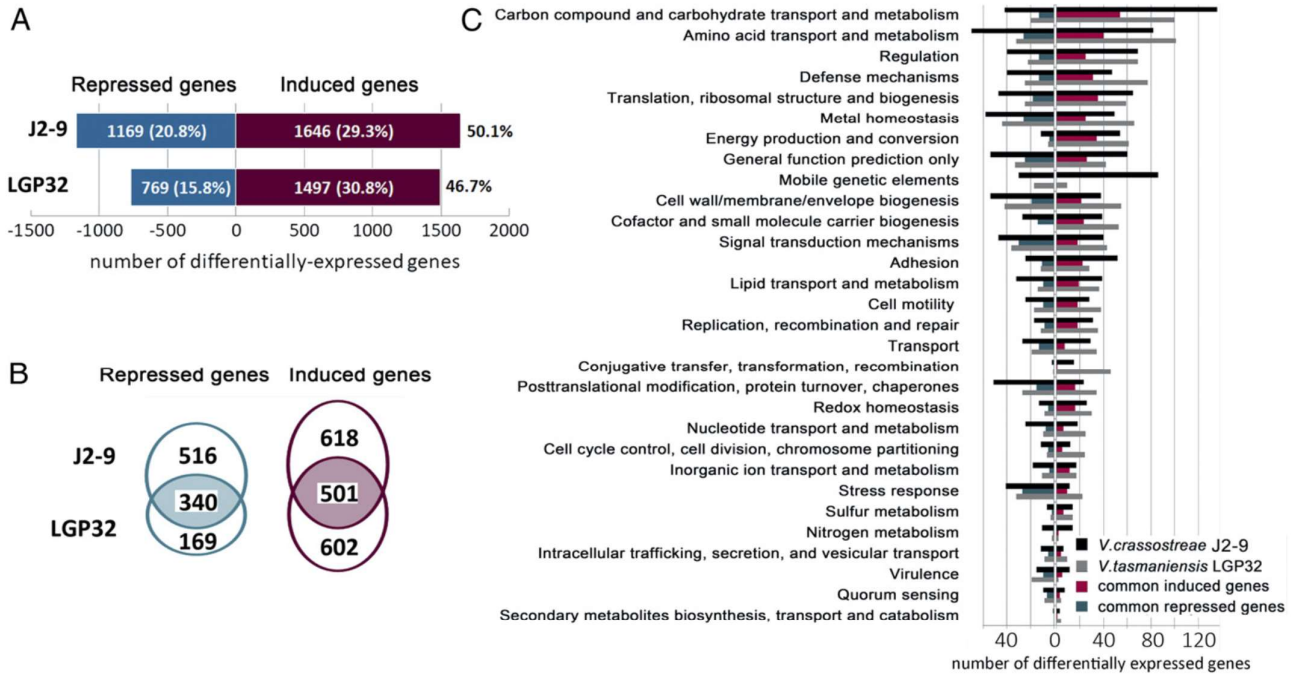

Fig. 5. Responses to host-imposed stresses revealed by within-host bacterial RNA-seq. Within-host transcriptomes of *V. tasmaniensis* LGP32 and *V. crassostreae* J2-9 (8 h after infection) were compared with bacterial transcriptomes before the infection (controls) in 3 independent experiments. Only those genes whose expression varied significantly by more than 2-fold were considered. (*A*) Number of bacterial genes significantly induced and repressed during host colonization. The proportion of differentially expressed genes over the entire transcriptome of LGP32 and J2-9 is given as a percentage of the total number of genes for each genome. Approximately half of the total bacterial transcriptome is altered during host colonization. Repressed and induced genes are showed in blue and purple, respectively. (*B*) Venn diagram showing the core response of pathogens during colonization (340 repressed genes and 501 induced genes, not including genes with an unknown function). The diagram was built on common orthologous genes differentially expressed upon host colonization in J2-9 and LGP32. (*C*) Functional distribution of the bacterial genes during LGP32 and J2-9 colonization process (genes without annotated function were not included; *SI Appendix*, Figs. S6 and S7 and Dataset S2).

host cells (45). Together, these examples indicate that phagocytes are a natural target for T6SS in *Vibrio* species. They demonstrate that T6SS functions to repress immune defenses in different hosts during critical intracellular stages of infection. Like in other Gram-negative bacteria adopting intracellular stages, we show here that T6SS plays a critical role in the success of vibrio infections (42, 43).

T6SS2 in *V. tasmaniensis* LGP32 was induced upon oyster colonization and reached maximum expression in dead oysters (*SI Appendix*, Fig. S7). However, this T6SS2 is absent from 2 other *V. tasmaniensis* virulent strains (J5-9 and J0-13; Fig. 1*A* and Dataset S4). Inactivation of T6SS2 did not alter LGP32 virulence and cytotoxicity (Fig. 6), indicating that it does not have a direct effect on host–pathogen interactions. Closer examination of the T6SS2 gene cluster revealed the absence of an evolved *vgrG* gene and the lack of a *paar* gene in proximity to *vgrG*. However, 7 genes encoding PAAR proteins and putative AHH endonucleases were present in tandem in a proximal region of the T6SS2 (*SI Appendix*, Figs. S10*B* and S11). This suggests that T6SS2 may play a role in interbacterial competition during colonization of oyster tissues, as shown for *V. fischeri* in its mutualistic association with squid (46). It could also be needed to exploit host resources after host death.

In *V. crassostreae* J2-9, the single T6SS was induced upon host colonization. This T6SS, carried by the plasmid pGV1512, is present in all *V. crassostreae* virulent strains (Fig. 1*A* and Dataset S4). As the encoded PAAR and VgrG proteins lack C-terminal effector domains (*SI Appendix*, Figs. S10 and S11), and because we were unable to identify any putative T6SS effector, the function of T6SS in *V. crassostreae* cannot presently be predicted. Even though it has previously been demonstrated that pGV1512 is necessary for J2-9 virulence (11), we did not observe any alteration in the cytotoxicity of J2-9 upon the loss of pGV1512 (Fig. 6*B*). Therefore, we have no evidence that T6SS could be involved in *V. crassostreae* cytotoxicity toward oyster hemocytes. Instead, one of the most highly induced J2-9 virulence genes inside the host, *r5.7* (Mage VCR9J2v1_730268; GenBank accession no. WP_048663858.1), was demonstrated to be necessary for cytotoxicity ($P < 0.001$; Fig. 6), and was also required for cytotoxicity in *V. crassostreae* strain J5-5 (*SI Appendix*, Fig. S13). Previous work has shown that R5.7 alone is not toxic toward oysters and suggested that the protein interacts with the external surface of *Vibrio* and/or its cellular targets in oysters (12). *r5.7* is a virulence gene widely distributed across the Splendidus clade, and we show here that it is a key determinant of *V. crassostreae* cell contact-dependent cytotoxicity to hemocytes, yet has been lost in *V. tasmaniensis* species. Thus, our results show that, in virulent species of the Splendidus clade in which the ancestral virulence gene *r5.7* has been lost, other mechanisms have been acquired (T6SS1 in *V. tasmaniensis*) that specifically target immune cells through cytotoxic mechanisms that enable successful host colonization.

Conclusion

Although cytotoxicity is widespread among *Vibrio* species pathogenic for humans and animals and is known to be important in disease progression, it has not been clearly associated with immune repression. Here, we demonstrate that the fate of vibrio infections in oysters, a natural host for marine *Vibrio* species, is determined by the specific mechanisms that have evolved in virulent strains to induce cytotoxicity. These mechanisms impair the host cellular defenses that normally prevent vibrios from causing systemic colonization of host tissues. Cytotoxicity toward immune cells was shown to be

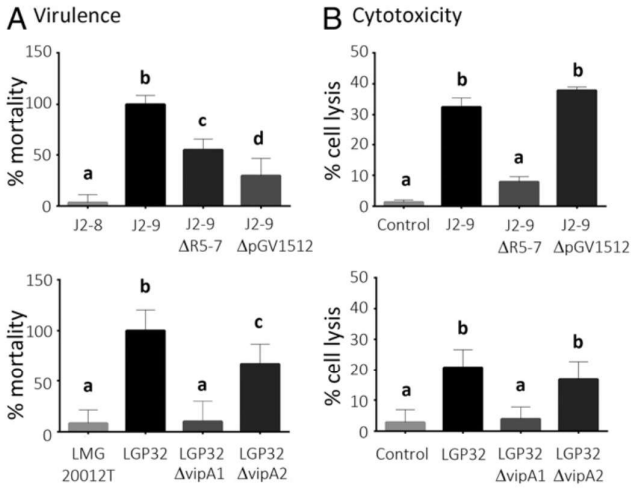

Fig. 6. Species-specific virulence factors are needed for immune cell lysis. (*A*) Virulence of *V. crassostreae* (*Upper*) and *V. tasmaniensis* (*Lower*) isogenic mutants was assessed by intramuscular injection of juvenile oysters. Mortalities were recorded at day 1. Data are expressed as percentage of mortality induced by the wild-type strains. (*B*) Cytotoxicity of vibrio isogenic mutants lacking virulence genes was determined on monolayers of hemocytes and monitored by the SYTOX Green assay. Cells were infected with bacteria at an MOI of 50:1. Maximum cytotoxicity displayed by vibrios is shown here. Error bars represent the SD of the mean (RM-ANOVA, $P < 0.001$; *SI Appendix*, Figs. S8 and S9).

dependent on distinct molecular determinants present in *V. crassostreae* and *V. tasmaniensis*, and other virulent species of *Vibrio* have been shown to be equipped with different specific virulence mechanisms. For example, in the Splendidus clade, MARTX toxins are found exclusively in *V. splendidus* and are necessary for virulence toward oysters (12). In more distant species from the Anguillarum clade, *Vibrio aestuarianus* uses a metalloprotease to evade hemocyte control (47, 48) and cause septicemia in oysters (49). Thus, *Vibrio* species that are pathogenic for oysters have evolved a diverse array of molecular mechanisms that all converge on the attenuation of the cellular defenses of their host, enabling subsequent tissue colonization (Fig. 7). As these mechanisms have been acquired independently during evolution in diverse species pathogenic for oysters, they could be a good indicator of the adaptation of these pathogenic species to oysters as a niche (50). Beyond oyster pathogens, a specific mechanism of phagocyte targeting has also been reported in *V. cholerae* (45). We believe more attention should be paid to *Vibrio* cytotoxicity in repressing host immunity, as this may be an insufficiently explored determinant of infection outcomes in metazoan hosts.

Materials and Methods

Strains, Plasmids, and Primers. All strains, plasmids and primers used or constructed in the present study are described in *SI Appendix, SI Materials and Methods* and Tables S6–S8.

Animals. *C. gigas* diploid oyster spat were used from 3 families of siblings (Decipher 1, 14, and 15) (10), and a batch of standardized Ifremer spats (NSI) were produced from a pool of 120 genitors (51). Spats were used for experimental infections and dual RNA-seq. Adults produced from a pool of 120 genitors (ASI) were used to collect hemolymph for cytotoxicity assays (*SI Appendix, SI Materials and Methods*).

Experimental Infections. Experimental infections were performed at 20 °C as in ref. 52 by injection at 7.5×10^7 CFU into oyster adductor muscle (details in *SI Appendix, SI Materials and Methods*). Statistical analyses were performed by using a nonparametric Kaplan–Meier test to estimate log-rank values for comparing conditions (GraphPad Prism 6).

Molecular Microbiology. *Vibrio* isolates were cultured as described in *SI Appendix, SI Materials and Methods*. Conjugation between *Escherichia coli* and *Vibrio* were performed at 30 °C as described previously (53). To label the strains with a fluorochrome, *gfp* gene was cloned in Apa1/Xho1 sites of the pMRB plasmid known to be stable in *Vibrio* spp. (54), resulting in a constitutive expression from a P_{lac} promoter. Gene inactivation was performed by cloning approximately 500 bp of the target gene in pSW23T (55) and selecting on Cm the suicide plasmid integration obtained by a single recombination (56). Mutants were screened for insertion of the suicide vector by PCR by using external primers flanking the different targeted genes (*SI Appendix*, Table S2).

Histology. Spats (1.5–2 cm) were injected with 7.5×10^7 CFU of GFP-expressing LGP32, J2-9, LMG20 012T, or J2-8. Noninjected oysters were used as controls. Spats were kept in seawater tanks at 20 °C, sampled, and fixed 8 h after injection. Histological sectioning was performed at HISTALIM (Montpellier, France). Longitudinal sections were immunostained with an anti-GFP primary antibody coupled to alkaline phosphatase (Abcam). Sections and hemocytes were observed as described in *SI Appendix, SI Materials and Methods*.

In Vitro Cytotoxicity Assays. Cytotoxicity of vibrios was measured on hemocyte monolayers according to procedures described in *SI Appendix, SI Materials and Methods*. Statistical analysis was performed by using RM-ANOVA.

Confocal Microscopy of Interaction Between Hemocytes and Vibrios in Vivo. Oysters were injected with 1.5×10^8 CFU of GFP-expressing vibrios (J2-8 or J2-9) a priori washed and resuspended in sterile seawater. Control oysters received an injection of an equal volume of sterile seawater. For each experimental condition, hemolymph was collected from 5 oysters at 2 h, 4 h, and 8 h after injection. Samples were fixed with 4% paraformaldehyde and stained with DAPI and Phalloidin-TRITC and observed by confocal microscopy as described in *SI Appendix, SI Materials and Methods*.

Dual RNA-Seq Experiments. 3 independent experimental infections were performed. For every experiment, 150 oysters (30 animals per condition) were injected with bacteria (10^7 CFU of LGP32, LMG20012T, J2-9, or J2-8) or sterile seawater (mock-infected oysters). In addition, both bacterial suspensions and 30 nontreated oysters were collected at time 0. For every experimental

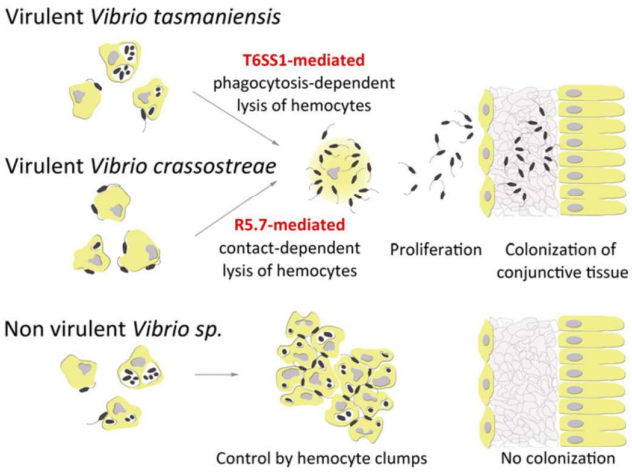

Fig. 7. Impairment of oyster cellular immunity as a common strategy of immune evasion in vibrios. Virulent strains of the species *V. tasmaniensis* and *V. crassostreae* exert cytotoxic activity toward immune cells. They thereby repress key cellular defenses, gain access to the conjunctive tissues, and cause systemic infection. In *V. crassostreae*, cytotoxicity is a rapid, contact-dependent phenotype that requires the R5.7 virulence factor, which is strongly induced inside the host. In *V. tasmaniensis*, which behaves as an intracellular pathogen, cytotoxicity is phagocytosis-dependent and requires the intracellular action of a constitutively expressed type 6 secretion system present on chromosome I. In contrast to virulent strains, nonvirulent strains of both species are controlled by hemocyte clumps in the hemolymph compartment, preventing them from causing systemic infection. We conclude that the outcome of the infection depends on independently evolved molecular determinants that impair oyster cellular defenses as a strategy of immune evasion.

condition, 30 oysters were then sampled 8 h after injection (i.e., before mortality occurred) before RNA extraction (*SI Appendix, SI Materials and Methods*). For oyster RNA-seq, library construction and sequencing were performed on polyadenylated mRNAs by Fasteris (Geneva, Switzerland; https://www.fasteris.com). Directional cDNA libraries were constructed and sequenced on an Illumina HiSeq system in paired-end reads of 2 × 75 bp. For bacterial RNA-seq, total RNA obtained from oyster tissues was used to prepare non–rRNA-bacterial RNA enriched libraries. After polyadenylated mRNAs (i.e., host mRNAs) were removed by using a MICROBEnrich Kit (Ambion), cDNA-oriented sequencing libraries were prepared starting from 100 ng enriched RNA by using an Ovation Universal RNA-Seq System kit (NuGEN). Library construction included a depletion step of abundant, nondesired sequences by using a Nugen-customized mixture of primers complementary to RNA sequences to be depleted, viz. oyster nuclear, mitochondrial, and ribosomal and bacterial ribosomal RNA sequences. The libraries were quantified by DeNovix dsDNA Broad Range Assay (DeNovix), and the quality was monitored by using an Agilent High Sensitivity DNA kit (Agilent Technologies). For each condition, 3 biological replicate libraries were prepared. Libraries were sequenced in paired-end mode (2 × 150 bp) by Fasteris on an Illumina HiSeq 4000 system to obtain ∼100 million reads per sample per run.

Oyster Transcriptome Analysis. Data were treated using the galaxy instance of the IHPE laboratory (57). Phred quality scores were checked by using the FastX toolkit galaxy interface (http://hannonlab.cshl.edu/fastx_toolkit/) and were greater than 26 for more than 90% of the read length for all of the sequences. All of the reads were thus kept for subsequent analyses. Mapping to the *C. gigas* reference genome [assembly version V9 (58)] was performed by using RNA STAR (Galaxy version 2.4.0d-2; ref. 59). HTSeq-count was used to count the number of reads overlapping annotated genes (mode Union; Galaxy Version v0.6.1) (60). The resulting files were used as input to determine differential expression for each feature between oysters injected with vibrios and mock-infected oysters by using DESeq2 (61). Fold changes in gene expression between test animals and controls were considered significant when the adjusted *P* value (P_{adj}) for multiple testing with the Benjamini–Hochberg procedure, which controls FDR, was <0.05. The same threshold was applied to fold changes in gene expression between mock-infected oysters and naïve controls. As genes for *C. gigas* antimicrobial peptides (AMPs) are not annotated in the *C. gigas* reference genome (assembly version V9; ref. 58), read counts for all AMPs were obtained by alignment to an in-house database of AMP protein sequences by using DIAMOND 0.7.9 (62) as described in *SI Appendix, SI Materials and Methods*. Oyster RNA-seq data have been made available through the SRA database (BioProject accession no. PRJNA515169) under SRA accession nos. SRR8551076–SRR8551093 (63).

***Vibrio* Transcriptome Analysis.** Raw Illumina sequencing reads were trimmed by Trimmomatic in paired-end mode (64) to remove sequences corresponding to the NuGEN-provided adapters, clipping part of reads having a quality score of below 20, and dropping reads of less than 36 nt. The 2 resulting files were used as input for Bowtie2 (65) to align the reads on *V. tasmaniensis* LGP32 or *V. crassostreae* J2-9 genome, respectively (*SI Appendix, SI Materials and Methods*). As the rate of read alignment on the bacterial genome was ∼2% for vibrios in oyster tissues, as opposed to >98% for the in vitro grown bacteria, we introduced a random down-sampling step of the aligned reads (http://broadinstitute.github.io/picard/command-line-overview.html#DownsampleSam; *SI Appendix, SI Materials and Methods*). Counts for each annotated feature (CDS + sRNAs) of *V. tasmaniensis* LGP32 or *V. crassostreae* J2-9 were then computed by using featureCounts (66). Differential expression was determined for each feature between oysters injected with vibrios and vibrios grown in vitro by DESeq2 (61). Genes were considered as differentially expressed between tested conditions and controls when |log2(fold change)| was ≥1 and P_{adj} for multiple testing with the Benjamini–Hochberg procedure was <0.05. Bacterial RNA-seq data have been made available through the SRA database: BioProject accession no. PRJNA521688 under SRA accession nos. SRR8567597–SRR8567602 (*V. crassostreae* J2-9) (67) and BioProject accession no. PRJNA521693 under SRA accession nos. SRR8573808–SRR8573813 (*V. tasmaniensis* LGP32) (68).

Functional Gene Ontology Annotations. For oyster genes, Blastx (69) comparison against NR database was performed for each set of genes with a maximum number of target hits of 20 and a minimal e-value of 0.001. XML blast result files were loaded onto Blast2GO (70) for GO mapping and annotation of the B2G database. Functional categories corresponding to significantly modulated genes (331 genes) were then determined manually; this was supported by background literature review. A heat map of the mean of log2 fold change in 3 independent experiments was then generated by using cluster 3.0 (http://bonsai.hgc.jp/~mdehoon/software/cluster/software.htm). For bacterial genes, annotations of differentially expressed genes (fold change ≥ 2 and $P_{adj} \leq 0.05$) were manually curated by using the MicroScope platform (71) and the MetaCyc database (72). Based on these curated annotations, each gene was assigned to 1 of 32 functional categories (the list of categories is provided in Fig. 5 and *SI Appendix*, Fig. S6). The MicroScope tools were used to compare genomes based on sequence and synteny conservation (*SI Appendix, SI Materials and Methods*).

RT-qPCR. RT-qPCR was performed on the same RNA samples as those used for deep sequencing to validate RNA-seq data (*SI Appendix*, Fig. S4) or on specific RNA samples to monitor the time course of bacterial gene expression in oysters (*SI Appendix*, Fig. S7). cDNA synthesis and real-time qPCR were performed as described in *SI Appendix, SI Materials and Methods*.

Specific Vibrio Quantification by qPCR. Genomic DNA was extracted with the DNA kit Promega (Wizard SV Genomic DNA Purification System) on the same oyster samples used for RNA-seq. Real-time qPCR was used to amplify monocopy genes from specific vibrio genomes (*SI Appendix*, Table S2). To quantify oyster genomes, *Cg*-BPI (GenBank accession no. AY165040) primers were used (*SI Appendix*, Table S2). The vibrio charge in oyster tissues was calculated as a number of vibrio genome copies per number of oyster genome copy (*SI Appendix, SI Material and Methods*).

***Vibrio* Genome Sequencing and Assembly.** Genomic DNA for J0-13, J5-13, and J5-9 was sequenced at the Bioenvironment platform (University of Perpignan, Cemeb) by using a NextSeq 550 instrument resulting in ∼100-fold coverage (*SI Appendix, SI Material and Methods*). Reads were assembled de novo by using Spades software. Computational prediction of coding sequences together with functional assignments was performed by using the automated annotation pipeline implemented in the MicroScope platform (73). The genome sequences of *V. tasmaniensis* J0-13, J5-13, and J5-9 were deposited in GenBank (BioProject accession no. PRJNA520819, nucleotide accession nos. SEOP00000000 (J0-13), SESM00000000 (J5-13), and SESL00000000 (J5-9) (74). The genome sequence of LMG20012T was given the BioProject accession no. PRJNA542263, nucleotide accession no. VARQ00000000 (75). Other *Vibrio* genomes presented in this study were previously deposited under the following accession numbers: J2-8 (PRJEB5890), J2-9 (PRJEB5876), J5-4 (PRJEB5877), LGP8 (PRJEB5884), J5-20 (PRJEB5882), and LGP32 (PRJEA32815).

ACKNOWLEDGMENTS. We thank Drs. François Bonhomme and Evelyne Bachère for fruitful discussions, Marc Leroy and Agnès Vergnes for precious technical assistance, and Jean-François Allienne at the Bioenvironment platform at University Perpignan Via Domitia for support in NGS library preparation and sequencing, and the qPHD platform/Montpellier genomix for access to qPCR. We thank Montpellier RIO Imaging (https://www.mri.cnrs.fr). A.J. thanks Emilie Drouineau and Claire Toffano-Nioche for advice on the use of bioinformatics tools. This work was supported by Agence Nationale de la Recherche (ANR) Grants Vibriogen ANR-11-BSV7-0023, Decipher ANR-14-CE19-0023, and Revenge ANR-16-CE32-0008-01; European Union's Horizon 2020 Research and Innovation Program Grant Vivaldi 678589; the University of Montpellier (Doctoral School Gaia; T.R.); Conicyt Pfcha/Doctorado En El Extranjero Becas Chile Grant 2016-72170430 (to D.O.); the Spanish Ministry of Science and Education Fellowship FPU13-0466 (to M.T.); the University of Granada Campus de Excelencia Internacional en Biosalud y Tecnologías de Información y Comunicación Grant CEI1-2015 (to M.T.); and the Chinese Scholarship Council (to X.L.). This study is set within the framework of the "Laboratoires d'Excellence (LABEX)" Tulip (ANR-10-LABX-41).

1. A. F. Takemura, D. M. Chien, M. F. Polz, Associations and dynamics of Vibrionaceae in the environment, from the genus to the population level. *Front. Microbiol.* **5**, 38 (2014).
2. N. Kremer *et al.*, Initial symbiont contact orchestrates host-organ-wide transcriptional changes that prime tissue colonization. *Cell Host Microbe* **14**, 183–194 (2013).
3. M. McFall-Ngai, Divining the essence of symbiosis: Insights from the squid-vibrio model. *PLoS Biol.* **12**, e1001783 (2014).
4. S. Chakraborty, G. B. Nair, S. Shinoda, Pathogenic vibrios in the natural aquatic environment. *Rev. Environ. Health* **12**, 63–80 (1997).
5. J. Dubert, J. L. Barja, J. L. Romalde, New insights into pathogenic vibrios affecting bivalves in hatcheries: Present and future prospects. *Front. Microbiol.* **8**, 762 (2017).
6. F. Le Roux, M. Blokesch, Eco-evolutionary dynamics linked to horizontal gene transfer in vibrios. *Annu. Rev. Microbiol.* **72**, 89–110 (2018).
7. F. L. Thompson, T. Iida, J. Swings, Biodiversity of vibrios. *Microbiol. Mol. Biol. Rev.* **68**, 403–431 (2004).
8. F. Le Roux, K. M. Wegner, M. F. Polz, Oysters and vibrios as a model for disease dynamics in wild animals. *Trends Microbiol.* **24**, 568–580 (2016).

9. P. Schmitt *et al.*, The antimicrobial defense of the pacific oyster, Crassostrea gigas. How diversity may compensate for scarcity in the regulation of resident/pathogenic microflora. *Front. Microbiol.* **3**, 160 (2012).
10. J. de Lorgeril *et al.*, Immune-suppression by OsHV-1 viral infection causes fatal bacteraemia in Pacific oysters. *Nat. Commun.* **9**, 4215 (2018).
11. M. Bruto *et al.*, Vibrio crassostreae, a benign oyster colonizer turned into a pathogen after plasmid acquisition. *ISME J.* **11**, 1043–1052 (2017).
12. M. Bruto *et al.*, Ancestral gene acquisition as the key to virulence potential in environmental Vibrio populations. *ISME J.* **12**, 2954–2966 (2018).
13. M. Gay, F. C. Berthe, F. Le Roux, Screening of Vibrio isolates to develop an experimental infection model in the Pacific oyster Crassostrea gigas. *Dis. Aquat. Organ.* **59**, 49–56 (2004).
14. A. Lemire *et al.*, Populations, not clones, are the unit of vibrio pathogenesis in naturally infected oysters. *ISME J.* **9**, 1523–1531 (2015).
15. M. Duperthuy *et al.*, Use of OmpU porins for attachment and invasion of Crassostrea gigas immune cells by the oyster pathogen Vibrio splendidus. *Proc. Natl. Acad. Sci. U.S.A.* **108**, 2993–2998 (2011).
16. A. S. Vanhove *et al.*, Copper homeostasis at the host vibrio interface: Lessons from intracellular vibrio transcriptomics. *Environ. Microbiol.* **18**, 875–888 (2016).
17. A. S. Vanhove *et al.*, Outer membrane vesicles are vehicles for the delivery of Vibrio tasmaniensis virulence factors to oyster immune cells. *Environ. Microbiol.* **17**, 1152–1165 (2015).
18. A. J. Westermann, L. Barquist, J. Vogel, Resolving host-pathogen interactions by dual RNA-seq. *PLoS Pathog.* **13**, e1006033 (2017).
19. C. T. Robb, E. A. Dyrynda, R. D. Gray, A. G. Rossi, V. J. Smith, Invertebrate extracellular phagocyte traps show that chromatin is an ancient defence weapon. *Nat. Commun.* **5**, 4627 (2014).
20. A. C. Poirier *et al.*, Antimicrobial histones and DNA traps in invertebrate immunity: Evidences in Crassostrea gigas. *J. Biol. Chem.* **289**, 24821–24831 (2014).
21. M. W. Hornef, M. J. Wick, M. Rhen, S. Normark, Bacterial strategies for overcoming host innate and adaptive immune responses. *Nat. Immunol.* **3**, 1033–1040 (2002).
22. L. E. Reddick, N. M. Alto, Bacteria fighting back: How pathogens target and subvert the host innate immune system. *Mol. Cell* **54**, 321–328 (2014).
23. B. Beutler, Tlr4: Central component of the sole mammalian LPS sensor. *Curr. Opin. Immunol.* **12**, 20–26 (2000).
24. M. Oldenburg *et al.*, TLR13 recognizes bacterial 23S rRNA devoid of erythromycin resistance-forming modification. *Science* **337**, 1111–1115 (2012).
25. I. C. McDowell *et al.*, Transcriptome of American oysters, Crassostrea virginica, in response to bacterial challenge: Insights into potential mechanisms of disease resistance. *PLoS One* **9**, e105097 (2014).
26. R. D. Rosa *et al.*, Big defensins, a diverse family of antimicrobial peptides that follows different patterns of expression in hemocytes of the oyster Crassostrea gigas. *PLoS One* **6**, e25594 (2011).
27. Y. S. Bae, M. K. Choi, W. J. Lee, Dual oxidase in mucosal immunity and host-microbe homeostasis. *Trends Immunol.* **31**, 278–287 (2010).
28. C. L. Bevins, N. H. Salzman, Paneth cells, antimicrobial peptides and maintenance of intestinal homeostasis. *Nat. Rev. Microbiol.* **9**, 356–368 (2011).
29. Z. Jia *et al.*, An integrin from oyster Crassostrea gigas mediates the phagocytosis toward Vibrio splendidus through LPS binding activity. *Dev. Comp. Immunol.* **53**, 253–264 (2015).
30. X. Pang *et al.*, Mosquito C-type lectins maintain gut microbiome homeostasis. *Nat. Microbiol.* **1**, 16023 (2016).
31. X. W. Wang, J. D. Xu, X. F. Zhao, G. R. Vasta, J. X. Wang, A shrimp C-type lectin inhibits proliferation of the hemolymph microbiota by maintaining the expression of antimicrobial peptides. *J. Biol. Chem.* **289**, 11779–11790 (2014).
32. P. Rosenstiel *et al.*, Regulation of DMBT1 via NOD2 and TLR4 in intestinal epithelial cells modulates bacterial recognition and invasion. *J. Immunol.* **178**, 8203–8211 (2007).
33. J. Li, M. M. E. Metruccio, D. J. Evans, S. M. J. Fleiszig, Mucosal fluid glycoprotein DMBT1 suppresses twitching motility and virulence of the opportunistic pathogen Pseudomonas aeruginosa. *PLoS Pathog.* **13**, e1006392 (2017).
34. Z. Lv *et al.*, Comparative study of three C1q domain containing proteins from pacific oyster Crassostrea gigas. *Dev. Comp. Immunol.* **78**, 42–51 (2018).
35. A. F. Takemura *et al.* Natural resource landscapes of a marine bacterium reveal distinct fitness-determining genes across the genome. *Environ. Microbiol.* **19**, 2422–2433 (2017).
36. M. Basler, Type VI secretion system: Secretion by a contractile nanomachine. *Philos. Trans. R. Soc. Lond. B Biol. Sci.* **370**, 20150021 (2015).
37. B. T. Ho, T. G. Dong, J. J. Mekalanos, A view to a kill: The bacterial type VI secretion system. *Cell Host Microbe* **15**, 9–21 (2014).
38. A. Joshi *et al.*, Rules of engagement: The type VI secretion system in Vibrio cholerae. *Trends Microbiol.* **25**, 267–279 (2017).
39. V. S. Nguyen *et al.*, Towards a complete structural deciphering of Type VI secretion system. *Curr. Opin. Struct. Biol.* **49**, 77–84 (2018).
40. A. B. Russell, S. B. Peterson, J. D. Mougous, Type VI secretion system effectors: Poisons with a purpose. *Nat. Rev. Microbiol.* **12**, 137–148 (2014).
41. X. Wang *et al.*, Edwardsiella tarda T6SS component evpP is regulated by esrB and iron, and plays essential roles in the invasion of fish. *Fish Shellfish Immunol.* **27**, 469–477 (2009).
42. H. Chen *et al.*, The bacterial T6SS effector EvpP prevents NLRP3 inflammasome activation by inhibiting the Ca^{2+}-dependent MAPK-jnk pathway. *Cell Host Microbe* **21**, 47–58 (2017).
43. J. Lennings, T. E. West, S. Schwarz, The *Burkholderia* type VI secretion system 5: Composition, regulation and role in virulence. *Front. Microbiol.* **9**, 3339 (2019).
44. A. T. Ma, J. J. Mekalanos, In vivo actin cross-linking induced by Vibrio cholerae type VI secretion system is associated with intestinal inflammation. *Proc. Natl. Acad. Sci. U.S.A.* **107**, 4365–4370 (2010).
45. A. T. Ma, S. McAuley, S. Pukatzki, J. J. Mekalanos, Translocation of a Vibrio cholerae type VI secretion effector requires bacterial endocytosis by host cells. *Cell Host Microbe* **5**, 234–243 (2009).
46. L. Speare *et al.*, Bacterial symbionts use a type VI secretion system to eliminate competitors in their natural host. *Proc. Natl. Acad. Sci. U.S.A.* **115**, E8528–E8537 (2018).
47. Y. Labreuche *et al.*, Cellular and molecular hemocyte responses of the Pacific oyster, Crassostrea gigas, following bacterial infection with Vibrio aestuarianus strain 01/32. *Microbes Infect.* **8**, 2715–2724 (2006).
48. Y. Labreuche *et al.*, Vibrio aestuarianus zinc metalloprotease causes lethality in the Pacific oyster Crassostrea gigas and impairs the host cellular immune defenses. *Fish Shellfish Immunol.* **29**, 753–758 (2010).
49. L. Parizadeh *et al.*, Ecologically realistic model of infection for exploring the host damage caused by Vibrio aestuarianus. *Environ. Microbiol.* **20**, 4343–4355 (2018).
50. S. F. Bailey, N. Rodrigue, R. Kassen, The effect of selection environment on the probability of parallel evolution. *Mol. Biol. Evol.* **32**, 1436–1448 (2015).
51. B. Petton, F. Pernet, R. Robert, P. Boudry, Temperature influence on pathogen transmission and subsequent mortalities in juvenile Pacific oysters Crassostrea gigas. (Translated from English). *Aquacult. Environ. Interact.* **3**, 257–273 (2013).
52. M. Duperthuy *et al.*, The major outer membrane protein OmpU of Vibrio splendidus contributes to host antimicrobial peptide resistance and is required for virulence in the oyster Crassostrea gigas. *Environ. Microbiol.* **12**, 951–963 (2010).
53. F. Le Roux, J. Binesse, D. Saulnier, D. Mazel, Construction of a Vibrio splendidus mutant lacking the metalloprotease gene vsm by use of a novel counterselectable suicide vector. *Appl. Environ. Microbiol.* **73**, 777–784 (2007).
54. F. Le Roux, B. M. Davis, M. K. Waldor, Conserved small RNAs govern replication and incompatibility of a diverse new plasmid family from marine bacteria. *Nucleic Acids Res.* **39**, 1004–1013 (2011).
55. G. Demarre *et al.*, A new family of mobilizable suicide plasmids based on broad host range R388 plasmid (IncW) and RP4 plasmid (IncPalpha) conjugative machineries and their cognate Escherichia coli host strains. *Res. Microbiol.* **156**, 245–255 (2005).
56. F. Le Roux *et al.*, Genome sequence of Vibrio splendidus: An abundant planctonic marine species with a large genotypic diversity. *Environ. Microbiol.* **11**, 1959–1970 (2009).
57. E. Afgan *et al.*, The galaxy platform for accessible, reproducible and collaborative biomedical analyses: 2018 update. *Nucleic Acids Res.* **46**, W537–W544 (2018).
58. G. Zhang *et al.*, The oyster genome reveals stress adaptation and complexity of shell formation. *Nature* **490**, 49–54 (2012).
59. A. Dobin *et al.*, STAR: Ultrafast universal RNA-seq aligner. *Bioinformatics* **29**, 15–21 (2013).
60. S. Anders, P. T. Pyl, W. Huber, HTSeq–A Python framework to work with high-throughput sequencing data. *Bioinformatics* **31**, 166–169 (2015).
61. M. I. Love, W. Huber, S. Anders, Moderated estimation of fold change and dispersion for RNA-seq data with DESeq2. *Genome Biol.* **15**, 550 (2014).
62. B. Buchfink, C. Xie, D. H. Huson, Fast and sensitive protein alignment using DIAMOND. *Nat. Methods* **12**, 59–60 (2015).
63. T. Rubio, E. Toulza, C. Chaparro, G. M. Charrière, D. Destoumieux-Garzón, *Crassostrea gigas* response to *Vibrio* strains J2-9, LGP32, J2-8 and LMG20012T, strain:Decipher Family 14 (Pacific oyster). BioProject. https://www.ncbi.nlm.nih.gov/bioproject/PRJNA515169. Deposited 15 January 2019.
64. A. M. Bolger, M. Lohse, B. Usadel, Trimmomatic: A flexible trimmer for Illumina sequence data. *Bioinformatics* **30**, 2114–2120 (2014).
65. B. Langmead, S. L. Salzberg, Fast gapped-read alignment with Bowtie 2. *Nat. Methods* **9**, 357–359 (2012).
66. Y. Liao, G. K. Smyth, W. Shi, FeatureCounts: An efficient general purpose program for assigning sequence reads to genomic features. *Bioinformatics* **30**, 923–930 (2014).
67. T. Rubio, X. Luo, G. M. Charrière, D. Destoumieux-Garzón, A. Jacq, Vibrio crassostreae strain:J2-9 response to oyster colonization. BioProject. https://www.ncbi.nlm.nih.gov/bioproject/PRJNA521688. Deposited 12 February 2019.
68. T. Rubio, X. Luo, G. M. Charrière, D. Destoumieux-Garzón, A. Jacq, Vibrio tasmaniensis strain: LGP32 response to oyster colonization. BioProject. https://www.ncbi.nlm.nih.gov/bioproject/PRJNA521693. Deposited 11 February 2019.
69. S. F. Altschul, W. Gish, W. Miller, E. W. Myers, D. J. Lipman, Basic local alignment search tool. *J. Mol. Biol.* **215**, 403–410 (1990).
70. A. Conesa *et al.*, Blast2GO: A universal tool for annotation, visualization and analysis in functional genomics research. *Bioinformatics* **21**, 3674–3676 (2005).
71. C. Médigue *et al.*, MicroScope-an integrated resource for community expertise of gene functions and comparative analysis of microbial genomic and metabolic data. *Brief. Bioinform.*, 10.1093/bib/bbx113 (2017).
72. R. Caspi *et al.*, The MetaCyc database of metabolic pathways and enzymes. *Nucleic Acids Res.* **46**, D633–D639 (2018).
73. D. Vallenet *et al.*, MicroScope–An integrated microbial resource for the curation and comparative analysis of genomic and metabolic data. *Nucleic Acids Res.* **41**, D636–D647 (2013).
74. M. Bruto, A. Lagorce, E. Toulza, F. Le Roux, D. Destoumieux-Garzón, Vibrio tasmaniensis, strains: J0-13, J5-13 and J5-9. BioProject. https://www.ncbi.nlm.nih.gov/bioproject/PRJNA520819. Deposited 4 February 2019.
75. M. Bruto, G. M. Charrière, F. Le Roux, D. Destoumieux-Garzón, Vibrio tasmaniensis strain:LMG 20012T. BioProject. https://www.ncbi.nlm.nih.gov/bioproject/?term=PRJNA542263. Deposited 5 May 2019.

II.2.1. SUPPLEMENTAL FIGURES

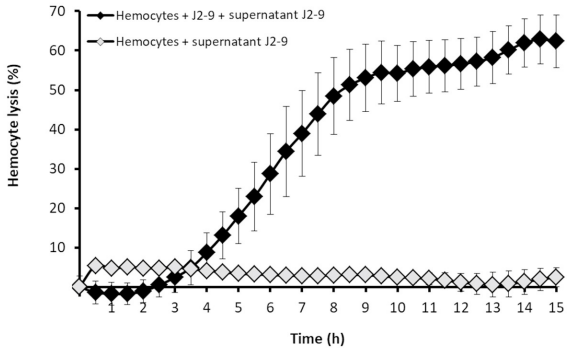

Figure S1 | Extracellular secretion products of J2-9 are not cytotoxic to hemocytes. Cytotoxicity of J2-9 was monitored on monolayers of hemocytes by measuring the fluorescence of Sytox green over 15 hours. At time 0, J2-9 cells (overnight culture) were added to hemocyte monolayers at a MOI of 50:1. Alternatively, an overnight culture supernatant of J2-9 devoid of bacteria (secretion products only) was added to hemocytes. The graph shows the time course of cytotoxicity of J2-9 (black diamonds) and the lack of cytotoxocity of J2-9 secretion products (grey diamonds). The error bars represent the standard deviation of technical triplicates. Data are representative of three independent experiments.

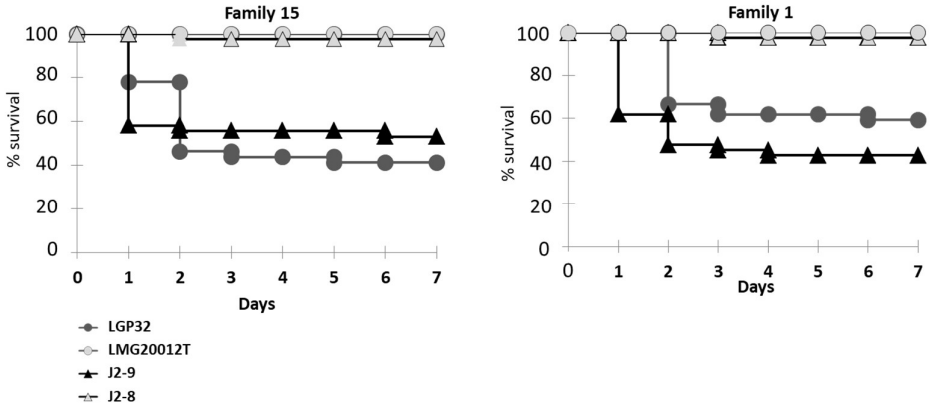

Figure S2 | Virulence of *V. tasmanienis* LGP32 and *V. crassotreae* J2-9 is independent on oyster genetic background. Kaplan Meier survival curves were generated from two additional families of biparental oysters injected with 7.5 x 10^7 CFU per oyster of LGP32, J2-9, LMG20012T or J2-8. Mortalities were monitored on 2 groups of 20 oysters per family (2 seawater tanks per condition) during 7 days after injection. (A) Mortalities on oyster Decipher family #15. LGP32, J2-9 and J2-8 induced 58.7%, 46% and 2.3% of mortalities of oysters respectively. LMG20012T did not induce mortalities. J2-9 and LGP32 conditions are not significantly different (Log-rank p-value=0.560). (B) Mortalities on oyster Decipher family #1. LGP32, J2-9 and J2-8 induced 40.7%, 57.1% and 3.3% of mortalities in oysters, respectively. LMG20012T did not induce mortalities. J2-9 and LGP32 conditions are not significantly different (Log-rank p-value=0.401).

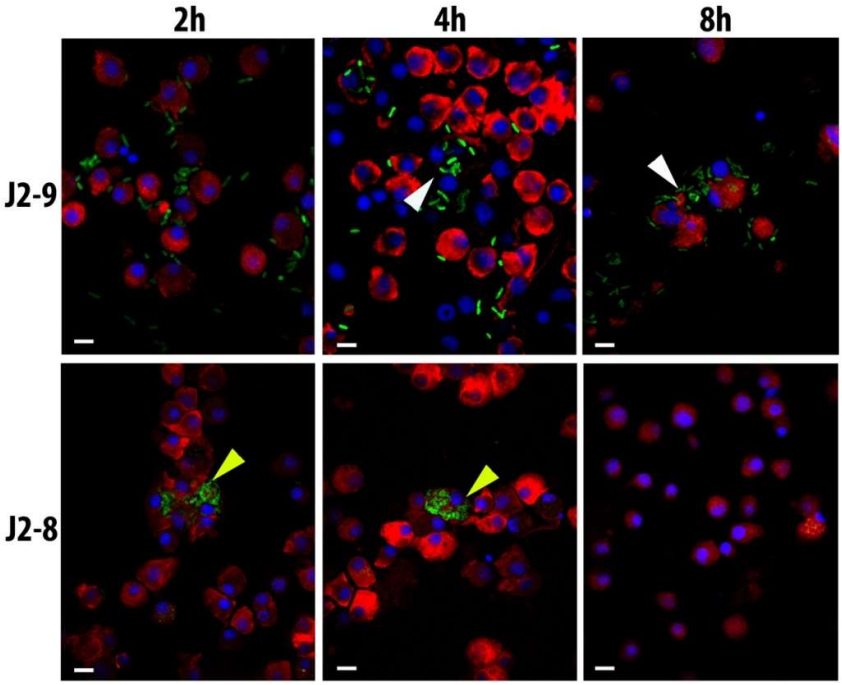

Figure S3 | **Only non-virulent vibrios are degraded by hemocyte phagocytosis**. Confocal microscopy of hemolymph collected from animals infected with *V. crassostrea* J2-9 or the non-virulent control J2-8. Juvenile oysters were injected with 1.5 x 10^8 CFU of GFP-expressing vibrios. For each experimental condition, hemolymph was withdrawn from five oysters, at 2, 4, and 8 h after injection. Hemocytes were observed by confocal microscopy on cytospin glass slides after the staining of nuclei and actin cytoskeleton with DAPI and phalloidin-TRITC, respectively. In oysters injected with J2-9, J2-9 cells were mostly extracellular and were detected at every time-point (white arrows). In contrast, the non-virulent J2-8 was massively phagocytized (yellow arrows) as soon as 2 h after infections showing loss of cell interatity at 4 h; they became almost undetectable after 8h in the oyster hemolymph. Scale bar: 10 µm.

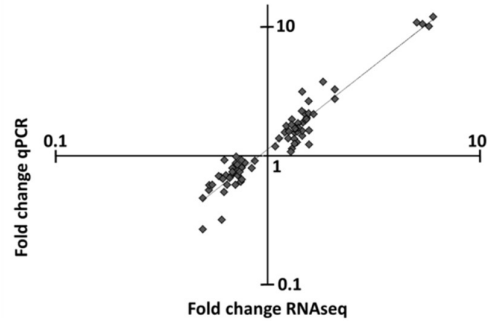

Figure S4 | **Validation of the RNAseq data using quantitative RT-PCR.** Nineteen oyster genes were selected and their expression (relative to the control genes *ef1, c23* and *RP56*) was quantified by qRT-

PCR in RNA samples used for each RNAseq condition. Expression data were compared to those obtained using the RNAseq approach (normalized read counts). Fold changes of RNAseq were fully validated by qPCR (R^2=0.926, p<0.001 linear regression test).

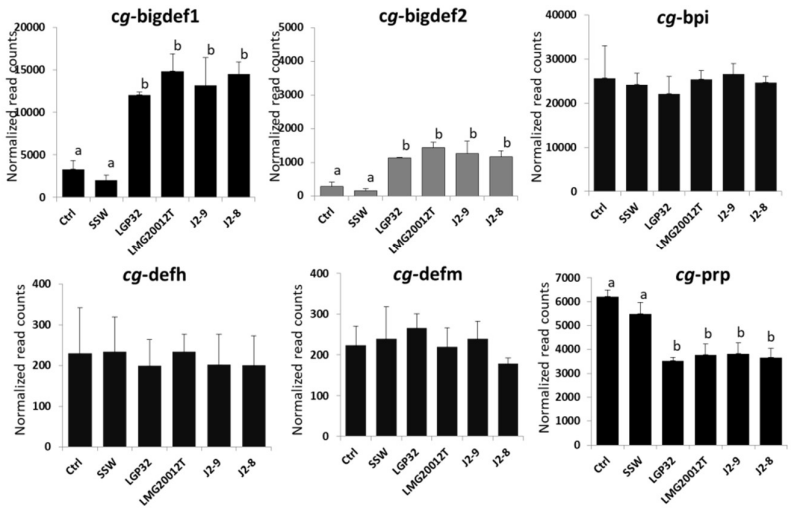

Figure S5 I Antimicrobial peptides respond similarly to virulent and non-virulent strains. Normalized read counts for AMP genes (*cg-bigdef1, cg-bigdef2, cg-bpi, cg-defh, cg-defm, cg-prp*) are plotted for vibrio-infected oysters (LGP32, LMG20012T, J2-9,J2-8), mock-infected oysters (sterile seawater, SSW) and naive oysters (Ctrl). *cg*-bigdef3 was absent from oyster family Decipher#14. Statistical analysis was performed using One-way ANOVA (p<0.001)

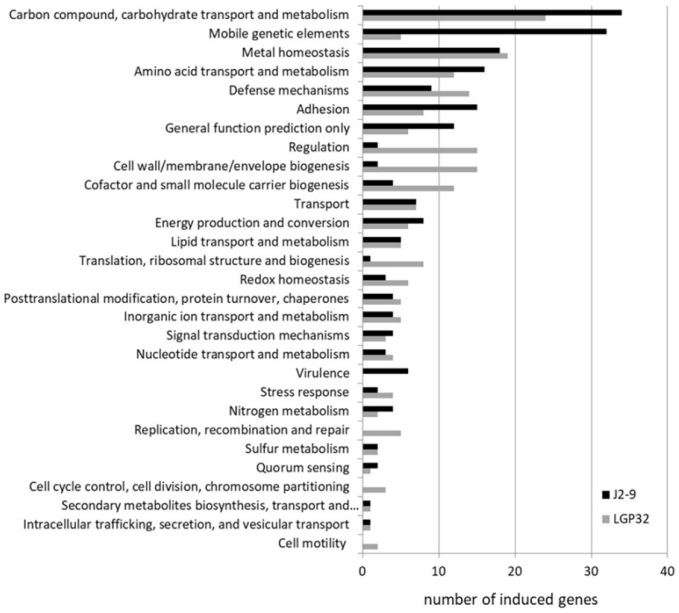

Figure S6 I Functional distribution of the 200 most induced *Vibrio* genes revealed by within host bacterial RNAseq. LGP32 and J2-9 transcripts were sorted according to foldchanges, the 200 most-induced genes during oyster colonization were then counted according to functional categories (genes without annotated function were not included).

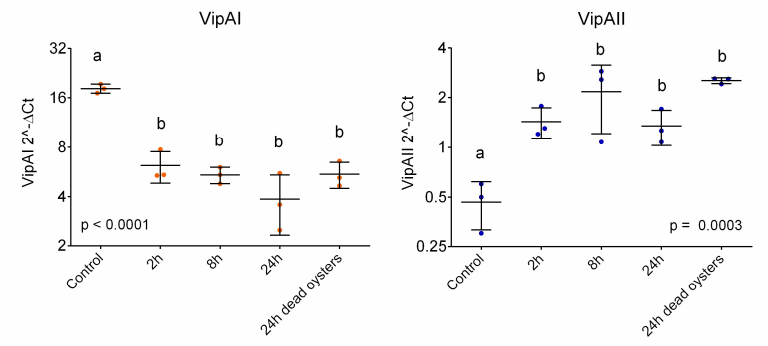

Figure S7 I qPCR monitoring of *vipA1* (VS-1332) and *vipA2* (VS_II0997) during host colonization. An overnight culture of *V. tasmaniensis* LGP32 was washed and resuspended in sterile seawater (SSW). Part of the bacterial suspension was immediately frozen for future RNA extraction (Control). In parallel, 300 juvenile oysters (NSI produced at Ifremer Argenton) were injected with the bacterial suspension (6 x 10^7 CFU per animal, 100 animals per tank). At each time point (2h, 8h, 24h), 10 live oysters and 10 dead oysters (for 24h only) were collected from each tank. Oysters were snap frozen in liquid nitrogen and grinded for RNA extraction. *vipA1* and *vipA2* expression were compared to the geometric mean of two reference genes 6PKF (VS_2913), MGS (VS_II1055). Data correspond to $2^{-\Delta Ct}$ values and Y-axis are in the log scale. Each dot represents a pool of 10 oysters. Data show that *vipA1* expression is frontloaded as opposed to the within-host induction of *vipA2*. Significance established by a One-way ANOVA with Tukey's multiple comparisons test.

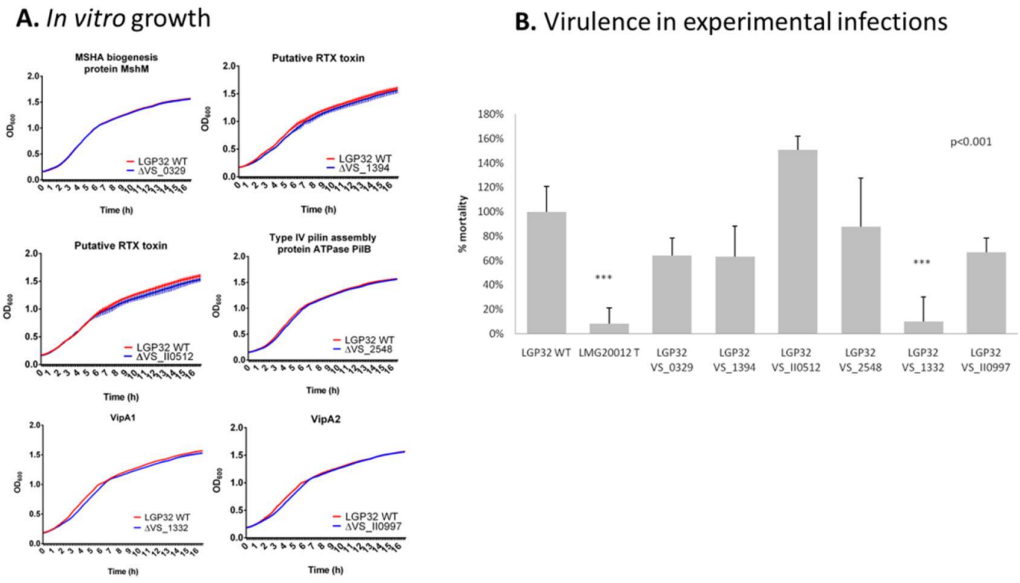

Figure S8 I Phenotyping of *V. tasmaniensis* LGP32 mutants. A. Growth curves of wild-type LGP32 and isogenic mutants. Cultures were made in LB NaCl 0.5M. OD_{600} was recorded in triplicate for each strain every 10 minutes after continuous orbital shaking in a TECAN M200 Infinite Pro plate reader, for a 16 hour

period at 20°C. B. Virulence in oyster experimental infections. Virulence was assessed by intramuscular injection of juvenile oysters in four independent experiments. LMG20012T was used as a negative control. Mortalities were recorded at day 1. Data are expressed as a percentage of the mortality induced by the wild-type strains. Strains or mutants significantly less virulent than the wild-type LGP32 are indicated by asterisks (Test Kruskal-Wallis, Dunn). ***p<0.001

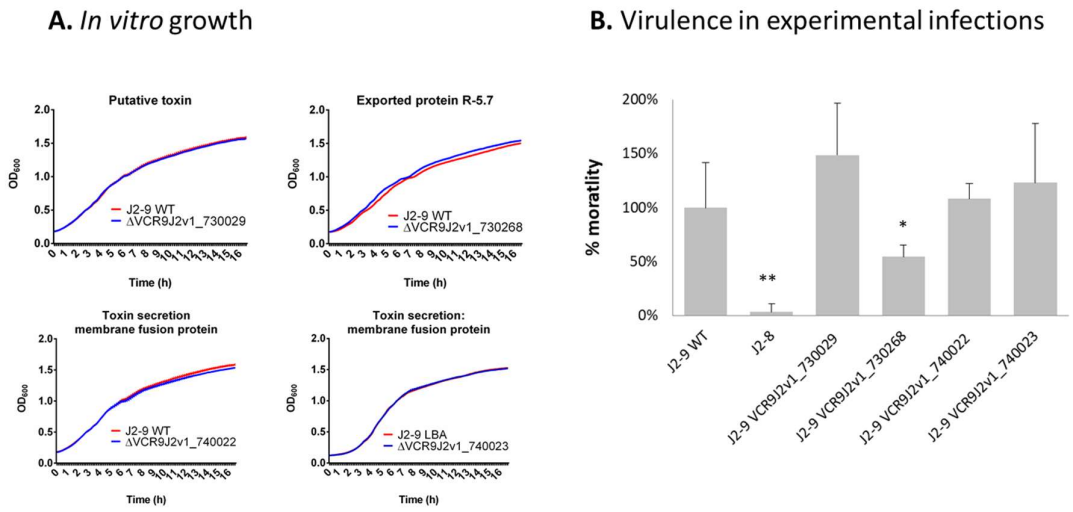

Figure S9 I Phenotyping of *V. crassostreae* J2-9 mutants. A. Growth curves of wild-type J2-9 and isogenic mutants. Cultures were made in LB NaCl 0.5M. OD_{600} was recorded in triplicate for each strain every 10 minutes after continuous orbital shaking in a TECAN M200 Infinite Pro plate reader, for a 16 hour period at 20°C. B. Virulence in oyster experimental infections. Virulence was assessed by intramuscular injection of juvenile oysters in three independent experiments. J2-8 was used as a negative control. Mortalities were recorded at day 1. Data are expressed as a percentage of the mortality induced by the wild-type strains. Strains or mutants significantly less virulent than the wild-type J2-9 are indicated by asterisks (Kruskal-Wallis test with Dunn's multiple comparison test). *p<0.05; **p<0.01

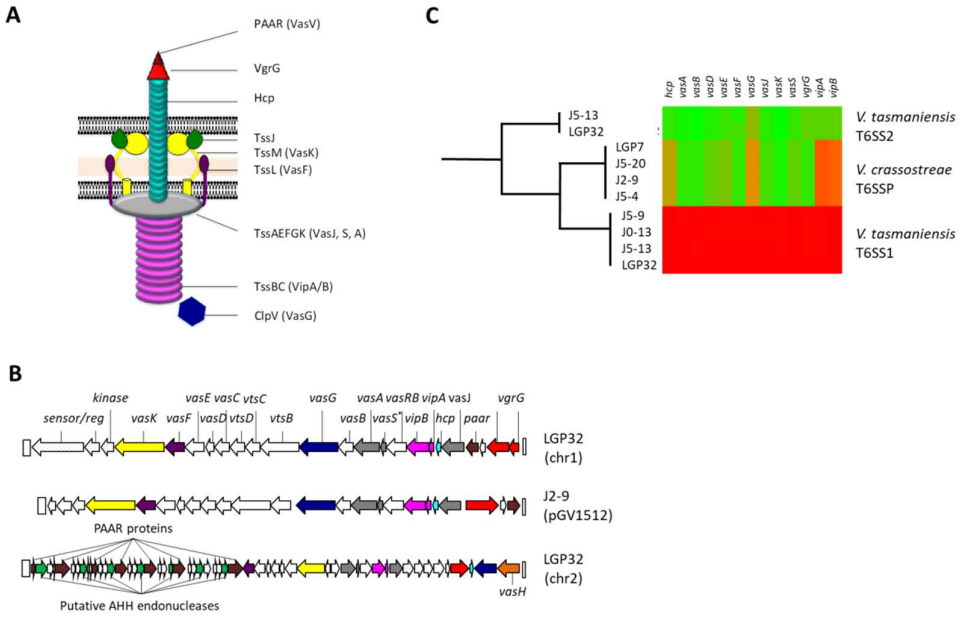

Figure S10 I The type 6 secretion system of *V. tasmaniensis* and *V. crassostreae*. A. Schematic representation of the assembled T6SS. The core-proteins of the T6SS are colored and named. B. Genes organization of the two T6SS of *V. tasmaniensis* LGP32 (chr1 : chromosome 1 ; chr2 : chromosome 2) and the T6SS of *V. crassostreae* J2-9 localized on a plasmid (pGV1512). The genes are named and colored in accordance to the previously shown schematic structure of the T6SS. C. Conservation of the core-proteins of the T6SSs in multiple strains of *V. tasmaniensis* and *V. crassostreae*.

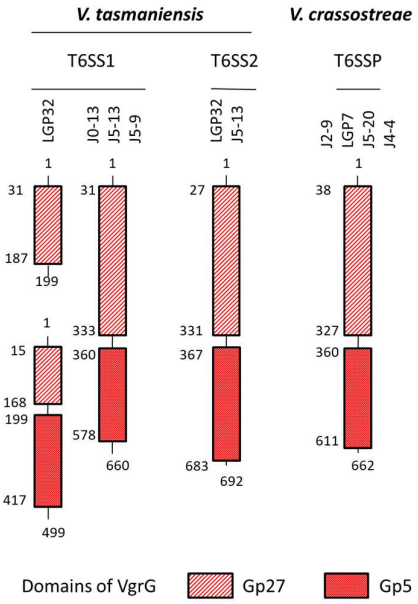

Figure S11 I Functional annotation of VgrG in the T6SSs of *V. tasmaniensis* and *V. crassostreae*. The different domains are indicated by squared with different motifs. The numbers indicate the beginning/end of the different domains.

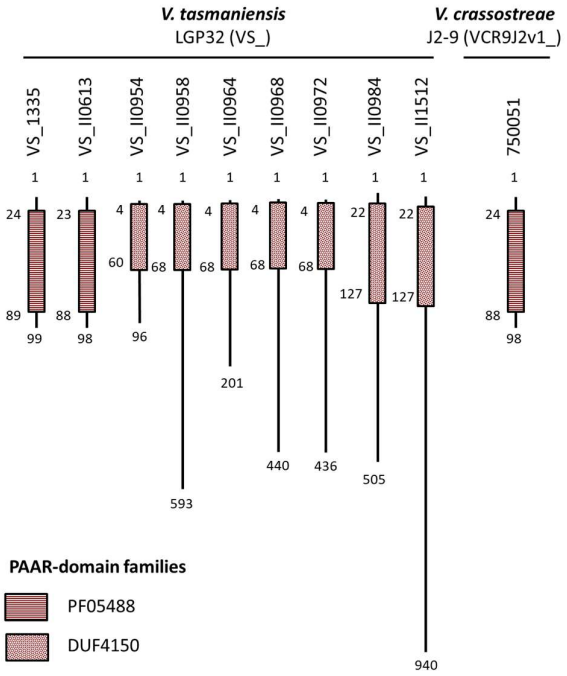

Figure S12 I Functional annotation of PAAR in the T6SSs of *V. tasmaniensis* and *V. crassostreae*. The different domains are indicated by squared with different motifs. The numbers indicate the beginning/end of the different domains.

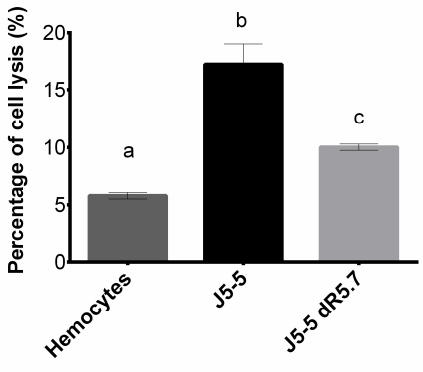

Figure S13 I Cytotoxicity of *V. crassostreae* J5-5 wild-type and isogenic mutant lacking the R5.7 virulence gene.

Cytotoxicity was determined on monolayers of hemocytes and monitored by the Sytox green assay. Cells were infected with bacteria at a MOI of 50:1. Maximum of cytotoxicity of vibrios is displayed. Error bars represent the standard deviation of the mean (RM-ANOVA p-value<0.001).

Table S1 | qPCR quantification of vibrios in oyster tissues.

Real-time qPCR was performed on 40ng/µl of DNA on the same samples using for RNAseq. Quantification of vibrios was calculated in number of vibrio genome copy per number of oyster genome copy because of Avogadro number and genome size of oyster and vibrios. These primers have been chosen because they are specific for each vibrio species. The ratio is the mean of 3 independent experiments.

Strains	Ratio: copy of vibrio genome/copy of oyster genome	Standard deviation
LGP32	0.045	0.037
LMG20 012T	0.015	0.005
J2-9	0.02	0.0014
J2-8	0.02	0.0038

Table S2. Bacterial strains

Strain	Description	Mutated gene	Reference
Π3813	*lacIQ, thi1, supE44, endA1, recA1, hsdR17, gyrA462, zei298::Tn10*, *DthyA::(erm-pir116)* [Tc^R Erm^R]		Le Roux et al., 2007
β3914	(F $^-$) RP4-2-Tc::Mu ΔdapA ::*(erm-pir116), gyrA462, zei298::Tn10* [Km^R Em^R Tc^R]		Le Roux et al., 2007
GV1508	J2-9, *V. crassostreae*		Lemire et al., 2015
GV1476	J2-9 + pMRB-P_{LAC}*gfp*		Bruto et al., 2017
GV1438	J2-9 *ΔpGV1512*		Bruto et al., 2017
GV1023	J2-9 *ΔR5.7*	VCR9J2v1_730268	Lemire et al., 2015
	J2-9 Δ*VCR9J2v1_740022::pSW23T* [Cm^R]	VCR9J2v1_740022	This study
	J2-9 Δ*VCR9J2v1_740023::pSW23T* [Cm^R]	VCR9J2v1_740023	This study
	J2-9 Δ*VCR9J2v1_730029::pSW23T* [Cm^R]	VCR9J2v1_730029	This study
GV1460	J2-8, *Vibrio sp.*		Lemire et al., 2015
GV1470	J2-8 + pMRB-P_{LAC}*gfp*		Bruto et al., 2017
	J5-4, *V. crassostreae*		Lemire et al., 2015
	J5-5, *V. crassostreae*		Lemire et al., 2015
GV1026	J5-5 *ΔR5.7*		Lemire et al., 2015
	J5-20, *V. crassostreae*		Lemire et al., 2015
	LGP8, *V. crassostreae*		Faury et al., 2005
	LGP32, *V. tasmaniensis*		Gay et al., 2004
	LGP32 + pMRB-P_{LAC}*gfp*		Vanhove et al., 2016
	LGP32 Δ*vipA T6SS1::pSW23T* [Cm^R]	VS_1332	This study
	LGP32 Δ*vipA T6SS2::pSW23T* [Cm^R]	VS_II0997	This study
	LGP32 Δ*mshM::pSW23T* [Cm^R]	VS_0329	This study
	LGP32 Δ*pilB::pSW23T* [Cm^R]	VS_2548	This study
	LGP32 Δ*rtx::pSW23T* [Cm^R]	VS_1394	This study
GV76	LGP32 Δ*rtx1*	VS_II0512	Binesse et al., 2008
	J0-13, *V. tasmaniensis*		Lemire et al., 2015
	J5-13, *V. tasmaniensis*		Lemire et al., 2016
	J5-9, *V. tasmaniensis*		Lemire et al., 2017
	LMG20012T, *V. tasmaniensis*		Thompson et al., 2003
	LMG20012T + pMRB-P_{LAC}*gfp*		Vanhove et al., 2016

Table S3. Plasmids

Plasmid	Description	Reference
pSW23T	*oriV*$_{R6K}$; *oriT*$_{RP4;}$ [Cm^R]	Demarre et al. 2005
pSWδVCR9J2v1_740022	pSW23T; *ΔVCR9J2v1_740022*	This study
pSWδVCR9J2v1_740023	pSW23T; *ΔVCR9J2v1_740023*	This study
pSWδVCR9J2v1_730029	pSW23T; *ΔVCR9J2v1_730029*	This study
pSWδmshM	pSW23T; *ΔmshM VS_0329*	This study
pSWδpilB	pSW23T; *ΔpilB VS_2548*	This study
pSWδrtx	pSW23T; *Δrtx VS_1394*	This study
pSWδvipAT6SS1T	pSW23T; *ΔvipA T6SS1*	This study
pSWδvipAT6SS2T	pSW23T; *ΔvipA T6SS2*	This study
pMRB-P$_{LAC}$*gfp*	*oriV*$_{R6Kg}$; *oriT*$_{RP4}$; *oriV*$_{pB1067;}$ P$_{LAC}$- *gfp* [Cm^R]	Le Roux et al., 2011

Table S4. Oligonucleotides

Oligonucleotide	Gene id	Sequence 5'-3'	Description	Organism	Use
CGI_10007949 F1	CGI_10007949	GGATGACGTGTTTCGTAGGG	B-1,3-galactosyltransferase brn	*C. gigas*	qRT-PCR of host genes
CGI_10007949 R1	CGI_10007949	TCAATGTCTGCCAACAGCTC	B-1,3-galactosyltransferase brn	*C. gigas*	qRT-PCR of host genes
CGI_10010688 F2	CGI_10010688	GACGGAAAGCTGGACACTGA	Bone-morphogenetic 1-like	*C. gigas*	qRT-PCR of host genes
CGI_10010688 R2	CGI_10010688	AGGTCATAGGGAGGGGCTTT	Bone-morphogenetic 1-like	*C. gigas*	qRT-PCR of host genes
CGI_10000441 F2	CGI_10000441	CCCAGGGTGCTCAACAATCA	Krueppel-like factor 5	*C. gigas*	qRT-PCR of host genes
CGI_10000441 R2	CGI_10000441	TGTGTTTTCGTATGTGGCGC	Krueppel-like factor 5	*C. gigas*	qRT-PCR of host genes
CGI_10000066 F2	CGI_10000066	TCTGCTCTGATTCGTGTCCA	Metallothionein	*C. gigas*	qRT-PCR of host genes
CGI_10000066 R2	CGI_10000066	TTGCAGTTTTCCGGTCCAGT	Metallothionein	*C. gigas*	qRT-PCR of host genes
CGI_10024165 F2	CGI_10024165	AGGATGAGACGGTTGCTCAG	Paired bov Pax-8-like isoform X1	*C. gigas*	qRT-PCR of host genes
CGI_10024165 R2	CGI_10024165	CCAACAACTTTGGCAGAACC	Paired bov Pax-8-like isoform X1	*C. gigas*	qRT-PCR of host genes
CGI_10020521 F1	CGI_10020521	CCACCTACACTCCAACGGAC	Zinc transporter 2-like	*C. gigas*	qRT-PCR of host genes
CGI_10020521R1	CGI_10020521	GGACGTGGATAAAGGCTGCT	Zinc transporter 2-like	*C. gigas*	qRT-PCR of host genes
CGI_10003627F1	CGI_10003627	AGATTGCCTGTCCAGTCACG	Metalloreductas STEAP4-like	*C. gigas*	qRT-PCR of host genes
CGI_10003627R1	CGI_10003627	AAACTTCATGGCTCCCTCCG	Metalloreductas STEAP4-like	*C. gigas*	qRT-PCR of host genes
CGI_10002304F1	CGI_10002304	TGTATCCGGTCGAGAGTGAG	Cyclin-G-associated kinase-like	*C. gigas*	qRT-PCR of host genes
CGI_10002304R1	CGI_10002304	TAACCGATTCCAGCTTGCGG	Cyclin-G-associated kinase-like	*C. gigas*	qRT-PCR of host genes
CGI_10010647F2	CGI_10010647	TACGTCGCCTTCACAGACAC	Heat shock 70	*C. gigas*	qRT-PCR of host genes
CGI_10010647R2	CGI_10010647	CGGCCAATGTTTCATGTCGG	Heat shock 70	*C. gigas*	qRT-PCR of host genes
CGI_10019038F2	CGI_10019038	TGGCCACATTGTCCCTTCAG	Arginine deiminase/G1/S-specific cyclin-E1	*C. gigas*	qRT-PCR of host genes
CGI_10019038 R2	CGI_10019038	CGAAGGACCAGTTGAGGAGG	Arginine deiminase/G1/S-specific cyclin-E1	*C. gigas*	qRT-PCR of host genes
CGI_10025754 F1	CGI_10025754	GCCCACGAATCTTGCTGAAC	Interleukin 17	*C. gigas*	qRT-PCR of host genes
CGI_10025754 R1	CGI_10025754	TTTGGGTAGCGGGTGGAAAG	Interleukin 17	*C. gigas*	qRT-PCR of host genes
CGI_10000478 F1	CGI_10000478	GACGACCCTATCCCAACACC	Neuronal acethylcholine receptor subunit α-6-like	*C. gigas*	qRT-PCR of host genes
CGI_10000478 R1	CGI_10000478	ATCTCGCCGATCCTTTTCCC	Neuronal acethylcholine receptor subunit α-6-like	*C. gigas*	qRT-PCR of host genes
CGI_10004930 F2	CGI_10004930	AAGTGGTCGAGAAACACCCG	NADPH oxidase 5	*C. gigas*	qRT-PCR of host genes
CGI_10004930 R2	CGI_10004930	CCGGGTCAGACGAACTCTTC	NADPH oxidase 5	*C. gigas*	qRT-PCR of host genes
CGI_10007268 F2	CGI_10007268	AGCAATGCTGGACACAACAG	Zinc transporter ZIP10-like isoform X1	*C. gigas*	qRT-PCR of host genes
CGI_10007268 R2	CGI_10007268	AATGGCGATGAAGCTGTACC	Zinc transporter ZIP10-like isoform X1	*C. gigas*	qRT-PCR of host genes
CGI_10009274 F2	CGI_10009274	AGCTGACAACACTGCCCAAT	Complement C1q tumor necrosis factor-related 7-like	*C. gigas*	qRT-PCR of host genes
CGI_10009274 R2	CGI_10009274	TTACTGGTTTCAGCTGTGCG	Complement C1q tumor necrosis factor-related 7-like	*C. gigas*	qRT-PCR of host genes
CGI_10000910 F2	CGI_10000910	AATGTCACAATGGGAAGCGC	Complement C1q4	*C. gigas*	qRT-PCR of host genes
CGI_10000910 R2	CGI_10000910	GGAGGTGGAATATGCGCTGT	Complement C1q4	*C. gigas*	qRT-PCR of host genes

CGI_10020815 F2	CGI_10020815	TGGCCAACATGAACATGTCC	Complement C1q2	*C. gigas*	qRT-PCR of host genes
CGI_10020815 R2	CGI_10020815	TGCTCCCACTGTTGTACCAA	Complement C1q2	*C. gigas*	qRT-PCR of host genes
CGI_10000960 F1	CGI_10000960	ACTGGGGAAAGAGGACGGAT	Frizzled-1	*C. gigas*	qRT-PCR of host genes
CGI_10000960 R1	CGI_10000960	ACACGCTTGGCTCCATGTAA	Frizzled-1	*C. gigas*	qRT-PCR of host genes
CGI_10020472 F2	CGI_10020472	TGATGGACTCGGCTCAGTTG	Deleted in malignant brain tumors 1-like	*C. gigas*	qRT-PCR of host genes
CGI_10020472 R2	CGI_10020472	TCAATGGCGGTTCTCTCACC	Deleted in malignant brain tumors 1-like	*C. gigas*	qRT-PCR of host genes
EFUfw	AB122066	GAGCGTGAACGTGGTATCAC	EF1	*C. gigas*	qRT-PCR of host genes
EFUrv	AB122066	ACAGCACAGTCAGCCTGTGA	EF1	*C. gigas*	qRT-PCR of host genes
C23fw	HS119070	AATCTTGCACCGTCATGCAG	C23	*C. gigas*	qRT-PCR of host genes
C23rv	HS119070	AATCAATCTCTGCTGATCTGC	C23	*C. gigas*	qRT-PCR of host genes
rp56F	FP004478	CAGAAGTGCCAGCTGACAGTC	RP56	*C. gigas*	qRT-PCR of host genes
rp56R	FP004478	AGAAGCAATCTCACACGGAC	RP56	*C. gigas*	qRT-PCR of host genes
OmpUS3	VS_2494	GTCCTACAGACAGCGATAGC	Porin OmpU	LGP32	qPCR quantification of vibrios
OmpUAS2	VS_2494	GTGGTAAGCCATGATATCGC	Porin OmpU	LGP32	qPCR quantification of vibrios
R5-2aF	VRSK9J2v1_730268	GGATGGGACCAACTACGGTG	Protein R5-2	J2-9	qPCR quantification of vibrios
R5-2aR	VRSK9J2v1_730268	CGTAGCCCGGAGGAAGAATC	Protein R5-2	J2-9	qPCR quantification of vibrios
LMG20012TF2	VTAS012-v1-10089	GGCGTTTCTTCACTTGCGAC	Exported protein of unknow function	LMG20012T	qPCR quantification of vibrios
LMG20012TR2	VTAS012-v1-10089	TTTGCGGAGAAGTGCTAGGG	Exported protein of unknow function	LMG20012T	qPCR quantification of vibrios
J2-8F2	VCR8J2v1-840028	GAGCTTGAGATGGAGAATCG	Anticodon nuclease	J2-8	qPCR quantification of vibrios
J2-8R2	VCR8J2v1-840028	ACCGTTTCTACTTCTGCACC	Anticodon nuclease	J2-8	qPCR quantification of vibrios
ΔmshM-1	VS_0329	CGGCGTTAGAAATGGGTGAG	MSHA biogenesis protein MshM	LGP32	Mutagenesis
ΔmshM-2	VS_0329	CCAAAGAAGAGCGCCAGATC	MSHA biogenesis protein MshM	LGP32	Mutagenesis
ΔpilB-1	VS_2548	GCCTGACTCAAGAACAAGCC	Type IV pilin assembly protein ATPase PilB	LGP32	Mutagenesis
ΔpilB-2	VS_2548	GATTGGCGAGCTCATCTTGG	Type IV pilin assembly protein ATPase PilB	LGP32	Mutagenesis
Δrtx-1	VS_1394	TCAAAGTCCATGATGCTGCG	Putative hemolysin-type RTX toxin	LGP32	Mutagenesis
Δrtx-2	VS_1394	CAAGGTTTGCTTTGCCAACG	Putative hemolysin-type RTX toxin	LGP32	Mutagenesis
ΔVCR9J2v1_730029-1	VCR9J2v1_730029	CCAATGGTTGGCGCTACTCC	Putative NAD(+)—arginine ADP ribosyltransferase	J2-9	Mutagenesis
ΔVCR9J2v1_730029-2	VCR9J2v1_730029	CGCTCTATCTGGGTGATTCG	Putative NAD(+)—arginine ADP ribosyltransferase	J2-9	Mutagenesis
ΔVCR9J2v1_740022-1	VCR9J2v1_740022	TGAGTTCGCTTCAGGTCGAG	Toxin secretion: membrane fusion protein (fragment)	J2-9	Mutagenesis
ΔVCR9J2v1_740022-2	VCR9J2v1_740022	TAA CCA TTC TAG GAG CGT GC	Toxin secretion: membrane fusion protein (fragment)	J2-9	Mutagenesis
ΔVCR9J2v1_740023-1	VCR9J2v1_740023	AACGCTAACAGGTCGCGTCG	Toxin secretion: membrane fusion protein (fragment)	J2-9	Mutagenesis

ΔVCR9J2v1_740023-2	VCR9J2v1_740023	GTCAAGGCGTATGGTGTTGG	Toxin secretion: membrane fusion protein (fragment)	J2-9	Mutagenesis
ΔvipAT6SS1-1	VS_1332	GtatcgataagcttgatatcgaattcTGACGTTGAGACTAATGGCG	VipA protein from T6SS1	LGP32	Mutagenesis
ΔvipAT6SS1-2	VS_1332	CccccgggctgcaggaattcTCGTGTCTGCACTTTGTAGAAC	VipA protein from T6SS1	LGP32	Mutagenesis
ΔvipAT6SS2-1	VS_II0997	GtatcgataagcttgatatcgaattcTTCCAGCGACAGGCGATGCG	VipA protein from T6SS2	LGP32	Mutagenesis
ΔvipAT6SS2-2	VS_II0997	CccccgggctgcaggaattcTCTTCATCTTGAAGAACAGCTGC	VipA protein from T6SS2	LGP32	Mutagenesis
Ext mshM-1	VS_0329	ATGTATCAAGCTCACTTTAG	MSHA biogenesis protein MshM	LGP32	Control of mutagenesis
Ext mshM-2	VS_0329	CCAACCCCACAGCATTGGCG	MSHA biogenesis protein MshM	LGP32	Control of mutagenesis
Ext pilB-1	VS_2548	GTGTGTAGTGCTAACCAACC	Type IV pilin assembly protein ATPase PilB	LGP32	Control of mutagenesis
Ext pilB-2	VS_2548	AGGGCATTGAGATAGAGCGC	Type IV pilin assembly protein ATPase PilB	LGP32	Control of mutagenesis
Ext rtx-1	VS_1394	GAAAGATGCCCAAGGTAACG	Putative hemolysin-type RTX toxin	LGP32	Control of mutagenesis
Ext rtx-2	VS_1394	ACTCAGTTTAACGCCATCCG	Putative hemolysin-type RTX toxin	LGP32	Control of mutagenesis
Ext VCR9J2v1_730029-1	VCR9J2v1_730029	GTTGTCTGAGCTTTACTGCC	Putative NAD(+)—arginine ADP ribosyltransferase	J2-9	Control of mutagenesis
Ext VCR9J2v1_730029-2	VCR9J2v1_730029	TGTACAAACGAGAGAGTGCC	Putative NAD(+)—arginine ADP ribosyltransferase	J2-9	Control of mutagenesis
Ext VCR9J2v1_740022-1	VCR9J2v1_740022	AAGCTGGCTTTTTAGTACGG	Toxin secretion: membrane fusion protein (fragment	J2-9	Control of mutagenesis
Ext VCR9J2v1_740022-2	VCR9J2v1_740022	AGCTCTGGGTAGAGGAAGG	Toxin secretion: membrane fusion protein (fragment	J2-9	Control of mutagenesis
Ext VCR9J2v1_740023-1	VCR9J2v1_740023	ATGTTATTTCGCCGACAAGTTC	Toxin secretion: membrane fusion protein (fragment	J2-9	Control of mutagenesis
Ext VCR9J2v1_740023-2	VCR9J2v1_740023	TTATTCGCTTCTTGGTATTC	Toxin secretion: membrane fusion protein (fragment	J2-9	Control of mutagenesis
Ext vipAT6SS1-1	VS_1332	ACGCGTAAGTAAGAACCGCG	VipA protein from T6SS1	LGP32	Control of mutagenesis
Ext vipAT6SS1-2	VS_1332	CCTAGCTCATCAGAAAGCGC	VipA protein from T6SS1	LGP32	Control of mutagenesis
Ext vipAT6SS2-1	VS_II0997	TGATGGCTCGGTGGCTCCG	VipA protein from T6SS2	LGP32	Control of mutagenesis
Ext vipAT6SS2-2	VS_II0997	TCGCCTTGGTCTGCACCAATG	VipA protein from T6SS2	LGP32	Control of mutagenesis
vipA1-F	VS_1332	GGTGATGACAGCCAGTTTGA	VipA protein from T6SS1	LGP32	qRT-PCR of bacterial genes
vipA1-R	VS_1332	CGAGAACGATCGGCTTTAGA	VipA protein from T6SS1	LGP32	qRT-PCR of bacterial genes
vipA2-F	VS_II0997	GCCTTGGTTGCATTAAAAGG	VipA protein from T6SS2	LGP32	qRT-PCR of bacterial genes
vipA2-R	VS_II0997	TGGTCTGCACCAATGCTAAG	VipA protein from T6SS2	LGP32	qRT-PCR of bacterial genes
6PKF-F	VS_2913	GCCGTCACTGTGGTGACCTT	6-phosphofructokinase	LGP32	qRT-PCR of bacterial genes
6PKF-R	VS_2913	TGCTTCTTGCCTTTCGCAAT	6-phosphofructokinase	LGP32	qRT-PCR of bacterial genes
MGS-F	VS_II1055	CTTTATGCAACGGGCACGAC	Methyl glyoxal synthase	LGP32	qRT-PCR of bacterial genes

MGS-	VS_II1055	GGTCGTGTGGTACGGCATTTA	Methyl glyoxal synthase	LGP32	qRT-PCR of bacterial genes

II.2.2. Supplementary Information Text

Materials and Methods

Strains, plasmids, and primers

Virulent strains used in this study were *V. tasmaniensis* LGP32 (1), *V. crassostreae* J2-9 (2). Non-virulent strains were *Vibrio sp.nov*. J2-8, close phylogenetic neighbor of the virulent *V. crassostreae* population (2) as well as the type strain of *V. tasmaniensis* LMG20 012T (3). Other strains, plasmids and primers used or constructed in the present study are described in SI Appendix Tables S2-S3-S4.

Animals

C. gigas diploid oyster spat were used from three families of siblings (referred to as Decipher #1, #14 and #15) (4) and a batch of standardized Ifremer spats (NSI) were produced from a pool of 120 genitors (5). Animals were from both sexes. Spats (4 to 6 months old) were used for experimental infections and dual RNA-seq. Adults (18 months old) produced from a pool of 120 genitors (ASI) were used to collect hemolymph for cytotoxicity assays. All oysters were produced at the Ifremer hatchery in Argenton, France. All families have been tested in experimental infections. The oysters of family #14 were chosen for the RNA-seq experiments.

Experimental infections

Experimental infections were performed at 20 °C by adapting a previously described procedure (6). Briefly, oysters were anesthetized for 3 h (7). Groups of 20 juvenile oysters (1.5-2 cm) were then distributed into tanks containing 3 L of seawater, per condition. Stationary phase cultures of bacteria (20 h at 20 °C) were washed by centrifugation (15 min, 1500 g, 20 °C) and resuspended in sterile seawater (SSW) before injecting at 7.5×10^7 CFU into oyster adductor muscle. Mortalities were monitored daily for 7 days. Two tanks were monitored per condition. Statistical analyses were performed using non-parametric Kaplan Meier test in order to estimate log-rank values for comparing conditions (GraphPad Prism 6). All experimental infections were performed according to the Ifremer animal care guidelines and policy.

Molecular microbiology

Vibrio isolates were grown at 20 °C in Zobell broth or agar (4 $g.l^{-1}$ bactopeptone and 1 $g.l^{-1}$ yeast extract in artificial seawater, pH 7.6), Luria-Bertani (LB) broth or LB-agar (LBA) containing 0.5 M NaCl. *Escherichia coli* strains were grown at 37°C in LB or on LBA for cloning and conjugation experiments. Chloramphenicol (Cm, 5, 10 or 25$\mu g.ml^{-1}$ depending on the strain), thymidine (0.3 mM) and diaminopimelate (0.3 mM) were added as supplements when

necessary. Conjugation between *E. coli* and *Vibrio* were performed at 30 °C as described previously (8). To label the strains with a fluorochrome, *gfp* gene was cloned in Apa1/Xho1 sites of the pMRB plasmid known to be stable in *Vibrio spp.* (9) resulting in a constitutive expression from a P_{lac} promoter. Gene inactivation was performed by cloning about 500 bp of the target gene in pSW23T (10) and selecting on Cm the suicide plasmid integration obtained by a single recombination (11). Mutants were screened for insertion of the suicide vector by PCR using external primers flanking the different targeted genes.

Histology

Groups of 10 spats (1.5-2 cm) were injected with 7.5 x 10^7 CFU of GFP-expressing LGP32 or J2-9. Groups of 5 spats were injected with 7.5 x 10^7 CFU of GFP-expressing LMG20 012T or J2-8 (controls). Two non-injected oysters were used as controls. Spats were distributed in one tank containing 3 L of seawater per condition, at 20 °C. Oysters were sampled and fixed 8 h after injection, in seawater Davidson (20% of formaldehyde, 30% of sterile seawater, 10% of glycerol and 30% of 95% ethanol). Histological sectioning was performed at HISTALIM, Montpellier, France. Briefly, oysters were extracted from the shell, tissues were dehydrated and included in paraffin with an inclusion automaton. Longitudinal sections were immunostained with an anti-GFP primary antibody coupled to alkaline phosphatase (Abcam). Revelation was performed with the PA-Red kit (Roche). Sections were scanned with slide scanner Hamamatsu NANOZOOMER. Hemocytes were observed with the ZEISS Z1 microscope equipped with Zeiss 63X/1.4 Plan-Apo Oil objective.

In vitro cytotoxicity assays

Hemocytes were plated in 96 well-plates (2 x 10^5 cells/well) or in 12 well-plates (5 x 10^5 cells/well) with a Transwell Permeable Support with a pore size of 0.4 µm. After 1 h, plasma was removed and 5 µg/µl Sytox Green (Molecular Probes) diluted in 200µl sterile seawater was added to each well. Vibrios, previously washed and opsonized in plasma for 1 h, were then added to the wells at a MOI of 50:1. Sytox fluorescence was monitored (λ_{ex} 480nm/λ_{em} 550nm) for 15 h using a TECAN microplate reader. Maximum cytolysis was determined by adding 0.1% Triton X-100 to hemocytes. To determine the role of phagocytosis in the vibrio-induced cytolysis of hemocytes, 5 µg/ml cytochalasin D was added to the wells 30 min before addition of vibrios. Statistical analysis was performed using RM-ANOVA.

Confocal microscopy of interaction between hemocytes and vibrios *in vivo*

Groups of 15 juvenile oysters (4-5 cm) were injected with 1.5 x 10^8 CFU of GFP-expressing vibrios (either J2-8 or J2-9) *a priori* washed and resuspended in sterile seawater. Control oysters received an injection of an equal volume of sterile seawater. For each experimental condition, hemolymph was collected from five oysters at 2 h, 4 h and 8 h after injection. Samples were fixed with 4% paraformaldehyde for 15 min and cytospun at 600 g for 10 min onto Superfrost glass slide. Glass slides were then washed with PBS and stained with 0.25 µg/ml DAPI (Sigma) and 1 µg/ml Phalloïdine-TRITC (Sigma) for 30 min at room temperature. Microscopy was performed using Leica DM 2500 confocal microscope with a Leica 63x ACS

APO 1.3 objective.

Dual RNA-seq experiments

Three independent experimental infections were performed on juvenile oysters from family Decipher#14 as described above. For every independent experiment, 150 oysters (30 animals per condition) were injected with either bacteria (10^7 CFUs of LGP32, LMG20012T, J2-9, J2-8 overnight cultures washed in sterile seawater), or sterile seawater (mock-infected oysters). In addition, both bacterial suspensions and 30 non-treated oysters were collected at time 0. For every experimental condition, 30 oysters were then sampled 8 h after injection (*i.e.* before mortality occurred). Oysters were extracted from shell and immediately frozen in liquid nitrogen. Pools of tissues from 30 oysters were ground by bead-beating (Retsch, Mixer Mill MM400) with a stainless-steel ball pre-chilled in liquid nitrogen. Both, oyster powder homogenates and bacterial suspensions, were lysed in 1.6 ml Trizol (Life technologies Inc.) and vortexed for 2.5 h at 4 °C. Samples were then stored at -80 °C until RNA extraction.

RNA was extracted from oyster tissues using the Direct-Zol RNA Miniprep kit from Proteigene, and according to the manufacturer's protocol. RNA concentration and purity were checked with a Nanodrop ND-1000 spectrometer (Thermo Scientific, Les Ulis, France; oyster RNA-seq) or a DS-11 Spectrophotometer (DeNovix Inc.; bacterial RNA-seq) and the integrity of the RNA was analyzed by capillary electrophoresis with an Agilent BioAnalyzer 2100. For oyster RNA-seq, library construction and sequencing were performed on polyadenylated mRNAs by the Fasteris Company (Switzerland, https://www.fasteris.com). Directional cDNA libraries were constructed and sequenced on an Illumina Hiseq, in paired-end reads of 2 x75 bp. For bacterial RNA-seq, total RNA obtained from oyster tissues was used to prepare non rRNA-bacterial RNA enriched libraries. After polyadenylated mRNAs (i.e. host mRNAs) were removed using MICROB*Enrich*™ Kit (Ambion), cDNA oriented sequencing libraries were prepared starting from 100 ng enriched RNA using Ovation Universal RNA-Seq System kit (NuGEN). Library construction included a depletion step of abundant, non-desired sequences, using a Nugen-customized mixture of primers complementary to RNA sequences to be depleted, viz. oyster nuclear, mitochondrial, and ribosomal and bacterial ribosomal RNA sequences. The libraries were quantified by DeNovix dsDNA Broad Range Assay (DeNovix Inc.) and the quality was monitored using Agilent High Sensitivity DNA kit (Agilent Technologies). For each condition, three biological replicate libraries were prepared. Libraries were sequenced in paired-end mode (2 × 150 bp) by Fasteris on an Illumina HiSeq 4000, to obtain ~ 100 million reads per sample/per run.

Oyster transcriptome analysis

For oyster RNA-seq data, data treatment was carried out using the galaxy instance of the IHPE lab (https://bioinfo.univ-perp.fr) (12). Phred quality scores were checked using the FastX toolkit galaxy interface (http://hannonlab.cshl.edu/fastx_toolkit/) and were higher than 26 for over 90% of the read length for all the sequences. All the reads were thus kept for subsequent analyses. Mapping to the *C. gigas* reference genome (assembly version V9 (13)) was performed using RNAstar (Galaxy Version 2.4.0d-2, (14)). HTSeq-count was used to count the number of reads overlapping annotated genes (mode Union) (Galaxy Version v0.6.1) (15).

The resulting files were used as input to determine differential expression for each feature between oysters injected with vibrios and mock-infected oysters using DESeq2 (16). Fold changes in gene expression between test animals and controls were considered significant when the adjusted *P*-value (P_{adj}) for multiple testing with the Benjamini-Hochberg procedure, which controls false discovery rate (FDR), was < 0.05. The same threshold was applied to fold changes in gene expression between mock-infected oysters and naïve controls. Oyster RNA-seq data has been made available through the SRA database (BioProject accession number PRJNA515169) under SRA accessions SRR8551076-SRR8551093.

As genes for *C. gigas* antimicrobial peptides (AMPs) are not annotated in the *C. gigas* reference genome (assembly version V9, (13)), read counts for all AMPs were obtained by alignment to an in-house database of AMP protein sequences using DIAMOND 0.7.9 (17). The AMPs database was prepared using diamond 'makedb' and the reads for each sample/replicate were compared to the database using diamond 'blastx'. Alignments were filtered for the best hit and e-value < 1e-6. Read counts for each AMP were normalized against the total sequence number for each sample/replicate.

Vibrio transcriptome analysis

For bacterial RNA-seq data, all the analyses but the last step (DESeq2) were carried out on a personal computer (Ubuntu 16.04 LTS), on which the necessary tools were executed from a docker container image (https://www.docker.com/why-docker). Raw Illumina® sequencing reads were trimmed by Trimmomatic in paired-end mode (18) to remove sequences corresponding to the NuGen provided adapters, clipping part of reads having a quality score of below 20, and dropping reads of less than 36 nt. The two resulting files containing the forward and reverse reads, respectively, of the paired-end reads, were used as input for Bowtie2 (19) to align the reads on *V. tasmaniensis* LGP32 or *V. crassostrea* J2-9 genome, respectively. In the case of LGP32, where the complete genome is available, the sequences of the two chromosomes were concatenated. In the case of J2-9, the genomic sequence corresponds to a concatenation of multiple contigs. In addition, whereas the rRNA operon was present in multiple copies in the genome of LGP32, it was unique in the J2-9 sequence file. We thus artificially duplicated the operon sequence in J2-9 so that reads corresponding to rRNA genes were listed by Bowtie2 as those with multiple alignments, and thus were eliminated as it was the case for LGP32.

As expected, in the case of bacterial RNA-seq samples resulting from oyster infection experiments, the rate of read alignment on the bacterial genome was ~2% at the most, whereas it was more than 98% in the case of the *in vitro* grown bacteria. To prevent a potential bias induced by this difference in the subsequent computational steps, we introduced a random downsampling step of the aligned reads of the control samples (*in vitro* growth). This was done using the command "downsampleSam" of the Picard tools (http://broadinstitute.github.io/picard/command-line-overview.html#DownsampleSam) with p= 0.02, leading to a number of aligned reads similar to what was obtained in case of the oyster infection samples. Counts for each annotated feature (CDS + sRNAs) of either *V. tasmaniensis* LGP32 or *V. crassostreae* J2-9 were then computed using featureCounts (20). The resulting files were used as input to determine differential expression for each feature between oyster injected with vibrios and vibrios grown *in vitro* by DESeq2 (16). DESeq2 was carried out on a Galaxy instance at the INRA migale bioinformatics platform:

http://migale.jouy.inra.fr/galaxy/. Genes were considered as differentially expressed between tested conditions and controls when |log2(fold change)| was ≥1 and adjusted *P*-value (P_{adj}) for multiple testing with the Benjamini-Hochberg procedure was < 0.05. Bacterial RNA-seq data has been made available through the SRA database: BioProject accession number PRJNA521688 under SRA accessions SRR8567597-SRR8567602 (*Vibrio crassostreae* J2-9) and BioProject accession number PRJNA521693 under SRA accessions SRR8573808-SRR8573813 (*Vibrio tasmaniensis* LGP32).

Functional gene ontology annotations

For oyster genes, Blastx (21) comparison against NR database was performed for each set of genes with a maximum number of target hits of 20 and a minimal e-value of 0.001. XML blast result files were loaded onto Blast2GO (22) for GO mapping and annotation of the B2G database. Functional categories corresponding to significantly modulated genes (331 genes), were then determined manually; this was supported by background literature review. A heatmap of the mean of log2 fold change in three independent experiments was then generated using cluster 3.0 (http://bonsai.hgc.jp/~mdehoon/ software /cluster/software.htm).

For bacterial genes, annotations of differentially expressed genes (fold change ≥ 2 and padj ≤ 0.05) were manually curated using the MicroScope platform (23) and the MetaCyc data base (24). Based on these curated annotations, each gene was assigned to one of 32 functional categories (see Figs 5 & S5 for the list of categories).

In addition, with the help of the tools provided by MicroScope, which allows for comparison between genomes based on sequence and synteny conservation; we identified genes which were common to both (J2-9 and LGP32) differential transcriptomes, with the exception of genes of unknown function. This subset of genes is defined as the intersection between the J2-9 and LGP32 differential transcriptomes.

RT-qPCR

RT-qPCR was performed either on the same RNA samples as those used for deep sequencing to validate RNAseq data (Fig. S3), or on specific RNA samples in order to monitor the time-course of bacterial gene expression in oysters (Fig S6). cDNA was synthetized using M-MLV RT (Invitrogen Inc.) using 1 µg of RNA and random primers (250 ng). Real-time qPCR was performed at the qPHd platform of qPCR in Montpellier using the Light-Cycler 480 System (Roche) and oyster gene specific primers (Table S8). The total Real-time qPCR reaction volume was 1.5 µl with 0.5 µl cDNA (40 ng μl^{-1}) and 1 µl LightCycler 480 SYBR Green I Master mix (Roche) containing 0.5 µM PCR primer (Eurogentec SA). Relative expression was calculated using the $2^{-\Delta\Delta Cq}$ method (Pfaffl, 2001), with normalization to the *C. gigas* reference genes, namely, *Cg*-RPL40 (GenBank FP004478), *Cg*-RPS6 (GenBank HS119070) and *Cg*-EF1a (GenBank AB123066). For understanding the time-course of the bacterial gene expression, 6-phosphofructokinase (VS_2913) and Methyl glyoxal synthase (VS_II1055) genes (Vanhove et al., 2016) were used as reference genes to monitor the relative expression of *vipA1* and *vipA2*.

Specific vibrio quantification by qPCR

Genomic DNA was extracted with the DNA kit Promega (Wizard SV Genomic DNA Purification System) on the same oyster samples used for RNA-seq. DNA concentration was measured using a NanoDrop 1000 Spectrophotometer (Thermo Fisher Scientific Inc.). Real-time qPCR was performed on a Light-Cycler 480 System (Roche). The total Real-time qPCR reaction volume was 1.5 µl with 0.5 µl cDNA (40 ng μl^{-1}) and 1 µl LightCycler 480 SYBR Green I Master mix (Roche) containing 0.5 µM PCR primer (Eurogenetec SA). Strain-specific primers were designed using Primer 3 plus (http://primer3plus.com/), to amplify monocopy genes from specific vibrio genomes (Table S8). Efficiency and specificity were checked on DNA extracted from six different vibrio strains. To quantify oyster genomes, *Cg*-BPI (GenBank: AY165040) primers were used (Table S8). The vibrio charge in oyster tissues was calculated as a number of vibrio genome copies per number of oyster genome copy considering the following genome sizes: *C. gigas* (637 Mbp), LGP32 (4.97 Mbp), LMG20012T (4.84 Mbp), J2-9 (5.79 Mbp), J2-8 (5.39 Mbp).

Vibrio genome sequencing and assembly

Genomic DNA for the J0-13, J5-13 and J5-9 strains was extracted with the NucleoSpin Tissue kit (Macherey-Nagel Inc.). Starting from 1 ng DNA, library construction was performed at the Bio-Environnement platform (University of Perpignan, France) with the Nextera XT kit (Illumina, USA) in paired-end mode (2 × 150 bp). Sequencing was carried out using a NextSeq 550 instrument resulting in ~100-fold coverage. Reads were assembled *de novo* using Spades software. Computational prediction of coding sequences together with functional assignments was performed using the automated annotation pipeline implemented in the MicroScope platform (25). The genome sequences of *V. tasmaniensis* J0-13, J5-13 and J5-9 were deposited in Genbank with the following accession numbers: SEOP00000000, SESM00000000 and SESL00000000.

References

1. Gay M, Berthe FC, & Le Roux F (2004) Screening of Vibrio isolates to develop an experimental infection model in the Pacific oyster Crassostrea gigas. (Translated from eng) *Dis Aquat Organ* 59(1):49-56 (in eng).
2. Lemire A*, et al.* (2015) Populations, not clones, are the unit of vibrio pathogenesis in naturally infected oysters. (Translated from English) *Isme Journal* 9(7):1523-1531 (in English).
3. Thompson FL, Thompson CC, & Swings J (2003) Vibrio tasmaniensis sp. nov., isolated from Atlantic salmon (Salmo salar L.). (Translated from eng) *Syst Appl Microbiol* 26(1):65-69 (in eng).
4. de Lorgeril J*, et al.* (2018) Immune-suppression by OsHV-1 viral infection causes fatal bacteraemia in Pacific oysters. (Translated from eng) *Nat Commun* 9(1):4215 (in eng).
5. Petton B, Pernet F, Robert R, & Boudry P (2013) Temperature influence on pathogen transmission and subsequent mortalities in juvenile Pacific oysters Crassostrea gigas. (Translated from English) *Aquaculture Environment Interactions* 3(3):257-273 (in English).
6. Duperthuy M*, et al.* (2010) The major outer membrane protein OmpU of Vibrio splendidus contributes to host antimicrobial peptide resistance and is required for virulence in the oyster Crassostrea gigas. (Translated from eng) *Environ Microbiol* 12(4):951-963 (in eng).
7. Suquet M*, et al.* (2009) Anesthesia in Pacific oyster, Crassostrea gigas. *Aquat. Living Resour.* 22 29-34.
8. Le Roux F, Binesse J, Saulnier D, & Mazel D (2007) Construction of a Vibrio splendidus mutant lacking the metalloprotease gene vsm by use of a novel counterselectable suicide vector.

(Translated from eng) *Appl Environ Microbiol* 73(3):777-784 (in eng).

9. Le Roux F, Davis BM, & Waldor MK (2011) Conserved small RNAs govern replication and incompatibility of a diverse new plasmid family from marine bacteria. (Translated from eng) *Nucleic Acids Res* 39(3):1004-1013 (in eng).

10. Demarre G*, et al.* (2005) A new family of mobilizable suicide plasmids based on broad host range R388 plasmid (IncW) and RP4 plasmid (IncPalpha) conjugative machineries and their cognate Escherichia coli host strains. (Translated from eng) *Res Microbiol* 156(2):245-255 (in eng).

11. Le Roux F*, et al.* (2009) Genome sequence of Vibrio splendidus: an abundant planctonic marine species with a large genotypic diversity. (Translated from eng) *Environ Microbiol* 11(8):1959-1970 (in eng).

12. Afgan E*, et al.* (2018) The Galaxy platform for accessible, reproducible and collaborative biomedical analyses: 2018 update. (Translated from eng) *Nucleic Acids Res* 46(W1):W537-W544 (in eng).

13. Zhang G*, et al.* (2012) The oyster genome reveals stress adaptation and complexity of shell formation. (Translated from eng) *Nature* 490(7418):49-54 (in eng).

14. Dobin A*, et al.* (2013) STAR: ultrafast universal RNA-seq aligner. (Translated from eng) *Bioinformatics* 29(1):15-21 (in eng).

15. Anders S, Pyl PT, & Huber W (2015) HTSeq--a Python framework to work with high-throughput sequencing data. (Translated from eng) *Bioinformatics* 31(2):166-169 (in eng).

16. Love MI, Huber W, & Anders S (2014) Moderated estimation of fold change and dispersion for RNA-seq data with DESeq2. (Translated from eng) *Genome Biol* 15(12):550 (in eng).

17. Buchfink B, Xie C, & Huson DH (2015) Fast and sensitive protein alignment using DIAMOND. (Translated from eng) *Nat Methods* 12(1):59-60 (in eng).

18. Bolger AM, Lohse M, & Usadel B (2014) Trimmomatic: a flexible trimmer for Illumina sequence data. (Translated from eng) *Bioinformatics* 30(15):2114-2120 (in eng).

19. Langmead B & Salzberg SL (2012) Fast gapped-read alignment with Bowtie 2. (Translated from eng) *Nat Methods* 9(4):357-359 (in eng).

20. Liao Y, Smyth GK, & Shi W (2014) featureCounts: an efficient general purpose program for assigning sequence reads to genomic features. (Translated from eng) *Bioinformatics* 30(7):923-930 (in eng).

21. Altschul SF, Gish W, Miller W, Myers EW, & Lipman DJ (1990) Basic local alignment search tool. (Translated from eng) *J Mol Biol* 215(3):403-410 (in eng).

22. Conesa A*, et al.* (2005) Blast2GO: a universal tool for annotation, visualization and analysis in functional genomics research. (Translated from eng) *Bioinformatics* 21(18):3674-3676 (in eng).

23. Medigue C*, et al.* (2017) MicroScope-an integrated resource for community expertise of gene functions and comparative analysis of microbial genomic and metabolic data. (Translated from eng) *Brief Bioinform* (in eng).

24. Caspi R*, et al.* (2018) The MetaCyc database of metabolic pathways and enzymes. (Translated from eng) *Nucleic Acids Res* 46(D1):D633-D639 (in eng).

25. Vallenet D*, et al.* (2013) MicroScope--an integrated microbial resource for the curation and comparative analysis of genomic and metabolic data. (Translated from eng) *Nucleic Acids Res* 41(Database issue):D636-647 (in eng).

II.3. COMPLEMENTARY RESULTS. ASSESSING THE ROLE OF AN EVPP ORTHOLOG AS A PUTATIVE T6SSCHR1-LGP32 EFFECTOR IN LGP32

Despite the many *in vivo*, *in vitro* and *in silico* global approaches that we have been using up to now, the nature of the effectors enabling *V. tasmaniensis* cytotoxicity have remained unknown four years after the description of LGP32 cytotoxicity towards hemocytes (Vanhove *et al*. 2016), a key determinant of its virulence to oysters. We have shown in article 2 that the T6SS encoded on *V. tasmaniensis* LGP32 chromosome 1 is essential for *V. tasmaniensis* virulence. We were therefore interested in characterizing the toxic effectors that are secreted through this system. As mentioned in article 2, the *vgrG* and *paar*-encoded domains, which form the tip of the T6SS to which effectors can form complexes and be delivered to the target cell. Moreover, the C-terminal domain of several of these VgrG and PAAR proteins have C-terminal domains with predicted enzymatic activity toxic for prokaryotic and eukaryotic cells (Shneider *et al*., 2013; Bondage *et ai.,* 2016). However, no potential C-terminal effectors domain could be identified in the VgrG and PAAR proteins found in all virulent strains of *V. tasmaniensis* (Rubio *et al*., 2019). Still, we identified *evpP,* a non-VgrG non PAAR T6SS effector characterized in the intracellular pathogen *Edwardsiella tarda* which is involved in cell invasion and inhibition of the host immune response (Chen *et al*., 2017). The effector EvpP secreted by the T6SS of *E. tarda* suppresses pyroptosis. The suppression of inflammasome activation and pyroptosis is suggested to be beneficial to *E. tarda* colonization in the host (Chen *et al*., 2017). Remarkably, in his thesis, Tristian Rubio showed that inhibition of caspases with z-vad tended to inhibit LGP32 cytotoxicity. As the effector subunit caspase-1 activates a pyroptotic cell-death pathway, it was hypothesized that LGP32-trigerred cell–death is due to pyroptosis (Rubio, 2017).

In order to determine, the potential role of *evpP* in the cytotoxicity and virulence of LGP32, Romain Guiraud (during his internship) and I constructed an *in-frame* deletion mutant for the coding sequence of *evpP* in *V. tasmaniensis* which we phenotyped both *in vitro* and *in vivo*.

Materials and methods

Construction of the suicide vector

An In-frame deletion of the targeted coding sequence was performed by allelic exchanged using the suicide plasmid pSW7848T according to (Le Roux *et al.* 2007).

Two 500 bp fragments flanking the region to delete were amplified with the following primers.

Table 1. Primers used for amplification of the regions flanking *evpP*
Sequence in bold: Homology with pSW7848T for cloning by Gibson assembly
Sequence underlined: Ecor1 restriction site
Sequence double underline homologies to allow fragment assembly during Gibson reaction

Primer	Sequence 5'-3'
5'evpPFw	**GTATCGATAAGCTTGATATC**GAATTC*CCTTTAGGTAGAAACATTGTG*
5'evpPRv	*GCTAGACCGGTACTGGT*GGTTTACAATATCACCACCAAGC
3'evpPFw	*GCTTGGTGGTGATATTGTAA*ACCACCAGTACCGGTCTAGC
3'evpPFw	**CCCCCGGGCTGCAG**GAATTCCATGCAGAGATTAGCGTTCC
pSWF	GAATTCCTGCAGCCCGGGGG
psWR	GAATTCGATATCAAGCTTATCGATAC

Two independent PCR amplifications were performed using 5'evpPFw + 5'evpPRv to amplify 500 bp upstream *evpP* and 3'evpPFw + 3'evpPFw for the 500 bp downstream *evpP*. The pSW7848T linear sequence was amplified by a PCR inside out using the vector DNA and the primers pSWF + psWR with a high-fidelity polymerase (Q5® High-Fidelity DNA Polymerase, NEB). The recombinant plasmid was then assembled using the Gibson assembly master mix (Nex England Biolabs) according to the provider's instructions. Correct insertion of the fragment with the correct size was verified by digestion with the restriction enzyme EcoRI and visualization of the digestion products by gel electrophoresis. Strains *E. coli* π3813 and *E. coli* β3914 were used as plasmid hosts for cloning and conjugation of the constructed vector, respectively (Le Roux et al., 2007)

Conjugation between *E. coli* β3914 with *V. tasmaniensis* LGP32

The donor strain *E. coli* β3914 carrying the pSW4878T:*evpP* was grown in LB media supplemented with chloramphenicol 35 ug/mL and 0.5 mM of diaminopimelic acid (DAP) and the recipient *V. tasmaniensis* in LB supplemented with 0.5 mM NaCl. Overnight cultures of both strains were diluted at 1:100 in culture media without antibiotic and grown at 30°C to an OD_{600nm} of 0.3. Conjugation was performed by a filter mating procedure described previously (Le Roux et al., 2007) with 1 ml donor and 10ml recipient. Conjugations were performed

overnight on filters incubated on LBA + NaCl 0.5N + diaminopimelic acid (DAP) plates at 30°C. Counter-selection the donor *E. coli* β3914, auxotrophic for DAP, was done by plating on a medium devoid of DAP, supplemented with chloramphenicol 5 ug/mL for selection of vibrio Cm^R trans-conjugants, and 1% glucose to suppress the expression of the ccdB toxin. For mutagenesis, Cm^R resistant colonies were grown in LB + NaCl 0.5N + glucose 1% up to late logarithmic phase and spread on plates containing 0.2% arabinose to induce the expression of the ccdB toxin and select for vector excision. Colonies susceptible to chloramphenicol, indicative of successful excision of pSW7848. Mutants were screened by PCR using external primers to verify the correct deletion of the target region (Figure 23).

Cytototoxicity assays and Experimental infections

Procedures are identical to materials and methods from article 2

Results

Two *evpP* deletion mutants were selected after PCR-verification of the correct gene deletion (Figure 23). They were first used on cytotoxicity assays against oyster hemocytes and compared to the wild-type LGP32 (cytotoxic) and the *vipA* mutant, which harbours a defective T6SS1 machinery and is devoid of cytotoxicity (Rubio *et al.*, 2019). Our results showed that both *evpP* mutants lacked cytotoxicity towards oyster hemocytes, similar to the *vipA* deletion mutant (Figure 24). Therefore, our results strongly suggest that *evpP* is a key effector of LGP32 T6SS1 cytotoxicity toward hemocytes.

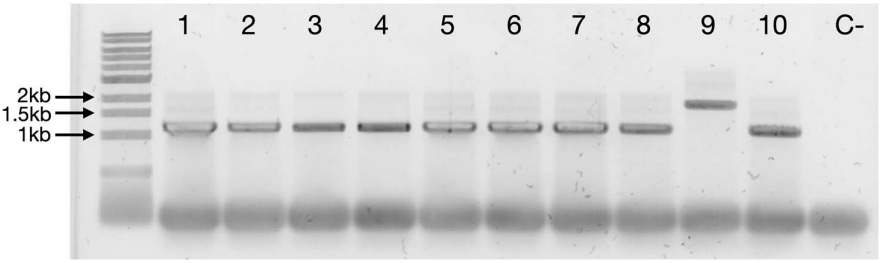

Figure 23. PCR verification of *evpP* deletion.

10 Clones susceptible to chloramphenicol after plasmid excision were tested by PCR to verify gene deletion. Primers upstream and dowstrem *evpP* sequence were used for PCR. Correct deletion of the *evpP* sequence should produce a fragment of 1082, bp while the wild type one of 1753 bp. 9 of the 10 clones tested corresponded to Δ*evpP* mutants while only one resulted in the *wild type* genotype after excision.

As they harbored identical phenotypes *in vitro*, we next tested one of the two deletion mutants in oyster experimental infection together with the wild-type LGP32 (virulent) and the LGP32 *vipA-i* mutant, which is non-virulent *in vivo* (Rubio *et al*., 2018). Our assays showed no impairment in virulence of the *evpP* mutant when injected into oysters (Figure 25) in contrast with the strong effect observed upon inhibition of the assembly of the T6SS **Chr1-LGP32** (LGP32 *vipA-i*). This suggests that *evpP* is not required for virulence *in vivo*.

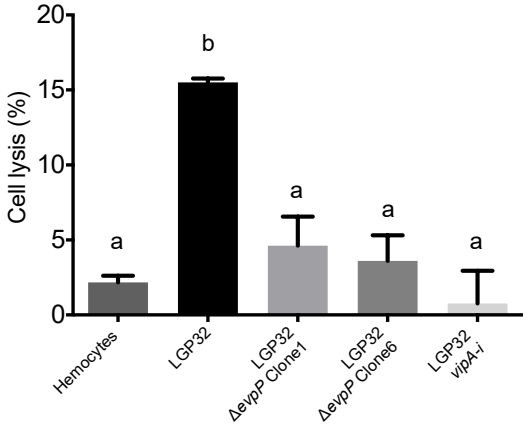

Figure 24. Cytotoxic activty of LGP32 Δ*evpP*.

Deletion of *evpP* induces loss of cytotoxicity toward immune cells in *V. tasmaniensis* LGP32. Cytotoxicity of LGP32 Δ*evpP* and LPG32 *vipA-i* as control *was* determined on monolayers of hemocytes and monitored by the SYTOX Green assay. Cells were infected with bacteria at an MOI of 50:1. Maximum cytotoxicity displayed by vibrios is shown here. Error bars represent the SD of the mean (RM-ANOVA, P < 0.001)

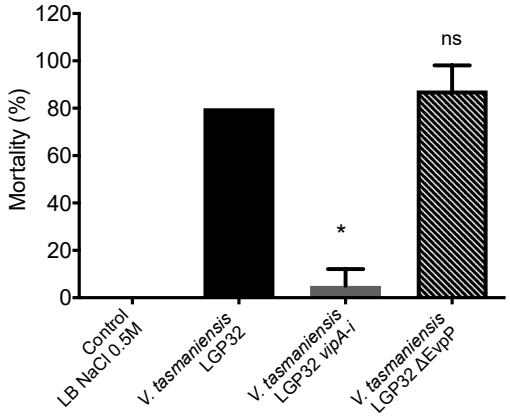

Figure 25. Contribution of *evpP* to *V. tasmaniensis virulence*.

Virulence of V. *tasmaniensis* isogenic mutant for *evpP* was assessed by intramuscular injection of 40

juvenile oysters [2]. Oysters, previously anaesthetized for 3 h by immersion in seawater with 50g L MgCl, were injected with 2 x10^7 CFU of each strain and mortalities were recorded at day 24 hrs in two independent experiments. Mean values are displayed ± SD. Different letters indicate a significant difference between them (ANOVA, $p < 0.05$ and Tukey HSD test)

These results highlight a dycotomy between cytotoxicity toward hemocytes and virulence, which we had never observed with our previous LGP32 mutants.

Noteworthy, the mortality induced by wild-type LGP32 control was particular high (80% after 24h) in our experimental infection. If the *evpP* effector is one effector among diverse T6SS effectors that contribute to virulence, the experiment should be repeated by injecting lower doses to oysters that help revealing more subtle phenotypes. This strategy was used for instance by Piel et al (2019) to reveal the role of T6SS in *V. crassostreae* cytotoxicity.

If *evpP* is indeed key for cytotoxicity but not required for virulence, it strongly suggest that other unidentified effectors secreted by this T6SS **Chr1-LGP32** are responsible for the virulence of LGP32. One possibility is that these other effectors, which may be acting on distinct cell types, are not revealed by our *in vitro* assays.

Further investigation of the *evpP* mutant, in particular complementation assays, are now needed to confirm our results and determine the role of *evpP* and/or other T6SS effectors in LGP32 pathogenesis. It will also be essential to determine whether and how *V. tasmaniensis evpP* relates to pyroptosis, since in *evpP* has been described as a pyroptosis suppressesor in *E. tarda*.

SECTION III. CHEATING BEHAVIOR IN VIBRIOS ASSOCIATED WITH POMS

III.1. CONTEXT AND OBJECTIVE OF THE STUDY

The Pacific Oyster Mortality Syndrome (POMS) has been extensively characterized in the French Atlantic environment where *Vibrio* species from the diverse Splendidus clade have been recurrently found associated with moribund oysters as secondary opportunistic colonizers that contribute significantly to the systemic infection leading to oyster death (Gay *et al.*, 2004; Saulnier *et al.*, 2010; Lemire *et al.*, 2015; Bruto *et al.*, 2017, 2018). Nonetheless, POMS affect oyster farming worldwide, and is observed in environments with different ecologies where variations in the composition of the *Vibrio* community are expected. Indeed, composition and abundance of *Vibrio* communities in the marine ecosystems are highly influenced by planktonic composition and environmental factors such as temperature, salinity, pH and dissolved oxygen (Turner *et al.*, 2009; Takemura *et al.*, 2014; Li *et al.*, 2020). Moreover, as shown by Bruto *et al.*, (2017) population structure of vibrio communities in the water column suffer local seasonal variations affecting as consequence *Vibrio* population assembly in oysters.

The Thau Lagoon is a Mediterranean marine ecosystem with significant oyster farming activity that has also suffered since 2008 from repeated episodes of POMS affecting juveniles with a strong presence of OsHV-1 restricted to the farming areas (20% of the total surface) (Pernet *et al.*, 2012). The Thau lagoon has an ecology that differs from the Atlantic coast, including higher salinity and a temperature regimen that during half of the years ranges between 16-30°C (Lopez-Joven *et al.*, 2018).

With the initial obsjective to characterize the vibrio community associated with POMS in the Mediterranean, we performed a series of *Vibrio* samplings, starting with a POMS episode during autumn of 2015, confirmed by the presence of OsHV-1 in moribund oysters. We characterized the population structure of vibrios in oysters and the water column and investigated the molecular basis underlying the observed associations.

In article 3 (in preparation), we present the results of the present study. Our data show that in the Thau Lagoon OsHV-1 infection was associated with a particular prevalence of members of the Harveyi clade, with strains taxonomically assigned to *Vibrio harveyi* and *V. rotiferianus* species preferentially associated with oyster tissues and *V. jasicida* and *V. owensii* species present in the water column excluded from moribund oysters. This preferential association of *V. harveyi* and V. *rotiferianus* to oysters could be confirmed experimentally by the reproduction of the polymicrobial infection in mesocosm experiments. The assessment of virulence potential and cytotoxic capacity, comparative genomics and functional assays led

us to conclude that two different strategies for colonization were present among these two vibrio species from the Thau Lagoon. On the one hand, the highly virulent *V. harveyi* suppressed the host cellular defenses through cytotoxic properties, as already observed in the Splendidus clade. On the other hand, we characterized the cheating strategy for iron acquisition of *V. rotiferianus* through non-cooperative siderophore uptake

III.2. ARTICLE N°3. KILLING OR CHEATING: TWO STRATEGIES TO COLONIZE AN OYSTER IN VIBRIO HARVEYI AND VIBRIO ROTIFERIANUS.

By Daniel Oyanedel*, Arnaud Lagorce*, Maxime Bruto*, Philippe Haffner, Marie-Agnès Travers, Benjamin Morga, Eve Toulza, Cristian Chaparro, Léa-lou Pimparé, Caroline Montagnani, Yannick Gueguen, Delphine Toubiez, Marc Leroy, Juliette Pouzadoux, Guillaume Mitta, Frédérique Le Roux, Guillaume Charrière, Delphine Destoumieux-Garzón.

* co-first authors

Manuscript in preparation

Killing or cheating: two strategies to colonize an oyster in *Vibrio harveyi* and *Vibrio rotiferianus*

Daniel Oyanedel*[1], Arnaud Lagorce*[1], Maxime Bruto*[2,3], Philippe Haffner[1], Marie-Agnès Travers[1], Benjamin Morga[4], Eve Toulza[1], Cristian Chaparro[1], Léa-lou Pimparé[1], Caroline Montagnani[1], Yannick Gueguen[1], Delphine Toubiez[4], Marc Leroy[1], Juliette Pouzadoux[1], Guillaume Mitta[1], Frédérique Le Roux[2,3], Guillaume Charrière[1], Delphine Destoumieux-Garzón[1#]

[1] IHPE, Univ Montpellier, CNRS, Ifremer, Université de Perpignan Via Domitia, Montpellier, France.

[2] Sorbonne Universités, UPMC Paris 06, CNRS, UMR 8227, Integrative Biology of Marine Models, Station Biologique de Roscoff, CS 90074, F-29688, Roscoff cedex, France.

[3] Ifremer, Unité Physiologie Fonctionnelle des Organismes Marins, ZI de la Pointe du Diable, CS 10070, F-29280 Plouzané, France

[4] Ifremer, SG2M-LGPMM, Laboratoire De Génétique Et Pathologie Des Mollusques Marins, La Tremblade, France.

Corresponding author

Tel. 04 67 14 46 25

Email. ddestoum@ifremer.fr

Running Head: Killing or cheating for oyster colonization

Introduction

Since 2008, the worldwide production of *Crassostreae gigas* oysters has been dramatically affected by the Pacific Oyster Mortality Syndrome (POMS), whose severity reached up to 100% mortality rates in French farms and expanded worldwide (Samain and Mccombie, 2008; EFSA, 2015; Burge *et al.*, 2020) This polymicrobial disease is caused by a Ostreid herpesvirus, OsHV-1 µVar, and opportunistic bacteria (de Lorgeril *et al.*, 2018) , among which members of the Vibrionaceae family (hereafter vibrios) are the best characterized (Lemire *et al.*, 2015; Petton *et al.*, 2015; Bruto *et al.*, 2017; Piel *et al.*, 2019). Oyster families susceptible to POMS present an overall lower basal expression of immune-related genes (Lorgeril *et al.*, 2020) and a delayed (inefficient) transcriptomic response to the OsHV-1 µVar infection, compared to resistant families (de Lorgeril *et al.*, 2018; Lafont *et al.*, 2020). Viral replication in susceptible oysters leads to the host entering an immune-compromised state, causing a dysbosis that evolves towards bacteremia (Lorgeril *et al.*, 2020)

Along the French Atlantic coastline, multiple *Vibrio* species of the highly diverse Splendidus clade (e.g. *Vibrio crassostreae*, *Vibrio splendidus*, *Vibrio tasmaniensis* and *Vibrio cyclitrophicus*) have been associated with POMS episodes and their virulence potential has been experimentally confirmed by Le Roux and collaborators (Gay *et al.*, 2004; Saulnier *et al.*, 2010; Lemire *et al.*, 2015; Bruto *et al.*, 2017, 2018) The repeated occurrence of the species *V. crassostreae* was evidenced during summer mortalities (Lemire *et al.*, 2015; Bruto *et al.*, 2017; de Lorgeril *et al.*, 2018) We recently showed that two virulent species associated with the disease, namely *V. crassostreae* and *V. tasmanienesis*, use species-specific cytotoxic properties to escape oyster cellular defenses and cause a systemic infection (Piel *et al.*, 2019; Rubio *et al.*, 2019)

Aside from the French Atlantic environment, POMS affect oyster farming in a large number of countries worldwide, which harbor diverse ecology and shellfish farming systems (Fuhrmann *et al.*, 2019). Recently, we showed that POMS is caused by two distinct viral populations of OsHV-1 µvar in French Atlantic and Mediterranean ecosystems (Delmotte *et al.*, 2020). Still, little is known on the population structure and distribution of vibrios co-occurring with OsHV-1 µvar in these other ecosystems. In addition, when vibrios are found associated with diseased animals, it is often difficult to disentangle vibrios with virulence potential from opportunistic colonizers. The underlying question is the role of *Vibrio* species in disease expression across environments.

Here, we took advantage of a Mediterranean marine ecosystem, the Thau lagoon (south of

France, N 43 °251, E 03 °391) hosting a significant oyster farming activity (20% of the total surface), whose ecology and farming practices highly differ from the Atlantic (Petton *et al.*, 2013; Pernet *et al.*, 2014b). In this environment, which also suffers from dramatic mortalities of juvenile oysters (Petton *et al.*, 2013; Pernet *et al.*, 2014b), mortality events occur twice a year, in spring and autumn, when the seawater temperature is in the 16-24°C range (Lopez-Joven *et al.*, 2018). We investigated the *Vibrio* community associated with the disease in the Thau lagoon by immersing specific pathogen-free juvenile oysters in the lagoon during the autumn 2015 mortalities. The *Vibrio* population structure showed a strong prevalence of the Harveyi clade in diseased oysters. *V. harveyi* and *V. rotiferianus* species were the most prevalent in oyster tissues, whereas *V. jasicida* and *V. owensii* were mainly associated with the water column. We confirmed further this association experimentally in a mesocosm experiment: OsHV-1 µVar enabled stable colonization by *V. harveyi* and *V. rotiferianus* but not *V. jasicida* and *V. owensii*. Colonization by *V. harveyi* and *V. rotiferianus* was facilitated by the virus-mediated immune suppression of oysters, as revealed by RNAseq analyses. Comparative genomics and functional assays were finally used to identify determinants of *Vibrio* colonization. The species *V. harveyi* was shown to carry virulence potential, being cytotoxic for oyster immune cells. It also produces vibrioferrin, a key siderophore that benefits to the oyster colonizer *V. rotiferianus,* which behaves as a cheater in this context. Our data unravel two strategies to colonize an oyster in *V. harveyi* and *V. rotiferianus*, one is the active dampening of oyster defenses whereas the other one relies on the use of key siderophores produced by the microbiota.

Results and discussion

***V. harveyi* and *V. rotiferianus* are two main *Vibrio* species associated with POMS in the Thau lagoon.**

We characterized the population structure of vibrios isolated from juvenile oysters and from the seawater during a mortality outbreak of juvenile oysters that occurred in October 2015 in the Thau lagoon, south of France. The oysters were positive for OsHV-1 µVar detection (Supplementary Table 1), revealing an on-going event of the POMS. A total of 472 bacterial isolates were sampled from oyster tissues and from the size-fractionated water column by plating on TCBS medium, selective for vibrios (Supplementary Table 2). Partial *hsp60* sequences were obtained for 448 isolates. Among them, 304 sequences (67.8 %) exhibited ≥ 95% identity with *Vibrio* type-strain sequences. Below this threshold, isolates were not included in the study. We found a strong association of the Harveyi clade to oyster tissues with 54 among the 55 isolates belonging to the species *V. harveyi*, *V. rotiferianus* and *V. owensii*

(Figure 1). Only one isolate from oyster, assigned to *V. chagasii* (Splendidus clade), fell outside the Harveyi clade. The water column showed a higher diversity of *Vibrio* species with Harveyi-related strains representing 21% of the total isolates (53/249) with a predominance of *V. jasicida* (39/53). The taxonomical assignation and phylogeny of the Harveyi-related strains were confirmed by a multi-locus sequence typing (MLST) based on 4 genes (*hsp60, rctB, topA* and *mreB*) (Figure 2A). A total of 104 isolates could be assigned to four main species: *V. harveyi* (n=63), *V. rotiferianus* (n=16), *V. jasicida* (n=15) and *V. owensii* (n=6), (Figure 2). Among them, *V. harveyi* and *V. rotiferianus* showed a positive association with oyster tissues whereas *V. jasicida* and *V. owensii* were almost exclusively associated with the water column (Figure 2A). The dominance of the Harveyi clade in POMS-diseased oysters was confirmed by PCR on three subsequent samplings, within and outside POMS episodes: Harveyi isolates, dominated by the species *V. harveyi,* were only associated with oysters infected with OsHV-1 µvar (Supplementary Table 1).

V. harveyi strains have been shown to cause disease in aquatic animals including marine fish and crustaceans (Kraxberger-Beatty *et al.*, 1990; Saeed, 1995; Hispano *et al.*, 1997; Diggles *et al.*, 2000; Alcaide *et al.*, 2001; Company *et al.*, 2002; Tendencia, 2002) In agreement with our data, Saulnier *et al.* isolated a virulent *V. harveyi* strain (03/082 2T1) in 2003 from *C. gigas* oyster spat during a mortality episode in the Thau lagoon (Saulnier *et al.*, 2010). More recently, *V. harveyi* was associated with mass mortalities of heat-stressed *C. gigas* in Australia (Green *et al.*, 2019) which agrees with the higher virulence of *V. harveyi* at high temperature (Montánchez *et al.*, 2019). However, contrary to our findings, no OsHV-1 could be detected in these diseased oysters (Green *et al.*, 2019), which suggests that oyster colonization by *V. harveyi* can be facilitated by stressors (e.g. high temperatures) other than a viral primary infection. The dominance of the Harveyi clade in our study contrasts markedly with known vibrios isolated from POMS-diseased oysters on the Atlantic coast, which mostly belong to the Splendidus clade (Lemire *et al.*, 2015; Bruto *et al.*, 2017). A possible reason for that difference is the preferential growth of *V. harveyi* in warm waters (Zhou *et al.*, 2012), such as those found the Thau lagoon (16-30°C) during half of the year (Lopez-Joven *et al.*, 2018)

V. harveyi isolates induce high mortality of juvenile oysters

To determine the virulence potential of the 104 Harveyi-related isolates, we performed experimental infections of juvenile oysters by injecting bacteria in the oyster adductor muscle (Figure 2A). We observed a clear correspondence between virulence (measured as the induced mortality rate) and species delineation. *V. harveyi* isolates were by far the most virulent with 50% of *V. harveyi* isolates inducing ≥ 50% mortality after 1 day (50% average mortality, Figure 2B). *V. harveyi* was statistically (Kruskal-Wallis and Mann-Whitney tests, $p < 0.0001$) more virulent than *V. rotiferianus*, *V. jasicida* and *V. owensii* species (Figure 2B). *V.*

rotiferianus isolates showed intermediate virulence with 0-30% mortality rate (13% average mortality, Figure 2B). *V. jasicida* isolates induced heterogeneous mortality rates with high contrast between isolates, from 0-44% mortality (18% average mortality, Figure 2B). Almost no mortality could be observed following injection of *V. owensii* and non-classified isolates of the Harveyi clade (Figure 2B). In conclusion, *V. harveyi* appears as a virulent species that colonizes oysters during a POMS event. Again, this result paralleled previous knowledge on the preferential association of virulent species to diseased oysters during Atlantic POMS episodes (Bruto et al, 2016). Still, the virulence potential does not always correlate with the colonization potential among species of the Harveyi clade. Indeed, *V. rotiferianus* isolates, that harbors low to moderate virulence, colonized oysters better than the virulent *V. jasicida* isolates (Figure 2A).

OsHV-1 µvar synergizes with vibrios of the Harveyi clade to kill oysters

We tested experimentally the synergy between species of the Harveyi clade and OsHV-1 µvar to kill oysters. For that, we performed a mesocosm experiment that enables to test infection with different pathogen combinations while using natural infection routes. Thus, oysters susceptible to the POMS were immersed into seawater containing either a reduced representation of the Harveyi phylogenetic and phenotypic diversity found in the field, or OsHV-1 µvar alone, or both. The bacterial community was composed of virulent isolates of *V. harveyi* (mortality rates 28-51%), isolates of *V. rotiferianus* and *V. jasicida* with contrasting virulence (mortality rates 0-44%), and non-virulent isolates of *V. owensii* (mortality rate 0%) (Supplementary Table 3). Mortalities were monitored over 6 days and individual oysters were collected over 2 days, until the first mortalities occurred, to monitor the *Vibrio* load and population structure over disease development. The load of total *Vibrio* was monitored in oysters by qPCR as a general approximation to the *Vibrio* dynamic within oysters.

No mortalities were observed when oysters were immersed in seawater containing only the Harveyi community (Figure 3A), indicating that the community is not sufficient to cause disease by natural routes of infections. A transient increase in *Vibrio* load was observed from 4h to 24h followed by a decreased at 48h, revealing a control of *Vibrio* colonization. In contrast, immersion into OsHV-1 µvar-containing seawater was sufficient to induce significant mortalities in juvenile oysters (85% mortality at day 6) with a progressive increase in *Vibrio* load observed over the first 2 days (Figure 3). The same phenomenon was earlier observed when pathogenic *V. crassostreae* (Atlantic isolate J2-9) was used to infect oysters in the presence/absence of OsHV-1 µvar (de Lorgeril *et al.*, 2018). Remarkably, mortalities were significantly enhanced (100% at day 4) when the Harveyi community and OsHV-1 µvar were combined into the mesocosm, as revealed by Kaplan-Meier survival curves (p=0.0018, Figure

3A). In this condition the *Vibrio* load in tissues of live oysters was 1-2 log higher than in other conditions at 2 day ($p < 0.001$, Figure 3B). This time point corresponds to an active replication phase for OsHV-1 µVar (Figure S1), earlier shown to trigger dysbiosis and bacteremia of opportunistic pathogens (de Lorgeril *et al.*, 2018). Thus, our results not only confirm that OsHV-1 µvar facilitates *Vibrio* colonization, but also evidence that interaction between OsHV-1 µvar and the Harveyi clade accelerates oyster death. This interaction, which results in enhanced disease compared to infections with microbes acting alone, is typical of synergies at play in polymicrobial diseases (Murray *et al.*, 2014)

OsHV-1 µvar modifies the oyster habitat to facilitate bacterial infection

To unveil the molecular bases of the different disease outcomes, we analyzed on the one hand the transcriptomic responses of oysters that develop the disease when exposed to both Harveyi and the OsHV-1 µvar virus (HV), and on the other hand, the transcriptomic responses of oysters exposed to Harveyi only (H), which control the infection. Three individuals from each condition were used for RNAseq. A total of 1467 genes were differentially expressed within all the libraries (FDR < 0.05, supplementary Table 3).

Oysters exposed to Harveyi only showed a limited number of differentially expressed genes (DEGs) when compared to the controls (DEGs, FDR < 0.05), with no genes common to all time points (Figure 4A); 21 were shared with the HV conditions (supplementary Table 3). DEGs were homologous to genes encoding proteins involved in interactions between host cells and bacteria (proteoglycans, mucins, agglutinin, von Willebrand factor) and a LPS-induced protein (supplementary Table 3). However, no induction of known immune genes was observed among DEGs. In agreement, we did not observe the induction of genes encoding antimicrobial peptides (AMPs) when performing a targeted alignment of oyster RNAseq reads to an in-house database of AMP sequences (data not shown), contrary to what we observed when we injected bacteria into oyster tissues, thereby breaching natural defenses (Rubio *et al.*, 2019). This suggests that resistance of oyster to colonization by vibrios does not result from an active induction of immune defenses that controls the microbiota, but it rather suggests that healthy oysters constitute a hostile habitat for vibrios (Destoumieux-Garzón *et al.*, 2020). It also indicates that oysters can tolerate transiently high *Vibrio* loads when acquired through natural routes.

On the opposite, a strong modification of oyster as a habitat for bacterial populations was observed in oysters exposed both OsHV-1 µvar and Harveyi. Significant transcriptomic changes were observed compared to untreated individuals with a total of 1468 DEGs (FDR < 0.05), 142 of which were common to all time points, and 384 DEGs common to 24 and 48 h,

representing 59% of common DEGs between these time points (Figure 4A). The transcriptional response increased gradually from 4 to 48 h with a discrete peak at 24 h (Figure 4B). A majority of the DEGs found in HV libraries were up-regulated (85% at HV4; 67% at HV24 and HV48). The response of oysters to this multipathogen exposure was consistent with the response to POMS (de Lorgeril et al., 2018), particularly in the late time-points (24 and 48h). Only one GO category, namely epithelial to mesenchymal transition, was significantly enriched at 4 h in HV libraries as revealed by a rank-based gene ontology analysis of the DEGs, (RGBOA with a false-discovery rate [FDR] < 0.05) (Figure 4C, Supplementary Table 4) and represented by two genes, a transcriptional regulator Erg-partial and a hepatocyte growth factor. A major shift in gene expression was observed at 24-48h (only ~20% of common DEGs with the 4h time point), when OsHV-1 µvar and *Vibrio* proliferated (Figure S1). At these late time points, significantly enriched GO categories were all related to the immune response (Figure 4C). Recognition of external stimulus, signal transduction, immunity, response to stress, and response to LPS were among the 13 biological processes modulated in diseased oysters. The corresponding 155 genes belong to gene families modulated during POMS in susceptible oysters (Figure 4B, supplementary Table 3) (de Lorgeril *et al.*, 2018; Lafont *et al.*, 2020).

Altogether our transcriptomic data suggest that oyster constitute a hostile habitat for vibrios which can be modified by the immunosuppressive OsHV-1 µvar virus to enable successful colonization.

OsHV-1 µVar favors colonization by *V. harveyi* and *V. rotiferianus* only

We next asked whether the immune suppression by the OsHV-1 µvar could similarly facilitate the colonization by the four species of the Harveyi clade found in the oyster environment. Individuals collected during the time course of the infection were therefore subjected to illumina Miseq sequencing of the *rctB* polymorphic region which discriminated the four species introduced into the mesocosm (Figure S2). The relative abundance of the 4 species remained stable in the oysters only exposed to the Harveyi community during 48 h, as revealed by *rctB* barcoding analysis (Figure 5, left panel). On the contrary, in the presence of OsHV-1 µvar, not only the total *Vibrio* load increased over time (Figure 3B) but there was also a significant enrichment of the species *V. harveyi* and *V. rotiferianus* at 48 h, after viral replication occurred (24h) (Figure 5, right panel). Investigations at an individual level revealed that the *Vibrio* population structure differed from one oyster to another, but *V. harveyi* and *V. rotiferianus* always dominated in relative abundance over the other 3 monitored species in all individuals. By this approach we were able to provide experimental evidence that the OsHV-1 µVar infection is sufficient to reproduce the differential association of Harveyi species found in the field. In this context the virulence potential found in *V. jasicida* isolates does not seem

to be a necessary trait that allows successful colonization through a natural route of infection. This shows that the capacity to colonize OsHV-1 µvar-infected oysters is highly dependent on bacterial determinants. It also shows that species-specific determinants rather than strain-specific virulence traits define the capacity of *V. harveyi* and *V. rotiferianus* to colonize oysters infected by OsHV-1 µvar.

***V. harveyi,* the strategy of a killer**

To gain access to genomic features that might be explanatory for the *V. harveyi* and *V. rotiferianus* colonization abilities, we sequenced 17 Harveyi-related genomes from our collection (4 *V. harveyi*, 5 *V. owensii*, 4 *V. jasicida* and 4 *V. rotiferianus* isolates) (Supplementary Table 5). Genome comparisons aimed to extract genes exclusively shared by the *V. harveyi* and *V. rotiferianus* gave as few as 15 genes, suggesting that species-specific determinants might be responsible for the colonization ability of these two species (Supplementary Table 6).

We first focused on *V. harveyi,* a species in which several virulence factors underlying the pathogenesis have been identified. These factors include adhesins, chitinases, extracellular polysaccharides involved in biofilm formation, haemolysins and proteases, siderophores and iron acquisition systems, Type III Secreting Systems (T3SS), and bacteriophage-mediated virulence (Darshanee Ruwandeepika *et al.*, 2012). Among the four species from the present study, *V. harveyi* was by far the species that gathered the greatest number of the virulence factors described so far. In particular, *V. harveyi* harbored a type 3 secretion system homologous to the *V. parahaemolyticus* T3SS1 (Supplementary Table 3), also present in *V. jasicida* (Supplementary Table 5; Figure S3). In *V. parahaemolyticus* T3SS1 is implicated in cytotoxicity on human cell lines while T3SS2 appears to act more specifically on intestinal cell lines (Ham and Orth, 2012). Among the effectors characterized as translocated by the T3SS1 (VopQ, VopR, VopS and VPA0450), we identified orthologs for VopQ (lysosome disruption and deacidification), VopR and VPA0450 (Plasma membrane-destabilizing inositol phosphatase (Broberg *et al.*, 2010) as well as an associated cargo chaperone orthologuous to VPA0451, which is needed for translocation of VPA0450 into the host cell membrane (Waddell *et al.*, 2014). By comparison, in *V. jasicida,* only two characterized secreted effectors were found, namely VopQ and the pro-apoptotic effector VopS (Bhattacharya, 2006). In addition, an arginine ADP ribosyltransferase (964 AA, 106kDa) only found in *V. harveyi* isolates was evidenced (gene 180147 of *V. harveyi* O-A1). This protein contains a 72 AA motif related to ExoToxin (a two-component protein complex known as AB toxin) like the cholera toxin (and in Clostridium, *Bacillus anthracis* toxins).

Besides, T6SS systems appeared widespread among our Harveyi strains (Supplementary Table 5). Orthologs of the T6SS1 and T6SS2 of the oyster pathogen *V. tasmaniensis* LGP32 were found. T6SS1 was present in all strains and T6SS2 only absent from *V. rotiferianus*. The T6SS1 has been already characterized as necessary for cytotoxicity towards hemocytes and virulence of *V. tasmaniensis* LGP32 while the role of the T6SS2 remains to be elucidated (Rubio et al., 2019). Similarly, in *V. cholerae,* a T6SS mediates cytotoxicity to macrophages by inducing actin cross-linking (Ma and Mekalanos, 2010)

Two other T6SS were found, the first named T6SS3 was found in all strains and a second one named T6SS4 was found associated with the *V. rotiferianus* species and to only one strain from the *V. harveyi* species (Supplementary Table 5).

The cytotoxic potential of *V. harveyi* was confirmed experimentally by comparing two strains representative of the four Harveyi species from our study. We found that *V. harveyi* strains exerted a potent cytotoxicity toward hemocytes, the oyster immune cells, 25-35% of which were lysed upon incubation with *V. harveyi* strains (Figure 6). By comparison, the three other species from the present study were significantly less cytotoxic (7-13% lysed hemocytes), $p < 0.001$ (One-way ANOVA test). Cytotoxic activtity was earlier described as the hallmark of two pathogenic *Vibrio* species (Splendidus clade) associated with the POMS in the Atlantic environment (Rubio *et al.*, 2019). From the present study, the Mediterranean *V. harveyi* isolates resemble the Atlantic *V. tasmanienis* and *V. crassostreae,* which are equipped with specific virulence/cytotoxicity factors that are needed to dampen oyster cellular defenses and cause systemic infections (Rubio *et al.*, 2019)

***V. rotiferianus,* the strategy of a cheater**

Unlike *V. harveyi, V. rotiferianus* (poorly virulent, good oyster colonizer) and *V. jasicida* (virulent, poor oyster colonizer) were poorly cytotoxic toward oyster immune cells. This indicates (i) that virulence in the Harveyi clade is multifactorial and (ii) that beyond cytotoxicity, other attributes determine the capacity to colonize oysters affected by the POMS. This was further explored by comparative genomics. Iron acquisition systems were a major difference between species (Supplementary Table 5). Indeed, *V. harveyi* was found to harbor a conserved set of genes responsible for the synthesis of vibrioferrin, a tricarboxylic acid siderophore derived from citric acid and for the synthesis of amphi-enterobactin. In contrast, *V. rotiferianus* does not exhibit known *Vibrionaceae* siderophore biosynthetic proteins but it carries the vibrioferrin receptor necessary for the siderophore uptake (Supplementary Table 5, Figure 7A). This receptor is present in both *V. harveyi* and *V. rotiferianus* (good colonizers) together with receptor proteins for aerobactin, enterobactin and deferoxamine B. In contrast, it is absent from the *V. owensii* and *V. jasicida* genomes

(poor colonizers), suggesting iron acquisition systems could determine the capacity of Harveyi species to colonize oysters. Iron acquisition systems are indeed well-known determinants of vibrio colonization in metazoan hosts as they determine their capacity to grow in iron-limited environments by the use of siderophores that bind poorly soluble iron and make it available to cells via active uptake (Arezes *et al.*, 2015). To investigate the role of vibrioferrin uptake, we compared the growth of *V. rotiferianus* (non-producer) in the presence/absence of two different doses of *V. harveyi* (producer) culture supernatant, which contains vibrioferrin. *V. harveyi* growth was not impaired in iron depleted media (EDDA used as iron chelator, Figure 7B), in agreement with its ability to produce siderophores. On the contrary, iron depletion significantly affected the growth of *V. rotiferianus*, $p < 0,01$ (Oneway ANOVA test). This growth defect was rescued in a dose-depended manner by the addition of cell-free culture supernatant from *V. harveyi* (Figure 7B). This demonstrates that *V. rotiferianus* is able to acquire important resources (most likely vibrioferrin) produced by *V. harveyi,* which are needed to grow in iron-poor environments. It also strongly supports the hypothesis that vibrioferrin uptake is a key determinant of *Vibrio* growth.

While *V. rotiferianus* has been described as a pathogen for the rainbow trout (Austin *et al.*, 2005), the present data indicate that the species does not participate actively to the POMS pathogenesis. Instead, our data highlight a cheating behavior of *V. rotiferianus* in siderophore utilization. Such a behavior has been reported in vibrios, the proportion of cheaters being higher in vibrios associated with large particles than in free-living vibrios (Cordero *et al.*, 2012). It is likely that the high bacterial loads that characterize the POMS fatal bacteriemia are very favorable to cheaters like *V. rotiferianus*, which benefit from the "public goods" (here the siderophores) produced by the dense *Vibrio* community, or other members of the microbiota, to grow in an iron-limited environment.

In conclusion, the present study shows that (i) healthy oyster constitute a rather hostile habitat that tolerates transiently high vibrio loads but does not allow stable colonization by vibrios. This habitat becomes permissive to specific vibrio species when immune defenses are altered by OsHV-1 µvar. (ii) The *Vibrio* community able to colonize OsHV-1 µvar-infected oysters varies according to ecosystems, but contains species that express the same capacity to dampen the oyster cellular defenses using cytotoxic activities. (iii) In the Thau lagoon, *V. harveyi* (adapted to elevated temperature) is a virulent species associated with POMS that synergizes with OsHV-1 µvar to accelerate oyster death. (iv) The *Vibrio* community associated with POMS is composed of both opportunistic pathogens, like *V. harveyi,* and simple opportunists (cheaters), like *V. rotiferianus*, benefiting from the activity of the pathogens, which dampen

the oyster immune defenses to facilitate the colonization and produce vibrioferrin, a siderophore that the cheaters can utilize for their own growth within diseased oysters.

Materials and methods

Oyster and bacterial sampling

In October 2015 (autumn mortality), 30 juvenile oysters (15 spats from Decipher family + 15 spats from France Naissain) and 40L of seawater were collected in the Mediterranean Thau lagoon (Languedoc-Roussillon, France; Supplementary Table 1). In 2016 and 2017, only juvenile oysters (NSI spats) were collected during mortality events (June 2016) or in absence of mortality (June 2016, march 2017, Table S1). OsHV-1 µvar DNA detection in oyster flesh using quantitative PCR as described by Lafont *et al.* (2017) showed that sampled oysters were infected by OsHV-1 µVar virus (Supplementary Table 1). Seawater was size-filtrated to collect zooplankton, large phytoplankton and organic molecules (60µm pore size filter), smaller organic particles (5 and 1µm) and free-living bacterial cells retained at 0.22µm (Bruto *et al.*, 2017).

Bacterial sampling

Oysters and the large seawater particles fraction were ground (Ultra-Turrax, IKA) and 100µL were plated on Vibrio selective media (thiosulfate-citrate-bile salts sucrose agar, TCBS, Difco DB, Le pont de Claix, France). The others filters (5, 1 and 0.22 µm) were directly placed on TCBS agar plate and incubated 2 days at 20°C. Around 100 colonies for each sample were randomly picked, re-steaked first on TCBS and then on Zobell agar (4g.l-1 bactopeptone, 1 g.l-1 yeast extract and 15g.l-1 agar in sterile seawater, pH 7.4) and stock cultures were stored at −80 °C in Zobell containing 15% glycerol (v/v). For subsequent molecular analyses, all isolates were grown overnight at 20 °C in liquid Zobell medium and DNA extracted using a DNA extraction kit (Nucleospin tissue, Macherey-Nagen) or using Whathman FTA cards (GE Healthcare).

Population structure analysis

All isolates from October 2015 were genotyped by *hsp60* partial gene sequence as described previously (Gob *et al.*, 1996; Hunt *et al.*, 2008) using primers *Hsp60* R and F generating a total of 448 *hsp60* sequences (Supplementary Table 2). The PCR conditions for *hsp60* amplification were: 3 min at 95°C followed by 30 cycles of 30 sec at 95°C, 30 sec at 37°C and 1min at 72°C with a final step of 5 min at 72°C. *hsp60* sequence ambiguities were corrected using 4peaks and Seaview software packages and received a taxonomic affiliation if the best blast-hit displays an identity superior to 95% with a type-strain. This resulted in the assignment of

304/448 isolates to 21 different species whereas the others were unknown species (Figure 2).

MLST genotyping

To identify and genotype isolates from October 2015 belonging to the Harveyi clade, 3 additional protein-coding genes have been sequenced (*rctB*, *topA* and *mreB*) (Supplementary Table 8). Once the 104 Harveyi-related strains identified, the *rctB, topA* and *mreB* sequences were amplified using rctB-F/rctB-R, VtopA400F/VtopA1200R and VmreB12F/VmreB999R primers, respectively (Sawabe *et al.*, 2007), (Supplementary Table 8). For *rctB*, the PCR program was: 2 min at 95°C followed by 30 cycles of 30 sec at 95°C, 1 min at 53°C and 1.45 min at 72°C with a final step of 5 min at 72°C For *topA* and *mreB*, the PCR conditions were: 2 min at 95°C followed by 30 cycles of 30 sec at 95°C, 30 sec at 50°C and 1min at 72°C with a final step of 5 min at 72°C. All PCR were performed using the Gotaq PCR polymerase (Gotaq G2 flexi, Promega) following the manufacturer's instructions. Genes were sequenced using the reverse PCR primer and sequencing was performed at GATC (https://www.gatc-biotech.com/fr).

On the bacterial strains isolated in the 3 other sampling points, the isolates were screened by PCR using rctB-F/rctB-R Vh-mreB-F/Vh-mreB-R primers designed to specifically hybridize with Harveyi-related *rctB* gene and *V. harveyi mreB* gene, respectively (Supplementary Table 8). For both detections, the PCR program was: 2 min at 95°C followed by 30 cycles of 30 sec at 95°C, 1 min at 53°C and 1.45 min at 72°C with a final step of 5 min at 72°C. Following this rational, 143 rctB+ isolates were considered as related to the Harveyi clade and related to *V. harveyi* species.

MLST *in silico* analyses

Sequences for each marker (*hsp60*, *rctB*, *topA* and *mreB*) were aligned with 8 V. harveyi superclade type strains using Muscle (Edgar, 2004). Alignments were concatenated with Seaview (Gouy et al., 2010). Phylogenetic trees were reconstructed with RAxML using a GTR model of evolution and Gamma law of rate heterogeneity. All other options were left at default values. Nodes support was assessed based on bootstraps with 100 replicates. Recombination can have profound effects on phylogenetic reconstruction, especially when the event is recent (Posada and Crandall, 2002). To determine if some markers recombined, each individual tree was manually inspected to search incongruent marker(s) for strains having long branches or low bootstrap support in the MLST tree. Incongruent markers were discarded in the alignment and strains having less than three non-recombinant markers were not considered. The final tree was reconstructed with RAxML as explained above with the filtered alignment.

Virulence studies on juvenile oysters

For injection procedures, bacteria were grown under agitation for 18 h at 20°C in Zobell liquid medium before dilution (with medium) to adjust the optical density (OD600) to 0.7. A volume of 40µL of each isolate was injected intramuscularly to 20 specific pathogen-free (SPF) juvenile *C. gigas* oysters (Petton *et al.*, 2015). *V. crassostreae* J2-9 (virulent strain), *V. tasmaniensis* LMG20012T (non-virulent strain) and sterile filtered seawater (negative control) were injected in parallel to pathogen free juvenile oysters. Animals were previously anesthetized in hexahydrate MgCl2 (50 g. L−1, 100 oysters/liter) for 14 to 16 h. Bacteria purity and concentration were checked by plating on Zobell agar. After injection, the juvenile oysters were transferred to aquaria (20 oysters per 1l aquarium) containing 400 mL of aerated seawater at 20 °C and kept under static conditions. Mortality was followed daily (24, 48 and 72hrs) and dead spats were removed from tanks.

Experimental infection in mesocosm

Seawater containing OsHV-1 µVar virions was produced by anesthetizing 90 oysters in hexahydrate MgCl2 (50 g. L−1, 100 oysters/liter) for 1-2 hrs, injecting them in the aductor muscle with 100 µl of a 0.2 µm filtrated viral suspension (10^8 genomic units mL^{-1}) and placed them in a 40 L tank for 24 hrs. After virions release, confirmed and quantified by qPCR, and previous to the mortality of donor oysters, contaminated was recover and used to fill the tanks for the different experimental conditions. Tanks with 2L of seawater and 10 oysters were prepared for sampling at different time points and tanks with 3L of seawater with 15 oysters to track the daily mortalities on each condition. Donor oysters were transferred to another tank to confirm mortalities. Clean seawater was used for the experimental conditions in absence of OsHV-1 µVar infection.

Bacterial strains were striked on Zobell agar and incubated at 20°C. Precultures were made by picking single colonies from the agar plates and growth in Zobell broth for 5h at 20°C in a rotary shaker. Zobell broth was seeded with the precultures and incubated for 18h at 20°C with agitation at 150 rpm. Cultures were centrifuged at 1500 x g for 10 min, the supernatant discarded and the pellet resuspended in sterile seawater. The OD600 of the bacterial suspension was measured and adjusted to OD600=1.

After placing the oysters in the tanks, bacterial suspension in seawater adjusted to OD600 = 1 (10^9 CFU/mL) were added to each tank to reach a final concentration of 10^7 CFU/mL. At each sampling time point, the oysters from the respective tank were taken together with a sample of 100 mL of seawater. The oyster flesh was removed from the shell, put into individual aluminum pockets and snap frozen in liquid nitrogen to be stored after at -80°C. Mortalities in

the monitoring tanks were recorded daily. 30 mL of seawater was filtered through 0.2um pore size and the filter stored individually at -80°C.Frozen individuals stored at -80°C were put into liquid nitrogen and transferred individually into stainless steel cylinders containing a stainless-steel ball cooled in liquid nitrogen, the cylinder was shacked at a frequency of 35 cycles/s for 30 s in a Retsch MM400 mixer mill. The pulverized tissue was transfer to a 2mL screw capped tube and stored at -80°C until further processing.

Nucleic acid extraction

Total DNA was extracted with the Nucleospin tissue DNA extraction kit (Machery Nagel, ref: 740952.250) with a modified protocol. Briefly, 20 mg of frozen tissue-powder, a pellet from 1 mL of stationary phase bacterial cultures or a 0.2um filter was added to a 2 mL screw capped tube containing Zirconium beads, lysis buffer and proteinase K and shaked for 12 min at a frequency of 35 cycles/s for in a Retsch MM400 mixer mill at room temperature. The samples were incubated for 1h 30min in a water bath at 56°C, after incubation RNAse A was added and the sample incubated were incubated for 5 min at 20°C and after for 10 min at 70°C. The following steps were carried out as recommended by the protocol provided by the manufacturer. DNA concentration and purity Nanodrop ND-1000 spectrometer (Thermo Scientific)

Total RNA was extracted from 20 mg of frozen tissue-powder using Direct-zol RNA extraction kit (Zymo research). Briefly, 20 mg of pulverized-frozen oyster tissue were resuspended in 1 mL of TRIzol and agitated at 150 rpm for 1.5 hrs. at 4°C. Trizol suspension was then incubated at 20°C for 5 minutes to finish the lysis. Next, 100 ul of chlorophorm were added, mixed by inversion and after 5 minutes tubes were centrifuged at 12.000 x g. The aqueous phase was recovered and the following steps were carried out as recommended by the protocol provided by the manufacturer. RNA concentration and purity were estimated using Nanodrop ND-1000 spectrometer (Thermo Scientific) and their integrity analyzed by capillary electrophoresis on a BioAnalyzer 2100 system (Agilent).

Vibrio genome sequencing

Genomic DNA for vibrio strains was extracted with the NucleoSpin Tissue kit (Macherey-Nagel Inc.). Individual genomic libraries were prepared at the Bio-Environment platform (University of Perpignan) using the nextera XT DNA Library Prep Kit (Illumina) according to the manufacturer's instructions starting from 1 ng of bacterial DNA and purified using AMPure XP beads. The quality of the libraries was checked using High Sensitivity DNA chip (Agilent) on a Bioanalyzer. Pooled libraries were sequenced in 2x150 paired-end mode on a NextSeq 550 (Illumina) resulting in ~100-fold coverage. Reads were assembled *de novo* using Spades

software. Computational prediction of coding sequences together with functional assignments and comparative genomics were performed using the MAGE software at the MicroScope platform (Vallenet *et al.*, 2013).

RNA sequencing and transcriptome analysis

RNA-seq library construction and sequencing were performed by the Fasteris Company (Switzerland). Directional cDNA libraries were constructed using the Ovation Complete Prokaryotic RNA-Seq (NuGen) and sequenced on a Novaseq system aiming to 100M reads in paired-end reads of 2 × 50 bp. Data treatment and analysis was performed with tools implemented under a Galaxy instance (Goecks *et al.*, 2010). All reads were kept for subsequent analysis as Phred scores determined by the Fastq-toolkit were higher than Q30 over 90% of the length for all the sequences. RNAstar (Galaxy Version 2.40d-2 [Dobin *et al.*, 2013]) was used to map reads to the *C. gigas* reference genome (assembly version V9 [Zhang *et al.*, 2012]. The number of reads overlapping annotated genes (mode Union) were determined by HTSeq-count (Galaxy Version v0.61 [Anders *et al.*, 2015]). Finally, differential gene expression was analyzed with the DESeq2 package (Love *et al.*, 2014). Fold changes between each time point of the kinetics and the control of un-treated oysters were considered to represent a differential gene expression when the adjusted p-value (Padj) for multiple testing with the Benjamini-Hochberk procedure to control the false discovery rate (FDR), was <0.05. The list of DEGs were represented on a heat map using a hierarchical clustering with uncentered Pearson correlation (MeV 4_9_0 software)

Enrichment analysis

DEGs were functionally annotated according to the database previously used by de Lorgeril *et al.* (2018). These annotated DEGs were used as input for GO enrichment analysis using an adaptive clustering and a rank-bases statistical analysis (Mann-Whitney U-test combined with adaptive clustering). The R and Perl scripts used can be downloaded [https://github.com/z0on/GO_MWU]. The parameters used for the adaptive clustering were: largest = 0.1, smallest = 10, and clusterCutHeight = 0.25. To combine both the significance of the differential expression and the level of expression into the analysis, the input table of continuous measures was generated by assigning the log2 fold-change values to those genes differentially expressed (FDR < 0.05) and a value of "0" to those genes with an FDR >0.05. A category was considered enriched with an FDR < 0.05

To represent the level of enrichment of modulated GO categories, a ratio was calculated for (i) upregulated enriched categories (number of genes significantly overexpressed in the category/total number of genes in this category) or (ii) for downregulated enriched

categories, -1 * (number of genes significantly downregulated in this category/total number of genes in this category) and represented on a heat map (MeV 4_9_0 software).

***Vibrio* quantification**

Quantification of total Vibrio in oysters was performed on DNA extracted from 20 mg of frozen tissue powders (see above) by targeting 16s rDNA.

Amplification reactions were carried out in duplicate, in a total volume of 20µl on Mx3000 and Mx3005 Thermocyclers (Agilent). Each well contained 5µl of genomic DNA (at 5 ng/µl), 10µl of the Brillant III Ultra-Fast SyberGreen Master Mix (Agilent), 0.060µl of each primer at 100µM (567F and 680R, table S8, [Thompson *et al.*, 2004], and distilled water. qPCR cycling conditions were as follows: 3 min at 95C, followed by 40 cycles of amplification at 95°C for 10 s and 60°C for 20 s.

Standard curves of known concentration of Vibrio genomes were generated using the relation between the concentration of DNA and the theoretical copy number of genomes, calculated on the basis of the DNA mass divided by molecular weight of the genome. They were also validated by the limit dilution method, assuming that the dilution at which 1 replicate in 10 was positive corresponds to 1 copy.

Absolute quantification of Vibrio genomes in oyster samples was then estimated by comparing the observed Ct values to known standards from 10^2 to 10^9 copies of Vibrio genomes. The absence of amplification (no Ct), or unquantifiable values (outside the standard range) were labelled as 1 copy and 10 copies respectively.

OsHV-1 µvar detection

Detection and quantification of OsHV-1 µvar DNA in oyster flesh was performed using quantitative PCR grounded oyster flesh (1.5mL) was centrifuged for 10 min at 4°C and 1500rpm and genomic DNA was extracted from 50µL of the supernatant using phenol: chloroform:isoamyl alcohol (25:24:1) and isopropanol precipitation. All amplification reactions were performed in duplicate using a Roche LightCycler 480 Real-Time thermocycler (qPHD-Montpellier GenomiX platform, Montpellier University). PCR reaction were performed in 6µL containing 3µL of LightCycler 480 SYBR Green I Master mix (Roche), 2µL (0.5µM) of pathogen specific primers and 100 ng of genomic DNA following a qPCR program with an initial denaturation step (95 °C for 10 min) and 40 cycles of denaturation (95 °C, 10 s), hybridization (60 °C, 20 s) and elongation step (72 °C, 25 s). Virus specific primer pairs targeting a region of the OsHV-1 µvar genome predicted to encode a DNA polymerase catalytic subunit (DP) were chosen as previously described: OsHVDPFor/OsHVDPRev (Table S6). Standard curves of

known concentration of DP plasmid were generated according to the Applied Biosystems manual of absolute real-time RT-PCR quantification. Absolute quantification of OsHV-1 µvar genome copies in oyster samples was then estimated by comparing the observed crossing point (Cp) values to known plasmid standards from 10^2 to 10^9 copies of DP. Oyster flesh samples exhibiting a viral load superior to 100 unit genome per ng of total DNA (UG/ng) were considered as infected by OsHV-1 µvar.

Barcoding

Locus-specific PCR primers including the required Illumina overhang adaptors were design to amplify a 573 bp region of the rctB gene in all our Harveyi strains, (rctB-Fw-I: 5'-TCGTCGGCAGCGTCAGATGTGTATAAGAGACAGYR-TGAATAGGCTCAAATTCGCCGTC-3'; rctB-Rv-I: 5'- GTCTCGTGGGCTCGGAGATGTGTATAAGAGACAGYR-CCWTCSTTCTWYGAAGAAYYGCT -3'). Two random bases, Y and R were added to the end of each of the Illumina overhang adaptors to increase sequencing efficiency has recommended by the GenSeq sequencing platform.

The PCR over the total DNA extracted from the sampled oysters (n=60) was carried out with a high fidelity Q5 polymerase in a total volume of 50 µl and a thermal cycler program with an initial step of 98°C for 25 s followed by 35 cycles of 98°C for 10 s, 51°C for 25 s and 72°C for 30 s. Final extension was performed at 72°C for 2 minutes. PCR products were resolved in a 1.5% gel electrophoresis, stained with gel red and visualized in a UV-photo capture system to confirm the presence of the 573 bp fragment.

Libraries were constructed with the 16S Metagenomic Sequencing Library Preparation (ref. 15044223) and sequenced in a MiSeq Illumina system to produce paired end reads 2x300 bp, by the GenSeq platform, University of Montpellier (ISEM), France.

The FROGS pipeline (Find Rapidly OTUs with Galaxy Solution) implemented into a Galaxy instance was used to process sequencing data and define Operation Taxonomic Units and taxonomic affiliations (Escudié *et al.*, 2018)

Paired reads were merged using FLASH (Magoč and Salzberg, 2011). Primer/adapter removal and denoising was done by cutadapt (Martin, 2011). Dereplicated sequences were used to perform de novo clustering using SWARM with an aggregation distance d = 3 (Mahé *et al.*, 2015). Chimera were removed using VSEARCH (de novo chimera detection) (Rognes *et al.*, 2016). OTUs generated were annotated using Blast+ against an in-house database containing the Harveyi rctB sequences to generate an OTU and affiliation table in standard

BIOM format. Affiliation and abundance data associated with each cluster was exported and used to estimate the relative abundance of the 4 different Harveyi species on each sample.

***In vitro* cytotoxicity assays**

Hemocytes were plated in 96 well-plates (2 x 105 cells/well) or in 12 well-plates (5 x 105 cells/well). After 1 h, plasma was removed and 5 µg/µl Sytox Green (Molecular Probes) diluted in 200µl sterile seawater was added to each well. Vibrios, previously washed and opsonized in plasma for 1 h, were then added to the wells at a MOI of 50:1. Sytox Green fluorescence was monitored (ƛex 480nm/ƛem 550nm) for 15 h using a TECAN microplate reader. Maximum cytolysis was determined by adding 0.1% Triton X-100 to hemocytes. Statistical analysis was performed using RM-ANOVA.

Iron depency growth of Harveyi

Growth experiments in iron depleted medium were performed with *V. harveyi* Th15_O_G11 and *V. rotiferianus* Th15_O_G10. Isolates were grown overnight at room temperature in minimal medium: 35g/L reef salts, 0.3% (wt/vol) casamino acids and vitamins: 0.1 µg/L vitamin B12, 2µg/L biotin, 5µg/L calcium pantothenate, 2µg/L folic acid, 5 µg/L nicotinamide, 10 µg/L pyridoxin hydrochloride, 5 µg/L riboflavin, 5 mg/L thiamin hydrochloride. Cultures were pelleted (2 min at 10,000 rpm in a microcentrifuge), the supernatant was discarded, and pellets were washed once in reef salts solution (35g/L). Cells were then inoculated (1:1,000) into minimal media with (iron-poor) or without (iron-replete) the iron-specific chelator EDDA (ethylenediamine-N,N'-diacetic acid). Cells were incubated at room temperature and the absorbance at 600 nm measured every hour for 24 h. The filtered *V. harveyi* Th15_O_G11 cell-free supernatant (3-kDa membrane using an Amicon Ultra centrifugal unit, Millipore) added to culture results from growth in iron-poor conditions (200µM EDDA).

References

Alcaide, E., Gil-Sanz, C., Sanjuán, E., Esteve, D., Amaro, C., Silveira, L., et al. (2001) Vibrio harveyi causes disease in seahorse, Hippocampus sp. *J Fish Dis* **24**: 311–313.

Anders, S., Pyl, P.T., and Huber, W. (2015) HTSeq-A Python framework to work with high-throughput sequencing data. *Bioinformatics* **31**: 166–169.

Arezes, J., Jung, G., Gabayan, V., Valore, E., Ruchala, P., Gulig, P.A., et al. (2015) Hepcidin-induced hypoferremia is a critical host defense mechanism against the siderophilic bacterium vibrio vulnificus. *Cell Host Microbe* **17**: 47–57.

Austin, B., Austin, D., Sutherland, R., Thompson, F., and Swings, J. (2005) Pathogenicity of vibrios to rainbow trout (Oncorhynchus mykiss, Walbaum) and Artemia nauplii. *Environ Microbiol* **7**: 1488–1495.

Bhattacharya, P.C. (2006) Economic development, gender inequality, and demographic outcomes: Evidence from India. *Popul Dev Rev* **32**: 263–292.

Broberg, C.A., Zhang, L., Gonzalez, H., Laskowski-Arce, M.A., and Orth, K. (2010) A Vibrio effector protein is an inositol phosphatase and disrupts host cell membrane integrity. *Science (80-)* **329**: 1660–1662.

Bruto, M., James, A., Petton, B., Labreuche, Y., Chenivesse, S., Alunno-Bruscia, M., et al. (2017) Vibrio crassostreae, a benign oyster colonizer turned into a pathogen after plasmid acquisition. *ISME J* **11**: 1043–1052.

Bruto, M., Labreuche, Y., James, A., Piel, D., Chenivesse, S., Petton, B., et al. (2018) Ancestral gene acquisition as the key to virulence potential in environmental Vibrio populations. *ISME J* **12**: 1.

Burge, C.A., Reece, K.S., Dhar, A.K., Kirkland, P., Morga, B., Dégremont, L., et al. (2020) First comparison of French and Australian OsHV-1 µvars by bath exposure. **138**: 137–144.

Company, R., Sitj, A., Pujalte, M.J., Garay, E., Alvarez-Pellitero, P., P, J., and P, J. (2002) Bacterial and parasitic pathogens in cultured common dentex, Dentex dentex L. *J Fish Dis* **22**: 299–309.

Cordero, O.X., Wildschutte, H., Kirkup, B., Proehl, S., Ngo, L., Hussain, F., et al. (2012) Ecological Populations of Bacteria Act as Socially Cohesive Units of Antibiotic Production and Resistance. *Science (80-)* **337**: 1228–1231.

Darshanee Ruwandeepika, H.A., Sanjeewa Prasad Jayaweera, T., Paban Bhowmick, P., Karunasagar, I., Bossier, P., and Defoirdt, T. (2012) Pathogenesis, virulence factors and virulence regulation of vibrios belonging to the Harveyi clade. *Rev Aquac* **4**: 59–74.

Delmotte, J., Chaparro, C., Galinier, R., Lorgeril, J. De, Petton, B., Stenger, P., et al. (2020) Contribution of Viral Genomic Diversity to Oyster Susceptibility in the Pacific Oyster Mortality Syndrome. *Front Microbiol* **11**: 1–17.

Destoumieux-Garzón, D., Canesi, L., Oyanedel, D., Travers, M.-A.A., Charrière, G.M., Pruzzo, C., and Vezzulli, L. (2020) Vibrio–bivalve interactions in health and disease. *Environ Microbiol*, doi.org/10.1111/1462-2920.15055

Diggles, B.K., Moss, G.A., Carson, J., and Anderson, C.D. (2000) Luminous vibriosis in rock lobster Jasus verreauxi (Decapoda: Palinuridae) phyllosoma larvae associated with infection by Vibrio harveyi. *Dis Aquat Organ* **43**: 127–137.

Dobin, A., Davis, C.A., Schlesinger, F., Drenkow, J., Zaleski, C., Jha, S., et al. (2013) STAR: Ultrafast universal RNA-seq aligner. *Bioinformatics* **29**: 15–21.

EFSA (2015) Oyster mortality. *EFSA J* **13**: 4122.

Escudié, F., Auer, L., Bernard, M., Mariadassou, M., Cauquil, L., Vidal, K., et al. (2018) FROGS: Find, Rapidly, OTUs with Galaxy Solution. *Bioinformatics* **34**: 1287–1294.

Fuhrmann, M., Richard, G., Quéré, C., Petton, B., and Pernet, F. (2019) Low pH reduced survival of the oyster Crassostrea gigas exposed to the Ostreid herpesvirus 1 by altering the metabolic response of the host. *Aquaculture* **503**: 167–174.

Gay, M., Renault, T., Pons, A.M., and Le Roux, F. (2004) Two Vibrio splendidus related strains collaborate to kill Crassostrea gigas: Taxonomy and host alterations. *Dis Aquat Organ* **62**: 65–74.

Gob, S.H., Potter, S., Wood, J.O., Hemmingsen, S.M., Reynolds, R.P., and Chow, A.W. (1996) HSP60 gene sequences as universal targets for microbial species identification: Studies with coagulase-negative staphylococci. *J Clin Microbiol* **34**: 818–823.

Goecks, J., Nekrutenko, A., Taylor, J., Afgan, E., Ananda, G., Baker, D., et al. (2010) Galaxy: a comprehensive approach for supporting accessible, reproducible, and transparent computational research in the life sciences. *Genome Biol* **11**:

Gouy, M., Guindon, S., and Gascuel, O. (2010) Sea view version 4: A multiplatform graphical user interface for sequence alignment and phylogenetic tree building. *Mol Biol Evol* **27**:

221–224.

Green, T.J., Siboni, N., King, W.L., Labbate, M., Seymour, J.R., and Raftos, D. (2019) Simulated Marine Heat Wave Alters Abundance and Structure of Vibrio Populations Associated with the Pacific Oyster Resulting in a Mass Mortality Event. *Microb Ecol* **77**: 736–747.

Hispano, C., Nebra, Y., and Blanch, A.R. (1997) Isolation of Vibrio harveyi from an ocular lesion in the short sunfish (Mola mola). *Bull Eur Assoc Fish Pathol* **17**: 104–107.

Hunt, D.E., David, L.A., Gevers, D., Preheim, S.P., Alm, E.J., and Polz, M.F. (2008) Resource Partitioning and Sympatric Differentiation Among Closely Related Bacterioplankton. *Science (80-)* **320**: 1081 LP – 1085.

Kraxberger-Beatty, T., McGarey, D.J., Grier, H.J., and Lim, D. V. (1990) Vibrio harveyi, an opportunistic pathogen of common snook, Centropomus undecimalis (Bloch), held in captivity. *J Fish Dis* **13**: 557–560.

Lafont, M., Petton, B., Vergnes, A., Pauletto, M., Segarra, A., Gourbal, B., and Montagnani, C. (2017) Long-lasting antiviral innate immune priming in the Lophotrochozoan Pacific oyster, Crassostrea gigas. *Sci Rep* **7**: 13143.

Lafont, M., Vergnes, A., Vidal-Dupiol, J., de Lorgeril, J., Gueguen, Y., Haffner, P., et al. (2020) A Sustained Immune Response Supports Long-Term Antiviral Immune Priming in the Pacific Oyster, Crassostrea gigas. *MBio* **11**: e02777-19.

Lemire, A., Goudenege, D., Versigny, T., Petton, B., Calteau, A., Labreuche, Y., et al. (2015) Populations, not clones, are the unit of vibrio pathogenesis in naturally infected oysters. *ISME J* **9**: 1523–1531.

Lopez-Joven, C., Rolland, J.-L., Haffner, P., Caro, A., Roques, C., Carré, C., et al. (2018) Oyster Farming, Temperature, and Plankton Influence the Dynamics of Pathogenic Vibrios in the Thau Lagoon . *Front Microbiol* **9**: 2530.

de Lorgeril, J., Lucasson, A., Petton, B., Toulza, E., Montagnani, C., Clerissi, C., et al. (2018) Immune-suppression by OsHV-1 viral infection causes fatal bacteraemia in Pacific oysters. *Nat Commun* **9**: 4215.

Lorgeril, J. De, Petton, B., Lucasson, A., Perez, V., Stenger, P., Dégremont, L., et al. (2020) Differential basal expression of immune genes confers Crassostrea gigas resistance to Pacific oyster mortality syndrome. **21**:1–14.

Love, M.I., Huber, W., and Anders, S. (2014) Moderated estimation of fold change and

dispersion for RNA-seq data with DESeq2. *Genome Biol* **15**: 1–21.

Ma, A.T. and Mekalanos, J.J. (2010) In vivo actin cross-linking induced by Vibrio cholerae type VI secretion system is associated with intestinal inflammation. *Proc Natl Acad Sci U S A* **107**: 4365–4370.

Magoč, T. and Salzberg, S.L. (2011) FLASH: Fast length adjustment of short reads to improve genome assemblies. *Bioinformatics* **27**: 2957–2963.

Mahé, F., Rognes, T., Quince, C., de Vargas, C., and Dunthorn, M. (2015) Swarmv2: Highly-scalable and high-resolution amplicon clustering. *PeerJ* **3**: 1–12.

Martin, M. (2011) Cutadapt removes adapter sequences from high-throughput sequencing reads. *EMBnet.journal* **17***: pp.*10-12

Montánchez, I., Ogayar, E., Plágaro, A.H., Esteve-Codina, A., Gómez-Garrido, J., Orruño, M., et al. (2019) Analysis of Vibrio harveyi adaptation in sea water microcosms at elevated temperature provides insights into the putative mechanisms of its persistence and spread in the time of global warming. *Sci Rep* **9**:

Murray, J.L., Connell, J.L., Stacy, A., Turner, K.H., and Whiteley, M. (2014) Mechanisms of synergy in polymicrobial infections. *J Microbiol* **52**: 188–199.

Pernet, F., Lagarde, F., Gall, P. Le, and D'Orbcastel, E.R. (2014a) Associations between farming practices and disease mortality of Pacific oyster Crassostrea gigas in a Mediterranean lagoon. *Aquac Environ Interact*. **5**: 99-106

Pernet, F., Lagarde, F., Jeanne, N., Daigle, G., Barret, J., Gall, P. Le, et al. (2014b) Spatial and Temporal Dynamics of Mass Mortalities in Oysters Is Influenced by Energetic Reserves and Food Quality. **9**: e88469

Petton, B., Bruto, M., James, A.A., Labreuche, Y., Alunno-Bruscia, M., and Le Roux, F.F. (2015) Crassostrea gigas mortality in France: The usual suspect, a herpes virus, may not be the killer in this polymicrobial opportunistic disease. *Front Microbiol* **6**: 1–10.

Petton, B., Pernet, F., Robert, R.R., and Boudry, P. (2013) Temperature influence on pathogen transmission and subsequent mortalities in juvenile Pacific oysters Crassostrea gigas. *Aquac Environ Interact* **3**: 257–273.

Piel, D., Bruto, M., James, A., Labreuche, Y., Lambert, C., Janicot, A., et al. (2019) Selection of Vibrio crassostreae relies on a plasmid expressing a type 6 secretion system cytotoxic for

host immune cells. *Environ Microbiol* doi.org/10.1111/1462-2920.14776.

Posada, D. and Crandall, K.A. (2002) The Effect of Recombination on the Accuracy of Phylogeny Estimation. *J Mol Evol* **54**: 396–402.

Rognes, T., Flouri, T., Nichols, B., Quince, C., and Mahé, F. (2016) VSEARCH: A versatile open source tool for metagenomics. *PeerJ* **2016**: 1–22.

Rubio, T., Oyanedel, D., Labreuche, Y., Toulza, E., Luo, X., Bruto, M., et al. (2019) Species-specific mechanisms of cytotoxicity toward immune cells determine the successful outcome of Vibrio infections. *Proc Natl Acad Sci* **116**: 14238–14247.

Saeed, M.O.O. (1995) Association of Vibrio harveyi with mortalities in cultured marine fish in Kuwait. *Aquaculture* **136**: 21–29.

Samain, J.-F. and Mccombie, H. (2008) Summer mortality of Pacific oyster Crassostrea gigas. *Morest Proj*.

Saulnier, D., De Decker, S., Haffner, P., Cobret, L., Robert, M., and Garcia, C. (2010) A Large-Scale Epidemiological Study to Identify Bacteria Pathogenic to Pacific Oyster Crassostrea gigas and Correlation Between Virulence and Metalloprotease-like Activity. *Microb Ecol* **59**: 787–798.

Sawabe, T., Kita-Tsukamoto, K., and Thompson, F.L. (2007) Inferring the evolutionary history of vibrios by means of multilocus sequence analysis. *J Bacteriol* **189**: 7932–7936.

Tendencia, E.A. (2002) Vibrio harveyi isolated from cage-cultured seabass Lates calcarifer Bloch in the Philippines. *Aquac Res* **33**: 455–458.

Thompson, J.R., Randa, M.A., Marcelino, L.A., Tomita-Mitchell, A., Lim, E., and Polz, M.F. (2004) Diversity and dynamics of a North Atlantic coastal Vibrio community. *Appl Environ Microbiol* **70**: 4103–4110.

Vallenet, D., Belda, E., Calteau, A., Cruveiller, S., Engelen, S., Lajus, A., et al. (2013) MicroScope - An integrated microbial resource for the curation and comparative analysis of genomic and metabolic data. *Nucleic Acids Res* **41**: 636–647.

Waddell, B., Southward, C.M., Mckenna, N., and Devinney, R. (2014) Identification of VPA0451 as the specific chaperone for the Vibrio parahaemolyticus chromosome 1 type III-secreted effector VPA0450. *FEMS Microbiol Lett* **353**: 141–150.

Zhang, G., Fang, X., Guo, X., Wang, JunLi, L., Luo, R., Xu, F., et al. (2012) The oyster genome

reveals stress adaptation and complexity of shell formation. *Nature* **490**: 49–54.

Zhou, K., Gui, M., Li, P., Xing, S., Cui, T., Peng, Z., et al. (2012) Effect of combined function of temperature and water activity on the growth of Vibrio harveyi. **43**: 1365–1375.

Figures

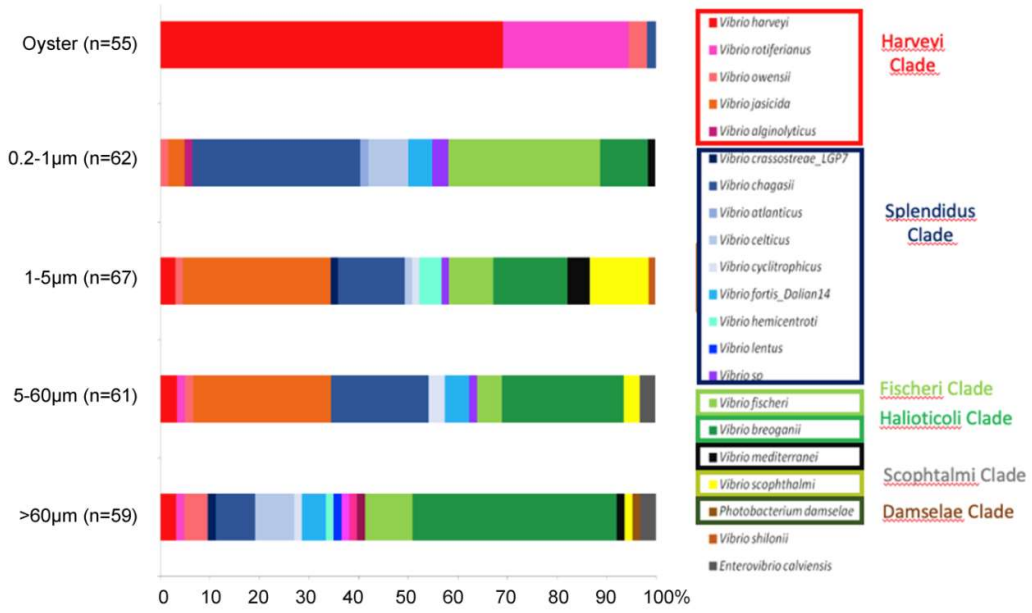

Figure 1. Population structure prediction of Vibrionaceae bacteria recovered from different seawater fractions or oyster flesh**.** The distribution (%) of vibrios isolated from oysters and size-filtered seawater fractions (>63um, 60-5um, 5-1um, 1-0.2um) in October 2015 during autumn mortality was analysed using the *hsp60* marker gene. Hsp60 sequences were blasted against sequences of *Vibrio* and an assignation was proposed if identity ≥ 95%. Altogether, 304 *hsp60* sequences display an identity ≥ 95% with *E. calviensis* DSM14347^{T}, *P. damselae* CIP102761^{T}, *V. alginolyticus* NBRC15630^{T}, *V. atlanticus* CECT7223^{T}, *V. breoganii* 1C10, *V. campbellii* CAIM519^{T}, *V. celticus* CECT7224^{T}, *V. chagasii* LMG21353^{T}, *V. crassostreae* LGP7^{T}, *V. cyclitrophicus* LMG21359^{T}, *V. fischeri* MJ11, *V. fortis* Dalian14, *V. harveyi* NBRC15634^{T}, *V. hemicentroti* CECT8714^{T}, *V. jasicida* CAIM1864^{T}, *V. lentus* CIP107166^{T}, *V. mediterranei* NBRC15635^{T}, *V. owensii* CAIM1854^{T}, *V. rotiferianus* CAIM577^{T}, *V. scophthalmi* LMG19158^{T}, *V. shilonii* AK1^{T}.`

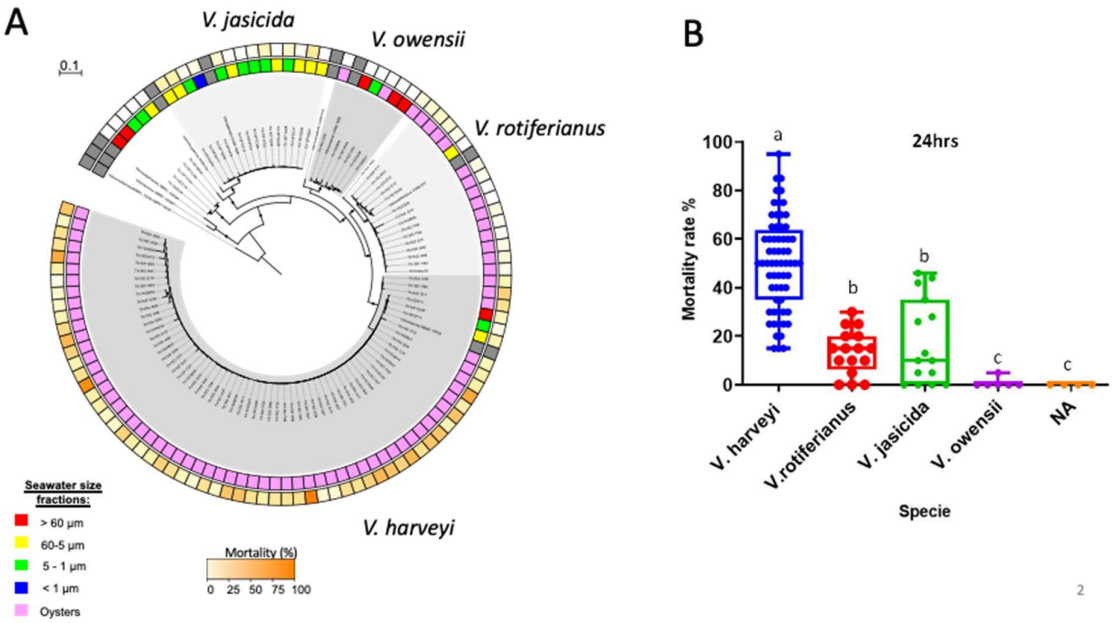

Figure 2. Harveyi clade population structure and virulence. (A) Phylogenetic tree based on *hsp60*, *rctB*, *topA* and *mreB* marker genes. Sequences were aligned using Muscle and concatenated with Seaview before tree reconstruction using a GTR model of evolution and Gamma law of rate heterogeneity. The inner ring indicates whether a strain was isolated from a specific seawater fraction or from oysters and the outer rings represents the mortality rates at 24hrs post-injection. Asterisks indicate the strains sequenced in this study. (B) Mortality rate following experimental infection with Harveyi-related isolates collected in the Thau lagoon in October 2015. Strains were individually injected into the muscle of 20 juvenile oysters and the mortality rate (%) scored after 24h. The effect of the vibrio species on oyster mortality rate was determined using Kruskal-Wallis test (p-value < 0.001). Significant differences between Vibrio species were performed with Mann-Whitney tests using the GraphPad Prism software (p-value < 0.001). *V. harveyi* (n=63), *V. rotiferianus* (n=16), *V. jasicida* (n=15), *V. owensii* (n=6), NA (not assigned, n=4).

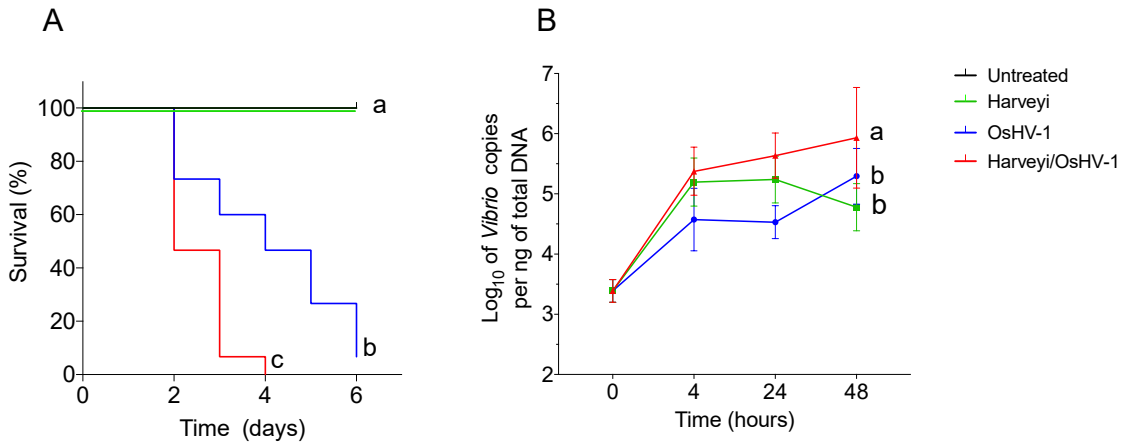

Figure 3. Colonization and mortality rate of OsHV-1 infected oysters by bacteria of the Harveyi clade. (A) Oyster mortalities were tracked daily over a 6-day period and Kaplan-Meier survival curves were generated with the data. No mortality was recorded in the untreated condition and for the oysters exposed to Harveyi only, until the last day of monitoring. A significant increase in the mortality rate was observed for oysters exposed to both Harveyi and OsHV-1 (log-rank test, P value = 0.0018). (B) Total Vibrio load was quantified on individual oysters by Vibrio-specific amplification of the 16S rRNA gene by qPCR. Total DNA for Vibrio quantification was extracted from frozen powder of whole oyster flesh. We quantified in average a 35-fold higher Vibrio load in oysters also exposed to OsHV-1 compared to the charge in oysters only exposed to bacteria (Kruskal-Wallis test, P value < 0.001). Total *Vibrio* load in untreated oysters was quantified only at time point 0

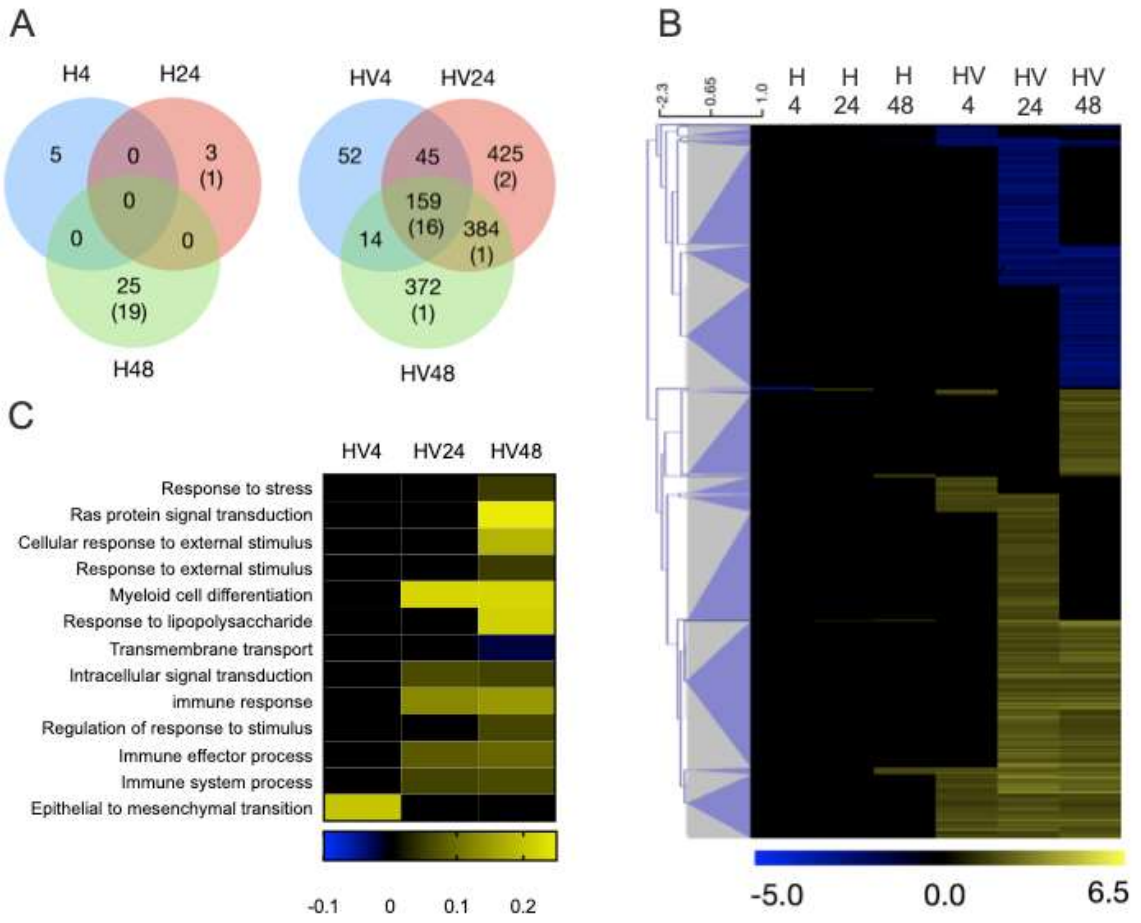

Figure 4. Oyster transcriptional response during infection by Harveyi and co-infection by OsHV-1. Differential expression analysis was performed between each sampling point from the two experimental condition and untreated oysters using the DEseq2 package (A) Venn diagram showing the distribution of the different DEGs (FDR < 0.05) among sampling points of the same experimental condition. The number of genes common to H and HV conditions is indicated in parenthesis. (B) Heat map of the log2 fold change values for the 1467 DEGs found in the bacteria/virus exposure condition and clustered according to the Pearson uncentered correlation (MeV_4_9_0 software). Clusters which participate on enriched biological functions are indicated with numbers from 1-8. (C) GO enrichment by a rank-bases statistical test (RGBOA) represented as a heatmap of biological function significantly enriched (FDR < 0.05) between each time point and the untreated control group. The intensity of enrichment for each GO category is represented by the ratio between the number of genes over-expressed (yellow) or under-expressed (blue) and the total number of genes belonging to the GO category. DEGs identified in HV24 and HV48 (diseased oysters) are characteristic of the response to

POMS: genes related to apoptosis (inhibitors of apoptosis (IAP), caspase, TNF receptors)), immune recognition receptors and proteins with putative antimicrobial activity (Scavenger receptor, LRR, TLR, β-1,3-Glucan recognition protein (βGRP), c-type lectins, C1q proteins, galectins, IL17R), antiviral genes (cGAs, RIG-like receptor [RLR], Tripartite motif-containing proteins [TRIM], E3 ubiquitin-protein ligase, ADAR), signaling pathways (JAK-STAT, IFN and NF-kB pathways), and effectors with antimicrobial (SOD, laccase, tyrosinase, alpha-2-macroglobulin) and antiviral functions (Interferon-stimulated genes, sacsin, viperin).

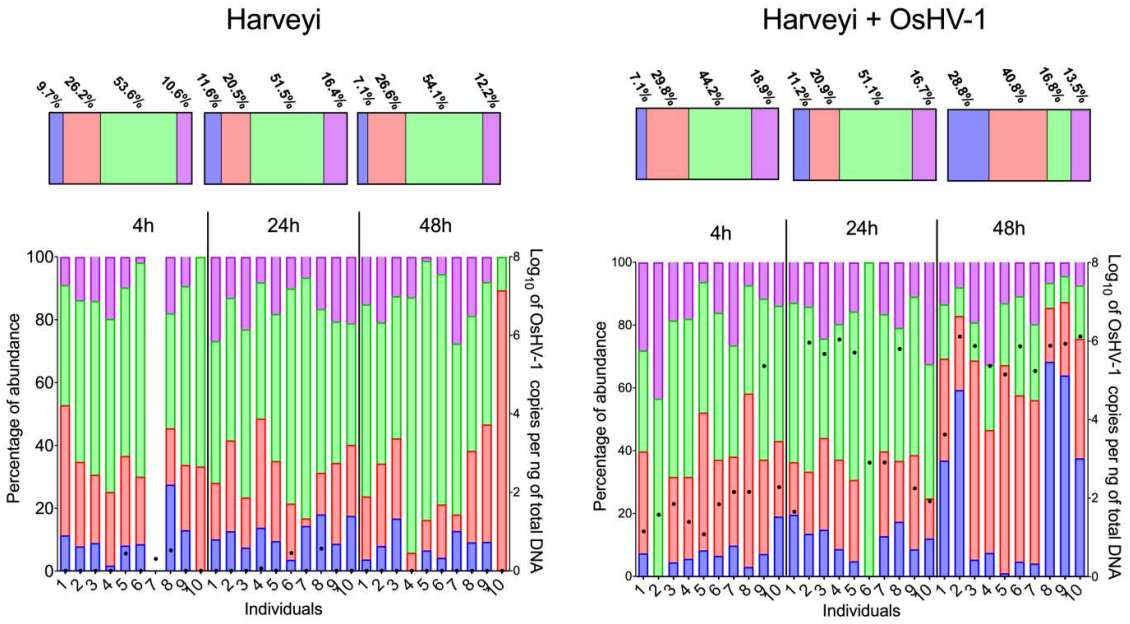

Figure 5. Analysis at the vibrio population level of the Vibrio colonizing oysters and OsHV-1 load. Vibrio populations inside oysters were analyzed by performing *rctB* gene-based barcoding by sequencing a 573 bp region of the *rctB* gene that allows phylogenetic resolution at the population level of the Harveyi clade. The PCR products were sequenced using Illumina Miseq system and data were used to estimate the relative abundance of each Harveyi population associated with individual oysters. Upper horizontal bars correspond to the average percentage of abundance of each Harveyi population for each time point (N=10 oysters). Lower charts show in vertical bars the relative abundance at the individual scale (left y-axis) together with black dots to represent the OsHV-1 load per individual (right y-axis) expressed has the $\log_{10}$ of the number of genome copies of OsHV-1 per ng of total DNA. Individuals used for RNAseq were H4 #2 #3 #4; H24 #1, #4, #10; H48 #1, #3, #6; HV4 #3 #4 #7; HV24 #2, #3, #4; HV48 #2, #8, #9.

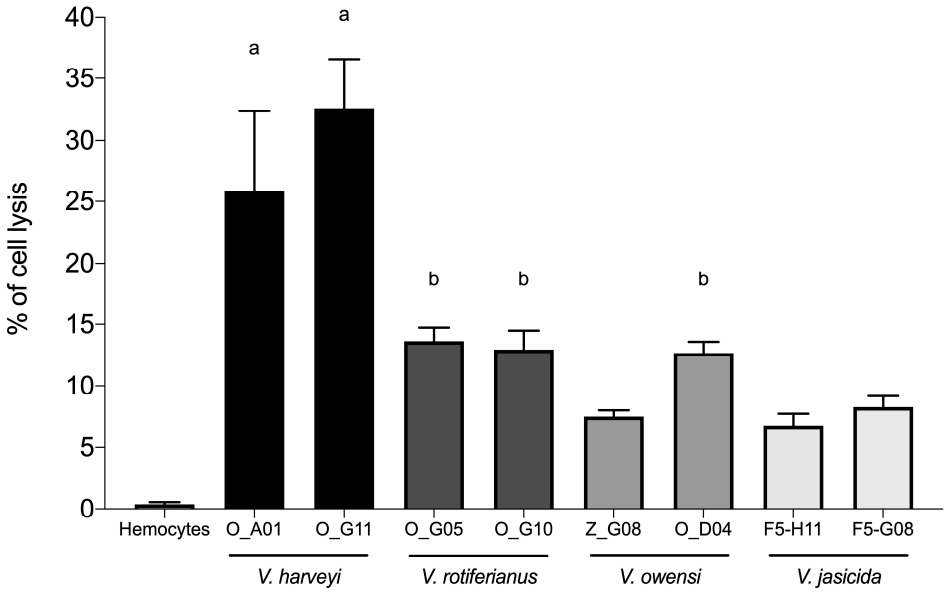

Figure 6. Cytotoxicity of Harveyi strains toward oyster immune cells. Cytotoxicity was determined on monolayers of hemocytes and monitored using the Sytox green labelling. Cells were infected with bacteria at a MOI of 50:1. Maximum of cytotoxicity of vibrios is displayed. Error bars represent the standard deviation of the mean, different letters indicate significant variation between conditions ($p<0,05$, One-way ANOVA with post-hoc Tukey HSD Test).

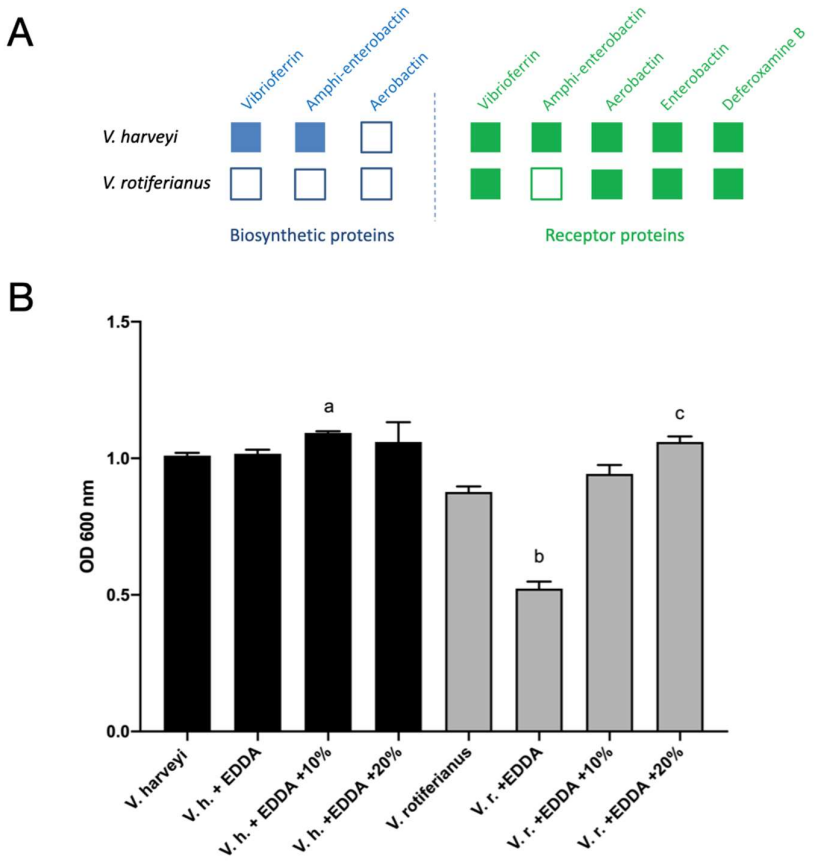

Figure 7. Siderophores distribution and growth of *V. harveyi* and *V. rotiferianus* in iron-depleted medium. (A) Known Vibrionaceae siderophore biosynthetic and receptor proteins in *V. harveyi* and *V. rotiferianus*. Biosynthetic proteins are indicated in blue and receptor proteins in green. Enterobactin and deferoxamine B are xenosiderophores produced by *E. coli* and *Streptomyces pilosus*, respectively. (B) Growth of the vibrioferrin producer *V. harveyi* O_G11 strain in minimal media (V.h.) and in media supplemented with 100 µM EDDA (V.h. EDDA), an iron-specific chelator. OD_{600} was measured after a 20 h growth. V.h. grew similarly in all media. By contrast, the non-producer *V. rotiferianus* O_G10 strain (V.r.), which only has specific receptors for vibrioferrin, showed a growth defect in the presence of 100 µM EDDA (V.r EDDA). This defect was completed by the addition of cell-free culture supernatant from *V. harveyi* O_G11 (10% or 20% vol/vol). The values are the mean of three independent cultures. Error bars represent the standard deviation of the mean, different letters indicate significant variation between conditions ($p<0,05$, One-way ANOVA with post-hoc Tukey HSD Test).

III.2.1. SUPPLEMENTAL FIGURES

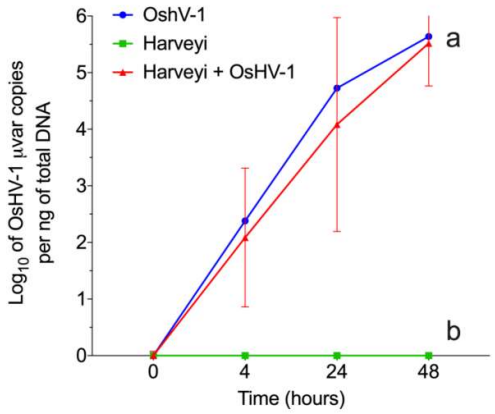

Figure S1. Total OsHV-1 µVar quantified on individual oysters by qPCR. Number of copies of OsHV-1 per ng of total DNA were $log_{10}(x+1)$ transformed. Final time points were compared by a Kruskal-Wallis test. Significative differences between conditions are noted with different letters (P value < 0.001)

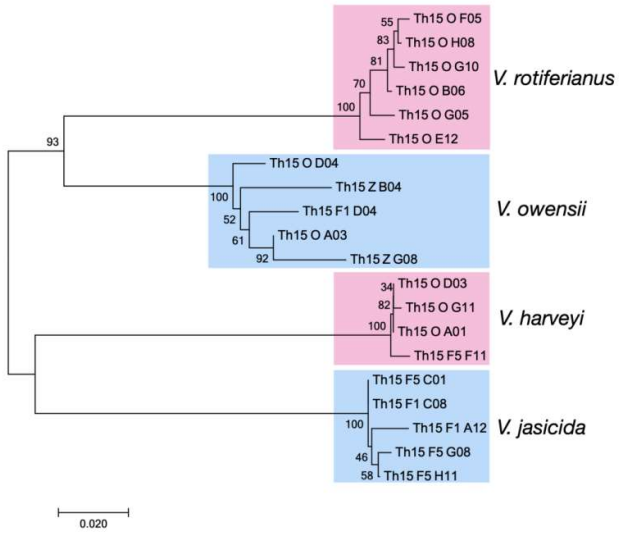

Figure S2. Discrimination of Harveyi species by *rctB* sequencing. Phylogenetical tree constructed using the Neighbor-Joining method, the optimal tree with the sum of branch length = 0.49310882 is shown. The percentage of replicate trees in which the associated taxa clustered together in the bootstrap test (1000 replicates) are shown next to the branches. The tree is drawn to scale, with branch lengths in the same units as those of the evolutionary distances used to infer the phylogenetic tree. The evolutionary distances were computed using the Maximum Composite Likelihood method and are in the units of the

number of base substitutions per site. The analysis involved 20 nucleotide sequences. All positions containing gaps and missing data were eliminated. There were a total of 494 positions in the final dataset. Evolutionary analyses were conducted in MEGA7.

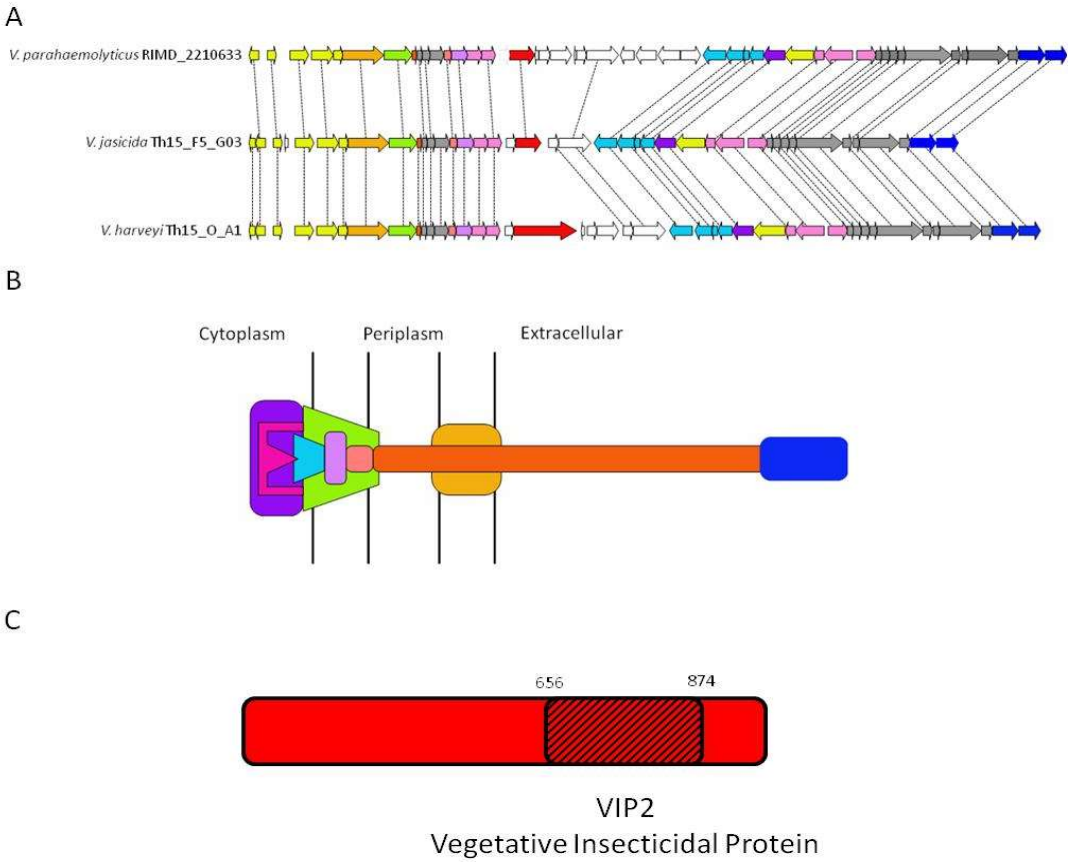

Figure S3. Arginine ADP-ribosyltransferase family protein and type three secretion system (T3SS) genetic organization in representative strains of the Harveyi super-clade. A. Synteny of the T3SS shared between *V. parahaemolyticus*, *V. jasicida* and *V. harveyi*. The effectors are indicated in red. In *V. harveyi*, the putative effector is an arginine ADP-ribosyltransferase. A dashed line connects to genes that share > 70% of identity. B. Typical structure of a T3SS. The colours used here are related to colours of genes in A. C. Vegetative insecticidal proteins 2 domain (VIP2) of the putative arginine ADP-ribosyltransferase in *V. harveyi*.

Table S1. Prevalence of the Harveyi clade in oyster flesh during Mediterranean POMS episodes. Oysters were collected during and outside POMS episodes in the Thau lagoon. At each sampling time, a total of 82 to 96 bacterial isolates obtained from oyster flesh were screened for the Harveyi clade (rctB-F/rctB-R primers) and the *V. harveyi* species (Vh-mreB-F/Vh-mreB-R primers). The oyster flesh was simultaneaouly tested for OsHV-1 detection (OsHVDPFor/OsHVDPRev primers)

Date	Field mortalities	OsHV-1 virus	% Harveyi clade	% *V. harveyi*
01/10/2015	Yes	positive	94.0	75.9
09/06/2016	No	negative	0.0	0.0
23/06/2016	Yes	positive	49.0	32.0
13/03/2017	No	negative	1.0	1.0

Table S2. Vibrio samplings in the Thau lagoon

Date	GPS coordinates	Temp	Mortality	Biological material	No of isolates
10/01/2015	43° 24' 49.058''N 3° 37' 54.005''E	18°C	yes	Oysters (n=30)	96
10/01/2015	43° 24' 49.058''N 3° 37' 54.005''E	18°C	yes	Water column > 60µm	96
10/01/2015	43° 24' 49.058''N 3° 37' 54.005''E	18°C	yes	Water column 5 µm	96
10/01/2015	43° 24' 49.058''N 3° 37' 54.005''E	18°C	yes	Water column 1µm	96
10/01/2015	43° 24' 49.058''N 3° 37' 54.005''E	18°C	yes	Water column 0,2µm	88
06/09/2016	43°22'44,8"N 3°34'17,5"E	24°C	no	Oysters (n=30)	76
06/23/2016	43° 23' 22.851''N 3° 35' 45.465"E	22°C	yes	Oysters (n=29)	96
03/13/2017	43°26.058'N 03°39'.878'E	12 .6°C	no	Oysters (n=12)	96

Table S3. List of oyster genes with significantly modulated expression. Log2 fold changes in gene expression were calculated relative to expression control oysters (not exposed to OsHV-1 µvar nor to the Harveyi community). Data are means of three independent individuals. Only significant values are displayed (FDR < 0.05). A *dash* indicates not significant values (FDR > 0.05).

		Log2 Foldchange					
CGI	**Gene**	**H4**	**H24**	**H48**	**HV4**	**HV24**	**HV48**
CGI_10001775	ankyrin repeat domain-containing 50-like	3.332	-	-	-	-	-
CGI_10010171	Heat shock Hsp20 domain containing	-2.127	-	-	-	-	-
CGI_10002497	4-coumarate-- ligase-like 7	-3.795	-	-	-	-	-
CGI_10008328	paramyosin-like isoform X1 [Crassostrea gigas]	-3.898	-	-	-	-	-
CGI_10009617	Myeloid leukemia factor partial	-4.026	-	-	-	-	-
CGI_10016962	glutathione S-transferase omega-1-like [Crassostrea gigas]	-	3.371	-	-	-	-
CGI_10005523	transmembrane 79-like	-	2.434	-	-	-	-
CGI_10027729	cell number regulator 3	-	-	2.773	-	-	-
CGI_10002102	complement C1q tumor necrosis factor-related 3-like	-	-	2.262	-	-	-
CGI_10028325	PREDICTED: uncharacterized protein LOC105325227 [Crassostrea gigas]	-	-	1.579	-	-	-
CGI_10024811	transport Sec31A isoform X2 [Cricetulus griseus]	-	-	-1.074	-	-	-
CGI_10010021	adenylate kinase mitochondrial isoform X2	-	-	-1.601	-	-	-
CGI_10010987	cytochrome P450 27C1-like [Crassostrea gigas]	-	-	-	3.082	-	-
CGI_10005397	temptin-like	-	-	-	2.734	-	-
CGI_10026598	Chondroitin proteoglycan-2	-	-	-	2.666	-	-
CGI_10019627	c-binding -like	-	-	-	2.453	-	-
CGI_10027853	multiple coagulation factor deficiency 2 homolog	-	-	-	2.441	-	-
CGI_10028418	Fbox domain containing [Acanthamoeba castellanii Neff]	-	-	-	2.380	-	-
CGI_10014080	mitochondrial amidoxime-reducing component 1-like	-	-	-	2.254	-	-
CGI_10005701	hypothetical protein CGI_10005701	-	-	-	2.050	-	-
CGI_10022810	NFX1-type zinc finger-containing 1	-	-	-	2.006	-	-
CGI_10009454	tetratricopeptide repeat 1	-	-	-	1.985	-	-
CGI_10005186	tRNA (guanine-N(7)-)-methyltransferase	-	-	-	1.969	-	-
CGI_10008630	Transmembrane [Xenopus laevis]	-	-	-	1.945	-	-
CGI_10006160		-	-	-	1.931	-	-
CGI_10005483	PREDICTED: uncharacterized protein LOC105325933	-	-	-	1.853	-	-
CGI_10019451	CRAL-TRIO domain-containing [Schistosoma haematobium]	-	-	-	1.838	-	-
CGI_10011753	phenylalanine--tRNA ligase beta subunit	-	-	-	1.821	-	-
CGI_10012207	dolichyl-diphosphooligosaccharide-- glycosyltransferase subunit STT3B	-	-	-	1.797	-	-
CGI_10007857	beta-N-acetylhexosaminidase [Photobacterium iliopiscarium]	-	-	-	1.785	-	-
CGI_10015268	PFC0760c-like isoform X1	-	-	-	1.736	-	-
CGI_10010738	myosin light chain smooth muscle-like [Limulus polyphemus]	-	-	-	1.642	-	-
CGI_10024100	estrogen receptor	-	-	-	1.618	-	-

CGI_10011402	chitin deacetylase isoform B	-	-	-	1.608	-	-
CGI_10016070	RISC-loading complex subunit tarbp2-like [Biomphalaria glabrata]	-	-	-	1.559	-	-
CGI_10017701	forkhead box L1	-	-	-	1.558	-	-
CGI_10014052	RER1 isoform X1 [Sinocyclocheilus grahami]	-	-	-	1.547	-	-
CGI_10008942	KH domain- RNA- signal transduction-associated 2-like	-	-	-	1.515	-	-
CGI_10020980	sarcoplasmic calcium-binding -like [Crassostrea gigas]	-	-	-	1.453	-	-
CGI_10020368	transmembrane 65-like	-	-	-	1.437	-	-
CGI_10025852	cyclin-dependent kinase 11B-like isoform X2	-	-	-	1.408	-	-
CGI_10017976	PREDICTED: uncharacterized protein LOC105346492 [Crassostrea gigas]	-	-	-	1.337	-	-
CGI_10025431	ELAV 3 isoform X8 [Lingula anatina]	-	-	-	1.307	-	-
CGI_10006896	sorting nexin-6-like	-	-	-	1.227	-	-
CGI_10011867	ataxin-1 isoform X1 [Monodelphis domestica]	-	-	-	1.221	-	-
CGI_10021833	pyridoxal-dependent decarboxylase domain-containing 2 isoform X2	-	-	-	1.148	-	-
CGI_10000487	Eukaryotic translation initiation factor 4E	-	-	-	1.094	-	-
CGI_10004762	40S ribosomal S27-like [Octopus bimaculoides]	-	-	-	0.964	-	-
CGI_10019620	lisH domain and HEAT repeat-containing KIAA1468 homolog isoform X1	-	-	-	-1.249	-	-
CGI_10025517	FAM43A-like [Lingula anatina]	-	-	-	-1.303	-	-
CGI_10006850	hypothetical protein CGI_10006850	-	-	-	-1.327	-	-
CGI_10007729	PREDICTED: uncharacterized protein LOC105332290	-	-	-	-1.508	-	-
CGI_10025350	Group 3 secretory phospholipase A2	-	-	-	-1.546	-	-
CGI_10015205	Mediator of RNA polymerase II transcription subunit 15	-	-	-	-1.666	-	-
CGI_10015863	Cyclin-dependent kinase inhibitor 1B	-	-	-	-1.755	-	-
CGI_10009829	hypothetical protein CGI_10009829	-	-	-	-1.789	-	-
CGI_10023357	E3 ubiquitin- ligase ARI3 [Crassostrea gigas]	-	-	-	-2.023	-	-
CGI_10016664	androgen-induced gene 1 -like isoform X3	-	-	-	-2.052	-	-
CGI_10011780	PREDICTED: uncharacterized protein LOC105334417 isoform X3	-	-	-	-2.108	-	-
CGI_10028397	oxidoreductase HTATIP2 isoform X3 [Callorhinchus milii]	-	-	-	-2.199	-	-
CGI_10011979	mutS homolog 4	-	-	-	-2.280	-	-
CGI_10001832	transmembrane 178B-like	-	-	-	-2.388	-	-
CGI_10014778	plexin-B1 isoform X1 [Poecilia formosa]	-	-	-	-2.516	-	-
CGI_10009791	mitogen-activated kinase kinase kinase partial	-	-	-	-2.598	-	-
CGI_10000207	partial	-	-	-	-2.950	-	-
CGI_10024431	N66 matrix -like	-	-	-	-	3.599	-
CGI_10020701	hypothetical protein CGI_10020701	-	-	3.808	-	3.517	-
CGI_10014333	Kielin chordin	-	-	-	-	3.339	-
CGI_10021409	Kinesin heavy chain	-	-	-	1.978	3.290	-
CGI_10020255	hypothetical protein CGI_10020255	-	-	-	-	3.264	-
CGI_10016026	proteoglycan 4-like	-	-	-	2.623	3.005	-
CGI_10017877	Solute carrier family 23 member 2	-	-	-	-	2.945	-
CGI_10003183	deoxynucleoside triphosphate triphosphohydrolase SAMHD1-like	-	-	-	-	2.929	-
CGI_10018797	PREDICTED: uncharacterized protein LOC105330395 [Crassostrea gigas]	-	-	-	-	2.907	-
CGI_10012708	hypothetical protein CGI_10012708	-	-	-	-	2.888	-
CGI_10018706	GTP-binding RAD [Crassostrea gigas]	-	-	-	-	2.869	-
CGI_10016805	hypothetical protein CGI_10016805	-	-	-	-	2.859	-
CGI_10014529	GATA zinc finger domain-containing 14-like	-	-	-	2.408	2.841	-

CGI_10003181	hypothetical protein CGI_10003181	-	-	-	-	2.826	-
CGI_10003430	von Willebrand factor D and EGF domain-containing -like	-	-	-	-	2.770	-
CGI_10017729	leucine-rich repeat-containing 15-like [Crassostrea gigas]	-	-	-	2.563	2.714	-
CGI_10012913	zinc finger 234 isoform X1 [Cercocebus atys]	-	-	-	-	2.593	-
CGI_10011215	hypothetical protein CGI_10011215	-	-	-	-	2.576	-
CGI_10016861	melanoma receptor tyrosine- kinase-like	-	-	-	1.772	2.573	-
CGI_10017426	Chorion peroxidase	-	-	-	2.506	2.547	-
CGI_10020509	5-hydroxytryptamine receptor 1-like [Crassostrea gigas]	-	-	-	-	2.544	-
CGI_10004239	PREDICTED: uncharacterized protein LOC105339532 [Crassostrea gigas]	-	-	-	-	2.544	-
CGI_10006348	LDLR chaperone MESD	-	-	-	-	2.542	-
CGI_10011837	complement C1q tumor necrosis factor-related 4	-	-	-	-	2.521	-
CGI_10005687	proline-rich transmembrane 1-like	-	-	-	-	2.507	-
CGI_10024897	Collagen alpha-1(XII) chain	-	-	-	-	2.497	-
CGI_10027921	perlucin 6	-	-	-	-	2.484	-
CGI_10008141	cyclin-G-associated kinase-like	-	-	-	-	2.475	-
CGI_10001711	tumor necrosis factor receptor superfamily member 27-like [Crassostrea gigas]	-	-	-	-	2.428	-
CGI_10018835	hypothetical protein CGI_10018835	-	-	-	-	2.425	-
CGI_10018572	hypothetical protein CGI_10018572	-	-	-	-	2.402	-
CGI_10006247	calmodulin variant 1	-	-	-	-	2.383	-
CGI_10020692	hypothetical protein CGI_10020692	-	-	-	-	2.381	-
CGI_10001977	hypothetical protein CGI_10001977	-	-	-	-	2.366	-
CGI_10015520	Multiple epidermal growth factor-like domains 10	-	-	-	-	2.353	-
CGI_10007514	retinol-binding 4-like	-	-	-	1.756	2.344	-
CGI_10018250	delta 4	-	-	-	1.757	2.344	-
CGI_10025372	seleno S-like	-	-	-	1.582	2.319	-
CGI_10025420	growth differentiation factor 8	-	-	-	-	2.318	-
CGI_10016695	ADAM family mig-17	-	-	-	-	2.313	-
CGI_10009371	girdin-like isoform X13	-	-	-	-	2.285	-
CGI_10013236	ADAM family mig-17	-	-	-	2.407	2.277	-
CGI_10005951	hypothetical protein CGI_10005951	-	-	-	-	2.245	-
CGI_10022372	E3 ubiquitin- ligase RNF213	-	-	-	-	2.241	-
CGI_10018175	PREDICTED: mucin-5AC-like	-	-	-	2.131	2.221	-
CGI_10018362	fibrocystin-L-like isoform X1	-	-	-	-	2.217	-
CGI_10005327	perlucin	-	-	-	-	2.214	-
CGI_10000894	disulfide-isomerase A5-like	-	-	-	-	2.211	-
CGI_10017289	Mediator of RNA polymerase II transcription subunit 19	-	-	-	2.367	2.206	-
CGI_10023163	delta D	-	-	-	-	2.206	-
CGI_10028286	kielin chordin	-	-	-	-	2.191	-
CGI_10026230	tyrosinase tyr-3	-	-	-	2.390	2.187	-
CGI_10014257	uncharacterized	-	-	-	1.599	2.174	-
CGI_10008546	excitatory amino acid transporter [Strongylocentrotus purpuratus]	-	-	-	-	2.168	-
CGI_10020314	complement C1q tumor necrosis factor-related 3-like isoform X2 [Crassostrea gigas]	-	-	-	-	2.158	-
CGI_10005884	toll-like receptor 3 isoform X1 [Crassostrea gigas]	-	-	-	-	2.154	-
CGI_10004628	nuclear transcription factor Y subunit gamma [Callorhinchus milii]	-	-	-	-	2.152	-
CGI_10005689	deoxyuridine 5 -triphosphate mitochondrial	-	-	-	-	2.145	-

CGI_10027907	Exonuclease 3 -5 domain-containing 1	-	-	-	-	2.140	-
CGI_10000646	Cytochrome b5	-	-	-	-	2.137	-
CGI_10026861	MAM and LDL-receptor class A domain-containing 1-like	-	-	-	-	2.135	-
CGI_10000434	microfibril-associated glyco 4-like	-	-	-	-	2.134	-
CGI_10007552	tolloid 2	-	-	-	-	2.134	-
CGI_10006327	RNMT-activating mini	-	-	-	-	2.131	-
CGI_10014279	laccase-1-like [Hydra vulgaris]	-	-	-	-	2.099	-
CGI_10019386	vitelline membrane outer layer 1-like	-	-	-	-	2.084	-
CGI_10012464	hypothetical protein CGI_10012464	-	-	-	-	2.075	-
CGI_10022879	deoxynucleoside triphosphate triphosphohydrolase SAMHD1	-	-	-	-	2.074	-
CGI_10011865	reticulocyte-binding 2 homolog a-like	-	-	-	-	2.065	-
CGI_10018297	serine ase [Ixodes scapularis]	-	-	-	-	2.044	-
CGI_10027808	galactose-specific lectin nattectin-like	-	-	-	-	2.040	-
CGI_10010868	probable phytanoyl- dioxygenase	-	-	-	-	2.038	-
CGI_10017070	ras-related RABF2b-like [Crassostrea gigas]	-	-	-	-	2.023	-
CGI_10021070	hypothetical protein CGI_10021070	-	-	-	-	2.006	-
CGI_10017844	Translation initiation factor eIF-2B subunit gamma	-	-	-	1.623	1.986	-
CGI_10013439	tctex1 domain-containing 1-like	-	-	-	-	1.982	-
CGI_10002628	Small nuclear ribonucleo polypeptide G [Homo sapiens]	-	-	-	-	1.970	-
CGI_10023095	cell wall DAN4-like	-	-	-	-	1.962	-
CGI_10022445	Seleno N	-	-	-	-	1.962	-
CGI_10005553	Mitogen-activated kinase kinase kinase 4	-	-	-	-	1.957	-
CGI_10007116	hypothetical protein CGI_10007116	-	-	-	-	1.946	-
CGI_10027749	WAS WASL-interacting family member 3-like	-	-	-	1.502	1.941	-
CGI_10004022	marginal zone B- and B1-cell-specific -like	-	-	-	-	1.936	-
CGI_10022775	coadhesin- partial	-	-	-	-	1.936	-
CGI_10010135	Laminin subunit alpha-1	-	-	-	-	1.934	-
CGI_10002598		-	-	-	-	1.920	-
CGI_10027768	cholecystokinin receptor type A-like [Crassostrea gigas]	-	-	-	-	1.917	-
CGI_10020128	glycine-rich domain-containing 2-like [Biomphalaria glabrata]	-	-	-	-	1.916	-
CGI_10023837	transmembrane matrix receptor MUP-4-like	-	-	-	-	1.912	-
CGI_10000050	succinate dehydrogenase [ubiquinone] iron-sulfur mitochondrial	-	-	-	-	1.910	-
CGI_10006015	myophilin [Echinococcus granulosus]	-	-	-	-	1.910	-
CGI_10027695	paired box Pax-6-like isoform X1 [Crassostrea gigas]	-	-	-	-	1.908	-
CGI_10018907	calmodulin 1 isoform X1 [Crassostrea gigas]	-	-	-	-	1.903	-
CGI_10023622	Tripartite motif-containing 2	-	-	-	-	1.901	-
CGI_10028116	39S ribosomal mitochondrial	-	-	-	2.015	1.896	-
CGI_10020176		-	-	-	-	1.896	-
CGI_10003794	hypothetical protein	-	-	-	-	1.887	-
CGI_10016842	cysteine and tyrosine-rich 1-like	-	-	-	-	1.887	-
CGI_10024321	Actin-related 2 3 complex subunit 3	-	-	-	-	1.880	-
CGI_10026502	universal stress -like isoform X1 [Biomphalaria glabrata]	-	-	-	-	1.878	-
CGI_10008396	hypothetical protein CGI_10008396	-	-	-	-	1.869	-
CGI_10017942	Matrilin-2 [Crassostrea gigas]	-	-	-	-	1.868	-
CGI_10026717	RNA-dependent RNA polymerase 1	-	-	-	-	1.868	-

CGI_10009732	DBH-like monooxygenase 1 [Crassostrea gigas]	-	-	-	-	1.863	-
CGI_10015750	membrane [Cecembia lonarensis]	-	-	-	-	1.846	-
CGI_10024013	hypothetical protein CGI_10024013	-	-	-	-	1.842	-
CGI_10009504	low-density lipo receptor-related 4-like	-	-	-	-	1.842	-
CGI_10026531	hypothetical protein CGI_10026531	-	-	-	-	1.841	-
CGI_10022626	macrophage mannose receptor 1-like	-	-	-	-	1.821	-
CGI_10008911	complement C1q tumor necrosis factor-related 4-like [Crassostrea gigas]	-	-	-	-	1.807	-
CGI_10018677	mucin-4-like isoform X2	-	-	-	2.072	1.796	-
CGI_10026975	ubiquitin [Capsaspora owczarzaki ATCC 30864]	-	-	-	-	1.792	-
CGI_10021446	Alkaline tissue-nonspecific isozyme	-	-	-	-	1.792	-
CGI_10022586	heat shock 70 kDa 12A-like [Crassostrea gigas]	-	-	-	-	1.786	-
CGI_10011533	salivary glue Sgs-3-like	-	-	-	-	1.781	-
CGI_10024591	mantle -like isoform X3	-	-	-	-	1.779	-
CGI_10018892	solute carrier family 13 member 5-like [Crassostrea gigas]	-	-	-	-	1.778	-
CGI_10023018	ubiquitin-conjugating enzyme E2 J1 isoform X1	-	-	-	-	1.771	-
CGI_10022955	Contactin	-	-	-	-	1.770	-
CGI_10012838	Sulfatase-modifying factor 1	-	-	-	-	1.765	-
CGI_10019692	calcitonin gene-related peptide type 1 receptor-like	-	-	-	-	1.759	-
CGI_10020541	hypothetical protein CGI_10020541	-	-	-	-	1.757	-
CGI_10010458	probable ATP-dependent RNA helicase DHX58	-	-	-	-	1.747	-
CGI_10009952	balbiani ring 3-like	-	-	-	-	1.731	-
CGI_10024389	Solute carrier organic anion transporter family member 4A1	-	-	-	-	1.727	-
CGI_10014092	aspartate cytoplasmic-like	-	-	-	-	1.723	-
CGI_10022249	Peptidyl-prolyl cis-trans isomerase B	-	-	-	-	1.723	-
CGI_10014831	Solute carrier family 12 member 2	-	-	-	-	1.721	-
CGI_10004524	5-hydroxytryptamine receptor 1-like [Crassostrea gigas]	-	-	-	-	1.715	-
CGI_10005749	mesenchyme-specific cell surface glyco -like	-	-	-	-	1.712	-
CGI_10018176	GH23898 [Drosophila grimshawi]	-	-	-	1.748	1.709	-
CGI_10006079	multiple epidermal growth factor-like domains 10	-	-	-	-	1.706	-
CGI_10015287	serine threonine- kinase ULK2-like isoform X3	-	-	-	-	1.690	-
CGI_10017403	eukaryotic translation initiation factor partial	-	-	-	1.492	1.690	-
CGI_10026789	28S ribosomal mitochondrial	-	-	-	-	1.676	-
CGI_10003927	hypothetical protein CGI_10003927	-	-	-	-	1.674	-
CGI_10021019	zinc finger CCCH domain-containing 13-like	-	-	-	-	1.673	-
CGI_10017177	amyloid beta A4 precursor -binding family A member 1-like isoform X1 [Crassostrea gigas]	-	-	-	-	1.670	-
CGI_10021718	28S ribosomal mitochondrial	-	-	-	-	1.667	-
CGI_10016467	deleted in malignant brain tumors 1 -like	-	-	-	-	1.664	-
CGI_10023174	MACRO domain-containing 2	-	-	-	-	1.664	-
CGI_10005896	C3a anaphylatoxin chemotactic receptor	-	-	-	-	1.662	-
CGI_10009192	hypothetical protein CGI_10009192	-	-	-	-	1.659	-
CGI_10020951	zinc finger 628	-	-	-	-	1.658	-
CGI_10004939	Cadherin EGF LAG seven-pass G-type receptor 2	-	-	-	-	1.653	-
CGI_10015700	inter-alpha-trypsin inhibitor heavy chain H3-like	-	-	-	-	1.653	-
CGI_10020961	40S ribosomal S16	-	-	-	-	1.649	-
CGI_10014236	multiple epidermal growth factor-like domains 10	-	-	-	-	1.649	-

CGI_10000852	baculoviral IAP repeat-containing 3-like [Crassostrea gigas]	-	-	-	-	1.646	-
CGI_10016752	Vacuolar sorting-associated 29	-	-	-	-	1.643	-
CGI_10009013	CREBRF homolog [Halyomorpha halys]	-	-	-	-	1.639	-
CGI_10004474	nucleolin-like isoform X1	-	-	-	1.680	1.637	-
CGI_10014200	RWD domain-containing 4	-	-	-	-	1.634	-
CGI_10020409	glutamine--fructose-6-phosphate aminotransferase [isomerizing] 2-like isoform X5	-	-	-	-	1.631	-
CGI_10016193	hypothetical protein CGI_10016193	-	-	-	-	1.630	-
CGI_10020253	Multiple epidermal growth factor-like domains 10	-	-	-	-	1.627	-
CGI_10027133	ADAM family mig-17	-	-	-	2.731	1.622	-
CGI_10012973	cytochrome P450 3A11-like [Crassostrea gigas]	-	-	-	-	1.610	-
CGI_10014307	dual specificity kinase splB-like [Hydra vulgaris]	-	-	-	-	1.590	-
CGI_10004072	HLA class II histocompatibility antigen gamma chain-like	-	-	-	-	1.590	-
CGI_10018828	Cat eye syndrome critical region 5	-	-	-	-	1.589	-
CGI_10018918	T-complex 1 subunit alpha	-	-	-	1.293	1.583	-
CGI_10026928	Glutamyl aminopeptidase	-	-	-	-	1.583	-
CGI_10002070	hypothetical protein CGI_10002070	-	-	-	-	1.581	-
CGI_10022978	early growth response 1-B-like	-	-	-	-	1.576	-
CGI_10019434	hypothetical protein CGI_10019434	-	-	-	1.548	1.573	-
CGI_10023734	hypothetical protein CGI_10023734	-	-	-	-	1.572	-
CGI_10022464	nidogen and EGF-like domain-containing 1	-	-	-	-	1.567	-
CGI_10009560	C-type lectin lectoxin-Lio3- partial	-	-	-	-	1.566	-
CGI_10008004	Leucine-rich repeat-containing 24	-	-	-	1.748	1.555	-
CGI_10023210	dual oxidase maturation factor 1-like	-	-	-	-	1.555	-
CGI_10026748	Collagen alpha-5(VI) chain	-	-	-	-	1.553	-
CGI_10023179	Collagen alpha-6(VI) chain	-	-	-	-	1.550	-
CGI_10010018	microfibril-associated glyco 4-like	-	-	-	-	1.542	-
CGI_10006768	Smaug homolog 1-like [Lingula anatina]	-	-	-	-	1.541	-
CGI_10014111	eukaryotic translation initiation factor 5A-1-like	-	-	-	-	1.539	-
CGI_10006579	transcription factor AP-1-like	-	-	-	-	1.530	-
CGI_10000751	MON2 homolog	-	-	-	-	1.527	-
CGI_10017761	beta-arrestin-1-like isoform X1 [Lingula anatina]	-	-	-	-	1.526	-
CGI_10023237	ubiquitin fusion degradation 1 homolog	-	-	-	-	1.524	-
CGI_10006881	F-box only 22-like	-	-	-	1.388	1.522	-
CGI_10012713	lateral signaling target 2 homolog	-	-	-	1.007	1.508	-
CGI_10016019	sodium-dependent glucose transporter 1A-like	-	-	-	-	1.503	-
CGI_10003866	zinc transporter ZIP12 isoform X3	-	-	-	-	1.495	-
CGI_10025144	A disintegrin and metallo ase with thrombospondin motifs 18-like	-	-	-	1.647	1.486	-
CGI_10008877	peroxiredoxin 6	-	-	-	-	1.484	-
CGI_10005111	solute carrier family 26 member 6-like [Lingula anatina]	-	-	-	-	1.482	-
CGI_10015065	proto-oncogene tyrosine- kinase Yrk-like isoform X2	-	-	-	-	1.475	-
CGI_10023366	mesencephalic astrocyte-derived neurotrophic factor-like	-	-	-	1.370	1.474	-
CGI_10018669	ETS domain-containing Elk-4-like isoform X2 [Biomphalaria glabrata]	-	-	-	-	1.472	-
CGI_10018118	UPF0469 KIAA0907 homolog	-	-	-	-	1.464	-
CGI_10024725	baculoviral IAP repeat-containing 7 isoform X2	-	-	-	-	1.456	-
CGI_10019647	Tripartite motif-containing 45	-	-	-	-	1.455	-

CGI_10020678	E3 ubiquitin- ligase MIB2	-	-	-	-	1.450	-
CGI_10024300	cyclic nucleotide-binding domain-containing 2-like	-	-	-	-	1.443	-
CGI_10003941	sodium-coupled monocarboxylate transporter 1-like	-	-	-	-	1.431	-
CGI_10005999	hypothetical protein CGI_10005999	-	-	-	-	1.428	-
CGI_10018378	F-box only 9	-	-	-	-	1.420	-
CGI_10002756	macrophage mannose receptor 1-like	-	-	-	-	1.419	-
CGI_10028623	rogdi-like isoform X2	-	-	-	-	1.414	-
CGI_10026413	copine-8-like isoform X2	-	-	-	-	1.414	-
CGI_10021322	microtubule-associated 1 light chain 3 alpha [synthetic construct]	-	-	-	-	1.411	-
CGI_10023128	calcium-binding P-like	-	-	-	-	1.410	-
CGI_10013086	major egg antigen-like [Octopus bimaculoides]	-	-	-	-	1.408	-
CGI_10021552	rap guanine nucleotide exchange factor 1-like isoform X1	-	-	-	-	1.405	-
CGI_10016401	MAM and LDL-receptor class A domain-containing 2-like	-	-	-	-	1.404	-
CGI_10013193	DAZ-associated 2-like isoform X1 [Crassostrea gigas]	-	-	-	-	1.398	-
CGI_10019166	WW domain-binding 2 isoform X2	-	-	-	-	1.394	-
CGI_10013840	Neurogenic locus notch 2	-	-	-	-	1.382	-
CGI_10008953	uncharacterized	-	-	-	-	1.374	-
CGI_10025652	BTB POZ domain-containing adapter for CUL3-mediated degradation 3-like [Biomphalaria glabrata]	-	-	-	-	1.354	-
CGI_10004140	TPR repeat-containing DDB_G0287407-like	-	-	-	-	1.343	-
CGI_10018618	MLP1-like isoform X4	-	-	-	-	1.341	-
CGI_10018743	hypothetical protein CGI_10018743	-	-	-	-	1.340	-
CGI_10007563	dnaJ homolog subfamily C member 3-like	-	-	-	1.444	1.339	-
CGI_10026441	E3 ubiquitin- ligase MIB2	-	-	-	-	1.331	-
CGI_10006535	ubiquilin-1 isoform X1	-	-	-	-	1.309	-
CGI_10023630	Prickle 2	-	-	-	1.173	1.308	-
CGI_10025509	Hepatocyte nuclear factor 3-beta	-	-	-	1.369	1.304	-
CGI_10009534	unconventional myosin-XVI	-	-	-	-	1.294	-
CGI_10027950	ATP-binding cassette sub-family A member 3-like [Biomphalaria glabrata]	-	-	-	1.524	1.292	-
CGI_10023337	dolichyl-diphosphooligosaccharide-- glycosyltransferase subunit STT3A	-	-	-	-	1.281	-
CGI_10006953	rho-related BTB domain-containing 2-like [Aplysia californica]	-	-	-	-	1.274	-
CGI_10023736	paramyosin-like isoform X1 [Crassostrea gigas]	-	-	-	-	1.263	-
CGI_10026962	hypothetical protein CGI_10026962	-	-	-	-	1.260	-
CGI_10018855	pleckstrin homology-like domain family B member 1 isoform X4	-	-	-	-	1.256	-
CGI_10002545	Casein kinase I isoform alpha	-	-	-	-	1.252	-
CGI_10003664	Mushroom body large-type Kenyon cell-specific 1	-	-	-	-	1.251	-
CGI_10014123	Golgi integral membrane 4-like isoform X4	-	-	-	1.191	1.244	-
CGI_10024279	threonine--tRNA cytoplasmic isoform X1 [Bactrocera oleae]	-	-	-	-	1.236	-
CGI_10025795	U2 snRNP-associated SURP motif-containing -like isoform X3	-	-	-	-	1.235	-
CGI_10021027	proline-rich 5-like isoform X2	-	-	-	-	1.232	-
CGI_10001793	3-hydroxyanthranilate 3,4-dioxygenase isoform X2	-	-	-	-	1.229	-
CGI_10021979	acid sphingomyelinase-like phosphodiesterase 3b	-	-	-	-	1.225	-
CGI_10006851	serine-rich adhesin for platelets-like	-	-	-	-	1.221	-
CGI_10010995	uncharacterized	-	-	-	1.328	1.218	-
CGI_10023852	naked cuticle like	-	-	-	-	1.214	-
CGI_10020967	piccolo-like [Crassostrea gigas]	-	-	-	-	1.201	-

CGI_10027590	synergin gamma-like isoform X1	-	-	-	-	1.195	-
CGI_10013081	Pleckstrin domain-containing family A member 5	-	-	-	-	1.192	-
CGI_10027733	voltage-dependent L-type calcium channel subunit beta-1-like isoform X3 [Crassostrea gigas]	-	-	-	-	1.182	-
CGI_10014240	dyslexia-associated KIAA0319 isoform X2	-	-	-	1.018	1.170	-
CGI_10016389	SH3 and multiple ankyrin repeat domains 3-like isoform X3 [Lingula anatina]	-	-	-	-	1.168	-
CGI_10026037	CDK5 and ABL1 enzyme substrate 1-like isoform X1	-	-	-	-	1.156	-
CGI_10014861	Ubiquitin-conjugating enzyme E2 N	-	-	-	-	1.149	-
CGI_10016663	1-phosphatidylinositol 3-phosphate 5-kinase	-	-	-	-	1.146	-
CGI_10026091	insulin receptor substrate 1 isoform X2	-	-	-	-	1.139	-
CGI_10006168	sprint-like isoform X1 [Crassostrea gigas]	-	-	-	-	1.130	-
CGI_10000865	zinc finger 318	-	-	-	1.112	1.120	-
CGI_10018167	integumentary mucin -like isoform X1	-	-	-	-	1.116	-
CGI_10023213	coiled-coil domain-containing R3HCC1L-like [Aplysia californica]	-	-	-	-	1.113	-
CGI_10017067	Lathosterol oxidase	-	-	-	-	1.109	-
CGI_10014107	lipoma-preferred partner homolog	-	-	-	-	1.106	-
CGI_10028872	Zinc finger 367	-	-	-	-	1.049	-
CGI_10012243	electroneutral sodium bicarbonate exchanger 1-like isoform X1 [Crassostrea gigas]	-	-	-	-	1.012	-
CGI_10018191	Syntaxin-6	-	-	-	-	0.955	-
CGI_10005796	kinesin KIF26B isoform X1 [Crassostrea gigas]	-	-	-	-	0.946	-
CGI_10026429	double C2-like domain-containing beta isoform X1 [Crassostrea gigas]	-	-	-	-	0.943	-
CGI_10027461	GON-4	-	-	-	-	0.940	-
CGI_10022667	golgin subfamily A member 6 22 [Biomphalaria glabrata]	-	-	-	-	-0.968	-
CGI_10015851	E3 ubiquitin- ligase HERC2-like	-	-	-	-0.874	-0.998	-
CGI_10016643	phosphatase 1L	-	-	-	-	-1.024	-
CGI_10008800	smg8	-	-	-1.138	-	-1.063	-
CGI_10015670	mitogen-activated kinase kinase kinase 4-like	-	-	-	-	-1.100	-
CGI_10019634	ras GTPase-activating IQGAP1 isoform X1 [Aplysia californica]	-	-	-	-	-1.111	-
CGI_10003423	Kyphoscoliosis peptidase [Crassostrea gigas]	-	-	-	-	-1.121	-
CGI_10009169	Kinesin KIF21A	-	-	-	-	-1.156	-
CGI_10019578	ral GTPase-activating subunit alpha-1-like isoform X4 [Biomphalaria glabrata]	-	-	-	-	-1.169	-
CGI_10021960	ras-related Rab-3-like isoform X4 [Crassostrea gigas]	-	-	-	-	-1.189	-
CGI_10022348	ATP-binding cassette sub-family C member 9-like	-	-	-	-	-1.207	-
CGI_10006173	ELKS Rab6-interacting CAST family member 1 isoform X5	-	-	-	-	-1.217	-
CGI_10022237	Choline mitochondrial	-	-	-	-	-1.245	-
CGI_10009595	neurobeachin 1	-	-	-	-	-1.249	-
CGI_10013349	Carnitine O-palmitoyltransferase liver isoform	-	-	-	-	-1.254	-
CGI_10019131	sperm flagellar 1-like isoform X1	-	-	-	-	-1.254	-
CGI_10002528	coiled-coil domain-containing 162- partial	-	-	-	-	-1.267	-
CGI_10021037	ACYPI004131 [Acyrthosiphon pisum]	-	-	-	-	-1.281	-
CGI_10024276	cholesterol 25-hydroxylase member 2	-	-	-	-	-1.284	-
CGI_10017721	probable phospholipid-transporting ATPase IIB isoform X2	-	-	-	-	-1.305	-
CGI_10028509	F-box-like WD repeat-containing TBL1XR1	-	-	-	-	-1.310	-
CGI_10008889	Usher syndrome type-1G -like	-	-	-	-	-1.320	-
CGI_10026539	phosphoacetylglucosamine mutase	-	-	-	-1.605	-1.320	-
CGI_10009117	FAM228B-like isoform X1 [Crassostrea gigas]	-	-	-	-	-1.352	-

CGI_10025179	RNA-binding 24-A-like isoform X1 [Octopus bimaculoides]	-	-	-	-	-1.357	-
CGI_10015855	rab effector -like isoform X2	-	-	-	-	-1.372	-
CGI_10008472	cytospin-A-like isoform X2 [Lingula anatina]	-	-	-	-	-1.375	-
CGI_10017381	multiple epidermal growth factor-like domains 6	-	-	-	-	-1.377	-
CGI_10000886	Multidrug resistance partial	-	-	-	-	-1.397	-
CGI_10015411	protocadherin-15 isoform X2 [Cimex lectularius]	-	-	-	-	-1.409	-
CGI_10025850	procollagen-lysine,2-oxoglutarate 5-dioxygenase 1-like isoform X2	-	-	-	-	-1.413	-
CGI_10007146	histone acetyltransferase KAT7 isoform X1	-	-	-	-	-1.416	-
CGI_10011708	guanine nucleotide-binding G(q) subunit alpha	-	-	-	-1.228	-1.424	-
CGI_10021851	Splicing factor U2AF 50 kDa subunit	-	-	-	-	-1.430	-
CGI_10021232	FAM49B-like isoform X1 [Crassostrea gigas]	-	-	-	-	-1.443	-
CGI_10022438	pre-mRNA-splicing factor RBM22-like	-	-	-	-	-1.444	-
CGI_10017399	uncharacterized	-	-	-	-	-1.445	-
CGI_10018771	E3 ubiquitin- ligase DZIP3-like isoform X1 [Acropora digitifera]	-	-	-	-	-1.456	-
CGI_10015333	WD repeat-containing 19-like	-	-	-	-	-1.456	-
CGI_10014997	transmembrane 132E-like	-	-	-	-	-1.461	-
CGI_10002432	hypothetical protein CGI_10002432	-	-	-	-	-1.469	-
CGI_10021963	patched homolog 1-like	-	-	-	-	-1.476	-
CGI_10010584	intersectin-1 [Halyomorpha halys]	-	-	-	-	-1.496	-
CGI_10008219	hypothetical protein CGI_10008219	-	-	-	-	-1.501	-
CGI_10007090	cilia- and flagella-associated 46-like	-	-	-	-	-1.502	-
CGI_10006390	neurotrimin-like [Crassostrea gigas]	-	-	-	-	-1.520	-
CGI_10012303	acetylcholine receptor subunit beta-like 1 isoform X1	-	-	-	-	-1.523	-
CGI_10028434	gem-associated 5-like	-	-	-	-	-1.529	-
CGI_10026046	WD repeat domain phosphoinositide-interacting 3-like	-	-	-	-	-1.531	-
CGI_10019925	Regulator of G- signaling 22	-	-	-	-	-1.536	-
CGI_10013413	allatostatin-A receptor-like isoform X1 [Crassostrea gigas]	-	-	-	-	-1.546	-
CGI_10018849	monocarboxylate transporter 9-like [Octopus bimaculoides]	-	-	-	-	-1.548	-
CGI_10016215	leucine-rich repeat and fibronectin type III domain-containing 1 [Lingula anatina]	-	-	-	-	-1.553	-
CGI_10008007	protocadherin-9-like isoform X1 [Crassostrea gigas]	-	-	-	-	-1.561	-
CGI_10009224	FTS and Hook-interacting -like isoform X1	-	-	-	-	-1.572	-
CGI_10009718	G- coupled receptor GRL101-like	-	-	-	-	-1.580	-
CGI_10025690	leucine-rich repeat-containing 23	-	-	-	-	-1.601	-
CGI_10009113	Frizzled-4	-	-	-	-	-1.610	-
CGI_10017261	transient receptor potential cation channel subfamily M member 2-like isoform X2 [Crassostrea gigas]	-	-	-	-1.671	-1.613	-
CGI_10009508	calpain-5 isoform X2 [Aquila chrysaetos canadensis]	-	-	-	-	-1.639	-
CGI_10019923	hypothetical protein CGI_10019923	-	-	-	-1.767	-1.647	-
CGI_10007632	trichohyalin-like isoform X1 [Biomphalaria glabrata]	-	-	-	-	-1.650	-
CGI_10006264	zinc finger and BTB domain-containing 5-like [Crassostrea gigas]	-	-	-	-	-1.655	-
CGI_10005168	sterile alpha motif domain-containing 9-like	-	-	-	-	-1.661	-
CGI_10017321	transmembrane 231-like	-	-	-	-	-1.667	-
CGI_10007407	Low-density lipo receptor-related partial	-	-	-	-	-1.673	-
CGI_10003173	GPI mannosyltransferase 3-like	-	-	-	-	-1.683	-
CGI_10011852	deleted in malignant brain tumors 1 -like	-	-	-	-	-1.687	-
CGI_10002311	Transaldolase	-	-	-	-	-1.688	-

CGI_10016527	Multidrug resistance-associated 7	-	-	-	-	-1.702	-
CGI_10017319	hypothetical protein CGI_10017319	-	-	-	-	-1.713	-
CGI_10008957	Sodium myo-inositol cotransporter partial	-	-	-	-	-1.720	-
CGI_10010716	HHIP 2	-	-	-	-	-1.725	-
CGI_10027862	transcriptional repressor YY1-like isoform X2	-	-	-	-	-1.729	-
CGI_10025600	neuronal acetylcholine receptor subunit alpha-3-like	-	-	-	-	-1.729	-
CGI_10021676	RNA binding fox-1 homolog 2-like isoform X7 [Biomphalaria glabrata]	-	-	-	-	-1.739	-
CGI_10011932	Calcitonin receptor	-	-	-	-	-1.755	-
CGI_10024580	very-long-chain enoyl- reductase-like	-	-	-	-	-1.757	-
CGI_10010634	N-alpha-acetyltransferase 20-like isoform X2 [Aplysia californica]	-	-	-	-	-1.761	-
CGI_10023646	PREDICTED: uncharacterized protein LOC105339977 [Crassostrea gigas]	-	-	-	-	-1.769	-
CGI_10021830	exocyst complex component 7 isoform X6	-	-	-	-	-1.785	-
CGI_10002689	gelsolin 2 [Crassostrea gigas]	-	-	-	-	-1.792	-
CGI_10016526	vasohibin-2-like isoform X1	-	-	-	-	-1.796	-
CGI_10028323	epidermal growth factor 8 isoform X2	-	-	-	-	-1.812	-
CGI_10020892	location of vulva defective 1-like	-	-	-	-	-1.814	-
CGI_10026002	spinster homolog 1-like [Callorhinchus milii]	-	-	-	-	-1.829	-
CGI_10023147	cytoplasmic tRNA 2-thiolation 1-like	-	-	-	-	-1.838	-
CGI_10013523	germ cell-less -like partial	-	-	-	-	-1.842	-
CGI_10013757	neuronal cell adhesion molecule-like isoform X2	-	-	-	-	-1.847	-
CGI_10028205	heparan sulfate glucosamine 3-O-sulfotransferase 5-like [Crassostrea gigas]	-	-	-	-	-1.847	-
CGI_10019525	WD repeat-containing 66-like	-	-	-	-	-1.848	-
CGI_10002030	enhancer of polycomb homolog 1-like	-	-	-	-	-1.858	-
CGI_10010334	Kyphoscoliosis peptidase [Crassostrea gigas]	-	-	-	-	-1.858	-
CGI_10018495	golgin subfamily A member 7-like	-	-	-	-	-1.883	-
CGI_10022702	centrosomal of 63 kDa-like isoform X5 [Crassostrea gigas]	-	-	-	-	-1.884	-
CGI_10024476	UDP-D-xylose:L-fucose alpha-1,3-D-xylosyltransferase 1-like isoform X2	-	-	-	-	-1.888	-
CGI_10005661	ankyrin repeat domain-containing 29-like	-	-	-	-	-1.889	-
CGI_10020867	116 kDa U5 small nuclear ribonucleo component	-	-	-	-	-1.896	-
CGI_10022560	histone-lysine N-methyltransferase 2D-like isoform X3	-	-	-	-	-1.903	-
CGI_10023417	brain-specific angiogenesis inhibitor 1-like	-	-	-	-	-1.907	-
CGI_10011691	phosphorylated CTD-interacting factor 1-like	-	-	-	-	-1.915	-
CGI_10019123	sodium leak channel non-selective -like	-	-	-	-	-1.916	-
CGI_10025205	angiopoietin-1 receptor-like	-	-	-	-	-1.945	-
CGI_10015994	hypothetical protein CGI_10015994	-	-	-	-	-1.956	-
CGI_10024732	Tripartite motif-containing 2	-	-	-	-	-1.960	-
CGI_10028804	tincar-like isoform X1 [Aplysia californica]	-	-	-	-	-1.967	-
CGI_10013965	Cytosolic endo-beta-N-acetylglucosaminidase	-	-	-	-	-2.006	-
CGI_10020780	p21-activated kinase-interacting 1	-	-	-	-	-2.015	-
CGI_10017928	hypothetical protein CGI_10017928	-	-	-	-	-2.016	-
CGI_10009731	cullin-4A-like	-	-	-	-	-2.029	-
CGI_10016633	leucine-rich repeat-containing 74B-like [Crassostrea gigas]	-	-	-	-	-2.037	-
CGI_10011138	Alpha-2C adrenergic receptor	-	-	-	-	-2.051	-
CGI_10011202	NC domain [Yersinia frederiksenii]	-	-	-	-	-2.052	-
CGI_10014869	PDF receptor	-	-	-	-	-2.053	-

CGI_10015549	glutamate receptor subunit 6 [Aplysia californica]	-	-	-	-	-2.061	-
CGI_10000209	hypothetical protein CGI_10000209	-	-	-	-2.354	-2.065	-
CGI_10018886	Partitioning defective 6 beta [Crassostrea gigas]	-	-	-	-	-2.072	-
CGI_10023779	beta-1,3-galactosyltransferase 1-like	-	-	-	-	-2.073	-
CGI_10003264	ADAM 17-like protease	-	-	-	-	-2.091	-
CGI_10018781	low-density lipo receptor-related 4-like	-	-	-	-	-2.109	-
CGI_10004693	Mitochondrial intermediate peptidase	-	-	-	-	-2.112	-
CGI_10002297	heparan-sulfate 6-O-sulfotransferase 2 [Stomoxys calcitrans]	-	-	-	-	-2.113	-
CGI_10026952	amiloride-sensitive sodium channel subunit alpha-like	-	-	-	-	-2.128	-
CGI_10023529	vang 2	-	-	-	-	-2.133	-
CGI_10018627	aquaporin-8-like isoform X1	-	-	-	-	-2.146	-
CGI_10018905	hypothetical protein CGI_10018905	-	-	-	-	-2.149	-
CGI_10015025	centrosomal of 135 kDa	-	-	-	-1.543	-2.149	-
CGI_10022146	transmembrane 201-like	-	-	-	-	-2.150	-
CGI_10025027	BTB POZ domain-containing 6-like [Crassostrea gigas]	-	-	-	-	-2.153	-
CGI_10012447	deleted in malignant brain tumors 1 -like	-	-	-	-	-2.157	-
CGI_10019146	kelch 36	-	-	-	-	-2.159	-
CGI_10021383	hypothetical protein CGI_10021383	-	-	-	-	-2.175	-
CGI_10009759	E3 ubiquitin- ligase XIAP [Cavia porcellus]	-	-	-	-	-2.175	-
CGI_10028361	Neuronal acetylcholine receptor subunit beta-3	-	-	-	-	-2.177	-
CGI_10022688	protocadherin Fat 4-like	-	-	-	-	-2.180	-
CGI_10022192	melanocortin receptor 4-like [Crassostrea gigas]	-	-	-	-	-2.185	-
CGI_10010582	synaptic vesicle glyco 2B-like	-	-	-	-	-2.185	-
CGI_10027401	F-box only 30	-	-	-	-	-2.186	-
CGI_10008685	F-box WD repeat-containing 7	-	-	-	-	-2.189	-
CGI_10017531	radial spoke head 14 homolog	-	-	-	-	-2.190	-
CGI_10000537	Exostosin-like 3	-	-	-	-	-2.196	-
CGI_10014478	thioredoxin domain-containing 15-like	-	-	-	-	-2.219	-
CGI_10023528	hypothetical protein CGI_10023528	-	-	-	-	-2.223	-
CGI_10015196	hypothetical protein CGI_10015196	-	-	-	-	-2.228	-
CGI_10009327	Thioredoxin domain-containing 5	-	-	-	-	-2.231	-
CGI_10001130	glyoxylate hydroxypyruvate reductase A-like isoform X3 [Cephus cinctus]	-	-	-	-	-2.236	-
CGI_10018264	histidine methyltransferase 1 homolog	-	-	-	-	-2.242	-
CGI_10003363	adrenodoxin-like isoform X1	-	-	-	-	-2.249	-
CGI_10024280	ARS-binding factor 1-like	-	-	-	-	-2.250	-
CGI_10002464	Serine threonine- kinase partial	-	-	-	-	-2.266	-
CGI_10028447	allene oxide synthase-lipoxygenase -like	-	-	-	-	-2.280	-
CGI_10013194	Low-density lipo receptor-related 5	-	-	-	-	-2.294	-
CGI_10024979	hypothetical protein CGI_10024979	-	-	-	-	-2.296	-
CGI_10005865	PREDICTED: uncharacterized protein LOC105334098 [Crassostrea gigas]	-	-	-	-	-2.302	-
CGI_10013627	PREDICTED: uncharacterized protein LOC105325888 [Crassostrea gigas]	-	-	-	-	-2.333	-
CGI_10019016	adenylate kinase isoenzyme 5-like	-	-	-	-	-2.342	-
CGI_10006657	transmembrane INAFM2	-	-	-	-	-2.342	-
CGI_10024473	3-mercaptopyruvate sulfurtransferase [Pantoea stewartii]	-	-	-	-	-2.342	-
CGI_10023795	derlin-1-like [Crassostrea gigas]	-	-	-	-	-2.343	-

CGI_10009131	ras and EF-hand domain-containing homolog [Lingula anatina]	-	-	-	-	-2.344	-
CGI_10020885	L-ascorbate oxidase	-	-	-	-	-2.355	-
CGI_10000340	solute carrier family 49 member 4	-	-	-	-	-2.356	-
CGI_10020976	Elongation of very long chain fatty acids 4	-	-	-	-	-2.359	-
CGI_10003593	calpain-2 catalytic subunit-like [Aplysia californica]	-	-	-	-	-2.362	-
CGI_10017595	sodium-coupled monocarboxylate transporter 1-like	-	-	-	-	-2.369	-
CGI_10003064	Dehydrogenase reductase SDR family member on chromosome X	-	-	-	-	-2.370	-
CGI_10016921	histone-lysine N-methyltransferase EHMT1	-	-	-	-	-2.372	-
CGI_10020514	patched domain-containing 3-like	-	-	-	-	-2.386	-
CGI_10023870	lipid phosphate phosphohydrolase 3-like [Crassostrea gigas]	-	-	-	-	-2.392	-
CGI_10004276	sodium-coupled monocarboxylate transporter 1-like	-	-	-	-	-2.393	-
CGI_10003966	MAM and LDL-receptor class A domain-containing 1-like	-	-	-	-	-2.399	-
CGI_10013592	CCAAT enhancer-binding zeta	-	-	-	-	-2.403	-
CGI_10008280	neuronal acetylcholine receptor subunit alpha-3-like	-	-	-	-	-2.403	-
CGI_10004345	Tripartite motif-containing 45	-	-	-	-	-2.419	-
CGI_10010850	hypothetical protein CGI_10010850	-	-	-	-	-2.422	-
CGI_10005469	nucleoredoxin 2	-	-	-	-	-2.435	-
CGI_10019330	S1 RNA-binding domain-containing 1	-	-	-	-	-2.454	-
CGI_10010757	Minor histocompatibility antigen H13	-	-	-	-	-2.470	-
CGI_10025921	hypothetical protein CGI_10025921	-	-	-	-	-2.500	-
CGI_10006379	Tripartite motif-containing 3	-	-	-	-	-2.510	-
CGI_10018374	Tripartite motif-containing 45	-	-	-	-	-2.527	-
CGI_10013252	serine threonine- kinase roco5	-	-	-	-	-2.531	-
CGI_10008102	hypothetical protein CGI_10008102	-	-	-	-	-2.532	-
CGI_10013251	ankyrin-3-like isoform X2 [Crassostrea gigas]	-	-	-	-	-2.558	-
CGI_10019664	alpha-mannosidase partial	-	-	-	-	-2.564	-
CGI_10010586	parkin coregulated gene homolog	-	-	-	-	-2.592	-
CGI_10025028	Survival of motor neuron-related-splicing factor 30	-	-	-	-	-2.592	-
CGI_10001170	pyruvate dehydrogenase E1 component subunit mitochondrial	-	-	-	-	-2.597	-
CGI_10020809	complement C1q 4	-	-	-	-	-2.598	-
CGI_10004201	FAM69C-like [Lingula anatina]	-	-	-	-	-2.616	-
CGI_10001356	transformation transcription domain-associated -like	-	-	-	-	-2.650	-
CGI_10006010	zinc finger ZFAT-like	-	-	-	-	-2.680	-
CGI_10028549	D-aspartate oxidase-like	-	-	-	-	-2.681	-
CGI_10003643	C-type mannose receptor 2	-	-	-	-	-2.689	-
CGI_10008295	bolA 2	-	-	-	-	-2.703	-
CGI_10018453	lipid droplet-associated hydrolase-like	-	-	-	-	-2.727	-
CGI_10008404	uncharacterized	-	-	-	-	-2.759	-
CGI_10024621	probable G- coupled receptor 158	-	-	-	-	-2.835	-
CGI_10007166	hypothetical protein CGI_10007166	-	-	-	-2.769	-2.842	-
CGI_10000936	estradiol 17-beta-dehydrogenase 8-like isoform X1 [Crassostrea gigas]	-	-	-	-	-2.845	-
CGI_10012196	DPH3 homolog	-	-	-	-	-2.866	-
CGI_10015601	Tubulin polymerization-promoting family member 2	-	-	-	-	-2.969	-
CGI_10005389	pyroglutamylated RFamide peptide receptor-like	-	-	-	-	-3.010	-
CGI_10022937	dual specificity phosphatase CDC14A-like	-	-	-	-	-3.094	-

CGI_10008714	WW domain-containing oxidoreductase	-	-	-	-	-3.164	-
CGI_10010235	heparan sulfate glucosamine 3-O-sulfotransferase 6-like	-	-	-	-	-3.297	-
CGI_10021777	Heat shock 70 kDa 12A	-	-	-	-	-3.371	-
CGI_10020590	Low-density lipo receptor-related 2	-	-	-	-	-3.436	-
CGI_10003809	E3 ubiquitin- ligase Midline-1 isoform X1 [Anser cygnoides domesticus]	-	-	-	-	-3.497	-
CGI_10007660	inner nuclear membrane Man1	-	-	-	-	-3.949	-
CGI_10016473	arrestin domain-containing 2-like [Biomphalaria glabrata]	-	-	-	-	-4.110	-
CGI_10004319	Tripartite motif-containing 2	-	-	-	-	6.011	5.336
CGI_10024054	PREDICTED: uncharacterized protein LOC105329159 [Crassostrea gigas]	-	-	-	-	5.593	5.301
CGI_10004922	IL17-5 [Crassostrea gigas]	-	-	-	-	5.309	5.188
CGI_10012722	myeloid differentiation primary response 88-like [Crassostrea gigas]	-	-	-	-	4.690	4.993
CGI_10021916	Uncharacterized protein C3orf59	-	-	-	1.801	4.363	4.409
CGI_10013925	cis-aconitate decarboxylase	-	-	-	-	3.449	4.319
CGI_10005393	Inhibitor of apoptosis	-	-	-	-	4.076	4.301
CGI_10028244	Tripartite motif-containing 2	-	-	-	1.796	4.382	4.275
CGI_10006118	Phosphatidylinositol-glycan-specific phospholipase D	-	-	-	-	3.022	4.239
CGI_10028360	signal CUB and EGF-like domain-containing 1	-	-	-	-	3.301	4.197
CGI_10025511	T9SS C-terminal target domain-containing	-	-	-	2.388	4.003	4.116
CGI_10016248	Group XV phospholipase A2	-	-	-	-	3.925	4.098
CGI_10000502	huntingtin-interacting 1-related - partial	-	-	-	1.882	3.887	4.072
CGI_10008241	C-type lectin domain family member A-like	-	-	-	-	2.308	4.070
CGI_10021170	Interferon regulatory factor 2	-	-	-	3.160	3.935	4.059
CGI_10004601	MAM and LDL-receptor class A domain-containing 1-like	-	-	-	2.235	3.609	4.026
CGI_10013924	phytanoyl- dioxygenase domain-containing 1-like	-	-	-	-	3.285	4.008
CGI_10000441	Krueppel-like factor 5 [Crassostrea gigas]	-	-	-	2.363	4.221	3.981
CGI_10024233	hemagglutinin amebocyte aggregation factor-like	-	-	-	-	2.397	3.898
CGI_10019228	cartilage matrix -like	-	-	-	-	4.411	3.888
CGI_10011447	hypothetical protein CGI_10011447	-	-	-	-	2.481	3.787
CGI_10012593	hypothetical protein CGI_10012593	-	2.905	-	-	4.826	3.722
CGI_10010240	Chorion peroxidase	-	-	-	-	-	3.668
CGI_10002396	Basic leucine zipper transcriptional factor ATF-like 3	-	-	-	-	2.970	3.664
CGI_10018753	deleted in malignant brain tumors 1 -like	-	-	-	-	2.507	3.646
CGI_10020743	alternative mitochondrial-like	-	-	-	2.879	3.189	3.598
CGI_10003321	mucin-5AC	-	-	-	-	3.645	3.530
CGI_10000144	helicase with zinc finger domain 2-like isoform X1 [Crassostrea gigas]	-	-	-	-	3.262	3.492
CGI_10026316	inhibitor of apoptosis	-	-	-	-	3.254	3.486
CGI_10001936	L-threonine 3- mitochondrial-like	-	-	-	1.764	3.303	3.483
CGI_10008621	Multiple epidermal growth factor-like domains 6	-	-	-	-	-	3.479
CGI_10017734	Ankyrin repeat domain-containing 50	-	-	-	-	2.990	3.473
CGI_10000080	Cytochrome b5	-	-	-	2.744	3.957	3.470
CGI_10007793	tyrosinase tyr-3	-	-	-	2.240	-	3.454
CGI_10028807	Fas ligand	-	-	-	-	4.022	3.440
CGI_10009106	hypothetical protein CGI_10009106	-	-	-	2.542	3.346	3.436
CGI_10002879	myb X isoform X1 [Crassostrea gigas]	-	-	-	2.400	3.849	3.432
CGI_10014565	mannose-P-dolichol utilization defect 1 -like	-	-	-	-	3.375	3.402

CGI_10015407	homeobox aristaless	-	-	-	-	3.696	3.356
CGI_10010438	huntingtin-interacting 1-related - partial	-	-	-	-	3.240	3.352
CGI_10028285	kielin chordin	-	-	-	-	3.399	3.325
CGI_10018986	hypothetical protein CGI_10018986	-	-	-	-	2.686	3.308
CGI_10001123	Chorion peroxidase	-	-	-	-	-	3.293
CGI_10018396	radical S-adenosyl methionine domain-containing 2	-	-	-	-	2.745	3.285
CGI_10019737	condensation domain [Leptospira fainei]	-	-	-	-	3.543	3.272
CGI_10024808	PREDICTED: uncharacterized protein LOC105331509 [Crassostrea gigas]	-	-	-	-	2.335	3.260
CGI_10005872		-	-	-	-	2.813	3.185
CGI_10015342	hypothetical protein CGI_10015342	-	-	-	2.529	2.483	3.158
CGI_10008727	nuclear 1	-	-	-	-	3.037	3.154
CGI_10017744	Leucine-rich repeats and immunoglobulin-like domains 3	-	-	-	-	3.603	3.149
CGI_10027441	helicase with zinc finger domain 2-like	-	-	-	1.350	2.945	3.144
CGI_10016254	Core-binding factor subunit beta	-	-	-	-	2.968	3.136
CGI_10004710		-	-	-	-	2.515	3.116
CGI_10005824	hypothetical protein CGI_10005824	-	-	-	-	2.349	3.086
CGI_10003823	COMM domain-containing 3	-	-	-	-	-	3.064
CGI_10013274	hypothetical protein CGI_10013274	-	-	-	-	2.979	3.061
CGI_10007670	PREDICTED: uncharacterized protein LOC105346062	-	-	-	2.577	2.257	3.026
CGI_10022263	proteoglycan 4-like [Crassostrea gigas]	-	-	2.440	3.172	3.345	3.024
CGI_10014497	von Willebrand factor type EGF and pentraxin domain-containing 1-like isoform X2 [Crassostrea gigas]	-	-	-	-	-	3.009
CGI_10006153	hypothetical protein CGI_10006153	-	-	-	-	2.697	3.003
CGI_10016403	hypothetical protein CGI_10016403	-	-	-	2.301	3.444	3.001
CGI_10003485	SLIT-ROBO Rho GTPase-activating 1-like	-	-	-	-	2.270	2.970
CGI_10007669	hypothetical protein CGI_10007669	-	-	-	-	-	2.965
CGI_10020900	hypothetical protein CGI_10020900	-	-	-	-	-	2.963
CGI_10019595	chitin synthase	-	-	-	2.507	3.021	2.948
CGI_10025307	hypothetical protein CGI_10025307	-	-	-	-	2.447	2.944
CGI_10014170	Nacrein F	-	-	-	-	-	2.923
CGI_10002657	hypothetical protein CGI_10002657	-	-	-	-	2.743	2.899
CGI_10000756	hypothetical protein CGI_10000756	-	-	-	-	-	2.890
CGI_10026674	DBH-like monooxygenase 1 [Crassostrea gigas]	-	-	-	-	-	2.886
CGI_10000167	astacin-like metalloprotease toxin 1	-	-	-	-	3.092	2.879
CGI_10012457	hypothetical protein CGI_10012457	-	-	1.625	2.270	3.073	2.847
CGI_10027672	fibrillin-2-like [Crassostrea gigas]	-	-	-	2.170	3.075	2.829
CGI_10017694	purine nucleoside phosphorylase-like	-	-	-	-	3.288	2.828
CGI_10009590	A-agglutinin anchorage subunit-like	-	-	2.075	2.334	2.082	2.818
CGI_10000860	hypothetical protein CGI_10000860	-	-	-	-	-	2.817
CGI_10007259	universal stress A [Crassostrea gigas]	-	-	1.351	2.034	2.188	2.802
CGI_10014448	transcription factor ETV7-like isoform X1 [Crassostrea gigas]	-	-	-	-	3.006	2.782
CGI_10005873	polyubiquitin 8-like [Acropora digitifera]	-	-	-	-	2.572	2.782
CGI_10014608	PREDICTED: uncharacterized protein LOC105337279 [Crassostrea gigas]	-	-	-	-	3.132	2.777
CGI_10009137	muscle M-line assembly unc-89-like	-	-	-	-	-	2.761
CGI_10017352	Tripartite motif-containing 2	-	-	-	2.023	3.779	2.757
CGI_10012786	tumor necrosis factor receptor superfamily member 27-like [Crassostrea gigas]	-	-	-	-	3.204	2.755

CGI_10002038	Mucosa-associated lymphoid tissue lymphoma translocation 1	-	-	-	-	2.604	2.734
CGI_10011916	tyrosinase tyr-3	-	-	-	-	2.166	2.732
CGI_10027442	helicase with zinc finger domain 2-like isoform X1 [Crassostrea gigas]	-	-	-	1.448	2.777	2.728
CGI_10002015	Kinesin heavy chain	-	-	-	-	3.811	2.713
CGI_10024162	LPS-induced TNF-alpha factor	-	-	2.097	2.459	3.458	2.708
CGI_10010566	Importin subunit alpha-2	-	-	-	-	3.116	2.702
CGI_10007657	solute carrier family 23 member 2-like [Crassostrea gigas]	-	-	-	-	3.159	2.700
CGI_10022693	Cysteine dioxygenase type 1	-	-	-	-	2.266	2.690
CGI_10027395	78 kDa glucose-regulated	-	-	-	-	-	2.670
CGI_10019164	FMRFamide receptor-like	-	-	-	-	2.271	2.662
CGI_10024893	PREDICTED: mucin-5AC-like	-	-	2.089	2.135	2.466	2.650
CGI_10018662	hypothetical protein CGI_10018662	-	-	-	2.441	2.625	2.645
CGI_10028806		-	-	-	-	2.725	2.644
CGI_10013941	hypothetical protein CGI_10013941	-	-	-	-	1.921	2.627
CGI_10017559	parathyroid hormone parathyroid hormone-related peptide receptor-like	-	-	-	1.864	3.520	2.624
CGI_10006899	Multiple epidermal growth factor-like domains 10	-	-	-	-	2.939	2.623
CGI_10002570	glutathione-specific gamma-glutamylcyclotransferase 1-like	-	-	-	-	-	2.621
CGI_10022061	hypothetical protein CGI_10022061	-	-	-	-	2.906	2.609
CGI_10026972	MFS-type transporter SLC18B1-like	-	-	-	-	-	2.597
CGI_10001622	hypothetical protein CGI_10001622	-	-	-	2.155	2.730	2.596
CGI_10004256	secretin receptor-like	-	-	-	-	-	2.595
CGI_10027370	nascent polypeptide-associated complex subunit muscle-specific form-like	-	-	-	2.507	2.743	2.588
CGI_10027091	hypothetical protein CGI_10027091	-	-	-	2.477	2.488	2.587
CGI_10014971	guanine nucleotide-binding G(s) subunit alpha-like	-	-	-	-	2.383	2.579
CGI_10019232	temptin-like	-	-	-	-	-	2.579
CGI_10012882	Transmembrane 2	-	-	-	-	2.403	2.576
CGI_10020787	PREDICTED: uncharacterized protein LOC105337946 [Crassostrea gigas]	-	-	-	1.751	2.949	2.574
CGI_10007753	tyrosinase tyr-3	-	-	-	-	-	2.572
CGI_10013239	Zonadhesin	-	-	-	2.011	1.978	2.561
CGI_10016723	hypothetical protein CGI_10016723	-	-	-	2.331	2.139	2.557
CGI_10015430	N-acetylated-alpha-linked acidic dipeptidase	-	-	-	1.793	3.224	2.551
CGI_10022826	Dynactin subunit 1	-	-	-	1.894	2.072	2.542
CGI_10018157	tyrosine- phosphatase non-receptor type 23-like	-	-	-	2.058	2.603	2.536
CGI_10008231	transmembrane 145 isoform X1	-	-	-	-	-	2.535
CGI_10018988	kielin chordin	-	-	-	2.750	2.708	2.534
CGI_10021010	hypothetical protein CGI_10021010	-	-	-	-	-	2.533
CGI_10021844	AGAP009899-PA [Anopheles gambiae PEST]	-	-	-	1.645	2.963	2.527
CGI_10007260	PREDICTED: colipase-like	-	-	-	2.062	1.657	2.524
CGI_10004864	Cysteine-rich secretory Mr30	-	-	-	-	2.201	2.522
CGI_10027842	Solute carrier family facilitated glucose transporter member 1	-	-	-	-	2.840	2.511
CGI_10008415	chromobox 8	-	-	-	-	2.443	2.508
CGI_10008804	PREDICTED: uncharacterized protein LOC105336910 isoform X1 [Crassostrea gigas]	-	-	-	-	2.447	2.507
CGI_10005029	Caprin-2 [Crassostrea gigas]	-	-	-	-	2.388	2.504
CGI_10010526	temptin-like	-	-	-	-	2.032	2.494
CGI_10012379	Deleted in malignant brain tumors 1	-	-	-	1.944	2.398	2.492

CGI_10009318	tyrosinase tyr-3	-	-	-	1.835	1.720	2.490
CGI_10013879	vesicular glutamate transporter 2	-	-	-	-	3.043	2.487
CGI_10003408	sialomucin core 24-like isoform X1	-	-	1.425	1.853	2.450	2.480
CGI_10021423	Collagen alpha-6(VI) chain	-	-	-	-	2.596	2.476
CGI_10007643	S-adenosylmethionine synthase isoform type-2	-	-	-	-	2.186	2.474
CGI_10015931	ADP-ribosylation factor 1	-	-	-	-	2.925	2.474
CGI_10014403	caspase-3-like [Crassostrea gigas]	-	-	-	1.556	2.092	2.469
CGI_10014865	hypothetical protein CGI_10014865	-	-	-	-	2.223	2.465
CGI_10011702	endoglucanase 13-like	-	-	-	-	-	2.465
CGI_10023336	mediator of RNA polymerase II transcription subunit 30 isoform X2	-	-	-	-	2.323	2.460
CGI_10012305	PREDICTED: uncharacterized protein LOC105344292 [Crassostrea gigas]	-	-	-	-	2.013	2.456
CGI_10004100	cell wall DAN4-like	-	-	-	-	-	2.453
CGI_10027377	protocadherin Fat 4-like	-	-	-	-	3.387	2.452
CGI_10000334	Chaperone dnaJ	-	-	-	-	2.663	2.446
CGI_10026671	sulfite oxidase-like	-	-	-	-	1.982	2.440
CGI_10004793	hypothetical protein CGI_10004793	-	-	-	-	2.047	2.433
CGI_10022976	hypothetical protein CGI_10022976	-	-	-	-	2.417	2.432
CGI_10004758	integumentary mucin -like	-	-	1.487	1.954	2.146	2.431
CGI_10007323	hypothetical protein CGI_10007323	-	-	-	1.472	2.871	2.428
CGI_10010445	chitin deacetylase - partial	-	-	-	1.863	2.351	2.427
CGI_10003083	probable ATP-dependent RNA helicase DHX58	-	-	-	2.066	-	2.425
CGI_10002355	hypothetical protein CGI_10002355	-	-	-	-	-	2.420
CGI_10019948	GTPase IMAP family member 7	-	-	-	2.586	-	2.417
CGI_10026443	TPR and ankyrin repeat-containing partial	-	-	-	1.219	3.532	2.413
CGI_10016148	hemicentin-2-like isoform X2 [Crassostrea gigas]	-	-	-	1.609	2.287	2.413
CGI_10028785	Tob1-like [Biomphalaria glabrata]	-	-	-	1.437	2.724	2.412
CGI_10006414	PREDICTED: uncharacterized protein DDB_G0283357-like isoform X1	-	-	-	-	2.948	2.408
CGI_10021734	chorion peroxidase-like	-	-	-	-	-	2.405
CGI_10007019	salivary glue Sgs-3-like	-	-	-	2.168	-	2.393
CGI_10018278	Beta-lactamase [Crassostrea gigas]	-	-	-	-	-	2.392
CGI_10004837	inhibitor of nuclear factor-kappaB	-	-	-	-	-	2.389
CGI_10001712	paramyosin-like isoform X1 [Crassostrea gigas]	-	-	-	-	2.184	2.379
CGI_10021136	Toll-like receptor 1	-	-	-	2.137	2.678	2.378
CGI_10013473	receptor-type tyrosine- phosphatase T-like	-	-	-	-	-	2.378
CGI_10018589	hypothetical protein CGI_10018589	-	-	-	-	-	2.378
CGI_10005518	transcriptional regulator Erg- partial	-	-	-	2.262	1.855	2.377
CGI_10000338	inhibitor of apoptosis	-	-	-	-	1.853	2.374
CGI_10017841	Excitatory amino acid transporter partial	-	-	-	-	2.952	2.373
CGI_10020195	glycogen-binding subunit 76A-like	-	-	-	-	2.016	2.371
CGI_10005650	ras-related Rab-11A-like	-	-	-	-	2.547	2.367
CGI_10024191	organic cation transporter -like isoform X1 [Crassostrea gigas]	-	-	-	-	-	2.365
CGI_10003270	interferon regulatory factor 8	-	-	-	-	2.152	2.363
CGI_10027957	ras-related GTP-binding A	-	-	-	-	-	2.362
CGI_10006931	peripheral myelin 22-like [Crassostrea gigas]	-	-	-	-	2.343	2.357
CGI_10026304	CCAAT enhancer binding	-	-	-	-	1.524	2.353

CGI_10016278	circumsporozoite -like	-	-	-	-	-	2.352
CGI_10016928	probable phytanoyl- dioxygenase	-	-	-	2.060	2.440	2.350
CGI_10018491	apolipo D-like	-	-	-	-	2.492	2.350
CGI_10020901	PREDICTED: uncharacterized protein LOC105347142 [Crassostrea gigas]	-	-	-	-	-	2.347
CGI_10028272	myeloperoxidase-like [Crassostrea gigas]	-	-	-	-	-	2.346
CGI_10009981	sodium- and chloride-dependent glycine transporter 1-like	-	-	-	-	2.688	2.345
CGI_10027906	Brain-specific angiogenesis inhibitor 1	-	-	-	-	-	2.344
CGI_10014532	interferon-induced 44-like [Crassostrea gigas]	-	-	-	-	2.952	2.343
CGI_10027659	ATP-binding cassette sub-family A member	-	-	-	-	2.560	2.340
CGI_10026432	ependymin-related 1-like	-	-	-	-	1.825	2.340
CGI_10017528	peptidyl-prolyl cis-trans isomerase FKBP4	-	-	-	-	2.352	2.336
CGI_10025112	cartilage matrix -like	-	-	-	2.541	2.466	2.334
CGI_10013387	PREDICTED: uncharacterized protein LOC105336172 [Crassostrea gigas]	-	-	-	-	-	2.332
CGI_10008477	memory suppression [Aplysia californica]	-	-	-	-	2.983	2.322
CGI_10017272	hypothetical protein CGI_10017272	-	-	-	-	2.225	2.318
CGI_10018472	PREDICTED: uncharacterized protein LOC105331338	-	-	-	-	2.424	2.318
CGI_10024302	hypothetical protein CGI_10024302	-	-	-	-	2.210	2.314
CGI_10012725	Myeloid differentiation primary response 88	-	-	-	-	2.705	2.313
CGI_10028347	transmembrane GTPase Marf-like	-	-	-	-	-	2.311
CGI_10008352	GTPase IMAP family member 4-like	-	-	-	2.132	2.280	2.304
CGI_10012215	histone acetyltransferase [Aspergillus flavus NRRL3357]	-	-	-	-	-	2.302
CGI_10002408	hypothetical protein CGI_10002408	-	-	-	-	-	2.301
CGI_10016804	myosin light chain smooth muscle isoform X4 [Monodelphis domestica]	-	-	-	-	2.082	2.301
CGI_10027378	collagen alpha-3(VI) chain- partial	-	-	-	-	2.226	2.300
CGI_10027602	mediator of DNA damage checkpoint 1-like isoform X1	-	-	-	-	-	2.299
CGI_10008090	tripartite motif-containing 2-like	-	-	-	-	-	2.298
CGI_10011201	N-acetylglucosamine-6-phosphate deacetylase [Crassostrea gigas]	-	-	-	-	-	2.295
CGI_10017847	ADAM 17-like protease	-	-	-	-	1.802	2.293
CGI_10008880	kyphoscoliosis peptidase-like	-	-	-	-	-	2.291
CGI_10006051	flocculation FLO10-like [Crassostrea gigas]	-	-	1.682	2.134	2.179	2.288
CGI_10004783	hypothetical protein CGI_10004783	-	-	-	-	2.460	2.285
CGI_10006287	Cytochrome P450 1A1	-	-	-	-	-	2.281
CGI_10002316	integumentary mucin -like	-	-	-	2.036	2.375	2.272
CGI_10027911	sacsin-like	-	-	-	-	2.146	2.271
CGI_10023465	multiple epidermal growth factor-like domains 10	-	-	-	-	-	2.269
CGI_10015817	phosphatidylinositol 4,5-bisphosphate 3-kinase catalytic subunit alpha isoform-like	-	-	-	-	2.485	2.268
CGI_10019528	suppressor of cytokine signaling 2-like	-	-	-	-	-	2.268
CGI_10028754	girdin-like [Crassostrea gigas]	-	-	-	-	2.541	2.266
CGI_10006428	hypothetical protein CGI_10006428	-	-	-	-	-	2.262
CGI_10023581	Calcium-binding NCS-1	-	-	-	-	-	2.261
CGI_10004027	epithelial-stromal interaction 1-like	-	-	-	-	1.828	2.258
CGI_10025999	mucin-2-like isoform X1	-	-	-	2.099	2.406	2.256
CGI_10024290	PREDICTED: uncharacterized protein LOC105321549 [Crassostrea gigas]	-	-	-	1.364	2.602	2.255
CGI_10017857	inter-alpha-trypsin inhibitor heavy chain H3-like	-	-	-	1.367	1.677	2.254
CGI_10005871	hypothetical protein CGI_10005871	-	-	-	-	2.075	2.247

CGI_10002610	Plasminogen	-	-	-	-	-	2.244
CGI_10021954	ATP-dependent RNA helicase chloroplastic-like [Parasteatoda tepidariorum]	-	-	-	1.651	2.190	2.243
CGI_10018711	chitin binding beak 1	-	-	-	-	-	2.243
CGI_10024612	hypothetical protein CGI_10024612	-	-	-	-	-	2.243
CGI_10002646	hypothetical protein CGI_10002646	-	-	-	1.843	2.238	2.241
CGI_10014320	mitochondrial amidoxime-reducing component 1-like	-	-	-	1.743	1.774	2.239
CGI_10026703	BAG family molecular chaperone regulator 4	-	-	-	-	1.910	2.238
CGI_10009634	spidroin-1-like [Crassostrea gigas]	-	-	-	-	-	2.238
CGI_10005710	RNA-dependent RNA polymerase 1	-	-	-	1.549	2.459	2.235
CGI_10019404	coiled-coil domain-containing 124	-	-	-	1.737	2.077	2.231
CGI_10001942	DNA polymerase lambda	-	-	-	-	-	2.229
CGI_10017716	neurotrophin receptor-interacting factor 2-like [Crassostrea gigas]	-	-	-	-	1.956	2.226
CGI_10026417	hypothetical protein CGI_10026417	-	-	-	-	2.630	2.219
CGI_10017882	endochitinase A-like [Crassostrea gigas]	-	-	-	3.201	3.371	2.219
CGI_10018952	AP-1 complex subunit gamma-1-like isoform X2	-	-	-	-	1.838	2.217
CGI_10011040	Phosphoinositide 3-kinase adapter 1	-	-	-	-	-	2.214
CGI_10016056	poly [ADP-ribose] polymerase 14-like	-	-	-	-	-	2.208
CGI_10023767	CD109 antigen-like	-	-	-	1.434	2.708	2.207
CGI_10017345	beta-lactamase 4	-	-	-	-	-	2.206
CGI_10010381	probable serine threonine- kinase pats1	-	-	-	-	1.650	2.199
CGI_10022861	PREDICTED: uncharacterized protein LOC105345884 [Crassostrea gigas]	-	-	-	-	2.549	2.198
CGI_10002524	DBH-like monooxygenase 1 [Crassostrea gigas]	-	-	-	-	-	2.193
CGI_10012001	nuclear transcription factor Y subunit alpha isoform X4	-	-	-	-	2.510	2.192
CGI_10009762	baculoviral IAP repeat-containing 7-like [Octopus bimaculoides]	-	-	-	-	1.927	2.189
CGI_10009892	Lupus brain antigen 1	-	-	-	-	1.746	2.189
CGI_10014482	voltage-dependent calcium channel subunit alpha-2 delta-2-like [Lingula anatina]	-	-	-	-	2.274	2.188
CGI_10020071	hypothetical protein CGI_10020071	-	-	2.060	2.295	3.244	2.188
CGI_10027603	mediator of DNA damage checkpoint 1-like isoform X1	-	-	-	-	-	2.178
CGI_10013950	Glutamine synthetase	-	-	-	-	-	2.175
CGI_10027032		-	-	-	2.124	2.990	2.175
CGI_10004798	membrane-attack complex perforin domain-containing [Eimeria acervulina]	-	-	-	-	1.971	2.169
CGI_10024590	mantle 9 [Salpingoeca rosetta]	-	-	-	-	1.561	2.167
CGI_10018604	Autophagy 5	-	-	-	-	-	2.167
CGI_10027104	cysteine--tRNA cytoplasmic-like	-	-	-	-	2.025	2.163
CGI_10020091	F-box only 40-like	-	-	-	-	-	2.160
CGI_10005072	ADAM 17-like protease	-	-	-	1.872	2.319	2.155
CGI_10004843	Kyphoscoliosis peptidase	-	-	-	-	-	2.152
CGI_10028827	peptidoglycan recognition SC2 [Drosophila melanogaster]	-	-	-	-	2.200	2.152
CGI_10016230	hypothetical protein CGI_10016230	-	-	-	1.566	1.777	2.152
CGI_10016651	deleted in malignant brain tumors 1 -like	-	-	-	2.681	2.585	2.152
CGI_10003979	von Willebrand factor C domain-containing 2-like	-	-	2.850	-	-	2.149
CGI_10021863	Annexin A7	-	-	-	-	1.945	2.148
CGI_10001437	Multiple epidermal growth factor-like domains 10	-	-	-	-	2.137	2.144
CGI_10020129	glycine-rich domain-containing 2-like [Biomphalaria glabrata]	-	-	-	-	2.760	2.140
CGI_10009891	TPR and ankyrin repeat-containing 1-like	-	-	-	-	1.633	2.139

CGI_10023661	Kazal-type serine protease inhibitor domain-containing	-	-	-	-	-	2.136
CGI_10010580	glucose dehydrogenase [quinone]-like	-	-	-	-	-	2.132
CGI_10001823	DNA topoisomerase 2-binding 1	-	-	-	2.051	2.278	2.129
CGI_10016807		-	-	-	-	2.218	2.126
CGI_10026034	probable serine threonine- kinase pats1	-	-	-	-	1.995	2.124
CGI_10023083	PREDICTED: uncharacterized protein LOC105330591 [Crassostrea gigas]	-	-	-	1.558	2.260	2.123
CGI_10024748	flocculation FLO10-like [Crassostrea gigas]	-	-	-	-	-	2.123
CGI_10013528	heat shock 70 kDa 12A-like [Crassostrea gigas]	-	-	-	-	-	2.121
CGI_10026399	PREDICTED: uncharacterized protein LOC105321645 [Crassostrea gigas]	-	-	-	-	1.686	2.117
CGI_10001246	probable E3 ubiquitin- ligase RNF144A	-	-	-	-	2.419	2.115
CGI_10020144	location of vulva defective 1-like	-	-	-	-	2.183	2.113
CGI_10024595	Complement C1q 4	-	-	-	-	-	2.109
CGI_10023871	Kunitz-like protease inhibitor precursor	-	-	-	-	-	2.109
CGI_10026718	hypothetical protein CGI_10026718	-	-	-	-	2.290	2.109
CGI_10019991	universal stress A	-	-	-	-	2.847	2.099
CGI_10017630	signal transducer and activator of transcription 5B [Ceratosolen solmsi marchali]	-	-	-	1.632	2.153	2.097
CGI_10027474		-	-	-	-	2.037	2.095
CGI_10011308	kyphoscoliosis peptidase-like	-	-	-	1.601	1.850	2.094
CGI_10003301	NFX1-type zinc finger-containing 1-like	-	-	-	-	1.812	2.094
CGI_10005392	Inhibitor of apoptosis	-	-	-	-	-	2.093
CGI_10013835	PREDICTED: uncharacterized protein LOC105340609	-	-	1.784	1.629	2.021	2.091
CGI_10014915	phosphoenolpyruvate cytosolic [GTP]-like	-	-	-	-	2.039	2.090
CGI_10021674	cytoplasmic A3a [Ceratitis capitata]	-	-	-	-	-	2.088
CGI_10011967	Exonuclease 3 -5 domain-containing 1	-	-	-	2.707	2.758	2.086
CGI_10002425	hypothetical protein CGI_10002425	-	-	-	-	-	2.084
CGI_10007411	hypothetical protein CGI_10007411	-	-	-	-	1.988	2.079
CGI_10021550	osteopetrosis associated transmembrane	-	-	-	-	2.933	2.078
CGI_10021893	E3 ubiquitin- ligase HERC2	-	-	-	-	1.952	2.060
CGI_10026991	Mediator of RNA polymerase II transcription subunit 27	-	-	-	1.783	2.378	2.059
CGI_10007403	Nuclear receptor subfamily 0 group B member partial	-	-	-	-	2.116	2.055
CGI_10012135	C-type lectin domain family 3 member A	-	-	-	-	-	2.052
CGI_10013999	tyrosinase tyr-3	-	-	-	-	2.066	2.050
CGI_10018865	collagen alpha-6(IV) chain-like	-	-	-	-	-	2.050
CGI_10013790	uncharacterized	-	-	-	-	2.295	2.044
CGI_10016716	ubiquitin-conjugating enzyme E2 H	-	-	-	-	2.008	2.044
CGI_10005366	runt-related transcription factor 1-like isoform X2 [Lingula anatina]	-	-	-	-	2.664	2.039
CGI_10005395	hypothetical protein CGI_10005395	-	-	-	-	-	2.038
CGI_10018512	insulin-like growth factor-binding complex acid labile subunit isoform X2 [Crassostrea gigas]	-	-	-	1.976	2.247	2.037
CGI_10008798	hypothetical protein CGI_10008798	-	-	-	-	2.189	2.035
CGI_10001539	Multiple epidermal growth factor-like domains 10	-	-	-	2.143	-	2.029
CGI_10011582	A disintegrin and metallo ase with thrombospondin motifs 1	-	-	-	-	1.956	2.028
CGI_10003305	aldose 1-epimerase-like	-	-	-	-	1.551	2.024
CGI_10015263	aryl hydrocarbon receptor nuclear translocator 1	-	-	-	-	1.422	2.023
CGI_10002191	sacsin-like [Acropora digitifera]	-	-	-	-	2.143	2.020
CGI_10024346	glyoxylate hydroxypyruvate reductase HPR3-like	-	-	-	-	-	2.019

CGI_10025208	ferric-chelate reductase 1	-	-	-	1.590	1.504	2.017
CGI_10016999	A disintegrin and metallo ase with thrombospondin motifs 16	-	-	-	1.414	1.746	2.007
CGI_10014228	cAMP-responsive element-binding -like 2	-	-	-	-	-	2.006
CGI_10015192	DNA-binding D-ETS-4-like isoform X2	-	-	-	-	2.296	2.006
CGI_10007405	Poly [ADP-ribose] polymerase partial	-	-	-	1.297	2.047	2.002
CGI_10016615	Exonuclease 3 -5 domain-containing 1	-	-	-	-	2.754	2.001
CGI_10012514	Toll-like receptor 13	-	-	-	-	-	1.998
CGI_10010457	Ddx58 partial	-	-	-	-	-	1.998
CGI_10001699	Proline-rich transmembrane 1	-	-	-	-	-	1.997
CGI_10019869	inhibitor of apoptosis	-	-	-	-	-	1.995
CGI_10007404	poly [ADP-ribose] polymerase 12-like	-	-	-	-	2.436	1.989
CGI_10020611	amidohydrolase ytcJ	-	-	-	-	-	1.988
CGI_10008901	PREDICTED: uncharacterized protein LOC105321918 [Crassostrea gigas]	-	-	-	-	-	1.986
CGI_10024194	follistatin-A-like isoform X1	-	-	-	1.982	2.465	1.986
CGI_10025319	hypothetical protein CGI_10025319	-	-	-	-	2.175	1.985
CGI_10015868	sestrin-3 isoform X1 [Wasmannia auropunctata]	-	-	-	-	1.791	1.983
CGI_10007774	Ubiquitin-like modifier-activating enzyme 1	-	-	-	-	2.060	1.981
CGI_10002821	complement C1q 4 [Crassostrea gigas]	-	-	-	-	1.967	1.981
CGI_10012111	transcription regulator BACH1-like	-	-	-	-	-	1.981
CGI_10006885	PREDICTED: uncharacterized protein LOC105337665	-	-	-	-	-	1.980
CGI_10021605	H ACA ribonucleo complex subunit 1	-	-	-	2.003	2.102	1.974
CGI_10024392	probable ATP-dependent RNA helicase DHX58	-	-	-	-	2.322	1.968
CGI_10017971	hypothetical protein CGI_10001622	-	-	-	-	2.236	1.967
CGI_10016836	dipeptidyl peptidase 1-like	-	-	-	1.808	2.077	1.960
CGI_10016016	von Willebrand factor type EGF and pentraxin domain-containing 1	-	-	-	-	1.611	1.957
CGI_10021984	PITH domain-containing CG6153 [Stomoxys calcitrans]	-	-	-	-	-	1.954
CGI_10012652	26S proteasome non-ATPase regulatory subunit 10-like	-	-	-	-	-	1.953
CGI_10020040	hypothetical protein CGI_10020040	-	-	-	1.701	1.949	1.946
CGI_10008089	1-acyl-sn-glycerol-3-phosphate acyltransferase alpha [Ceratitis capitata]	-	-	-	-	-	1.943
CGI_10016684	hypothetical protein CGI_10016684	-	-	-	-	1.892	1.942
CGI_10026568	sodium- and chloride-dependent glycine transporter 2-like	-	-	-	-	2.274	1.941
CGI_10005216	Galactose-1-phosphate uridylyltransferase	-	-	-	-	2.216	1.935
CGI_10005488	HRAS-like suppressor 3	-	-	-	-	-	1.933
CGI_10005874	ubiquitin carboxyl-terminal hydrolase 26-like	-	-	-	-	-	1.931
CGI_10003342	GTP cyclohydrolase 1-like	-	-	-	2.124	-	1.929
CGI_10019553	PRKCA-binding partial	-	-	-	-	2.319	1.925
CGI_10006248	tRNA 2 -phosphotransferase 1	-	-	-	-	1.538	1.910
CGI_10027779	ovomucoid-like [Crassostrea gigas]	-	-	-	1.622	1.918	1.909
CGI_10018381	FAM63B- partial	-	-	-	-	1.724	1.905
CGI_10005032	Caprin-2 [Crassostrea gigas]	-	-	-	-	-	1.905
CGI_10022009	required for meiotic nuclear division 1 homolog	-	-	-	1.710	2.894	1.904
CGI_10026835	low-density lipo receptor-related 4-like	-	-	-	-	2.130	1.896
CGI_10002587	ras suppressor 1 isoform X2 [Callorhinchus milii]	-	-	-	-	-	1.894
CGI_10026281	prominin-1-A-like isoform X2	-	-	-	-	2.120	1.893
CGI_10005263	AT-rich interactive domain-containing 1B-like	-	-	-	-	-	1.892

CGI_10024740	7-alpha-hydroxycholest-4-en-3-one 12-alpha-hydroxylase-like	-	-	-	-	1.868	1.889
CGI_10028227	UBA-like domain-containing 2	-	-	-	-	2.200	1.887
CGI_10024671	inhibitor of apoptosis	-	-	-	-	1.901	1.884
CGI_10009319	tyrosinase tyr-3	-	-	-	-	-	1.884
CGI_10024378	proto-oncogene c-Fos-like	-	-	-	-	-	1.881
CGI_10016998	serine threonine- kinase 26- partial	-	-	-	-	2.459	1.878
CGI_10010178	PIF- partial	-	-	-	-	2.395	1.877
CGI_10017629	Signal transducer and transcription activator 6	-	-	-	1.407	2.021	1.876
CGI_10008126	hypothetical protein CGI_10008126	-	-	-	-	-	1.876
CGI_10015343	hypothetical protein CGI_10015343	-	-	-	-	-	1.874
CGI_10009816	annexin B9-like isoform X2	-	-	-	1.923	1.599	1.874
CGI_10014276	laccase-like [Octopus bimaculoides]	-	-	-	-	-	1.871
CGI_10024173	WD repeat-containing 91	-	-	-	1.755	1.921	1.870
CGI_10004252	ankyrin repeat and KH domain-containing 1-like [Biomphalaria glabrata]	-	-	-	-	1.915	1.869
CGI_10028079	tyrosinase tyr-3	-	-	-	-	-	1.867
CGI_10027512	Toll-like receptor 13	-	-	-	-	1.835	1.867
CGI_10026416	PREDICTED: uncharacterized protein LOC105326467 isoform X3 [Crassostrea gigas]	-	-	-	-	2.608	1.867
CGI_10001532	nuclear speckle splicing regulatory 1-like	-	-	-	1.753	-	1.866
CGI_10010092	chondroitin proteoglycan 2-like	-	-	1.644	1.646	2.211	1.864
CGI_10007476	cysteine and tyrosine-rich 1-like	-	-	-	1.860	2.523	1.863
CGI_10012830	hypothetical protein CGI_10012830	-	-	-	1.484	2.170	1.858
CGI_10023950	galectin-5- partial	-	-	-	-	2.053	1.855
CGI_10007265	poly [ADP-ribose] polymerase 14-like	-	-	-	1.374	2.208	1.853
CGI_10016583	Aggrecan core	-	-	-	-	1.644	1.851
CGI_10015018	solute carrier family 26 member 6-like [Lingula anatina]	-	-	-	-	3.678	1.848
CGI_10012458	atrial natriuretic peptide-converting enzyme isoform X2	-	-	-	1.482	2.202	1.846
CGI_10019372	baculoviral IAP repeat-containing 7	-	-	-	-	1.532	1.846
CGI_10023396	NFX1-type zinc finger-containing 1-like	-	-	-	-	1.963	1.844
CGI_10010588	cathepsin L1-like isoform X1 [Crassostrea gigas]	-	-	-	-	-	1.841
CGI_10013436	fos-related antigen 1-like	-	-	-	-	2.206	1.839
CGI_10026868	Retinal dehydrogenase 1	-	-	-	-	-	1.837
CGI_10012998	Double-stranded RNA-specific adenosine deaminase	-	-	-	-	-	1.832
CGI_10026006	hypothetical protein CGI_10026006	-	-	-	-	1.784	1.832
CGI_10023765	CD109 antigen-like	-	-	-	-	2.332	1.830
CGI_10015747	FMRFamide receptor-like [Crassostrea gigas]	-	-	-	-	1.467	1.827
CGI_10026604	probable chitinase 3	-	-	-	1.416	1.864	1.826
CGI_10005474	NFX1-type zinc finger-containing 1-like	-	-	-	-	1.852	1.826
CGI_10007107	gastrula zinc finger - partial	-	-	-	-	1.913	1.825
CGI_10025356	arrestin domain-containing 3-like	-	-	-	-	1.471	1.824
CGI_10008900	cysteine-rich and transmembrane domain-containing 1-like	-	-	-	-	-	1.823
CGI_10028023	PREDICTED: uncharacterized protein LOC105325168 [Crassostrea gigas]	-	-	-	-	1.817	1.822
CGI_10026425	transcriptional repressor p66-beta-like isoform X2 [Crassostrea gigas]	-	-	-	1.381	1.701	1.818
CGI_10018575	aldehyde dimeric NADP-preferring isoform X4 [Diuraphis noxia]	-	-	-	-	-	1.818
CGI_10018142	Transcription factor p65	-	-	-	-	1.642	1.802
CGI_10001365	DD3-3-like	-	-	-	-	1.468	1.801

CGI_10022007	4-hydroxyphenylpyruvate dioxygenase-like	-	-	-	1.567	2.084	1.799
CGI_10014131	alkaline phosphatase-like isoform X1 [Crassostrea gigas]	-	-	-	-	-	1.799
CGI_10024719	cysteine- acidic integral membrane -like	-	-	-	-	1.401	1.798
CGI_10027102	SET and MYND domain-containing 5-like	-	-	-	-	1.582	1.797
CGI_10013044	hypothetical protein CGI_10013044	-	-	-	-	1.656	1.797
CGI_10021872	iron-sulfur cluster assembly enzyme mitochondrial	-	-	-	-	-	1.797
CGI_10023824	fatty acid hydroxylase domain-containing 2	-	-	-	-	-	1.796
CGI_10010459	probable ATP-dependent RNA helicase DDX58	-	-	-	-	1.669	1.795
CGI_10020475	inhibitor of nuclear factor-kappaB	-	-	-	-	1.649	1.793
CGI_10005761	uncharacterized	-	-	-	-	2.251	1.791
CGI_10026543	membrane progestin receptor gamma-B-like	-	-	-	1.594	2.034	1.788
CGI_10022931	Sox8 [Xenopus laevis]	-	-	-	1.769	1.809	1.786
CGI_10017861	endothelial PAS domain-containing 1	-	-	-	-	1.781	1.784
CGI_10003117	atrial natriuretic peptide receptor 1-like	-	-	-	-	-	1.772
CGI_10026493	Toll-like receptor 13	-	-	-	-	2.100	1.772
CGI_10024609	GTPase-activating Rap Ran-GAP domain 3 isoform X2	-	-	-	-	1.379	1.767
CGI_10018883	Ral guanine nucleotide dissociation stimulator-like 1	-	-	-	1.114	1.457	1.767
CGI_10022746	Fibronectin type III domain-containing 1	-	-	-	1.666	2.086	1.767
CGI_10006058	complement C1q tumor necrosis factor-related 3-like	-	-	-	-	-	1.764
CGI_10015483	E3 ubiquitin- ligase MIB2	-	-	-	-	-	1.763
CGI_10020257	BAG family molecular chaperone regulator 3-like isoform X2	-	-	1.544	1.427	1.796	1.761
CGI_10016949	Nuclear Factor of Kappa light polypeptide gene enhancer in b(B)-cells n [Caenorhabditis elegans]	-	-	-	-	2.163	1.757
CGI_10015320	carboxylesterase type B	-	-	-	-	1.742	1.757
CGI_10005050	tRNA 2 -phosphotransferase 1	-	-	-	-	-	1.755
CGI_10028398	dimethylaniline monooxygenase [N-oxide-forming] 5 isoform X2	-	-	-	-	-	1.755
CGI_10013286	TBC1 domain family member 13 isoform X1	-	-	-	2.385	2.066	1.752
CGI_10024393	Interferon-induced helicase C domain-containing 1	-	-	-	-	-	1.748
CGI_10022260	L-aminoadipate-semialdehyde dehydrogenase large subunit-like	-	-	-	2.074	1.909	1.748
CGI_10023094	hypothetical protein CGI_10023094	-	-	-	-	1.774	1.747
CGI_10008698	relA-associated inhibitor-like	-	-	-	1.955	1.971	1.744
CGI_10013530	heat shock 70 kDa 12A-like [Crassostrea gigas]	-	-	-	-	-	1.743
CGI_10001126	Annexin A7	-	-	-	1.215	1.893	1.741
CGI_10023414	UPF0515 C19orf66 homolog isoform X2	-	-	-	-	2.135	1.739
CGI_10019898	sacsin-like	-	-	-	1.946	2.415	1.739
CGI_10014708	ETS translocation variant 4-like isoform X3	-	-	-	-	1.740	1.734
CGI_10007459	surfeit locus 2	-	-	-	-	-	1.733
CGI_10024084	homeobox Hox-A1-like	-	-	-	-	2.153	1.733
CGI_10004183	purine nucleoside phosphorylase-like	-	-	-	-	1.814	1.733
CGI_10015691	homocysteine-responsive endoplasmic reticulum-resident ubiquitin-like domain member 2	-	-	-	1.249	1.746	1.732
CGI_10005182	double-stranded RNA-specific adenosine deaminase-like	-	-	-	-	1.626	1.732
CGI_10024602	Fibrinogen C domain-containing 1	-	-	-	1.682	1.642	1.726
CGI_10013061	serine protease inhibitor Cvsi-1-like	-	-	1.602	-	1.913	1.721
CGI_10007713	hypothetical protein CGI_10007713	-	-	-	-	1.995	1.720
CGI_10027283	Vesicle-associated membrane 7	-	-	-	1.549	1.926	1.716
CGI_10003650	substance-K receptor-like [Crassostrea gigas]	-	-	-	-	-	1.715

CGI_10009620	poly [ADP-ribose] polymerase 12-like [Coturnix japonica]	-	-	-	-	2.239	1.707
CGI_10005003	signal transducer and transcription activator isoform X5 [Stomoxys calcitrans]	-	-	-	-	1.839	1.704
CGI_10025815	thiopurine S-methyltransferase isoform X2	-	-	-	-	-	1.703
CGI_10000612	hypothetical protein CGI_10000612	-	-	-	1.605	1.964	1.702
CGI_10019891	growth hormone-inducible transmembrane	-	-	-	-	1.861	1.701
CGI_10014162	steroid 17-alpha-hydroxylase 17,20 lyase-like [Aplysia californica]	-	-	-	-	1.693	1.700
CGI_10020090	stimulated by retinoic acid gene 6 homolog	-	-	-	-	-	1.697
CGI_10018329	Astacin-like metalloendopeptidase	-	-	-	-	-	1.695
CGI_10023327	tyrosine- phosphatase non-receptor type 23-like	-	-	-	-	1.624	1.694
CGI_10007959	dyslexia susceptibility 1 candidate gene 1 isoform X1	-	-	-	-	1.842	1.690
CGI_10022911	Tripartite motif-containing 3	-	-	-	-	-	1.688
CGI_10007380	transcription factor SUM-1-like	-	-	-	-	1.928	1.687
CGI_10026457	primary amine liver isozyme-like	-	-	-	-	-	1.685
CGI_10013531	heat shock 70 kDa 12A-like	-	-	-	-	1.467	1.683
CGI_10025133	uncharacterized	-	-	-	-	1.732	1.680
CGI_10020847	Nicotinamide riboside kinase 1	-	-	-	-	1.528	1.679
CGI_10012081	probable inactive serine threonine- kinase DDB_G0274613 [Crassostrea gigas]	-	-	-	1.174	1.279	1.674
CGI_10023115	collagen alpha-6(VI) chain-like isoform X1 [Lepisosteus oculatus]	-	-	-	2.185	2.488	1.673
CGI_10024889	ceramide kinase-like isoform X2	-	-	-	-	-	1.672
CGI_10014492		-	-	-	-	1.391	1.671
CGI_10006343	fructose-1,6-bisphosphatase 1-like	-	-	-	-	2.302	1.667
CGI_10028027	arylsulfatase B-like	-	-	-	-	1.789	1.662
CGI_10027975	midnolin [Chrysemys picta bellii]	-	-	-	-	2.435	1.661
CGI_10005238	immediate early response gene 5	-	-	-	-	1.551	1.658
CGI_10019374	hypothetical protein CGI_10019374	-	-	-	1.708	2.229	1.656
CGI_10022075	scaffold salvador-like [Biomphalaria glabrata]	-	-	-	1.504	1.991	1.655
CGI_10021811	transcription factor Sox-11-like	-	-	-	-	1.937	1.653
CGI_10021445	Tripartite motif-containing 2	-	-	-	-	-	1.645
CGI_10019135	spermine oxidase	-	-	-	-	1.775	1.644
CGI_10006759	retinoic acid receptor gamma-like isoform X1 [Crassostrea gigas]	-	-	-	-	2.070	1.638
CGI_10028911	WD repeat and FYVE domain-containing 2-like	-	-	-	1.415	1.481	1.636
CGI_10012084	Alpha-crystallin B chain	-	-	-	-	1.896	1.635
CGI_10023394	zinc finger 675-like isoform X1 [Crassostrea gigas]	-	-	-	-	1.701	1.632
CGI_10014502	von Willebrand factor type EGF and pentraxin domain-containing 1-like isoform X2 [Crassostrea gigas]	-	-	-	-	-	1.632
CGI_10021719	hypothetical protein CGI_10021719	-	-	-	-	2.139	1.630
CGI_10022522	succinate dehydrogenase [ubiquinone] flavo mitochondrial	-	-	-	1.584	1.765	1.627
CGI_10028773	heterochromatin 1-binding 3-like	-	-	-	-	1.606	1.624
CGI_10020220	hypothetical protein CGI_10020220	-	-	1.886	1.883	1.787	1.624
CGI_10004708	zinc metallo ase nas-12-like	-	-	-	-	1.832	1.622
CGI_10019612	hypothetical protein CGI_10019612	-	-	-	-	1.428	1.620
CGI_10023781	Alpha-amylase 1	-	-	-	1.654	2.138	1.616
CGI_10027197	60S ribosomal L35	-	-	-	1.650	1.973	1.615
CGI_10015633	von Willebrand factor D and EGF domain-containing partial	-	-	-	1.473	1.995	1.614
CGI_10016891	Cell adhesion molecule 3	-	-	-	-	1.667	1.610
CGI_10016154	tumor necrosis factor alpha-induced 3	-	-	-	-	1.608	1.603

CGI_10004070	ATP synthase F(0) complex subunit mitochondrial-like	-	-	-	1.690	2.062	1.602
CGI_10010963	cell wall DAN4-like isoform X1	-	-	-	1.574	1.927	1.602
CGI_10026220	XK-related 6-like [Biomphalaria glabrata]	-	-	-	-	1.425	1.602
CGI_10027689	beta-1,3-glucan-binding -like	-	-	-	-	-	1.602
CGI_10016167	monocarboxylate transporter 12 [Orussus abietinus]	-	-	-	-	-	1.601
CGI_10010444	Hepatocyte growth factor	-	-	-	1.598	2.830	1.599
CGI_10003407	PREDICTED: uncharacterized protein LOC105320765 [Crassostrea gigas]	-	-	-	-	-	1.598
CGI_10007955	universal stress A [Crassostrea gigas]	-	-	-	-	-	1.598
CGI_10014345	Tyrosine- phosphatase non-receptor type 23	-	-	-	-	1.588	1.597
CGI_10026947	hypothetical protein CGI_10026947	-	-	-	-	2.006	1.597
CGI_10020276	insoluble matrix shell 5-like	-	-	-	-	-	1.596
CGI_10013372	PHD finger 13	-	-	-	-	1.639	1.595
CGI_10014539	Aminopeptidase N	-	-	-	-	1.925	1.593
CGI_10021475	slowpoke-binding -like	-	-	-	-	1.419	1.592
CGI_10014540	aminopeptidase N-like	-	-	-	-	1.896	1.591
CGI_10011735	insulin-like growth factor-binding complex acid labile subunit	-	-	-	-	-	1.589
CGI_10012085	Maltase- intestinal	-	-	-	-	1.919	1.587
CGI_10025610	eukaryotic elongation factor 2 kinase-like isoform X2	-	-	-	-	1.561	1.585
CGI_10005978	collagen alpha-6(VI) chain-like	-	-	-	-	-	1.583
CGI_10017458	ankyrin repeat [Trichomonas vaginalis G3]	-	-	-	-	1.307	1.580
CGI_10023096	Enterin neuropeptide	-	-	-	1.560	1.922	1.578
CGI_10007201	hypothetical protein CGI_10007201	-	-	-	-	1.715	1.577
CGI_10014171	cytochrome P450 family partial	-	-	-	-	1.412	1.576
CGI_10024091	homeobox Hox-B4a-like	-	-	-	-	-	1.576
CGI_10019154	sacsin isoform X1 [Corvus cornix cornix]	-	-	-	-	2.114	1.572
CGI_10028487	probable secreted beta-glucosidase adg3 isoform X1	-	-	-	-	-	1.570
CGI_10006027	CREB-binding -like isoform X2	-	-	-	-	-	1.562
CGI_10021178	SH2 domain-containing adapter F	-	-	-	-	-	1.562
CGI_10018375	hypothetical protein CGI_10018375	-	-	-	1.096	1.560	1.558
CGI_10005031	Caprin-2 [Crassostrea gigas]	-	-	-	-	-	1.557
CGI_10004110	sequestosome-1 isoform X2	-	-	-	-	-	1.554
CGI_10013827	DD3-3-like	-	-	-	-	1.832	1.550
CGI_10028513	sucrase- intestinal	-	-	-	-	1.630	1.550
CGI_10009148	von Willebrand factor type EGF and pentraxin domain-containing 1	-	-	-	1.565	1.596	1.549
CGI_10016496	FAM8A1-like	-	-	-	-	1.660	1.544
CGI_10005452	E3 ubiquitin- ligase RNF213-like	-	-	-	-	1.579	1.536
CGI_10016017	von Willebrand factor type EGF and pentraxin domain-containing 1-like isoform X2 [Crassostrea gigas]	-	-	-	-	-	1.530
CGI_10014005	Dual specificity phosphatase 4	-	-	-	-	1.585	1.525
CGI_10008274	FAM13A-like isoform X1 [Biomphalaria glabrata]	-	-	-	1.474	-	1.520
CGI_10022376	shisa-5-like [Crassostrea gigas]	-	-	-	1.522	1.728	1.511
CGI_10025809	LIM domain [Trichinella spiralis]	-	-	-	1.429	1.818	1.508
CGI_10008681	ABC transporter F family member 4-like isoform X2	-	-	-	-	1.594	1.506
CGI_10014285	forkhead box P1-like isoform X3 [Crassostrea gigas]	-	-	-	-	1.541	1.505
CGI_10024566	mediator of RNA polymerase II transcription subunit 8-like [Biomphalaria glabrata]	-	-	-	-	1.860	1.505
CGI_10005931	delta(3,5)-Delta(2,4)-dienoyl- mitochondrial-like	-	-	-	-	-	1.502

CGI_10000440	insoluble matrix shell 5-like	-	-	-	-	-	1.501
CGI_10022777	Tripartite motif-containing 3	-	-	-	-	1.732	1.498
CGI_10009933	glycoside hydrolase family 3 [Trichoderma atroviride IMI 206040]	-	-	-	1.591	1.438	1.493
CGI_10022803	urea-proton symporter DUR3-like	-	-	-	-	1.480	1.493
CGI_10001203	copper-transporting ATPase 1-like isoform X1	-	-	-	-	1.674	1.492
CGI_10026051	ecdysone-induced 78C-like isoform X8 [Crassostrea gigas]	-	-	-	1.322	1.653	1.490
CGI_10023537	PR domain zinc finger 5-like [Crassostrea gigas]	-	-	-	-	1.960	1.478
CGI_10023902	ras guanyl-releasing 3-like isoform X1 [Biomphalaria glabrata]	-	-	-	-	1.414	1.475
CGI_10016266	cingulin-like isoform X6	-	-	-	1.384	1.302	1.474
CGI_10017807	ras-related M-Ras-like	-	-	-	-	-	1.467
CGI_10002462	mucin-5AC-like isoform X1	-	-	-	1.286	1.663	1.458
CGI_10017943	28S ribosomal mitochondrial	-	-	-	1.743	1.476	1.454
CGI_10007980	forkhead box O-like	-	-	-	1.303	1.687	1.454
CGI_10016596	sacsin-like [Acropora digitifera]	-	-	-	-	-	1.453
CGI_10015083	zinc finger C3H1 type-like 1	-	-	-	-	1.521	1.451
CGI_10006016	myophilin isoform X1	-	-	-	-	1.434	1.449
CGI_10006640	alkaline tissue-nonspecific isozyme isoform X1 [Equus asinus]	-	-	-	-	-	1.449
CGI_10021672	ribosomal S2-like isoform 3 [Callorhinchus milii]	-	-	-	-	-	1.444
CGI_10021171	interferon regulatory factor 2	-	-	-	-	-	1.439
CGI_10006556	GRB2-associated-binding 1-like isoform X2	-	-	-	-	1.833	1.434
CGI_10014466	intraflagellar transport 74 homolog	-	-	-	-	1.304	1.430
CGI_10026352	hypothetical protein CGI_10026352	-	-	-	-	-	1.424
CGI_10016629	zinc finger -like 1	-	-	1.507	1.625	1.718	1.414
CGI_10024520	phosphorylase b kinase gamma catalytic skeletal muscle heart isoform isoform X2	-	-	-	-	-	1.409
CGI_10027721	proto-oncogene tyrosine- kinase Src isoform X2	-	-	-	-	1.661	1.408
CGI_10027385	homeobox Hox-A9-like isoform X1 [Crassostrea gigas]	-	-	-	-	2.046	1.403
CGI_10009497	caspase recruitment domain-containing 9-like	-	-	-	-	-	1.394
CGI_10011420	vascular endothelial growth factor A-like	-	-	-	-	-	1.389
CGI_10008906	complement C1q tumor necrosis factor-related 4-like [Crassostrea gigas]	-	-	-	-	1.911	1.387
CGI_10000174	60S ribosomal L37a	-	-	-	-	1.620	1.381
CGI_10012829	PX domain-containing kinase	-	-	-	-	1.581	1.370
CGI_10005449	golgin subfamily B member 1-like	-	-	-	-	-	1.368
CGI_10006196	Poly [ADP-ribose] polymerase 14	-	-	-	-	-	1.361
CGI_10023913	hypothetical protein CGI_10023913	-	-	-	-	-	1.356
CGI_10020778	vacuolar sorting-associated 37A-like	-	-	-	1.433	1.381	1.352
CGI_10023583	PREDICTED: uncharacterized protein LOC105336505	-	-	-	-	1.317	1.350
CGI_10017042	hexokinase-2-like isoform X5 [Aplysia californica]	-	-	-	-	-	1.341
CGI_10028634	Rho-related GTP-binding	-	-	-	-	2.107	1.339
CGI_10002108	iron zinc purple acid phosphatase [Crassostrea gigas]	-	-	-	-	-	1.338
CGI_10021948	DNA-directed RNA polymerase II subunit RPB1	-	-	-	-	1.488	1.336
CGI_10016441	INO80 complex subunit D isoform X2 [Cercocebus atys]	-	-	-	-	1.700	1.325
CGI_10028440	sex comb on midleg 2 isoform X1	-	-	-	-	1.553	1.325
CGI_10012662	WAS/WASL-interacting protein family member 1	-	-	-	-	1.495	1.324
CGI_10007222	ubiquitin-conjugating enzyme E2-17 kDa [Bactrocera oleae]	-	-	-	-	-	1.323
CGI_10022778	tyrosine- kinase ZAP-70 [Strongylocentrotus purpuratus]	-	-	-	-	1.227	1.320

CGI_10006574	ubiquinol-cytochrome c reductase subunit partial [Mytilus edulis]	-	-	-	-	-	1.320
CGI_10009756	TFG isoform X2	-	-	-	1.444	1.541	1.317
CGI_10015211	Inositol-pentakisphosphate 2-kinase	-	-	-	-	-	1.317
CGI_10018985	Na(+) H(+) exchange regulatory cofactor NHE-RF1-like	-	-	-	-	1.153	1.314
CGI_10010173	transcription factor SPT20 homolog	-	-	-	-	-	1.309
CGI_10018446	hypothetical protein CGI_10018446	-	-	-	1.317	-	1.307
CGI_10007794	zinc finger MYND domain-containing 15-like	-	-	-	-	-	1.297
CGI_10008003	Leucine-rich repeat-containing 24	-	-	-	2.093	1.796	1.295
CGI_10021883	receptor-type tyrosine- phosphatase delta- partial	-	-	-	-	-	1.275
CGI_10003481	Ras-related Rab-11A	-	-	-	1.295	1.491	1.270
CGI_10028226	E3 ubiquitin- ligase MGRN1-like isoform X2	-	-	-	-	1.700	1.267
CGI_10002331	paramyosin-like isoform X1 [Crassostrea gigas]	-	-	-	1.062	-	1.264
CGI_10018945	E3 ubiquitin- ligase AMFR	-	-	-	-	1.521	1.263
CGI_10016263	heat shock 70 kDa 12A-like	-	-	-	-	1.141	1.262
CGI_10017572	serine arginine repetitive matrix 1-like isoform X1	-	-	-	-	1.096	1.258
CGI_10022102	acidic mammalian chitinase-like	-	-	-	1.193	1.286	1.254
CGI_10019068	CUE domain-containing 1-like	-	-	-	-	1.576	1.252
CGI_10018403	probable helicase with zinc finger domain	-	-	-	-	1.042	1.248
CGI_10019893	40S ribosomal S28 [Salmo salar]	-	-	-	1.326	1.143	1.235
CGI_10009433	ERO1 alpha isoform X4	-	-	-	-	-	1.228
CGI_10026035	E3 ubiquitin- ligase MIB1-like isoform X1	-	-	-	-	1.277	1.227
CGI_10006667	microphthalmia-associated transcription factor isoform X1	-	-	-	-	1.177	1.227
CGI_10017227	glutamate dehydrogenase mitochondrial	-	-	-	-	-	1.220
CGI_10006521	WD repeat-containing 27	-	-	-	-	-	1.218
CGI_10017066	probable ATP synthase subunit g mitochondrial	-	-	-	-	-	1.216
CGI_10009991	cathepsin D	-	-	-	-	-	1.215
CGI_10021213	Low-density lipo receptor-related 11	-	-	-	-	0.986	1.180
CGI_10004546	trichohyalin-like isoform X1 [Crassostrea gigas]	-	-	-	-	-	1.175
CGI_10001554	eukaryotic initiation factor 4A-I-like	-	-	-	-	1.452	1.163
CGI_10017944	collagen alpha-1(VII) chain-like [Lingula anatina]	-	-	-	-	-	1.160
CGI_10018006	histone deacetylase 4-like	-	-	-	-	1.291	1.157
CGI_10008751	hypothetical protein CGI_10008751	-	-	-	-	1.263	1.153
CGI_10017308	pre-mRNA-splicing regulator WTAP-like [Lingula anatina]	-	-	-	-	1.120	1.132
CGI_10024107	E3 ubiquitin- ligase rififylin	-	-	-	-	1.191	1.131
CGI_10015061	mucolipin-3-like isoform X2	-	-	-	-	0.941	1.120
CGI_10020202	lysine-specific demethylase 6A-like isoform X1	-	-	-	-	1.447	1.117
CGI_10006989	radial spoke head 1 homolog	-	-	-	1.313	0.997	1.095
CGI_10016438	signal transducing adapter molecule 1-like	-	-	-	-	1.156	1.086
CGI_10021701	myocyte-specific enhancer factor 2A-like isoform X1 [Lingula anatina]	-	-	-	-	1.087	1.078
CGI_10013694	dual specificity phosphatase 16-like isoform X1 [Lingula anatina]	-	-	-	-	1.518	1.062
CGI_10026305	CCAAT enhancer-binding gamma	-	-	-	-	1.146	1.037
CGI_10026720	Translocon-associated subunit beta	-	-	-	-	0.974	1.009
CGI_10009323	subfamily B member 5	-	-	-	-	1.007	1.000
CGI_10010276	5 -AMP-activated kinase subunit gamma-1-like isoform X2 [Aplysia californica]	-	-	-	-	0.999	0.985
CGI_10003308	MAP kinase-activated kinase 2	-	-	-	-	1.163	0.984

CGI_10007096	1-phosphatidylinositol 4,5-bisphosphate phosphodiesterase epsilon-1-like	-	-	-	-	1.065	0.934
CGI_10012818	slit homolog 2 -like isoform X1	-	-	-	-	-	-0.891
CGI_10004570	rapamycin-insensitive companion of mTOR-like	-	-	-	-	-0.854	-0.891
CGI_10002921	tyrosine- kinase SRK2-like isoform X2 [Crassostrea gigas]	-	-	-	-	-	-0.910
CGI_10002456	tubulin alpha chain-like	-	-	-	-	-	-0.964
CGI_10028320	FRAS1-related extracellular matrix 2-like	-	-	-	-	-1.316	-0.971
CGI_10025934	receptor for activated C kinase 1	-	-	-	-	-	-1.003
CGI_10003777	sodium channel 1 brain-like isoform X2	-	-	-	-	-	-1.019
CGI_10012864	dedicator of cytokinesis 3 isoform X2	-	-	-	-1.090	-1.018	-1.025
CGI_10019526	WD repeat-containing 66	-	-	-	-	-1.052	-1.040
CGI_10018712	Leucine-rich repeats and immunoglobulin-like domains 3	-	-	-	-	-	-1.089
CGI_10019262	dual specificity testis-specific kinase 2-like	-	-	-	-	-	-1.097
CGI_10026557	glyco 3-alpha-L-fucosyltransferase A [Cimex lectularius]	-	-	-	-	-1.140	-1.104
CGI_10022074	radial spoke head 4 homolog A-like	-	-	-	-	-	-1.111
CGI_10027502	rootletin-like isoform X2	-	-	-	-	-1.084	-1.119
CGI_10025239	poly(rC)-binding 3-like isoform X1 [Crassostrea gigas]	-	-	-	-	-1.157	-1.134
CGI_10003348	dynein heavy chain domain-containing 1-like	-	-	-	-	-	-1.138
CGI_10011731	serine threonine- kinase pats1	-	-	-	-	-	-1.148
CGI_10025394	dynein regulatory complex subunit 5	-	-	-	-	-	-1.174
CGI_10016472	coiled-coil domain-containing 180-like	-	-	-	-	-	-1.182
CGI_10002069	von Willebrand factor D and EGF domain-containing -like	-	-	-	-	-1.201	-1.190
CGI_10008512	ankyrin and armadillo repeat-containing -like	-	-	-	-	-1.353	-1.197
CGI_10017631	EF-hand calcium-binding domain-containing 6	-	-	-	-	-	-1.200
CGI_10015576	tektin-2 [Chrysemys picta bellii]	-	-	-	-	-1.071	-1.204
CGI_10010713	metastasis-associated MTA3-like	-	-	-	-	-	-1.205
CGI_10015332	WD repeat-containing 19 isoform X1 [Chrysemys picta bellii]	-	-	-	-1.188	-1.177	-1.211
CGI_10006111	poly(ADP-ribose) polymerase pme-5-like	-	-	-	-	-	-1.219
CGI_10020015	Dynein heavy chain axonemal	-	-	-	-	-	-1.230
CGI_10011755	cilia- and flagella-associated 74	-	-	-	-	-1.459	-1.232
CGI_10002806	dynein heavy chain domain-containing 1-like	-	-	-	-	-	-1.239
CGI_10019387	Sn1-specific diacylglycerol lipase alpha	-	-	-	-	-1.409	-1.241
CGI_10015959	Laminin subunit beta-1	-	-	-	-	-1.224	-1.256
CGI_10020454	Choline transporter 1	-	-	-	-	-1.307	-1.257
CGI_10005381	dynein beta ciliary-like	-	-	-	-	-	-1.260
CGI_10010994	dynein heavy chain axonemal-like	-	-	-	-	-	-1.264
CGI_10006978	cilia- and flagella-associated 47	-	-	-	-	-	-1.287
CGI_10002893	tetratricopeptide repeat 28-like	-	-	-	-	-	-1.296
CGI_10008053	zinc finger [Ixodes scapularis]	-	-	-	-	-1.586	-1.298
CGI_10024972	zinc finger ush-like [Crassostrea gigas]	-	-	-	-	-1.164	-1.304
CGI_10020680	ribosome biogenesis NSA2 homolog	-	-	-	-	-	-1.307
CGI_10019697	RNA-binding single-stranded-interacting 3-like isoform X9 [Crassostrea gigas]	-	-	-	-	-	-1.323
CGI_10015728	nesprin-1-like isoform X1	-	-	-	-	-	-1.329
CGI_10010486	beta-1-syntrophin-like	-	-	-	-	-	-1.353
CGI_10005619	vacuolar sorting-associated 51 homolog	-	-	-	-	-1.602	-1.356
CGI_10024636	Potassium voltage-gated channel Shaw [Trichinella britovi]	-	-	-	-	-	-1.359

CGI_10013748	Kielin chordin	-	-	-	-	-	-1.377
CGI_10004929	transient receptor potential cation channel subfamily M member 3-like isoform X1 [Crassostrea gigas]	-	-	-	-	-	-1.385
CGI_10013577	coiled-coil domain-containing 81-like	-	-	-	-	-	-1.388
CGI_10013398	furin-like isoform X2	-	-	-	-	-	-1.390
CGI_10017264	sphingosine-1-phosphate phosphatase 1	-	-	-	-	-1.997	-1.392
CGI_10005337	Regulator of G- signaling 22	-	-	-	-	-	-1.397
CGI_10010015	gamma-glutamyltransferase isoform X3 [Alligator mississippiensis]	-	-	-	-	-1.644	-1.399
CGI_10006803	PREDICTED: uncharacterized protein C7orf72-like isoform X2 [Crassostrea gigas]	-	-	-	-	-1.293	-1.404
CGI_10014711	mitochondria-eating -like isoform X2	-	-	-	-	-	-1.405
CGI_10025496	Serine threonine- kinase Nek9	-	-	-	-	-	-1.409
CGI_10024919	dynein heavy chain axonemal-like	-	-	-	-	-	-1.411
CGI_10011842	neuronal acetylcholine receptor subunit alpha-6-like	-	-	-	-	-	-1.417
CGI_10008691	sine oculis-binding homolog isoform X1	-	-	-	-	-2.031	-1.427
CGI_10013124	Extracellular matrix FRAS1	-	-	-	-	-1.562	-1.428
CGI_10001604	G -coupled receptor kinase 5	-	-	-	-	-	-1.430
CGI_10002900	Coiled-coil domain-containing 65	-	-	-	-	-1.494	-1.448
CGI_10018327	Organic cation transporter [Crassostrea gigas]	-	-	-	-	-1.584	-1.454
CGI_10015394	hypothetical protein CGI_10015394	-	-	-	-	-1.574	-1.465
CGI_10002649	tetratricopeptide repeat 40 isoform X1 [Chrysemys picta bellii]	-	-	-	-	-1.281	-1.466
CGI_10013654	ovo isoform X2	-	-	-	-	-	-1.482
CGI_10020178	GRIP1-associated protein 1	-	-	-	-	-	-1.489
CGI_10011794	nucleolar 9-like	-	-	-	-	-	-1.495
CGI_10025447	multidrug resistance-associated 1-like isoform X1	-	-	-	-	-1.846	-1.498
CGI_10023897	jagged- partial	-	-	-	-	-1.612	-1.504
CGI_10008057	histone H2B-like [Crassostrea gigas]	-	-	-	-	-	-1.509
CGI_10008179	protocadherin-9-like [Crassostrea gigas]	-	-	-	-	-1.465	-1.515
CGI_10007561	Mo25-like [Octopus bimaculoides]	-	-	-	-1.271	-1.289	-1.522
CGI_10020952	leucine-rich repeat soc-2-like [Lingula anatina]	-	-	-	-	-	-1.529
CGI_10021162	nucleoside diphosphate kinase homolog 5-like	-	-	-	-	-	-1.530
CGI_10023187	PREDICTED: uncharacterized protein LOC105331822 isoform X4 [Crassostrea gigas]	-	-	-	-	-	-1.534
CGI_10016659	leucine-rich repeat-containing 15-like	-	-	-	-	-	-1.539
CGI_10015301	A disintegrin and metallo ase with thrombospondin motifs 18	-	-	-	-	-1.627	-1.555
CGI_10007130	neutral cholesterol ester hydrolase 1-like [Crassostrea gigas]	-	-	-	-	-	-1.577
CGI_10009931	dynein intermediate chain ciliary-like isoform X2	-	-	-	-1.019	-1.430	-1.586
CGI_10011332	transient receptor potential cation channel subfamily M member 2-like isoform X2	-	-	-	-	-1.984	-1.586
CGI_10011831	X-ray radiation resistance-associated 1	-	-	-	-	-1.711	-1.595
CGI_10014601	EF-hand calcium-binding domain-containing 6-like	-	-	-	-	-1.420	-1.601
CGI_10018306	cysteine-rich motor neuron 1 isoform X2	-	-	-	-	-	-1.620
CGI_10014864	Tetratricopeptide repeat 25	-	-	-	-	-	-1.624
CGI_10007659	c-binding -like	-	-	-	-	-	-1.633
CGI_10015111	potassium voltage-gated channel subfamily A member 1-like isoform X1 [Crassostrea gigas]	-	-	-	-1.450	-1.507	-1.643
CGI_10016538	hypothetical protein CGI_10016538	-	-	-	-	-1.169	-1.645
CGI_10004801	monocarboxylate transporter 13-like [Priapulus caudatus]	-	-	-	-	-	-1.647
CGI_10009679	cilia- and flagella-associated 20	-	-	-	-	-	-1.661
CGI_10000478	neuronal acetylcholine receptor subunit alpha-6-like	-	-	-	-	-2.114	-1.662

CGI_10009522	solute carrier family facilitated glucose transporter member 6 [Oreochromis niloticus]	-	-	-	-	-1.714	-1.662
CGI_10005399	nmrA-like family domain-containing 1	-	-	-	-	-	-1.668
CGI_10006796	c-binding -like	-	-	-	-	-	-1.671
CGI_10020388	unconventional myosin-IXb isoform X2 [Halyomorpha halys]	-	-	-	-	-	-1.674
CGI_10024262	Sodium-dependent noradrenaline transporter	-	-	-	-	-2.546	-1.675
CGI_10002359	hypothetical protein CGI_10002359	-	-	-	-	-	-1.683
CGI_10026740	hypothetical protein CGI_10026740	-	-	-	-	-	-1.689
CGI_10009992	carboxypeptidase Y-like	-	-	-	-	-	-1.693
CGI_10008753	T-box transcription factor TBX1-like	-	-	-	-	-1.431	-1.693
CGI_10025613	ankyrin repeat and fibronectin type-III domain-containing 1-like isoform X1 [Crassostrea gigas]	-	-	-	-	-1.767	-1.694
CGI_10005859	Chitin synthase 8	-	-	-	-1.762	-2.488	-1.746
CGI_10007803	dynein beta flagellar outer arm-like	-	-	-	-	-	-1.749
CGI_10020242	zinc transporter ZIP9	-	-	-	-	-	-1.752
CGI_10020064	Partner of Y14 and partial	-	-	-	-	-	-1.752
CGI_10006473	partial [Drosophila miranda]	-	-	-	-	-	-1.759
CGI_10017254	dead ringer homolog	-	-	-	-	-1.377	-1.763
CGI_10009873	Alpha-1,3-mannosyl-glyco 4-beta-N-acetylglucosaminyltransferase B	-	-	-	-	-	-1.771
CGI_10021564	leucine-rich repeat and death domain-containing 1	-	-	-	-	-1.491	-1.776
CGI_10022694	multiple C2 and transmembrane domain-containing 1-like	-	-	-	-	-	-1.783
CGI_10022740	CD2-associated [Mus musculus]	-	-	-	-	-	-1.786
CGI_10017638	serine protease inhibitor	-	-	-	-	-	-1.786
CGI_10017607	yellow-like [Harpegnathos saltator]	-	-	-	-	-	-1.786
CGI_10007466	UPF0394 inner membrane yeeE [Crassostrea gigas]	-	-	-	-	-	-1.796
CGI_10012742	Tubulin polyglutamylase complex subunit 1	-	-	-	-	-	-1.807
CGI_10027576	von Willebrand factor D and EGF domain-containing -like	-	-	-	-	-2.017	-1.808
CGI_10028321	FRAS1-related extracellular matrix 3	-	-	-	-1.592	-2.848	-1.817
CGI_10001457	tetraspanin-4 isoform X2	-	-	-	-	-	-1.818
CGI_10012712	Stabilin- partial	-	-	-	-	-	-1.819
CGI_10026357	WD repeat-containing 63-like	-	-	-	-	-	-1.819
CGI_10001938	rho guanine nucleotide exchange factor 10	-	-	-	-2.106	-2.097	-1.820
CGI_10004787	E3 ubiquitin- ligase RNF123-like	-	-	-	-	-	-1.821
CGI_10010564	Neurogenic locus notch	-	-	-	-	-	-1.821
CGI_10012772	ankyrin repeat [Trichomonas vaginalis G3]	-	-	-	-	-	-1.821
CGI_10006605	IWS1 homolog isoform X1 [Crassostrea gigas]	-	-	-	-	-	-1.848
CGI_10020437	T-box transcription factor TBX20	-	-	-	-	-1.528	-1.851
CGI_10019643	testis-expressed protein 45	-	-	-	-	-	-1.857
CGI_10012029	Xanthine dehydrogenase oxidase	-	-	-	-	-	-1.862
CGI_10018731	apolipophorins-like	-	-	-	-	-	-1.867
CGI_10023840	low affinity immunoglobulin epsilon Fc receptor-like isoform X2	-	-	-	-	-1.798	-1.875
CGI_10015298	Sal 1	-	-	-	-	-1.725	-1.876
CGI_10028062	cyclin-dependent kinase 17-like isoform X2 [Crassostrea gigas]	-	-	-	-	-1.864	-1.877
CGI_10016240	transient receptor potential cation channel subfamily M member 2-like	-	-	-	-	-	-1.880
CGI_10011654	WD repeat-containing on Y chromosome-like isoform X4	-	-	-	-	-	-1.890
CGI_10011806	tyrosine- kinase transmembrane receptor Ror-like	-	-	-	-	-	-1.896
CGI_10005416	uncharacterized threonine-rich GPI-anchored glyco -like isoform X1	-	-	-	-	-	-1.896

CGI_10003005	G patch domain-containing partial	-	-	-	-	-	-1.899
CGI_10021544	glutathione S-transferase 3-like [Crassostrea gigas]	-	-	-	-	-	-1.903
CGI_10027134	dimethylaniline monooxygenase [N-oxide-forming] 2-like [Crassostrea gigas]	-	-	-	-	-1.367	-1.916
CGI_10001488	E3 ubiquitin- ligase UBR3	-	-	-	-	-	-1.917
CGI_10026808	multiple epidermal growth factor-like domains 6	-	-	-	-	-	-1.924
CGI_10022022	Multiple epidermal growth factor-like domains 10	-	-	-	-	-	-1.927
CGI_10004593	Multiple epidermal growth factor-like domains 10	-	-	-	-	-	-1.927
CGI_10004288	Formimidoyltransferase-cyclodeaminase	-	-	-	-	-2.146	-1.928
CGI_10016600	skeletal receptor tyrosine- kinase	-	-	-	-	-	-1.928
CGI_10026174	hypothetical protein CGI_10026174	-	-	-	-	-	-1.932
CGI_10011556	uncharacterized	-	-	-	-	-1.319	-1.941
CGI_10009681	coiled-coil domain-containing 113-like	-	-	-	-	-	-1.965
CGI_10011950	PRA1 family 3-like	-	-	-	-	-	-1.965
CGI_10010790	Krueppel-like factor 6	-	-	-	-	-	-1.970
CGI_10024224	PR domain zinc finger 1-like isoform X1	-	-	-	-	-	-1.973
CGI_10022509	sugar transporter SWEET1	-	-	-	-	-	-1.984
CGI_10010870	hypothetical protein CGI_10010870	-	-	-	-	-	-1.989
CGI_10020465	transmembrane 183-like	-	-	-	-	-	-1.996
CGI_10021116	hypothetical protein CGI_10021116	-	-	-	-	-	-1.999
CGI_10009336	glucose dehydrogenase [quinone]-like [Crassostrea gigas]	-	-	-	-	-	-2.007
CGI_10024419	von Willebrand factor A domain-containing 5A	-	-	-	-	-2.846	-2.011
CGI_10020146	insulin-like growth factor 2 mRNA-binding 1 isoform X1	-	-	-	-2.133	-1.920	-2.015
CGI_10026143	ferric-chelate reductase 1	-	-	-	-	-	-2.016
CGI_10024956	PREDICTED: uncharacterized protein LOC105322838 [Crassostrea gigas]	-	-	-	-	-	-2.019
CGI_10015306	helicase ARIP4-like	-	-	-	-2.096	-	-2.025
CGI_10016175	inversin-B-like isoform X1 [Priapulus caudatus]	-	-	-	-	-	-2.033
CGI_10016173	probable domain-containing histone demethylation 2C isoform X1	-	-	-	-	-	-2.037
CGI_10013488	PREDICTED: uncharacterized protein LOC105321461 [Crassostrea gigas]	-	-	-	-	-2.267	-2.041
CGI_10025197	prolactin-releasing peptide receptor-like [Lingula anatina]	-	-	-	-	-	-2.043
CGI_10007149	Cytochrome P450 2B19	-	-	-	-	-	-2.046
CGI_10013775	hypothetical protein CGI_10013775	-	-	-	-	-	-2.053
CGI_10003800	pancreatic triacylglycerol lipase-like	-	-	-	-	-	-2.058
CGI_10021572	FAM227B-like isoform X2	-	-	-	-	-	-2.060
CGI_10023089	hypothetical protein CGI_10023089	-	-	-	-	-	-2.064
CGI_10009864	carbonic anhydrase-related 10-like	-	-	-	-	-	-2.077
CGI_10028821	myosin heavy fast skeletal muscle-like	-	-	-	-	-	-2.079
CGI_10027606	hypothetical protein CGI_10027606	-	-	-	-	-	-2.083
CGI_10028311	cytochrome P450 2C14-like isoform X2 [Crassostrea gigas]	-	-	-	-	-1.799	-2.084
CGI_10005085	PREDICTED: uncharacterized protein LOC105347200 isoform X6 [Crassostrea gigas]	-	-	-	-	-	-2.097
CGI_10023644	arylsulfatase I-like	-	-	-	-	-	-2.099
CGI_10008129	coiled-coil domain-containing 89-like	-	-	-	-	-	-2.099
CGI_10012018	cGMP-inhibited 3 ,5 -cyclic phosphodiesterase A-like	-	-	-	-2.621	-2.762	-2.100
CGI_10014450	Otopetrin-2 [Crassostrea gigas]	-	-	-	-	-2.679	-2.116
CGI_10004647	Protection of telomeres 1	-	-	-	-	-	-2.117
CGI_10010898	white-like isoform X2	-	-	-	-	-	-2.138

CGI_10017171	placenta-specific gene 8 -like	-	-	-	-	-	-2.142
CGI_10001524		-	-	-	-	-	-2.148
CGI_10014323	Transient receptor potential cation channel subfamily M member 3	-	-	-	-	-	-2.152
CGI_10020740	antho-RFamide neuropeptides-like isoform X2 [Biomphalaria glabrata]	-	-	-	-	-	-2.155
CGI_10004471	Tubulin polyglutamylase TTLL13	-	-	-	-	-	-2.156
CGI_10027212	intraflagellar transport 80 homolog	-	-	-	-	-	-2.160
CGI_10024531	fibrillin-2-like [Athalia rosae]	-	-	-	-	-	-2.162
CGI_10016977	sodium calcium exchanger 1-like isoform X1 [Lingula anatina]	-	-	-	-	-1.554	-2.165
CGI_10021345	Ras-related C3 botulinum toxin substrate 1	-	-	-	-	-	-2.170
CGI_10007588	acetylcholine receptor subunit beta-like	-	-	-	-	-	-2.171
CGI_10001552	diacylglycerol kinase delta-like isoform X1	-	-	-	-	-2.344	-2.172
CGI_10012075	c-binding -like	-	-	-	-	-	-2.176
CGI_10019546	DNA (cytosine-5)-methyltransferase 3B-like isoform X1 [Octopus bimaculoides]	-	-	-	-	-2.725	-2.191
CGI_10027243	C2 domain-containing 2-like isoform X5	-	-	-	-	-2.370	-2.193
CGI_10018075	coiled-coil domain-containing 105-like	-	-	-	-	-0.989	-2.193
CGI_10012988	L-ascorbate oxidase	-	-	-	-	-1.861	-2.195
CGI_10009234	SSUH2 homolog	-	-	-	-	-1.844	-2.209
CGI_10024669	hypothetical protein CGI_10024669	-	-	-	-	-	-2.210
CGI_10014167	VWFA and cache domain-containing 1	-	-	-	-	-2.219	-2.223
CGI_10019646	Cohesin subunit SA-1	-	-	-	-	-	-2.224
CGI_10009477	fas apoptotic inhibitory molecule 1-like isoform X1 [Crassostrea gigas]	-	-	-	-	-	-2.227
CGI_10027466	sodium calcium exchanger 2-like isoform X3 [Crassostrea gigas]	-	-	-	-	-1.720	-2.228
CGI_10005836	GQ-coupled-like [Lingula anatina]	-	-	-	-	-	-2.233
CGI_10022605	Transposon Tf2-6 poly	-	-	-	-	-	-2.245
CGI_10003259	transient receptor potential cation channel subfamily V member 5-like	-	-	-	-	-	-2.245
CGI_10005783	hypothetical protein CGI_10005783	-	-	-	-	-2.274	-2.247
CGI_10000904	plexin-B1-like [Oryzias latipes]	-	-	-	-	-	-2.265
CGI_10013284	hypothetical protein CGI_10013284	-	-	-	-	-	-2.268
CGI_10013556	ATP-dependent DNA helicase Q-like SIM	-	-	-	-	-2.376	-2.269
CGI_10024668	BTB POZ domain-containing 2	-	-	-	-1.296	-2.266	-2.272
CGI_10011075	latrophilin-2-like [Crassostrea gigas]	-	-	-	-	-	-2.273
CGI_10028757	PREDICTED: uncharacterized protein LOC105323477 [Crassostrea gigas]	-	-	-	-	-	-2.280
CGI_10008555	15-hydroxyprostaglandin dehydrogenase [NAD(+)]-like	-	-	-	-	-2.466	-2.286
CGI_10004293	tRNA (adenine(58)-N(1))-methyltransferase catalytic subunit TRMT61A	-	-	-	-	-2.269	-2.293
CGI_10014977	sorting nexin-14-like isoform X2	-	-	-	-	-	-2.297
CGI_10019459	TBC1 domain family member 19	-	-	-	-	-	-2.297
CGI_10004886	probable dolichyl pyrophosphate Glc1Man9 c2 alpha-1,3-glucosyltransferase	-	-	-	-	-	-2.298
CGI_10005803	Tripartite motif-containing 3	-	-	-	-1.720	-	-2.298
CGI_10028902	hypothetical protein CGI_10028902	-	-	-	-	-	-2.306
CGI_10009667	hypothetical protein CGI_10009667	-	-	-	-	-	-2.307
CGI_10017480	E3 ubiquitin- ligase UHRF1	-	-	-	-	-	-2.318
CGI_10016023	Complement C1q 2	-	-	-	-	-	-2.321
CGI_10022485	multiple epidermal growth factor-like domains 10	-	-	-	-	-	-2.328
CGI_10013692	rho GTPase-activating 20-like isoform X2	-	-	-	-	-2.375	-2.330
CGI_10024583	collagen alpha-1(IX) chain isoform X1	-	-	-	-	-2.597	-2.344

CGI_10000329	Down syndrome cell adhesion molecule 1 partial	-	-	-	-	-	-2.346
CGI_10027097	hypothetical protein CGI_10027097	-	-	-	-	-	-2.355
CGI_10002018	clavesin-2-like [Lingula anatina]	-	-	-	-	-	-2.357
CGI_10009310	pyruvate dehydrogenase E1 component subunit mitochondrial	-	-	-	-	-	-2.364
CGI_10018187	short-chain collagen C4-like	-	-	-	-	-	-2.379
CGI_10017639	serine protease inhibitor dipetalogastin-like	-	-	-	-	-	-2.384
CGI_10015927	thrombospondin type-1 domain-containing 4-like	-	-	-	-1.776	-	-2.386
CGI_10004719	pseudouridylate synthase 7 homolog	-	-	-	-	-	-2.392
CGI_10000783	uncharacterized	-	-	-	-	-	-2.398
CGI_10003810	sodium- and chloride-dependent glycine transporter 1-like	-	-	-	-	-	-2.400
CGI_10012515	C-type lectin mannose-binding isoform-like	-	-	-	-	-	-2.403
CGI_10019747	Calcium homeostasis endoplasmic reticulum	-	-	-	-	-	-2.403
CGI_10004692	hypothetical protein CGI_10004692	-	-	-	-	-	-2.404
CGI_10002352	heat shock 70 kDa 12A-like [Crassostrea gigas]	-	-	-	-	-	-2.416
CGI_10011862	Tumor suppressor p53-binding 1	-	-	-	-	-	-2.420
CGI_10025616	kelch-like ECH-associated 1	-	-	-	-	-	-2.421
CGI_10001792	hypothetical protein CGI_10001792	-	-	-	-	-4.254	-2.422
CGI_10016976	sodium calcium exchanger 1-like isoform X1 [Lingula anatina]	-	-	-	-	-	-2.428
CGI_10013708	hypothetical protein CGI_10013708	-	-	-	-	-	-2.428
CGI_10017751	lipopolysaccharide-induced tumor necrosis factor-alpha factor homolog [Crassostrea gigas]	-	-	-	-	-	-2.435
CGI_10010358	PREDICTED: uncharacterized protein LOC105333557 [Crassostrea gigas]	-	-	-	-	-	-2.438
CGI_10026834	glucosyltransferase [Yersinia aldovae]	-	-	-	-	-	-2.443
CGI_10007864	Epidermal growth factor receptor	-	-	-	-	-	-2.450
CGI_10015757	S1 RNA-binding domain-containing partial	-	-	-	-	-	-2.457
CGI_10012073	hemicentin-1 isoform X3	-	-	-	-	-	-2.459
CGI_10010065	uncharacterized	-	-	-	-	-	-2.465
CGI_10009294	uncharacterized	-	-	-	-	-	-2.468
CGI_10009593	uncharacterized	-	-	-	-	-	-2.490
CGI_10019413	ADP-ribosylation factor 2 [Cucumis melo]	-	-	-	-	-	-2.491
CGI_10008294	seleno O-like	-	-	-	-	-	-2.510
CGI_10019987	hypothetical protein CGI_10019987	-	-	-	-	-	-2.511
CGI_10025340	Collagen alpha-4(VI) chain	-	-	-	-	-	-2.521
CGI_10006685	Gamma-tubulin complex component 4	-	-	-	-	-	-2.523
CGI_10001542	MAP kinase-activating death domain	-	-	-	-	-1.877	-2.530
CGI_10013256	chitin binding beak 1	-	-	-	-	-	-2.535
CGI_10011703	leucine-rich repeat-containing 74B-like	-	-	-	-	-2.327	-2.542
CGI_10026272	monocarboxylate transporter 14-like isoform X1 [Crassostrea gigas]	-	-	-	-	-3.060	-2.543
CGI_10018117	Baculoviral IAP repeat-containing 2	-	-	-	-	-	-2.545
CGI_10012300	acetylcholine receptor subunit alpha-like isoform X2	-	-	-	-	-	-2.570
CGI_10016021	Complement C1q 2	-	-	-	-	-	-2.582
CGI_10021809	Tripartite motif-containing 2	-	-	-	-	-	-2.587
CGI_10016500	family transcriptional regulator [Streptomyces CFMR 7]	-	-	-	-	-	-2.619
CGI_10018956	hypothetical protein CGI_10018956	-	-	-	-	-	-2.625
CGI_10012931	myc box-dependent-interacting 1-like	-	-	-	-	-2.419	-2.632
CGI_10000304	eukaryotic initiation factor 4A-I	-	-	-	-4.234	-3.034	-2.643

CGI_10021313	tripartite motif-containing 55-like [Crassostrea gigas]	-	-	-	-	-	-2.654
CGI_10028375	neuronal acetylcholine receptor subunit alpha-3-like	-	-	-	-	-	-2.664
CGI_10015207	Aldo-keto reductase family 1 member B10	-	-	-	-	-2.654	-2.668
CGI_10024575	tctex1 domain-containing 2-like [Crassostrea gigas]	-	-	-	-	-	-2.684
CGI_10016505	triadin-like [Crassostrea gigas]	-	-	-	-	-2.185	-2.684
CGI_10022101	Collagen alpha-5(VI) chain	-	-	-	-2.373	-	-2.688
CGI_10026221	non-symbiotic hemoglobin 1-like	-	-	-	-	-	-2.700
CGI_10015913	hypothetical protein CGI_10015913	-	-	-	-	-1.836	-2.705
CGI_10027054	TP53-regulating kinase	-	-	-	-	-	-2.716
CGI_10002586	probable cytosolic iron-sulfur assembly CIAO1 [Python bivittatus]	-	-	-	-	-	-2.730
CGI_10022423	gastrula zinc finger [Danio rerio]	-	-	-	-	-	-2.739
CGI_10018532	Neurochondrin	-	-	-	-	-	-2.744
CGI_10005082	peripheral myelin 22-like [Crassostrea gigas]	-	-	-	-	-2.866	-2.773
CGI_10002233	tyrosine- kinase Fer-like	-	-	-	-	-	-2.796
CGI_10008526	hypothetical protein CGI_10008526	-	-	-	-	-	-2.797
CGI_10013443	proton-coupled folate transporter-like	-	-	-	-	-	-2.803
CGI_10002450	alpha-centractin [Crassostrea gigas]	-	-	-	-	-	-2.810
CGI_10017945	neuronal acetylcholine receptor subunit alpha-3-like	-	-	-	-	-	-2.811
CGI_10011295	calmodulin-A-like isoform X1	-	-	-	-	-2.699	-2.822
CGI_10007762	LIM domain only 3-like	-	-	-	-	-2.828	-2.830
CGI_10020352	AGAP002739-PA [Anopheles gambiae PEST]	-	-	-	-	-3.161	-2.854
CGI_10012330	Tubulin beta chain	-	-	-2.866	-2.806	-3.303	-2.895
CGI_10002011	alanine and glycine-rich -like [Crassostrea gigas]	-	-	-	-	-3.199	-2.909
CGI_10000794	hypothetical protein CGI_10000794	-	-	-	-	-	-2.960
CGI_10004742	zinc finger CCCH domain-containing 11A-like	-	-	-	-	-	-2.980
CGI_10014688	vezatin isoform X2	-	-	-	-	-	-3.021
CGI_10007871	PIH1 domain-containing 2-like	-	-	-	-	-	-3.080
CGI_10008330	hypothetical protein CGI_10008330	-	-	-	-	-	-3.113
CGI_10007795	nuclear receptor ROR-beta-like [Crassostrea gigas]	-	-	-	-	-2.538	-3.148
CGI_10014880	UPF0364 C6orf211 homolog	-	-	-	-	-	-3.160
CGI_10012074	c-binding -like	-	-	-	-	-	-3.230
CGI_10009342	partial	-	-	-	-	-	-3.259
CGI_10027027	mediator of RNA polymerase II transcription subunit 2-like [Crassostrea gigas]	-	-	-	-	-2.209	-3.271
CGI_10006879	glycosyl hydrolase	-	-	-	-	-	-3.308
CGI_10013014	schlafen 1	-	-	-	-	-	-3.321
CGI_10000695	E3 ubiquitin- ligase MIB2	-	-	-	-	-	-3.358
CGI_10009843	Centrosomal of 76 kDa	-	-	-	-	-2.553	-3.584
CGI_10025718	Synaptic vesicle 2-related	-	-	-	-	-	-3.593
CGI_10012465	PREDICTED: uncharacterized protein LOC105338963 [Crassostrea gigas]	-	-	-	-	-3.024	-3.774

Table S4. RGBOA analysis

Enriched Biological functions at 4 hours			
Biological function	**p.adj**	**Log2 FC**	**Annotation**
epithelial to mesenchymal transition	3.56E-07		
CGI_10005518		2.26	transcriptional regulator Erg- partial
CGI_10010444		1.60	Hepatocyte growth factor
Enriched Biological functions at 24hours			
Biological function	**p.adj**	**Log2 FC**	**Annotation**
myeloid cell differentiation	0.01426		
CGI_10027197		1.97	60S ribosomal L35
CGI_10016254		2.97	Core-binding factor subunit beta
CGI_10026305		1.15	CCAAT enhancer-binding gamma
CGI_10006667		1.18	microphthalmia-associated transcription factor isoform X1
intracellular signal transduction	0.01748		
CGI_10021170		3.94	Interferon regulatory factor 2
CGI_10010459		1.67	probable ATP-dependent RNA helicase DDX58
CGI_10021954		2.19	ATP-dependent RNA helicase chloroplastic-like [Parasteatoda tepidariorum]
CGI_10003183		2.93	deoxynucleoside triphosphate triphosphohydrolase SAMHD1-like
CGI_10010458		1.75	probable ATP-dependent RNA helicase DHX58
CGI_10024392		2.32	probable ATP-dependent RNA helicase DHX58
CGI_10003270		2.15	interferon regulatory factor 8
CGI_10005182		1.63	double-stranded RNA-specific adenosine deaminase-like
CGI_10007096		1.06	1-phosphatidylinositol 4,5-bisphosphate phosphodiesterase epsilon-1-like
CGI_10023902		1.41	ras guanyl-releasing 3-like isoform X1 [Biomphalaria glabrata]
CGI_10022146		-2.15	transmembrane 201-like
CGI_10017070		2.02	ras-related RABF2b-like [Crassostrea gigas]
CGI_10021960		-1.19	ras-related Rab-3-like isoform X4 [Crassostrea gigas]
CGI_10003481		1.49	Ras-related Rab-11A
CGI_10014532		2.95	interferon-induced 44-like [Crassostrea gigas]
CGI_10026034		2.00	probable serine threonine- kinase pats1
CGI_10015931		2.93	ADP-ribosylation factor 1
CGI_10006953		1.27	rho-related BTB domain-containing 2-like [Aplysia californica]
CGI_10018706		2.87	GTP-binding RAD [Crassostrea gigas]
CGI_10028634		2.11	Rho-related GTP-binding
CGI_10014971		2.38	guanine nucleotide-binding G(s) subunit alpha-like
CGI_10018396		2.74	radical S-adenosyl methionine domain-containing 2
CGI_10015817		2.49	phosphatidylinositol 4,5-bisphosphate 3-kinase catalytic subunit alpha isoform-like
CGI_10021019		1.67	zinc finger CCCH domain-containing 13-like

CGI_10025133		1.73	[Nematostella vectensis]
CGI_10005650		2.55	ras-related Rab-11A-like
CGI_10022879		2.07	deoxynucleoside triphosphate triphosphohydrolase SAMHD1
CGI_10027441		2.95	helicase with zinc finger domain 2-like
CGI_10000144		3.26	helicase with zinc finger domain 2-like isoform X1 [Crassostrea gigas]
CGI_10004570		-0.85	rapamycin-insensitive companion of mTOR-like
CGI_10022075		1.99	scaffold salvador-like [Biomphalaria glabrata]
CGI_10003308		1.16	MAP kinase-activated kinase 2
CGI_10014861		1.15	Ubiquitin-conjugating enzyme E2 N
CGI_10023630		1.31	Prickle 2
immune response	0.01748		
CGI_10018396		2.74	radical S-adenosyl methionine domain-containing 2
CGI_10027512		1.83	Toll-like receptor 13
CGI_10027721		1.66	proto-oncogene tyrosine- kinase Src isoform X2
CGI_10026305		1.15	CCAAT enhancer-binding gamma
CGI_10028827		2.20	peptidoglycan recognition SC2 [Drosophila melanogaster]
CGI_10028806		2.73	[Nematostella vectensis]
CGI_10006667		1.18	microphthalmia-associated transcription factor isoform X1
immune effector process	0.01426		
CGI_10021170		3.94	Interferon regulatory factor 2
CGI_10010459		1.67	probable ATP-dependent RNA helicase DDX58
CGI_10003183		2.93	deoxynucleoside triphosphate triphosphohydrolase SAMHD1-like
CGI_10003270		2.15	interferon regulatory factor 8
CGI_10005182		1.63	double-stranded RNA-specific adenosine deaminase-like
CGI_10014532		2.95	interferon-induced 44-like [Crassostrea gigas]
CGI_10017629		2.02	Signal transducer and transcription activator 6
CGI_10005003		1.84	signal transducer and transcription activator isoform X5 [Stomoxys calcitrans]
CGI_10017630		2.15	signal transducer and activator of transcription 5B [Ceratosolen solmsi marchali]
CGI_10018396		2.74	radical S-adenosyl methionine domain-containing 2
CGI_10021019		1.67	zinc finger CCCH domain-containing 13-like
CGI_10025133		1.73	[Nematostella vectensis]
CGI_10022879		2.07	deoxynucleoside triphosphate triphosphohydrolase SAMHD1
CGI_10026305		1.15	CCAAT enhancer-binding gamma
CGI_10024321		1.88	Actin-related 2 3 complex subunit 3
immune system process	0.02906		
CGI_10021170		3.94	Interferon regulatory factor 2
CGI_10010459		1.67	probable ATP-dependent RNA helicase DDX58
CGI_10021954		2.19	ATP-dependent RNA helicase chloroplastic-like [Parasteatoda tepidariorum]
CGI_10003183		2.93	deoxynucleoside triphosphate triphosphohydrolase SAMHD1-like
CGI_10010458		1.75	probable ATP-dependent RNA helicase DHX58
CGI_10024392		2.32	probable ATP-dependent RNA helicase DHX58
CGI_10003270		2.15	interferon regulatory factor 8
CGI_10005182		1.63	double-stranded RNA-specific adenosine deaminase-like

CGI_10017943	1.48	28S ribosomal mitochondrial
CGI_10014532	2.95	interferon-induced 44-like [Crassostrea gigas]
CGI_10018396	2.74	radical S-adenosyl methionine domain-containing 2
CGI_10021019	1.67	zinc finger CCCH domain-containing 13-like
CGI_10025133	1.73	[Nematostella vectensis]
CGI_10022879	2.07	deoxynucleoside triphosphate triphosphohydrolase SAMHD1
CGI_10028827	2.20	peptidoglycan recognition SC2 [Drosophila melanogaster]
CGI_10016154	1.61	tumor necrosis factor alpha-induced 3
CGI_10027441	2.95	helicase with zinc finger domain 2-like
CGI_10000144	3.26	helicase with zinc finger domain 2-like isoform X1 [Crassostrea gigas]
CGI_10016921	-2.37	histone-lysine N-methyltransferase EHMT1
CGI_10010444	2.83	Hepatocyte growth factor
CGI_10003308	1.16	MAP kinase-activated kinase 2
CGI_10014861	1.15	Ubiquitin-conjugating enzyme E2 N
CGI_10012725	2.70	Myeloid differentiation primary response 88
CGI_10008714	-3.16	WW domain-containing oxidoreductase
CGI_10027721	1.66	proto-oncogene tyrosine- kinase Src isoform X2
CGI_10024321	1.88	Actin-related 2 3 complex subunit 3
CGI_10026305	1.15	CCAAT enhancer-binding gamma
CGI_10005518	1.85	transcriptional regulator Erg- partial
CGI_10020437	-1.53	T-box transcription factor TBX20
CGI_10006667	1.18	microphthalmia-associated transcription factor isoform X1
CGI_10017629	2.02	Signal transducer and transcription activator 6
CGI_10005003	1.84	signal transducer and transcription activator isoform X5 [Stomoxys calcitrans]
CGI_10017630	2.15	signal transducer and activator of transcription 5B [Ceratosolen solmsi marchali]
CGI_10016254	2.97	Core-binding factor subunit beta
CGI_10027512	1.83	Toll-like receptor 13
CGI_10028806	2.73	[Nematostella vectensis]
CGI_10000304	-3.03	eukaryotic initiation factor 4A-I

Enriched Biological functions at 48hours

Biological function	**p.adj**	**Log2 FC**	**Annotation**
Response to stress			
CGI_10018604		2.17	Autophagy 5
CGI_10003083		2.43	probable ATP-dependent RNA helicase DHX58
CGI_10021170		4.06	Interferon regulatory factor 2
CGI_10012725		2.31	Myeloid differentiation primary response 88
CGI_10010459		1.80	probable ATP-dependent RNA helicase DDX58
CGI_10004742		-2.98	zinc finger CCCH domain-containing 11A-like
CGI_10018142		1.80	Transcription factor p65
CGI_10024393		1.75	Interferon-induced helicase C domain-containing 1
CGI_10003270		2.36	interferon regulatory factor 8
CGI_10005182		1.73	double-stranded RNA-specific adenosine deaminase-like
CGI_10024233		3.90	hemagglutinin amebocyte aggregation factor-like
CGI_10007793		3.45	tyrosinase tyr-3

CGI_10001123	3.29	Chorion peroxidase
CGI_10010240	3.67	Chorion peroxidase
CGI_10021734	2.40	chorion peroxidase-like
CGI_10028272	2.35	myeloperoxidase-like [Crassostrea gigas]
CGI_10005474	1.83	NFX1-type zinc finger-containing 1-like
CGI_10014276	1.87	laccase-like [Octopus bimaculoides]
CGI_10016651	2.15	deleted in malignant brain tumors 1 -like
CGI_10027957	2.36	ras-related GTP-binding A
CGI_10014532	2.34	interferon-induced 44-like [Crassostrea gigas]
CGI_10004922	5.19	IL17-5 [Crassostrea gigas]
CGI_10024595	2.11	Complement C1q 4
CGI_10023765	1.83	CD109 antigen-like
CGI_10017629	1.88	Signal transducer and transcription activator 6
CGI_10005003	1.70	signal transducer and transcription activator isoform X5 [Stomoxys calcitrans]
CGI_10001942	2.23	DNA polymerase lambda
CGI_10017630	2.10	signal transducer and activator of transcription 5B [Ceratosolen solmsi marchali]
CGI_10018396	3.29	radical S-adenosyl methionine domain-containing 2
CGI_10007774	1.98	Ubiquitin-like modifier-activating enzyme 1
CGI_10003823	3.06	COMM domain-containing 3
CGI_10012135	2.05	C-type lectin domain family 3 member A
CGI_10023840	-1.88	low affinity immunoglobulin epsilon Fc receptor-like isoform X2
CGI_10025133	1.68	[Nematostella vectensis]
CGI_10006027	1.56	CREB-binding -like isoform X2
CGI_10001792	-2.42	hypothetical protein CGI_10001792
CGI_10012514	2.00	Toll-like receptor 13
CGI_10024612	2.24	hypothetical protein CGI_10024612
CGI_10012722	4.99	myeloid differentiation primary response 88-like [Crassostrea gigas]
CGI_10026174	-1.93	hypothetical protein CGI_10026174
CGI_10026493	1.77	Toll-like receptor 13
CGI_10021136	2.38	Toll-like receptor 1
CGI_10027512	1.87	Toll-like receptor 13
CGI_10021345	-2.17	Ras-related C3 botulinum toxin substrate 1
CGI_10014497	3.01	von Willebrand factor type EGF and pentraxin domain-containing 1-like isoform X2 [Crassostrea gigas]
CGI_10028827	2.15	peptidoglycan recognition SC2 [Drosophila melanogaster]
CGI_10021171	1.44	interferon regulatory factor 2
CGI_10019528	2.27	suppressor of cytokine signaling 2-like
CGI_10012515	-2.40	C-type lectin mannose-binding isoform-like
CGI_10012379	2.49	Deleted in malignant brain tumors 1
CGI_10018753	3.65	deleted in malignant brain tumors 1 -like
CGI_10008241	4.07	C-type lectin domain family member A-like
CGI_10011916	2.73	tyrosinase tyr-3
CGI_10009318	2.49	tyrosinase tyr-3
CGI_10007753	2.57	tyrosinase tyr-3
CGI_10009319	1.88	tyrosinase tyr-3
CGI_10028079	1.87	tyrosinase tyr-3

CGI_10027395		2.67	78 kDa glucose-regulated
CGI_10016583		1.85	Aggrecan core
CGI_10023950		1.86	galectin-5- partial
CGI_10012829		1.37	PX domain-containing kinase
CGI_10003308		0.98	MAP kinase-activated kinase 2
CGI_10027721		1.41	proto-oncogene tyrosine- kinase Src isoform X2
CGI_10010457		2.00	Ddx58 partial
CGI_10003301		2.09	NFX1-type zinc finger-containing 1-like
CGI_10023396		1.84	NFX1-type zinc finger-containing 1-like
CGI_10026305		1.04	CCAAT enhancer-binding gamma
CGI_10012998		1.83	Double-stranded RNA-specific adenosine deaminase
CGI_10017480		-2.32	E3 ubiquitin- ligase UHRF1
CGI_10016804		2.30	myosin light chain smooth muscle isoform X4 [Monodelphis domestica]
CGI_10024107		1.13	E3 ubiquitin- ligase rififylin
Ras protein signal transduction	0.00496		
CGI_10023902		1.47	ras guanyl-releasing 3-like isoform X1 [Biomphalaria glabrata]
CGI_10006027		1.56	CREB-binding -like isoform X2
CGI_10005650		2.37	ras-related Rab-11A-like
cellular response to external stimulus	0.03371		
CGI_10018604		2.17	Autophagy 5
CGI_10027957		2.36	ras-related GTP-binding A
CGI_10006027		1.56	CREB-binding -like isoform X2
CGI_10027395		2.67	78 kDa glucose-regulated
CGI_10012725		2.31	Myeloid differentiation primary response 88
CGI_10021345		-2.17	Ras-related C3 botulinum toxin substrate 1
response to external stimulus	0.03371		
CGI_10003083		2.43	probable ATP-dependent RNA helicase DHX58
CGI_10021170		4.06	Interferon regulatory factor 2
CGI_10010459		1.80	probable ATP-dependent RNA helicase DDX58
CGI_10021954		2.24	ATP-dependent RNA helicase chloroplastic-like [Parasteatoda tepidariorum]
CGI_10004742		-2.98	zinc finger CCCH domain-containing 11A-like
CGI_10024393		1.75	Interferon-induced helicase C domain-containing 1
CGI_10024392		1.97	probable ATP-dependent RNA helicase DHX58
CGI_10003270		2.36	interferon regulatory factor 8
CGI_10005182		1.73	double-stranded RNA-specific adenosine deaminase-like
CGI_10001246		2.12	probable E3 ubiquitin- ligase RNF144A
CGI_10026035		1.23	E3 ubiquitin- ligase MIB1-like isoform X1
CGI_10021893		2.06	E3 ubiquitin- ligase HERC2
CGI_10000695		-3.36	E3 ubiquitin- ligase MIB2
CGI_10015483		1.76	E3 ubiquitin- ligase MIB2
CGI_10014532		2.34	interferon-induced 44-like [Crassostrea gigas]
CGI_10017629		1.88	Signal transducer and transcription activator 6
CGI_10005003		1.70	signal transducer and transcription activator isoform X5 [Stomoxys calcitrans]
CGI_10017630		2.10	signal transducer and activator of transcription 5B [Ceratosolen solmsi marchali]
CGI_10018945		1.26	E3 ubiquitin- ligase AMFR

CGI_10018396		3.29	radical S-adenosyl methionine domain-containing 2
CGI_10025133		1.68	[Nematostella vectensis]
CGI_10004787		-1.82	E3 ubiquitin- ligase RNF123-like
CGI_10001488		-1.92	E3 ubiquitin- ligase UBR3
CGI_10028226		1.27	E3 ubiquitin- ligase MGRN1-like isoform X2
CGI_10021171		1.44	interferon regulatory factor 2
CGI_10019528		2.27	suppressor of cytokine signaling 2-like
CGI_10005873		2.78	polyubiquitin 8-like [Acropora digitifera]
CGI_10005452		1.54	E3 ubiquitin- ligase RNF213-like
CGI_10027441		3.14	helicase with zinc finger domain 2-like
CGI_10000144		3.49	helicase with zinc finger domain 2-like isoform X1 [Crassostrea gigas]
CGI_10027442		2.73	helicase with zinc finger domain 2-like isoform X1 [Crassostrea gigas]
CGI_10010457		2.00	Ddx58 partial
CGI_10012998		1.83	Double-stranded RNA-specific adenosine deaminase
CGI_10017480		-2.32	E3 ubiquitin- ligase UHRF1
CGI_10024107		1.13	E3 ubiquitin- ligase rififylin
CGI_10023765		1.83	CD109 antigen-like
CGI_10003823		3.06	COMM domain-containing 3
CGI_10012135		2.05	C-type lectin domain family 3 member A
CGI_10023840		-1.88	low affinity immunoglobulin epsilon Fc receptor-like isoform X2
CGI_10014497		3.01	von Willebrand factor type EGF and pentraxin domain-containing 1-like isoform X2 [Crassostrea gigas]
CGI_10028827		2.15	peptidoglycan recognition SC2 [Drosophila melanogaster]
CGI_10012515		-2.40	C-type lectin mannose-binding isoform-like
CGI_10016583		1.85	Aggrecan core
CGI_10023950		1.86	galectin-5- partial
CGI_10003308		0.98	MAP kinase-activated kinase 2
CGI_10006027		1.56	CREB-binding -like isoform X2
CGI_10000304		-2.64	eukaryotic initiation factor 4A-I
CGI_10018604		2.17	Autophagy 5
CGI_10012725		2.31	Myeloid differentiation primary response 88
CGI_10027957		2.36	ras-related GTP-binding A
CGI_10021345		-2.17	Ras-related C3 botulinum toxin substrate 1
CGI_10027395		2.67	78 kDa glucose-regulated
CGI_10010444		1.60	Hepatocyte growth factor
myeloid cell differentiation	0.00197		
CGI_10027197		1.62	60S ribosomal L35
CGI_10016254		3.14	Core-binding factor subunit beta
CGI_10026305		1.04	CCAAT enhancer-binding gamma
CGI_10006667		1.23	microphthalmia-associated transcription factor isoform X1
response to lipopolysaccharide	0.01619		
CGI_10003308		0.98	MAP kinase-activated kinase 2
CGI_10006027		1.56	CREB-binding -like isoform X2
CGI_10027395		2.67	78 kDa glucose-regulated
transmembrane transport	0.03371		

CGI_10011332		-1.59	transient receptor potential cation channel subfamily M member 2-like isoform X2
CGI_10014323		-2.15	Transient receptor potential cation channel subfamily M member 3
CGI_10016240		-1.88	transient receptor potential cation channel subfamily M member 2-like
CGI_10015111		-1.64	potassium voltage-gated channel subfamily A member 1-like isoform X1 [Crassostrea gigas]
CGI_10024636		-1.36	Potassium voltage-gated channel Shaw [Trichinella britovi]
CGI_10016977		-2.16	sodium calcium exchanger 1-like isoform X1 [Lingula anatina]
CGI_10027466		-2.23	sodium calcium exchanger 2-like isoform X3 [Crassostrea gigas]
CGI_10004070		1.60	ATP synthase F(0) complex subunit mitochondrial-like
CGI_10026671		2.44	sulfite oxidase-like
CGI_10003777		-1.02	sodium channel 1 brain-like isoform X2
CGI_10017857		2.25	inter-alpha-trypsin inhibitor heavy chain H3-like
CGI_10026568		1.94	sodium- and chloride-dependent glycine transporter 2-like
CGI_10025447		-1.50	multidrug resistance-associated 1-like isoform X1
CGI_10017841		2.37	Excitatory amino acid transporter partial
CGI_10003810		-2.40	sodium- and chloride-dependent glycine transporter 1-like
CGI_10009981		2.35	sodium- and chloride-dependent glycine transporter 1-like
CGI_10024262		-1.68	Sodium-dependent noradrenaline transporter
CGI_10009522		-1.66	solute carrier family facilitated glucose transporter member 6 [Oreochromis niloticus]
CGI_10027842		2.51	Solute carrier family facilitated glucose transporter member 1
immune response	0.00046		
CGI_10018396		3.29	radical S-adenosyl methionine domain-containing 2
CGI_10027512		1.87	Toll-like receptor 13
CGI_10027721		1.41	proto-oncogene tyrosine- kinase Src isoform X2
CGI_10010457		2.00	Ddx58 partial
CGI_10026305		1.04	CCAAT enhancer-binding gamma
CGI_10028827		2.15	peptidoglycan recognition SC2 [Drosophila melanogaster]
CGI_10028806		2.64	[Nematostella vectensis]
CGI_10006667		1.23	microphthalmia-associated transcription factor isoform X1
regulation of response to stimulus	0.01456		
CGI_10003083		2.43	probable ATP-dependent RNA helicase DHX58
CGI_10021170		4.06	Interferon regulatory factor 2
CGI_10012725		2.31	Myeloid differentiation primary response 88
CGI_10010459		1.80	probable ATP-dependent RNA helicase DDX58
CGI_10021954		2.24	ATP-dependent RNA helicase chloroplastic-like [Parasteatoda tepidariorum]
CGI_10004742		-2.98	zinc finger CCCH domain-containing 11A-like
CGI_10024393		1.75	Interferon-induced helicase C domain-containing 1
CGI_10024392		1.97	probable ATP-dependent RNA helicase DHX58
CGI_10003270		2.36	interferon regulatory factor 8
CGI_10005182		1.73	double-stranded RNA-specific adenosine deaminase-like
CGI_10017943		1.45	28S ribosomal mitochondrial
CGI_10027957		2.36	ras-related GTP-binding A
CGI_10014532		2.34	interferon-induced 44-like [Crassostrea gigas]
CGI_10018396		3.29	radical S-adenosyl methionine domain-containing 2

CGI_10025133		1.68	[Nematostella vectensis]
CGI_10006027		1.56	CREB-binding -like isoform X2
CGI_10021345		-2.17	Ras-related C3 botulinum toxin substrate 1
CGI_10028827		2.15	peptidoglycan recognition SC2 [Drosophila melanogaster]
CGI_10021171		1.44	interferon regulatory factor 2
CGI_10020437		-1.85	T-box transcription factor TBX20
CGI_10016154		1.60	tumor necrosis factor alpha-induced 3
CGI_10027395		2.67	78 kDa glucose-regulated
CGI_10009679		-1.66	cilia- and flagella-associated 20
CGI_10021162		-1.53	nucleoside diphosphate kinase homolog 5-like
CGI_10027441		3.14	helicase with zinc finger domain 2-like
CGI_10000144		3.49	helicase with zinc finger domain 2-like isoform X1 [Crassostrea gigas]
CGI_10010444		1.60	Hepatocyte growth factor
CGI_10003308		0.98	MAP kinase-activated kinase 2
CGI_10027721		1.41	proto-oncogene tyrosine- kinase Src isoform X2
CGI_10010457		2.00	Ddx58 partial
CGI_10011040		2.21	Phosphoinositide 3-kinase adapter 1
CGI_10025934		-1.00	receptor for activated C kinase 1
CGI_10012998		1.83	Double-stranded RNA-specific adenosine deaminase
CGI_10009497		1.39	caspase recruitment domain-containing 9-like
CGI_10024107		1.13	E3 ubiquitin- ligase rififylin
CGI_10015817		2.27	phosphatidylinositol 4,5-bisphosphate 3-kinase catalytic subunit alpha isoform-like
CGI_10005650		2.37	ras-related Rab-11A-like
CGI_10021178		1.56	SH2 domain-containing adapter F
CGI_10005518		2.38	transcriptional regulator Erg- partial
CGI_10011295		-2.82	calmodulin-A-like isoform X1
CGI_10026305		1.04	CCAAT enhancer-binding gamma
CGI_10006667		1.23	microphthalmia-associated transcription factor isoform X1
CGI_10001126		1.74	Annexin A7
CGI_10021863		2.15	Annexin A7
CGI_10007222		1.32	ubiquitin-conjugating enzyme E2-17 kDa [Bactrocera oleae]
CGI_10022740		-1.79	CD2-associated [Mus musculus]
immune effector process	0.00052		
CGI_10003083		2.43	probable ATP-dependent RNA helicase DHX58
CGI_10021170		4.06	Interferon regulatory factor 2
CGI_10010459		1.80	probable ATP-dependent RNA helicase DDX58
CGI_10004742		-2.98	zinc finger CCCH domain-containing 11A-like
CGI_10024393		1.75	Interferon-induced helicase C domain-containing 1
CGI_10003270		2.36	interferon regulatory factor 8
CGI_10005182		1.73	double-stranded RNA-specific adenosine deaminase-like
CGI_10014532		2.34	interferon-induced 44-like [Crassostrea gigas]
CGI_10017629		1.88	Signal transducer and transcription activator 6
CGI_10005003		1.70	signal transducer and transcription activator isoform X5 [Stomoxys calcitrans]
CGI_10017630		2.10	signal transducer and activator of transcription 5B [Ceratosolen solmsi marchali]

CGI_10018396		3.29	radical S-adenosyl methionine domain-containing 2
CGI_10025133		1.68	[Nematostella vectensis]
CGI_10021171		1.44	interferon regulatory factor 2
CGI_10019528		2.27	suppressor of cytokine signaling 2-like
CGI_10010457		2.00	Ddx58 partial
CGI_10012998		1.83	Double-stranded RNA-specific adenosine deaminase
CGI_10026305		1.04	CCAAT enhancer-binding gamma
immune system process	0.00303		
CGI_10003083		2.43	probable ATP-dependent RNA helicase DHX58
CGI_10021170		4.06	Interferon regulatory factor 2
CGI_10010459		1.80	probable ATP-dependent RNA helicase DDX58
CGI_10021954		2.24	ATP-dependent RNA helicase chloroplastic-like [Parasteatoda tepidariorum]
CGI_10004742		-2.98	zinc finger CCCH domain-containing 11A-like
CGI_10024393		1.75	Interferon-induced helicase C domain-containing 1
CGI_10024392		1.97	probable ATP-dependent RNA helicase DHX58
CGI_10003270		2.36	interferon regulatory factor 8
CGI_10005182		1.73	double-stranded RNA-specific adenosine deaminase-like
CGI_10017943		1.45	28S ribosomal mitochondrial
CGI_10014532		2.34	interferon-induced 44-like [Crassostrea gigas]
CGI_10018396		3.29	radical S-adenosyl methionine domain-containing 2
CGI_10025133		1.68	[Nematostella vectensis]
CGI_10028827		2.15	peptidoglycan recognition SC2 [Drosophila melanogaster]
CGI_10021171		1.44	interferon regulatory factor 2
CGI_10016154		1.60	tumor necrosis factor alpha-induced 3
CGI_10021162		-1.53	nucleoside diphosphate kinase homolog 5-like
CGI_10027441		3.14	helicase with zinc finger domain 2-like
CGI_10000144		3.49	helicase with zinc finger domain 2-like isoform X1 [Crassostrea gigas]
CGI_10010444		1.60	Hepatocyte growth factor
CGI_10003308		0.98	MAP kinase-activated kinase 2
CGI_10010457		2.00	Ddx58 partial
CGI_10011040		2.21	Phosphoinositide 3-kinase adapter 1
CGI_10012998		1.83	Double-stranded RNA-specific adenosine deaminase
CGI_10012725		2.31	Myeloid differentiation primary response 88
CGI_10027957		2.36	ras-related GTP-binding A
CGI_10006027		1.56	CREB-binding -like isoform X2
CGI_10021345		-2.17	Ras-related C3 botulinum toxin substrate 1
CGI_10009679		-1.66	cilia- and flagella-associated 20
CGI_10027721		1.41	proto-oncogene tyrosine- kinase Src isoform X2
CGI_10009497		1.39	caspase recruitment domain-containing 9-like
CGI_10026305		1.04	CCAAT enhancer-binding gamma
CGI_10022740		-1.79	CD2-associated [Mus musculus]
CGI_10005518		2.38	transcriptional regulator Erg- partial
CGI_10020437		-1.85	T-box transcription factor TBX20
CGI_10006667		1.23	microphthalmia-associated transcription factor isoform X1
CGI_10017629		1.88	Signal transducer and transcription activator 6

CGI_10005003		1.70	signal transducer and transcription activator isoform X5 [Stomoxys calcitrans]
CGI_10017630		2.10	signal transducer and activator of transcription 5B [Ceratosolen solmsi marchali]
CGI_10016254		3.14	Core-binding factor subunit beta
CGI_10027512		1.87	Toll-like receptor 13
CGI_10019528		2.27	suppressor of cytokine signaling 2-like
CGI_10028806		2.64	[Nematostella vectensis]
CGI_10000304		-2.64	eukaryotic initiation factor 4A-I
intracellular signal transduction	0.03371		
CGI_10003083		2.43	probable ATP-dependent RNA helicase DHX58
CGI_10021170		4.06	Interferon regulatory factor 2
CGI_10010459		1.80	probable ATP-dependent RNA helicase DDX58
CGI_10021954		2.24	ATP-dependent RNA helicase chloroplastic-like [Parasteatoda tepidariorum]
CGI_10004742		-2.98	zinc finger CCCH domain-containing 11A-like
CGI_10024393		1.75	Interferon-induced helicase C domain-containing 1
CGI_10024392		1.97	probable ATP-dependent RNA helicase DHX58
CGI_10003270		2.36	interferon regulatory factor 8
CGI_10005182		1.73	double-stranded RNA-specific adenosine deaminase-like
CGI_10007096		0.93	1-phosphatidylinositol 4,5-bisphosphate phosphodiesterase epsilon-1-like
CGI_10023902		1.47	ras guanyl-releasing 3-like isoform X1 [Biomphalaria glabrata]
CGI_10017807		1.47	ras-related M-Ras-like
CGI_10003481		1.27	Ras-related Rab-11A
CGI_10014532		2.34	interferon-induced 44-like [Crassostrea gigas]
CGI_10011731		-1.15	serine threonine- kinase pats1
CGI_10026034		2.12	probable serine threonine- kinase pats1
CGI_10015931		2.47	ADP-ribosylation factor 1
CGI_10028634		1.34	Rho-related GTP-binding
CGI_10019413		-2.49	ADP-ribosylation factor 2 [Cucumis melo]
CGI_10014971		2.58	guanine nucleotide-binding G(s) subunit alpha-like
CGI_10018396		3.29	radical S-adenosyl methionine domain-containing 2
CGI_10015817		2.27	phosphatidylinositol 4,5-bisphosphate 3-kinase catalytic subunit alpha isoform-like
CGI_10025133		1.68	[Nematostella vectensis]
CGI_10006027		1.56	CREB-binding -like isoform X2
CGI_10021345		-2.17	Ras-related C3 botulinum toxin substrate 1
CGI_10005650		2.37	ras-related Rab-11A-like
CGI_10021171		1.44	interferon regulatory factor 2
CGI_10019528		2.27	suppressor of cytokine signaling 2-like
CGI_10027441		3.14	helicase with zinc finger domain 2-like
CGI_10000144		3.49	helicase with zinc finger domain 2-like isoform X1 [Crassostrea gigas]
CGI_10004570		-0.89	rapamycin-insensitive companion of mTOR-like
CGI_10022075		1.66	scaffold salvador-like [Biomphalaria glabrata]
CGI_10003308		0.98	MAP kinase-activated kinase 2
CGI_10010457		2.00	Ddx58 partial
CGI_10012998		1.83	Double-stranded RNA-specific adenosine deaminase

CHAPTER 3. GENERAL DISCUSSION AND FUTURE PROSPECTS

The overall objective of the present thesis was to characterize the mechanisms underpinning the association of the oyster *Crassostrea gigas* with vibrio populations in health and disease. Oysters possess a remarkable ability to maintain an immune homeostasis in presence of an abundant and diverse microbiota, which paradoxically is in close contact with immunocompetent tissues (Schmitt et al. 2012). In this state, preferential and positive associations of vibrio populations can be sustained within oysters without the development of disease. However, abiotic and biotic stressors acting on the oyster holobiont (the oyster and its associated microbiota) can trigger a dysbiosis in which the proliferation of opportunistic vibrio species leads to oyster death. In this thesis we have been interested in characterizing these two different states, which both question the tolerance of the oyster immune system and its manipulation by vibrios. The following section will discuss the thesis main results in perspective with the available literature and the future prospects derived from our conclusions.

CYTOTOXICITY AS A MEAN FOR VIBRIOS TO DAMPEN OF OYSTER IMMUNE DEFENSES

Over the past years, significant attention has been paid to the vibrio populations associated with the Pacific Oyster Mortality Syndrome (POMS) (Lemire *et al.,* 2015; Bruto *et al.,* 2017; Piel *et al.,* 2019). We studied here vibrios associated with POMS isolated from two different marine coastal environments that host important oyster farming activity, namely the bay of Brest on the French Atlantic coast and the Thau Lagoon, on the Mediterranean coast. Vibrio species pathogenic for oysters belong to the the Splendidus clade in the Atlantic (Lemire *et* al., 2015; Bruto *et* al., 2017) and to the Harveyi clade in the Thau lagoon (Oyanedel *in prep*). Remarkably in both clades, we found that virulent populations of vibrios express cytotoxicity toward oyster immune cells, the hemocytes (Rubio *et al*., 2019, Oyanedel in prep). Inside a given environment virulent vibrio species vary with time (Bruto *et al*., 2017). However, our results from **article 2**, showed that the virulent vibrio species, *V. crassostreae* and *V. tasmaniensis* are characterized by species-specific mechanisms to suppress the cellular defenses and enable systemic infections. On the opposite, non-cytotoxic strains from the same vibrio species are rapidly controlled by hemocytes through phagocytosis and cell clumping, thus preventing systemic infection. This ability to suppress oyster cellular defenses was also evidenced in *V. harveyi* **(article 3)**, a species that efficiently colonizes OsHV-1 infected oysters both in the field and in mesocosm experiments. Virulence and cytotoxicity

therefore appear closely related, probably because they determine colonization success, as we demonstrated in the Splendidus clade (Rubio *et al*., 2019).

VIBRIO SPECIES-SPECIFIC WEAPONS TO SUPPRESS OYSTER IMMUNE CELLS

Subversion of the host defenses is achieved by bacteria through several strategies including the avoidance or degradation of antimicrobial peptides, disguising of their MAMPs and manipulation of signaling pathways and vital cellular functions (Reddick and Alto, 2014), but also through more aggressive mechanisms that aim directly at the annihilation of the antimicrobial functions of the central mediator of the innate immunity, the hemocytes, achieved through the activity of toxins that are exported by bacteria into the extracellular milieu, or either injected or intracellularly delivered into target cells through specialized secretion systems (A.T. Ma *et al.*, 2009; Osorio, 2018).

As developed in article 2, determinants of cytotoxicity towards the hemocytes are species–specific and have independently evolved in *V. crassostreae* and *V. tasmaniensis*. In *V. crassostreae,* we found that cytotoxicity and virulence are highly dependent on the protein R5.7 (absent from *V. tasmaniensis*); whereas in *V. tasmaniensis* virulence and cytotoxicity are highly dependent on a type VI secretion system present in chromosome 1 ($T6SS_{Chr1\text{-}LGP32}$) (Rubio *et al*., 2019).

Bruto *et al.* (2018), evidenced that the **r5.7 gene** is ancestral in the Splendidus clade. The protein itself is not cytotoxic (Bruto *et al*., 2018); however, to mediate cytotoxicity, we found that R5.7-expressing *V. crassostreae* require physical **contact with hemocytes** (Rubio *et al*., 2019). Still, as an **extracellular pathogen,** *V. crassotreae* did not depend on internalization through phagocytosis to express cytotoxicity. Interestingly, we found that upon the loss of the ancestral *r5.7* gene, *V. tasmaniensis,* which is a **facultative intracellular pathogen of oyster hemocytes** (Duperthuy 2011), has acquired a **$T6SS_{Chr1\text{-}LGP32}$** that delivers cytotoxic effectors to oyster hemocytes intracellularly upon phagocytosis. These findings shed light on the mechanisms of *V. tasmaniensis* cytotoxicity and virulence, which both require the OmpU-mediated mechanism of phagocyte internalization and depend on the resistance of *V. tasmaniensis* to intra-phagolysosomal degradation, as necessary for this facultative intracellular pathogen (Duperthuy *et al.*, 2011; Vanhove *et al.*, 2015, 2016). So far, in the search for the putative effectors associated with the set of T6SSs identified on both species we constructed a mutant for the *evpP* ortholog identified as a potential $T6SS_{Chr1\text{-}LGP32}$ effector present in all virulent strains of *V. tasmaniensis*. EvpP is one of the three proteins secreted by the T6SS and essential for the virulence of the fish pathogen *Edwardsiella tarda* (Hu *et al.*, 2014). However, the mutant did not show any attenuation in virulence during experimental

infections but only lost cytotoxicity potential (complementary data, section II.3).

Whether or not a T6SS also participates in the cytotoxicity of *V. crassostreae* has been debated. In *V. crassostreae*, a T6SS is carried on the virulence plasmid called pGV1512, required for virulence. In our assays, we could not evidence any role of pGV1512 in *V. crassoatreae* cytotoxicity. However, the team of Frédérique Le Roux recently demonstrated the contribution of the T6SS encoded in pGV1512 to cytotoxicity, by using an alternative cytotoxicity assay that involves the contact of bacteria with the total hemocyte population in suspension (Piel *et al.*, 2019), in contrast with our assay that relies on a monolayer of adherent cells that was standardized for the phagocytosis-dependent cytotoxicity of *V. tasmaniensis* (Vanhove *et al.*, 2016). While no putative secreted effectors have been identified so far based on genomic analysis for the *V. crassostreae* $T6SS_{pGV1512}$ the authors showed that T6SS and R5.7 act independently but additively to produce cytotoxicity (Piel *et al.*, 2019).

In the cytotoxic species *V. harveyi* associated with POMS in the Thau lagoon, we have not been able to produce isogenic mutants so far, preventing us from clarifying the molecular basis of the species virulence and cytotoxicity. However, comparative genomics between populations of the Harveyi clade allowed us to hypothesize that the differential distribution of a type III secretion system in chromosome 1 (T3SS1) and putative associated cytotoxic effectors previously identified in *V. parahaemolyticus* (Broberg *et al.*, 2010; Osorio, 2018; Wu *et al.*, 2020), could contribute to the contrasted difference in cytotoxicity between *V. harveyi* and the other three populations from the same clade. Briefly, this T3SS cluster and associated putative effectors are absent from the low cytotoxic *V. rotiferianus* and *V. owensii*. In *V. harveyi* and *V. jasicida,* which both contain the T3SS structural genes, but display contrasted cytotoxicity (*V. jasicida* is not cytotoxic), the main difference that we could identify is the higher number of putative cytotoxic effector present in *V. harveyi* (Arginin ADP-ribosyl transferase, VopQ, VopR, VopS, and VPA0450) relative to *V. jasicida* (VopQ and VopS). Targeted gene deletion or invalidation of structural elements of this T3SS1 and associated putative effectors will help to clarify their respective roles in cytotoxicity and virulence. The available methods for genetic manipulation, by transfer of non-replicative suicide plasmids through conjugation, that we used in article 1 and 2, has been optimized for the Splendidus clade in model strains such as *V. tasmaniensis* LGP32 and *V. crassostreae* J2-9, therefore, similar optimization is necessary to be applied to our Harveyi collection. Recently, methods for genetic manipulation of *V. harveyi* have been successfully developed (Delavat *et al.*, 2018) which should be considered for future work in gene manipulations in Harveyi strains of interest.

Altogether our data on distinct *Vibrio* populations (*V. tasmaniensis, V. crassostreae, V. harveyi*) show that species-specific weapons are used to suppress oyster immune cells during

POMS pathogenesis. This suggests that *V. tasmaniensis, V. crassostreae,* and *V. harveyi* should be considered as opportunistic pathogens, and not simple colonizers benefiting from OsHV-1 immune suppression.

NOT ONLY VIBRIO KILLERS CAN BENEFIT FROM OSHV-1 INFECTION

In the course of the present thesis, the polymicrobial nature of the POMS was demonstrated in our laboratory (de Lorgeril *et al.,* 2018). This prompted us to adapt our infection protocols. We therefore used mesocosms as ecologically realistic experimental infections in which oysters were exposed to seawater containing the OsHV-1 virus and a *Vibrio* community, instead of classical intramuscular injections of given pathogens. This modification of our procedures allowed us to unveil novel behaviors among the vibrios associated with POMS. As we worked in a polymicrobial framework, it can happen that multiple host-bacteria and bacteria-bacteria interactions alter the within-host selective pressures acting on potential colonizers (Alizon, 2013). In article 3, our results showed that not all vibrios able to colonize oysters are cytotoxic, but some of them can benefit from the activity of the microbiota, which not only dampens the oyster immune defenses but also produces "public goods" that can be utilize by opportunistic cheaters.

We evidenced here a cheating behavior for iron acquisition (Kramer *et al.*, 2020) through vibrioferrin uptake in *V. rotiferianus*. This species, which colonizes efficiently oysters, is not cytotoxic and it has lost the vibrioferrin synthesis cluster present in *V. harveyi* while retaining the gene coding for the cognate receptor, an example of evolution of dependencies through adaptive gene loss, also known as the black queen hypothesis (Morris, 2015). We confirmed *in vitro* that growth can be restored under iron-limiting condition by the cell free extracellular products of *V. harveyi,* a vibrioferrin producer. This result leads us to propose that, as a moderately virulent and cytotoxic population, *V. rotiferianus* benefits from the compromised physiological state of the host caused by highly virulent populations like *V. harveyi* but also from the non-cooperative acquisition of public goods such as siderophores to colonize the oyster through a purely opportunistic strategy.

It will now be necessary to perform additional mesocosm experiments with isolated and specific combination of populations to answer two pending questions. (i) Does the colonization of the host by *V. rotiferianus* result of an opportunistic strategy that depends on the presence of *V. harveyi*? If so, this would confirm that the oyster could serve as a niche for the development of dependency between vibrio populations (here, killers and cheaters). (ii) What factors explain the exclusion of *V. owensii* and *V. jasicida* from oysters? Is it due to intrinsic potential disadvantages (e.g. metaolic requirements) specific or common to both populations or does it result from the interaction with the other two Harveyi populations (as

neither *V. owensii* nor *V. jasicida* express the vibrioferrin siderophore and cognate receptor synthesis genes, unlike *V. harveyi* and *V. rotiferianus*)?

SYNERGISM BETWEEN VIBRIO POPULATIONS AND OSHV-1 VIRUS

We have shown here that two of the Harveyi populations (*V. harveyi* and *V. rotiferianus*) are capable, through virulence or public good-exploitation traits, to colonize oysters under POMS. If vibrios alone did not cause mortality in our mesocosm experiments, they significantly worsened the mortality rate of oysters compared to the OsHV-1 only condition. Such a synergistic effect is a typically expected (Murray *et* al., 2014) but rarely demonstrated in ecologically-realistic experimental set-ups recapitulating the complexity of polymicrobial diseases. We have shown that OsHV-1 (de Lorgeril *et al.,* 2018) and vibrios (Rubio *et ai.,* 2019, Oyanedel, *in prep*) are pathogens that respectively manipulate or lyse hemocytes, the oyster immune cells. However, as described in Chapter 1, populations of hemocytes are diverse and still poorly characterized. Understanding synergism will now require to identify the hemocytes populations targeted by both pathogens, and the key functions consequently altered. For that, we propose the use of single cell RNAseq that should be of high interest to address these two specific questions and better understand the cellular and molecular determinants of pathogen synergism.

OSHV-1 IMMUNOSUPPRESSION AND MODIFICATION OF OYSTER AS A HABITAT

We observed here a contrasted dynamic of oyster-vibrio interaction when OsHV-1 was absent from the mesocosm (article 3). In this case, vibrio load only transiently increased in oyster tissues to later decrease by 48h without changes in the relative abundance of each of the four species of vibrio. Moreover, no significant differential gene expression was observed between naive and bacteria-only exposed oysters, as if the oyster immune system did not sense high vibrio loads when acquired through natural infection routes. This contrasts with our results in article 2, where strong transcriptional responses were induced by the injection of either virulent or non-virulent vibrios. The reason why vibrios do not induce the immune response in natural infection set-ups remains ignored. One possible hypothesis is the host production of PGRPs with amidase activity (PGRP-LB), which has been shown to suppress immune signaling confering tolerance to the microbiota, in other invertebrates (Zaidman-Rémy *et al.,* 2006).

In the absence of host transcriptomic changes, the refractiveness of oysters to a stable colonization by exogenous vibrios prompted us to speculate that the oyster represents a

highly hostile habitat to be colonized by foreign vibrios without the disruptive effect of additional factors such as the immunosuppression by OsHV-1. This is supported by our supplementary data on copper, zinc and ROS tolerance (Chapter 2, Section I,4) and discussed in more details in our minireview (article 4). This hypothesis is further supported by the transcriptional reprogramming of oysters in the presence of OsHV-1, which enables stable vibrio colonization. The observed transcriptomic response was reminiscent of POMS (de Lorgeril *et al*., 2018) with confounded responses towards OsHV-1 and vibrios. To help clarify the degree of association achieved by vibrios in healthy oysters, we now propose to track the histological localization of GFP-tagged bacteria in healthy and POMS-affected oysters, during the kinetic of exposure in the same manner than vibrios were localized by immuno-histological investigations in article 2.

CYTOTOXICITY IN *V. SPLENDIDUS* COLONIZING HEALTHY OYSTERS: A COLONIZATION RATHER THAN A VIRULENCE DETERMINANT

Bruto *et al.* (2017) determined how vibrio populations assemble from the environment into oysters during POMS episodes but also in the spring season with no occurrence of mass mortalities of farmed juvenile oysters. Through our collaboration with the team of Frédérique Le Roux, we could access to a collection of six vibrio populations distributed across seasons, that were phylogenetically characterized, genome sequenced, and with preferential potential habitats identified. Population structure of vibrios was strongly influenced by the season of isolation with a strong predominance of the virulent population *V. crassostreae* in the summer. Nonetheless, the spring season was also characterized by the positive association of *V. splendidus* populations to the oyster in a context where colonization occurs without the immunosuppressive effect of OsHV-1 and the recurrent development of disease and population structure is not biased towards the selection of phenotypes of high virulence.

We focused here on population #23 taxonomically assigned to the species *V. splendidus* (Pop#23). This population presented a moderate virulence potential compared to populations of *V. crassostreae* or the closely related but collected from summer season and carrier of the plasmid pGV1512, population *V. splendidus* #24. All the strains of Pop#23 were cytotoxic towards hemocytes *in vitro* including the strain 4G1_4 considered non-virulent (oyster survival >82% six days after injection). This strain was characterized by the absence of two loci coding for effector delivery systems, a MARTX complex and a T6SS that we show to be linked to an even higher survival of injected oysters when invalidated in a moderately virulent strain, but had no effect on cytotoxicity. We have not gone further in the frame of article 1 into the characterization of the cytoxicity determinants of *V. splendidus*. However, it

is likely that R5.7 plays a key role. In *V. crassostreae*, another species of Splendidus clade, R5.7 is not sufficient but necessary for full virulence (Bruto *et al.*, 2017, 2018) and acts independently of the presence of the $T6SS_{pGV1512}$ to cause hemocyte cytotoxicity (Piel *et al.*, 2019). As R5.7 is present in all the strains of Pop#23, we speculate that it could be responsible for cytotoxicity. While the determinants of Pop#23 cytotoxicity remains to be elucidated, we have identified that cytotoxicity towards hemocytes and the dampening of the cellular defenses of the oysters is also present in vibrios belonging to the microbiota of healthy oysters and not exclusive of highly virulent vibrios that recurrently cause systemic infection in diseased oysters. These findings further support that cytotoxicity is key in vibrios of the Splendidus clade to colonize oysters, but they also indicate that cytotoxicity is not a sufficient indicator of virulence; it rather contributes to modify the oyster towards a less hostile habitat.

TRADE-OFFS ON VIRULENCE ACTING ON VIBRIOS COLONIZING HEALTHY OYSTERS

We were intrigued by the strains of the Pop#23 that displays moderately virulence while carrying virulence factors such as an MARTX and a $T6SS_{4G4\_4}$. Comparative genomic among Pop#23 strains allowed us to identify differences in the gene content of the *wbe* cluster responsible for the synthesis of the O-antigen of the LPS. This *wbe* region is a hypervariable locus susceptible to extensive gene exchange through HGT that contributes to structural variation of the O-antigen. Due to its localization in the outer membrane, the O-antigen is subjected to selective pressures by environmental predators, and by the antimicrobial effectors of metazoan hosts (Wildschutte *et al.*, 2004; March *et al.*, 2013).

We demonstrated that while the O-antigen structure shared by moderately virulent strains confers resistance to predation by amoeba, it constrained the colonization efficiency and virulence potential of these strains. This was evidenced by the mutation of the *wbe* region that on the one hand, lowered the immunogenicity of the strain, increasing its colonization capacity and virulence potential in the oyster, but on the other hand, made it susceptible to predation by amoeba.

These results suggest that the selection for resistance to predation through O-antigen modifications can be in conflicting selection with virulence, in contrast with the coincidental selection identified in *V. tasmaniensis* LGP32 (Robino *et al*., 2019). POMS seems to select predominantly highly virulent phenotypes that seem better adapted to benefit from immunosuppressed oysters, with the exception of opportunistic cheaters identified in the Mediterranean environment (article 3). Considering that OsHV-1 rapidly transmits among susceptible populations of oysters, it is expected that in this context, host rapid killing will promote pathogen transmission to proximal permissive individuals ensuring new replicative niches for virulent populations to thrive (Fleury *et al*., 2020). In contrast, healthy juvenile oysters

are hostile to new colonizers and therefore the expression of high virulence potential leading to the killing of the host can be in this case maladaptive (Alizon and Michalakis, 2015) as it will eliminate the bacterial niche forcing vibrios to undergo colonization of immunocompetent hosts with an established and stable microbiota. Therefore, the evolution towards a moderate virulence and resistance to predation, exemplified by Pop#23, could result in a higher overall fitness than the selection for higher virulence in this particular context of association with oysters.

OPPORTUNISTIC PATHOGENS OF POMS OUTSIDE THE *VIBRIO* GENUS

Recently, culture independent studies of massive mortality episodes of oysters have allowed to identify that although vibrios are indeed present in diseased animals they are not the only bacterial group that thrive in diseased oysters affected by biotic and abiotic environmental stressors such as the OsHV-1 or high temperatures (de Lorgeril *et al.*, 2018; Green *et al.*, 2019; King *et al.*, 2019). Among them, *Arcobacter* has been recurrently found more represented in diseased oysters and also capable to benefit from the disturbance of the microbiota and physiology of the host caused by a *Vibrio* injection to dominate the microbiota associated with the hemolymph. *Arcobacter* is considered as an emerging food and waterborne pathogen capable to cause gastroenteritis in humans. *Arcobacter* species have been found in human stool samples as well as livestock and raw food from animal origin (Sekhar *et al.*, 2017) including edible mollusks with a general prevalence of 40% with the highest values in surf clams (87.4%) and the lowest in oysters (18%) (Collado *et al.*, 2014). Among *Arcobacter* spp., antimicrobial and metal resistance together with virulence factors with cytotoxic effects towards mammalian cells have been described (Brückner *et al.*, 2020). Given these characteristics it is likely that *Arcobacter* could functionally replace *Vibrio* as secondary opportunist of diseased oysters. Still, to date our knowledge of *Arcobacter* is very limited and much more investigation would be needed to demonstrate their role in disease expression. We still ignore whether strains associated with POMS express virulence potential or have an opportunistic behavior through resources acquisition. So far, the ubiquity, ease of isolation and genetic manipulability of vibrios, together with the evidences about their involvement in oyster diseases has driven the research efforts towards this group contributing without question to the understanding of disease of complex etiology such as POMS. Nonetheless, non-targeted culture-independent approximations of the dynamics of the oyster microbiota highlight the importance to consider higher order interactions and other microbial taxon when studying diseases in oysters. With the development of metatranscriptomics applied to POMS by Annick Jacq (CNRS, Orsay, France) in collaboration with Eve Toulza in our laboratory, we expect to learn more on the functional complementarity / cooperation of microbial populations contributing to the fatal outcome of POMS.

GENERAL CONCLUSION

The objective of the present thesis was to characterize the mechanisms underpinning the association of the oyster *Crassostrea gigas* with vibrio populations in health and disease. Oysters possess a remarkable ability to maintain an immune homeostasis in presence of an abundant and diverse microbiota, which paradoxically is in close contact with immunocompetent tissues (Schmitt *et al*. 2012). In this state, preferential and positive associations of vibrio populations can be sustained within oysters without the development of disease. However, abiotic and biotic stressors acting on the oyster holobiont (the oyster and its associated microbiota) can trigger a dysbiosis in which the proliferation of opportunistic vibrio species leads to oyster death (de Lorgeril, *et al*. 2018). In this thesis we have been interested in characterizing these two states, which question both the tolerance of the oyster immune system and its manipulation by vibrios.

The study of the homeostatic state led us to characterize a *V. splendidus* population associated with healthy oysters (**article 1**). We identified this population as moderately virulent, and found that the O-antigen, a major membrane determinant of Gram-negative bacteria, is subjected to important selection pressures in *V. splendidus,* which are exerted by both the host immune system and environmental predators (grazers). We indeed found that O-antigen structures that favor resistance to environmental predators result in an increased activation of the oyster immune system and a reduced virulence in that host. Our results suggest an evolution of *V. splendidus* towards moderate virulence as a compromise between fitness in the oyster as a host, and resistance to its predators in the environment. We found that not only Vibrio species are able to modulate their O-antigen structure to reduce immunogenicity but some species are also rather resistant to the host immune effectors. However, by comparing *Vibrio* species positively and negatively associated with oyster tissues we found that resistance to host antimicrobial defenses is not sufficient to colonize a healthy oyster.

In parallel, we investigated the association of vibrios when homeostasis between the immunity and the microbiota of the oyster is disrupted. We focused on several vibrio populations associated with the Pacific Oyster Mortality Syndrome. We first developed a comparative study of the mechanisms of virulence in two species *V. crassostreae* and *V. tasmaniensis* (Splendidus clade) associated with POMS in the Atlantic marine ecosystem (**article 2**). This study led to the characterization of *Vibrio* cytotoxicity as a key determinant of oyster colonization, which enables to escape from the potent host cellular defenses. We found that different species from the Splendidus clade harbor different weapons that enable

similar dampening of host immune defenses and enable systemic infections. In *V. tasmaniensis* and *V. crassotreae,* these mechanisms involve a T6SS and the protein R5.7 of unknown function, respectively. An effector of T6SS-mediated cytotoxicity toward immune cells was identified in *V. tasmaniensis.*

Finally, by characterizing vibrio populations associated with POMS in a Mediterranean oyster-farming site (**article 3**), we found that vibrios able to colonize OsHV-1 µvar-infected oysters vary according to ecosystems, but include species that express the same capacity to dampen the oyster cellular defenses using cytotoxic activities. In particular in the Thau lagoon, *V. harveyi* (adapted to elevated temperature) is a virulent species associated with POMS that synergizes with OsHV-1 µvar to accelerate oyster death. Moreover, we showed that the *Vibrio* community associated with POMS is composed of both opportunistic pathogens, like *V. harveyi*, and simple opportunists (cheaters), like *V. rotiferianus*, benefiting from the activity of the pathogens, which dampen the oyster immune defenses to facilitate the colonization and produce vibrioferrin, a siderophore that the cheaters can utilize for their own growth within diseased oysters.

Article 4 (annexe 1) provides a synthesis of our current understanding of Vibrio-bivalve interactions, which integrates the results of the present thesis and draws hypothesis that may explain the higher virulence of *Vibro* species in oysters as opposed to mussels

REFERENCES

-A-

Abdelaziz, M., Ibrahem, M.D., Ibrahim, M.A., Abu-Elala, N.M., and Abdel-moneam, D.A. (2017) Monitoring of Different Vibrio Species Affecting Marine Fishes in Lake Qarun and Gulf of Suez: Phenotypic and Molecular Characterization. *Egypt J Aquat Res* **43**: 141–146.

Alcaide, E., Gil-Sanz, C., Sanjuán, E., Esteve, D., Amaro, C., Silveira, L., et al. (2001) Vibrio harveyi Causes Disease in Seahorse, Hippocampus sp. J Fish Dis 24: 311–313.

Alizon, S. (2013) Co-infection and Super-infection Models in Evolutionary Epidemiology. *Interface Focus* **3**: 1-13.

Amaro, C. and Biosca, E.G. (1996) Vibrio vulnificus Biotype 2, Pathogenic for Eels, si Also an Opportunistic Pathogen for Humans. *Appl Environ Microbiol* **62**: 1454–1457.

-B-

Bachère, E., Gueguen, Y., Gonzalez, M., De Lorgeril, J., Garnier, J., and Romestand, B. (2004) Insights into the Anti-microbial Defense of Marine Invertebrates: The Penaeid Shrimps and the Oyster Crassostrea gigas. *Immunol Rev* **198**: 149–168.

Bachère, E., Rosa, R.D., Schmitt, P., Poirier, A.C., Merou, N., Charrière, G.M., and Destoumieux-Garzón, D. (2015) The New Insights into the Oyster Antimicrobial Defense: Cellular, Molecular and Genetic View. *Fish Shellfish Immunol* **46**: 50–64.

Baker, S.M. and Mann, R. (1994) Description of Metamorphic Phases in the Oyster Crassostrea virginica and Effects of Hypoxia on Metamorphosis. *Mar Ecol Prog Ser* **104**: 91–99.

Balebona, M.C., Moriñigo, M.A., and Borrego, J.J. (1995) Role of Extracellular Products in the Pathogenicity of Vibrio strains on Cultured Gilt-head Seabream (Sparus aurata). *Microbiologia* **11**: 439-446.

Banerjee, S.K. and Farber, J.M. (2018) Trend and Pattern of Antimicrobial Resistance In Molluscan Vibrio species Sourced to Canadian Estuaries. *Antimicrob Agents Chemother* **62**: 1–9.

Ben Cheikh, Y., Travers, M.-A., Morga, B., Godfrin, Y., Rioult, D., and Le Foll, F. (2016) First Evidence for a Vibrio strain Pathogenic to Mytilus edulis Altering Hemocyte Immune Capacities. *Dev Comp Immunol* **57**: 107–119.

Beutler, B. (2004) Innate Immunity: an Overview. *Mol Immunol* **40**: 845–859.

Bisharat, N., Agmon, V., Finkelstein, R., Raz, R., Ben-Dror, G., Lerner, L., et al. (1999) Clinical, epidemiological, and microbiological features of Vibrio vulnificus biogroup 3 causing outbreaks of wound infection and bacteraemia in Israel. Lancet 354: 1421–1424.

Binesse, J., Delsert, C., Saulnier, D., Champomier-Vergès, M.-C.C., Zagorec, M., Munier-Lehmann, H., et al. (2008) Metalloprotease Vsm Is the Major Determinant of Toxicity for Extracellular Products of Vibrio splendidus. *Appl Environ Microbiol* **74**: 7108–7117.

Bingle, C.D. and Craven, C.J. (2004) Meet the Relatives: A Family of BPI- and LBP-Related Proteins. *Trends Immunol* **25**: 53–55.

Blokesch, M. (2016) Natural Competence for Transformation. *Curr Biol* **26**: 1126–1130.

Blokesch, M. and Schoolnik, G.K. (2007) Serogroup Conversion of Vibrio cholerae in Aquatic Reservoirs. *PLoS Pathog* **3**: 733–742.

Bohannan, B.J.M. and Lenski, R.E. (2000) Linking Genetic Change to Community Evolution: Insights From Studies of Bacteria and Bacteriophage. *Ecol Lett* **3**: 362–377.

Boyd, E.F., Carpenter, M.R., Chowdhury, N., Cohen, A.L., Haines-Menges, B.L., Kalburge, S.S., et al. (2015) Post-Genomic Analysis of Members of the Family Vibrionaceae. *Microbiol Spectr* **3**: 1-26.

Brameyer, S., Rösch, T.C., El Andari, J., Hoyer, E., Schwarz, J., Graumann, P.L., and Jung, K. (2019) DNA-Binding Directs the Localization of a Membrane-Integrated Receptor of the ToxR Family. *Commun Biol* **2**: 1-10.

Broberg, C.A., Zhang, L., Gonzalez, H., Laskowski-Arce, M.A., and Orth, K. (2010) A Vibrio Effector Protein is an Inositol Phosphatase and Disrupts Host Cell Membrane Integrity. *Science* **329**: 1660–1662.

Brooks, J.F., Gyllborg, M.C., Cronin, D.C., Quillin, S.J., Mallama, C. A, Foxall, R., et al. (2014) Global Discovery of Colonization Determinants in the Squid Symbiont Vibrio fischeri. *Proc Natl Acad Sci* **111**: 17284-17289.

Broquard, C., Martinez, A.S., Maurouard, E., Lamy, J.B., and Dégremont, L. (2020) Sex Determination in the Oyster Crassostrea gigas: A large Longitudinal Study of Population Sex Ratios and Individual Sex Changes. *Aquaculture* **515**: 734555.

Bruto, M., James, A., Petton, B., Labreuche, Y., Chenivesse, S., Alunno-Bruscia, M., et al. (2017)

Vibrio crassostreae, a Benign Oyster Colonizer Turned into a Pathogen After Plasmid Acquisition. *ISME J* **11**: 1043–1052.

Bruto, M., Labreuche, Y., James, A., Piel, D., Chenivesse, S., Petton, B., et al. (2018) Ancestral Gene Acquisition as the Key to Virulence Potential in Environmental Vibrio Populations. *ISME J* **12**: 2954-2966.

-C-

Cardinaud, M., Barbou, A., Capitaine, C., Bidault, A., Dujon, A.M., Moraga, D., and Paillard, C. (2014) Vibrio harveyi Adheres to and Penetrates Tissues of the European Abalone Haliotis tuberculata Within the First Hours of Contact. *Appl Environ Microbiol* **80**: 6328–6333.

Castillo, D., Alvise, P.D., Xu, R., Zhang, F., Middelboe, M., and Gram, L. (2017) Comparative Genome Analyses of Vibrio anguillarum Strains Reveal a Link with Pathogenicity Traits. *mSystems* **2**: 1–14.

Castillo, D., Kauffman, K., Hussain, F., Kalatzis, P., Rørbo, N., Polz, M.F., and Middelboe, M. (2018) Widespread Distribution of Prophage-Encoded Virulence Factors in Marine Vibrio Communities. *Sci Rep* **8**: 2–10.

Ceccarelli, D., Amaro, C., Romalde, J.L., Suffredini, E., Vezzulli, L., and Powell, J.L. (2019) Vibrio species. In *Food Microbiology*. Doyle, M. P., Diez-González, F., and Hill, C. (eds). Washington DC: ASM Press, pp. 347–388.

Chapman, C., Henry, M., A. Bishop Lilly, K., Joy, A., Adam, B., Wagner, T., et al. (2015) Scanning the Landscape of Genome Architecture of Non-o1 and Non-o139 Vibrio cholerae by Whole Genome Mapping Reveals Extensive Population Genetic Diversity. *PLoS One* **10**: 1–15.

Chen, Y., Dai, J., Morris, J.G., and Johnson, J.A. (2010) Genetic Analysis of the Capsule Polysaccharide (K antigen) and Exopolysaccharide Genes in Pandemic Vibrio parahaemolyticus O3:K6. *BMC Microbiol* **10**: 1-10.

Chiang, Y.N., Penadés, J.R., and Chen, J. (2019) Genetic Transduction by Phages and Chromosomal Islands: The New and Noncanonical. *PLoS Pathog* **15**: 1–7.

Chibani, C.M., Roth, O., Liesegang, H., and Wendling, C.C. (2020) Genomic Variation Among Closely Related Vibrio alginolyticus Strains is Located on Mobile Genetic Elements. *BMC Genomics* **21**: 1-14.

Childers, B.M. and Klose, K.E. (2007) Regulation of Virulence in Vibrio cholerae: The ToxR

Regulon. *Future Microbiol* **2**: 335–344.

Chow, J., Lee, S.M., Shen, Y., Khosravi, A., and Mazmanian, S.K. (2010) Host-bacterial Symbiosis in Health and Disease. *Adv Immunol* **107**: 243–274.

Chow, J. and Mazmanian, S.K. (2010) A Pathobiont of the Microbiota Balances Host Colonization and Intestinal Inflammation. *Cell Host Microbe* **7**: 265–276.

Cognie, B., Haure, J., and Barillé, L. (2006) Spatial Distribution in a Temperate Coastal Ecosystem of the Wild Stock of the Farmed Oyster Crassostrea gigas (Thunberg). *Aquaculture* **259**: 249–259.

Cooper, N.R. (1985) The Classical Complement Pathway: Activation and Regulation of the First Complement Component. *Adv in Inmunol* **37**: 151-207.

Company, R., Sitj, A., Pujalte, M.J., Garay, E., Alvarez-Pellitero, P., P, J., et al. (2002) Bacterial and Parasitic Pathogens in Cultured Common dentex, Dentex dentex L. J *Fish Dis* **22**: 299–309.

Cordero, Otto X., Ventouras, L.A., DeLong, E.F., and Polz, M.F. (2012a) Public Good Dynamics Drive Evolution of Iron Acquisition Strategies in Natural Bacterioplankton Populations. *Proc Natl Acad Sci USA* **109**: 20059–20064.

Cordero, O. X., Wildschutte, H., Kirkup, B., Proehl, S., Ngo, L., Hussain, F., et al. (2012b) Ecological Populations of Bacteria Act as Socially Cohesive Units of Antibiotic Production and Resistance. *Science* **337**: 1228–1231.

Corzett, C.H., Elsherbini, J., Chien, D.M., Hehemann, J.H., Henschel, A., Preheim, S.P., et al. (2018) Evolution of a Vegetarian Vibrio: Metabolic Specialization of Vibrio breoganii to Macroalgal Substrates. *J Bacteriol* **200**: 1–10.

Cota, I., Sánchez-Romero, M.A., Hernández, S.B., Pucciarelli, M.G., García-Del Portillo, F., and Casadesús, J. (2015) Epigenetic Control of Salmonella enterica O-Antigen Chain Length: A Tradeoff between Virulence and Bacteriophage Resistance. *PLoS Genet* **11**: 1-18.

Crisan, C. V., Chande, A.T., Williams, K., Raghuram, V., Rishishwar, L., Steinbach, G., et al. (2019) Analysis of Vibrio cholerae genomes identifies new type VI secretion system gene clusters. Genome Biol 20: 1–14.

-D-

Darshanee Ruwandeepika, H.A., Karunasagar, I., Bossier, P., and Defoirdt, T. (2015) Expression and Quorum Sensing Regulation of Type III Secretion System Genes of Vibrio harveyi During Infection of Gnotobiotic Brine Shrimp. *PLoS One* **10**: 1–11.

Davidson, S.K., Koropatnick, T.A., Kossmehl, R., Sycuro, L., and McFall-Ngai, M.J. (2004) NO Means "Yes" in the Squid-Vibrio Symbiosis: Nitric oxide (NO) During the Initial Stages of a Beneficial Association. *Cell Microbiol* **6**: 1139–1151.

Davis, J.W. and Sizemore, R.K. (1982) Incidence of Vibrio Species Associated With Blue Crabs (Callinectes sapidus) Collected From Galveston Bay, Texas. *Appl Environ Microbiol* **43**: 1092–1097.

Davison, A.J., Trus, B.L., Cheng, N., Steven, A., Watson, M.S., Cunningham, C., et al. (2005) A Novel Class of Herpesvirus With Bivalve Hosts. *J Gen Virol* **86**: 41–53.

Defoirdt, T. and Sorgeloos, P. (2012) Monitoring of Vibrio harveyi Quorum Sensing Activity in Real Time During Infection of Brine Shrimp Larvae. *ISME J* **6**: 2314–2319.

Dégremont, L., Azéma, P., Maurouard, E., and Travers, M.-A. (2020) Enhancing Resistance to Vibrio aestuarianus in Crassostrea gigas by Selection. *Aquaculture* **526**: 735429.

Delavat, F., Bidault, A., Pichereau, V., and Paillard, C. (2018) Rapid and Efficient Protocol to Introduce Exogenous DNA in Vibrio harveyi and Pseudoalteromonas sp. *J Microbiol Methods* **154**: 1–5.

Deng, Y., Xu, H., Su, Y., Liu, S., Xu, L., Guo, Z., et al. (2019) Horizontal Gene Transfer Contributes to Virulence and Antibiotic Resistance of Vibrio harveyi 345 Based on Complete Genome Sequence Analysis. *BMC Genomics* **20**: 1–19.

Diederich, S., Nehls, G., van Beusekom, J.E., and Reise, K. (2005) Introduced Pacific Oysters (Crassostrea gigas) in the Northern Wadden Sea: Invasion Accelerated by Warm Summers? *Helgol Mar Res* **59**: 97–106.

Diggles, B.K., Moss, G.A., Carson, J., and Anderson, C.D. (2000) Luminous Vibriosis in Rock Lobster Jasus verreauxi (Decapoda: Palinuridae) Phyllosoma Larvae Associated with Infection Vibrio harveyi. *Dis Aquat Organ* **43:** 127–137.

Dryselius, R., Kurokawa, K., and Iida, T. (2007) Vibrionaceae, a Versatile Bacterial Family with Evolutionarily Conserved Variability. *Res Microbiol* **158**: 479–486.

Dubert, J., Barja, J.L., and Romalde, J.L. (2017) New Insights into Pathogenic Vibrios Affecting

Bivalves in Hatcheries: Present and Future Prospects. *Front Microbiol* **8**: 762.

Duinker, A. and Cranford, P.J. (2012) Variability in Particle Retention Efficiency by the Mussel mytilus Edulis. *J Exp Mar Bio Eco* **412**: 96–102.

Duperthuy, M. (2010) Effecteurs moléculaires de lassociation Crassostrea gigas / Vibrio splendidus. Rôle de la porine OmpU dans les mécanismes de résistance et déchappement à la réponse immunitaire de lhôte.

Duperthuy, M., Binesse, J., Le Roux, F., Romestand, B., Caro, A., Got, P., et al. (2010) The major outer membrane protein OmpU of Vibrio splendidus contributes to host antimicrobial peptide resistance and is required for virulence in the oyster Crassostrea gigas. Environ Microbiol 12: 951–963.

Duperthuy, M., Schmitt, P., Garzón, E., Caro, A., Rosa, R.D., Le Roux, F., et al. (2011) Use of OmpU Porins for Attachment and Invasion of Crassostrea gigas Immune Cells by the Oyster Pathogen Vibrio splendidus. *Proc Natl Acad Sci* **108**: 2993–2998.

Dupont, S., Lokmer, A., Corre, E., Auguet, J., Petton, B., Toulza, E., et al. (2020) Oyster Hemolymph is a Complex and Dynamic Ecosystem Hosting Bacteria, Protists and Viruses. *Anim Microb* **2**: 1-16.

Dy, R.L., Richter, C., Salmond, G.P.C., and Fineran, P.C. (2014) Remarkable Mechanisms in Microbes to Resist Phage Infections. *Annu Rev Virol* **1**: 307–331.

-E-

Eiler, A., Gonzalez-Rey, C., Allen, S., and Bertilsson, S. (2007) Growth Response of Vibrio cholerae and Other Vibrio spp. to Cyanobacterial Dissolved Organic Matter and Temperature in Brackish Water. *FEMS Microbiol Ecol* **60**: 411–418.

Eilers, H., Pernthaler, J., Glöckner, F.O., and Amann, R. (2000) Culturability and In Situ Abundance of Pelagic Bacteria from the North Sea. *Appl Environ Microbiol* **66**: 3044–3051.

EFSA AHAW Panel (EFSA Panel on Animal Health and Welfare), 2015. Scientific opinion on oyster mortality. *EFSA Journal* 2015; **13**:4122, 59 pp. doi:10.2903/j.efsa.2015.4122

Escapa, M., Isacch, J.P., Daleo, P., Alberti, J., Iribarne, O., Borges, M., et al. (2004) The Distribution and Ecological Effects of the Introduced Pacific Oyster Crassostrea gigas (Thunberg, 1793) in Northern Patagonia. *J Shellfish Res* **23**: 765–772.

Espejo, R.T., García, K., and Plaza, N. (2017) Insight Into the Origin and Evolution of the Vibrio parahaemolyticus Pandemic Strain. *Front Microbiol* **8**: 1397.

Evseev, G.A., Yakovlev, Y.M., and Li, X. (1996) The Anatomy of the Pacific Oyster, Crassostrea gigas (Thurnberg)(Bivalvia : Ostreidae). *Publ Seto Mar Biol Lab* **37**: 239–255.

-F-

Fabioux, C., Huvet, A., Le Souchu, P., Le Pennec, M., and Pouvreau, S. (2005) Temperature and Photoperiod Drive Crassostrea gigas Reproductive Internal Clock. *Aquaculture* **250**: 458–470.

Farmer J.J., III, Janda J.M., Brenner F.W., Cameron D.N., Birkhead K.M. (2005) Genus 1. *Vibrio* Pacini 1854, 411AL, In Bergey's Manual of Systematic Bacteriology. Brenner D.J., Krieg N.R., Staley J.T.(eds). New York, NY, USA: Springer, pp. 494–546.

Fleury, E., Barbier, P., Petton, B., Normand, J., Thomas, Y., Pouvreau, S., et al. (2020) Latitudinal drivers of oyster mortality: deciphering host, pathogen and environmental risk factors. Sci Rep 10: 1–12.

Fleury, E. and Huvet, A. (2012) Microarray Analysis Highlights Immune Response of Pacific Oysters as a Determinant of Resistance to Summer Mortality. *Mar Biotechnol* **14**: 203–217.

Fuhrmann, M., Delisle, L., Petton, B., Corporeau, C., and Pernet, F. (2018) Metabolism of the Pacific Oyster, Crassostrea gigas, is Influenced by Salinity and Modulates Survival to the Ostreid Herpesvirus OsHV-1. *Biol Open* **7**: 1-10.

-G-

Gabriel, M.W., Matsui, G.Y., Friedman, R., and Lovell, C.R. (2014) Optimization of Multilocus Sequence Analysis for Identification of Species in the Genus Vibrio. *Appl Environ Microbiol* **80**: 5359–5365.

Gay, M., Renault, T., Pons, A.M., and Le Roux, F. (2004) Two Vibrio splendidus Related Strains Collaborate to Kill Crassostrea gigas: Taxonomy and Host Alterations. *Dis Aquat Organ* **62**: 65–74.

Gerdol, M., Greco, S., and Pallavicini, A. (2019) Extensive Tandem Duplication Events Drive the Expansion of the C1q-Domain-Containing Gene Family in Bivalves. *Mar Drugs* **17**: 1–13.

Gerdol, M., Venier, P., and Pallavicini, A. (2015) The Genome of the Pacific Oyster Crassostrea gigas Brings New Insights on the Massive Expansion of the C1q Gene Family in Bivalvia.

Dev Comp Immunol **49**: 59–71.

Gillis, M., Vandamme, P., De Vos, P., Swings, J., and Kersters, K. (2015) Polyphasic Taxonomy. In Bergey's Manual of Systematics and Archaea and Bacteria. Whitman, W. B. (ed). New Jersey: John Wiley & Sons, pp. 1-10.

Ginger, K.W.K., Vera, C.B.S., R, D., Dennis, C.K.S., Adela, L.J., Yu, Z., and Thiyagarajan, V. (2013) Larval and Post-Larval Stages of Pacific Oyster (Crassostrea gigas) Are Resistant to Elevated CO2. *PLoS One* **8**: 1–12.

Go, J., Deutscher, A.T., Spiers, Z.B., Dahle, K., Kirkland, P.D., and Jenkins, C. (2017) Mass Mortalities of Unknown Aetiology in Pacific Oysters Crassostrea gigas in Port Stephens, New South Wales, Australia. *Dis Aquat Organ* **125**: 227–242.

Godfrey, L.R. (2005) General Anatomy. In *The Laboratory Primate*. Wolfe-Coote, S. (ed). United Kingdom: Elsevier, pp. 29–45.

Gomez-Gil, B., Thompson, C., Matsumura, Y., Sawabe, T., Iida, T., Christen, R., and Thompson, F. (2014) The Famlily Vibrionaceae. In *The Prokaryotes: Gammaproteobacteria*. Rosenberg, E., DeLong, E. F., Lory, S., Stackenbrandt, E., and Thompson, F. Berlin: Springer, pp. 659–747.

Gonzalez, M., Gueguen, Y., Destoumieux-Garzón, D., Romestand, B., Fievet, J., Pugnière, M., et al. (2007) Evidence of a Bactericidal Permeability Increasing Protein in an Invertebrate, the Crassostrea gigas Cg-BPI. *Proc Natl Acad Sci* **104**: 17759–17764.

Gonzalez, M., Romestand, B., Fievet, J., Huvet, A., Lebart, M.C., Gueguen, Y., and Bachère, E. (2005) Evidence in Oyster of a Plasma Extracellular Superoxide Dismutase which Binds LPS. *Biochem Biophys Res Commun* **338**: 1089–1097.

Gooday, G.W. (1990) Physiology of Microbial Degradation of Chitin and Chitosan. *Biodegradation* **1**: 177–190.

Gosling, E. (2015) Morphology of Bivalves. In *Marine Bivalve Molluscs*. New Jersey: John Wiley & Sons, pp.12–43.

Goudenège, D., Travers, M.-A., Lemire, A., Petton, B., Haffner, P., Labreuche, Y., et al. (2015) A Single Regulatory Gene is Sufficient to Alter Vibrio aestuarianus Pathogenicity in Oysters. *Environ Microbiol* **17**: 4189–4199.

Green, T.J., Helbig, K., Speck, P., and Raftos, D.A. (2016) Primed for Success: Oyster Parents Treated with Poly(I:C) Produce Offspring with Enhanced Protection Against Ostreid

Herpesvirus Type I Infection. *Mol Immunol* **78**: 113–120.

Green, E.R. and Mecsas, J. (2016) Bacterial Secretion Systems: An Overview. *Microbiol Spectr* **4**: 1–19.

Green, T.J., Raftos, D., Speck, P., and Montagnani, C. (2015) Antiviral Immunity in Marine Molluscs. *J Gen Virol* **96**: 2471–2482.

Green, T.J., Siboni, N., King, W.L., Labbate, M., Seymour, J.R., and Raftos, D. (2019) Simulated Marine Heat Wave Alters Abundance and Structure of Vibrio Populations Associated with the Pacific Oyster Resulting in a Mass Mortality Event. *Microb Ecol* **77**: 736–747.

Grimes, D.J. (2020) The Vibrios : Scavengers, Symbionts, and Pathogens from the Sea. *Microb Ecol: 1-6*.

Grize, H. and Héra, M. (1991) Introduction into France of the Japanese Oyster (Crassostrea gigas). *ICES J Mar Sci* **47**: 388–403.

Gueguen, Y., Romestand, B., Fievet, J., Schmitt, P., Destoumieux-Garzón, D., Vandenbulcke, F., et al. (2009) Oyster Hemocytes Express a Proline-Rich Peptide Displaying Synergistic Antimicrobial Activity with a Defensin. *Mol Immunol* **46**: 516–522.

-H-

Hasegawa, H., Lind, E.J., Boin, M.A., and Häse, C.C. (2008) The Extracellular Metalloprotease of Vibrio Tubiashii is a Major Virulence Factor for Pacific Oyster (Crassostrea gigas) Larvae. *Appl Environ Microbiol* **74**: 4101–4110.

Hauton, C. and Smith, V.J. (2007) Adaptive Immunity in Invertebrates: A Straw House Without a Mechanistic Foundation. *BioEssays* **29**: 1138–1146.

Henke, J.M. and Bassler, B.L. (2004) Quorum Sensing Regulates Type III Secretion in. *J Bacteriol* **186**: 3794–3805.

Hernández-Cabanyero, C. and Amaro, C. (2020) Phylogeny and life cycle of the zoonotic pathogen Vibrio vulnificus. *Environ Microbiol* doi.org/10.1111/1462-2920.15137

Herrera, C.M., Crofts, A.A., Henderson, J.C., Pingali, S.C., Davies, B.W., Stephen, M., and Trent, M.S. (2014) The Vibrio cholerae VprA-VprB Two-Component System Controls Virulence Through Endotoxin Modification. *MBio* **5**: 1-13.

Hispano, C., Nebra, Y., and Blanch, A.R. (1997) Isolation of Vibrio harveyi From an Ocular

Lesion in the Short Sunfish (Mola mola). *Bull Eur Assoc Fish Pathol* **17**: 104–107.

Hiyoshi, H., Wangdi, T., Lock, G., Saechao, C., Raffatellu, M., Cobb, B.A., and Bäumler, A.J. (2018) Mechanisms to Evade the Phagocyte Respiratory Burst Arose by Convergent Evolution in Typhoidal Salmonella serovars. *Cell Rep* **22**: 1787–1797.

Hood, M.I. and Skaar, E.P. (2012) Nutritional Immunity: Transition Metals at the Pathogen-Host Interface. *Nat Rev Microbiol* **10**: 525–537.

Hu, W., An, G., Sivaraman, J., Leung, K.Y., and Mok, Y.K. (2014) A Disordered Region in the EvpP Protein from the Type VI Secretion System of Edwardsiella Tarda is Essential for EvpC Binding. *PLoS One* **9**: 1–11.

Huang, B., Zhang, L., Xu, F., Tang, X., Li, L., Wang, W., et al. (2019) Oyster Versatile IKKa/βs Are Involved in Toll-Like Receptor and RIG-I-Like Receptor Signaling for Innate Immune Response. *Front Immunol* **10**: 1826.

Hubert, C.L. and Michell, S. (2020) A Universal Oyster Infection Model Demonstrates that Vibrio vulnificus Type 6 Secretion Systems Have Antibacterial Activity in vivo. *Environ Microbiol* doi.org/10.1111/1462-2920.15123

Hunt, D.E., David, L.A., Gevers, D., Preheim, S.P., Alm, E.J., and Polz, M.F. (2008) Resource Partitioning and Sympatric Differentiation Among Closely Related Bacterioplankton. *Science* **320**: 1081–1085.

Hussa, E.A., O'Shea, T.M., Darnell, C.L., Ruby, E.G., and Visick, K.L. (2007) Two-Component Response Regulators of Vibrio fischeri: Identification, Mutagenesis, and Characterization. *J Bacteriol* **189**: 5825–5838.

-I-

Itoh, N., Kamitaka, R., Takahashi, K.G., and Osada, M. (2010a) Identification and Characterization of Multiple β-glucan Binding Proteins in the Pacific Oyster, Crassostrea gigas. *Dev Comp Immunol* **34**: 445–454.

Itoh, N., Okada, Y., Takahashi, K.G., and Osada, M. (2010b) Presence and Characterization of Multiple Mantle lysozymes in the Pacific Oyster, Crassostrea gigas. *Fish Shellfish Immunol* **29**: 126–135.

Itoh, N. and Takahashi, K.G. (2008) Distribution of Multiple Peptidoglycan Recognition Proteins in the Tissues of Pacific Oyster, Crassostrea gigas. *Comp Biochem Physiol - B Biochem Mol*

Biol **150**: 409–417.

Izutsu, K., Kurokawa, K., Tashiro, K., Kuhara, S., Hayashi, T., Honda, T., and Iida, T. (2008) Comparative Genomic Analysis Using Microarray Demonstrates a Strong Correlation Between the Presence of the 80-Kilobase Pathogenicity Island and Pathogenicity in Kanagawa Phenomenon-Positive Vibrio parahemolyticus Strains. *Infect Immun* **76**: 1016–1023.

-J-

Jana, B., Fridman, C.M., Bosis, E., and Salomon, D. (2019) A Modular Effector with a DNase Domain and a Marker for T6SS Substrates. *Nat Commun* **10**: 3595.

Jani, A.J. and Cotter, P.A. (2010) Type VI Secretion: Not Just for Pathogenesis Anymore. *Cell Host Microbe* **8**: 2–6.

Jemaa, M., Morin, N., Cavelier, P., Cau, J., Strub, J.M., and Delsert, C. (2014) Adult Somatic Progenitor Cells and Hematopoiesis in Oysters. *J Exp Biol* **217**: 3067–3077.

Jia, Z., Zhang, H., Jiang, S., Wang, M., Wang, L., and Song, L. (2016) Comparative Study of Two Single CRD C-Type Lectins, CgCLec-4 and CgCLec-5, from Pacific Oyster Crassostrea gigas. *Fish Shellfish Immunol* **59**: 220–232.

Jiang, S., Jia, Z., Zhang, T., Wang, L., Qiu, L., Sun, J., and Song, L. (2016) Functional Characterisation of Phagocytes in the Pacific Oyster Crassostrea gigas. *PeerJ* **4**: 1-18.

Johnson, C.N. (2013) Fitness Factors in Vibrios: A Mini-review. *Microb Ecol* **65**: 826–851.

Johnson, T.L., Fong, J.C., Rule, C., Rogers, A., Yildiz, F.H., and Sandkvist, M. (2014) The Type II Secretion System Delivers Matrix Proteins for Biofilm Formation by Vibrio cholerae. *J Bacteriol* **196**: 4245–4252.

Jones, M.K. and Oliver, J.D. (2009) Vibrio vulnificus: Disease and Pathogenesis. *Infect Immun* **77**: 1723–1733.

Jung, K., Fabiani, F., Hoyer, E., and Lassak, J. (2018) Bacterial Transmembrane Signalling Systems and their Engineering for Biosensing. *Open Biol* **8**: 1-12.

-K-

Kashimoto, T., Ueno, S., Hanajima, M., Hayashi, H., Akeda, Y., Miyoshi, S., et al. (2003) Vibrio vulnificus Induces Macrophage Apoptosis In Vitro and In Vivo. *Infect Immun* **71**: 533–535.

Kennedy, R.J. and Roberts, D. (1999) A Survey of the Current Status of the Flat Oyster Ostrea edulis in Strangford Lough, Northern Ireland, with a View to the Restoration of its Oyster Beds. *Biol Environ* **99**: 79–88.

Keyhani, N.O. and Roseman, S. (1999) Physiological Aspects of Chitin Catabolism in Marine Bacteria. *Biochim Biophys Acta - Gen Subj* **1473**: 108–122.

King, W.L., Jenkins, C., Go, J., Siboni, N., Seymour, J.R., and Labbate, M. (2019) Characterisation of the Pacific Oyster Microbiome During a Summer Mortality Event. *Microb Ecol* **77**: 502–512.

Knirel, Y.A., Prokhorov, N.S., Shashkov, A.S., Ovchinnikova, O.G., Zdorovenko, E.L., Liu, B., et al. (2015) Variations in O-antigen biosynthesis and O-acetylation Associated with Altered Phage Sensitivity in Escherichia coli 4s. *J Bacteriol* **197**: 905–912.

Konovalova, A., Petters, T., and Søgaard-Andersen, L. (2010) Extracellular Biology of Myxococcus xanthus. *FEMS Microbiol Rev* **34**: 89–106.

Kramer, J., Özkaya, Ö., and Kümmerli, R. (2020) Bacterial Siderophores in Community and Host Interactions. *Nat Rev Microbiol* **18**: 152–163.

Kraxberger-Beatty, T., McGarey, D.J., Grier, H.J., Lim, D. V., T., K.-B., McGarey, D.J., et al. (1990) Vibrio harveyi, an Opportunistic Pathogen of Common Snook, Centropomus Undecimalis (Bloch), held in captivity. *J Fish Dis* **13**: 557–560.

-L-

Labreuche, Y., Lambert, C., Soudant, P., Boulo, V., Huvet, A., and Nicolas, J.-L.L. (2006a) Cellular and Molecular Hemocyte Responses of the Pacific Oyster, Crassostrea gigas, Following Bacterial Infection with Vibrio aestuarianus Strain 01/32. *Microbes Infect* **8**: 2715–2724.

Labreuche, Y., Le Roux, F., Henry, J., Zatylny, C., Huvet, A., Lambert, C., et al. (2010) Vibrio aestuarianus Zinc Metalloprotease Causes Lethality in the Pacific Oyster Crassostrea gigas and Impairs the Host Cellular Immune Defenses. *Fish Shellfish Immunol* **29**: 753–758.

Labreuche, Y., Soudant, P., Gonçalves, M., Lambert, C., and Nicolas, J.-L. (2006b) Effects of Extracellular Products from the Pathogenic Vibrio aestuarianus Strain 01/32 on Lethality and Cellular Immune Responses of the Oyster Crassostrea gigas. *Dev Comp Immunol* **30**: 367–379.

Lafont, M., Goncalves, P., Guo, X., Montagnani, C., Raftos, D., and Green, T. (2019)

Transgenerational Plasticity and Antiviral Immunity in the Pacific Oyster (Crassostrea gigas) Against Ostreid Herpesvirus 1 (OsHV-1). *Dev Comp Immunol* **91**: 17–25.

Lafont, M., Petton, B., Vergnes, A., Pauletto, M., Segarra, A., Gourbal, B., and Montagnani, C. (2017) Long-Lasting Antiviral Innate Immune Priming in the Lophotrochozoan Pacific Oyster, Crassostrea gigas. *Sci Rep* **7**: 13143.

Lafont, M., Vergnes, A., Vidal-Dupiol, J., de Lorgeril, J., Gueguen, Y., Haffner, P., et al. (2020) A Sustained Immune Response Supports Long-Term Antiviral Immune Priming in the Pacific Oyster, Crassostrea gigas. *MBio* **11**: e02777-19.

Lasa, A., di Cesare, A., Tassistro, G., Borello, A., Gualdi, S., Furones, D., et al. (2019) Dynamics of the Pacific Oyster Pathobiota During Mortality Episodes in Europe Assessed by 16S rRNA Gene Profiling and a New Target Enrichment Next-Generation Sequencing Strategy. *Environ Microbiol* **21**: 4548–4562.

Law Whyte, L., David, G., Rothery, B., Law Whyte, L., David, G., and Rothery, B. (2018) Antimicrobial Peptides of Multicellular Organisms. *Universe Exp* **415**: 63–74.

Le Roux, F. and Blokesch, M. (2018) Eco-evolutionary Dynamics Linked to Horizontal Gene Transfer in Vibrios. *Annu Rev Microbiol* **72**: 89–110.

Le Roux, F., Wegner, K.M., Baker-Austin, C., Vezzulli, L., Osorio, C.R., Amaro, C., et al. (2015) The Emergence of Vibrio Pathogens in Europe: Ecology, Evolution, and Pathogenesis (Paris, 11–12th March 2015). *Front Microbiol* **6**: 830.

Le Roux, F., Wegner, K.M., and Polz, M.F. (2016) Oysters and Vibrios as a Model for Disease Dynamics in Wild Animals. *Trends Microbiol* **24**: 568–580.

Lee, C. Te, Chen, I.T., Yang, Y.T., Ko, T.P., Huang, Y.T., Huang, J.Y., et al. (2015) The Opportunistic Marine Pathogen Vibrio parahaemolyticus Becomes Virulent by Acquiring a Plasmid that Expresses a Deadly Toxin. *Proc Natl Acad Sci U S A* **112**: E5445.

Lee, K.K., Liu, P.C., and Huang, C.Y. (2003) Vibrio parahaemolyticus Infectious for Both Humans and Edible Mollusk Abalone. *Microbes Infect* **5**: 481–485.

Lemire, A., Goudenege, D., Versigny, T., Petton, B., Calteau, A., Labreuche, Y., et al. (2015) Populations, not Clones, are the Unit of Vibrio Pathogenesis in Naturally Infected Oysters. *ISME J* **9**: 1523–1531.

Lepuschitz, S., Baron, S., Larvor, E., Granier, S.A., Pretzer, C., Mach, R.L., et al. (2019) Phenotypic and Genotypic Antimicrobial Resistance Traits of Vibrio cholerae Non-

O1/Non-O139 Isolated From a Large Austrian Lake Frequently Associated With Cases of Human Infection. *Front Microbiol* **10**: 1–9.

Li, G. and Wang, M.Y. (2020) The Role of Vibrio Vulnificus Virulence Factors and Regulators in its Infection-Induced Sepsis. *Folia Microbiol* **65**: 265–274.

Li, H., Kong, N., Sun, J., Wang, W., Li, M., Gong, C., et al. (2019) A C1qDC (CgC1qDC-6) with a Collagen-Like Domain Mediates Hemocyte Phagocytosis and Migration in Oysters. *Dev Comp Immunol* **98**: 157–165.

Li, J., Zhang, Y.Y., Zhang, Y.Y., Xiang, Z., Tong, Y., Qu, F., and Yu, Z. (2014) Genomic Characterization and Expression Analysis of Five Novel IL-17 Genes in the Pacific Oyster, Crassostrea gigas. *Fish Shellfish Immunol* **40**: 455–465.

Li, Y., Song, X., Wang, W., Wang, L., Yi, Q., Jiang, S., et al. (2017) The Hematopoiesis in Gill and its Role in the Immune Response of Pacific Oyster Crassostrea gigas Against Secondary Challenge with Vibrio splendidus. *Dev Comp Immunol* **71**: 59–69.

Li, Y., Sun, J., Zhang, Y., Wang, M., Wang, L., and Song, L. (2019) CgRel Involved in Antibacterial Immunity by Regulating the Production of CgIL17s and CgBigDef1 in the Pacific Oyster Crassostrea gigas. *Fish Shellfish Immunol*.

Lindell, K., Fahlgren, A., Hjerde, E., Willassen, N.-P., Fällman, M., and Milton, D.L. (2012) Lipopolysaccharide O-antigen Prevents Phagocytosis of Vibrio anguillarum by Rainbow Trout (Oncorhynchus mykiss) Skin Epithelial Cells. *PLoS One* **7**: e37678–e37678.

Lo, H.R., Lin, J.H., Chen, Y.H., Chen, C.L., Shao, C.P., Lai, Y.C., and Hor, L.I. (2011) RTX Toxin Enhances the Survival of Vibrio vulnificus During Infection by Protecting the Organism from Phagocytosis. *J Infect Dis* **203**: 1866–1874.

Lokmer, A., Goedknegt, M.A., Thieltges, D.W., Fiorentino, D., Kuenzel, S., Baines, J.F., and Wegner, K.M. (2016a) Spatial and Temporal Dynamics of Pacific Oyster Hemolymph Microbiota across Multiple Scales. *Front Microbiol* **7**: 1367.

Lokmer, A., Kuenzel, S., Baines, J.F., and Wegner, K.M. (2016b) The Role of Tissue-Specific Microbiota in Initial Establishment Success of Pacific Oysters. *Environ Microbiol* **18**: 970–987.

Lokmer, A. and Mathias Wegner, K. (2015) Hemolymph Microbiome of Pacific Oysters in Response to Temperature, Temperature Stress and Infection. *ISME J* **9**: 670–682.

de Lorgeril, J., Lucasson, A., Petton, B., Toulza, E., Montagnani, C., Clerissi, C., et al. (2018)

Immune-Suppression by OsHV-1 Viral Infection Causes Fatal Bacteraemia in Pacific Oysters. *Nat Commun* **9**: 4215.

de Lorgeril, J. De, Petton, B., Lucasson, A., Perez, V., Stenger, P., Dégremont, L., et al. (2020) Differential Basal Expression of Immune Genes Confers Crassostrea gigas Resistance to Pacific Oyster Mortality Syndrome. *BMC Genomics* **21** :63

de Lorgeril, J., Zenagui, R., Rosa, R.D., Piquemal, D., and Bachère, E. (2011) Whole Transcriptome Profiling of Successful Immune Response to Vibrio Infections in the Oyster Crassostrea gigas by Digital Gene Expression Analysis. *PLoS One* **6**: e23142–e23142.

Lu, J., Shi, Y., Cai, S., and Feng, J. (2017) Metabolic Responses of Haliotis Diversicolor to Vibrio parahaemolyticus Infection. *Fish Shellfish Immunol* **60**: 265–274.

Lupo, C., Travers, M.-A., Tourbiez, D., Barthélémy, C.F., Beaunée, G., and Ezanno, P. (2019) Modeling the Transmission of Vibrio gestuarianus in Pacific Oysters Using Experimental Infection Data. *Front Vet Sci* **6**: 1–15.

Lv, Z., Qiu, L., Wang, M., Jia, Z., Wang, W., Xin, L., et al. (2018) Comparative Study of Three C1q Domain Containing Proteins from Pacific Oyster Crassostrea gigas. *Dev Comp Immunol* **78**: 42–51.

-M-

Ma, A.T., McAuley, S., Pukatzki, S., and Mekalanos, J.J. (2009) Translocation of a Vibrio cholerae Type VI Secretion Effector Requires Bacterial Endocytosis by Host Cells. *Cell Host Microbe* **5**: 234–243.

Ma, Z., Jacobson, F.E., and Giedroc, D.P. (2009) Metal Transporters and Metal Sensors: How Coordination Chemistry Controls Bacterial Metal Homeostasis. *October* **109**: 4644–4681.

Maeshima, N. and Fernandez, R.C. (2013) Recognition of Lipid A Variants by the TLR4-MD-2 Receptor Complex. *Front Cell Infect Microbiol* **4**: 1–13.

Makino, K., Oshima, K., Kurokawa, K., Yokoyama, K., Uda, T., Tagomori, K., et al. (2003) Genome Sequence of Vibrio parahaemolyticus: A Pathogenic Mechanism Distinct from that of V cholerae. *Lancet* **361**: 743–749.

Martins, N.E. (2020) Towards a Mechanism for Poly(I.C) Antiviral Priming in Oysters. *MBio* **11**: 1–4.

Matsumoto, T., Nakamura, A.M., and Takahashi, K.G. (2006) Cloning of cDNAs and

Hybridization Analysis of Lysozymes from Two Oyster Species, Crassostrea gigas and Ostrea edulis. *Comp Biochem Physiol - B Biochem Mol Biol* **145**: 325–330.

Matz, C. and Kjelleberg, S. (2005) Off the Hook - How Bacteria Survive Protozoan Grazing. *Trends Microbiol* **13**: 302–307.

Melillo, D., Marino, R., Italiani, P., and Boraschi, D. (2018) Innate Immune Memory in Invertebrate Metazoans: A Critical Appraisal. *Front Immunol* **9**:1915.

Merrell, D.S. and Falkow, S. (2004) Frontal and Stealth Attack Strategies in Microbial Pathogenesis. *Nature* **430**: 250–256.

Metzger, L.C. and Blokesch, M. (2016) Regulation of Competence-Mediated Horizontal Gene Transfer in the Natural Habitat of Vibrio cholerae. *Curr Opin Microbiol* **30**: 1–7.

Milton, D.L. (2006) Quorum Sensing in Vibrios: Complexity for Diversification. *Int J Med Microbiol* **296**: 61–71.

Milutinović, B. and Kurtz, J. (2016) Immune Memory in Invertebrates. *Semin Immunol* **28**: 328–342.

Minamino, T. and Imada, K. (2015) The Bacterial Flagellar Motor and its Structural Diversity. *Trends Microbiol* **23**: 267–274.

Mohamad, N., Amal, M.N.A., Saad, M.Z., Yasin, I.S.M., Zulkiply, N.A., Mustafa, M., and Nasruddin, N.S. (2019) Virulence-Associated Genes and Antibiotic Resistance Patterns of Vibrio spp. Isolated from Cultured Marine Fishes in Malaysia. *BMC Vet Res* **15**: 1–13.

Montagnani, C., Kappler, C., Reichhart, J.M., and Escoubas, J.M. (2004) Cg-Rel, the First Rel/NF-κB Homolog Characterized in a Mollusk, the Pacific Oyster Crassostrea gigas. *FEBS Lett* **561**: 75–82.

Morris, R.J. (2015) Black Queen hypothesis. *ISME J* **3**: 2085-2091.

Mouriño-Pérez, R.R., Worden, A.Z., and Azam, F. (2003) Growth of Vibrio cholerae O1 in Red Tide Waters off California. *Appl Environ Microbiol* **69**: 6923–6931.

Mukhopadhyay, S. and Gordon, S. (2004) The Role of Scavenger Receptors in Pathogen Recognition and Innate Immunity. *Immunobiology* **209**: 39–49.

Mukhtar, M.S., Carvunis, A., Dreze, M., Epple, P., Steinbrenner, J., Moore, J., et al. (2011) Plant Immune System Network. *Science* **333**: 596–601.

Munro, J., Oakey, J., Bromage, E., and Owens, L. (2003) Experimental Bacteriophage-Mediated Virulence in Strains of Vibrio harveyi. *Dis Aquat Organ* **54**: 187–194.

Murray, J.L., Connell, J.L., Stacy, A., Turner, K.H., and Whiteley, M. (2014) Mechanisms of synergy in polymicrobial infections. J Microbiol 52: 188–199.

-N-

Nakasone, N. and Iwanaga, M. (1998) Characterization of Outer Membrane Protein OmpU of Vibrio cholerae O1. *Infect Immun* **66**: 4726–4728.

Nasu, H., Iida, T., Sugahara, T., Yamaichi, Y., Park, K.S., Yokoyama, K., et al. (2000) A Filamentous Phage Associated with Recent Pandemic Vibrio parahaemolyticus O3:K6 Strains. *J Clin Microbiol* **38**: 2156–2161.

Navarro-Garcia, F., Ruiz-Perez, F., Cataldi, Á., and Larzábal, M. (2019) Type VI Secretion System in Pathogenic Escherichia coli: Structure, Role in Virulence, and Acquisition. *Front Microbiol* **10**: 1–17.

Nyholm, S. V. and McFall-Ngai, M.J. (2004) The Winnowing: Establishing the Squid - Vibrios Symbiosis. *Nat Rev Microbiol* **2**: 632–642.

-O-

Okada, K., Iida, T., Kita-Tsukamoto, K., and Honda, T. (2005) Vibrios Commonly Possess Two Chromosomes. *J Bacteriol* **187**: 752–757.

O'Shea, Y.A. and Boyd, E.F. (2002) Mobilization of the Vibrio Pathogenicity Island between Vibrio cholerae Isolates Mediated by CP-T1 Generalized Transduction. *FEMS Microbiol Lett* **214**: 153–157.

Osorio, C.R. (2018) T3SS Effectors in Vibrios: Homology in Sequence, Diversity in Biological Functions? *Virulence* **9**: 721–723.

Osunla, C.A. and Okoh, A.I. (2017) Vibrio Pathogens: A Public Health Concern in Rural Water Resources in Sub-Saharan Africa. *Int J Environ Res Public Health* **14**: 1–27.

-P-

Payne, S.M., Mey, A.R., and Wyckoff, E.E. (2016) Vibrio Iron Transport: Evolutionary Adaptation to Life in Multiple Environments. *Microbiol Mol Biol Rev* **80**: 69–90.

Peña-Navarro, N., Castro-Vásquez, R., Vargas-Leitón, B., and Dolz, G. (2020) Molecular

Detection of Acute Hepatopancreatic Necrosis Disease (AHPND) in Penaeus vannamei Shrimps in Costa Rica. *Aquaculture* **523**: 735190.

Pernet, F., Barret, J., Le Gall, P., Corporeau, C., Dégremont, L., Lagarde, F., et al. (2012) Mass Mortalities of Pacific Oysters Crassostrea gigas Reflect Infectious Diseases and Vary with Farming Practices in the Mediterranean Thau Lagoon, France. *Aquac Environ Interact* **2**: 215-237.

Pernet, F., Lagarde, F., Gall, P. Le, and D'Orbcastel, E.R. (2014) Associations Between Farming Practices and Disease Mortality of Pacific Oyster Crassostrea gigas in a Mediterranean Lagoon. *Aquac Environ Interact*.

Pernthaler, J. (2005) Predation on Prokaryotes in the Water Column and its Ecological Implications. *Nat Rev Microbiol* **3**: 537–546.

Petton, B., Boudry, P., Alunno-Bruscia, M., and Pernet, F. (2015) Factors Influencing Disease-Induced Mortality of Pacific Oysters Crassostrea gigas. *Aquac Environ Interact* **6**: 205–222.

Petton, B., de Lorgeril, J., Mitta, G., Daigle, G., Pernet, F., and Alunno-Bruscia, M. (2019) Fine-Scale Temporal Dynamics of Herpes Virus and Vibrios in Seawater During a Polymicrobial Infection in the Pacific Oyster Crassostrea gigas. *Dis Aquat Organ* **135**: 97–106.

Petton, B., Pernet, F., Robert, R.R., and Boudry, P. (2013) Temperature Influence on Pathogen Transmission and Subsequent Mortalities in Juvenile Pacific Oysters Crassostrea gigas. *Aquac Environ Interact* **3**: 257–273.

Piel, D., Bruto, M., James, A., Labreuche, Y., Lambert, C., Janicot, A., et al. (2019) Selection of Vibrio crassostreae Relies on a Plasmid Expressing a Type 6 Secretion System Cytotoxic for Host Immune Cells. *Environ Microbiol*: 1-14.

Popovic, T., Fields, P.I., Olsvik, O., Wells, J.G., Evins, G.M., Cameron, D.N., et al. (1995) Molecular Ubtyping of Toxigenic Vibrio cholerae o139 Causing Epidemic Cholera in India and Bangladesh, 1992-1993. *J Infect Dis* **171**: 122–127.

Preheim, S.P., Boucher, Y., Wildschutte, H., David, L.A., Veneziano, D., Alm, E.J., and Polz, M.F. (2011a) Metapopulation Structure of Vibrionaceae Among Coastal Marine Invertebrates. *Environ Microbiol* **13**: 265–275.

Preheim, S.P., Timberlake, S., and Polz, M.F. (2011b) Merging Taxonomy with Ecological Population Prediction in a Case Study of Vibrionaceae. *Appl Environ Microbiol* **77**: 7195–

7206.

Pruzzo, C., Gallo, G., and Canesi, L. (2005) Persistence of Vibrios in Marine Bivalves: The Role of Interactions with Haemolymph Components. *Environ Microbiol* **7**: 761–772.

Pukatzki, S., Ma, A.T., Sturtevant, D., Krastins, B., Sarracino, D., Nelson, W.C., et al. (2006) Identification of a Conserved Bacterial Protein Secretion System in Vibrio cholerae Using the Dictyostelium Host Model System. *Proc Natl Acad Sci U S A* **103**: 1528–1533.

-R-

Randall, R.E. and Goodbourn, S. (2008) Interferons and Viruses: An Interplay Between Induction, Signalling, Antiviral Responses and Virus countermeasures. *J Gen Virol* **89**: 1–47.

Reddick, L.E. and Alto, N.M. (2014) Bacteria Fighting Back: How Pathogens Target and Subvert the Host Innate Immune System. *Mol Cell* **54**: 321–328.

Reen, F.J., Almagro-Moreno, S., Ussery, D., and Boyd, E.F. (2006) The Genomic Code: Inferring Vibrionaceae Niche Specialization. *Nat Rev Microbiol* **4**: 697–704.

Rehnstam, A.S., Bäckman, S., Smith, D.C., Azam, F., and Hagström, Å. (1993) Blooms of Sequence-Specific Culturable Bacteria in the Sea. *FEMS Microbiol Lett* **102**: 161–166.

Renault, T. (2016) Malacoherpesviruses of Mollusks, In Aquaculture Virology. Kibenge, F. S. B. and Godoy, M. G. (eds). United Kingdom: Elsevier, pp.513-524.

Ringgaard, S., Yang, W., Alvarado, A., Schirner, K., and Briegel, A. (2018) Chemotaxis Arrays in Vibrio Species and their Intracellular Positioning by the ParC/ParP System. *J Bacteriol* **200**: 1–15.

Roberts, S., Gueguen, Y., de Lorgeril, J., and Goetz, F. (2008) Rapid Accumulation of an Interleukin 17 Homolog Transcript in Crassostrea Gigas Hemocytes Following Bacterial Exposure. *Dev Comp Immunol* **32**: 1099–1104.

Robino, E., Poirier, A.C., Amraoui, H., Le Bissonnais, S., Perret, A., Lopez-Joven, C., et al. (2019) Resistance of the Oyster Pathogen Vibrio tasmaniensis LGP32 Against Grazing by Vannella sp. Marine Amoeba Involves Vsm and CopA Virulence Factors. *Environ Microbiol* doi:10.1111/1462-2920.14770.

Robinson, A.N. and Green, T.J. (2020) Fitness Costs Associated with Maternal Immune Priming in the Oyster. *Fish Shellfish Immunol* **103**: 32–36.

Rodrigues, S., Paillard, C., Van Dillen, S., Tahrioui, A., Berjeaud, J.M., Dufour, A., and Bazire, A.

(2018) Relation Between Biofilm and Virulence in Vibrio tapetis: A Transcriptomic Study. *Pathogens* **7**: 1–15.

Romalde, J.L., Diéguez, A.L., Lasa, A., and Balboa, S. (2014) New Vibrio Species Associated to Molluscan Microbiota: A Review. *Front Microbiol* **4**: 1–11.

Rowley, A.F. and Powell, A. (2007) Invertebrate Immune Systems–Specific, Quasi-Specific, or Nonspecific? *J Immunol* **179**: 7209–7214.

Ruby, E.G. and Lee, K.H. (1998) The Vibrio fischeri-Euprymna Scolopes Light Organ Association: Current Ecological Paradigms. *Appl Environ Microbiol* **64**: 805–812.

Russell, A.B., Peterson, S.B., and Mougous, J.D. (2014) Type VI Secretion System Effectors: Poisons with a Purpose. *Nat Rev Microbiol* **12**: 137–148.

Ruwandeepika, H.A.D., Bhowmick, P.P., Karunasagar, I., Bossier, P., and Defoirdt, T. (2011) Quorum Sensing Regulation of Virulence Gene Expression in Vibrio harveyi In Vitro and In Vivo During Infection of Gnotobiotic Brine Shrimp Larvae. *Environ Microbiol Rep* **3**: 597–602.

-S-

Sadler, A.J. and Williams, B.R.G. (2008) Interferon-Inducible Antiviral Effectors. *Nat Rev Immunol* **8**: 559–568.

Saeed, M.O.O. (1995) Association of Vibrio harveyi with Mortalities in Cultured Marine Fish in Kuwait. *Aquaculture* **136**: 21–29.

Sanchez, A. and Gore, J. (2013) Feedback Between Population and Evolutionary Dynamics Determines the Fate of Social Microbial Populations. *PLoS Biol* **11**: e1001547.

Satake, H. and Sekiguchi, T. (2012) Toll-Like Receptors of Deuterostome Invertebrates. *Front Immunol* **3**: 1–7.

Saulnier, D., De Decker, S., Haffner, P., Cobret, L., Robert, M., and Garcia, C. (2010) A Large-Scale Epidemiological Study to Identify Bacteria Pathogenic to Pacific Oyster Crassostrea gigas and Correlation Between Virulence and Metalloprotease-Like Activity. *Microb Ecol* **59**: 787–798.

Sawabe T (2006) The Mutual Partnership Between Vibrio halioticoli and Abalones. In: The biology of Vibrios. Thompson FL, Austin B, Swings J (eds). Washington, D.C: ASM Press, pp. 219–230.

Sawabe, T., Kita-Tsukamoto, K., and Thompson, F.L. (2007) Inferring the Evolutionary History of Vibrios by Means of Multilocus Sequence Analysis. *J Bacteriol* **189**: 7932–7936.

Sawabe, T.T., Ogura, Y., Matsumura, Y., Feng, G., Rohul Amin, A.K.M., Mino, S., et al. (2013) Updating the Vibrio Clades Defined by Multilocus Sequence Phylogeny: Proposal of Eight New Clades, and the Description of Vibrio tritonius sp. nov. *Front Microbiol* **4**: 1–14.

Scarano, C., Spanu, C., Ziino, G., Pedonese, F., Dalmasso, A., Spanu, V., et al. (2014) Antibiotic Resistance of Vibrio Species Isolated from Sparus aurata Reared in Italian Mariculture. *New Microbiol* **37**: 329–337.

Schleicher, T.R. and Nyholm, S. V. (2011) Characterizing the Host and Symbiont Proteomes in the Association Between the Bobtail Squid, Euprymna scolopes, and the bacterium, Vibrio fischeri. *PLoS One* **6**: e25649.

Schmitt, P., Duperthuy, M., Montagnani, C., Bachère, E., and Destoumieux-Garzón, D. (2011) Immune Responses in the Pacific Oyster Crassostrea gigas: An Overview with Focus on Summer Mortalities. In *Oysters: Physiology, Ecological dristribution and Mortality*. Qin, J. G. (ed). New York: Nova Science Publishers, pp. 227-273.

Schmitt, P., de Lorgeril, J., Gueguen, Y., Destoumieux-Garzón, D., and Bachère, E. (2012a) Expression, Tissue Localization and Synergy of Antimicrobial Peptides and Proteins in the Immune Response of the Oyster Crassostrea gigas. *Dev Comp Immunol* **37**: 363–370.

Schmitt, P., Rosa, R.D., Duperthuy, M., de Lorgeril, J., Bachère, E., Destoumieux-Garzón, D., et al. (2012b) The Antimicrobial Defense of the Pacific Oyster, Crassostrea gigas. How Diversity May Compensate for Scarcity in the Regulation of Resident/Pathogenic Microflora. *Front Microbiol* **3**: 160.

Schwartzman, J.A., Lynch, J.B., Flores Ramos, S., Zhou, L., Apicella, M.A., Yew, J.Y., and Ruby, E.G. (2019) Acidic pH Promotes Lipopolysaccharide Modification and Alters Colonization in a Bacteria–Animal Mutualism. *Mol Microbiol* **112**: 1326–1338.

Schaller, G.E., Shiu, S.H., and Armitage, J.P. (2011) Two-component systems and their co-option for eukaryotic signal transduction. *Curr Biol* **21**: R320–R330.

Lo Scrudato, M. and Blokesch, M. (2012) The Regulatory Network of Natural Competence and Transformation of Vibrio cholerae. *PLoS Genet* **8**: e1002778.

Nguyen, A.N., Disconzi, E., Charrière, G.M., Destoumieux-Garzón, D., Bouloc, P., et al. (2018) csrB Gene Duplication Drives the Evolution of Redundant Regulatory Pathways

Controlling Expression of the Major Toxic Secreted Metalloproteases in Vibrio tasmaniensis LGP32. *mSphere* **3**: e00582-18.

Segarra, A., Pépin, J.F., Arzul, I., Morga, B., Faury, N., and Renault, T. (2010) Detection and Description of a Particular Ostreid Herpesvirus 1 Genotype Associated with Massive Mortality Outbreaks of Pacific Oysters, Crassostrea gigas, in France in 2008. *Virus Res* **153**: 92–99.

Shapiro, B.J., Friedman, J., Cordero, O.X., Preheim, S.P., Timberlake, S.C., Szabó, G., et al. (2012) Population Genomics of Early Events in the Ecological Differentiation of Bacteria. *Science* **336**: 48–51.

Shapiro, B.J. and Polz, M.F. (2015) Microbial Speciation. *Cold Spring Harb Perspect Biol* **7**: 1–22.

Sikora, A.E. (2013) Proteins Secreted Via the Type II Secretion System: Smart Strategies of Vibrio cholerae to Maintain Fitness in Different Ecological Niches. *PLoS Pathog* **9**: (2)

Silva, A.J., Pham, K., and Benitez, J.A. (2003) Haemagglutinin/Protease Expression and Mucin Gel Penetration in El Tor Biotype Vibrio cholerae. *Microbiology* **149**: 1883–1891.

Sloup, R.E., Konal, A.E., Severin, G.B., Korir, M.L., Bagdasarian, M.M., Bagdasarian, M., and Waters, C.M. (2017) Cyclic Di-GMP and VpsR Induce the Expression of Type II Secretion in Vibrio cholerae. *J Bacteriol* **199**: e00106-17.

Song, X., Wang, H., Chen, H., Sun, M., Liang, Z., Wang, L., and Song, L. (2016) Conserved Hemopoietic Transcription Factor Cg-SCL Delineates Hematopoiesis of Pacific Oyster Crassostrea gigas. *Fish Shellfish Immunol* **51**: 180–188.

de Souza Santos, M. and Orth, K. (2014) Intracellular Vibrio parahaemolyticus Escapes the Vacuole and Establishes a Replicative Niche in the Cytosol of Epithelial Cells. *MBio* **5**: e01506-14.

Sozhamannan, S., Deng, Y.K., Li, M., Sulakvelidze, A., Kaper, J.B., Johnson, J.A., et al. (1999) Cloning and Sequencing of the Genes Downstream of the wbf Gene Cluster of Vibrio cholerae Serogroup O139 and Analysis of the Junction Genes in Other Serogroups. *Infect Immun* **67**: 5033–5040.

Speare, L., Cecere, A.G., Guckes, K.R., Smith, S., Wollenberg, M.S., Mandel, M.J., et al. (2018) Bacterial Symbionts use a Type VI Secretion System to Eliminate Competitors in their Natural Host. *Proc Natl Acad Sci* **115**: E8528–E8537.

Sperandio, V., Giron, J.A., Silveira, W.D., and Kaper, J.B. (1995) The OmpU Outer Membrane

Protein, A Potential Adherence Factor of Vibrio cholerae. *Infect Immun* **63**: 4433–4438.

Spohn, R., Daruka, L., Lázár, V., Martins, A., Vidovics, F., Grézal, G., et al. (2019) Integrated Evolutionary Analysis Reveals Antimicrobial Peptides with Limited Resistance. *Nat Commun* **10**: 1–13.

Stabili, L., Acquaviva, M.I., and Cavallo, R.A. (2005) Mytilus Galloprovincialis Filter Feeding on the Bacterial Community in a Mediterranean Coastal Area (Northern Ionian Sea, Italy). *Water Res* **39**: 469–477.

Stagličić, N., Šegvić-Bubić, T., Ezgeta-Balić, D., Bojanić Varezić, D., Grubišić, L., Žuvić, L., et al. (2020) Distribution Patterns of Two Co-Existing Oyster Species in the Northern Adriatic Sea: The Native European Flat Oyster Ostrea edulis and the Non-Native Pacific Oyster Magallana gigas. *Ecol Indic* **113**: 106233.

Steimle, A., Autenrieth, I.B., and Frick, J.S. (2016) Structure and Function: Lipid A Modifications in Commensals and Pathogens. *Int J Med Microbiol* **306**: 290–301.

Stones, D.H. and Krachler, A.M. (2016) Against the Tide: The Role of Bacterial Adhesion in Host Colonization. *Biochem Soc Trans* **44**: 1571–1580.

Strand, Å., Waenerlund, A., and Lindegarth, S. (2011) High Tolerance of the Pacific Oyster (Crassostrea gigas, Thunberg) to Low Temperatures. *J Shellfish Res* **30**: 733–735.

Strom, M.S. and Paranjpye, R.N. (2000) Epidemiology and Pathogenesis of Vibrio vulnificus. *Microbes Infect* **2**: 177–188.

Sullivan, T.J. and Neigel, J.E. (2018) Effects of Temperature and Salinity on Prevalence and Intensity of Infection of Blue Crabs, Callinectes sapidus, by Vibrio cholerae, V. parahaemolyticus, and V. vulnificus in Louisiana. *J Invertebr Pathol* **151**: 82–90.

Sun, J., Wang, L, Wu, Z., Han, S., Wang, L, Li, M., et al. (2019) P38 is Involved in Immune Response by Regulating Inflammatory Cytokine Expressions in the Pacific Oyster Crassostrea gigas. *Dev Comp Immunol* **91**: 108–114.

Sun, S., Kjelleberg, S., and McDougald, D. (2013) Relative Contributions of Vibrio Polysaccharide and Quorum Sensing to the Resistance of Vibrio cholerae to Predation by Heterotrophic Protists. *PLoS One* **8**: e56338–e56338.

Sun, Y., Zhou, Z., Wang, L., Yang, C., Jianga, S., and Song, L. (2014) The Immunomodulation of a Novel Tumor Necrosis Factor (CgTNF-1) in Oyster Crassostrea gigas. *Dev Comp*

Immunol **45**: 291–299.

-T-

Takahashi, K.G., Izumi-Nakajima, N., and Mori, K. (2017) Unique Phagocytic Properties of Hemocytes of Pacific Oyster Crassostrea gigas Against Yeast and Yeast Cell-Wall Derivatives. *Fish Shellfish Immunol* **70**: 575–582.

Takemura, A.F., Chien, D., and Polz, M. (2014) Associations and Dynamics of Vibrionaceae in the Environment, From the Genus to the Population Level. *Front Microbiol* **5**: 38.

Takemura, A.F., Corzett, C.H., Hussain, F., Arevalo, P., Datta, M., Yu, X., et al. (2017) Natural Resource Landscapes of a Marine Bacterium Reveal Distinct Fitness-Determining Genes Across the Genome. *Environ Microbiol* **19**: 2422–2433.

Takeuchi, T., Koyanagi, R., Gyoja, F., Kanda, M., Hisata, K., Fujie, M., et al. (2016) Bivalve-Specific Gene Expansion in the Pearl Oyster Genome: Implications of Adaptation to a Sessile Lifestyle. *Zool Lett* **2**: 1–13.

Tendencia, E.A. (2002) Vibrio harveyi Isolated from Cage-cultured Seabass Lates calcarifer Bloch in the Philippines. *Aquac Res* **33**: 455–458.

Tamplin, M.L. and Capers, G.M. (1992) Persistence of Vibrio vulnificus in tissues of Gulf Coast oysters, Crassostrea virginica, exposed to seawater disinfected with UV light. Appl Environ Microbiol 58: 1506–1510.

Thompson, C.C., Vicente, A.C.P., Souza, R.C., Vasconcelos, A.T.R., Vesth, T., Alves, N., et al. (2009) Genomic Taxonomy of Vibrios. *BMC Evol Biol* **9**: 1–16.

Tirapé, A., Bacque, C., Brizard, R., Vandenbulcke, F., and Boulo, V. (2007) Expression of Immune-Related Genes in the Oyster Crassostrea gigas During Ontogenesis. *Dev Comp Immunol* **31**: 859–873.

Travers, M.-A., Boettcher Miller, K., Roque, A., and Friedman, C.S. (2015) Bacterial Diseases in Marine Bivalves. *J Invertebr Pathol* **131**: 11–31.

-U-

Ubertini, M., Lagarde, F., Mortreux, S., Gall, P. Le, Chiantella, C., Fiandrino, A., et al. (2017) Gametogenesis, Spawning Behavior and Larval Abundance of the Pacific Oyster Crassostrea gigas in the Thau Lagoon: Evidence of an Environment-Dependent Strategy.

Aquaculture **473**: 51–61.

Ulrich, L.E. and Koonin, E. V (2005) One-Component Systems Dominate Signal Transduction in Prokaryotes. *Trends Microbiol* **13**: 52–56.

Uribe-Quero, E. and Rosales, C. (2017) Control of Phagocytosis by Microbial Pathogens. *Front Immunol* **8**: 1–23.

-V-

Vanhove, A.S., Duperthuy, M., Charrière, G.M., Le Roux, F., Goudenège, D., Gourbal, B., et al. (2015) Outer Membrane Vesicles are Vehicles for the Delivery of Vibrio tasmaniensis Virulence Factors to Oyster Immune Cells. *Environ Microbiol* **17**: 1152–1165.

Vanhove, A.S., Rubio, T.P., Nguyen, A.N., Lemire, A., Roche, D., Nicod, J., et al. (2016) Copper Homeostasis at the Host Vibrio Interface: Lessons from Intracellular Vibrio Transcriptomics. *Environ Microbiol* **18**: 875–888.

VanInsberghe, D., Arevalo, P., Chien, D., and Polz, M.F. (2020) How Can Microbial Population Genomics Inform Community Ecology? *Philos Trans R Soc B Biol Sci* **375**:.

Vaughn, C.C. and Hoellein, T.J. (2018) Bivalve Impacts in Freshwater and Marine Ecosystems. *Annu Rev Ecol Evol Syst* **49**: 183–208.

Veldhoen, M. (2017) Interleukin 17 is a Chief Orchestrator of Immunity. *Nat Immunol* **18**: 612–621.

Verma, J., Bag, S., Saha, B., Kumar, P., Ghosh, T.S., Dayal, M., et al. (2019) Genomic Plasticity Associated with Antimicrobial Resistance in Vibrio cholerae. *Proc Natl Acad Sci U S A* **116**: 6226–6231.

Verma, S.C. and Miyashiro, T. (2013) Quorum sensing in the squid-Vibrio symbiosis. *Int J Mol Sci* **14**: 16386–16401.

Vezzulli, L., Stagnaro, L., Grande, C., Tassistro, G., Canesi, L., and Pruzzo, C. (2018) Comparative 16SrDNA Gene-Based Microbiota Profiles of the Pacific Oyster (Crassostrea gigas) and the Mediterranean Mussel (Mytilus galloprovincialis) from a Shellfish Farm (Ligurian Sea, Italy). *Microb Ecol* **75**: 495–504.

Vigneron, V., Solliec, G., Montanié, H., and Renault, T. (2004) Detection of Ostreid Herpesvirus 1 (OsHV-1) DNA in Seawater by PCR: Influence of Water Parameters in Bioassays. *Dis Aquat Organ* **62**: 35–44.

Visick, K.L. and Skoufos, L.M. (2001) Two-Component Sensor Required for Normal Symbiotic Colonization of Euprymna scolopes by Vibrio fischeri. *J Bacteriol* **183**: 835–842.

Vogt, G. (2012). Hidden Treasures in Stem Cells of Indeterminately Growing Bilaterian Invertebrates. Stem. *Cell. Rev*. **8**: 305-317

-W-

Wang, H., Naseer, N., Chen, Y., Zhu, A.Y., Kuai, X., Galagedera, N., et al. (2017) OxyR2 Modulates OxyR1 Activity and Vibrio cholerae Oxidative Stress Response. *Infect Immun* **85**: e00929-16.

Wang, L., Huang, M., Zhang, H., and Song, L. (2011) The Immune Role of C-Type Lectins in Molluscs. *ISJ-Invertebrate Surviv J* **8**: 241–246.

Wang, L., Song, X., and Song, L. (2018) The Oyster Immunity. *Dev Comp Immunol* **80**: 99–118.

Wang, L., Zhang, H., Wang, M., Zhou, Z., Wang, W., Liu, R., et al. (2019) The Transcriptomic Expression of Pattern Recognition Receptors: Insight into Molecular Recognition of Various Invading Pathogens in Oyster Crassostrea gigas. *Dev Comp Immunol* **91**: 1–7.

Wang, L., Zhang, H., Wang, L., Zhang, D., Lv, Z., Liu, Z., et al. (2017) The RNA-Seq Analysis Suggests a Potential Multi-Component Complement System in *Oyster* Crassostrea gigas. *Dev Comp Immunol* **76**: 209–219.

Wang, W., Li, M., Wang, L., Chen, H., Liu, Z., Jia, Z., et al. (2017) The Granulocytes are the Main Immunocompetent Hemocytes in Crassostrea gigas. *Dev Comp Immunol* **67**: 221–228.

Wang, W., Liu, R., Zhang, T., Zhang, R., Song, X., Wang, L., and Song, L. (2015) A Novel Phagocytic Receptor (CgNimC) from Pacific Oyster Crassostrea gigas with Lipopolysaccharide and Gram-Negative Bacteria Binding Activity. *Fish Shellfish Immunol* **43**: 103–110.

Wang, W., Wang, L., Liu, Z., Song, X., Yi, Q., Yang, C., and Song, L. (2020) The Involvement of TLR Signaling and Anti-Bacterial Effectors in Enhanced Immune Protection of Oysters After Vibrio splendidus Pre-Exposure. *Dev Comp Immunol* **103**: 103498.

Wang, W., Zhang, T., Wang, L., Xu, J., Li, M., Zhang, A., et al. (2016) A New Non-Phagocytic TLR6 with Broad Recognition Ligands from Pacific Oyster Crassostrea gigas. *Dev Comp Immunol* **65**: 182–190.

Watve, S., Barrasso, K., Jung, S.A., Davis, K.J., Hawver, L.A., Khataokar, A., et al. (2020) Parallel

Quorum-Sensing System in Vibrio cholerae Prevents Signal Interference Inside the Host. *PLoS Pathog* **16**: 1–27.

Weil, A. A. and LaRocque, R.C. (2012) Cholera and Other Vibrios. In Hunter's Tropical Medicine and Emerging Infectious Diseases. Ryan, E. T., Solomon, T., Endy, T. P., Hill, D. R., and Aronson, N. E. (eds). United Kingdom: Elsevier, pp. 486-491.

Weynberg, K.D., Voolstra, C.R., Neave, M.J., Buerger, P., and Van Oppen, M.J.H. (2015) From Cholera to Corals: Viruses as Drivers of Virulence in a Major Coral Bacterial Pathogen. *Sci Rep* **5**: 1–9.

Whitaker, W.B., Parent, M.A., Boyd, A., Richards, G.P., and Boyd, E.F. (2012) The Vibrio parahaemolyticus ToxRS Regulator is Required for Stress Tolerance and Colonization in a Novel Orogastric Streptomycin-Induced Adult Murine Model. *Infect Immun* **80**: 1834–1845.

Wildschutte, H., Preheim, S.P., Hernandez, Y., and Polz, M.F. (2010) O-Antigen Diversity and Lateral Transfer of the wbe Region Among Vibrio splendidus Isolates. *Environ Microbiol* **12**: 2977–2987.

Williams, T.C., Blackman, E.R., Morrison, S.S., Gibas, C.J., and Oliver, J.D. (2014) Transcriptome Sequencing Reveals the Virulence and Environmental Genetic Programs of Vibrio vulnificus Exposed to Host and Estuarine Conditions. *PLoS One* **9**: 1–27.

Worden, A.Z., Seidel, M., Smriga, S., Wick, A., Malfatti, F., Bartlett, D., and Azam, F. (2006) Trophic Regulation of Vibrio cholerae in Coastal Marine Waters. *Environ Microbiol* **8**: 21–29.

Wu, C., Zhao, Z., Liu, Y., Zhu, X., Liu, M., Luo, P., and Shi, Y. (2020) Type III Secretion 1 Effector Gene Diversity Among Vibrio Isolates From Coastal Areas in China. *Front Cell Infect Microbiol* **10**: 1–11.

-X-

Xin, L., Zhang, H., Zhang, R., Li, H., Wang, W., Wang, L., et al. (2015) CgIL17-5, An Ancient Inflammatory Cytokine in Crassostrea gigas Exhibiting the Heterogeneity Functions Compared with Vertebrate Interleukin17 Molecules. *Dev Comp Immunol* **53**: 339–348.

-Y-

Yamaura, K., Takahashi, K.G., and Suzuki, T. (2008) Identification and Tissue Expression Analysis of C-type Lectin and Galectin in the Pacific Oyster, Crassostrea gigas. *Comp Biochem*

Physiol - B Biochem Mol Biol **149**: 168–175.

Yang, X., Long, M., and Shen, X. (2018) Effector–Immunity Pairs Provide the T6SS Nanomachine its Offensive and Defensive Capabilities. *Molecules* **23**: 1009.

Yildiz, F.H. and Visick, K.L. (2009) Vibrio Biofilms: So Much the Same Yet so Different. *Trends Microbiol* **17**: 109–118.

-Z-

Zhang, L., Li, L., Guo, X., Litman, G.W., Dishaw, L.J., and Zhang, G. (2015) Massive Expansion and Functional Divergence of Innate Immune Genes in a Protostome. *Sci Rep* **5**: 1–11.

Zhang, L.L., Li, L., and Zhang, G.F. (2012) Sequence Variability of Fibrinogen-Related Proteins (FREPs) in Crassostrea gigas. *Chinese Sci Bull* **57**: 3312–3319.

Zhang, T., Qiu, L., Sun, Z., Wang, L., Zhou, Z., Liu, R., et al. (2014) The Specifically Enhanced Cellular Immune Responses in Pacific Oyster (Crassostrea gigas) Against Secondary Challenge with Vibrio splendidus. *Dev Comp Immunol* **45**: 141–150.

Zhang, Y., He, X., Li, X., Fu, D., Chen, J., and Yu, Z. (2011) The Second Bactericidal Permeability Increasing Protein (BPI) and its Revelation of the Gene Duplication in the Pacific Oyster, Crassostrea gigas. *Fish Shellfish Immunol* **30**: 954–963.

Zhang, H., Wang, L., Song, L., Song, X., Wang, B., Mu, C., and Zhang, Y. (2009) A Fibrinogen-related Protein from Bay Scallop Argopecten irradians Involved in Innate Immunity as Pattern Recognition Receptor. *Fish Shellfish Immunol* **26**: 56–64.

Zhang, Y.Y., Yu, F., Li, J., Tong, Y., Zhang, Y.Y., and Yu, Z. (2014) The First Invertebrate RIG-I-Like Receptor (RLR) Homolog Gene in the Pacific Oyster Crassostrea gigas. *Fish Shellfish Immunol* **40**: 466–471.

Zhang, S.M., Zeng, Y., and Loker, E.S. (2008) Expression Profiling and Binding Properties of Fibrinogen-related Proteins (FREPs), Plasma Proteins from the Schistosome Snail Host Biomphalaria glabrata. *Innate Immun* **14**: 175–189.

Zhu, S., Nishikino, T., Hu, B., Kojima, S., Homma, M., and Liu, J. (2017) Molecular Architecture of the Sheathed Polar Flagellum in Vibrio alginolyticus. *Proc Natl Acad Sci USA* **114**: 10966–10971.

ANNEXE 1 ARTICLE N°4 *VIBRIO*-BIVALVE INTERACTIONS IN HEALTH AND DISEASE

By Delphine Destoumieux-Garzón[1*], Laura Canesi[2], **Daniel Oyanedel[1]**, Marie-Agnès Travers[1], Guillaume M. Charrière[1], Carla Pruzzo[2], Luigi Vezzulli[2*]

environmental microbiology

Environmental Microbiology (2020) **00**(00), 00–00 doi:10.1111/1462-2920.15055

Special Issue Article

Vibrio–bivalve interactions in health and disease

Delphine Destoumieux-Garzón,[1*] **Laura Canesi**,[2] **Daniel Oyanedel**,[1] **Marie-Agnès Travers**,[1] **Guillaume M. Charrière**,[1] **Carla Pruzzo**[2] **and Luigi Vezzulli**[2*]

[1]*IHPE, Université de Montpellier, CNRS, Ifremer, Université de Perpignan Via Domitia, Montpellier, France.*

[2]*DISTAV, Department of Earth, Environment and Life Sciences, University of Genoa, Genoa, Italy.*

Summary

In the marine environment, bivalve mollusks constitute habitats for bacteria of the *Vibrionaceae* family. Vibrios belong to the microbiota of healthy oysters and mussels, which have the ability to concentrate bacteria in their tissues and body fluids, including the hemolymph. Remarkably, these important aquaculture species respond differently to infectious diseases. While oysters are the subject of recurrent mass mortalities at different life stages, mussels appear rather resistant to infections. Thus, *Vibrio* species are associated with the main diseases affecting the worldwide oyster production. Here, we review the current knowledge on *Vibrio*–bivalve interaction in oysters (*Crassostrea* sp.) and mussels (*Mytilus* sp.). We discuss the transient versus stable associations of vibrios with their bivalve hosts as well as technical issues limiting the monitoring of these bacteria in bivalve health and disease. Based on the current knowledge of oyster/mussel immunity and their interactions with *Vibrio* species pathogenic for oyster, we discuss how differences in immune effectors could contribute to the higher resistance of mussels to infections. Finally, we review the multiple strategies evolved by pathogenic vibrios to circumvent the potent immune defences of bivalves and how key virulence mechanisms could have been positively or negatively selected in the marine environment through interactions with predators.

Received 30 March, 2020; revised 28 April, 2020; accepted 29 April, 2020. *For correspondence. E-mail ddestoum@ifremer.fr E-mail luigi.vezzulli@unige.it; Tel. +33 467 14 46 25

Introduction

Animal–bacteria association has a long evolutionary history that could go as far back as to the origins of multicellularity (McFall-Ngai *et al*., 2013). The presence of complex host-associated microbial communities is a characteristic shared by most animal species (Fraune and Bosch, 2010) and the type of interactions that they establish with their host can range from mutualistic to pathogenic. The capacity for microbes to colonize a host depends on both host and microbial determinants. On the one hand, healthy metazoans control their microbial environment with physical and chemical barriers, which from early stages of development shape the assemblage of their associated microbiota [for review see (Bevins and Salzman, 2011; McFall-Ngai *et al*., 2013)]. On the other hand, microbes have evolved strategies to overcome a series of innate immune mechanisms conserved across metazoans, which control both infections and host–microbiome homeostasis (Brennan and Gilmore, 2018).

In marine environments, metazoans constitute habitats for bacteria of the *Vibrionaceae* family (vibrios). These γ-proteobacteria are ubiquitous in marine and brackish environments representing one of the most abundant culturable fraction of the marine microbial community (Ceccarelli *et al*., 2019). They possess a high colonization potential partially due to their metabolic versatility and genetic variability (Le Roux *et al*., 2016). Their associations with plants, algae, zooplankton and other animals have been widely documented (Takemura *et al*., 2014; Le Roux and Blokesch, 2018). In particular, some species of mollusks have established very intimate associations with *Vibrio* species, as illustrated by the mutualistic symbiosis of the squid *Euprymna scolopes* (Cephalopod) and *Vibrio fischeri* (McFall-Ngai, 2014). Bivalves, such as the oyster *Crassostrea gigas*, were shown to host a diversity of *Vibrio* populations, defined as members of the same species sharing a common gene pool and habitat (Le Roux *et al*., 2016), in both health and disease (Bruto *et al*., 2017). *Vibrio* associations with bivalves can be also

neutral. Indeed, as filter feeders straining food particles from the seawater, bivalves accumulate exogenous bacteria, often transiently (Froelich and Oliver, 2013). Moreover, *Vibrio* species attach to the chitinaceous surfaces of invertebrates, which provide a nutrient-rich habitat (Hunt *et al*., 2008a, 2008b), but do not always colonize their tissues. However, intimate interactions have also been described. Recently, evidence of co-evolution between vibrios and bivalves has been acquired in natural oyster beds (Wegner *et al*., 2019).

Parasitic interactions are among the most documented *Vibrio*–bivalve associations, as they cause major damages to the host (Goudenège *et al*., 2015; Lemire *et al*., 2015; Bruto *et al*., 2018; Dias *et al*., 2018), with important consequences on the sustainability of the shellfish farming industry (Travers *et al*., 2015). A key question for predicting and managing disease is whether *Vibrio* associations with bivalves result from specific (genome-encoded) abilities or disability to colonize these animal species and how much they depend on environmental constraints. A series of genetic determinants favouring bivalve colonization and disease expression have been identified in vibrios so far (Duperthuy *et al*., 2011; Lemire *et al*., 2015; Bruto *et al*., 2017; Rubio *et al*., 2019). They will be reviewed here in detail. Among environmental factors, the temperature is known to significantly affect the *Vibrio* communities associated with bivalves (Alfaro *et al*., 2019). In fact, vibrios are strongly thermo-dependent and many species thrive in warm water exceeding 17°C (Stauder *et al*., 2010; Ceccarelli *et al*., 2019). The threat posed by vibrios to the shellfish industry can be thus exacerbated by the impact of climate change, in particular sea surface warming, on their global spread (Vezzulli *et al*., 2016; Baker-Austin *et al*., 2017). Additional effects include the temperature-dependent expression of virulence factors and the modifications of host physiology (reproductive effort, immune status, etc.) (Travers *et al*., 2009), which in bivalves can indirectly favour colonization by opportunistic vibrios (Le Roux *et al*., 2016).

In this review, we will focus on the oyster *Crassostrea gigas* and the mussels *Mytilus edulis* and *Mytilus galloprovincialis*, which are bivalves of economic interest and ecological relevance with widely documented interactions with a diversity of vibrios. We will discuss successively *Vibrio* associations with bivalves, the key role of bivalve cellular defences in controlling vibrios, the multiple adaptive strategies of vibrios to their bivalve hosts, and the role of the biotic environment in the selection (both positive and negative) of adapted genotypes.

Vibrios as key components of bivalve microbiota

Vibrios account for a significant proportion of bacteria found in healthy and diseased bivalves, where they can reach concentrations about 100-fold higher than those in ambient water (DePaola *et al*., 1990; Šolić *et al*., 1999; Shen *et al*., 2009). Approaches to study *Vibrio* communities include both culture-dependent protocols and global DNA sequencing approaches. Whole-body homogenates or single tissues (e.g. hemolymph, gut and hepatopancreas) are often analysed. A large fraction of these bacteria might go undetected using culture-dependent methods due to metabolic requirements and culture conditions (e.g. food source, temperature and generation time). Sequencing-based approaches allow to overcome most of the problems related to cultivation (Lokmer and Mathias Wegner, 2015; Lokmer *et al*., 2016a, 2016b) and to access hidden non-culturable vibrios. However, species-level resolution among genetically related *Vibrio* species is often poor using the most commonly employed 16S rRNA marker, thereby limiting the fine-scale evaluation of taxonomic heterogeneity within the genus (Poretsky *et al*., 2014; King *et al*., 2019). Additional phylogenetic markers such as the heat shock protein hsp60 (Jesser and Noble, 2018; King *et al*., 2019) were proposed as alternatives to 16S-barcoding to discriminate members of the *Vibrio* genus more precisely. Still, one single marker often provides insufficient resolution, due to the high genomic plasticity of vibrios (Le Roux and Blokesch, 2018), and culture-dependent methods coupled to multiple locus sequence analyses (MLSA) or core gene phylogenies are generally required for finest resolution analysis (Sawabe *et al*., 2013).

Vibrios associated with bivalves

Over the past 30 years, many studies carried out in different geographical areas have highlighted the complex structure of *Vibrio* populations commonly associated with bivalves (Romalde *et al*., 2014; Chen *et al*., 2016; Bruto *et al*., 2017). Species belonging to the clades Splendidus and Harveyi are among the most frequently found in association with healthy oysters and mussels (Romalde *et al*., 2014; Le Roux *et al*., 2016). Their concentration, diversity and dynamics depend strongly on environmental parameters, such as temperature and salinity (Romalde *et al*., 2014).

Most of our knowledge on vibrios associated with bivalves derives from studies focusing on pathological contexts. Indeed, a number of bacterial species, which include many *Vibrio* species, have been associated with mortality outbreaks of cultivated bivalves (oysters, clams and mussels) (Saulnier *et al*., 2010; Travers *et al*., 2015; Le Roux *et al*., 2016; Dubert *et al*., 2017). These *Vibrio* species can be primary pathogens, e.g. capable of causing pathological changes associated with disease in a healthy bivalve, or opportunistic pathogens, which cause

disease when bivalves are compromised by a break in protective barriers or immunosuppression.

Expression of *Vibrio* diseases depends on host factors, essentially host genetics (species, population), life stage (larval, juvenile or adult form) and life-history traits, e.g. co-infection by other pathogens (viruses as for example), the weakening of immune capacity due to environmental stressors (Zannella *et al*., 2017), or immune priming following the previous encounter with vibrios (Zhang *et al*., 2014; Rey-Campos *et al*., 2019).

Thanks to highly developed oyster production systems that go from hatcheries to nurseries and grow-out farming, we have a good knowledge of *Vibrio* species infecting different developmental stages of *Crassostrea* sp. Vibrios associated with diseases in oyster spat and/or larvae include bacteria belonging to the species *V. anguillarum*, *V. alginolyticus*, *V. tubiashii*/*V. europaeus*, *V. ostreicida*, *V. coralliilyticus*, *V. neptunius*, *V. bivalvicida*, and to the Splendidus clade (for review see Romalde and Barja, 2010; Travers *et al*., 2015; Dubert *et al*., 2017). Closely related species of the Splendidus clade (e.g. *V. splendidus*, *V. tasmaniensis*, *V. cyclitrophicus* and *V. crassostreae*) have been repeatedly isolated from *C. gigas* juveniles (<12 months old) affected by the Pacific Oyster Mortality Syndrome (POMS) triggered by the Ostreid herpesvirus OsHV-1 µVar (Lemire *et al*., 2015; Bruto *et al*., 2017; de Lorgeril *et al*., 2018). *Vibrio aestuarianus* (Anguillarum clade) was found to cause mass mortality of adult *C. gigas* in France since 2001 and since 2011 in Ireland, Scotland and Spain (Garnier *et al*., 2008; Garcia *et al*., 2014; Travers *et al*., 2017)

High taxonomic resolution analysis of the bivalve pathobiota applied on healthy and diseased *C. gigas* samples using a new target enrichment next-generation sequencing approach revealed the dominance of primary pathogens such as *V. aestuarianus* or OsHV-1 in tissues of diseased *C. gigas* collected during mass mortality events affecting juveniles and/or adults at different European farming sites (Lasa *et al*., 2019). Albeit at lower relative abundance, other bacterial species were exclusively identified in infected oysters, particularly *Vibrio* sp. (*V. alginolyticus*, *V. coralliilyticus*, *V. crassostreae*, *V. splendidus* and *V. tasmaniensis*) and *Arcobacter* sp.

Thorough studies on vibrios pathogenic for oysters have shown that the functional unit of pathogenesis can be a clone (e.g. *V. aestuarianus*), a population (e.g. *V. crassostreae*) or a consortium, and this is further complicated by *Vibrio* interactions with the host microbiota (Le Roux *et al*., 2016). Recently, de Lorgeril and colleagues (2018) demonstrated that the POMS is caused by multiple infections with an initial and necessary step involving OsHV-1 µVar. The virus leads the host to enter an immuno-compromised state preceding the invasion by opportunistic pathogenic bacteria (including pathogenic vibrios) that kill the oyster. It can be speculated that POMS-associated mortalities are caused by multiple species/populations of pathogens (e.g. *Vibrio*, *Arcobacter* sp.) that collaborate to kill oysters (Russell and Cavanaugh, 2017; de Lorgeril *et al*., 2018), but the role of the non-virulent microbiota should not be neglected as non-virulent *Vibrio* strains have the potential to dramatically increase the host damages caused by virulent strains (Lemire *et al*., 2015). The role of these bacterial consortia should be deeply analysed in future functional studies to shed light on the mechanisms underlying polymicrobial infections in bivalves (Lasa *et al*., 2019).

In contrast to oyster diseases, less information is available on pathogenic *Vibrio* diseases affecting mussels (*Mytilus* spp.), which are also other important farmed bivalves. Actually, although mussels can concentrate vibrios in their tissues (Stabili *et al*., 2005), they are considered particularly resistant to microbial infections, in particular vibrioses (Lupo and Le Bouquin, 2019). They rarely experience mass mortalities (Domeneghetti *et al*., 2014; Romero *et al*., 2014) although recent outbreaks of unknown aetiology have been reported (Charles *et al*., 2020a). Among the rare reported cases of *Vibrio* infection, *V. splendidus*-related strains were isolated from diseased *Mytilus edulis* adults and the isolated strains induced mortalities when injected to mussels (Ben Cheikh *et al*., 2016, 2017). Strains identified as *V. splendidus* and *V. coralliilyticus*/*neptunius*-like caused high mortality rates in larvae of the greenshell mussel *Perna canalicula* (*Mytilidae*) (Kesarcodi-Watson *et al*., 2009). Moreover, strains of *V. coralliilyticus* isolated from bleached corals (Wilson *et al*., 2013) had strong and concentration-dependent immunotoxicity and embryotoxicity in mussel *in vitro* (Balbi *et al*., 2019). Interestingly, the susceptibility of mussels to vibrios of the Splendidus clade (oyster pathogens) was shown to be dependent on host physiology (Charles *et al*., 2020b). Whether or not vibrios are causal agents in mussel mortalities observed in the field remains unclear (Charles *et al*., 2020a).

A recent study investigated possible links between the different susceptibility to *Vibrio* infection of oysters and mussels and their microbiota (Vezzulli *et al*., 2018). Using 16S rRNA gene-based analysis, the authors provided the first comparison of microbiota profiles associated with hemolymph and digestive gland of *C. gigas* and *M. galloprovincialis* co-cultured at the same aquaculture site. Vibrios accounted for a larger fraction of the microbiota in *C. gigas* compared with *M. galloprovincialis*, suggesting that oysters might provide better conditions than mussels for the survival of these bacteria. More recently, Pierce and Ward (2019), by comparing the gut microbiome of the oyster *C. virginica* and the mussel *M.*

edulis, found that while the two bivalves harbour microbial communities with similar composition, on a functional level, the microbial community varies according to host species and season. The authors suggested that host species intrinsic factors affect the composition of the bivalve microbiota independently of environmental conditions and diet.

In addition to vibrios pathogenic for bivalves, both oysters and mussels can concentrate within their tissues other vibrios pathogenic for humans. Since edible bivalves, especially oysters, are often eaten raw or undercooked, they represent an important vehicle for the transmission of these pathogens to humans. Most relevant *Vibrio* species associated with seafood-related diseases are *V. parahaemolyticus*, *V. vulnificus* and, to a lesser extent, non-toxigenic *V. cholerae* (Jones *et al*., 2014; Froelich and Noble, 2016; Williams *et al*., 2017; Tack *et al*., 2019). These species, as far as we know, do not affect bivalve health but represent a serious and growing threat to public health (Tack *et al*., 2019).

Stable versus transient associations

It has been debated whether the presence of vibrios in bivalves results from stable associations or from the non-specific uptake of vibrios from food or seawater. In a pioneer study, Hunt and colleagues (2008a, 2008b) analysed *Vibrio* population structures in mussels and in the water column. The diversity and frequency of populations identified by MLSA were similar in mussels and water samples, suggesting that mussels do not represent a strongly selective habitat for vibrios. However, population structure does not imply the absence of selection in mussel but suggests that selection is balanced by migration and/or adaptation to different environments (Preheim *et al*., 2011). More recently, Le Roux and collaborators have deeply analysed *Vibrio* associations with oysters and relationships between vibrios in the water column and in oyster tissues (Le Roux *et al*., 2016; Bruto *et al*., 2017). By comparing the frequency and abundance between *Vibrio* populations in these two compartments, Bruto and colleagues (2017) showed that several populations were unequally distributed. Among them, *V. crassostreae* and some *V. splendidus* populations were positively and preferentially associated with oyster tissues.

Because of habitat preferences related to their metabolic requirements, resistance/tolerance mechanisms and specific colonization determinants, distinct *Vibrio* species can colonize diverse tissues in bivalves. Total bacterial 16S has proven that hemolymph, which carries the bivalve immune cells, harbours a microbiota highly distinct from the rest of the tissues (Lokmer *et al*., 2016b). Strikingly, vibrios can survive in this immune tissue, which is likely a colonization route toward deeper tissues. Outside pathological contexts, hemolymph colonization is rapidly controlled by hemocytes, the bivalve immune cells (Rubio *et al*., 2019). In contrast, pathogenic vibrios escape from hemocyte control and colonize the connective tissue, which appears as a site of proliferation leading to fatal bacteremia (Parizadeh *et al*., 2018; Rubio *et al*., 2019) (Fig. 1).

New technologies such as metagenomics-based tools combined with manipulative ecological and physiological approaches are expected to significantly increase our current knowledge on *Vibrio* association with bivalves and their colonization mechanisms.

Vibrios facing bivalve cellular defences

Upon host colonization, microbes are recognized by pattern-recognition receptors that initiate cellular-based signal transduction cascades connecting microbe recognition signals to expression and secretion of immunomodulatory cytokines and chemokines (Reddick and Alto, 2014) and contribute to control infections by triggering the expression of immune effectors that modify the microbe habitat. Effectors of metazoan innate immunity include antimicrobial peptides (AMPs), reactive oxygen species (ROS), nitric oxide (NO) and heavy metals (copper, zinc), present at epithelial/mucosal surfaces, in phagocytes and body fluids, which create a hostile environment for microbes (Hood and Skaar, 2012; Franzenburg *et al*., 2013). These conserved innate immune mechanisms are key components of the defence of bivalves against infections.

The key role of hemocytes

Bivalves are endowed with a powerful innate immune system, mainly based on the activity of circulating immune cells, the hemocytes, soluble plasma factors, as well as on tissue-mediated immune responses (Bachère *et al*., 2015; Canesi and Pruzzo, 2016; Gerdol *et al*., 2018), creating a hostile environment for vibrios (Schmitt *et al*., 2012b; Destoumieux-Garzón *et al*., 2014). Due to the presence of an open circulatory system, bivalve hemocytes are not only circulating in the hemolymph but they also infiltrate tissues.

Hemocytes of both oysters and mussels can kill vibrios through phagocytosis, production of highly reactive ROS and NO, as well as a number of AMPs and hydrolytic enzymes (Canesi *et al*., 2002; Bachère *et al*., 2015; Canesi and Pruzzo, 2016) (Fig. 1). Hemocytes populations (granular, semi-granular, or agranular cells) (Bachère *et al*., 1988; Chagot *et al*., 1992) vary according to bivalve species, physiological status and environmental factors (Smith *et al*., 2016). In *C. gigas*, specialized

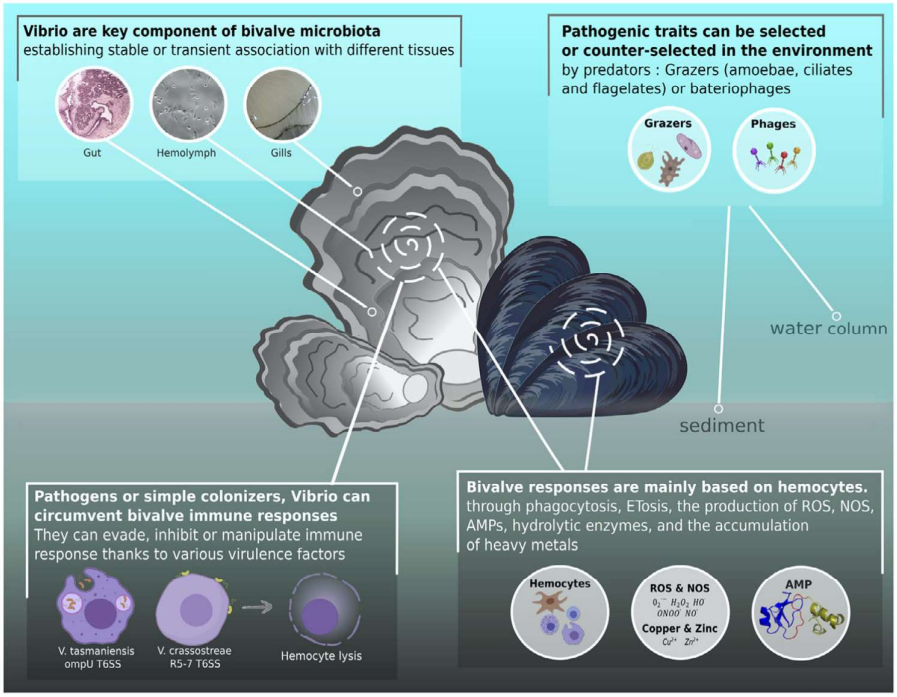

Fig 1. *Vibrio*–bivalve interactions and the biotic environment. Vibrios belong to the natural microbiota of oysters and mussels, establishing both transient and stable interactions. Outside pathogenic contexts, vibrio communities are controlled in the hemolymph by key hemocyte responses that include phagocytosis, ETosis and the production/accumulation of microbicidal compounds (ROS, NOS, AMPs, copper and zinc). However, vibrios can overcome these potent antimicrobial defences by inducing the lysis of bivalve hemocytes. Different mechanisms have been evolved by vibrio species leading to this common end. The required effectors can be delivered extracellularly by contact with the hemocyte membrane or intracellularly inside the phagosome. This enables vibrios to colonize deeper tissues and cause systemic infections. Interactions with predators (phages and amoeba) could favour the selection of mechanisms of virulence (cytotoxicity, resistance to bivalve antimicrobial defences) in the environment as they confer resistance to grazing; in contrast, some surface determinants could be counter-selected as they confer an advantage in colonizing oysters but an increased susceptibility to predators.

populations of semi-granular and granular cells harbour strong phagocytic capacity and produce highly reactive molecules (ROS and NO) in response to *V. splendidus*; they also express lysozymes and AMPs in agreement with their immunological roles (Bachère *et al*., 2015; Wang *et al*., 2017). Similarly, in *M. galloprovincialis*, granular and semi-granular cells harbour phagocytic activity, they produce ROS and NO; small hyaline cells produce NO only (García-García *et al*., 2008). Enzymes involved in oxidative stress (dual oxidases, NADPH oxidases) and hydrolases including lysozymes, which participate in the killing of phagocytized bacteria by degrading bacterial peptidoglycan (Costa *et al*., 2009; Itoh *et al*., 2010; Xue *et al*., 2010) are expressed by hemocytes of mussels and oysters (Rosa *et al*., 2012; Campos *et al*., 2015; Wang *et al*., 2017; de Lorgeril *et al*., 2018; Jiang *et al*., 2018). The respiratory burst generated by hemocytes is a major microbicidal reaction in bivalves, which also triggers the formation of DNA Extracellular traps (ETosis). In oysters and mussels, ETosis contributes to control *Vibrio* infections (Altincicek *et al*., 2008; Poirier *et al*., 2014; Romero *et al*., 2020).

Recently, mechanisms involved in heavy metal homeostasis have been shown to play a key role in the antibacterial response of oysters (Vanhove *et al*., 2015; Rubio *et al*., 2019; Shi *et al*., 2019). Copper/zinc redistribution upon *Vibrio* infections is accompanied in hemocytes by changes in the expression levels of metallothioneins as well as copper and zinc transporter genes (Ctr1, ATP7A, ZIP1 and Znt2), which across animal species mediate the uptake of heavy metals and their accumulation in intracellular compartments for intracellular killing of phagocytized bacteria (Neyrolles *et al*., 2015). It is worth noting that bivalves have widely differing concentrations of heavy metals in their tissues, with oysters (*Crassostrea* sp.) showing the highest body burden of copper and zinc (Pan and Wang, 2009; Shi *et al*., 2019). Although in mussels the role of heavy metals in the immune response to vibrios has been not investigated in such detail, sequences of ATP7A, Ctr1, ZIP1, Znt1 and Znt2 belonging to evolutionarily conserved metal transport systems are present in the genome of *M. galloprovincialis* (Gerdol M., pers. comm.), which suggests they could play a similar role in mussel

defence. So far in *Mytilus* sp., available data indicates that metal exposure can result in increases or decreases in hemocyte immune parameters, depending on the exposure conditions (Parry and Pipe, 2004; Höher *et al*., 2013). In this light, the role of copper/zinc homeostasis in mussel immune response deserves further investigation.

A high number of highly diversified AMPs have also been identified in oysters and mussels, in which they are expressed by hemocytes and/or epithelia. Some of them, but not all, have been purified and characterized for their various immune functions. Remarkably, mussels and oysters show contrasting antimicrobial responses. Indeed, AMP expression is potent in mussel (Pallavicini *et al*., 2008) as opposed to mild in oysters (Schmitt *et al*., 2012b). Both species express highly diversified Csαβ-defensins (Hubert *et al*., 1996; Mitta *et al*., 1999; Gueguen *et al*., 2006; Schmitt *et al*., 2010) and big defensins (Rosa *et al*., 2012; Gerdol *et al*., 2019, 2020; Loth *et al*., 2019) as well as bactericidal/permeability-increasing proteins (Gonzalez *et al*., 2007). These AMPs/proteins are expressed in hemocytes and/or epithelia either constitutively or in response to bacterial challenge (Schmitt *et al*., 2012b). Although the multiple mechanisms of action of bivalve AMPs are far from being uncovered, activities against vibrios have been evidenced, ranging from potent (e.g. big-defensins) to weak (e.g. defensins) (Duperthuy *et al*., 2010; Schmitt *et al*., 2012a; Loth *et al*., 2019). Remarkably, beyond these shared peptide families, the AMP repertoire of oysters and mussels contains species-specific AMP families. In *M. galloprovincialis*, these families include myticins, mytilins and mytimicins, which are also the most expressed AMPs (Pallavicini *et al*., 2008). Similarly, in *C. gigas*, they include proline-rich peptides, molluscidins and a macrophage expressed gene 1-like (for review see Bachère *et al*., 2015). However, some AMP families like mussel myticins are likely not involved in the response to vibrios but other functions such as antiviral responses (Balseiro *et al*., 2011) or wound healing (Rey-Campos *et al*., 2020).

Environmental factors are known to significantly affect immune responses. Thus, immune parameters of mussels and oysters (total hemocyte counts, the proportion of hemocyte populations, immune gene expression) vary with temperature and exposure to pollutants, including heavy metals and nanoparticles (Parry and Pipe, 2004; Höher *et al*., 2013; Wendling and Wegner, 2015; Canesi and Corsi, 2016; Auguste *et al*., 2020), which may have important consequences on bivalve susceptibility to pathogens. In addition, recent studies have revealed that previous encounter with pathogens is a life-history trait that defines the resistance/tolerance of bivalves to infections (i.e. immune priming). In the oyster *C. gigas*, priming of the antiviral response conferred long-term protection against the OsHV-1 virus, which was controlled by a sustained antiviral response (Lafont *et al*., 2017, 2020); moreover, a primary stimulation with *V. splendidus* enhanced immune signalling and conferred higher phagocytosis capacities to oyster hemocytes (Zhang *et al*., 2014; Wang *et al*., 2020). In the mussel *M. galloprovincialis*, priming with vibrios modified immune responses allowing mussels to tolerate the infection (Rey-Campos *et al*., 2019). Interestingly, Wendling and Wegner (2015) showed that in selective environments, i.e. at elevated temperatures reflecting patterns of disease outbreaks in natural populations, oysters can rapidly adapt to widespread communities of pathogenic vibrios. Oysters showing higher resistance to sympatric vibrios showed higher hemocyte counts and phagocytosis rates.

Responses to vibrios in oysters and mussels

Long-term records on mussels (*Mytilus* spp.) and oysters (*Crassostrea* spp.) have revealed they experience rare or frequent pathologies respectively, in particular in relation to *Vibrio* diseases. Although no data on species-specific comparison are available, the main immune mechanisms and effectors seem to be shared by the hemocytes of different mollusks, as reported in Escoubas and colleagues (2016). Experimental infections with different *Vibrio* species and strains have revealed how the complex machinery of immune pathways in hemocytes, together with soluble plasma factors, is activated when facing a *Vibrio* challenge. Here, some examples of responses of mussels and oysters to challenge with pathogenic vibrios are summarized. Oyster pathogens have been often used to challenge both species of bivalves. Thus, most data have been collected on the responses to the oyster pathogens *V. tasmaniensis* LGP32, *V. crassostreae* J2-9 (both from the Splendidus clade) and *V. aestuarianus* 01/032 (Anguillarum clade) (Labreuche *et al*., 2006a; Balbi *et al*., 2013; Green *et al*., 2016; Vanhove *et al*., 2016; Rubio *et al*., 2019).

One important question is whether the host can discriminate commensals from pathogenic strains. A recent study in which vibrios of the Splendidus clade were injected to oysters revealed that all *Vibrio* strains were recognized by oyster hemocytes independently of their virulence status (Rubio *et al*., 2019). They induced three major immune signalling pathways, namely the interleukin 17, tumour necrosis factor and Toll-like receptor (TLR) pathways. They also induced the production of AMPs (big defensins), ROS (dual oxidase expression), and heavy metals (metallothioneins and metal transporters). However, pathogenic strains were also shown to manipulate bivalve immune responses for successful colonization. These species-specific mechanisms are detailed below.

Responses to V. tasmaniensis. *Vibrio tasmaniensis* LGP32 was isolated from moribund *C. gigas* oysters by Gay and colleagues (2004). LGP32 interactions with its natural host have been widely documented. LGP32 is a facultative intracellular pathogen of oyster immune cells (Duperthuy *et al*., 2011). In *C. gigas*, LGP32 uses the major outer membrane protein OmpU to attach to and enter the hemocytes; opsonization is mediated by the major plasma protein *Cg*-EcSOD recognized by β-integrins at the hemocyte surface (Fig. 2). Consistent with a manipulation of hemocyte phagocytosis, LGP32 infection leads to an altered expression of oyster genes involved in cytoskeleton dynamics (Rubio *et al*., 2019). As LGP32 is recognized by the oyster immune system, it induces antimicrobial defences based on AMPs (big defensins), ROS (dual oxidase) and heavy metals (Rubio *et al*., 2019). However, inside the phagosome, it escapes from host cellular defences by avoiding acidic vacuole formation and by limiting the production of ROS (Duperthuy *et al*., 2011). This is accompanied by a repression of the NADPH-oxidase expression (Rubio *et al*., 2019) and the activation of mechanisms of resistance/tolerance to antimicrobials (see **Multifaceted adaptive responses of vibrios to their molluscan hosts** section). Inside the hemocytes, LGP32 induces lysosomal disruption (Balbi *et al*., 2013) and causes hemocyte lysis through the intracellular delivery of type 6 secretion system (T6SS) effectors (Vanhove *et al*., 2016; Rubio *et al*., 2019) (Fig. 2).

In mussels, LGP32 shows a lower pathogenic potential and induces lower hemocyte damage than in oysters (Balbi *et al*., 2013). LGP32 is rapidly phagocytized by *M. galloprovincialis* hemocytes, although phagocytosis does not require opsonization by plasma components, and it elicits the release of hemocyte antibacterial effectors (Balbi *et al*., 2013) (Fig. 2). When internalized, LGP32 remains viable within intracellular vacuoles, escaping lysosomal degradation. Accordingly, *V. splendidus* is able to proliferate in mussel hemolymph *in vivo*. The observed resistance of LGP32 to the bactericidal activity of mussel hemocytes was related to alterations of PI-3 Kinase signalling, leading to impairment of the endo-lysosomal system, which suggests that LGP32 could interfere with host cell signalling pathways, thereby escaping its bactericidal activity. In agreement, in *M. galloprovincialis* infected with LGP32, hemocytes show an altered expression of genes involved in innate immune response, inflammatory response, cell migration

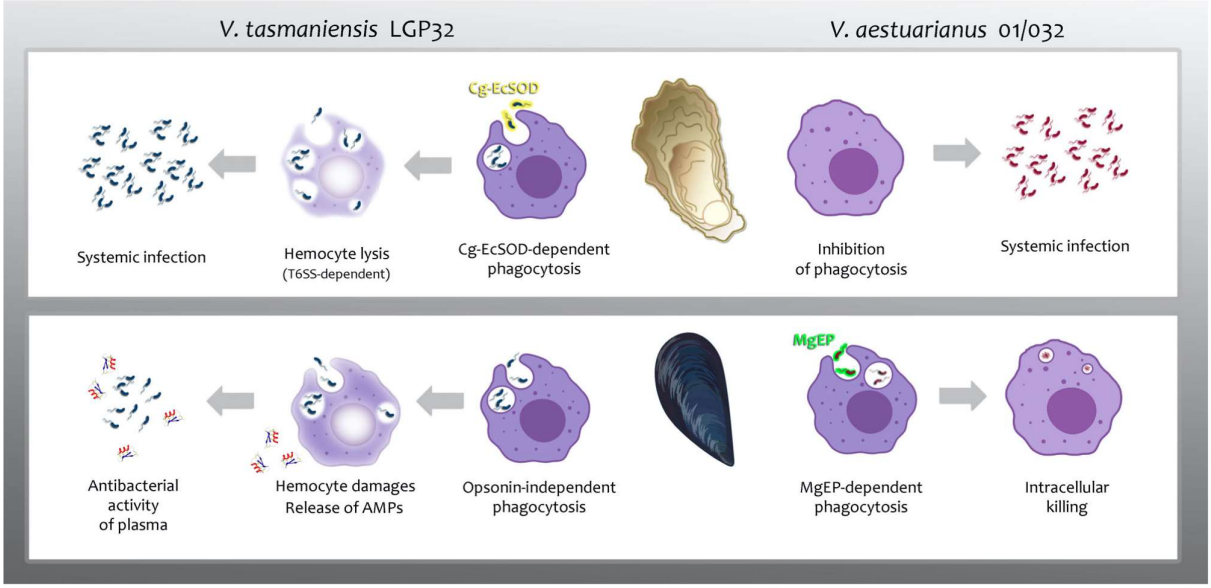

Fig 2. A simplified view of hemocyte–vibrio interactions. The interaction of the oyster pathogens *V. tasmaniensis* LGP32 and *V. aestuarianus* 01/032 with hemocytes of *C. gigas* and *M. galloprovincialis* has been characterized in independent studies. Data highlights different interactions in both species. Left panel: *V. tasmaniensis* LGP32 is readily phagocytized by both oyster and mussel hemocytes, but entry pathways differ. Opsonisation by the major plasma protein Cg-EcSOD is only required in oyster, in which it mediates uptake through β-integrin recognition. LGP32 survives intracellularly in both species (see Stable versus transient associations section for mechanisms of resistance) and causes hemocyte damages. Hemocyte lysis dampens cellular defences and is associated with pathogenicity in oyster only. Hemocytes show less damage lower in mussel and respond to LGP32 infection by the release of antibacterial effectors in the plasma. The potent AMPs of mussel hemocytes may play a key role in the control of LGP32 infection. Right panel: *V. aestuarianus* 01/032 secretes extracellular products that inhibit phagocytosis by oyster hemocytes and enable bacterial proliferation. In contrast, in mussels, the plasma protein MgEP recognizes 01/032 and promotes its phagocytosis; 01/032 is then degraded intracellularly. Opsonisation with MgEP is sufficient to restore uptake and killing of 01/032 by oyster hemocytes. MgEP appears as a key factor in the resistance of mussels to 01/032 infections.

not the observed repression of immune genes is related to the vibrio-triggered lysis of specific hemocyte populations remains to be clarified. Similar to other pathogenic vibrios, *V. splendidus* 10/068, which was isolated from moribund mussels in France in 2010 (Ben Cheikh *et al.*, 2017), was shown to alter different functions of hemocytes including motility, adhesion, ROS production, phagosome maturation and viability. Moreover, its ECPs inhibited cellular responses such as ROS production (Ben Cheikh *et al.*, 2016) through an unknown mechanism.

Overall, current insights into *Vibrio*–bivalve interactions show a key role of hemocytes in controlling infections through phagocytosis and its associated arsenal of antimicrobial compounds (ROS, heavy metals and AMPs). Hemocyte reactions also include ETosis, which is triggered by the oxidative burst and could participate in containing vibrios inside the hemolymph compartment. While the cellular defence arsenal is generally comparable in oyster and mussels, it appears to mainly differ in the AMPs expressed by immune cells and tissues and in the major soluble components present in the plasma, which serve as opsonins. Both AMPs and soluble plasma factors might contribute to the distinct susceptibility of oysters and mussels to infections.

Multifaceted adaptive responses of vibrios to their molluscan hosts

According to natural selection, microbes adapted for growth in metazoan hosts have selected strategies to evade, inhibit, or manipulate immune responses (Stubbendieck *et al.*, 2016). Commonly, counter-measures to host innate immunity include active dampening of immune defences, i.e. immune suppression, escape from host recognition (usually by disguising their immunogenic surface components), or resistance/tolerance to antimicrobials (Hornef *et al.*, 2002; Reddick and Alto, 2014). This evasion/tolerance scenario applies to species belonging to the resident microbiota of metazoans as well as to new invaders. In *Vibrio* species infecting or simply colonizing bivalves several of these strategies have been recently identified. These recent data highlight the multifaceted nature of immune evasion in *Vibrio* populations positively associated with bivalves.

Resistance/tolerance to host antimicrobials has been evidenced as a key determinant of *Vibrio* infectivity in oysters. Most data were obtained in the facultative intracellular pathogen *V. tasmaniensis* (Duperthuy *et al.*, 2011). In this species, resistance to ROS and heavy metals was identified as essential. Indeed, both antioxidants (SodA, AhpCF, catalase) and copper efflux machineries (CopA, CusABC) were highly induced upon contact with hemocytes and they determined *Vibrio* resistance to intracellular killing (Vanhove *et al.*, 2016). Mechanisms that confer increased resistance to oyster AMPs were also evidenced (Destoumieux-Garzón *et al.*, 2014). Inside the phagosomes of oyster hemocytes, *V. tasmaniensis* LGP32 was shown to release outer membrane vesicles (OMVs) that entrap AMPs and increase antimicrobial resistance (Vanhove *et al.*, 2015). An OmpU-mediated protection against AMPs was also evidenced in *V. tasmaniensis* LGP32 (Duperthuy *et al.*, 2010), which likely results from the OmpU-mediated induction of the envelope stress response, as demonstrated in *V. cholerae* (Mathur and Waldor, 2004; Mathur *et al.*, 2007). However, up to now potent mechanisms that modify the electronegativity of the lipopolysaccharides (LPS) and increase resistance to AMPs (Hankins *et al.*, 2011, 2012; Cullen *et al.*, 2015) have not been identified in *Vibrio* strains associated with bivalves. RND efflux machineries that detoxify *Vibrio* cells from the host antimicrobials (Bina *et al.*, 2008) are present in the genomes of *Vibrio* strains colonizing bivalves, but their role has not been studied. Moreover, *Vibrio* strains positively and negatively associated with oysters could not be discriminated on the basis of their resistance to AMPs (Oyanedel *et al.*, unpublished). Therefore, it is unclear how much resistance to AMPs contributes to colonization success in oysters. This may differ for *Vibrio* species associated with mussels, which express AMPs in large amounts (Mitta *et al.*, 2000; Pallavicini *et al.*, 2008), or with oysters, which express AMPs in small amounts (Schmitt *et al.*, 2012a).

Mechanisms of immune cell lysis needed to escape from hemocyte control were identified in *V. tasmaniensis* and *V. crassostreae* (Vanhove *et al.*, 2016; Piel *et al.*, 2019; Rubio *et al.*, 2019). Such an active dampening of oyster cellular defences was shown to depend on distinct molecular effectors: a chromosome-encoded T6SS active against eukaryotic cells in *V. tasmaniensis*, and the ancestral R5-7 virulence factor together with a T6SS carried by a plasmid (T6SSpGV) in *V. crassostreae* (Piel *et al.*, 2019; Rubio *et al.*, 2019). Both mechanisms enable virulent *Vibrio* to escape hemocyte control and cause systemic infections (Fig. 1). Recently, strains of *V. splendidus* able to colonize oyster tissues were also found to be cytotoxic toward hemocytes (Oyanedel *et al.*, 2020). Similar evolution toward cytotoxic phenotypes illustrates the importance for successful colonizers to overcome the major cellular defences of oysters: they create a less hostile habitat that enables colonization of oyster tissues. Cytotoxicity is therefore an important determinant of strain infectivity, which enables virulence expression when *Vibrio* strains harbour virulence factors.

Some bacterial species have acquired the capacity to escape from host recognition by becoming less immunogenic or by reducing the host immune responses elicited

by the release of microbe-associated molecular patterns such as LPS and peptidoglycan (Charroux *et al*., 2018). Such mechanisms of immune evasion remain poorly described in *Vibrio* species. However, in a recent study of a *V. splendidus* population associated with oysters, distinct structures of LPS O-antigen were identified. Manipulations of the *wbe* hypervariable genomic region, which determines the O-antigen structure in *V. splendidus* (Wildschutte *et al*., 2010) lead to less immunogenic structures that favoured oyster colonization (Oyanedel *et al*., 2020). This identifies immune evasion as a novel adaptive mechanism underpinning colonization in *Vibrio* associated with bivalves.

Within metazoan hosts, microbes are also engaged in interbacterial competition for survival among the diverse resident microbial communities and against new colonizers (Fraune *et al*., 2015). Bacteria have adapted to growth with neighbours (Stubbendieck and Straight, 2016). Tools for competition between bacteria can point to the fight for vital resources, growth inhibition, or direct killing of rivals by the delivery of toxins and AMPs such as bacteriocins (Stubbendieck and Straight, 2016). The fight for iron, present in limiting concentrations within metazoan hosts, was evidenced in the transcriptomic activity of vibrios colonizing bivalves with a major induction of siderophore biosynthesis and iron-uptake machineries (Vanhove *et al*., 2016; Rubio *et al*., 2019). This likely has a major impact on colonization success, as earlier shown in *V. vulnificus* infecting mice (Arezes *et al*., 2015). While several studies have evidenced bacteria harbouring antimicrobial activity in the hemolymph of bivalves (Defer *et al*., 2013; Desriac *et al*., 2014), the production of bacteriocins and resistance to such non-host-derived immune effectors remains a poorly explored aspect of *Vibrio* infectivity. However, it was suggested that cooperation exists within *Vibrio* populations based on bacteriocin production and uptake (Cordero *et al*., 2012). Similarly, recent studies have revealed the broad distribution of interbacterial T6SS in *Vibrio* species, a killing mechanism that uses contact-dependent toxin delivery and toxin-resistance mechanism to inhibit competitors (Ho *et al*., 2015). In *Vibrio* species pathogenic for oysters such T6SS systems are induced upon host colonization although a formal role in interbacterial competition has not been demonstrated (Rubio *et al*., 2019). Such a demonstration was achieved in *V. vulnificus*, in which two T6SS are involved in interspecies/intraspecies competition within oyster hosts (Hubert, 2019), and in *V. fischeri*, in which a T6SS controls competitions during squid colonization (Speare *et al*., 2018).

Altogether, recent advances in *Vibrio*–bivalve interactions highlight the adaptive potential of bivalve colonizers, which have not only developed strategies to circumvent the potent cellular defences of their natural hosts but also tools for competition with the abundant microbial communities hosted by bivalves.

The selection of adapted genotypes in bivalves and the aquatic environment

As free-living and non-obligatory parasites, vibrios engage in diverse biotic interactions in the environment outside of their bivalve hosts. Among these biotic interactions, they encounter two major groups of bacterial predators, i.e. bacteriophages and bacterivorous protists (grazers), i.e. ciliates, flagellates and amoebozoae (Pernthaler, 2005). As predator–prey interactions are some of the strongest forces driving rapid co-evolution of both partners, often referred to as an arm-race (Dawkins *et al*., 1979), predator–prey interactions in bacterial communities significantly influence and shape bacterial adaptive strategies and favour the selection of predation resistance traits.

Grazers can be found in most ecological niches inhabited by bacterial communities, and their predation activity shares similar cellular and molecular processes with their metazoan immune cells counterparts, the phagocytes, i.e. the hemocytes in the case of bivalves. Phagocytosis and intracellular antimicrobial processes are indeed highly conserved from protozoans to mammals (Boulais *et al*., 2010). Hence, bacterial predation by grazers has often been suggested to favour the co-incidental selection of bacterial virulence factors, including in *Vibrionaceae* (Erken *et al*., 2013). A diversity of survival adaptations against predation by grazers can be found in bacteria and classified into two main groups: either pre-ingestional or post-ingestional adaptations (Matz and Kjelleberg, 2005). Pre-ingestional adaptions including high motility, filamentation, surface masking or toxin release are commonly found in extracellular pathogens; whereas post-ingestional adaptations including digestion resistance through vacuolar trafficking inhibition or vacuolar escape, and intracellular toxin release are commonly found for intracellular pathogens and tend to favour bacterial growth (Matz and Kjelleberg, 2005).

Escape from phagocytosis. Among pre-ingestional adaptations, some are widely shared by *Vibrionaceae* as they are flagellated and highly motile. In addition, some of them can form biofilms, as e.g. *V. cholerae* that produces *Vibrio* polysaccharides favouring resistance to grazing (Sun *et al*., 2013; Van der Henst *et al*., 2018a). Interestingly the oyster *V. tasmaniensis* LGP32 has been suggested to form biofilms (Vezzulli *et al*., 2015), although a potential role of this process in resistance to grazers remains to be investigated.

Cytotoxic activities. Toxin/protease release and cytotoxic activities can both play a role as pre-ingestional or post-ingestional adaptations to grazers (Matz and Kjelleberg, 2005). Protease secretion is widespread among vibrios and it has been described for most strains pathogenic toward bivalves (Binesse *et al*., 2008; Labreuche *et al*., 2010). Some of these proteases favour resistance to grazing by amoeba and ciliates as shown for the metalloprotease Vsm secreted by *V. tasmaniensis* LGP32 (Robino *et al*., 2019) and the protease PrtV secreted by *V. cholerae* (Vaitkevicius *et al*., 2006). To date in vibrios, they represent some of the best examples of factors under environmental selective pressure that contribute to virulence/toxicity in a metazoan host. *Vibrio tasmaniensis* and *V. crassostreae* also harbour cytotoxic capacities that are necessary for their pathogenicity (Rubio *et al*., 2019), among them MARTX toxins and T6SS components (Bruto *et al*., 2017; Piel *et al*., 2019; Rubio *et al*., 2019). However, none of these systems have been shown toprotect bivalve pathogens against grazing so far. The role of MARTX toxins in resistance to grazing was shown for *V. vulnificus*, in which a MARTX involved in eel infection confers protection against amoeba grazing (Lee *et al*., 2013), but remain to be investigated in bivalve pathogens still. Similarly, the T6SS of *V. cholerae* has shown cytotoxic activity on the slime mould *Dictyostelium discoideum* during its actively grazing unicellular life stage (Pukatzki *et al*., 2006). However, in the oyster pathogen *V. tasmaniensis* LGP32, where a T6SS determines cytotoxicity toward oyster hemocytes (Rubio *et al*., 2019), no effect was found in the interaction with the amoebae *Vannella* sp. 1411 (Robino *et al*., 2019). Hence a potential role for T6SS in biotic interactions outside bivalves remains to be identified.

Resistance to heavy metals. Evidence of post-ingestional adaptations in vibrios are limited to a number of pathogenic strains that adopt intracellular stages and survive intracellular digestion (Rosenberg and Falkovitz, 2004; Ma *et al*., 2009; Vidal-Dupiol *et al*., 2011; Ritchie *et al*., 2012; de Souza Santos and Orth, 2014; Van der Henst *et al*., 2016), as shown for *V. tasmaniensis* LGP32 in hemocytes of bivalves (Duperthuy *et al*., 2011; Balbi *et al*., 2013; Vanhove *et al*., 2016; Rubio *et al*., 2019). Such properties are rather unusual for pathogenic vibrios and potentially reminiscent of post-ingestional adaptation to grazers predation. Indeed, LGP32 was found resistant to grazing by the free-living amoeba *Vannella* and some virulence factors, such as the p-ATPase copper efflux pump CopA, were found to play a role in this resistance (Robino *et al*., 2019). Interestingly the CopA-mediated resistance to copper is also necessary for *V. fischeri* colonization in the bobtail squid (Brooks *et al*., 2014). Therefore, copper resistance favouring resistance to amoeba predation is also a key determinant of *Vibrio* associations with molluscan hosts, both in parasitic and mutualistic interactions.

Adsorption inhibition. In addition to grazers, bacteriophages are an important class of predators, which are abundant and highly diverse in marine environments; they contribute to the evolution of bacteria by mediating horizontal gene transfer and genomic rearrangements, as well as by bactericidal selection (Dy *et al*., 2014). A critical step in their interaction with bacteria is the attachment to cell wall components (membrane receptors, porins, LPS, flagella and pili) thus exerting an important selective pressure on cell wall composition and cell wall plasticity. Hence bacteria adaptation to phage predation can share similarities with pre-ingestional masking strategies to avoid recognition by grazers. Among adaptations to phages that have been described for vibrios, LPS modifications (Seed *et al*., 2012) play a key role and OMVs release can be used as decoy strategy (Manning and Kuehn, 2011) in a similar manner than OMVs play a role as a decoy against AMPs during bivalve immune response (Vanhove *et al*., 2015). Interestingly OMVs are involved in *V. cholerae* resistance to phages (Reyes-Robles *et al*., 2018) as well as in resistance against the amoeba *Acanthamoebae castellanii* (Valeru *et al*., 2014)

The LPS structure under multiple selective pressures. Some virulence traits can be under adverse selection in different biotic interactions and generate a tradeoff equilibrium. In a recent study of a *V. splendidus* population associated with oysters, we identified distinct structures of LPS O-antigen encoded by the wbe hypervariable genomic region, which determines the O-antigen structure in *V. splendidus* (Wildschutte *et al*., 2010). Interestingly less immunogenic structures of LPS O-antigen that favoured oyster colonization led to attenuated resistance to grazing by the *Vannella* sp. AP1411 free-living marine amoebae, suggesting a tradeoff between grazing resistance and oyster colonization (Oyanedel *et al*., 2020). Such a tradeoff between virulence and resistance to predators was also reported for *V. cholerae* O-antigen structure, which is under epigenetic control: phase variants of the wbe region defective in producing O-antigen are indeed highly resistant to phage infection, but severely attenuated in terms of virulence (Seed *et al*., 2012). Altogether these studies highlight the critical role of LPS O-antigen in biotic interactions involving vibrios, strains pathogenic for bivalve being no exception. The extreme variability of this major membrane structure is controlled by genetic or epigenetic determinants

favouring environmental persistence but leading to attenuated virulence in bivalves.

Altogether these recent studies show that the multiple biotic interactions of vibrios in the environment can lead to either positive (coincidental selection), neutral (relaxed selection), or negative (conflicting selection) effects on the selection of *Vibrio* traits required for virulence expression in bivalves (Mikonranta *et al*., 2012) (Fig. 1). Predation could favour the selection of some virulence factors that participate to pathogenicity in bivalve host (Adiba *et al*., 2010). However, as illustrated in the well-known intracellular pathogen *L. pneumophila*, hundreds of virulence factors can interact with a diversity of hosts, without having similar importance in each interaction (Boamah *et al*., 2017; Ghosh and O'Connor, 2017; Park *et al*., 2020). Thus, in *V. cholerae*, some virulence factors involved in the resistance to grazing by *A. castellanii* have a minor role in pathogenesis in human (Van der Henst *et al*., 2018b). They can also have adverse effects as recently illustrated in a *V. splendidus* moderately virulent for oysters (Oyanedel *et al*., 2020). Vibrios being mostly opportunistic pathogens, they appear to have acquired, on the one hand, 'generalist' virulence factors involved in multiple biotic interactions, and on the other hand, 'specialist' virulence factors involved in interactions with a particular host, with possible trade-offs on other interactions.

Concluding remarks

This review highlights the multifaceted nature of *Vibrio* interactions with mussels and oysters, aquaculture species showing contrasting resistance to infections. While only a limited number of vibrios pathogenic for mussels have been described, the current literature shows that oyster pathogens tend to interact differently with major components of oyster/mussel plasma and with their key immune cells, the hemocytes, which perform phagocytosis and produce highly microbicidal reactive oxygen/nitrogen species and accumulate heavy metals. The potent production of AMPs in mussels, as opposed to oysters, could be an important factor controlling disease outcomes. Plasma-soluble recognition proteins specific of the bivalve species also appear to have a critical role. However, understanding the higher susceptibility of oysters to infections requires a more systematic comparison of *Vibrio* interactions with mussels and oysters. Thanks to their successful colonization of oysters, different strategies of immune evasion and tolerance/resistance have been evidenced in vibrios pathogenic for oysters. These mechanisms include tolerance to the main cellular defences of oysters (ROS, AMPs and heavy metals), active dampening of cellular immunity through cytolytic mechanisms (toxins, T6SS) as well as reduced antigenic properties through modifications of LPS, a major and hypervariable component of *Vibrio* outer membrane. Recent knowledge on the interactions of vibrios with environmental predators (phages, grazers) highlights possible mechanisms of coincidental selection as well as tradeoffs acting on these important determinants of *Vibrio* virulence (Fig. 1).

Acknowledgements

We are grateful to Prof. Marco Gerdol (University of Trieste) for precious genomic data on mussels. This work was supported by the European Union's Horizon 2020 Research and Innovation Program Grant Vivaldi 678589; the CNRS, PEPS Blanc 2016 (project Like Inhospitality); CONICYT PFCHA/Doctorado En El Extranjero Becas Chile/2016-72170430 to D.O.; AMIBADAPT project funded by LABEX CeMEB. This study is set within the framework of the 'Laboratoires d'Excellence (LABEX)' Tulip (ANR-10-LABX-41).

References

Adiba, S., Nizak, C., van Baalen, M., Denamur, E., and Depaulis, F. (2010) From grazing resistance to pathogenesis: the coincidental evolution of virulence factors. *PLoS One* **5**: e11882.

Alfaro, A.C., Nguyen, T.V., and Merien, F. (2019) The complex interactions of Ostreid herpesvirus 1, Vibrio bacteria, environment and host factors in mass mortality outbreaks of *Crassostrea gigas*. *Rev Aquac* **11**: 1148–1168.

Altincicek, B., Stötzel, S., Wygrecka, M., Preissner, K.T., and Vilcinskas, A. (2008) Host-derived extracellular nucleic acids enhance innate immune responses, induce coagulation, and prolong survival upon infection in insects. *J Immunol* **181**: 2705–2712.

Arezes, J., Jung, G., Gabayan, V., Valore, E., Ruchala, P., Gulig, P.A., *et al*. (2015) Hepcidin-induced hypoferremia is a critical host defense mechanism against the siderophilic bacterium *Vibrio vulnificus*. *Cell Host Microbe* **17**: 47–57.

Auguste, M., Balbi, T., Ciacci, C., Canonico, B., Papa, S., Borello, A., *et al*. (2020) Immune training after repeated exposure to nanoplastics in the marine bivalve *Mytilus*. *Front Immunol* **11**(426), 1–11. https://doi.org/10.3389/fimmu.2020.00426.

Azéma, P., Travers, M.-A., De Lorgeril, J., Tourbiez, D., and Dégremont, L. (2015) Can selection for resistance to OsHV-1 infection modify susceptibility to *Vibrio aestuarianus* infection in *Crassostrea gigas*? First insights from experimental challenges using primary and successive exposures. *Vet Res* **46**: 139.

Bachère, E., Chagot, D., and Grizel, H. (1988) Separation of *Crassostrea gigas* hemocytes by density gradient centrifugation and counterflow centrifugal elutriation. *Dev Comp Immunol* **12**: 549–559.

Bachère, E., Rosa, R.D., Schmitt, P., Poirier, A.C., Merou, N., Charrière, G.M., and Destoumieux-Garzón, D. (2015) The new insights into the oyster antimicrobial defense: cellular, molecular and genetic view. *Fish Shellfish Immunol* **46**: 50–64.

Baker-Austin, C., Trinanes, J., Gonzalez-Escalona, N., and Martinez-Urtaza, J. (2017) Non-cholera vibrios: the microbial barometer of climate change. *Trends Microbiol* **25**: 76–84.

Balbi, T., Auguste, M., Cortese, K., Montagna, M., Borello, A., Pruzzo, C., *et al*. (2019) Responses of *Mytilus galloprovincialis* to challenge with the emerging marine pathogen *Vibrio coralliilyticus*. *Fish Shellfish Immunol* **84**: 352–360.

Balbi, T., Fabbri, R., Cortese, K., Smerilli, A., Ciacci, C., Grande, C., *et al*. (2013) Interactions between *Mytilus galloprovincialis* hemocytes and the bivalve pathogens *Vibrio aestuarianus* 01/032 and *Vibrio splendidus* LGP32. *Fish Shellfish Immunol* **35**: 1906–1915.

Balseiro, P., Falcó, A., Romero, A., Dios, S., Martínez-López, A., Figueras, A., *et al*. (2011) *Mytilus galloprovincialis* Myticin C: a chemotactic molecule with antiviral activity and immunoregulatory properties. *PLoS One* **6**: e23140.

Ben Cheikh, Y., Travers, M.-A., and Le Foll, F. (2017) Infection dynamics of a *V. splendidus* strain pathogenic to *Mytilus edulis*: in vivo and in vitro interactions with hemocytes. *Fish Shellfish Immunol* **70**: 515–523.

Ben Cheikh, Y., Travers, M.-A., Morga, B., Godfrin, Y., Rioult, D., and Le Foll, F. (2016) First evidence for a Vibrio strain pathogenic to *Mytilus edulis* altering hemocyte immune capacities. *Dev Comp Immunol* **57**: 107–119.

Bevins, C.L., and Salzman, N.H. (2011) The potter's wheel: the host's role in sculpting its microbiota. *Cell Mol Life Sci* **68**: 3675–3685.

Bina, X.R., Provenzano, D., Nguyen, N., and Bina, J.E. (2008) *Vibrio cholerae* RND family efflux systems are required for antimicrobial resistance, optimal virulence factor production, and colonization of the infant mouse small intestine. *Infect Immun* **76**: 3595–3605.

Binesse, J., Delsert, C., Saulnier, D., Champomier-Vergès, M.C., Zagorec, M., Munier-Lehmann, H., *et al*. (2008) Metalloprotease Vsm is the major determinant of toxicity for extracellular products of *Vibrio splendidus*. *Appl Environ Microbiol* **74**: 7108–7117.

Boamah, D.K., Zhou, G., Ensminger, A.W., and O'Connor, T.J. (2017) From many hosts, one accidental pathogen: the diverse protozoan hosts of *Legionella*. *Front Cell Infect Microbiol* **7**: 477.

Boulais, J., Trost, M., Landry, C.R., Dieckmann, R., Levy, E. D., Soldati, T., *et al*. (2010) Molecular characterization of the evolution of phagosomes. *Mol Syst Biol* **6**: 423.

Brennan, J.J., and Gilmore, T.D. (2018) Evolutionary origins of toll-like receptor signaling. *Mol Biol Evol* **35**: 1576–1587.

Brooks, J.F., Gyllborg, M.C., Cronin, D.C., Quillin, S.J., Mallama, C.A., Foxall, R., *et al*. (2014) Global discovery of colonization determinants in the squid symbiont *Vibrio fischeri*. *Proc Natl Acad Sci U S A* **111**: 17284–17289.

Bruto, M., James, A., Petton, B., Labreuche, Y., Chenivesse, S., Alunno-Bruscia, M., *et al*. (2017) *Vibrio crassostreae*, a benign oyster colonizer turned into a pathogen after plasmid acquisition. *ISME J* **11**: 1043–1052.

Bruto, M., Labreuche, Y., James, A., Piel, D., Chenivesse, S., Petton, B., *et al*. (2018) Ancestral gene acquisition as the key to virulence potential in environmental Vibrio populations. *ISME J* **12**: 1.

Campos, A., Apraiz, I., da Fonseca, R.R., and Cristobal, S. (2015) Shotgun analysis of the marine mussel *Mytilus edulis* hemolymph proteome and mapping the innate immunity elements. *Proteomics* **15**: 4021–4029.

Canesi, L., and Corsi, I. (2016) Effects of nanomaterials on marine invertebrates. *Sci Total Environ* **565**: 933–940.

Canesi, L., Gallo, G., Gavioli, M., and Pruzzo, C. (2002) Bacteria–hemocyte interactions and phagocytosis in marine bivalves. *Microsc Res Tech* **57**: 469–476.

Canesi, L., and Pruzzo, C. (2016) . In *Chapter 6 - Specificity of Innate Immunity in Bivalves: A Lesson from Bacteria*, Ballarin, L., and Cammarata, M.B.T.-L.Cambridge, MA, USA: (eds): Academic Press, pp. 79–91.

Ceccarelli D, Amaro C, Romalde J, Suffredini E, Vezzulli L. (2019). Vibrio Species, p 347-388. In Doyle M, Diez-Gonzalez F, Hill C (ed), Food Microbiology: Fundamentals and Frontiers, 5th Edition. ASM Press, Washington, DC. doi: 10.1128/9781555819972.ch13.

Chagot, D., Boulo, V., Hervio, D., Mialhe, E., Bachere, E., Mourton, C., and Grizel, H. (1992) Interactions between *Bonamia ostreae* (Protozoa: Ascetospora) and hemocytes of *Ostrea edulis* and *Crassostrea gigas* (Mollusca: Bivalvia): entry mechanisms. *J Invertebr Pathol* **59**: 241–249.

Charles, M., Bernard, I., Villalba, A., Oden, E., Burioli, E., Allain, G., *et al*. (2020a) High mortality of mussels in northern Brittany - evaluation of the involvement of pathogens, pathological conditions and pollutants. *J Invertebr Pathol* **170**: 107308.

Charles, M., Trancart, S., Oden, E., and Houssin, M. (2020b) Experimental infection of *Mytilus edulis* by two *Vibrio splendidus*-related strains: determination of pathogenicity level of strains and influence of the origin and annual cycle of mussels on their sensitivity. *J Fish Dis* **43**: 9–21.

Charroux, B., Capo, F., Kurz, C.L., Peslier, S., Chaduli, D., Viallat-lieutaud, A., and Royet, J. (2018) Cytosolic and secreted peptidoglycan-degrading enzymes in *Drosophila* respectively control local and systemic immune responses to microbiota. *Cell Host Microbe* **23**: 215–228.e4.

Chen, H., Liu, Z., Shi, Y., and Ding, H.H. (2016) Microbiological analysis and microbiota in oyster: a review. *Invertebr Survival J* **13**: 374–388.

Cordero, O.X., Wildschutte, H., Kirkup, B., Proehl, S., Ngo, L., Hussain, F., *et al*. (2012) Ecological populations of bacteria act as socially cohesive units of antibiotic production and resistance. *Science* **337**: 1228–1231.

Costa, M.M., Prado-Alvarez, M., Gestal, C., Li, H., Roch, P., Novoa, B., and Figueras, A. (2009) Functional and molecular immune response of Mediterranean mussel (*Mytilus galloprovincialis*) haemocytes against pathogen-associated molecular patterns and bacteria. *Fish Shellfish Immunol* **26**: 515–523.

Cullen, T.W., Schofield, W.B., Barry, N.A., Putnam, E.E., Rundell, E.A., Trent, M.S., *et al*. (2015) Antimicrobial peptide resistance mediates resilience of prominent gut commensals during inflammation. *Science* **347**: 170–175.

Dawkins, R., Krebs, J.R., Maynard Smith, J., and Holliday, R. (1979) Arms races between and within species. *Proc R Soc London Ser B Biol Sci* **205**: 489–511.

de Lorgeril, J., Lucasson, A., Petton, B., Toulza, E., Montagnani, C., Clerissi, C., *et al*. (2018) Immune-suppression by OsHV-1 viral infection causes fatal bacteraemia in Pacific oysters. *Nat Commun* **9**: 4215.

de Lorgeril, J., Zenagui, R., Rosa, R.D., Piquemal, D., and Bachère, E. (2011) Whole transcriptome profiling of successful immune response to Vibrio infections in the oyster *Crassostrea gigas* by digital gene expression analysis. *PLoS One* **6**: e23142.

de Souza Santos, M., and Orth, K. (2014) Intracellular *Vibrio parahaemolyticus* escapes the vacuole and establishes a replicative niche in the cytosol of epithelial cells. *MBio* **5**: e01506-14.

Defer, D., Desriac, F., Henry, J., Bourgougnon, N., Baudy-Floc'h, M., Brillet, B., *et al*. (2013) Antimicrobial peptides in oyster hemolymph: the bacterial connection. *Fish Shellfish Immunol* **34**: 1439–1447.

DePaola, A., Hopkins, L.H., Peeler, J.T., Wentz, B., and McPhearson, R.M. (1990) Incidence of *Vibrio parahaemolyticus* in U.S. coastal waters and oysters. *Appl Environ Microbiol* **56**: 2299–2302.

Desriac, F., Le Chevalier, P., Brillet, B., Leguerinel, I., Thuillier, B., Paillard, C., and Fleury, Y. (2014) Exploring the hologenome concept in marine bivalvia: haemolymph microbiota as a pertinent source of probiotics for aquaculture. *FEMS Microbiol Lett* **350**: 107–116.

Destoumieux-Garzón, D., Duperthuy, M., Vanhove, A.S., Schmitt, P., Wai, S.N., and Shafer, W.M. (2014) Resistance to antimicrobial peptides in vibrios. *Antibiotics* **3**: 540–563.

Dias, G.M., Bidault, A., Le Chevalier, P., Choquet, G., Der Sarkissian, C., Orlando, L., *et al*. (2018) *Vibrio tapetis* displays an original type IV secretion system in strains pathogenic for bivalve Molluscs. *Front Microbiol* **9**: 227.

Domeneghetti, S., Varotto, L., Civettini, M., Rosani, U., Stauder, M., Pretto, T., *et al*. (2014) Mortality occurrence and pathogen detection in *Crassostrea gigas* and *Mytilus galloprovincialis* close-growing in shallow waters (Goro lagoon, Italy). *Fish Shellfish Immunol* **41**: 37–44.

Dubert, J., Barja, J.L., and Romalde, J.L. (2017) New insights into pathogenic vibrios affecting bivalves in hatcheries: present and future prospects. *Front Microbiol* **8**: 762.

Duperthuy, M., Binesse, J., Le Roux, F., Romestand, B., Caro, A., Got, P., *et al*. (2010) The major outer membrane protein OmpU of *Vibrio splendidus* contributes to host antimicrobial peptide resistance and is required for virulence in the oyster *Crassostrea gigas*. *Environ Microbiol* **12**: 951–963.

Duperthuy, M., Schmitt, P., Garzon, E., Caro, A., Rosa, R. D., Le Roux, F., *et al*. (2011) Use of OmpU porins for attachment and invasion of *Crassostrea gigas* immune cells by the oyster pathogen *Vibrio splendidus*. *Proc Natl Acad Sci U S A* **108**: 2993–2998.

Dy, R.L., Richter, C., Salmond, G.P.C., and Fineran, P.C. (2014) Remarkable mechanisms in microbes to resist phage infections. *Annu Rev Virol* **1**: 307–331.

Erken, M., Lutz, C., and McDougald, D. (2013) The rise of pathogens: predation as a factor driving the evolution of human pathogens in the environment. *Microb Ecol* **65**: 860–868.

Escoubas, J.-M., Destoumieux-Garzón, D., Montagnani, C., Gourbal, B., Duval, D., Green, T., and Charrière, G. (2016) Immunity in molluscs. In *Encyclopedia of Immunobiology*, Ratcliffe, M.J. (ed), pp. 417–436). Cambridge, MA, USA: .Academic press.

Franzenburg, S., Fraune, S., Altrock, P.M., Künzel, S., Baines, J.F., Traulsen, A., and Bosch, T.C.G. (2013) Bacterial colonization of Hydra hatchlings follows a robust temporal pattern. *ISME J* **7**: 781–790.

Fraune, S., Anton-Erxleben, F., Augustin, R., Franzenburg, S., Knop, M., Schröder, K., *et al*. (2015) Bacteria–bacteria interactions within the microbiota of the ancestral metazoan Hydra contribute to fungal resistance. *ISME J* **9**: 1543–1556.

Fraune, S., and Bosch, T.C.G. (2010) Why bacteria matter in animal development and evolution. *BioEssays* **32**: 571–580.

Froelich, B., and Oliver, J.D. (2013) The interactions of *Vibrio vulnificus* and the oyster *Crassostrea virginica*. *Microb Ecol* **65**: 807–816.

Froelich, B.A., and Noble, R.T. (2016) Vibrio bacteria in raw oysters: managing risks to human health. *Philos Trans R Soc Lond B Biol Sci* **371**: 20150209.

Garcia, C., Lupo, C., Travers, M.-A., Arzul, I., Tourbiez, D., Haffner, P., *et al*. (2014) *Vibrio aestuarianus* and Pacific oyster in France: a review of 10 years of surveillance. *J Shellfish Res* **6**: 142.

García-García, E., Prado-Álvarez, M., Novoa, B., Figueras, A., and Rosales, C. (2008) Immune responses of mussel hemocyte subpopulations are differentially regulated by enzymes of the PI 3-K, PKC, and ERK kinase families. *Dev Comp Immunol* **32**: 637–653.

Garnier, M., Labreuche, Y., Garcia, C., Robert, M., and Nicolas, J.-L. (2007) Evidence for the involvement of pathogenic bacteria in Summer mortalities of the pacific oyster *Crassostrea gigas*. *Microb Ecol* **53**: 187–196.

Garnier, M., Labreuche, Y., and Nicolas, J.-L. (2008) Molecular and phenotypic characterization of *Vibrio aestuarianus* subsp. *francensis* subsp. nov., a pathogen of the oyster *Crassostrea gigas*. *Syst Appl Microbiol* **31**: 358–365.

Gay, M., Renault, T., Pons, A.M., and Le Roux, F. (2004) Two *Vibrio splendidus* related strains collaborate to kill *Crassostrea gigas*: taxonomy and host alterations. *Dis Aquat Organ* **62**: 65–74.

Gerdol, M., Gomez-Chiarri, M., Castillo, M.G., Figueras, A., Fiorito, G., Moreira, R., *et al*. (2018) Immunity in molluscs: recognition and effector mechanisms, with a focus on bivalvia BT. In *Advances in Comparative Immunology*, Cooper, E.L. (ed). Cham: Springer International Publishing, pp. 225–341.

Gerdol, M., Moreira, R., Cruz, F., Gomez, J., Vlasova, A., Rosani, U., *et al*. (2019) Massive gene presence/absence variation in the mussel genome as an adaptive strategy: first evidence of a pan-genome in Metazoa. https://doi.org/10.1101/781377.

Gerdol, M., Schmitt, P., Venier, P., Rocha, G., Rosa, R.D., and Destoumieux-Garzón, D. (2020) Functional insights from the evolutionary diversification of big defensins. *Front Immunol* **11**(758), 1–16. https://doi.org/10.3389/fimmu.2020.00758.

Ghosh, S., and O'Connor, T.J. (2017) Beyond paralogs: the multiple layers of redundancy in bacterial pathogenesis. *Front Cell Infect Microbiol* **7**: 467.

Gonzalez, M., Gueguen, Y., Destoumieux-Garzón, D., Romestand, B., Fievet, J., Pugnière, M., *et al*. (2007) Evidence of a bactericidal permeability increasing protein in an invertebrate, the *Crassostrea gigas* Cg-BPI. *Proc Natl Acad Sci U S A* **104**: 17759–17764.

Goudenège, D., Travers, M.A., Lemire, A., Petton, B., Haffner, P., Labreuche, Y., *et al*. (2015) A single regulatory gene is sufficient to alter *Vibrio aestuarianus* pathogenicity in oysters. *Environ Microbiol* **17**: 4189–4199.

Green, T.J., Vergnes, A., Montagnani, C., and De Lorgeril, J. (2016) Distinct immune responses of juvenile and adult oysters (*Crassostrea gigas*) to viral and bacterial infections. *Vet Res* **47**: 1–11.

Gueguen, Y., Herpin, A., Aumelas, A., Garnier, J., Fievet, J., Escoubas, J.-M., *et al*. (2006) Characterization of a defensin from the oyster *Crassostrea gigas*: recombinant production, folding, solution structure, antimicrobial activities, and gene expression. *J Biol Chem* **281**: 313–323.

Hankins, J.V., Madsen, J.A., Giles, D.K., Brodbelt, J.S., Trent, M.S., and Tor, E. (2012) Amino acid addition to *Vibrio cholerae* LPS establishes a link between surface remodeling in Gram-positive and Gram-negative bacteria. *Proc Natl Acad Sci U S A* **109**: 8722–8727.

Hankins, J.V., Madsen, J.A., Giles, D.K., Childers, B.M., Klose, K.E., Brodbelt, J.S., and Trent, M.S. (2011) Elucidation of a novel *Vibrio cholerae* lipid A secondary hydroxy-acyltransferase and its role in innate immune recognition. *Mol Microbiol* **81**: 1313–1329.

Ho, B.T., Dong, T.G., and Mekalanos, J.J. (2015) A view to a kill: the bacterial type 6 secretion system. *Cell Host Microbe* **15**: 9–21.

Höher, N., Regoli, F., Dissanayake, A., Nagel, M., Kriews, M., Köhler, A., and Broeg, K. (2013) Immunomodulating effects of environmentally realistic copper concentrations in *Mytilus edulis* adapted to naturally low salinities. *Aquat Toxicol* **140–141**: 185–195.

Hood, M.I., and Skaar, E.P. (2012) Nutritional immunity: transition metals at the pathogen-host interface. *Nat Rev Microbiol* **10**: 525–537.

Hornef, M.W., Wick, M.J., Rhen, M., and Normark, S. (2002) Bacterial strategies for overcoming host innate and adaptive immune responses. *Nat Immunol* **3**: 1033–1040.

Hubert, C. (2019) *V. vulnificus* type VI secretion System (T6SS) interactions in an oyster in vivo model and their impact on Vibrio ecology. In *International Conference on Biology of Vibrios*, November 17–20, 2019, Montreal, Quebec, Canada.

Hubert, F., Noël, T., and Roch, P. (1996) A member of the arthropod defensin family from rdible mediterranean mussels (*Mytilus galloprovincialis*). *Eur J Biochem* **240**: 302–306.

Hunt, D.E., David, L.A., Gevers, D., Preheim, S.P., Alm, E. J., and Polz, M.F. (2008a) Resource partitioning and sympatric differentiation among closely related bacterioplankton. *Science* **320**: 1081–1085.

Hunt, D.E., Gevers, D., Vahora, N.M., and Polz, M.F. (2008b) Conservation of the chitin utilization pathway in the *Vibrionaceae*. *Appl Environ Microbiol* **74**: 44–51.

Itoh, N., Okada, Y., Takahashi, K.G., and Osada, M. (2010) Presence and characterization of multiple mantle lysozymes in the Pacific oyster, *Crassostrea gigas*. *Fish Shellfish Immunol* **29**: 126–135.

Jesser, K.J., and Noble, R.T. (2018) Vibrio ecology in the Neuse river estuary, North Carolina, characterized by next-generation amplicon sequencing of the gene encoding heat shock protein 6. *Appl Environ Microbiol* **84**: e00333-18.

Jiang, S., Qiu, L., Wang, L., Jia, Z., Lv, Z., Wang, M., *et al*. (2018) Transcriptomic and quantitative proteomic analyses provide insights into the phagocytic killing of hemocytes in the oyster *Crassostrea gigas*. *Front Immunol* **9**: 1280.

Jones, J.L., Lüdeke, C.H.M., Bowers, J.C., DeRosia-Banick, K., Carey, D.H., and Hastback, W. (2014) Abundance of *Vibrio cholerae*, *V. vulnificus*, and *V. parahaemolyticus* in oysters (*Crassostrea virginica*) and clams (*Mercenaria mercenaria*) from Long Island sound. *Appl Environ Microbiol* **80**: 7667–7672.

Kesarcodi-Watson, A., Kaspar, H., Lategan, M.J., and Gibson, L. (2009) Two pathogens of Greenshel mussel larvae, *Perna canaliculus*: *Vibrio splendidus* and a *V. coralliilyticus/neptunius*-like isolate. *J Fish Dis* **32**: 499–507.

King, W.L., Siboni, N., Kahlke, T., Green, T.J., Labbate, M., and Seymour, J.R. (2019) A new high throughput sequencing assay for characterizing the diversity of natural Vibrio communities and its application to a pacific oyster mortality even. *Front Microbiol* **10**: 2907.

Labreuche, Y., Lambert, C., Soudant, P., Boulo, V., Huvet, A., and Nicolas, J.-L.L. (2006a) Cellular and molecular hemocyte responses of the Pacific oyster, *Crassostrea gigas*, following bacterial infection with *Vibrio aestuarianus* strain 01/32. *Microbes Infect* **8**: 2715–2724.

Labreuche, Y., Le Roux, F., Henry, J., Zatylny, C., Huvet, A., Lambert, C., *et al*. (2010) *Vibrio aestuarianus* zinc metalloprotease causes lethality in the Pacific oyster *Crassostrea gigas* and impairs the host cellular immune defenses. *Fish Shellfish Immunol* **29**: 753–758.

Labreuche, Y., Soudant, P., Gonçalves, M., Lambert, C., and Nicolas, J.-L. (2006b) Effects of extracellular products from the pathogenic *Vibrio aestuarianus* strain 01/32 on lethality and cellular immune responses of the oyster *Crassostrea gigas*. *Dev Comp Immunol* **30**: 367–379.

Lafont, M., Petton, B., Vergnes, A., Pauletto, M., Segarra, A., Gourbal, B., and Montagnani, C. (2017) Long-lasting antiviral innate immune priming in the Lophotrochozoan Pacific oyster, *Crassostrea gigas*. *Sci Rep* **7**: 13143.

Lafont, M., Vergnes, A., Vidal-Dupiol, J., de Lorgeril, J., Gueguen, Y., Haffner, P., *et al*. (2020) A sustained immune response supports long-term antiviral immune priming in the Pacific oyster, *Crassostrea gigas*. *MBio* **11**: e02777-19.

Lasa, A., di Cesare, A., Tassistro, G., Borello, A., Gualdi, S., Furones, D., *et al*. (2019) Dynamics of the Pacific oyster pathobiota during mortality episodes in Europe assessed by 16S rRNA gene profiling and a new target enrichment next-generation sequencing strategy. *Environ Microbiol* **21**: 4548–4562.

Le Roux, F., and Blokesch, M. (2018) Eco-evolutionary dynamics linked to horizontal gene transfer in *Vibrios*. *Annu Rev Microbiol* **72**: 89–110.

Le Roux, F., Wegner, K.M., and Polz, M.F. (2016) Oysters and *Vibrios* as a model for disease dynamics in wild animals. *Trends Microbiol* **24**: 568–580.

Lee, C.-T., Pajuelo, D., Llorens, A., Chen, Y.-H., Leiro, J.M., Padrós, F., *et al*. (2013) MARTX of *Vibrio vulnificus* biotype 2 is a virulence and survival factor. *Environ Microbiol* **15**: 419–432.

Lemire, A., Goudenege, D., Versigny, T., Petton, B., Calteau, A., Labreuche, Y., and Le Roux, F. (2015) Populations, not clones, are the unit of vibrio pathogenesis in naturally infected oysters. *ISME J* **9**: 1523–1531.

Lokmer, A., Goedknegt, M.A., Thieltges, D.W., Fiorentino, D., Kuenzel, S., Baines, J.F., and Wegner, K. M. (2016a) Spatial and temporal dynamics of pacific oyster hemolymph microbiota across multiple scales. *Front Microbiol* **7**: 1367.

Lokmer, A., Kuenzel, S., Baines, J.F., and Wegner, K.M. (2016b) The role of tissue-specific microbiota in initial establishment success of Pacific oysters. *Environ Microbiol* **18**: 970–987.

Lokmer, A., and Mathias Wegner, K.M. (2015) Hemolymph microbiome of Pacific oysters in response to temperature, temperature stress and infection. *ISME J* **9**: 670–682.

Loth, K., Vergnes, A., Barreto, C., Voisin, S.N., Meudal, H., Da Silva, J., *et al*. (2019) The ancestral N-terminal nomain of big Defensins drives bacterially triggered assembly into antimicrobial nanonets. *MBio* **10**: e01821–e01819.

Lupo, C. and Le Bouquin, S. (2019) Revue systématique de la littérature relative aux facteurs de risque de mortalité des moules exploitées en France, IFREMER, PDG-RBE-SGMM-LGPMM, Station de La Tremblade, Avenue de Mus de Loup, F-17390 La Tremblade, France.

Lv, Z., Qiu, L., Wang, M., Jia, Z., Wang, W., Xin, L., *et al*. (2018) Comparative study of three C1q domain containing proteins from pacific oyster *Crassostrea gigas*. *Dev Comp Immunol* **78**: 42–51.

Ma, A.T., McAuley, S., Pukatzki, S., and Mekalanos, J.J. (2009) Translocation of a *Vibrio cholerae* type VI secretion effector requires bacterial endocytosis by host cells. *Cell Host Microbe* **5**: 234–243.

Manning, A.J., and Kuehn, M.J. (2011) Contribution of bacterial outer membrane vesicles to innate bacterial defense. *BMC Microbiol* **11**: 258.

Mathur, J., Davis, B.M., and Waldor, M.K. (2007) Antimicrobial peptides activate the *Vibrio cholerae* σE regulon through an OmpU-dependent signalling pathway. *Mol Microbiol* **63**: 848–858.

Mathur, J., and Waldor, M.K. (2004) The *Vibrio cholerae* ToxR-regulated porin OmpU confers resistance to antimicrobial peptides. *Infect Immun* **72**: 3577–3583.

Matz, C., and Kjelleberg, S. (2005) Off the hook - how bacteria survive protozoan grazing. *Trends Microbiol* **13**: 302–307.

McFall-Ngai, M. (2014) Divining the essence of symbiosis: insights from the squid-vibrio model. *PLoS Biol* **12**: e1001783.

McFall-Ngai, M., Hadfield, M.G., Bosch, T.C.G., Carey, H.V., Domazet-Lošo, T., Douglas, A.E., *et al*. (2013) Animals in a bacterial world, a new imperative for the life sciences. *Proc Natl Acad Sci U S A* **110**: 3229–3236.

Mikonranta, L., Friman, V.-P., and Laakso, J. (2012) Life history trade-offs and relaxed selection can decrease bacterial virulence in environmental reservoirs. *PLoS One* **7**: e43801.

Mitta, G., Vandenbulcke, F., Hubert, F., and Roch, P. (1999) Mussel defensins are synthesised and processed in granulocytes then released into the plasma after bacterial challenge. *J Cell Sci* **112**: 4233–4242.

Mitta, G., Vandenbulcke, F., Noel, T., Romestand, B., Beauvillain, J.C., Salzet, M., and Roch, P. (2000) Differential distribution and defence involvement of antimicrobial peptides in mussel. *J Cell Sci* **113**: 2759–2769.

Neyrolles, O., Wolschendorf, F., Mitra, A., and Niederweis, M. (2015) Mycobacteria, metals, and the macrophage. *Immunol Rev* **264**: 249–263.

Oyanedel, D., Labreuche, Y., Bruto, M., Amraoui, H., Robino, E., Haffner, P., *et al*. (2020) Vibrio splendidus O-antigen structure: a trade-off between virulence to oysters and resistance to grazers. *Environ Microbiol*. https://doi.org/10.1111/1462-2920.14996.

Pallavicini, A., del Mar Costa, M., Gestal, C., Dreos, R., Figueras, A., Venier, P., and Novoa, B. (2008) High sequence variability of myticin transcripts in hemocytes of immune-stimulated mussels suggests ancient host–pathogen interactions. *Dev Comp Immunol* **32**: 213–226.

Pan, K., and Wang, W.-X. (2009) Biodynamics to explain the difference of copper body concentrations in five marine bivalve species. *Environ Sci Technol* **43**: 2137–2143.

Parizadeh, L., Tourbiez, D., Garcia, C., Haffner, P., Dégremont, L., Le Roux, F., and Travers, M.-A. (2018) Ecologically realistic model of infection for exploring the host damage caused by *Vibrio aestuarianus*. *Environ Microbiol* **20**: 4343–4355.

Park, J.M., Ghosh, S., and O'Connor, T.J. (2020) Combinatorial selection in amoebal hosts drives the evolution of the human pathogen *Legionella pneumophila*. *Nat Microbiol* **5**: 599–609. https://doi.org/10.1038/s41564-019-0663-7.

Parry, H.E., and Pipe, R.K. (2004) Interactive effects of temperature and copper on immunocompetence and disease susceptibility in mussels (*Mytilus edulis*). *Aquat Toxicol* **69**: 311–325.

Pernthaler, J. (2005) Predation on prokaryotes in the water column and its ecological implications. *Nat Rev Microbiol* **3**: 537–546.

Pezzati, E., Canesi, L., Damonte, G., Salis, A., Marsano, F., Grande, C., *et al*. (2015) Susceptibility of *Vibrio aestuarianus* 01/032 to the antibacterial activity of *Mytilus* haemolymph: identification of a serum opsonin involved in mannose-sensitive interactions. *Environ Microbiol* **17**: 4271–4279.

Piel, D., Bruto, M., James, A., Labreuche, Y., Lambert, C., Janicot, A., *et al*. (2019) Selection of *Vibrio crassostreae* relies on a plasmid expressing a type 6 secretion system cytotoxic for host immune cells. *Environ Microbiol*. https://doi.org/10.1111/1462-2920.14776.

Pierce, M.L., and Ward, J.E. (2019) Gut microbiomes of the eastern oyster *Crassostrea virginica* and the blue mussel *Mytilus edulis*: temporal variation and the influence of

marine aggregate-associated microbial communities. *mSphere* **4**: e00730-19.

Poirier, A.C., Schmitt, P., Rosa, R.D., Vanhove, A.S., Kieffer-Jaquinod, S., Rubio, T.P., *et al*. (2014) Antimicrobial histones and DNA traps in invertebrate immunity: evidences in *Crassostrea gigas*. *J Biol Chem* **289**: 24821–24831.

Poretsky, R., Rodriguez-R, L.M., Luo, C., Tsementzi, D., and Konstantinidis, K.T. (2014) Strengths and limitations of 16S rRNA gene amplicon sequencing in revealing temporal microbial community dynamics. *PLoS One* **9**: e93827.

Preheim, S.P., Boucher, Y., Wildschutte, H., David, L.A., Veneziano, D., Alm, E.J., and Polz, M.F. (2011) Metapopulation structure of *Vibrionaceae* among coastal marine invertebrates. *Environ Microbiol* **13**: 265–275.

Pruzzo, C., Gallo, G., and Canesi, L. (2005) Persistence of vibrios in marine bivalves: the role of interactions with haemolymph components. *Environ Microbiol* **7**: 761–772.

Pukatzki, S., Ma, A.T., Sturtevant, D., Krastins, B., Sarracino, D., Nelson, W.C., *et al*. (2006) Identification of a conserved bacterial protein secretion system in *Vibrio cholerae* using the *Dictyostelium* host model system. *Proc Natl Acad Sci U S A* **103**: 1528–1533.

Reddick, L.E., and Alto, N.M. (2014) Bacteria fighting back: how pathogens target and subvert the host innate immune system. *Mol Cell* **54**: 321–328.

Rey-Campos, M., Moreira, R., Gerdol, M., Pallavicini, A., Novoa, B., and Figueras, A. (2019) Immune tolerance in *Mytilus galloprovincialis* hemocytes after repeated contact with *Vibrio splendidus*. *Front Immunol* **10**: 1–15.

Rey-Campos, M., Moreira, R., Romero, A., Medina-Gali, R. M., Novoa, B., Gasset, M., and Figueras, A. (2020) Transcriptomic analysis reveals the wound healing activity of mussel Myticin C. *Biomolecules* **10**: 133.

Reyes-Robles, T., Dillard, R.S., Cairns, L.S., Silva-Valenzuela, C.A., Housman, M., Ali, A., *et al*. (2018) *Vibrio cholerae* outer membrane vesicles inhibit bacteriophage infection. *J Bacteriol* **200**: e00792-17.

Ritchie, J.M., Rui, H., Zhou, X., Iida, T., Kodoma, T., Ito, S., *et al*. (2012) Inflammation and disintegration of intestinal villi in an experimental model for *Vibrio parahaemolyticus*-induced diarrhea. *PLoS Pathog* **8**: e1002593.

Robino, E., Poirier, A.C., Amraoui, H., Le Bissonnais, S., Perret, A., Lopez-Joven, C., *et al*. (2019) Resistance of the oyster pathogen *Vibrio tasmaniensis* LGP32 against grazing by *Vannella* sp. marine amoeba involves Vsm and CopA virulence factors. *Environ Microbiol*. https://doi.org/10.1111/1462-2920.14770.

Romalde, J.L., and Barja, J.L. (2010) Bacteria in molluscs: good and bad guys. *Curr Res Technol Educ Top Appl Microbiol Microb Biotechnol*, **1**, 136–147.

Romalde, J.L., Diéguez, A.L., Lasa, A., and Balboa, S. (2014) New *Vibrio* species associated to molluscan microbiota: a review. *Front Microbiol* **4**: 1–11.

Romero, A., Costa, M., Forn-Cuni, G., Balseiro, P., Chamorro, R., Dios, S., *et al*. (2014) Occurrence, seasonality and infectivity of *Vibrio* strains in natural populations of mussels *Mytilus galloprovincialis*. *Dis Aquat Organ* **108**: 149–163.

Romero, A., Novoa, B., and Figueras, A. (2020) Extracellular traps (ETosis) can be activated through NADPH-dependent and -independent mechanisms in bivalve mollusks. *Dev Comp Immunol* **106**: 103585.

Rosa, R.D., de Lorgeril, J., Tailliez, P., Bruno, R., Piquemal, D., and Bachère, E. (2012) A hemocyte gene expression signature correlated with predictive capacity of oysters to survive *Vibrio* infections. *BMC Genomics* **13**: 252.

Rosenberg, E., and Falkovitz, L. (2004) The Vibrio shiloi/Oculina patagonica model system of coral bleaching. *Annu Rev Microbiol* **58**: 143–159.

Rubio, T., Oyanedel, D., Labreuche, Y., Toulza, E., Luo, X., Bruto, M., *et al*. (2019) Species-specific mechanisms of cytotoxicity toward immune cells determine the successful outcome of *Vibrio* infections. *Proc Natl Acad Sci U S A* **116**: 14238–14247.

Russell, S.L., and Cavanaugh, C.M. (2017) Intrahost genetic diversity of bacterial symbionts exhibits evidence of mixed infections and recombinant haplotypes. *Mol Biol Evol* **34**: 2747–2761.

Saulnier, D., De Decker, S., Haffner, P., Cobret, L., Robert, M., and Garcia, C. (2010) A large-scale epidemiological study to identify bacteria pathogenic to Pacific oyster *Crassostrea gigas* and correlation between virulence and metalloprotease-like activity. *Microb Ecol* **59**: 787–798.

Sawabe, T., Ogura, Y., Matsumura, Y., Feng, G., Rohul Amin, A.K.M., Mino, S., *et al*. (2013) Updating the *Vibrio* clades defined by multilocus sequence phylogeny: proposal of eight new clades, and the description of *Vibrio tritonius* sp. nov. *Front Microbiol* **4**: 1–14.

Schmitt, P., de Lorgeril, J., Gueguen, Y., Destoumieux-Garzón, D., and Bachère, E. (2012a) Expression, tissue localization and synergy of antimicrobial peptides and proteins in the immune response of the oyster *Crassostrea gigas*. *Dev Comp Immunol* **37**: 363–370.

Schmitt, P., Gueguen, Y., Desmarais, E., Bachère, E., and De Lorgeril, J. (2010) Molecular diversity of antimicrobial effectors in the oyster *Crassostrea gigas*. *BMC Evol Biol* **10**: 12.

Schmitt, P., Rosa, R.D., Duperthuy, M., de Lorgeril, J., Bachère, E., Destoumieux-Garzón, D., *et al*. (2012b) The antimicrobial defense of the Pacific oyster, *Crassostrea gigas*. How diversity may compensate for scarcity in the regulation of resident/pathogenic microflora. *Front Microbiol* **3**: 160.

Seed, K.D., Faruque, S.M., Mekalanos, J.J., Calderwood, S. B., Qadri, F., and Camilli, A. (2012) Phase variable o-antigen biosynthetic genes control expression of the major protective antigen and bacteriophage receptor in *Vibrio cholerae* O1. *PLoS Pathog* **8**: e1002917.

Shen, X., Cai, Y., Liu, C., Liu, W., Hui, Y., and Su, Y.-C. (2009) Effect of temperature on uptake and survival of *Vibrio parahaemolyticus* in oysters (*Crassostrea plicatula*). *Int J Food Microbiol* **136**: 129–132.

Shi, B., Wang, T., Zeng, Z., Zhou, L., You, W., and Ke, C. (2019) The role of copper and zinc accumulation in defense against bacterial pathogen in the Fujian oyster (*Crassostrea angulata*). *Fish Shellfish Immunol* **92**: 72–82.

Smith, V.J., Accorsi, A., and Malagoli, D. (2016) Chapter 1 - Hematopoiesis and hemocytes in Pancrustacean and Molluscan models. In *The Evolution of the Immune System:*

Conservation and Diversification, Malagoli, D.Cambridge, MA, USA: (ed): Academic Press, pp. 1–28.

Šolić, M., Krstulović, N., Jozić, S., and Curać, D. (1999) The rate of concentration of faecal coliforms in shellfish under different environmental conditions. *Environ Int* **25**: 991–1000.

Speare, L., Cecere, A.G., Guckes, K.R., Smith, S., Wollenberg, M.S., Mandel, M.J., *et al*. (2018) Bacterial symbionts use a type VI secretion system to eliminate competitors in their natural host. *Proc Natl Acad Sci U S A* **115**: E8528–E8537.

Stabili, L., Acquaviva, M.I., and Cavallo, R.A. (2005) *Mytilus galloprovincialis* filter feeding on the bacterial community in a Mediterranean coastal area (Northern Ionian Sea, Italy). *Water Res* **39**: 469–477.

Stubbendieck, R.M., and Straight, P.D. (2016) Multifaceted interfaces of bacterial competition. *J Bacteriol* **198**: 2145–2155.

Stubbendieck, R.M., Vargas-Bautista, C., and Straight, P.D. (2016) Bacterial communities: interactions to scale. *Front Microbiol* **7**: 1234.

Sun, S., Kjelleberg, S., and McDougald, D. (2013) Relative contributions of *Vibrio* polysaccharide and quorum sensing to the resistance of *Vibrio cholerae* to predation by heterotrophic protists. *PLoS One* **8**: e56338.

Tack, D.M., Marder, E.P., Griffin, P.M., Cieslak, P.R., Dunn, J., Hurd, S., *et al*. (2019) Preliminary incidence and trends of infections with pathogens transmitted commonly through food - foodborne diseases active surveillance network, 10 U.S. sites, 2015-2018. *Morb Mortal Wkly Rep* **68**: 369–373.

Takemura, A., Chien, D., and Polz, M. (2014) Associations and dynamics of *Vibrionaceae* in the environment, from the genus to the population level. *Front Microbiol* **5**: 38.

Tanguy, M., Gauthier-Clerc, S., Pellerin, J., Danger, J.-M., and Siah, A. (2018) The immune response of *Mytilus edulis* hemocytes exposed to *Vibrio splendidus* LGP32 strain: a transcriptomic attempt at identifying molecular actors. *Fish Shellfish Immunol* **74**: 268–280.

Tanguy, M., McKenna, P., Gauthier-Clerc, S., Pellerin, J., Danger, J.-M., and Siah, A. (2013) Functional and molecular responses in *Mytilus edulis* hemocytes exposed to bacteria, *Vibrio splendidus*. *Dev Comp Immunol* **39**: 419–429.

Travers, M.-A., Basuyaux, O., Le Goic, N., Huchette, S., Nicolas, J.-L., Koken, M., and Paillard, C. (2009) Influence of temperature and spawning effort on *Haliotis tuberculata* mortalities caused by *Vibrio harveyi*: an example of emerging vibriosis linked to global warming. *Glob Chang Biol* **15**: 1365–1376.

Travers, M.-A., Boettcher Miller, K., Roque, A., and Friedman, C.S. (2015) Bacterial diseases in marine bivalves. *J Invertebr Pathol* **131**: 11–31.

Travers, M.-A., Tourbiez, D., Parizadeh, L., Haffner, P., Kozic-Djellouli, A., Aboubaker, M., *et al*. (2017) Several strains, one disease: experimental investigation of *Vibrio aestuarianus* infection parameters in the Pacific oyster, *Crassostrea gigas*. *Vet Res* **48**: 32.

Vaitkevicius, K., Lindmark, B., Ou, G., Song, T., Toma, C., Iwanaga, M., *et al*. (2006) A *Vibrio cholerae* protease needed for killing of *Caenorhabditis elegans* has a role in protection from natural predator grazing. *Proc Natl Acad Sci U S A* **103**: 9280–9285.

Valeru, S.P., Shanan, S., Alossimi, H., Saeed, A., Sandström, G., and Abd, H. (2014) Lack of outer membrane protein A enhances the release of outer membrane vesicles and survival of *Vibrio cholerae* and suppresses viability of *Acanthamoeba castellanii*. *Int J Microbiol* **2014**: 610190.

Van der Henst, C., Scrignari, T., Maclachlan, C., and Blokesch, M. (2016) An intracellular replication niche for *Vibrio cholerae* in the amoeba *Acanthamoeba castellanii*. *ISME J* **10**: 897–910.

Van der Henst, C., Vanhove, A.S., Carolina, N., Dörr, D., Stutzmann, S., Stoudmann, C., *et al*. (2018a) Molecular insights into *Vibrio choleraea* intra-amoebal host-pathogen interactions. *Nat Commun* **9**: 3460.

Van der Henst, C., Vanhove, A.S., Drebes Dörr, N.C., Stutzmann, S., Stoudmann, C., Clerc, S., *et al*. (2018b) Molecular insights into *Vibrio cholerae*'s intra-amoebal host-pathogen interactions. *Nat Commun* **9**: 3460.

Vanhove, A.S., Duperthuy, M., Charrière, G.M., Le Roux, F., Goudenège, D., Gourbal, B., *et al*. (2015) Outer membrane vesicles are vehicles for the delivery of *Vibrio tasmaniensis* virulence factors to oyster immune cells. *Environ Microbiol* **17**: 1152–1165.

Vanhove, A.S., Rubio, T.P., Nguyen, A.N., Lemire, A., Roche, D., Nicod, J., *et al*. (2016) Copper homeostasis at the host vibrio interface: lessons from intracellular vibrio transcriptomics. *Environ Microbiol* **18**: 875–888.

Vezzulli, L., Grande, C., Reid, P.C., Hélaouët, P., Edwards, M., Höfle, M.G., *et al*. (2016) Climate influence on *Vibrio* and associated human diseases during the past half-century in the coastal North Atlantic. *Proc Natl Acad Sci U S A* **113**: E5062–E5071.

Vezzulli, L., Pezzati, E., Stauder, M., Stagnaro, L., Venier, P., and Pruzzo, C. (2015) Aquatic ecology of the oyster pathogens *Vibrio splendidus* and *Vibrio aestuarianus*. *Environ Microbiol* **17**: 1065–1080.

Vezzulli, L., Stagnaro, L., Grande, C., Tassistro, G., Canesi, L., and Pruzzo, C. (2018) Comparative 16SrDNA gene-based microbiota profiles of the Pacific oyster (*Crassostrea gigas*) and the mediterranean mussel (*Mytilus galloprovincialis*) from a shellfish farm (Ligurian Sea, Italy). *Microb Ecol* **75**: 495–504.

Vidal-Dupiol, J., Ladriere, O., Destoumieux-Garzon, D., Sautiere, P.-E., Meistertzheim, A.-L., Tambutte, E., *et al*. (2011) Innate immune responses of a scleractinian soral to vibriosis. *J Biol Chem* **286**: 22688–22698.

Wang, W., Li, M., Wang, L., Chen, H., Liu, Z., Jia, Z., *et al*. (2017) The granulocytes are the main immunocompetent hemocytes in *Crassostrea gigas*. *Dev Comp Immunol* **67**: 221–228.

Wang, W., Wang, L., Liu, Z., Song, X., Yi, Q., Yang, C., and Song, L. (2020) The involvement of TLR signaling and anti-bacterial effectors in enhanced immune protection of oysters after *Vibrio splendidus* pre-exposure. *Dev Comp Immunol* **103**: 103498.

Wegner, K.M., Piel, D., Bruto, M., John, U., Mao, Z., Alunno-Bruscia, M., *et al*. (2019) Molecular targets for coevolutionary interactions between Pacific oyster larvae and their sympatric vibrios. *Front Microbiol* **10**: 1–13.

Wendling, C.C., and Wegner, K.M. (2015) Adaptation to enemy shifts: rapid resistance evolution to local vibrio spp. in invasive pacific oysters. *Proc R Soc B Biol Sci* **282**: 20142244.

Wildschutte, H., Preheim, S.P., Hernandez, Y., and Polz, M. F. (2010) O-antigen diversity and lateral transfer of the wbe region among *Vibrio splendidus* isolates. *Environ Microbiol* **12**: 2977–2987.

Williams, T.C., Froelich, B.A., Phippen, B., Fowler, P., Noble, R.T., and Oliver, J.D. (2017) Different abundance and correlational patterns exist between total and presumed pathogenic *Vibrio vulnificus* and *V. parahaemolyticus* in shellfish and waters along the North Carolina coast. *FEMS Microbiol Ecol*, **93**(6), 1–11.

Xue, Q., Hellberg, M.E., Schey, K.L., Itoh, N., Eytan, R.I., Cooper, R.K., and La Peyre, J.F. (2010) A new lysozyme from the eastern oyster, *Crassostrea virginica*, and a possible evolutionary pathway for i-type lysozymes in bivalves from host defense to digestion. *BMC Evol Biol* **10**: 213.

Zannella, C., Mosca, F., Mariani, F., Franci, G., Folliero, V., Galdiero, M., *et al*. (2017) Microbial diseases of bivalve mollusks: infections, immunology and antimicrobial defense. *Mar Drugs* **15**(182), 1–36.

Zhang, T., Qiu, L., Sun, Z., Wang, L., Zhou, Z., Liu, R., *et al*. (2014) The specifically enhanced cellular immune responses in Pacific oyster (*Crassostrea gigas*) against secondary challenge with *Vibrio splendidus*. *Dev Comp Immunol* **45**: 141–150.

Wilson, B., Muirhead, A., Bazanella, M., Huete-Stauffer, C., Vezzulli, L., & Bourne, D.G. (2013). An Improved Detection and Quantification Method for the Coral PathogenVibrio coralliilyticus. *Plos One*, **8**(12), e81800

Stauder, M., Vezzulli, L., Pezzati, E., Repetto, B., & Pruzzo, C. (2010). Temperature affects Vibrio cholerae O1 El Tor persistence in the aquatic environment via an enhanced expression of GbpA and MSHA adhesins. *Env Microbiol Rep*, **2**(1), 140–144.

Bases moléculaires et cellulaires des interactions *Vibrio* / *Crassostrea gigas* en contexte sain et pathologique.

Les bactéries du genre *Vibrio* sont ubiquitaires dans les milieux aquatiques. Elles adoptent des modes de vie libres et associés. Elles établissent des symbioses mutualistes, commensales et parasitaires avec de nombreux métazoaires. Chez l'huître *Crassostrea gigas* saine, un microbiote abondant et diversifié qui comprend de nombreux *Vibrio* est maintenu sous homéostasie immunitaire. Toutefois, sous l'influence de stress biotiques ou abiotiques une dysbiose se crée favorisant la prolifération d'espèces opportunistes de *Vibrio* qui peuvent induire la mort des huîtres. C'est notamment le cas lors du syndrome de mortalité des huîtres du Pacifique (POMS) provoqué par un virus immunosuppresseur, OsHV-1 µvar. Nous avons ici caractérisé les interactions *Vibrio* / *C. gigas* en contexte sain et pathologique. Nous montrons que chez des populations de *V. splendidus* associées à des huîtres saines, la virulence et la capacité de colonisation peuvent être contraintes par la sélection de structures de l'antigène O qui sont plus facilement reconnues par le système immunitaire de l'hôte mais qui confèrent une résistance au broutage par des amibes marines. Ce compromis entre la capacité à coloniser son hôte et la persistance environnementale est vraisemblablement à l'origine de la grande diversité structurale observée pour l'antigène O dans cette espèce. En contexte pathologique, nous avons montré que les espèces associées à l'huître sont en grande majorité cytotoxiques pour les cellules immunitaires de leur hôte, et ce, quel que soit l'environnement considéré (Atlantique, Méditerranée). Cette cytotoxicité est un déterminant clé de l'échappement aux puissantes défenses cellulaires de l'huître et du succès infectieux. Nous avons observé que les bases moléculaires de la cytotoxicité sont spécifiques à chaque espèce de *Vibrio* étudiée. Enfin, au-delà des agents pathogènes opportunistes qui utilisent la cytotoxicité (*V. tasmaniensis, V. crassostreae, V. splendidus, V. harveyi*), nous avons identifié de simples opportunistes, comme *V. rotiferianus*, qui non seulement bénéficient de l'activité immunosuppressive des autres agents pathogènes mais également adoptent des stratégies d'acquisition non coopérative de biens publics, tels que les sidérophores produits par la communauté microbienne hébergée par leur hôte.

Cellular and molecular bases of *Vibrio* interactions with *Crassostrea gigas* oysters in health and disease

Bacteria of the genus *Vibrio* are ubiquitous in aquatic environments. They adopt free and associated lifestyles. They establish mutualistic, commensal and parasitic symbioses with numerous metazoa. In the healthy *Crassostrea gigas* oyster, an abundant and diverse microbiota that includes many *Vibrio* is maintained under immune homeostasis. However, under the influence of biotic or abiotic stressors a dysbiosis is created favoring the proliferation of opportunistic *Vibrio* species, which can induce the death of oysters. This occurs during the Pacific Oyster Mortality Syndrome (POMS), which is caused by an immunosuppressive virus, OsHV-1 µvar. We have here characterized the *Vibrio* / *C. gigas* interactions in health and disease. We show that in populations of *V. splendidus* associated with healthy oysters, virulence and colonization capacity can be constrained by the selection of O-antigen structures that are more easily recognized by the host immune system but which confer resistance to grazing by marine amoebae. This trade-off between the ability to colonize its host and environmental persistence is likely the cause of the great structural diversity observed for the O-antigen in this species. In a pathological context, we have shown that the species associated with the oyster are for the most part cytotoxic for the immune cells of their host, regardless of the environment considered (Atlantic, Mediterranean). This cytotoxicity is a key determinant of the escape from the oyster's powerful cellular defenses and determines the infectious success. We observed that the molecular bases of cytotoxicity are specific to each *Vibrio* species studied. Finally, beyond opportunistic pathogens that use cytotoxicity (*V. tasmaniensis, V. crassostreae, V. splendidus, V. harveyi*), we have identified simple opportunists, such as *V. rotiferianus,* which not only benefit from the immunosuppressive activity of other pathogens but also adopt strategies of non-cooperative acquisition of public goods, such as siderophores produced by the microbial community hosted by their host.